Viral Hepatitis and Fatty Liver Disease in Liver Cancer: two sides of the coin

Jiaye Liu

Cover layout: the author of the thesis

Cover design: Edith Luethi

Source of image: https://pixabay.com/photos/art-abstract-painting-abstract-art-3028303/

Printed by: Ridderprint BV, the Netherlands

Financial support for printing this thesis was kindly provided by

Erasmus MC – University Medical Center Rotterdam

ISBN: 978-94-6416-322-3

Viral Hepatitis and Fatty Liver Disease in Liver Cancer: two sides of the coin

Virale hepatitis en leververvetting bij leverkanker: twee kanten van dezelfde medaille

---

Thesis

To obtain the degree of Doctor from the
Erasmus University Rotterdam
by command of the
rector magnificus

Prof. dr. R.C.M.E. Engels

and in accordance with the decision of the Doctorate Board

The public defense shall be held on

Tuesday 15th December 2020 at 9:30

by

Jiaye Liu

Born in Chongqing Province, China

Erasmus University Rotterdam

DOCTORAL COMMITTEE

Promotor

Prof. dr. M.P. Peppelenbosch

Inner Committee

Prof dr. R.A. de Man

Prof dr. A.J. Moshage

Prof dr. R.P.J. Oude Elferink

Co-promotor

Dr. Q. Pan

Contents

CHAPTER 1

General Introduction and Aim of This Thesis

The liver is a vertebrate-specific structure essential for all member species of this subphylum, including humans, for detoxification, homeostasis, digestion and growth. It is an accessory digestive organ, producing bile (an alkaline fluid containing cholesterol and bile acids), which aids absorption of fat and fat-soluble micronutrients. The liver consists mostly of hepatocytes which perform a wide variety of high-volume biochemical reactions, including the synthesis and breakdown of small and complex biomolecules, many of which are necessary for normal vital functions. Estimates regarding the organ's total number of functions vary, but a common number listed in textbooks is it being around 500. Although, or maybe because of, being essential for life, it is also the location of many diseases. In this thesis I have pursued to obtain more insight in the disease of the liver.

Hepatitis C

Liver disease often involves hepatitis (inflammation of the liver). Although there are many etiologies that underlie hepatitis, the viral infection is probably the most common cause of hepatitis. In this thesis I provide special attention to Hepatitis C virus (HCV), which can be labelled as an import global health problem as chronic HCV infection is the second most common risk factor for hepatocellular carcinoma (HCC) and is responsible for 10–25% of all HCC cases.[1] Hence there is an urgent to better understand the dynamics of HCV infection and the factors that underlie HCC development in such patients.

An important factor should be taken into account in this respect are developments with respect to treatment of HCV infection. Interferon (IFN)-α and pegylated (PEG) recombinant human IFN were approved for treating HCV infection in 90th century. Although not fully satisfactory, the rate of sustained virologic response (SVR) achieved more than 80% when using response-guided PEG-IFNα plus ribavirin (PR) therapy.[2] Rapid advances in therapy with oral direct-acting antivirals (DAAs) have resulted in further significant improvements in SVR which exceed 95%.[3] Reaching SVR significantly reduces the risk of developing hepatoma, as was already known from the IFN era, so one may have expected that with the newer DAAs, such a risk would be minimized to an occasional event, but several reports from the wider clinical applications of the new treatments were worrying.[4-6] They observed much higher rate HCC development than previous reports on IFN responders which called more attention on the application of DAAs to HCV eradication. Therefor it was important to further investigate whether DAAs would affect HCC development and to evaluate the efficacy and safety in some special cohort of patients.

Hepatitis E

Hepatitis E (HEV) is a single-strand positive-sense RNA virus belongs to the Orthohepevirus genus within the Hepeviridae family and at least four types can produce human infection. It is the most common causative agent for acute viral

hepatitis worldwide and although often hardly symptomatic, it is still estimated that there are around 56000 HEV-related deaths annually.[7] HEV genotype 1 and 2 are indigenous predominantly in countries of the developing world, especially in Asia and Africa. They are transmitted via a fecal-oral route through contaminated water sources in conjunction with poor sanitary conditions, thus these genotypes responsible for many of the water-borne outbreaks of HEV. In contrast, HEV genotypes 3 and 4 infect humans and animals alike and with transmission to humans from animal reservoirs (like pigs) being responsible for the infectious pressure on the human population and human-to-human infection being not important if present at all.[8] The latter strains are mainly restricted to developing countries.[9] In general, HEV causes a self-limiting infection with low mortality. However, fulminant hepatitis may develop and a high mortality rate (as high as 20%-30%) is reported in pregnant women.[10, 11] Chronic HEV infections are increasingly documented in immunocompromised patients, individuals with HIV infection and hemodialysis patients. As thus, HEV constitutes as an important threat to global health and further research into the factors driving disease progression as well as how its best managed is required.

NAFLD and MAFLD

Apart, from infections of pathogens, also lifestyle may be responsible for important pathology in the liver. Maybe nonalcoholic fatty liver disease (NAFLD, also called metabolic dysfunction-associated fatty liver disease [MAFLD]) is one of the most important liver diseases. This condition, to a certain extent, can be considered as a hepatic manifestation of metabolic syndrome, in turn the consequence of an unhealthy diet and sedentary behavioral style.[12] Practically, NAFLD is defined as the presence of 5% of hepatic steatosis in the absence of competing liver disease etiologies, such as chronic viral hepatitis, use of medications that induce steatosis (such as amiodarone or tamoxifen), or other chronic liver diseases, such as autoimmune hepatitis, hemochromatosis, Wilson's disease, or significant alcohol consumption. Although NAFLD is very common and not an overly serious condition, a subgroup of patients progresses to nonalcoholic steatohepatitis (NASH), which is a more serious type of liver disease. NASH is defined histologically by presence of hepatic steatosis with evidence for hepatocyte damage (ballooning hepatocytes).[12] NASH is associated with a multitude of pathological events, but hepatic fibrosis and cirrhosis are especially problematic.[13-15] Indeed, NASH has been recognized as one of the leading causes of cirrhosis in adults in the United States.[16-18]

Moreover, HCC has been linked to NAFLD. A comparative study from USA documented the yearly cumulative incidence of HCC was 2.6% in patients with NASH-associated cirrhosis.[19] In parallel, a large US health care database study identified NAFLD or NASH as the most common underlying risk factor for HCC, being present in 59% of cases, and NAFLD-associated HCC was recognized as an emerging indication for liver transplantation in the USA.[20, 21] Accordingly, the

number of individuals with NAFLD potentially at risk for developing HCC may be much larger than previously thought. This presents a compelling need to understand the epidemiological information of NAFLD and review potential strategies for HCC prevention and surveillance in the affected population.

Liver cancer

Apart from viral infection and steatosis, genetic transformation and subsequent uncontrolled growth of tumor cells are also important sources of liver disease. Liver cancer has a relatively high prevalence and in combination with a paucity of curative and therapeutic options, it remains a leading cause of mortality worldwide.[22] With increasing age, the incidence of liver cancer increases and thus the globally rising life expectancy will further provoke more cases of this deadly disease.[23, 24] According to the GLOBOCAN 2018 survey, an estimated 18.1 million new cases of liver cancer occurred, while 9.6 million cancer deaths were a consequence of this disease.[25] It is thus evident that liver cancer is a major health problem warranting further research.

Liver cancer is a term that groups various subtypes of disease, including HCC (the most prevalent form), cholangiocarcinoma (CCA) and various other rare types. In conjunction they constitute the fourth leading cause of cancer-related death.[25] HCC accounts for 75% - 85% of liver cancer and is often the consequence of other etiologies that provoke chronic inflammatory liver diseases, finally culminating in oncogenic transformation including viral hepatitis and liver steatosis.[26] In the principle this would provide a window for prevention and early diagnosis of disease at a potentially curative stage, but unfortunately effective prevention, timely diagnosis and treatment remain challenging. Main issues in this respect are the absence of symptoms and liver cancer progresses silently without specific manifestations, whereas once disease has been established it is highly resistant to therapy.[27] Insights into the characteristics of the cells that initiate the disease, how the cells involved acquire their resistance towards therapeutic intervention, and how physiology of these cells is different from non-transformed cells may all proof necessary to devise novel avenues for the rational treatment of disease. These are all aspects of liver cancer I have aimed to explore in thesis.

Based on the above I decided to explore in this thesis Hepatitis C, fatty liver disease and liver cancer. In order to be able the field forward (which is fairly competitive) I realized I had to exploit the possibilities provided by novel tools, which I shall discuss below.

LGR5 and Organoids

As also evident from the above, liver biology studies are required, but such studies are very challenging in animal models and particularly in humans. Use of immortal transformed cell lines has been abundant, also by my own host laboratory,[28] but the general opinion among professionals is that their use has proven inadequate with respect to capturing the clinical situation as encountered by oncologists and other physicians. However, progress in stem cell culture achieved in the last decade has made it possible to derive in vitro 3D tissue cultures called organoids.[29] Although organoids are stem cell derived, they are organ-like in many respects. Their use has been extensively described by colleagues in various recent publications.[30, 31] Organoids system not only offer a promising platform for stem cell study but could also be used for modeling a wide range of diseases.[32] In the present thesis I shall do so for various liver diseases, including NAFLD.

Stem cells in cancer are considered to be responsible for tumor initiation and growth, therapy resistance and tumor recurrence due to their unique feature of self-renewal capacity that enables such cells to give birth to offspring of which a substantial fraction retains the stemness.[33] Their physiology remains only partly understood and also markers identifying these cells have not yet been conclusively defined. With regard to liver cancer, analogous to other systems, LGR5 (leucine-rich-repeat-containing G-protein-coupled receptor 5) may mark a group of stem cells proliferating after liver injury induced by carbon tetrachloride (CCL4).[31] Generally, this marked population has high tumorigenesis, evident by their remarkable capacity to form tumors when transplanted into immunodeficient mice.[34] Although cancer stem cells fuel the tumor initiation and tumor growth, making them attractive cancer targets[33], many adult stem cells resemble such cells with respect to marker expression, making it difficult to target cancer stem cells without killing important healthy cells. Encouraging results, however, have been obtained with antibody-drug conjugates. Anti-LGR5-antibody-drug conjugates selectively target and deplete LGR5 stem cells in colon cancer and impede the growth of the primary tumor without a major effect on normal stem cell pool.[35] These observations make LGR5-targeting an attractive novel strategy for combating cancer stem cells and the current thesis I have explored this possibility with respect to liver cancer.

Cancer associated fibroblasts

Apart from cancer stem cells, supporting cell types may also represent a valuable novel target for therapy of liver cancer. In this context cancer-associated fibroblasts (CAFs) attract attention, as they are a major component of the tumor microenvironment. It is thought that they played an important role in cancer progression and drug resistance.[36] Research of the interaction between CAFs and the cancer cells remained challenging. Potentially, in vitro models that involve co-cultures of CAFs and cancer cells may be exploited to determine in a potentially more clinically relevant tumor model medication effects and such cultures may

better mimic the actual situation *in vivo.* Diverse sorts of co-culture systems exploiting the mutual interaction between CAFs and tumor cells have been investigated in previous studies and have gained interest in the cancer research field, stimulating me to further explore possibilities here.[37-39] Important cellular interactions within the tumor microenvironment include the interaction between (presumptive) tumor cells and fibroblasts are known to further promote tumor initiation, progression and metastasis in much of the cancer types investigated.[36, 40, 41] Such models have also been implemented for testing anticancer agents, but unfortunately progress is impeded by the reliance on tumor cell lines and/or fibroblast cell lines and thus current experimentation has not permitted to fully capture the mechanistic details of the mutual interactions involved. Hence, in the present thesis I endeavored to determine how isolated CAFs promote the proliferation and also the angiogenesis of liver cancer in an organoid system that mimics tumors much better as compared to earlier approaches. I find that such organoid systems may be useful for imitating liver cancer and allow long-term cultures for expanding cancer cells, e.g. for precision medicine approaches aimed at extracting personalized information with respect to response to therapy and also for further exploring the properties of cancer cells in general especially the stem cell population defined by LGR5 positivity in particular. With respect to the latter, I addressed my hypothesis that targeting cancer stem cells directly potentially yields improved therapy.

Aim of the thesis

Lipid droplets are an often-ignored ultrastructural feature of cells but may have important roles in explaining pathophysiological mechanisms. With regard to liver disease, their role remains undefined. Hence in chapter 2, I set out to perform a deep study with respect to the body of current biomedical literature in this respect. I find that lipid droplets are closely correlated to lipid storage, lipid metabolism, membrane biosynthesis, cell signaling, inflammation, pathogen-host interaction and cancer development.

Hepatitis C, is the diseases in which lipid droplets may be involved. Recently, lipid droplets have been linked to the action of DAAs with respect to their action in Hepatitis C.[42] Research into Hepatitis C is important as the number of HCV-related cirrhosis has doubled in the last 10 years and is projected to reach peak levels in the next decade. Although the number of decompensated cirrhotic patients has continued to increase, the organ donor pool has remained static over the last decade, resulting in increased liver transplant waitlist mortality. Moreover, HCV occurrence or recurrence is commonly observed in transplant recipients post liver transplantation. DAA therapies, however, have changed the landscape of HCV due to their excellent safety profile and cure rates. In chapter 3, I compared the efficacy and safety of different combinations of DAAs in transplant recipients with HCV

genotype 1 (GT1) infection in order to provide more information for clinical treatment.

Inspired by my results described in chapter 3, in chapter 4 of this thesis, I further built on the observation that IFN-free all-oral DAAs have replaced IFN-based therapy as the standard of care for HCV infection worldwide because of the higher SVR rate and lower incidence of adverse effects. By using currently approved DAA regimens, HCV can be eradicated in more than 95% of infected hosts, regardless of their disease severity. Results with respect to the development of HCC in former HCV patients are, however, more ambiguous. Since 2016, the risk of de novo occurrence or recurrence of HCC in hepatitis C patients receiving DAAs has been debated following a report identifying an unexpected high early tumor recurrence rate in such patients. It is possible that alternative DAA regimens may improve outcomes, possibly also because of different interactions with lipid droplets (see chapter 2). Hence, I initiated an in vitro study on the effects of different concentrations of Sofosbuvir in tumor cells. Intriguingly, I observe a moderate stimulation of proliferation, possibly related to DAA effects with respect to liver cancer.

DAAs (which I investigated in chapter 3 and 4) have revolutionized the management of Hepatitis C, but based on case reports, may have promise in Hepatitis E as well.[43] In order to understand to which extent such strategies might become important, I decided to obtain more insight into the prevalence of Hepatitis E, and the study involved is described in chapter 5. Hepatitis E is the fifth known human viral hepatitis and is probably the most common cause of acute viral hepatitis in the world. Despite being an important cause of hepatitis and being widely studied, the HEV remains poorly understood, with little comprehension about its prevalence in general population, HIV infected individuals, people with acute hepatitis as well as hemodialysis patients. Although chronic HEV infection is not a classical cause of HCC, some case reports have indicated that HEV joins hepatitis B/C viruses as a potential cause of HCC in chronically infected patients.[44] In Chapter 5, I performed a systematic review and meta-analysis in order to pooled estimate the prevalence of HEV in these subgroups.

As explained above, not only viral infection is a substantial health problem, but the lifestyle-associated fatty liver disease is so as well, prompting investigation, especially as the pathophysiology of NAFLD relates to the lipid droplet research described in chapter 2. In chapters 6-8, thus NAFLD becomes the center of my attention. Fatty liver disease has gained high prevalence and a growing contribution to the burden of end-stage liver disease in the general population. In chapter 6 this notion is objectified by investigating the prevalence, incidence, and risk factors for NAFLD in the general population. In addition, I explored the disease progression and clinical outcomes of NAFLD. In view of the results obtained in chapter 7-8, I further investigated the MAFLD prevalence in overweight or obese children/adults. The results provide an up-to-date description of the problem of fatty liver disease

and rationalize further efforts to adequately model this disease for defining rational treatment.

Potential sequela of both viral infection as well as fatty liver disease are the liver cancers that may develop in such patients. As explained above, the (cancer) stem cell compartment may be an attractive target for clinical management of liver cancer. Thus prompted, in chapter 9 and chapter 10, I aim to investigate the interrelationship of the proliferative LGR5 stem cells in liver cancer. In chapter 9, I aim to establish malignant organoids models from mouse injury primary liver tumors and whereas in chapter 10 I demonstrate their applications for liver cancer research. Unfortunately, however, I discovered that the studies involved did not yet fully capture the influence of stromal component in the liver cancer process and thus I decided to explore these aspects better in the last chapter of this thesis.

In chapter 11, I decided to investigate the interaction of the cancer with the stroma and for this purpose I exploit an organoid-based co-culture model that combines CAFs with tumor organoids. CAFs that were activated by tumor cells in a co-culture condition, displayed increases in α-SMA expression and migratory activity. Tumor cell proliferation was significantly increased in the co-culture group when contrasted to the control group. I also showed the presence of a reciprocal interaction between fibroblasts and tumor organoids and their relation to the components of the microenvironment surrounding these two cell types. I conclude that the co-culture system might allow study of the tumor microenvironment and may permit evaluation of drug screening. Especially in combination with other strategies these findings may open the way for improved treatment.

In conjunction, in this thesis I explore the epidemiology of inflammatory disease in liver, the stem cell compartment leading to liver cancer development and the interactions of liver cancer cells with environment (fibroblasts and immune system). I hope to with this multifaceted approach to have contributed to better understanding and care of this deadly disease.

Reference

1. Ghouri YA, Mian I, Rowe JH. Review of hepatocellular carcinoma: Epidemiology, etiology, and carcinogenesis. J Carcinog 2017;16:1.
2. Fried MW, Shiffman ML, Reddy KR, et al. Peginterferon alfa-2a plus ribavirin for chronic hepatitis C virus infection. N Engl J Med 2002;347:975-82.
3. Kohli A, Shaffer A, Sherman A, et al. Treatment of hepatitis C: a systematic review. JAMA 2014;312:631-40.
4. Conti F, Buonfiglioli F, Scuteri A, et al. Early occurrence and recurrence of hepatocellular carcinoma in HCV-related cirrhosis treated with direct-acting antivirals. J Hepatol 2016;65:727-733.
5. Reig M, Marino Z, Perello C, et al. Unexpected high rate of early tumor recurrence in patients with HCV-related HCC undergoing interferon-free therapy. J Hepatol 2016;65:719-726.
6. Kozbial K, Moser S, Schwarzer R, et al. Unexpected high incidence of hepatocellular carcinoma in cirrhotic patients with sustained virologic response following interferon-free direct-acting antiviral treatment. J Hepatol 2016;65:856-858.
7. Blasco-Perrin H, Abravanel F, Blasco-Baque V, et al. Hepatitis E, the neglected one. Liver Int 2016;36 Suppl 1:130-4.
8. Hakim MS, Wang W, Bramer WM, et al. The global burden of hepatitis E outbreaks: a systematic review. Liver Int 2017;37:19-31.
9. Dalton HR. Hepatitis e: the 'new kid on the block' or an old friend? Transfus Med Hemother 2014;41:6-9.
10. Tsega E, Krawczynski K, Hansson BG, et al. Hepatitis E virus infection in pregnancy in Ethiopia. Ethiop Med J 1993;31:173-81.
11. Strand RT, Franque-Ranque M, Bergstrom S, et al. Infectious aetiology of jaundice among pregnant women in Angola. Scand J Infect Dis 2003;35:401-3.
12. Chalasani N, Younossi Z, Lavine JE, et al. The diagnosis and management of non-alcoholic fatty liver disease: practice guideline by the American Gastroenterological Association, American Association for the Study of Liver Diseases, and American College of Gastroenterology. Gastroenterology 2012;142:1592-609.
13. Younossi ZM, Stepanova M, Rafiq N, et al. Pathologic criteria for nonalcoholic steatohepatitis: interprotocol agreement and ability to predict liver-related mortality. Hepatology 2011;53:1874-82.
14. Ekstedt M, Hagstrom H, Nasr P, et al. Fibrosis stage is the strongest predictor for disease-specific mortality in NAFLD after up to 33 years of follow-up. Hepatology 2015;61:1547-54.
15. Angulo P, Kleiner DE, Dam-Larsen S, et al. Liver Fibrosis, but No Other Histologic Features, Is Associated With Long-term Outcomes of Patients With Nonalcoholic Fatty Liver Disease. Gastroenterology 2015;149:389-97 e10.
16. Vernon G, Baranova A, Younossi ZM. Systematic review: the epidemiology and natural history of non-alcoholic fatty liver disease and non-alcoholic steatohepatitis in adults. Aliment Pharmacol Ther 2011;34:274-85.
17. Charlton MR, Burns JM, Pedersen RA, et al. Frequency and outcomes of liver transplantation for nonalcoholic steatohepatitis in the United States. Gastroenterology 2011;141:1249-53.
18. Wong RJ, Aguilar M, Cheung R, et al. Nonalcoholic steatohepatitis is the second leading etiology of liver disease among adults awaiting liver transplantation in the United States. Gastroenterology 2015;148:547-55.
19. Sanyal A, Poklepovic A, Moyneur E, et al. Population-based risk factors and resource utilization for HCC: US perspective. Curr Med Res Opin 2010;26:2183-91.
20. Baffy G, Brunt EM, Caldwell SH. Hepatocellular carcinoma in non-alcoholic fatty liver disease: an emerging menace. J Hepatol 2012;56:1384-91.
21. Wong RJ, Cheung R, Ahmed A. Nonalcoholic steatohepatitis is the most rapidly growing indication for liver transplantation in patients with hepatocellular carcinoma in the U.S. Hepatology 2014;59:2188-95.
22. Gravitz L. Liver cancer. Nature 2014;516:S1.
23. Petrick JL, Braunlin M, Laversanne M, et al. International trends in liver cancer incidence, overall and by histologic subtype, 1978-2007. Int J Cancer 2016;139:1534-45.
24. Wang F, Mubarik S, Zhang Y, et al. Long-Term Trends of Liver Cancer Incidence and Mortality in China 1990-2017: A Joinpoint and Age-Period-Cohort Analysis. Int J Environ Res Public Health 2019;16.
25. Bray F, Ferlay J, Soerjomataram I, et al. Global cancer statistics 2018: GLOBOCAN estimates of incidence and mortality worldwide for 36 cancers in 185 countries. CA Cancer J Clin 2018;68:394-424.
26. Gores GJ. Decade in review-hepatocellular carcinoma: HCC-subtypes, stratification and sorafenib. Nat Rev Gastroenterol Hepatol 2014;11:645-7.
27. Llovet JM, Montal R, Sia D, et al. Molecular therapies and precision medicine for hepatocellular carcinoma. Nat Rev Clin Oncol 2018;15:599-616.
28. Hernanda PY, Pedroza-Gonzalez A, van der Laan LJ, et al. Tumor promotion through the mesenchymal stem cell compartment in human hepatocellular carcinoma. Carcinogenesis 2013;34:2330-40.
29. Clevers H. Modeling Development and Disease with Organoids. Cell 2016;165:1586-1597.
30. Cao W, Liu J, Wang L, et al. Modeling liver cancer and therapy responsiveness using organoids derived from primary mouse liver tumors. Carcinogenesis 2019;40:145-154.
31. Cao W, Li M, Liu J, et al. LGR5 marks targetable tumor-initiating cells in mouse liver cancer. Nat Commun 2020;11:1961.
32. Dutta D, Heo I, Clevers H. Disease Modeling in Stem Cell-Derived 3D Organoid Systems. Trends Mol Med 2017;23:393-410.
33. Greten FR. Cancer: Tumour stem-cell surprises. Nature 2017;543:626-627.
34. de Sousa e Melo F, Kurtova AV, Harnoss JM, et al. A distinct role for Lgr5(+) stem cells in primary and metastatic colon cancer. Nature 2017;543:676-680.
35. Junttila MR, Mao W, Wang X, et al. Targeting LGR5+ cells with an antibody-drug conjugate for the treatment of colon cancer. Sci Transl Med 2015;7:314ra186.
36. Kalluri R. The biology and function of fibroblasts in cancer. Nat Rev Cancer 2016;16:582-98.
37. Cadamuro M, Nardo G, Indraccolo S, et al. Platelet-derived growth factor-D and Rho GTPases regulate recruitment of cancer-associated fibroblasts in cholangiocarcinoma. Hepatology 2013;58:1042-53.
38. Awaji M, Futakuchi M, Heavican T, et al. Cancer-Associated Fibroblasts Enhance Survival and Progression of the Aggressive Pancreatic Tumor Via FGF-2 and CXCL8. Cancer Microenviron 2019;12:37-46.
39. Chen S, Giannakou A, Wyman S, et al. Cancer-associated fibroblasts suppress SOX2-induced dysplasia in a lung squamous cancer coculture. Proc Natl Acad Sci U S A 2018;115:E11671-E11680.
40. Friedrich J, Seidel C, Ebner R, et al. Spheroid-based drug screen: considerations and practical approach. Nat Protoc 2009;4:309-24.

41. Aref AR, Huang RY, Yu W, et al. Screening therapeutic EMT blocking agents in a three-dimensional microenvironment. Integr Biol (Camb) 2013;5:381-9.
42. Park SB, Boyer A, Hu Z, et al. Discovery and characterization of a novel HCV inhibitor targeting the late stage of HCV life cycle. Antivir Ther 2019;24:371-381.
43. Wahid B. Successful treatment of HBV, HCV, & HEV, with 12-week long use of tenofovir, sofosbuvir, daclatasvir, and ribavirin: A case report. J Infect Public Health 2020;13:149-150.
44. Borentain P, Colson P, Bolon E, et al. Hepatocellular carcinoma complicating hepatitis E virus-related cirrhosis. Hepatology 2018;67:446-448.

CHAPTER 2

Lipid Droplets and Interactions with Other Organelles in Liver Diseases

Ling Wang, **Jiaye Liu**, Zhijiang Miao, Qiuwei Pan, Wanlu Cao

In preparation

Abstract

Lipid droplets (LDs) are cellular organelles for lipid storage with a hydrophobic core of neutral lipid enclosed by a phospholipid monolayer. Besides in fat tissue, LDs are also widely present in hepatocytes, and play key roles in health and disease of the liver. LDs dynamically interact with other cellular organelles to exert a variety of biological functions. Besides lipid storage, they are also involved in lipid metabolism, membrane biosynthesis, cell signaling, inflammation, pathogen-host interaction and cancer development. In this review, we aim to concisely decipher the interactions of LDs with other organelles and their functional implications in the important liver diseases, including fatty liver disease, viral hepatitis and liver cancer.

Keywords: lipid droplet, lipid biogenesis, organelle, liver disease

1. Introduction

Lipid droplets (LDs) are newly-recognized cellular organelles found in many types of cells and tissues [1]. It has a hydrophobic core with neutral lipid, usually consisting of triacylglycerols and sterol esters, and encircled by a phospholipid monolayer with integral and peripheral proteins (Fig. 1). Initially, LDs were thought only as lipid deposition in all organisms without biological functions, whereas accumulating research found that different proteins in the surface of LDs endow them various functions (Fig. 1).

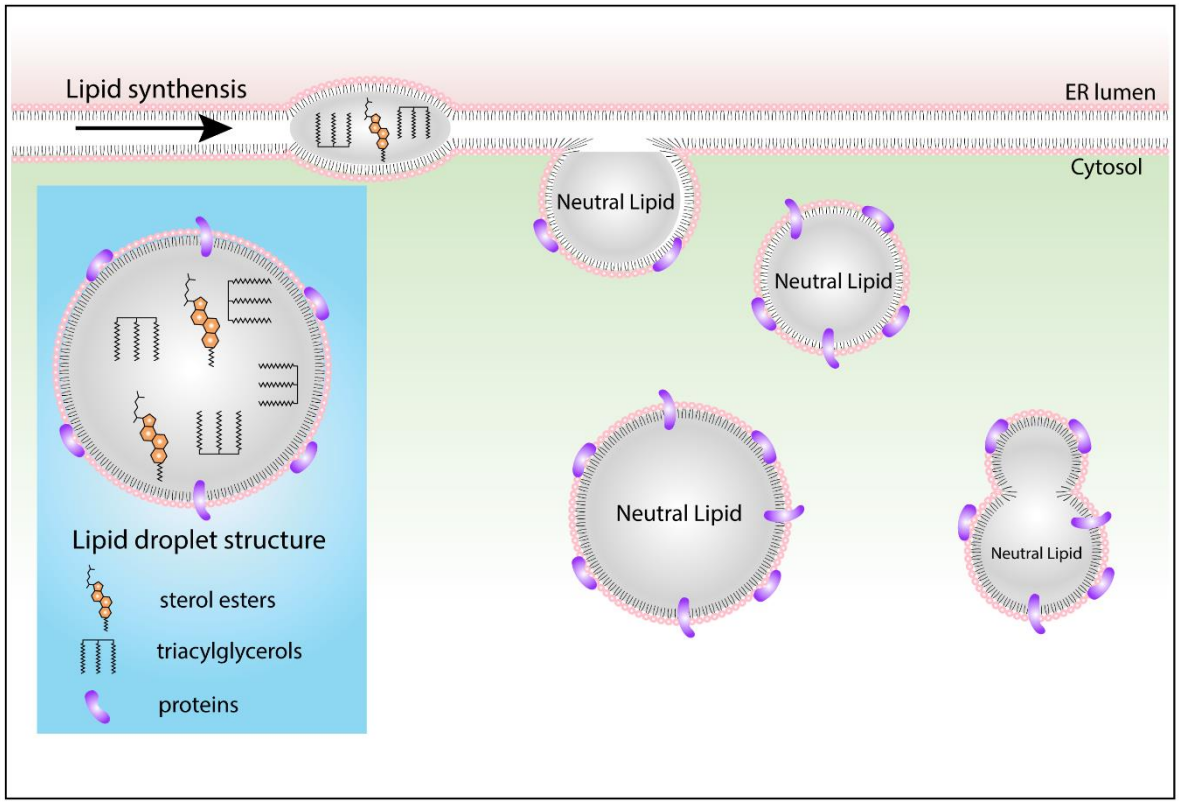

Figure 1. The structure and biogenesis of lipid droplets.

Acting as a dynamic hub in lipid metabolism, energy homeostasis and cellular signaling [2], LDs play essential roles in health and diseases. Because of drastic changes in life style and environment, obesity has grown into a global pandemic during the past decades, accompanied with comorbidities including insulin resistance, type 2 diabetes mellitus, hypertension, cardiovascular disease and dyslipidemia [3]. Thus, research on LDs mainly focused on fat cells of adipose tissue, which is the largest energy reservoir of the body.

In fact, the liver is a metabolically active organ serving as a center for lipid metabolism, and dysfunction of lipid metabolism is inevitably associated with hepatic physiopathology [4]. For example, hepatic impairment of lipid metabolism such as lipid overload attributes to the development of fatty liver disease. The epidemic of fatty liver

disease parallels the obesity pandemic. Intriguingly, LDs closely connect and interact with other cellular organelles including endoplasmic reticulum (ER), mitochondria, peroxisomes and lysosomes [5]. In this review, we aim to decipher LD biogenesis, their multifaceted interactions with other cellular organelles and functional implications in the context of the most important liver diseases.

2. Biogenesis of lipid droplets

The liver, in particular hepatocytes, plays a key role in lipid metabolism, and is considered as the hub of fatty acid synthesis and lipid circulation. Accumulation of LDs in hepatocytes is almost universal albert at variable amount. The level of LDs presenting in hepatocytes is intimately related to the metabolic status. The biogenesis and turnover of LDs in hepatocytes are highly regulated and coordinated. Although the exact process of LD biogenesis remains to be further defined, this roughly involves four main steps (Fig. 1)

2.1 Lipid synthesis and lens formation

Neutral lipids, as the core of LDs, are initially generated in ER. The classical model of LD biogenesis is based on ER-budding through multiple steps. Firstly, it is the synthesis of triacylglycerols and sterol esters in the ER, where enzymes for catalysis are located. For triacylglycerols synthesis, fatty acids use fatty acyl-CoA as acyl donors to synthesize diacylglycerols either via the glycerol phosphate or monoacylglycerol pathway. Diacylglycerols are catalyzed by diacylglycerol acyltransferase enzymes (DGAT) to produce triacylglycerols [6]. For synthesis of sterol esters, sterols are catalyzed by acyl-CoA:cholesterol acyl transferase (ACAT) [7]. Subsequently, when neutral lipid concentration increases, free neutral lipids distributed in the leaflets of ER bilayer will coalesce to form an oil len in the ER bilayer [8].

2.2 Expansion and budding of neutral lipid lens

Upon neutral lipid accumulation, lens will grow and bud into a nearly spherical droplet from ER membrane. ER bilayer phospholipid composition and surface tension are key parameters in the process of budding. The different phospholipid composition of ER membrane and/or surface tension will form different sizes of LDs [9]. LD budding also facilitates the recruitment and function of many proteins. For example, seipin essentially involved in LD biogenesis is an ER membrane protein. Seipin is stably associated with nascent ER-LD contacts [10], which supports the formation of ER-LD contacts and promotes delivery of triacylglycerols from ER to LDs [11]. The cooperation between phospholipids and proteins contributes to LDs emergence. Their composition dictates ER membrane asymmetricity which guides directionality in the process of LD budding [12].

2.3 Proteins targeting to lipid droplets

There are more than 100 proteins on the phospholipid monolayer surface of LDs which endow LDs distinct functions. How proteins specifically target to LDs remains largely elusive. Two major pathways help to understand the basic mechanisms of proteins targeting LDs, which are associated with two categories of proteins, including class I and II [13].

Class I proteins translocate from the ER bilayer with a hydrophobic hairpin structure to LDs via membrane bridges. These proteins, such as GPAT4, DGAT2, appear to lack ER luminal domains which may help them to insert into ER membrane or LD monolayer [13, 14, 15]. Class II proteins are translated in the cytosol, and subsequently bind to the LD surface. Most class II proteins, such as the perilipin/ADRP/TIP47 (PAT) proteins, bind to LDs through amphipathic helices or short stretches of hydrophobic residues [13, 16, 17, 18]. Amphipathic interfacial α-helical in monolayer-integrated proteins may be a common motif that directs membrane integration for monotopic integral proteins [19].

2.4 Growth of lipid droplets

The sizes of LDs vary among different cell types. In white adipocytes, the size ranges from 0.1 μm to 100 μm in diameter [20]. There are two main pathways mediating LD growth, including triacylglycerol synthesis and LD fusion or coalescence. In the triacylglycerol synthesis pathway, newly synthesized triacylglycerols laterally diffuse to LDs attaching to ER. Triacylglycerols and proteins are transported via vesicular transport when LDs are separated from the ER [21]. In this pathway, GPAT4 and other triacylglycerol synthesis enzymes can relocalize from ER to LDs to mediate LD growth [14]. In the second pathway, many proteins contribute to LD growth. Fsp27, an LD-associated protein, can promote LD growth via the LD contact sites [22]. CTP:phosphocholine cytidylyltransferase regulates phospholipid hemostasis to maintain LD expansion [23, 24].

3. Biological functions of lipid droplets and interactions with other organelles

LDs were initially thought to merely deposit fat in adipose tissue without major biological functions. Later on, they were considered as cellular organelles that regulate storage and hydrolysis of neutral lipids and serve as a reservoir for cholesterol and acyl-glycerols for membrane formation and maintenance. Recently, LDs were recognized as highly dynamic organelles that essentially regulates intracellular lipid storage and metabolism, as well as many other functions. In non-adipocytes, such as hepatocytes, LDs protect cells from lipotoxicity by storage of fatty acids as neutral triacylglycerols.

The development of stat-of-the-art imaging techniques has revealed new insight into physical interactions of LDs with other organelles with specific functional implications (Fig. 2). This has extended the understanding of LD biology beyond the classical lipid-related functions, but also various other cellular signaling including inflammatory responses [25, 26].

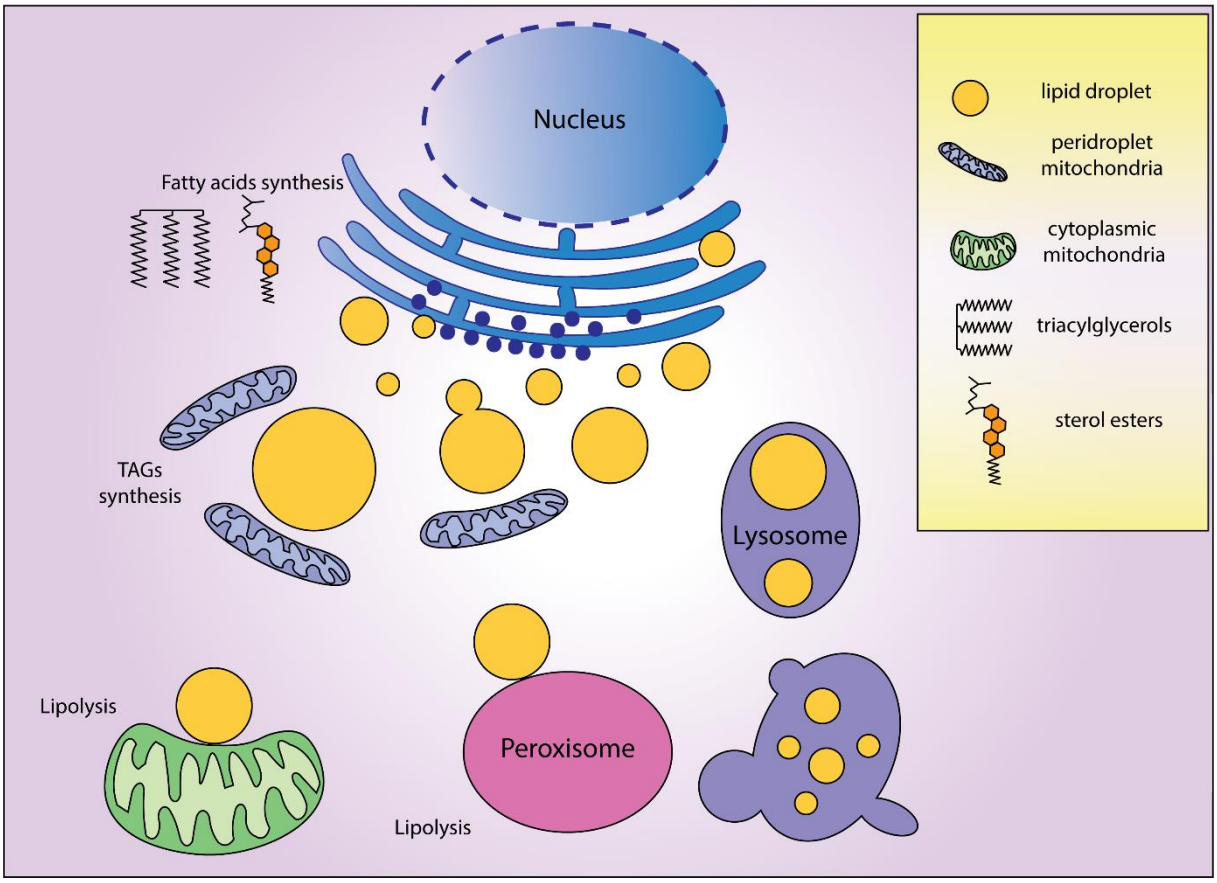

Figure 2. Interactions between lipid droplet and other cellular organelles. A) ER is the place to formate LDs, and LD-ER contacts transport lipid and proteins. B) Mitochondria can be divided into two subpopulations: peridroplet mitochondria that binds to LDs support triacylglycerol synthesis and conversely reduce β-oxidation activity, and cytoplasmic mitochondria that take place lipolysis to supply energy. C) Peroxisomes exert lipolysis through catabolization of fatty acid β-oxidation. D) Lysosomes degrade fatty acids by autophagy. ER: endoplasmic reticulum; LDs: lipid droplets.

3.1 LD-ER interaction

ER is the primary site for generating LDs. The interactions between ER and LD maintain lipid homeostasis and protect against lipotoxicity. LD-ER contacts not only transport lipids, but also proteins. Upon free fatty acids transported from ER and assembled in LDs, proteins bind with LDs to format a unique phospholipid monolayer [27]. After LD degradation, the level of neutral lipids declines. Some integral droplet proteins such as AAM-B and UBXD8 will return back to ER [28]. Some secretory proteins are transported to Golgi complex for assembly and secretion [29]. Other LD proteins are degraded via ubiquitin-proteasome system (UPS) or autophagy [30].

3.2 LD-mitochondrion interaction

Besides ER, mitochondrion is the most common interacting partner of LDs [31]. In mammalian cells, lipolysis of LD-derived fatty acids take place in mitochondrion through β-oxidation to supply energy [32, 33]. During nutrient starvation, LD-mitochondrion interactions are further increased and LD-derived fatty acids are supplied to mitochondrial fatty acid oxidation via AMPK activation [34]. Direct connections between LDs and mitochondria are required to enable flux of fatty acids into mitochondria [35].

Based on whether or not interacting with LDs, mitochondria can be divided into two subpopulations, peridroplet mitochondria that binds to LDs and cytoplasmic mitochondria, with distinct role in lipid metabolism [36]. Peridroplet mitochondria are segregated with unique protein composition and structure. They can support triacylglycerol synthesis and conversely reduce β-oxidation activity [37].

The perilipin protein family, belonging to PAT proteins, are surface scaffolds and regulators in LDs [38]. The members of perilipin family interact with mitochondrion to exert functions in lipid metabolism. Perilipin 5 (Plin5), only present in mammals, essentially mediates LD-mitochondrion interactions. Plin5 recruits mitochondria to the LD surface through a C-terminal region and protects mitochondrion from excessive fatty acid exposure by regulating LD hydrolysis and controlling local fatty acid flux [39]. In addition to lipid metabolism regulation and lipotoxicy defense, Plin5 also has antioxidant role to alleviate oxidative damage, whereas oxidative stress is intimately associated with mitochondrial electron transport chain [40].

Some aspects of LD-mitochondrion interaction also involve ER. For example, MIGA2, an outer mitochondrial membrane protein links mitochondria to LDs, but also binds to the membrane proteins VAP-A or VAP-B of ER. Through multifaceted links among mitochondria, ER and LDs, MIGA2 promotes *de novo* lipogenesis from non-lipid precursors and stores lipids in LDs [41].

3.3 LD-peroxisome

Peroxisomes are membrane-bound organelles present in the cytoplasm of all eukaryotic cells. They are essential in metabolism of lipids and reactive oxygen species. In the liver, peroxisomes also catabolize bile acid intermediates. Both LDs and peroxisomes are formed in the ER. This is thought to occur at the same ER subdomains where the reticulon homology domain of the multiple C2 domain containing transmembrane protein is located. This indicates intrinsic interactions between LDs and peroxisomes already during their biogenesis [42]. The best known example for illustrating the functional implication of LD-peroxisome interaction is probably β-oxidation of fatty acids. This crosstalk links lipolysis mediated by LDs to catabolize fatty acid β-oxidation within the peroxisomes [43].

Because both LDs and peroxisomes biogenesis occurs at ER, there could be communication and proteins/lipids trafficking among these three organelles [44]. Coordination and interaction among LDs, peroxisomes and mitochondria have been reported in adipocytes of mouse model to regulate energy consumption via CIDE-ATGL-PPARα pathway [45]. These multi-organelle interactions are likely occur at the membrane contact sites, but their precise protein composition and physiological function remain largely undefined.

3.4 LD-lysosome

Lysosomes, the single-lipid-bilayer membrane organelles, are considered as waste disposal systems of the cells. They contain a variety of enzymes that enable to digest various engulfed biomolecules including lipids. Lysosomes are closely linked to one of the LD catabolism pathways. LD catabolism has two major pathways including lipolysis and autophagy. Autophagy is the degradation pathway in lysosome, and has been termed as lipophagy when referring to the specific degradation of lipids. Lysosome regulates lipid metabolism through autophagy, and inhibition of autophagy results in increased amount of triacylglycerols and LDs [46]. For example, defects in specific autophagy gene will lead to accumulation of LDs in cytoplasm because of defective lipid catabolism [46].

In the liver, involvement of autophagy in lipid catabolism is most prominent during fasting or nutrient deprivation, although lipophagy also maintains constitutive lipid degradation. Defects of key autophagy genes are associated with increased levels of triacylglycerols in liver [47, 48]. Conversely, accumulation of intracellular LDs promotes autophagy. LDs provide lipid precursors for autophagosome biogenesis, more specifically for autophagosomal membrane formation [49]. Furthermore, ER can also contribute to the interactions between LD and autophagy [50].

4. Lipid droplets in major liver diseases

Dysregulation and imbalance of lipid metabolism in liver inevitably causes pathogenesis. The most prominently related disorder is fatty liver disease. Fatty liver disease is a leading etiology of primary liver cancer, and altered hepatic lipid metabolism can fuel hepatic carcinogenesis (Fig. 3). Interestingly, intracellular pathogens, including hepatitis viruses, can exploit LDs to sustain their life cycle.

4.1 Metabolic dysfunction-associated fatty liver disease

Metabolic dysfunction-associated fatty liver disease (MAFLD) is a new nomenclature updated from the previous known non-alcoholic fatty liver disease (NAFLD). Diagnosis of MAFLD is proposed to be based on detection of hepatic steatosis in addition to one

of the three conditions, including overweight/obesity, presence of type 2 diabetes mellitus, or evidence of metabolic dysregulation [51]. Although the precise epidemiology of MAFLD remains unknown as a new terminology, the prevalence of NAFLD has been estimated as 25% of the global population [52].

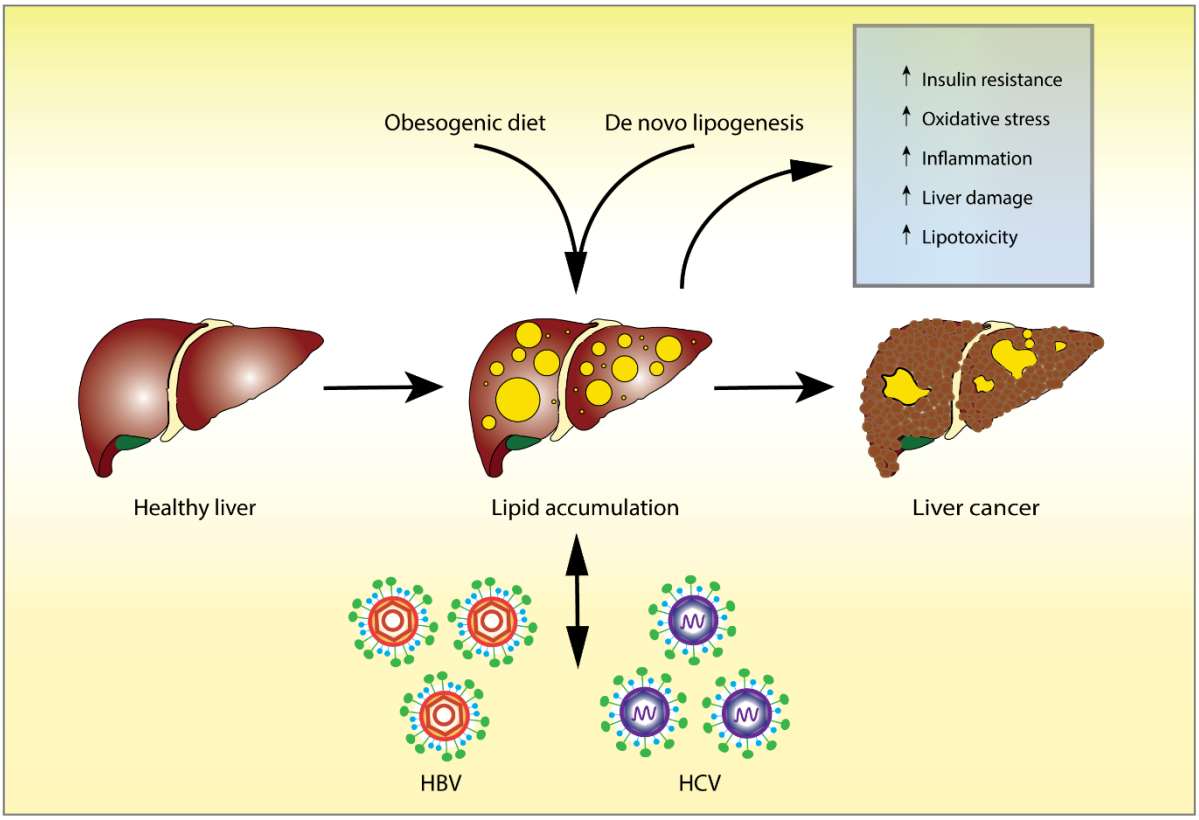

Figure 3. Lipid droplets in major liver diseases. Excessive fatty acids lead to lipid metabolic disorder. Imbalance of lipid homeostasis will trigger LDs formation that promotes devolopment of metabolic dysfunction-associated fatty liver disease. Similarly, hepatitis virus infections, especially HBV and HCV, accelerate lipid accumulation and cause inflammation in liver. In turn, LDs support the life cycle of hepatitis viruses. Fatty acids sustain HCC cell growthand create a supportive microenvironment for cancer stem cells. LDs: lipid droplets; HBV: hepatitis B virus; HCV: hepatitis C virus; HCC: hepatocellular carcinoma.

Steatosis, featured by lipid accumulation as either microvesicular or macrovesicular LDs in hepatocytes, is the hallmark of fatty liver disease. Fatty acids in the liver are derived from diet uptake, de novo lipogenesis and endogenous lipid catabolism. Imbalance in lipid anabolism and catabolism causes excessive fatty acids storage in hepatocytes as LDs, promoting the emergency of fatty liver disease. Fatty acids can also be converted to lipid intermediates that impair insulin signaling, referring as lipid-induced insulin resistance and lipotoxicity. Hepatic steatosis is often associated with insulin resistance, which in turn exacerbates the pathogenesis of MAFLD [53]. Accumulated LDs will trigger further hepatic oxidative stress and inflammation, resulting in continued liver damage and more advanced disease stage such as steatohepatitis [54].

At molecular level, several proteins are known to regulate LDs in fatty liver disease. The PAT family proteins located on LD surface include perilipin, adipophilin, TIP47, S3-12 and OXPAT. They differentially expressed in fatty compared to normal liver. Perilipin, adipophilin and TIP47 are associated with different sizes of LDs. TIP47 affects nascent LDs, while perilipin and adipophilin are important for maturation and maintenance of LDs in hepatocytes [55]. CIDEA and Fsp27 are LD-associated proteins that promote LD fusion and regulate lipid storage. Their expression is dramatically upregulated in hepatic steatosis [56]. This process may be mediated by MKP5. Because loss of MKP5 in mice activates p38, resulting in increased expression of CIDEA and Fsp27 [57]. 17β-hydroxysteroid dehydrogenase-13 (17β-HSD13), a newly identified LD-associated protein, has been demonstrated as a pathogenic protein in MAFLD. 17β-HSD13 controls the number and size of LDs and is causative for fatty liver phenotype [58]. High expression of 17β-HSD13 in fatty liver has been shown to be induced by liver X receptor α through SREBP-1c [59].

4.2 Viral hepatitis

Viral hepatitis are caused by the five hepatotropic viruses including hepatitis A, B, C, D and E. Globally, about 500 million people are chronically infected with hepatitis B (HBV) or C (HCV) virus. The link of HBV to LDs is mainly through the viral HBx protein, which causes lipid accumulation by upregulation of the liver X receptor and its lipogenic target genes [60, 61]. HBV viral particle production has been shown to impair LD expansion associated with inhibition of the expression of CIDE proteins. Because CIDE proteins support HBV production; this may serve as negative feedback loop for maintaining persistent infection [62].

HCV is the best known pathogen with close connections to LDs. LDs serve as putative sites for viral assembly during HCV replication [63]. The process of infectious HCV particle assembly consists of nucleocapsid formation, budding into the ER, and virion maturation. The capsid Core protein closely associates with LDs, and further recruits nonstructural proteins around LDs to participate in virus production [63]. HCV assembly likely takes place at the sites requiring interactions of ER and LDs [64]. Recent high-resolution imaging study indicates selective recruitment of ER membranes wrapping LDs to form membranous structure coupling HCV replication and assembly [65]. HCV Core can also be efficiently targeted to LDs outside the context of virion assembly, and induce LD redistribution and hepatic steatosis [66, 67]. This partially explains why MAFLD is a prominent feature of chronic hepatitis C patients, and eradication of HCV by antiviral treatment dramatically decreases liver steatosis [68].

4.3 Liver cancer

MAFLD and viral hepatitis are the leading etiologies of primary liver cancer, namely hepatocellular carcinoma (HCC). Enhanced lipogenesis is a metabolic hallmark of cancer cells, and aberrant lipid metabolism universally occurs in HCC cells [69]. Fat-containing liver lesions are commonly seen in HCC patients [70]. In HCC, lipogenesis pathway is activated, while fatty acid oxidation is downregulated [71, 72]. With a high rate of growth, HCC cells acquire fatty acids to support their proliferation [73]. Recent evidence indicate the essential involvement of lipid metabolism in cancer stem cells (CSCs). Activation of intrinsic lipid pathways in CSCs upregulates fatty acid de novo synthesis [74]. Furthermore, the lipid context in tumor microenvironment, in particular the stem cell niche, regulates CSC behavior [75]. Liver tumors are known to harbor CSCs [76], and the role of LDs and lipid metabolism in this unique cancer cell population deserves to be further studied.

Conlusion

LDs are highly dynamic organelles closely associated and interacting with other celleular organelles for exerting a variety of biological functions. The liver is a central organ in lipid metabolism and LDs are widely present in hepatocytes. LDs play key roles in health and diseases of the liver, involving in lipid metabolism, energy homeostasis, cell signaling, inflammation, pathogen-host interaction and carcinogenesis. Mechnistically decipering the role of LDs in liver shall help to better understand pathegensis of the major liver diseases inclduing MAFLD, viral hepattis and cancer, as well as to facilitate therapeutic development.

References

1. Guo, Y., et al., *Lipid droplets at a glance.* J Cell Sci, 2009. **122**(Pt 6): p. 749-52.
2. Collaborators, G.B.D.O., et al., *Health Effects of Overweight and Obesity in 195 Countries over 25 Years.* N Engl J Med, 2017. **377**(1): p. 13-27.
3. Gluchowski, N.L., et al., *Lipid droplets and liver disease: from basic biology to clinical implications.* Nat Rev Gastroenterol Hepatol, 2017. **14**(6): p. 343-355.
4. Olzmann, J.A. and P. Carvalho, *Dynamics and functions of lipid droplets.* Nat Rev Mol Cell Biol, 2019. **20**(3): p. 137-155.
5. Jackson, C.L., *Lipid droplet biogenesis.* Curr Opin Cell Biol, 2019. **59**: p. 88-96.
6. Yen, C.L., et al., *Thematic review series: glycerolipids. DGAT enzymes and triacylglycerol biosynthesis.* J Lipid Res, 2008. **49**(11): p. 2283-301.
7. Korber, M., I. Klein, and G. Daum, *Steryl ester synthesis, storage and hydrolysis: A contribution to sterol homeostasis.* Biochim Biophys Acta Mol Cell Biol Lipids, 2017. **1862**(12): p. 1534-1545.
8. Ben M'barek, K., et al., *ER Membrane Phospholipids and Surface Tension Control Cellular Lipid Droplet Formation.* Dev Cell, 2017. **41**(6): p. 591-604 e7.
9. Salo, V.T., et al., *Seipin regulates ER-lipid droplet contacts and cargo delivery.* Embo J, 2016. **35**(24): p. 2699-2716.
10. Salo, V.T., et al., *Seipin Facilitates Triglyceride Flow to Lipid Droplet and Counteracts Droplet Ripening via Endoplasmic Reticulum Contact.* Dev Cell, 2019. **50**(4): p. 478-493 e9.
11. Chorlay, A., et al., *Membrane Asymmetry Imposes Directionality on Lipid Droplet Emergence from the ER.* Dev Cell, 2019. **50**(1): p. 25-42 e7.
12. Kory, N., R.V. Farese, Jr., and T.C. Walther, *Targeting Fat: Mechanisms of Protein Localization to Lipid Droplets.* Trends Cell Biol, 2016. **26**(7): p. 535-546.
13. Wilfling, F., et al., *Triacylglycerol synthesis enzymes mediate lipid droplet growth by relocalizing from the ER to lipid droplets.* Dev Cell, 2013. **24**(4): p. 384-99.
14. Kuerschner, L., C. Moessinger, and C. Thiele, *Imaging of lipid biosynthesis: how a neutral lipid enters lipid droplets.* Traffic, 2008. **9**(3): p. 338-52.
15. Prévost, C., et al., *Mechanism and Determinants of Amphipathic Helix-Containing Protein Targeting to Lipid Droplets.* Dev Cell, 2018. **44**(1): p. 73-86 e4.
16. Sztalryd, C. and D.L. Brasaemle, *The perilipin family of lipid droplet proteins: Gatekeepers of intracellular lipolysis.* Biochim Biophys Acta Mol Cell Biol Lipids, 2017. **1862**(10 Pt B): p. 1221-1232.
17. Ozeki, S., et al., *Rab18 localizes to lipid droplets and induces their close apposition to the endoplasmic reticulum-derived membrane.* J Cell Sci, 2005. **118**(Pt 12): p. 2601-11.
18. Pataki, C.I., et al., *Proteomic analysis of monolayer-integrated proteins on lipid droplets identifies amphipathic interfacial α-helical membrane anchors.* Proc Natl Acad Sci U S A, 2018. **115**(35): p. E8172-E8180.
19. Murphy, D.J. and J. Vance, *Mechanisms of lipid-body formation.* Trends in Biochemical Sciences, 1999. **24**(3): p. 109-115.
20. Thiam, A.R., R.V. Farese, Jr., and T.C. Walther, *The biophysics and cell biology of lipid droplets.* Nat Rev Mol Cell Biol, 2013. **14**(12): p. 775-86.
21. Gong, J., et al., *Fsp27 promotes lipid droplet growth by lipid exchange and transfer at lipid droplet contact sites.* J Cell Biol, 2011. **195**(6): p. 953-63.
22. Krahmer, N., et al., *Phosphatidylcholine synthesis for lipid droplet expansion is mediated by localized activation of CTP:phosphocholine cytidylyltransferase.* Cell Metab, 2011. **14**(4): p. 504-15.
23. Guo, Y., et al., *Functional genomic screen reveals genes involved in lipid-droplet formation and utilization.* Nature, 2008. **453**(7195): p. 657-61.
24. Valm, A.M., et al., *Applying systems-level spectral imaging and analysis to reveal the organelle interactome.* Nature, 2017. **546**(7656): p. 162-167.
25. Greenberg, A.S., et al., *The role of lipid droplets in metabolic disease in rodents and humans.* J Clin Invest, 2011. **121**(6): p. 2102-10.
26. Tauchi-Sato, K., et al., *The surface of lipid droplets is a phospholipid monolayer with a unique Fatty Acid composition.* J Biol Chem, 2002. **277**(46): p. 44507-12.
27. Zehmer, J.K., et al., *Targeting sequences of UBXD8 and AAM-B reveal that the ER has a direct role in the emergence and regression of lipid droplets.* Journal of cell science, 2009. **122**(Pt 20): p. 3694-3702.
28. Olofsson, S.-O., et al., *Lipid droplets as dynamic organelles connecting storage and efflux of lipids.* Biochimica et Biophysica Acta (BBA) - Molecular and Cell Biology of Lipids, 2009. **1791**(6): p. 448-458.
29. Bersuker, K. and J.A. Olzmann, *Establishing the lipid droplet proteome: Mechanisms of lipid droplet protein targeting and degradation.* Biochimica et biophysica acta Molecular and cell biology of lipids, 2017. **1862**(10 Pt B): p. 1166-1177.
30. Wang, H., et al., *Analysis of lipid droplets in cardiac muscle.* Methods Cell Biol, 2013. **116**: p. 129-49.
31. Tarnopolsky, M.A., et al., *Influence of endurance exercise training and sex on intramyocellular lipid and mitochondrial ultrastructure, substrate use, and mitochondrial enzyme activity.* Am J Physiol Regul Integr Comp Physiol, 2007. **292**(3): p. R1271-8.
32. Shaw, C.S., D.A. Jones, and A.J. Wagenmakers, *Network distribution of mitochondria and lipid droplets in human muscle fibres.* Histochem Cell Biol, 2008. **129**(1): p. 65-72.
33. Herms, A., et al., *AMPK activation promotes lipid droplet dispersion on detyrosinated microtubules to increase mitochondrial fatty acid oxidation.* Nat Commun, 2015. **6**: p. 7176.
34. Rambold, Angelika S., S. Cohen, and J. Lippincott-Schwartz, *Fatty Acid Trafficking in Starved Cells: Regulation by Lipid Droplet Lipolysis, Autophagy, and Mitochondrial Fusion Dynamics.* Developmental Cell, 2015. **32**(6): p. 678-692.
35. Benador, I.Y., et al., *Mitochondria Bound to Lipid Droplets: Where Mitochondrial Dynamics Regulate Lipid Storage and Utilization.* Cell Metabolism, 2019. **29**(4): p. 827-835.
36. Benador, I.Y., et al., *Mitochondria Bound to Lipid Droplets Have Unique Bioenergetics, Composition, and Dynamics that Support Lipid Droplet Expansion.* Cell metabolism, 2018. **27**(4): p. 869-885.e6.
37. Wang, H. and C. Sztalryd, *Oxidative tissue: perilipin 5 links storage with the furnace.* Trends in Endocrinology & Metabolism, 2011. **22**(6): p. 197-203.
38. Wang, H., et al., *Perilipin 5, a lipid droplet-associated protein, provides physical and metabolic linkage to mitochondria.* Journal of lipid research, 2011. **52**(12): p. 2159-2168.

39. Zhu, Y., et al., *Perilipin 5 Reduces Oxidative Damage Associated With Lipotoxicity by Activating the PI3K/ERK-Mediated Nrf2-ARE Signaling Pathway in INS-1 Pancreatic β-Cells.* Frontiers in endocrinology, 2020. **11**: p. 166-166.
40. Freyre, C.A.C., et al., *MIGA2 Links Mitochondria, the ER, and Lipid Droplets and Promotes De Novo Lipogenesis in Adipocytes.* Molecular Cell, 2019. **76**(5): p. 811-825.e14.
41. Joshi, A.S., et al., *Lipid droplet and peroxisome biogenesis occur at the same ER subdomains.* Nature Communications, 2018. **9**(1): p. 2940.
42. Shai, N., M. Schuldiner, and E. Zalckvar, *No peroxisome is an island - Peroxisome contact sites.* Biochim Biophys Acta, 2016. **1863**(5): p. 1061-9.
43. Joshi, A.S. and S. Cohen, *Lipid Droplet and Peroxisome Biogenesis: Do They Go Hand-in-Hand?* Front Cell Dev Biol, 2019. **7**: p. 92.
44. Zhou, L., et al., *Coordination Among Lipid Droplets, Peroxisomes, and Mitochondria Regulates Energy Expenditure Through the CIDE-ATGL-PPARα Pathway in Adipocytes.* Diabetes, 2018. **67**(10): p. 1935-1948.
45. Singh, R., et al., *Autophagy regulates lipid metabolism.* Nature, 2009. **458**(7242): p. 1131-1135.
46. Yang, L., et al., *Defective hepatic autophagy in obesity promotes ER stress and causes insulin resistance.* Cell Metab, 2010. **11**(6): p. 467-78.
47. Jaber, N., et al., *Class III PI3K Vps34 plays an essential role in autophagy and in heart and liver function.* Proc Natl Acad Sci U S A, 2012. **109**(6): p. 2003-8.
48. Settembre, C. and A. Ballabio, *Lysosome: regulator of lipid degradation pathways.* Trends Cell Biol, 2014. **24**(12): p. 743-50.
49. Velázquez, A.P., et al., *Lipid droplet–mediated ER homeostasis regulates autophagy and cell survival during starvation.* Journal of Cell Biology, 2016. **212**(6): p. 621-631.
50. Eslam, M., et al., *A new definition for metabolic dysfunction-associated fatty liver disease: An international expert consensus statement.* J Hepatol, 2020.
51. Younossi, Z.M., et al., *Global epidemiology of nonalcoholic fatty liver disease-Meta-analytic assessment of prevalence, incidence, and outcomes.* Hepatology, 2016. **64**(1): p. 73-84.
52. Zhang, C.H., et al., *Molecular mechanisms of hepatic insulin resistance in nonalcoholic fatty liver disease and potential treatment strategies.* Pharmacol Res, 2020: p. 104984.
53. Chen, K., et al., *Advancing the understanding of NAFLD to hepatocellular carcinoma development: From experimental models to humans.* Biochim Biophys Acta Rev Cancer, 2019. **1871**(1): p. 117-125.
54. Straub, B.K., et al., *Differential pattern of lipid droplet-associated proteins and de novo perilipin expression in hepatocyte steatogenesis.* Hepatology, 2008. **47**(6): p. 1936-1946.
55. Zhou, L., et al., *Cidea promotes hepatic steatosis by sensing dietary fatty acids.* Hepatology, 2012. **56**(1): p. 95-107.
56. Tang, P., et al., *Protective Function of Mitogen-Activated Protein Kinase Phosphatase 5 in Aging- and Diet-Induced Hepatic Steatosis and Steatohepatitis.* Hepatology communications, 2019. **3**(6): p. 748-762.
57. Su, W., et al., *Comparative proteomic study reveals 17β-HSD13 as a pathogenic protein in nonalcoholic fatty liver disease.* Proc Natl Acad Sci U S A, 2014. **111**(31): p. 11437-42.
58. Su, W., et al., *Liver X receptor α induces 17β-hydroxysteroid dehydrogenase-13 expression through SREBP-1c.* American Journal of Physiology-Endocrinology and Metabolism, 2017. **312**(4): p. E357-E367.
59. Kim, K.H., et al., *Hepatitis B virus X protein induces hepatic steatosis via transcriptional activation of SREBP1 and PPARgamma.* Gastroenterology, 2007. **132**(5): p. 1955-67.
60. Na, T.Y., et al., *Liver X receptor mediates hepatitis B virus X protein-induced lipogenesis in hepatitis B virus-associated hepatocellular carcinoma.* Hepatology, 2009. **49**(4): p. 1122-31.
61. Yasumoto, J., et al., *Hepatitis B virus prevents excessive viral production via reduction of cell death-inducing DFF45-like effectors.* J Gen Virol, 2017. **98**(7): p. 1762-1773.
62. Miyanari, Y., et al., *The lipid droplet is an important organelle for hepatitis C virus production.* Nature Cell Biology, 2007. **9**(9): p. 1089-1097.
63. Filipe, A. and J. McLauchlan, *Hepatitis C virus and lipid droplets: finding a niche.* Trends Mol Med, 2015. **21**(1): p. 34-42.
64. Lee, J.Y., et al., *Spatiotemporal Coupling of the Hepatitis C Virus Replication Cycle by Creating a Lipid Droplet- Proximal Membranous Replication Compartment.* Cell Rep, 2019. **27**(12): p. 3602-3617 e5.
65. Camus, G., et al., *The hepatitis C virus core protein inhibits adipose triglyceride lipase (ATGL)-mediated lipid mobilization and enhances the ATGL interaction with comparative gene identification 58 (CGI-58) and lipid droplets.* The Journal of biological chemistry, 2014. **289**(52): p. 35770-35780.
66. Boulant, S., et al., *Hepatitis C Virus Core Protein Induces Lipid Droplet Redistribution in a Microtubule- and Dynein-Dependent Manner.* Traffic, 2008. **9**(8): p. 1268-1282.
67. Tada, T., et al., *Viral eradication reduces both liver stiffness and steatosis in patients with chronic hepatitis C virus infection who received direct-acting anti-viral therapy.* Aliment Pharmacol Ther, 2018. **47**(7): p. 1012-1022.
68. Hu, B., et al., *Aberrant lipid metabolism in hepatocellular carcinoma cells as well as immune microenvironment: A review.* Cell Prolif, 2020. **53**(3): p. e12772.
69. Balci, N.C., et al., *Fat containing HCC: findings on CT and MRI including serial contrast-enhanced imaging.* Acad Radiol, 2009. **16**(8): p. 963-8.
70. Yamashita, T., et al., *Activation of lipogenic pathway correlates with cell proliferation and poor prognosis in hepatocellular carcinoma.* Journal of Hepatology, 2009. **50**(1): p. 100-110.
71. Björnson, E., et al., *Stratification of Hepatocellular Carcinoma Patients Based on Acetate Utilization.* Cell Reports, 2015. **13**(9): p. 2014-2026.
72. Menendez, J.A. and R. Lupu, *Fatty acid synthase and the lipogenic phenotype in cancer pathogenesis.* Nat Rev Cancer, 2007. **7**(10): p. 763-77.
73. Yasumoto, Y., et al., *Inhibition of Fatty Acid Synthase Decreases Expression of Stemness Markers in Glioma Stem Cells.* PLoS One, 2016. **11**(1): p. e0147717.
74. Nieman, K.M., et al., *Adipocytes promote ovarian cancer metastasis and provide energy for rapid tumor growth.* Nat Med, 2011. **17**(11): p. 1498-503.
75. Cao, W., et al., *LGR5 marks targetable tumor-initiating cells in mouse liver cancer.* Nat Commun, 2020. **11**(1): p. 1961.

CHAPTER 3

Direct-acting antiviral agents for liver transplant recipients with recurrent genotype 1 hepatitis C virus infection: Systematic review and meta-analysis

Jiaye Liu, Buyun Ma, Wanlu Cao, Meng Li, Wichor M. Bramer, Maikel P. Peppelenbosch and Qiuwei Pan

Transpl Infect Dis. 2019 Apr; 21(2): e13047.

Abstract

Background: Comprehensive evaluation of safety and efficacy of different combinations of direct-acting antivirals (DAAs) in liver transplant recipients with genotype 1 (GT1) hepatitis C virus (HCV) recurrence remains limited. Therefore, we performed this systematic review and meta-analysis in order to evaluate the clinical outcome of DAA treatment in liver transplant patients with HCV GT1 recurrence.

Methods: Studies were included if they contained information of 12 weeks sustained virologic response (SVR12) after DAA treatment completion as well as treatment related complications for liver transplant recipients with GT1 HCV recurrence.

Results: We identified 16 studies comprising 885 patients. The overall pooled estimate proportion of SVR12 was 93% (95% confidence interval (CI): 0.89, 0.96), with moderate heterogeneity observed (τ^2=0.01, P<0.01, I^2=75%). High tolerability was observed in liver transplant recipients reflected by serious adverse events (sAEs) with pooled estimate proportion of 4% (95% CI: 0.01, 0.07; τ^2=0.02, P<0.01, I^2=81%). For subgroup analysis, a total of five different DAA regimens were applied for treating these patients. Sofosbuvir/Ledipasvir (SOF/LDV) led the highest pooled estimate SVR12 proportion, followed by Paritaprevir/Ritonavir/Ombitasivir/Dasabuvir (PrOD), Daclatasvir (DCV)/Simeprevir (SMV) ± Ribavirin (RBV), and SOF/SMV ± RBV, Asunaprevir (ASV)/DCV. There was a tendency for favoring a higher pooled SVR12 proportion in patients with METAVIR Stage F0-F2 of 93% (95% CI: 0.89, 0.96) compared to 83% (95% CI: 0.75, 0.88) for stage F3-F4 (p<0.01). There was no significant difference between LT recipients treated with or without RBV (p=0.23).

Conclusions: DAA treatment is highly effective and well tolerated in liver transplant recipients with recurrent GT1 HCV infection.

Key words: Direct-acting antiviral; HCV; Liver transplantation; Genotype 1; Recurrence.

Introduction

Liver cirrhosis and hepatocellular carcinoma (HCC) secondary to hepatitis C virus (HCV) infection are the leading causes for liver transplantation (LT) worldwide.(1, 2) However, recurrent HCV infection post LT is a unique and difficult medical dilemma which occurs in over 90% of patients, and severe recurrent infection is observed in nearly 30% of patients within 3 to 5 years.(3, 4) Thus, the allograft and recipient survival is closely correlated with the successful eradication of HCV.

Until very recently, interferon-based therapy was the only treatment option and rate of sustained virological response (SVR) in these transplant recipients was merely 20%-30%.(5, 6) The combination of direct-acting antiviral agents, in the form of a first generation protease inhibitor, telaprevir or boceprevir, doubled the SVR rate at the expense of a series of adverse events (AEs) and serious adverse events (sAEs).(7, 8) These included rashes, cytopenias, allograft rejection, severe anemia, and a mortality rate of 9% in one series. At the end of year of 2013, the US Food and Drug Administration (FDA) and European Medicines Agency (EMA) approvals of simeprevir (SMV) and sofosbuvir (SOF) heralded a new era in direct-acting antiviral (DAA) therapy of HCV-related liver diseases. Consequently, the launches of several other second generation of interferon-free DAAs have opened a new scenario which revolutionized the treatment of chronic HCV infection in the general infected population. With a very favorable safety profile and high rates of SVR of over 95%,(9) the newer and all-oral DAA-based regimens have provided an unprecedented opportunity to cure HCV. Although HCV disease burden remains substantial for the time being, however it is estimated that, within next decade, most patients with HCV infection would likely to attend SVR. Furthermore, SVR may forestall the progression of liver diseases with subsequent reduction in liver-related complications including hepatocellular carcinoma (HCC), hepatic decompensation, and both liver related as well as all-cause mortality.

HCV genotype 1 (GT1) is the most prevalent recurrence affecting the majority of patients post LT.(10, 11) However, the effectiveness and tolerability of various of combinations of DAAs on specific genotype of HCV recurrence in LT recipients remain largely unknown.(12) In this study, we performed a systematic review and meta-analysis in order to provide a comprehensive, reliable, and up-to-date assessment of DAA treatment for GT1 HCV recurrence post transplantation. Our results may provide additional guidance for clinical practice and future research.

Materials and Methods

Literature search

We have conducted a systematic search of various electronic databases, including Ovid Medline, EMBASE, Web of Science, Cochrane Database and Google Scholar for relevant studies published from inception until July, 2018. The search was designed and conducted by an experienced medical librarian with input from the study investigators, using controlled vocabulary supplemented with keywords (“sofosbuvir” OR “ribavirin” OR “ritonavir” OR “asunaprevir” OR “simeprevir” OR “daclatasvir” OR “ombitasvir” OR “ledipasvir” OR “velpatasvir” OR “grazoprevir” OR “elbasvir” OR “DAA”

OR “direct-acting antivirals” AND “liver transplantation” AND “hepatitis C” OR “HCV” AND “Genotype 1” OR “GT1”) (Supplementary method 1). In addition, the bibliographies of relevant review articles and all included studies were manually reviewed to identify relevant studies. No restrictions were applied to language due to the limited number of manuscripts. Abstracts from conferences were excluded in our database search. Besides, the reference lists of included articles and relevant systematic reviews were manually searched.

Inclusion and exclusion criteria

All records identified through database searches were downloaded and duplicate records were removed. The title and abstract of remaining records were screened for relevance to liver disease and human subjects. After this initial screening, the lists of selected studies were cross-checked to resolve discrepancies. Subsequently, full articles were retrieved for detailed assessment.

Reports were included if they were original studies which contained at least 5 patients, presented effectiveness of treatment of second generation of interferon-free DAA regimens for at least 12 weeks in adult LT recipients with GT1 HCV recurrence. In addition, these included studies should present proportion of SVR12 after the end of the treatment. We excluded studies that enrolled LT recipients featured coinfection with hepatitis A, B, D, E virus or human immunodeficiency virus (HIV). Besides, studies without reporting AEs and/or sAEs were also excluded.

Study selection and data extraction

Two reviewers (J.L. and B.M.) worked independently to determine whether a study met inclusion criteria, abstracted information to assess the methodological validity of each candidate study, and extracted data with structured data collection forms. The reviewers resolved discrepancies by jointly reviewing the study in question. If no consensus was reached, a third reviewer (Q.P.), unaware of prior determinations, functioned as an arbiter.

Extracted information for this study include study design, immunosuppression protocols, dosage adjust, DAA combinations, collaboration (single or multicenter) and patient demographics including age, gender, ethnicity, viral load, degree of fibrosis. We also obtained data of treatment outcomes of SVR12. In addition, data about the tolerability of DAA treatment were also collected.

Quality assessment

The quality of included studies was rated using the institute of Health Economics (IHE) quality appraisal checklist, which is usually employed for assessment of the quality of case series. As all of the included studies were single-arm reports, an assessment tool for case series is more suitable than the Newcastle Ottawa Scale (NOS). In this 20-item checklist, both risk of bias and quality of reporting were scored by yes, no or partial/unclear answers. Eight quality parameters including study objective (0-1 points), study design (0-3 points), study population (0-3 points), intervention and co-intervention (0-2 points), outcome measure (0-4 points), statistical analysis (0-1 points),

results and conclusions (0-5 points) and competing interests and sources of support (0-1 points) were used to assess included studies. In our analysis, studies with 0-2, 3-5, 6-8 and ≥9 points were considered as having low, moderate, high and very high risk of bias, respectively. Quality assessment was done by two independent authors (J.L. and B.M.), and disagreements were solved by the third author (Q.P.).

Statistical analysis

After checking for consistency, the Metaprop module in the R-3.4.2 statistical software package was used for the meta-analysis. Given that, the SVR12 proportion in many articles are close to 100%. So the proportion of SVR12 reported in each study was Free-Turkey double arcsine transformed prior to compute the pooled estimate rate. 95% confidence interval (CI) were estimated using Wilson score method. We performed meta-analysis of proportion to compute the pooled estimate proportions by using a random-effect model (DerSimonian-Laird Method). Heterogeneity across the included studies was assessed using the Cochran Q-statistics and I2 statistics, with I2 statistics 25%-50%, 50%-75% and >75% considered as mild, moderate and severe heterogeneity, respectively. Based on the available data, subgroup meta-analysis were performed by using the Q test to determine whether the pooled estimate proportion of SVR12 varied by study type (retrospective study or perspective study), with or without Ribavirin (RBV), METAVIR score (F0-F2 or F3-F4), and different kinds of regimens SOF/SMV with or without RBV, SOF/Ledipasvir (LDV), Asunaprevir (ASV)/SMV, DCV/SMV with or without RBV and Paritaprevir/Ritonavir/Ombitasivir/Dasabuvir (PrOD). Funnel plots and Egger regression test were used to assess potential publication biases.

Ethical approval or inform consent from patients was not required, because our data were extracted from previous studies. Nevertheless, the included studies in our review did obtain patient consent and each study was approved by ethics committee.

Results

Literature search

Our search strategy identified 2747 articles for inclusion. After removing duplicate studies, 2655 studies were further evaluated for eligibility. Of these, 1593 studies were excluded, which had no DAA, HCV GT1 or LT related items. After screening the titles and abstracts, another 950 studies were excluded; 744 studies of them included ineligible study participants, 206 with small sample size. 112 studies were retrieved and evaluated in full text. Of those reviewed in detail, 96 studies were excluded due to duplicate publication, improper study design, or incomplete information of effectiveness and tolerability. Eventually, 16 studies, published until July 2018, involving 885 patients were eligible for the qualitative and quantitative synthesis as detailed in Figure 1. Based on the Institute of Health Economics (IHE) quality appraisal checklist, six studies were of low risk of bias compared to 10 studies with moderate risk of bias. To date, no randomized controlled trial has been published exploring the efficacy and tolerability of DAAs on recurrence of post LT. The 16 included studies

were performed by five different countries. Among them, 62.5% were conducted in USA, 18.75% in Japan, 6.25% in UK, 6.25% in Germany and 6.25% in Spain. Ten of the included studies were multi-center studies and six were single-center studies. All of these studies were published in full text.

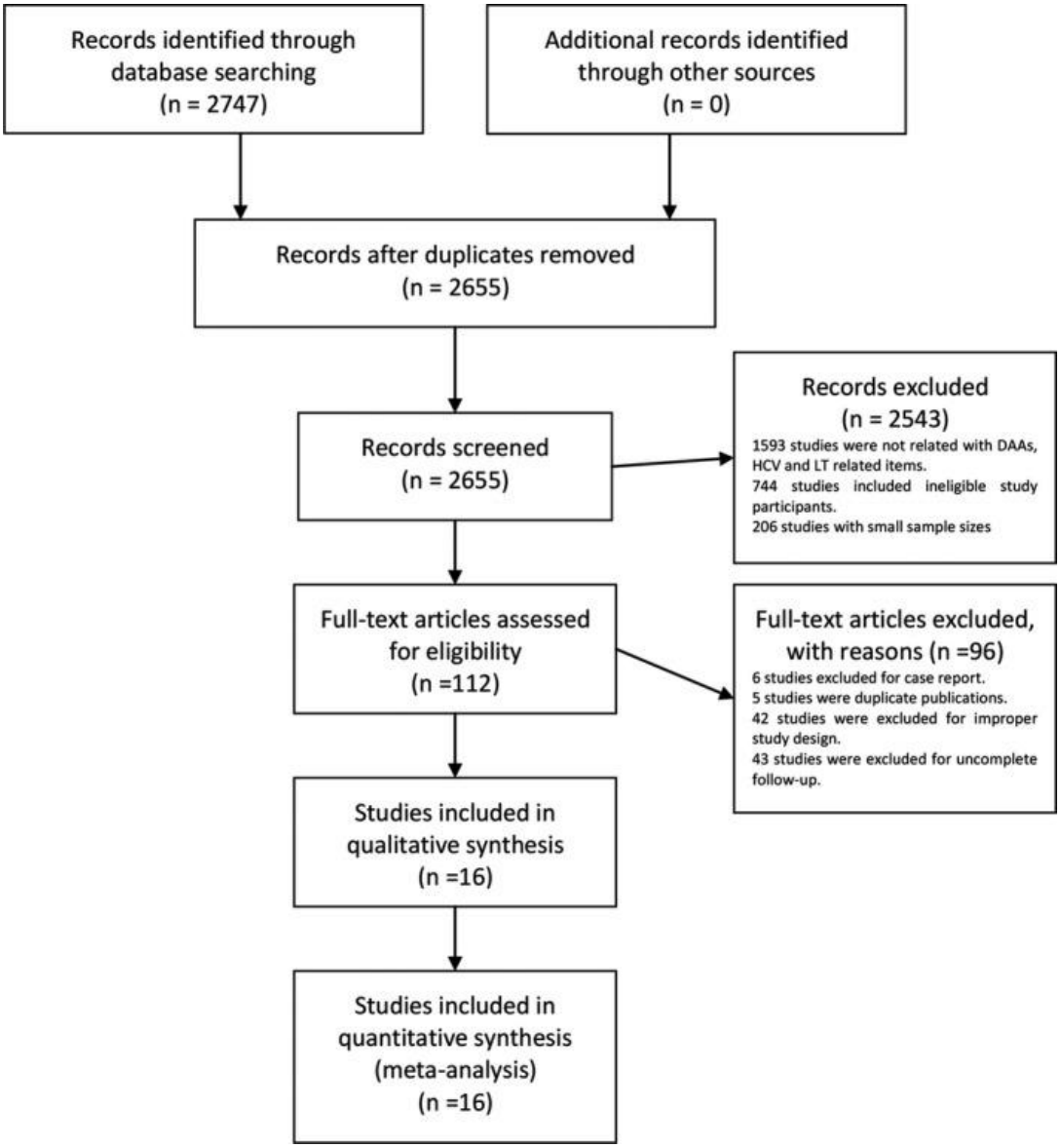

Figure 1. Study selection.

Baseline characteristics

Table 1 and 2 summarize the baseline patient demographic and clinical characteristics. Except one study (13) that did not report patient ethnicity, the majority of patients were Caucasian, male, with a mean age of approximately 60-year-old, had GT1a HCV recurrence, and received tacrolimus as part of their immunosuppressive treatment. Five different DAA combination protocols were described: SOF/SMV with or without RBV (n=8);(13-20) SOF/LDV (n=3);(21-23) ASV/SMV (n=2);(24, 25) DCV/SMV with or without RBV (n=2);(26, 27) PrOD (n=1).(28) Detailed baseline characteristics of the included studies are provided in Table 1 and 2.

Table 1. Basic characteristic of studies included.

Author	Year	Cases	Study design	Ethnicity (C/B/A/H/O)	Genotype 1a (%)	Male (%)	Age(Years)	Collaboration
Jacqueline	2016	46	Prospective	37/8/1/0/0	33 (71.7%)	34 (73.9%)	60 (49-68)	Multiple-center-
Robert	2016	151	Prospective	118/14/0/0/19	87 (57.6%)	112 (74.2%)	61 (46-78)	Multiple-center
Lutchman	2016	50	Retrospective	25/0/0/16/9	32 (64.0%)	42 (84.0%0	61.3 ± 7.1	Single-center
Suraki	2015	123	Retrospective	91/12/0/12/8	74 (60.2%)	93 (75.6%)	61 ± 6	Multiple-center
Saro	2015	32	Retrospective	11/0/2/19/0	22 (68.8%)	21 (65.6%)	58 (47-71)	Single-center
Jackson	2016	67	Retrospective	-	23 (34.3%)	46 (68.7%)	61.5 ± 6.6	Multiple-center
Punzalan	2015	42	Retrospective	34/1/1/6/0	33 (78.6%)	28 (66.7%)	58	Single-center
Toru	2017	74	Retrospective	0/0/74/0/0	-	32 (43.2%)	62.7 ± 4.5	Multiple-center
Kerstin	2015	6	Retrospective	6/0/0/0/0	5 (83.3%)	5 (83.3%)	58.5 (50-63)	Single-center
Masaki	2017	9	Retrospective	0/0/9/0/0	-	5 (55.6%)	64.7 ± 0.85	Single-center
Neil	2015	56	Retrospective	48/0/0/0/8	44 (78.6%)	42 (75.0%)	61	Multiple-center
Paul	2014	34	Prospective	29/4/0/0/1	29 (85.3%)	27 (79.4%)	59.6 ± 6.6	Multiple-center
Yoshihide	2017	54	Retrospective	0/0/54/0/0	-	25 (46.3%)	64 (47-77)	Multiple-center
Mohamed	2017	60	Retrospective	53/0/0/0/7	47 (78.3%)	42 (70.0%)	59.9 ± 7.25	Single-center
Mohamed A	2016	46	Retrospective	32/0/0/0/14	26 (56.5%)	32 (69.6%)	62.0 ± 8	Multiple-center
Xavier	2016	35	Prospective	34/0/0/0/1	-	22 (62.9%)	62 (27-69)	Multiple-center

A, Asian; B, black; C, Causian; H, Hispanic; O, others.

Table 2. Basic characteristics of the studies included.

Author	Immunosuppressive protocols	Dosage adjust	Viral Load Log IU/mL	DAAs protocol	Duration of DAA treatment	Duration from LT (M)
Jacqueline	TAC 89%, MMF 41%, SIR 11%	15 pts underwent dosage adjust	5.8	SOF+SMV ±RBV	12/24 wk	54 (9-171)
Robert s.	TAC 80%, CsA 10%, both 0.6%; MMF/MPA 40%	NR	-	SOF+SMV±RBV	12 wk	60 (0-276)
Lutchman	96% TAC	1 pts changed cyclosporin into TAC	6.3 ± 1.2	SOF+SMV	12 wk	-
Suraki	TAC 91%,CsA 8%	NR	-	SOF+SMV+RBV	12 wk	57 ± 65
Saro	TAC 66%, CsA 3%, RAP 3%, TAC+MMF 25%, CsA+MMF 3%	NR	6.58	SOF+SMV	12 wk	48 (7-166)
Jackson	TAC 84%, CsA 6%, SIR 6%	NR	-	SOF+SMV	12 wk	-
Punzalan	TAC 88%,CsA 7%,RAP 5%	7 pts TAC dosage decreased	-	SOF+SMV	12 wk	-
Toru	TAC 45%, TAC+MMF 45%, TAC+MMF+STE 45%, MMF 4%, CsA 1%	NR	6.3	ASV+DCV	24 wk	-
Kerstin	-	No change	6.06	DCV+SMV	24 wk	15 (6-162)
Masaki	TAC 56%+MMF, MMF 22%, TAC 11%, CsA+PRED 11%	NR	6.11	ASV+DCV	24 wk	70 (3-121)
Neil	CsA 9%, TAC 71%, MPA 2%, SIR 18%	8pts TAC dosage increased, 9 pts decreased; 2pts CsA dosage decreased; 3 pts SIR dosage increased, 3pts decreased	-	SOF+SMV±RBV	12 wk	53
Paul	TAC 85%, CsA 15%, MMF 32%, PRED 6%	No change	6.6	PrOD	12 wk	-
Yoshihide	TAC 75%, MMF 46%, PRED 28%	NR	6.5	LDV+SOF	12 wk	61 (1-158)
Mohamed	-	NR	-	LDV+SOF	12 wk	42 (11-113)
Mohamed A	TAC 76%, SIR 13%, CsA 9%, EVR 2%, MMF 33%	Minimal changed but details not report	7.79	LDV+SOF	12/24 wk	30 (2-117)
Xavier 2016	TAC 71%, CsA 29%	NR	6.9	SMV+DCV+RBV	24 wk	47 (14-114)

ASV, Asunaprevir; CsA, Cyclosporine A; DAAs, direct-acting antivirals; DCV, Daclatavir; EVR, Everolimus; LDV, Ledipasvir; m, months; MMF, Mycophenolate Mofetil; MPA, Mycophenolic Acid; PrOD, Paritaprevir/Ritonavir/Ombitasivir/Dasabuvir; Pts, patients; PRED, Prednisone; RAP, Rapamune; RBV, Ribavirin; SIR, Sirolimus; STE, Steroid; SOF, Sofosbuvir; SMV, Simeprevir; TAC, Tacrolimus.

Outcomes

The efficacy and tolerability of DAA treatment.

Once DAA treatment completed, patients were followed up for evaluating SVR12 proportion. In total, 805 out of 885 (91.0%) patients successfully achieved SVR12. The pooled estimate SVR12 proportion among all LT recipients were 93% (95% CI: 0.89, 0.96), with moderate heterogeneity observed in a random-effects model (tau^2=0.01, p<0.001, I^2=75%, Figure 2). The expected shape observed in the funnel plots and results of the Egger's test (p=0.44) indicated no significant publication bias (Supplementary Figure 1 and 2). AEs commonly occurred in these patients. General symptoms including fever, fatigue and dizziness were the most common AEs with pooled estimate rate of 37% (95% CI: 0.14, 0.64; tau^2=0.30, p<0.01, I^2 =98%, Random-effects model, Supplementary figure 3). Pooled estimate incidence rate of gastrointestinal AEs was 10% (95% CI: 0.02, 0.23; tau^2=0.11, p<0.01, I^2 =96%, Random-effects model, Supplementary figure 4) and pooled estimate incidence rate of skin problems was 7% (95% CI: 0.02, 0.15; tau^2=0.06, p<0.01, I^2 =93%, Random-effects model, Supplementary figure 5). SAEs were mainly associated with kidney injury, were reported in 45 patients, and 12 patients died during the treatment period (Table 3). The pooled estimate rate of sAEs was 4% (95% CI: 0.01, 0.07, tau^2=0.02, p<0.01, I^2 =81%, Random-effects model, Figure 3).

Study Design

Twelve retrospective and four prospective studies were included. There was no significant difference in pooled estimate SVR12 proportion when comparing studies of prospective, 91% (95% CI: 0.87, 0.95), versus retrospective, 93% (95% CI: 0.88, 0.97) (*P*=0.44, Figure S6, Random effects model).

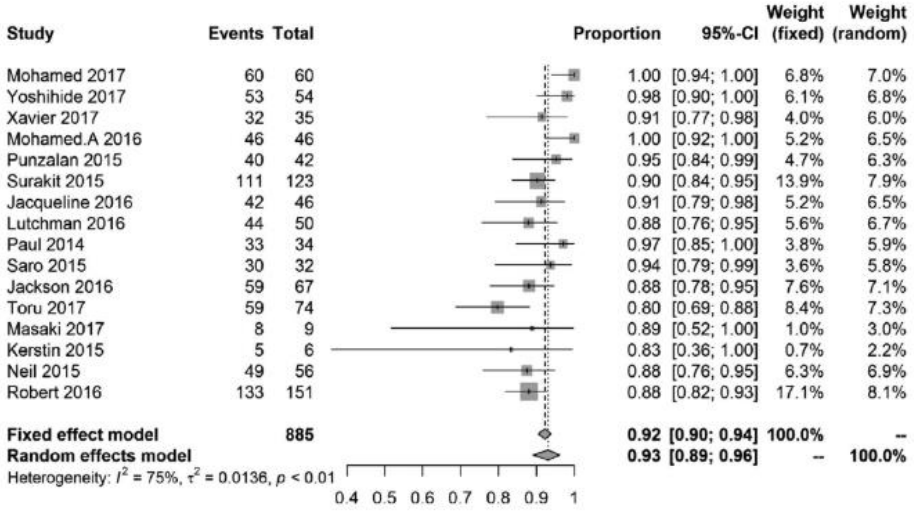

Figure 2. Pooled estimate proportion of 12 weeks sustained virological response after treatment completion and 95% confidence interval after directing-acting treatment of GT1 HCV recurrence post

liver transplantation from 16 studies. Abbreviations: Events, the number of patients who reached SVR12; Total, the number of patients analyzed.

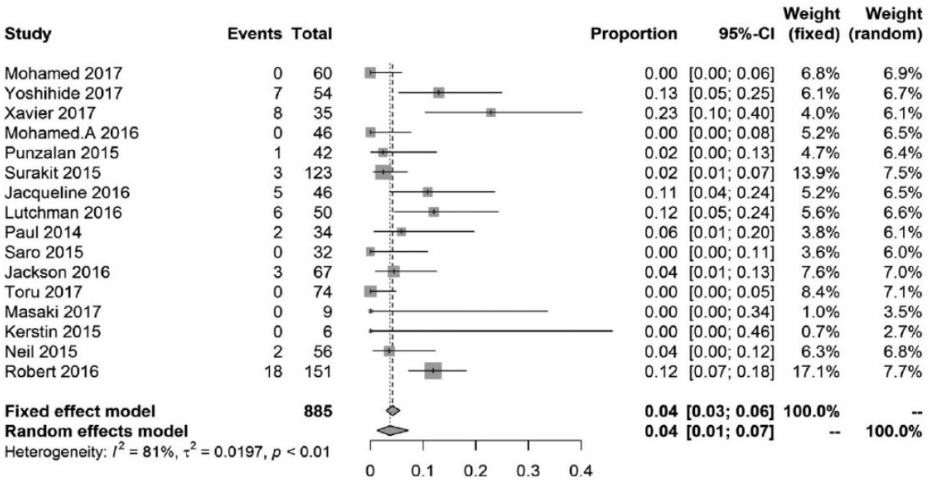

Figure 3. Pooed estimate proportion of serious adverse events and 95% confidence interval after direct-acting antivirals of GT1 HCV recurrence post liver transplantation form 16 studies. Abbreviations: Events, the number of patients who reached SVR12; Total, the number of patients analyzed.

3.3.3 Degree of liver cirrhosis. The METAVIR Fibrosis Score, simply put, is a evaluate system to determine the level of liver fibrosis.(29) The METAVIR Fibrosis Score grades the degree of fibrosis on a 5-point scale from 0 to 4. Fibrosis scores range from F0-F4 (F0 stage, no fibrosis; F1 stage, portal fibrosis without septa; F2 stage, portal fibrosis with septa; F3 stage, numerous septa without cirrhosis; F4 stage, cirrhosis). A total of eight studies evaluated levels of fibrosis and cirrhosis of patients according to METAVIR Fibrosis Score. The pooled SVR12 rate estimates among patients with METAVIR Fibrosis Score F0-F2 stage was 93% (95% CI: 0.89, 0.96) compared to 83% (95% CI: 0.75, 0.88) for stage F3-F4. There was a trend for a higher SVR12 rate in patients with F0-F2 stage than patients with F3-F4 stage (p<0.01, Figure 4, Random-effects model).

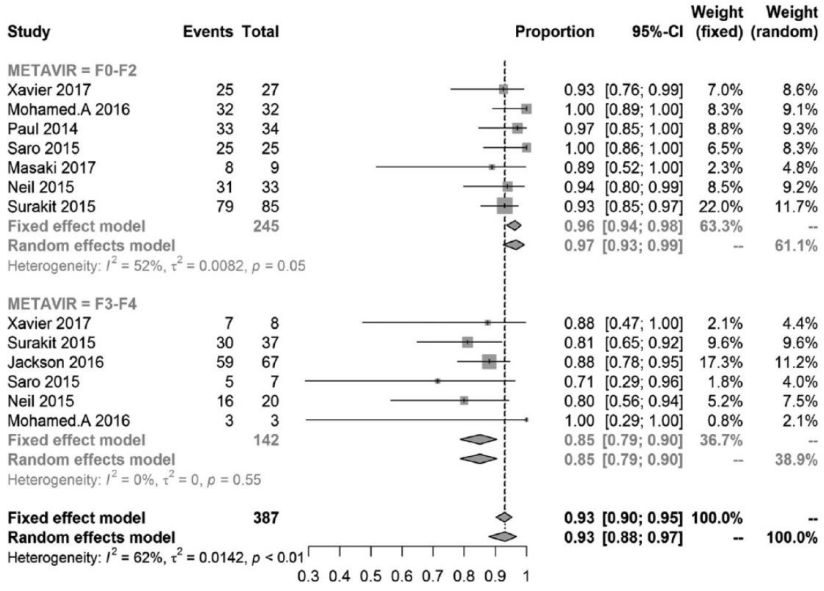

Figure 4. Comparison of pooled estimate proportion of 12 weeks sustained virological response after treatment completion and 95% confidence interval between METAVIR Fibrosis Stages F0-F2 and F3-F4 after direct-acting antivirals treatment of hepatitis C virus genotype 1 recurrence post liver transplantation. Abbreviations: Events, the number of patients who reached SVR12; Total, the number of patients analyzed.

Different combination of DAA regimens

Sixteen studies which contained five different DAA regimens were administered into clinical treatment of LT recipients with recurrent GT1 HCV infection. The pooled estimate SVR12 proportion were 97% (95 CI: 0.89, 1.00), 81% (95% CI: 0.72, 0.89), 100% (95% CI: 0.98, 1.00), 90% (95% CI: 0.80, 0.97), and 90% (95% CI: 0.87, 0.92) among patients who underwent treatment of PrOD, ASV/DCV, LDV/SOF, SMV/DCV with or without RBV and SMV/SOF with or without RBV, respectively (Figure S7, Random effects model).

With or without RBV

A total of 124 LT recipients used RBV as combinational treatment compared to 761 recipients without. The pooled estimate SVR12 proportion of recipients treated with RBV was 90% (95%CI: 0.84, 0.94). For recipients treated without RBV, the pooled proportion was 94% (95%CI: 0.89, 0.97). There was no significant difference in SVR12 proportion between LT recipients treated with or without RBV (*P*=0.23, Figure S8, Random effects model).

Discussion

The current systematic review and meta-analysis included 16 studies comprising 885 patients to assess the outcome of DAA treatment for liver transplant recipients with recurrent GT1 HCV infection. Overall, the pooled SVR12 and sAEs proportion were 93% and 4%, representing a rather good outcome. Subgroup analyses revealed clear difference in SVR12 rates for different treatment strategies. The pooled estimate proportion for combination of LDV/SOF appears much higher than the other four combinations. In addition, the efficacy of DAA treatment is closely associated with fibrosis or cirrhosis levels, which highlights the necessity of early initiation of DAA treatment in these patients.

The pooled estimate results of SVR12 provided evidence that DAA treatment was clinically effective in eradicating GT1 HCV recurrence post LT. This is comparable to the pooled estimate results from a recent meta-analysis that contained all HCV GTs.(30) Of note, the unbalanced application of DAAs for GT1 HCV recurrence exists among different regions. There is a trend that the first-class of DAAs are commonly used in European or North American countries. For many countries, even like Japan, cost-effectiveness other than SVR rate is the first consideration for clinicians.(24, 25) However, in Asia-pacific or Africa countries, HCV has distinct epidemiology. Furthermore, DAA availability has been delayed due to economic constraints and regulatory rules.(31) Although two studies from Japan suggested that DAA treatment

is effective in Asian patients, multi-regional and systematic studies should be combined to further confirm the effectiveness of DAA treatment for different regions.

The average time of progression from initial HCV infection to cirrhosis is about 30 years, but 20-30% of liver transplant recipients develop cirrhosis within 5 years.(32) Re-transplantation is the only option to achieve long-term survival of patients with decompensated cirrhosis. However, due to organ shortage and poor clinical outcome, re-transplantation is clearly not a sustainable solution.(33) In our subgroup analysis of liver transplant recipients with SVR12 rate and fibrosis data (METAVIR Fibrosis Score), our detailed analysis supports the latest evidence-based guidelines that DAAs also can be effectively used in eradicating HCV in patients with advanced fibrosis or cirrhosis post LT.(34) We observed a higher SVR12 pooled estimate proportion in patients with mild fibrosis compared with those of advanced fibrosis or cirrhosis, with a trend favoring SVR12 in patients with mild fibrosis. Our results indicated that the capability of HCV eradication by DAAs may be correlated with the levels of liver fibrosis or cirrhosis. Therefore, DAA treatment is recommended to be initiated early after transplantation.

Five different combinations of DAA treatment were identified in our systematic review and meta-analysis. There are important differences among the strategies, such as addition of RBV, duration of treatment and potential drug interactions. Among these regimens, SMV/SOF with or without RBV were most commonly used with a pooled estimate SVR12 proportion of 90%, which is comparable with a recent study reporting SVR12 rate of 88%.(30) A number of studies have pointed out that SMV may interact with Cyclosporine A (CsA), and therefore the immunosuppressant tacrolimus is recommended to be used.(35) In general, the combination of SMV and SOF with or without RBV seems to be a safe regimen even at the early stage of post-transplantation, when constant changes of immunosuppressive medication are often required and the patients are vulnerable to side effects. The combination of LDV and SOF has been used in three studies. The safety and efficacy of combination of LDV and SOF was firstly confirmed in a US-based SOLAR-2 study with a SVR12 rate of 96% and SVR24 rate of 98%.(36) The pooled estimate SVR12 proportion of LDV and SOF from our study is as high as 100%. Only one study reported their results for the DAA combination regimen of PrOD in GT1 HCV recurrence post LT with SVR12 proportion of 97%. Unfortunately, PrOD is contraindicated in patients with cirrhosis and has a potential to increase the plasma cyclosporine A (CsA) levels by 5-6 folds and tacrolimus levels by 60-85 folds, which limited its clinical application.(28) In addition, efficacy and safety were not established for shorter duration therapy, or more advanced fibrosis/cirrhosis in a real world setting. Combination of ASV and DCV were administered by two Japanese studies with the lowest pooled estimate SVR12 proportion of 81%. Although this combination had a cost-effective advantage, increased transaminase levels were commonly associated with ASV.(37, 38) Two studies have reported a pooled estimate SVR12 proportion of 90% with DAA combination of SMV/DCV with or without RBV. Although the pooled estimate SVR12 proportion was satisfactory, two limitations including small sample size and prolonged treatment period of 24 weeks in these two studies should be noted.

There is ongoing debate whether adding RBV to interferon-free treatment strategy is necessary for treating HCV recurrence after LT.(16) RBV has been used for over 40 years in combination for treating HCV with an obscure understanding of its mechanism-of-action.(39, 40) What is clear, however, is adverse effects. Hemolytic anemia has been observed in about one third of the patients. Lymphopenias, pruritus and rash also commonly occur. Thus, patients treated with RBV often need a close monitoring and dose adjustment, especially for those with chronic kidney disease. It is also recommended that patients treated with RBV should undergo at least 6-month washout period due to the possible teratogenic and embryocidal effects.(40-42) In current study, we observed an increased pooled estimate incidence rate of sAEs in patients treated with RBV, in accordance with the results from previous studies. Given that a number of studies have pointed out RBV were not correlated with an increased SVR12 rate,(13, 16, 20, 43) we compared patients treated or not treated with this medication. Our results also indicated that RBV was not correlated with an increased pooled estimate SVR12 proportion. We also assessed the tolerability of DAA treatment by analyzing pooled estimate proportion of AEs and sAEs. General symptoms, gastro-intestinal symptoms, and skin complaints were presented with a pooled estimate incidence rate of 37%, 10% and 7%, respectively. SAEs including death caused by hepatic or renal failure, pneumonia, bone marrow failure, acute kidney, liver or other major organ infection, hepatic decompensation, spontaneous bacterial peritonitis, and sepsis, were analyzed with a pooled estimate incidence rate of 4% (I^2 =81%).

Among them, renal dysfunction was reported in 45 patients, and 12 patients died during the treatment period. Impaired renal function commonly occurred in liver transplant recipients with the prevalence ranging from 17% to 95%.(44, 45) Approximately 40% of these patients had already experienced a hepatorenal syndrome pre-transplantation.(46) In addition, toxic reasons, ischemia reperfusion and CNI-associated nephropathy were account for renal dysfunction post-transplantation.(47) Although the exact pathophysiological mechanisms are not fully understood, HCV infection may influence renal function through different pathways.(48) A recent study documented that patients with HCV recurrence after LT will absolutely benefit from HCV elimination but will be at a higher risk for renal dysfunction or failure associated with antiviral drugs like SOF.(49) Unlike most DAAs, the nucleotide analogue NS5B polymerase inhibitor SOF was renally excreted. For area under the curves (AUCs) of SOF, patients with end-stage renal diseases was 45-fold and 35-fold higher compared to normal renal function when dosed 1 hour before or 1 hour after hemodialysis, respectively.(50) However, there are conflicting data about the application of SOF in clinical treatment. Saxena et al (51) evaluated the safety and efficacy of SOF-based therapy in HCV-infected patients with impaired renal function. High SVR rate of 83% was achieved with high rate of renal dysfunction and sAEs observed. A prospective multicenter cohort study enrolled 50 patients with GFR < 35 mL/min per 1.73 m^2 for treatment with a SOF-based therapy. All genotypes were included and more than half of them were cirrhotic patients. The results indicated that there is no significant change in GFR for patients who were not on dialysis.(52) More recently, Teegen et al (49) also documented that a dose reduction for SOF did not seem to be necessary to prevent

further renal damage. Thus, additional data are still needed to further assess the safety of SOF in transplant recipients.

CNIs are the backbone of immunosuppressive treatment of LT. Eighty percent of liver transplant recipients were using tacrolimus alone or in combination with mycophenolate 1 year post transplantation.(53) Although CNIs can reduce the incidence of acute injection and improve overall survival, they are inevitably associated with nephrotoxicity which is reflected in tubular atrophy, interstitial fibrosis, and glomerulosclerosis on kidney biopsy.(54) However, so far, the use of a CNI-free regimen is still challenging and the trend in LT was to use regimens that minimize the use of CNIs in combination with mycophenolate mofetil (MMF) or mammalian target of rapamycin inhibitors. One important observation, the use of everolimus with reduced tacrolimus exposure helped to preserve renal function after 3-year follow up which indicated that consideration should be given to minimize the dose of CNIs or switch to MMF or everolimus for these patients.(55, 56)

This study has exclusively focused on the effectiveness and tolerability of DAA treatment. Thus, a control group is not included, such as patients treated with DAAs before LT or treated with interferon post LT. Thus, without such a control, we cannot conclude whether treatment post LT has any advantage than treatment prior to LT or interferon treated recipients. Besides, most studies were from developed regions, including North American or European countries. Hence, multi-regional studies are still needed to substantiate the comprehensive information for better clinical guidance globally. Last but not the least, the field of HCV treatment is a dynamic and constantly changing landscape. A number of new agents or combination approaches may still in clinical trials or just licensed.

In summary, our results support DAAs as treatment for eradicating GT1 HCV recurrence in liver transplant recipients. They are highly effective and well-tolerated. However, fine-tuning is essential for achieving the optimal outcome, given considerations of drug availability, potential drug-drug interactions, the fibrotic or cirrhotic stage of the patients and regional/social factors.

Table 3. Incidence of adverse events and serious adverse events during direct-acting antivirals treatment for patients of hepatitis C virus genotype 1 recurrence post liver transplantation.

	Jacqueline 2016	Robert 2016	Lutchman 2016	Suraki 2015	Saro 2015	Jackson 2016	Punzalan 2015
GI Symptoms							
Nausea	23.9%	11.3%	4.4%	5.0%	3.0%	11.3%	
Diarrhea	21.7%						
Vomitting	17.4%						
Constipation	10.9%						
De-or increased appetite	13.0%		4.4%		3.0%		
General Symptoms							
Perspiration							
Cough							
Insomnia	13.0%		35.9%	2.0%			
Dizziness					9.0%		
Fever					3.0%		
Headache	37.0%	18.5%	8.7%	5.0%	25.0%	18.5%	
Fatigue	34.8%	25.2%	44.6%	13.0%	22.0%	25.2%	2.4%
Skin Problems							
Photosensitivity, pruritus, rash	21.7%	13.9%	44.6%	6.0%	6.0%	13.9%	12.0%
Anemia	10.6%			77.0%		10.6%	
Dysnoea	28.2%			4.0%			
Infection and infestation		14.6%				14.6%	
Joint or muscle pain			4.4%		9.0%		2.4%
Others		11.9%		14.0%			21.5%
sAEs	10.9%	11.9%	6.5%	2.4%	0	11.9%	2.4%

Toru 2017	Kerstin 2015	Masaki 2017	Neil 2015	Paul 2014	Yoshihide 2017	Mohamed 2017	Mohamed A.2016	Xavier 2016
			36.0%	24.0%		3.0%		
				26.0%	2.0%			14.0%
	30.0%		21.0%					
	17.0%							
				32.0%				14.0%
			21.0%	26.0%			5.0%	
			7.0%	18.0%				
			36.0%	44.0%		23.0%	5.0%	14.0%
	50.0%		71.0%	50.0%		20.0%	6.0%	9.0%
			35.0%	21.0%				31.0%
	30.0%			29.0%				54.0%
								11.0%
					2.0%			
			7.0%	39.0%				
20.2%		22.2%	28.0%	42.0%	10.0%			
0	0	0	3.6%	6.0%	13.0%	0	0	23.0%

GI, gastrointestinal; sAEs, serious adverse events.

Reference

1. Brown RS. Hepatitis C and liver transplantation. Nature 2005; 436(7053): 973-978.
2. Gane EJ, Portmann BC, Naoumov NV et al. Long-term outcome of hepatitis C infection after liver transplantation. N Engl J Med 1996; 334(13): 815-820.
3. Gane E. The natural history and outcome of liver transplantation in hepatitis C virus-infected recipients. Liver Transpl 2003; 9(11): S28-34.
4. Berenguer M, Ferrell L, Watson J et al. HCV-related fibrosis progression following liver transplantation: increase in recent years. J Hepatol 2000; 32(4): 673-684.
5. Gane EJ and Agarwal K. Directly acting antivirals (DAAs) for the treatment of chronic hepatitis C virus infection in liver transplant patients: "a flood of opportunity". Am J Transplant 2014; 14(5): 994-1002.
6. Berenguer M, Palau A, Aguilera V, Rayon JM, Juan FS, and Prieto M. Clinical benefits of antiviral therapy in patients with recurrent hepatitis C following liver transplantation. Am J Transplant 2008; 8(3): 679-687.
7. Garg V, van Heeswijk R, Lee JE, Alves K, Nadkarni P, and Luo X. Effect of telaprevir on the pharmacokinetics of cyclosporine and tacrolimus. Hepatology 2011; 54(1): 20-27.
8. Hulskotte E, Gupta S, Xuan F et al. Pharmacokinetic interaction between the hepatitis C virus protease inhibitor boceprevir and cyclosporine and tacrolimus in healthy volunteers. Hepatology 2012; 56(5): 1622-1630.
9. Hull MW, Yoshida EM, and Montaner JS. Update on Current Evidence for Hepatitis C Therapeutic Options in HCV Mono-infected Patients. Curr Infect Dis Rep 2016; 18(7): 22.
10. Nguyen LH and Nguyen MH. Systematic review: Asian patients with chronic hepatitis C infection. Aliment Pharmacol Ther 2013; 37(10): 921-936.
11. Kao JH, Ahn SH, Chien RN et al. Urgency to treat patients with chronic hepatitis C in Asia. J Gastroenterol Hepatol 2017; 32(5): 966-974.
12. Messina JP, Humphreys I, Flaxman A et al. Global distribution and prevalence of hepatitis C virus genotypes. Hepatology 2015; 61(1): 77-87.
13. Jackson WE, Hanouneh M, Apfel T et al. Sofosbuvir and simeprevir without ribavirin effectively treat hepatitis C virus genotype 1 infection after liver transplantation in a two-center experience. Clin Transplant 2016; 30(6): 709-713.
14. O'Leary JG, Fontana RJ, Brown K et al. Efficacy and safety of simeprevir and sofosbuvir with and without ribavirin in subjects with recurrent genotype 1 hepatitis C postorthotopic liver transplant: the randomized GALAXY study. Transpl Int 2017; 30(2): 196-208.
15. Punzalan CS, Barry C, Zacharias I et al. Sofosbuvir plus simeprevir treatment of recurrent genotype 1 hepatitis C after liver transplant. Clin Transplant 2015; 29(12): 1105-1111.
16. Crittenden NE, Buchanan LA, Pinkston CM et al. Simeprevir and sofosbuvir with or without ribavirin to treat recurrent genotype 1 hepatitis C virus infection after orthotopic liver transplantation. Liver Transpl 2016; 22(5): 635-643.
17. Pungpapong S, Aqel B, Leise M et al. Multicenter experience using simeprevir and sofosbuvir with or without ribavirin to treat hepatitis C genotype 1 after liver transplant. Hepatology 2015; 61(6): 1880-1886.
18. Khemichian S, Lee B, Kahn J et al. Sofosbuvir and Simeprevir Therapy for Recurrent Hepatitis C Infection After Liver Transplantation. Transplant Direct 2015; 1(6): e21.
19. Lutchman G, Nguyen NH, Chang CY et al. Effectiveness and tolerability of simeprevir and sofosbuvir in nontransplant and post-liver transplant patients with hepatitis C genotype 1. Aliment Pharmacol Ther 2016; 44(7): 738-746.
20. Brown RS, Jr., O'Leary JG, Reddy KR et al. Interferon-free therapy for genotype 1 hepatitis C in liver transplant recipients: Real-world experience from the hepatitis C therapeutic registry and research network. Liver Transpl 2016; 22(1): 24-33.
21. Ueda Y, Ikegami T, Akamatsu N et al. Treatment with sofosbuvir and ledipasvir without ribavirin for 12 weeks is highly effective for recurrent hepatitis C virus genotype 1b infection after living donor liver transplantation: a Japanese multicenter experience. J Gastroenterol 2017; 52(8): 986-991.
22. Elfeki MA, Abou Mrad R, Modaresi Esfeh J et al. Sofosbuvir/Ledipasvir Without Ribavirin Achieved High Sustained Virologic Response for Hepatitis C Recurrence After Liver Transplantation: Two-Center Experience. Transplantation 2017; 101(5): 996-1000.
23. Shoreibah M, Orr J, Jones D, Zhang J, Venkata K, and Massoud O. Ledipasvir/sofosbuvir without ribavirin is effective in the treatment of recurrent hepatitis C virus infection post-liver transplant. Hepatol Int 2017; 11(5): 434-439.
24. Ikegami T, Ueda Y, Akamatsu N et al. Asunaprevir and daclatasvir for recurrent hepatitis C after liver transplantation: A Japanese multicenter experience. Clin Transplant 2017; 31(11).
25. Honda M, Sugawara Y, Watanabe T et al. Outcomes of treatment with daclatasvir and asunaprevir for recurrent hepatitis C after liver transplantation. Hepatol Res 2017; 47(11): 1147-1154.
26. Herzer K, Papadopoulos-Kohn A, Walker A et al. Daclatasvir, Simeprevir and Ribavirin as a Promising Interferon-Free Triple Regimen for HCV Recurrence after Liver Transplant. Digestion 2015; 91(4): 326-333.
27. Forns X, Berenguer M, Herzer K et al. Efficacy, safety, and pharmacokinetics of simeprevir, daclatasvir, and ribavirin in patients with recurrent hepatitis C virus genotype 1b infection after orthotopic liver transplantation: The Phase II SATURN study. Transpl Infect Dis 2017; 19(3).
28. Kwo PY, Mantry PS, Coakley E et al. An interferon-free antiviral regimen for HCV after liver transplantation. N Engl J Med 2014; 371(25): 2375-2382.
29. Rousselet MC, Bedossa P, Pilette C, Oberti F, and Cales P. Metavir score reflects liver fibrosis in chronic alcoholic diseases. Hepatology 1999; 30(4): 586a-586a.
30. Nguyen NH, Yee BE, Chang C et al. Tolerability and effectiveness of sofosbuvir and simeprevir in the post-transplant setting: systematic review and meta-analysis. BMJ Open Gastroenterol 2016; 3(1): e000066.
31. Lim SG, Aghemo A, Chen PJ et al. Management of hepatitis C virus infection in the Asia-Pacific region: an update. Lancet Gastroenterol Hepatol 2017; 2(1): 52-62.
32. Berenguer M, Prieto M, Rayon JM et al. Natural history of clinically compensated hepatitis C virus-related graft cirrhosis after liver transplantation. Hepatology 2000; 32(4 Pt 1): 852-858.
33. Carrion JA, Navasa M, and Forns X. Retransplantation in patients with hepatitis C recurrence after liver transplantation. J Hepatol 2010; 53(5): 962-970.
34. European Association for the Study of the Liver. Electronic address eee. EASL Recommendations on Treatment of Hepatitis C 2016. J Hepatol 2017; 66(1): 153-194.

35. Perumpail RB, Wong RJ, Ha LD et al. Sofosbuvir and simeprevir combination therapy in the setting of liver transplantation and hemodialysis. Transpl Infect Dis 2015; 17(2): 275-278.
36. Manns M, Samuel D, Gane EJ et al. Ledipasvir and sofosbuvir plus ribavirin in patients with genotype 1 or 4 hepatitis C virus infection and advanced liver disease: a multicentre, open-label, randomised, phase 2 trial. Lancet Infect Dis 2016; 16(6): 685-697.
37. Lok AS, Gardiner DF, Lawitz E et al. Preliminary study of two antiviral agents for hepatitis C genotype 1. N Engl J Med 2012; 366(3): 216-224.
38. Fujii Y, Uchida Y, and Mochida S. Drug-induced immunoallergic hepatitis during combination therapy with daclatasvir and asunaprevir. Hepatology 2015; 61(1): 400-401.
39. Feld JJ and Hoofnagle JH. Mechanism of action of interferon and ribavirin in treatment of hepatitis C. Nature 2005; 436(7053): 967-972.
40. Thomas E, Ghany MG, and Liang TJ. The application and mechanism of action of ribavirin in therapy of hepatitis C. Antiviral Chemistry & Chemotherapy 2012; 23(1): 1-12.
41. Gentile I, Borgia F, Buonomo AR, Castaldo G, and Borgia G. A novel promising therapeutic option against hepatitis C virus: an oral nucleotide NS5B polymerase inhibitor sofosbuvir. Current Medicinal Chemistry 2013; 20(30): 3733-3742.
42. Fried MW. Side effects of therapy of hepatitis C and their management. Hepatology 2002; 36(5 Suppl 1): S237-244.
43. Saab S, Greenberg A, Li E et al. Sofosbuvir and simeprevir is effective for recurrent hepatitis C in liver transplant recipients. Liver International 2015; 35(11): 2442-2447.
44. Barri YM, Sanchez EQ, Jennings LW et al. Acute kidney injury following liver transplantation: definition and outcome. Liver Transpl 2009; 15(5): 475-483.
45. Ojo AO, Held PJ, Port FK et al. Chronic renal failure after transplantation of a nonrenal organ. N Engl J Med 2003; 349(10): 931-940.
46. Gambato M, Lens S, Navasa M, and Forns X. Treatment options in patients with decompensated cirrhosis, pre- and post-transplantation. J Hepatol 2014; 61(1 Suppl): S120-131.
47. Weber ML, Ibrahim HN, and Lake JR. Renal dysfunction in liver transplant recipients: evaluation of the critical issues. Liver Transpl 2012; 18(11): 1290-1301.
48. Husing A, Kabar I, Schmidt HH, and Heinzow HS. Hepatitis C in Special Patient Cohorts: New Opportunities in Decompensated Liver Cirrhosis, End-Stage Renal Disease and Transplant Medicine. Int J Mol Sci 2015; 16(8): 18033-18053.
49. Teegen EM, Durr M, Maurer MM et al. Evaluation of histological dynamics, kidney function and diabetes in liver transplant patients after antiviral treatment with direct-acting antivirals: Therapy of HCV-recurrence. Transpl Infect Dis 2018: e13020.
50. Glead Siences Inc These highlights do not include all the information needed to use SOVALDI safely and effectively. See full prescribing information for SOVALDI.<http://www.gilead.com/~/media/Files/pdfs/medicines/liverdisease/sovaldi/sovaldi_pi.pdf> 2017.08.02.
51. Saxena V, Koraishy FM, Sise ME et al. Safety and efficacy of sofosbuvir-containing regimens in hepatitis C-infected patients with impaired renal function. Liver International 2016; 36(6): 807-816.
52. Dumortier J, Bailly F, Pageaux GP et al. Sofosbuvir-based antiviral therapy in hepatitis C virus patients with severe renal failure. Nephrol Dial Transplant 2017; 32(12): 2065-2071.
53. Kim WR, Smith JM, Skeans MA et al. OPTN/SRTR 2012 Annual Data Report: liver. Am J Transplant 2014; 14 Suppl 1: 69-96.
54. Flechner SM, Kobashigawa J, and Klintmalm G. Calcineurin inhibitor-sparing regimens in solid organ transplantation: focus on improving renal function and nephrotoxicity. Clin Transplant 2008; 22(1): 1-15.
55. Saliba F, De Simone P, Nevens F et al. Renal function at two years in liver transplant patients receiving everolimus: results of a randomized, multicenter study. Am J Transplant 2013; 13(7): 1734-1745.
56. Sterneck M, Kaiser GM, Heyne N et al. Everolimus and early calcineurin inhibitor withdrawal: 3-year results from a randomized trial in liver transplantation. Am J Transplant 2014; 14(3): 701-710.

Supplementary data for

Direct-acting antiviral agents for liver transplant recipients with recurrent hepatitis C virus genotype 1 infection: systematic review and meta-analysis

Table of contents

Supplementary method 1. Searching strategy for direct-acting antivirals for treatment of hepatitis C virus genotype 1 recurrence post liver transplantation.

Embase.com 1106

('direct acting antiviral'/exp OR 'sofosbuvir'/de OR 'ribavirin'/de OR 'ritonavir'/de OR 'asunaprevir'/de OR 'simeprevir'/de OR 'daclatasvir'/de OR 'ombitasvir'/de OR 'dasabuvir plus ombitasvir plus paritaprevir plus ritonavir'/de OR 'ledipasvir'/de OR 'ledipasvir plus sofosbuvir'/de OR 'velpatasvir'/de OR 'sofosbuvir plus velpatasvir'/de OR 'elbasvir plus grazoprevir'/de OR 'grazoprevir'/de OR 'elbasvir'/de OR ((direct* NEAR/3 (antiviral* OR anti-viral*)) OR daas OR daa OR sofosbuvir* OR ribavirin* OR Ritonavir* OR Asunaprevir* OR Simeprevir* OR daclatasvir* OR ombitasvir* OR prod OR ledipasvir* OR velpatasvir* OR Grazoprevir* OR Elbasvir* OR Sunvepra* OR interferon-free OR ifn-free):kw,de,ab,ti) AND ('liver transplantation'/exp OR 'organ transplantation'/de OR transplantation/de OR 'graft recipient'/de OR 'patient history of liver transplantation'/de OR (((liver OR hepat* OR organ OR organs) AND (transplant* OR graft* OR allotransplant* OR allograft* OR autotransplant* OR autograft* OR recipient*))):kw,de,ab,ti) AND ('Hepatitis C virus genotype 1'/exp OR (('Hepatitis C virus'/exp OR 'Hepatitis C'/exp) AND genotype/de) OR (((Hepatitis-C OR hcv OR Hepacivirus) AND ((genotyp* OR gt OR subtyp*)) OR gt1 OR g1)):kw,de,ab,ti) NOT ([Conference Abstract]/lim OR [Letter]/lim OR [Note]/lim OR [Editorial]/lim) AND [english]/lim

Medline Ovid 662

(sofosbuvir/ OR ribavirin/ OR ritonavir/ OR asunaprevir/ OR simeprevir/ OR daclatasvir/ OR ombitasvir/ OR ledipasvir/ OR ledipasvir plus sofosbuvir/ OR velpatasvir/ OR grazoprevir/ OR elbasvir/ OR ((direct* ADJ3 (antiviral* OR anti-viral*)) OR daas OR daa OR sofosbuvir* OR ribavirin* OR Ritonavir* OR Asunaprevir* OR Simeprevir* OR daclatasvir* OR ombitasvir* OR prod OR ledipasvir* OR velpatasvir* OR Grazoprevir* OR Elbasvir* OR Sunvepra* OR interferon-free OR ifn-free).kw,ab,ti.) AND (liver transplantation/ OR liver/tr OR organ transplantation/ OR transplantation/ OR graft recipient/ OR (((liver OR hepat* OR organ OR organs) AND (transplant* OR graft* OR allotransplant* OR allograft* OR autotransplant* OR autograft* OR recipient*))).kw,ab,ti.) AND (((Hepacivirus/ OR Hepatitis C/) AND genotype/) OR (((Hepatitis-C OR hcv OR Hepacivirus) AND ((genotyp* OR gt OR subtyp*)) OR gt1 OR g1)).kw,ab,ti.) NOT (letter OR news OR comment OR editorial OR congresses OR abstracts).pt. AND english.la.

Cochrane CENTRAL 134

(((direct* NEAR/3 (antiviral* OR anti-viral*)) OR daas OR daa OR sofosbuvir* OR ribavirin* OR Ritonavir* OR Asunaprevir* OR Simeprevir* OR daclatasvir* OR ombitasvir* OR prod OR ledipasvir* OR velpatasvir* OR Grazoprevir* OR Elbasvir* OR Sunvepra* OR interferon-free OR ifn-free):ab,ti) AND ((((liver OR hepat* OR organ OR organs) AND (transplant* OR graft* OR allotransplant* OR allograft* OR autotransplant* OR autograft* OR recipient*))):ab,ti) AND ((((Hepatitis-C OR hcv OR Hepacivirus) AND ((genotyp* OR gt OR subtyp*)) OR gt1 OR g1)):ab,ti)

Web of science 645

TS=((((direct* NEAR/2 (antiviral* OR anti-viral*)) OR daas OR daa OR sofosbuvir* OR ribavirin* OR Ritonavir* OR Asunaprevir* OR Simeprevir* OR daclatasvir* OR ombitasvir* OR prod OR ledipasvir* OR velpatasvir* OR Grazoprevir* OR Elbasvir* OR Sunvepra* OR interferon-free OR ifn-free)) AND ((((liver OR hepat* OR organ OR organs) AND (transplant* OR graft* OR allotransplant* OR allograft* OR autotransplant* OR autograft* OR recipient*)))) AND ((((Hepatitis-C OR hcv OR Hepacivirus) AND ((genotyp* OR gt OR subtyp*)) OR gt1 OR g1)))) AND DT=(article) AND LA=(english)

Google scholar

"direct antiviral"|"direct*antiviral"|"direct acting anti"|sofosbuvir|ribavirin|"interferon|ifn free" "liver|hepatic transplantation|graft|recipient" "Hepatitis-C"|Hepacivirus "genotype|gt|subtype 1"

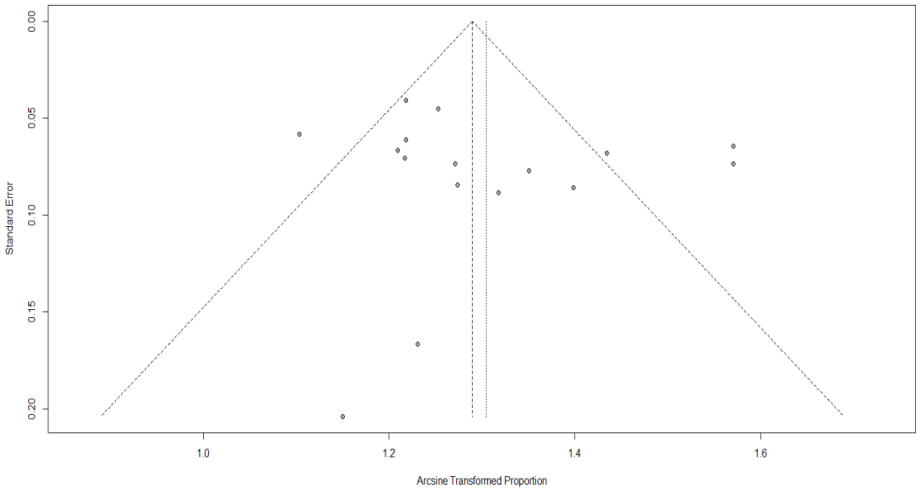

Supplementary figure 1. The Begg funnel plot for 12 weeks sustained virologic response after direct-acting antivirals treatment of hepatitis C virus genotype 1 recurrence post liver transplantation from 16 studies.

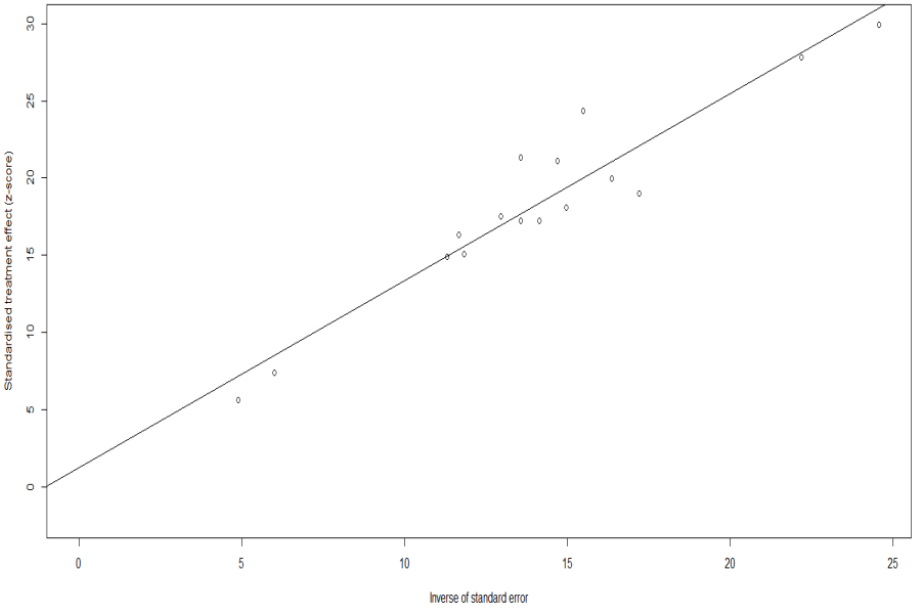

Supplementary figure 2. The Egger regression test for 12 weeks sustained virologic response after direct-acting antivirals treatment of hepatitis C virus genotype 1 recurrence post liver transplantation from 16 studies.

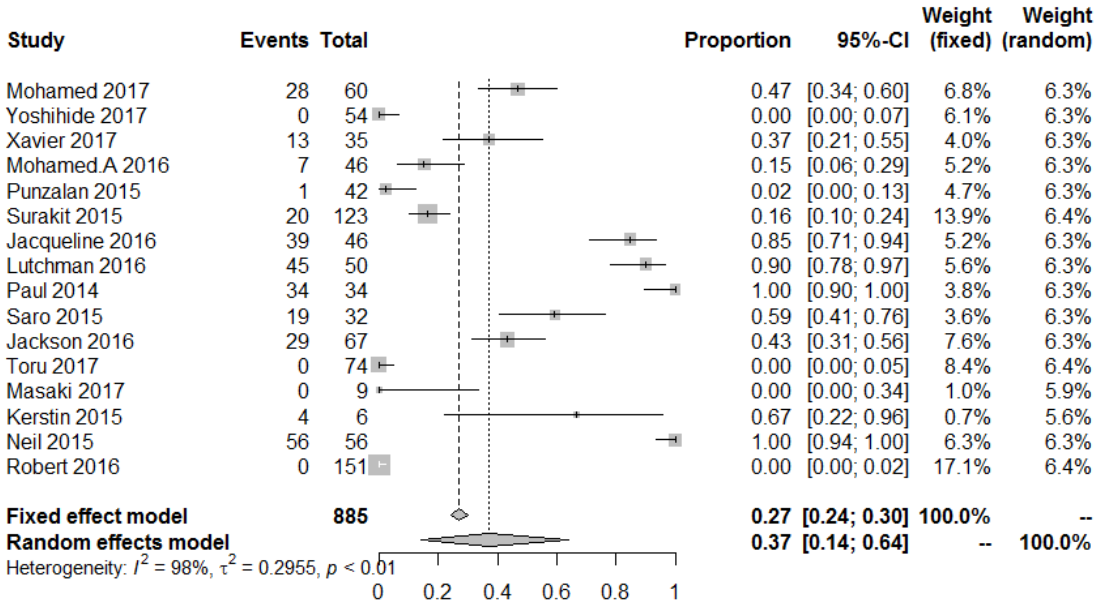

Supplementary figure 3. Pooled estimate proportion of general symptoms incidence and 95% confidence interval after direct-acting antivirals of hepatitis C virus genotype 1 recurrence post liver transplantation from 16 studies. Abbreviations: CI, confidence interval; Events, the number of patients who reached SVR12; Total, the number of patients analyzed.

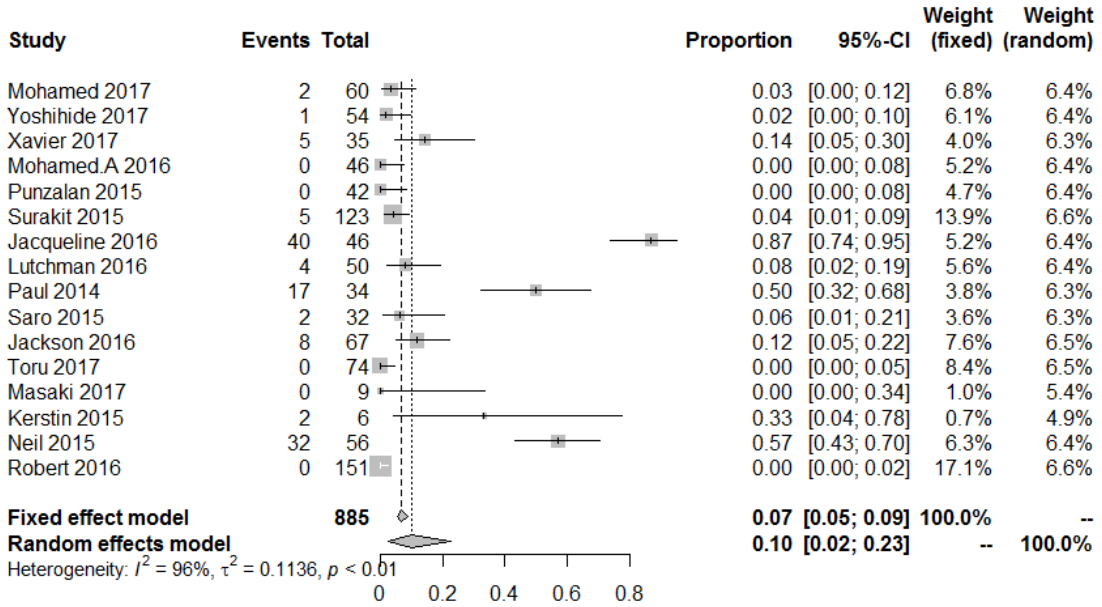

Supplementary Figure 4. Pooled estimate proportion of gastrointestinal symptoms incidence and 95% confidence interval after direct-acting antivirals of hepatitis C virus genotype 1 recurrence post liver transplantation from 16 studies. Abbreviations: CI, confidence interval; Events, the number of patients who reached SVR12; Total, the number of patients analyzed.

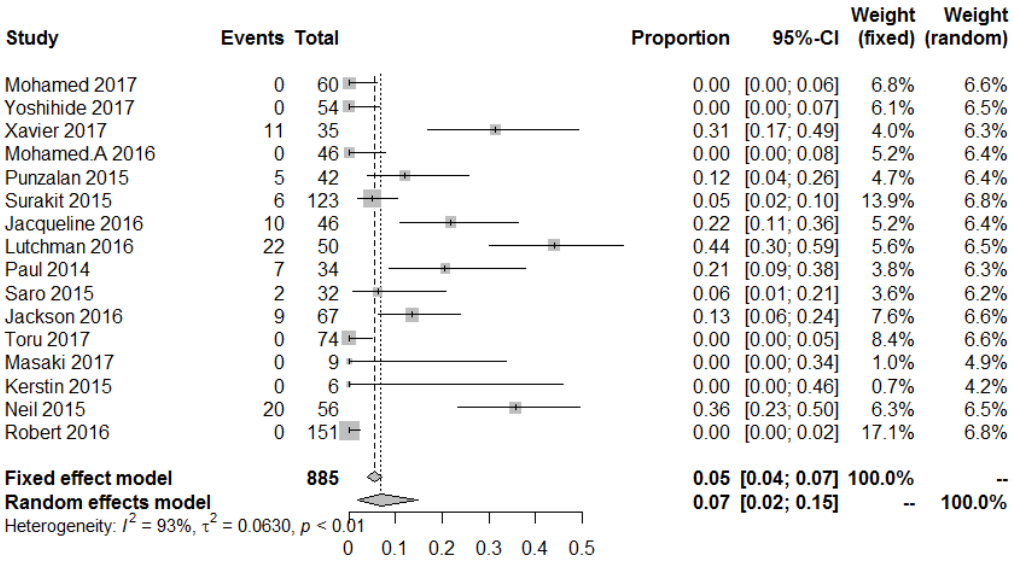

Supplementary figure 5. Pooled estimate proportion of skin problems incidence and 95% confidence interval after direct-acting antivirals of hepatitis C virus genotype 1 recurrence post liver transplantation from 16 studies. Abbreviations: CI, confidence interval; Events, the number of patients who reached SVR12; Total, the number of patients analyzed.

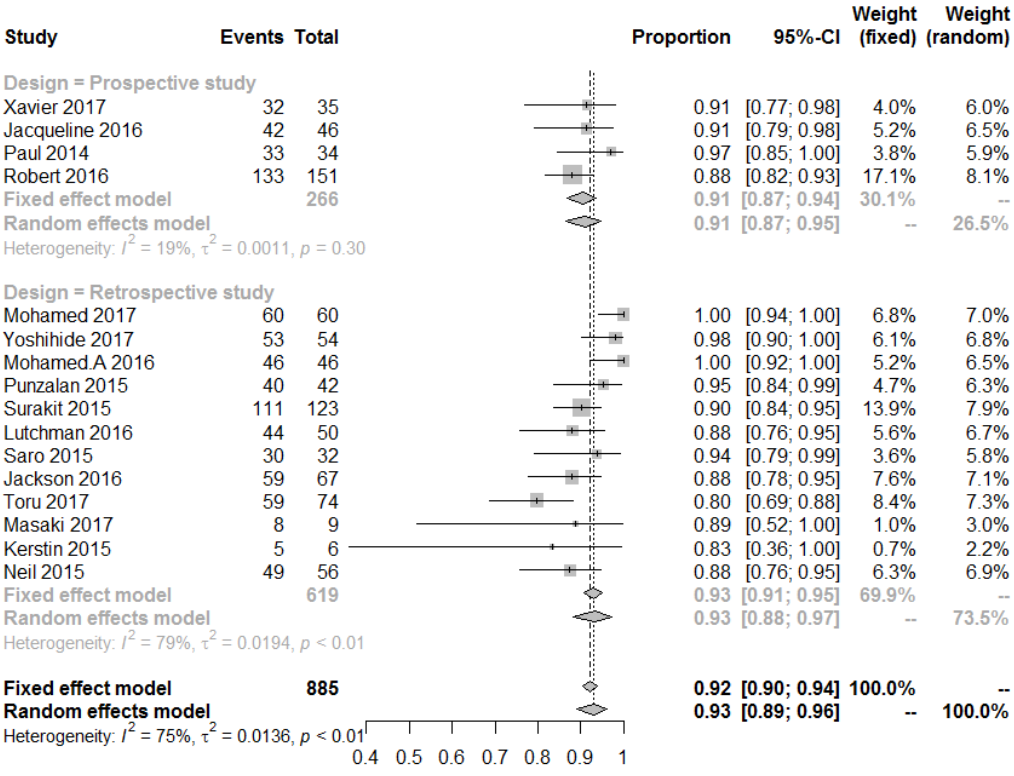

Supplementary figure 6. Comparison of pooled estimate proportion of 12 weeks sustained virologic response after treatment completion and 95% confidence interval between prospective studies and retrospective studies after direct-acting antivirals treatment of hepatitis C virus genotype 1 recurrence post liver transplantation. Abbreviations: CI, confidence interval; Events, the number of patients who reached SVR12; Total, the number of patients analyzed.

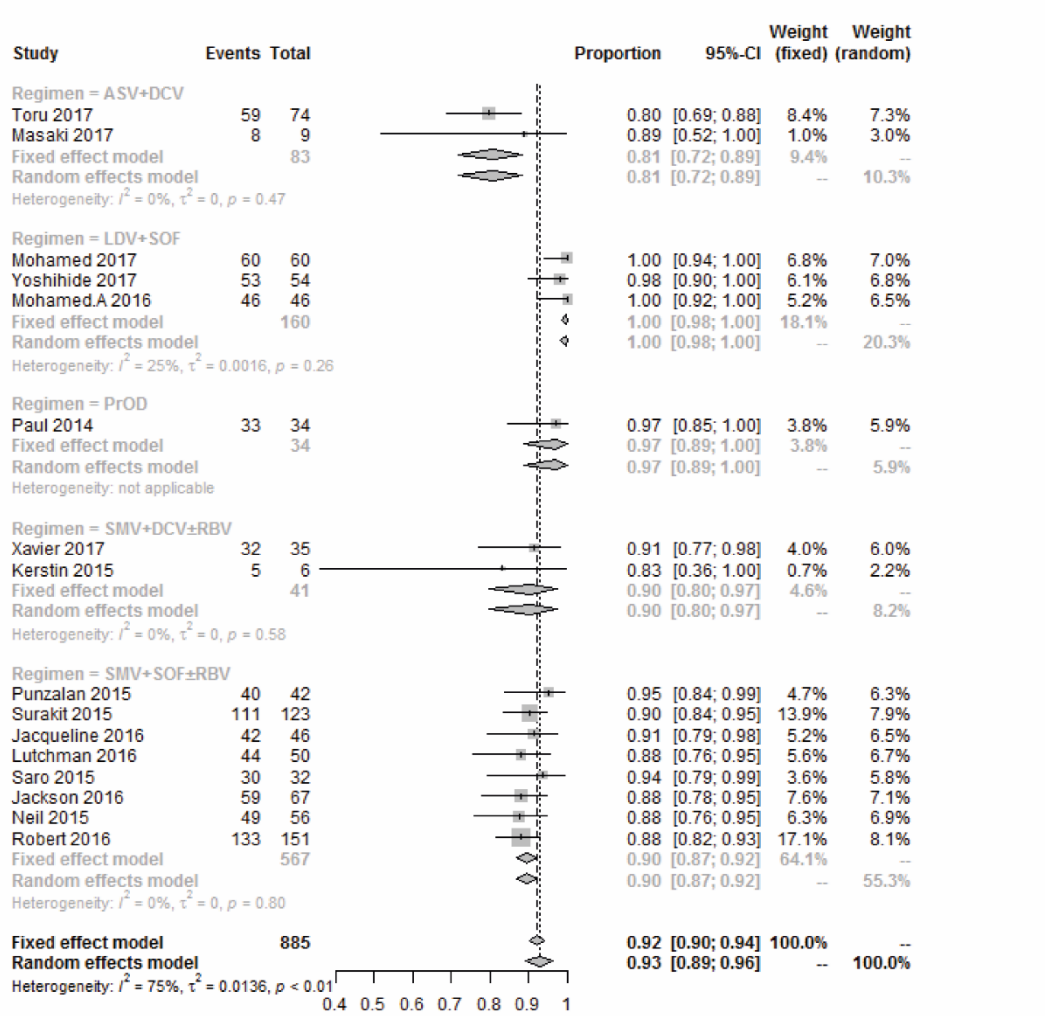

Supplementary figure 7. Comparison of pooled estimate proportion of 12 weeks sustained virologic response after treatment completion and 95% confidence interval among five different direct-acting antivirals regimens for treatment of hepatitis C virus genotype 1 recurrence post liver transplantation. Abbreviations: CI, confidence interval; Events, the number of patients who reached SVR12; Total, the number of patients analyzed; PrOD, Paritaprevir/Ritonavir/Ombitasivir/Dasabuvir; ASV+DCV, Asunaprevir/Daclatavir; SOF+LDV, Sofosbuvir/Ledipasvir; DCV+SMV±RBV, Daclatavir/Simeprevir with or without Ribavirin; SOF+SMV±RBV, Sofosbuvir/Simeprevir with or without Ribavirin.

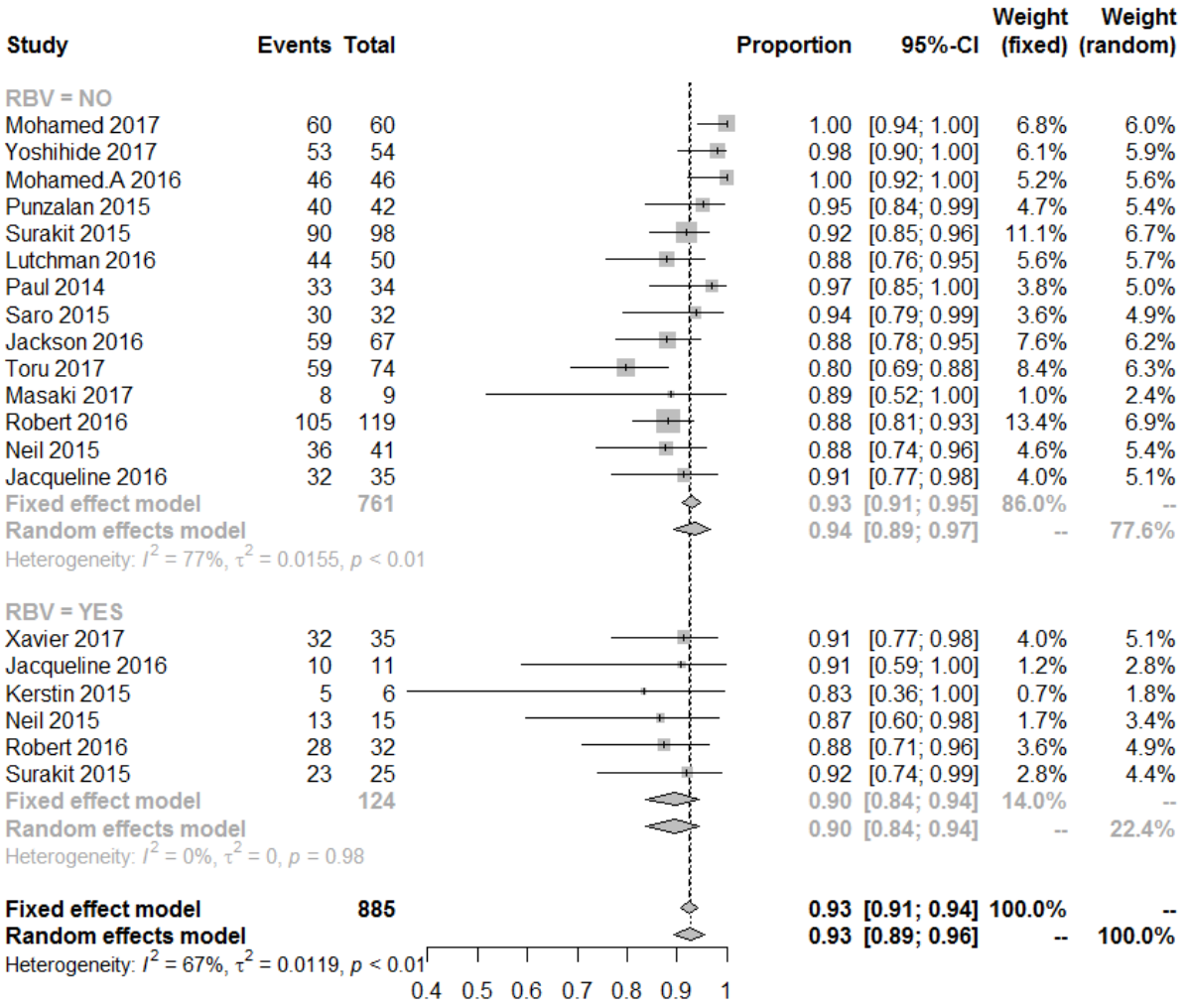

Supplementary figure 8. Comparison of pooled estimate proportion of 12 weeks sustained virologic response after treatment completion and 95% confidence interval for treatment with or without Ribavirin of hepatitis C virus genotype 1 recurrence post liver transplantation. Abbreviations: CI, confidence interval; Events, the number of patients who reached SVR12; Total, the number of patients analyzed.

CHAPTER 4

Sofosbuvir Directly Promotes the Clonogenic Capability of Human Hepatocellular Carcinoma Cells

Jiaye Liu, Wanlu Cao, Buyun Ma, Meng Li, Maikel P. Peppelenbosch and Qiuwei Pan

Clin Res Hepatol Gastroenterol. 2019 Oct;43(5).

The recent launch of several types of direct-acting antiviral agents (DAAs) has opened a new scenario for treating chronic hepatitis C virus (HCV) infection. Extremely satisfactory sustained virological response (SVR) rates have been achieved in DAA treated HCV patients, leading to the extensive use of these regimens worldwide [1]. Because HCV is one of the leading causes of hepatocellular carcinoma (HCC), successful eradication of the infection is expected to dramatically reduce the risk of HCC development in these patients. Counterintuitively, several recent studies have reported an unexpected high rate of HCC development after DAA treatment [2,3]; whereas others did not observe such a risk [4]. However, it remains challenge to make definitive conclusion on this issue because of the heterogeneous populations and methodologies applied in the different studies. Regardless of this ongoing debate, a popular hypothesis has emerged that tumor development is likely attributed to the indirect effect of DAA treatment by disrupting cancer immunosurveillance, for instance through decreasing natural killer (NK) cell activation and inhibiting its cytotoxic function [5]. These immunological changes could be responsible for reduced immunosurveillance of neoplastic clone growing and spreading. Interestingly, a recent study [6] has profiled the levels of immune mediators including cytokines, growth factors and apoptosis markers in serum of HCV patients treated with DAA and studied the association with the development of HCC. They observed that the indirect effect of immune modulation by DAAs may have little impact on HCC development, although the immune background before treatment could already have a potential effect. In contrast, we have investigated whether DAAs have direct effect on HCC cells. Sofosbuvir (SOF), targeting the HCV RNA-dependent RNA polymerase, is widely used DAAs for HCV treatment. Importantly, most reported cases with HCC development were treated with SOF-based regimens. To evaluate the direct effect, four human HCC cell lines including Huh7, Huh6, HepG2 and SNU449 were treated with serial concentrations of SOF (0, 0.01, 0.1, 1M), which are clinically relevant. As expected, SOF potently inhibited HCV replication in Huh7-based subgenomic replicon (Supplementary Figure 1). No major effect was observed on the growth of bulk of HCC cells by SOF treatment for 48 or 72 hours determined by MTT and Alamar blue assays (Supplementary Figure 2 and 3). But, surprisingly, SOF increased single cell-based clonogenic capability in all four HCC cell lines. This is reflected by the significantly increased number and size of formed colonies (Fig. 1). In contrast, placebo treatment has no such effect (Supplementary Figure 4). Thus, we have clearly demonstrated a direct promoting effect of SOF on single HCC cell-based clonogenic initiation and expansion, but not on the growth of the bulk of HCC cells. We interpret that these unexpected results may bear important implications in explaining the clinical observations. In fact, higher risk of HCC development has been mostly observed from HCV patients with advanced diseases (e.g. cirrhosis), [3] or previously treated for HCC (e.g. ablation, resection, chemoembolization [2] or liver transplantation [7]). Although these studies are often blamed for the bias in selection of these particular patient groups, our results however may indicate a direct promoting effect of DAAs on the rare preexisting transformed tumor cells in the cirrhotic liver, the residual HCC cells that are not completely eradicated by treatment, or the circulating tumor cells in the transplant

patients. Despite the low number of these tumor cells, they are likely resemble the so called cancer stem cells that are resistance to chemo- or radiotherapy but responsible for tumor initiation, treatment relapse and recurrence after surgical operation [8]. Thus, DAAs are likely not to have a universal but rather specific effects on particular patients in respect to the risk of HCC development; whereas the current clinical studies are unable to fully resolve the ongoing debate. Nevertheless, neither our findings nor the previous study6 shall exclude the possibility of an indirect effect of DAAs on triggering HCC development, as tumor micro-environment was a complicated and evolving field. We believe that the joint efforts of future experimental and clinical research are necessary to clarify this alarming issue and to gain mechanistic insight.

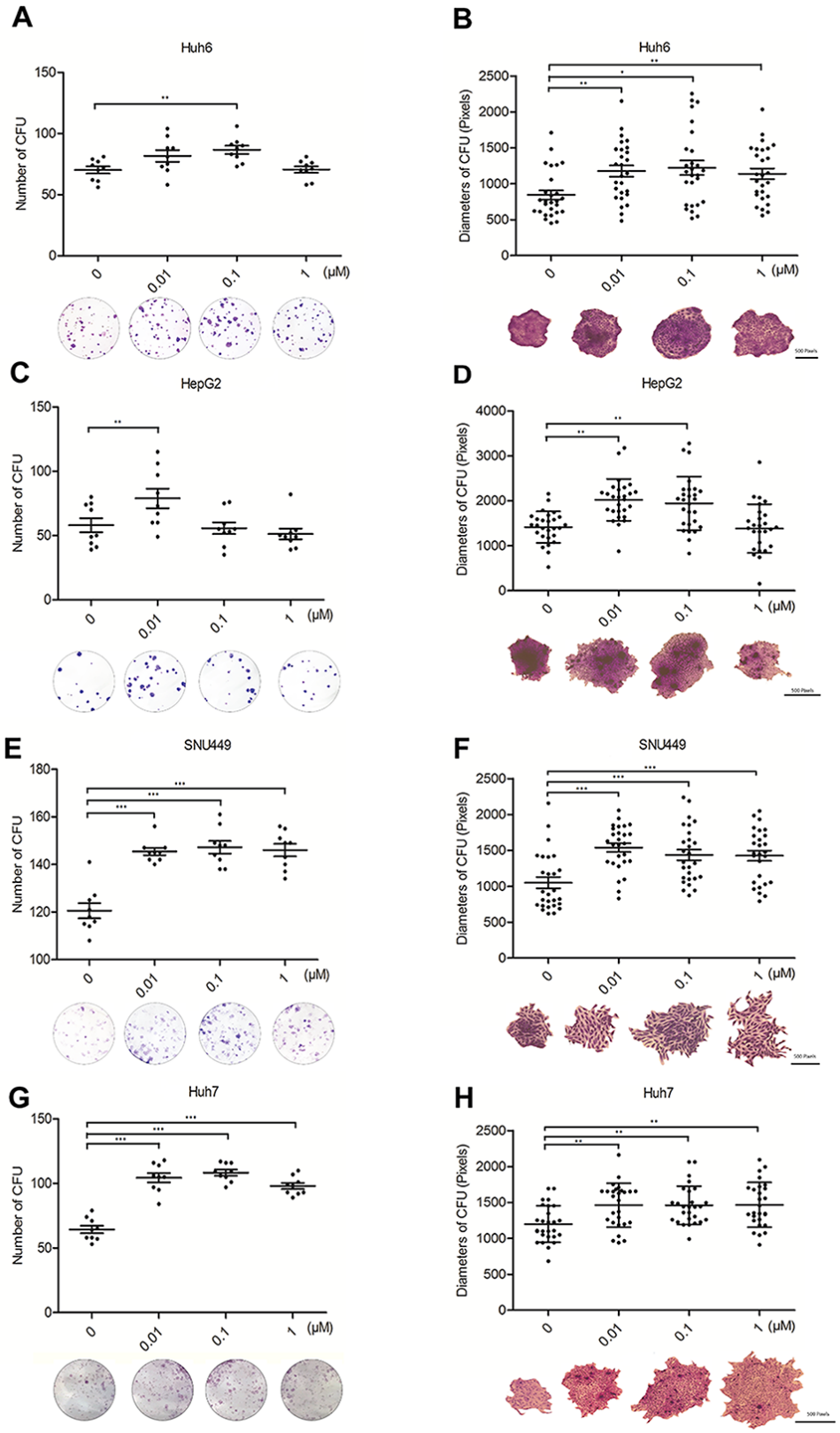

Figure 1. Sofosbuvir (SOF) treatment promotes the clonogenic capability of human hepatocellular carcinoma cells. (A, C, E, F) The number of colonies/1000 cells of HepG2, SNU449, Huh6 and Huh7 after SOF treatment (mean ± SEM, n=9); (B, D, G, H). The diameters of colony formation units (CFUs). Every three random colonies from nine independent wells were measured (mean ± SEM, n=27). Mann-Whitney test; *P<0.05, **P<0.01, ***P<0.001.

Reference

[1] Bourlière M, Bronowicki J-P, de Ledinghen V, Hézode C, Zoulim F, Mathurin P, et al. Ledipasvir-sofosbuvir with or without ribavirin to treat patients with HCV genotype 1 infection and cirrhosis non-responsive to previous protease-inhibitor therapy: a randomised, double-blind, phase 2 trial (SIRIUS). Lancet Infect Dis 2015;15(4):397—404.

[2] Conti F, Buonfiglioli F, Scuteri A, Crespi C, Bolondi L, Caraceni P, et al. Early occurrence and recurrence of hepatocellular carcinoma in HCV-related cirrhosis treated with direct-acting antivirals. J Hepatol 2016;65(4):727—33 [Epub 2016/06/29].

[3] Reig M, Marino˜ Z, Perelló C, Inarrairaegui ˜ M, Ribeiro A, Lens S, et al. Unexpected high rate of early tumor recurrence in patients with HCV-related HCC undergoing interferon-free therapy. J Hepatol 2016;65(4):719—26.

[4] Khaliq S, Jahan S, Pervaiz A. Sequence variability of HCV Core region: Important predictors of HCV induced pathogenesis and viral production. Infec Genet Evol 2011;11(3):543—56.

[5] Debes JD, Janssen HLA, Boonstra A. Hepatitis C treatment and liver cancer recurrence: cause for concern? Lancet Gastroenterol Hepatol 2017;2(2):78—80.

[6] Debes JD, van Tilborg M, Groothuismink ZMA, Hansen BE, Schulze zur Wiesch J, von Felden J, et al. Levels of cytokines in serum associate with development of hepatocellular carcinoma in patients with HCV infection treated with direct-acting antivirals. Gastroenterology.

[7] Yang JD, Aqel BA, Pungpapong S, Gores GJ, Roberts LR, Leise MD. Direct acting antiviral therapy and tumor recurrence after liver transplantation for hepatitis C-associated hepatocellular carcinoma. J Hepatol 2016;65(4):859—60.

[8] Batlle E, Clevers H. Cancer Stem Cell Revisited. 2017;23:1124.

Supplementary data for

Sofosbuvir directly promotes the clonogenic capability of human hepatocellular carcinoma cells

Table of contents

1 Supplementary materials and methods

1.1 Reagents

Sofosbuvir (SOF; PSI-7977) was purchased from Chemscene and were dissolved in dimethyl sulfoxide (DMSO) in a concentration of 10 mMol/L. Sorafenib was obtained from Bioconnect. 3-(4,5-Dimethylthiazol-2-yl)-2,5-Diphenyltetrazolium Bromide (MTT) was from Sigma-Aldrich. Alamar blue reagent was from Invitrogen.

1.2 HCC cells culture

Human hepatocellular carcinoma cells (Huh7, Huh6, SNU449 and HepG2) were cultured with Dulbecco's modified Eagle's medium (Invitrogen, Carlsbad, CA) supplemented with 10% fetal bovine serum (Sigma-Aldrich) and 1% Penicillin/Streptomycin (Gibco, Bleiswijk, The Netherlands).

1.3 HCV cell culture model

HCV subgenomic replicon model (Huh7-HCV-Luc) was on the basis of Huh7 cells containing a subgenomic HCV bicistronic replicon (I389/NS3-3V/LucUbiNeo-ET) which contains the non-structural coding sequence of HCV and the firefly luciferase gene. Huh7-HCV-Luc cells were cultured in the presence of 250 µg/mL G418 (Sigma-Aldrich).

1.4 Measurement of Luciferase activity

Huh7-HCV-Luc luciferase activity was quantified by adding luciferin potassium salt (100 mM, Sigma-Aldrich) to the cells and then incubating for 30 minutes at 37^{o}C. Then firefly luciferase activities were quantified with a LumiStar Optima luminescence counter (BMG labTech, Offenburg, Germany).

1.5 MTT assay

The cells were seeded in a 96-well plate, at a concentration of 6×10^{3} cells/well in 100 µl medium. Then they were incubated overnight to attach to the bottom of the wells and then treated with serials dilutions of SOF (0, 0.01, 0.1, 1 µM). Cell viability was analyzed by adding 10 mM MTT. Subsequently, the cells were incubated at 37 C with 5% CO_2 for 4 hours. The culture medium was then replaced by 100 µl of DMSO for each well. The absorbance of each well was read in a microplate absorbance reader (Bio-Rad, Japan) at wavelength of 490 nm. All measures performed in triplicates.

1.6 Alamar blue assay

The cells were harvested and then seeded in 96-well plate. Alamar blue reagent was firstly diluted into DMEM medium in 1:20 ratio. After removing supernatant, 100 µl diluted Alamar blue medium was added into each well. The plate was then moved to incubator at 37 C with 5% CO_2 for 2 hours. Fluorescence was measured using Varioskan Flash Microplate Multimode Readers with an excitation wavelength of 530 nm and an emission wavelength of 590 nm. All measures performed in triplicates.

1.7 Colony formation assay

The cells were harvested and suspended in medium, then seeded into 12 well plate (1000 cells/well). Cells were incubated overnight to attach to the bottom of the wells and then treated with serial dilutions of SOF (0, 0.01, 0.1, 1 µM). Formed colonies were stained by crystal violet solution (Sigmal-Aldrich). Colony numbers were counted and their diameters were measured microscopically trough digital image analysis.

1.8 Statistical analysis

Statistical analysis was performed by using the nonpaired, nonparametric test (Mann-Whitney test; GraphPad Prism software, GraphPad Software Inc., La Jolla, CA). Difference were considered with significant difference at P values < 0.05.

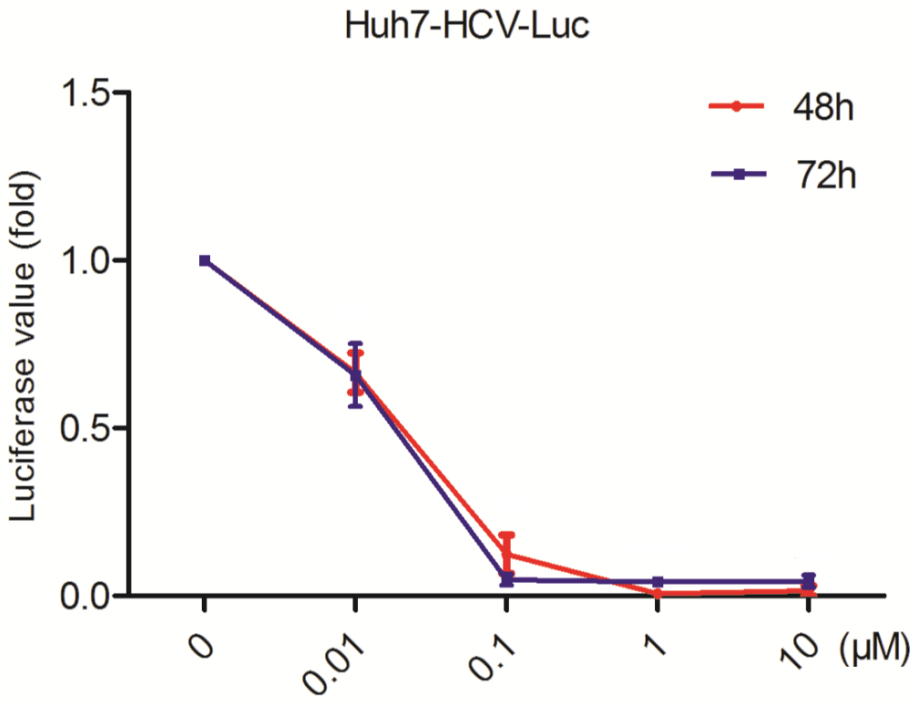

Supplementary figure 1. In the Huh7-HCV-Luc cells, treatment with clinically relevant concentrations of sofosbuvir (SOF) potently inhibited hepatitis C (HCV) replication-related luciferase activity (mean ± SEM, n = 5).

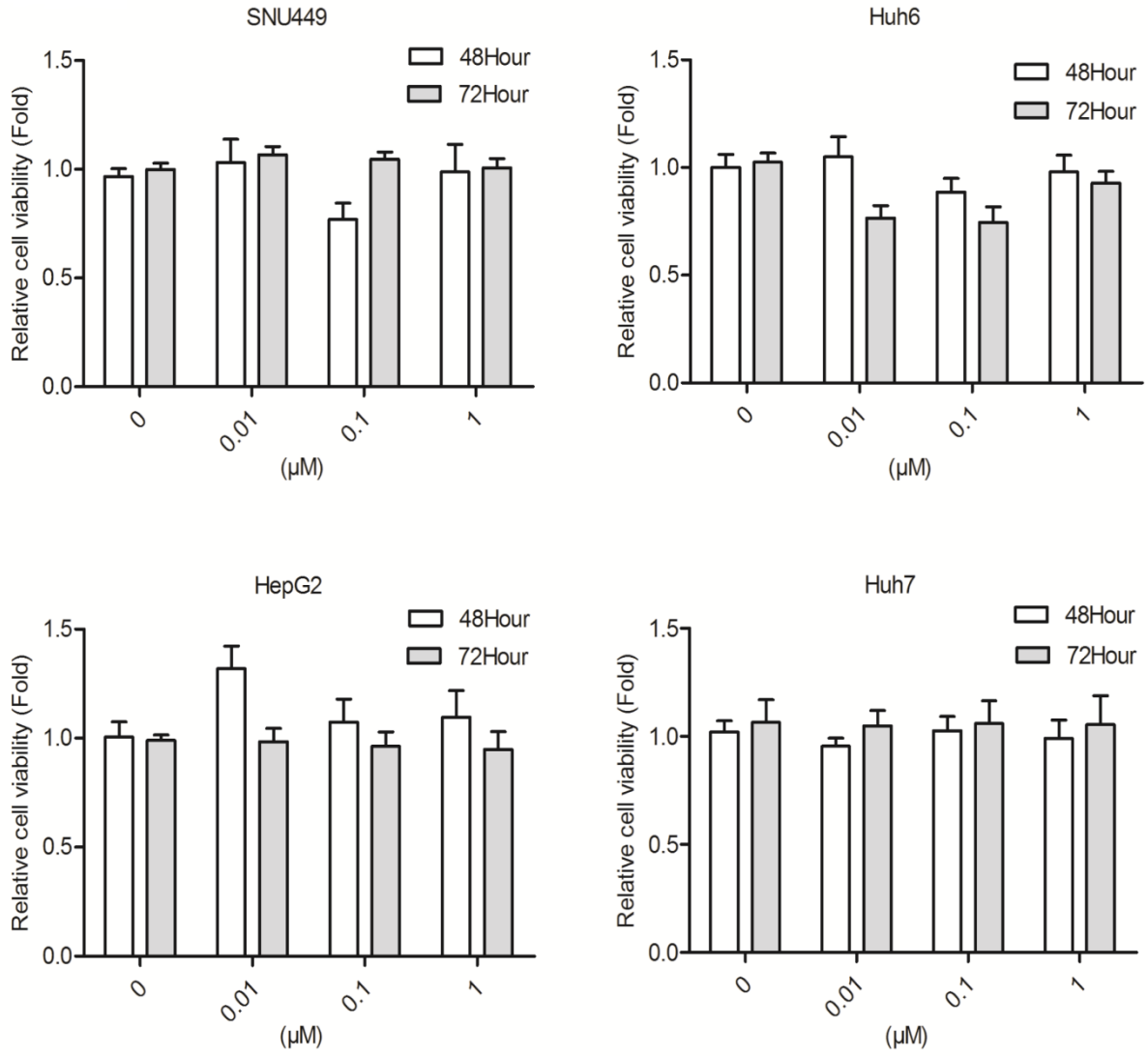

Supplementary figure 2. No major effect was observed on the metabolic activity of hepatocellular carcinoma (HCC) cells by sofosbuvir (SOF) treatment for 48 and 72 hours with clinically relevant concentrations in MTT assay (mean ± SEM, n = 9).

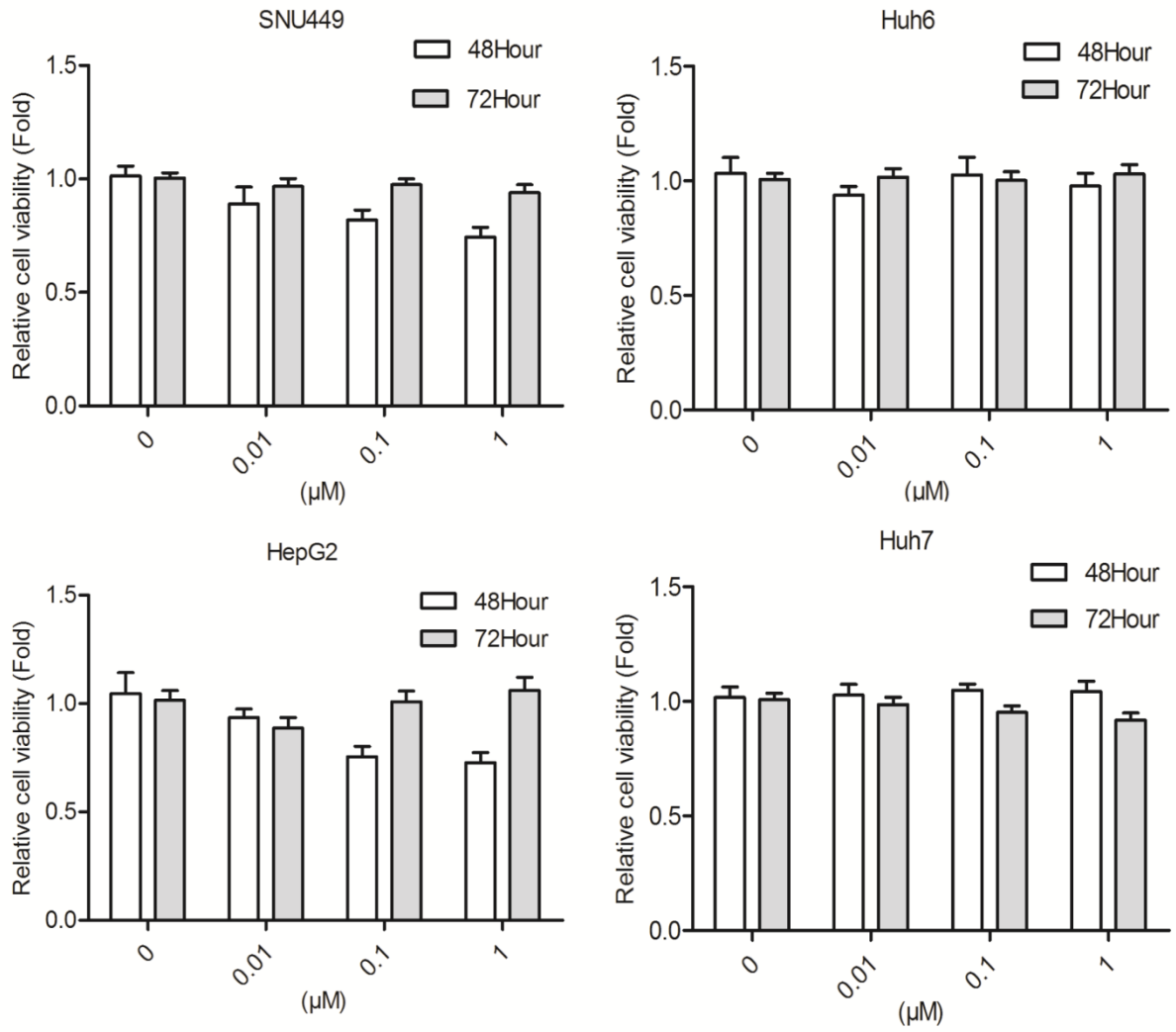

Supplementary figure 3. No major effect was observed on the growth of the bulk of hepatocellular carcinoma (HCC) cells by sofosbuvir (SOF) treatment for 48 and 72 hours with clinically relevant concentrations in Alamar blue assay (mean ± SEM, n = 9).

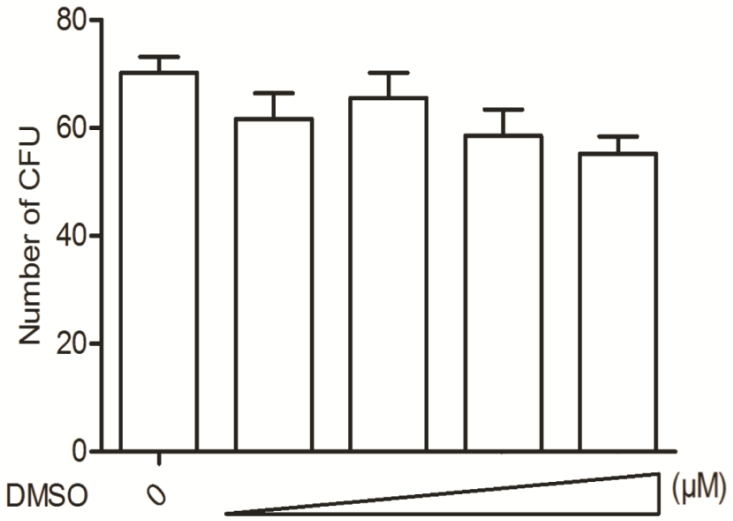

Supplementary figure 4. DMSO as placebo in accordance with the dilution contained in the sofosbuvir (SOF) treatment did not affect the number of colony formation units in Huh6 cells (mean ± SEM, n = 9).

CHAPTER 5

The global epidemiology of hepatitis E virus infection: A systematic review and meta-analysis

Pengfei Li***, Jiaye Liu*#,** Yang Li, Junhong Su, Zhongren Ma, Wichor. M. Bramer, Wanlu Cao, Robert. A de Man, Maikel P. Peppelenbosch, Qiuwei Pan#

Liver Int. 2020;40;1516-1528

Abstract

Background and Aims: Hepatitis E virus (HEV) as an emerging zoonotic pathogen is a leading cause of acute viral hepatitis worldwide, with a high risk of developing chronic infection in immunocompromised patients. However, the global epidemiology of HEV infection has not been comprehensively assessed. This study aims to map the global prevalence and identify the risk factors of HEV infection by performing a systematic review and meta-analysis.

Methods: A systematic searching of articles published in Medline, Embase, Web of science, Cochrane and Google scholar databases till July 2019 to identify studies with HEV prevalence data. Pooled prevalence among different countries and continents were estimated. HEV IgG seroprevalence of subgroups were compared and risk factors for HEV infection were evaluated using odd ratios.

Results: We identified 419 related studies which comprised of 1519872 individuals. A total of 1099717 participants pooled from 287 studies of general population estimated a globally anti-HEV IgG seroprevalence of 12.47% (95% CI 10.42-14.67; I^2=100%). Notably, the use of ELISA kits from different manufactures has a substantial impact on the global estimation of anti-HEV IgG seroprevalence. The pooled estimates of anti-HEV IgM seroprevalence based on 98 studies is 1.47% (95% CI 1.14-1.85; I^2=99%). The overall estimate of HEV viral RNA positive rate in general population is 0.20% (95% CI 0.15-0.25; I^2=98%). Consumption of raw meat (p=0.0001), exposure to soil (p<0.0001), blood transfusion (p=0.0138), traveling to endemic areas (p=0.0244), contacting with dogs (p=0.0416), living in rural areas (p=0.0349) and receiving education less than elementary school (p<0.0001) were identified as risk factors for anti-HEV IgG positivity.

Conclusions: Globally, approximately 939 million corresponding to 1 in 8 individuals have ever experienced HEV infection. 15-110 million individuals have recent or ongoing HEV infection. Our study highlights the substantial burden of HEV infection and calls for increasing routine screening and preventive measures.

INTRODUCTION

Hepatitis E virus (HEV) as a single-stranded positive-sense RNA virus is a leading cause of acute viral hepatitis worldwide. The infection is usually asymptomatic or self-limiting in the general population. However, acute infection in pregnant women may cause severe clinical outcomes, including fulminant hepatic failure with high mortality rate reaching up to 20-30%.[1] These patients are mostly from resource-limited regions. In European countries, HEV infection has been frequently reported to bear high risk of developing into chronic hepatitis in immunocompromised individuals, in particular organ transplant patients.[2,3] Thus, HEV is truly imposing a global health burden in both developing and developed countries.

Currently, eight distinct genotypes of HEV have been classified.[4] Genotype (GT) 1-4 are known to be the main threat to humans. GT 1 and 2 are restricted to human and mainly transmit through contaminated water causing acute hepatitis. GT 3 and 4 are zoonotic and have been identified in a wide spectrum of hosts, including human, swine, wild boar, goat, cattle, deer, camel and yak.[5] Both GT 3 and 4 can cause chronic infection in organ transplant patients,[2,6] and consumption of raw or undercooked animal meat has been recognized as the main routes of causing sporadic cases in developed countries.[7] In fact, the host range of HEV is ever expanding and the implications of the rare genotypes and the newly discovered strains in human health remain largely uncertain.[7] This further complicates the transmission and the risk of HEV infection. In addition to the classical waterborne and foodborne transmission routes, blood transfusion-mediated transmission has been reported in organ transplant patients.[8] Person-to-person transmission has also been proposed.[9] Intriguingly, recent evidence has indicated that pet animals including dogs, cats, rabbits and horses might be accidental hosts for HEV and constitute a potential source for transmitting to human.[10,11] Thus, there is an urgent need to comprehensively understand the risks for HEV infection, in order to device preventive measures.

Globally, it has been roughly estimated that one third of the population are living in HEV endemic areas.[12] More recently, substantial efforts have been dedicated to systematically evaluate HEV prevalence in different continents (e.g. the Americas and Europe),[13,14] different countries (e.g. industrialized countries, China, Iran, Brazil and Somalia),[15-17] and special populations or settings (e.g. blood donors, swine workers and outbreak setting).[18-20] Most of these studies are based on seropositivity of anti-HEV IgG antibody. Anti-HEV IgG antibody developed post-infection usually persists for many years, and is thus regarded as a marker for past infection.[21,22] In contrast, anti-HEV IgM antibody is short-lived up to a few months, thus considered as evidence of recent or current infection. Detection of HEV RNA is a *bona fide* marker for active ongoing infection. In this study, we aimed to systematically estimate the global burden of HEV infection. More specifically, we have mapped the global prevalence of past, recent and ongoing HEV infection and evaluated the key risk factors of infection.

METHODS

Data sources and searches

A systematic search was conducted in Medline, Embase, Web of science, Cochrane CENTRAL and Google scholar. Databases were searched for articles in the English language from inception until July 2019. All searches from database were performed by a biomedical information specialist of the medical library, with an exhaustive set of search terms related to hepatitis E virus infection and epidemiology (The full search strategies are provided in the Supplementary file S1). This study is reported in accordance with the Preferred Reporting Items for Systematic Reviews and Meta-Analysis (PRISMA).[23] No institutional review board approval was required for this meta-analysis because our study only included data which had been published previously.

Study selection

Studies were included if they met following criteria: i) Studies which contained data about seroprevalence of anti-HEV IgG, anti-HEV IgM or HEV RNA positivity. ii) Studies contained mixed population were excluded unless they clearly and explicitly reported the prevalence for each group. iii) Studies contained information of risk factors related to HEV infection. iv) Studies which focused on the HEV prevalence in human beings. Studies were excluded if they met following criteria: i) Studies are systematic review, meta-analysis, case reports, perspectives and abstracts. ii) None human studies. iii) No primary data or incomplete data. iv) Duplicate data. v) Studies with less than 50 individuals were excluded in order to decrease bias caused by small population. vi) Studies concerning about HEV outbreaks, since the prevalence and outcome of HEV infection in these studies would dramatically differ from those of the general population. Two reviewers (PL and JL) worked independently to determine whether a study met inclusion criteria, abstracted information to assess the methodological validity of each candidate study, and extracted data with structured data collection forms. The reviewers resolved discrepancies by jointly reviewing the study in question. If no consensus was reached, a third reviewer (QP), unaware of prior determinations, functioned as an arbiter.

Data extraction and quality assessment

Eligible studies were further divided into three study populations: general population, occupational population and special population. General population included people without apparent risk factors and could be comprised of blood donors, pregnant women, healthy individuals and hospital attendants. For general population, individuals were further divided into subgroups by gender, different age ranges, study period (1993-2006 or 2007-2019), country development classification (developing and developed countries), gross national income classification of each country (high, upper-middle, lower middle and low income) and ELISA kit manufacturers. More importantly, odd ratios (OR) analysis of anti-HEV IgG seropositivity was conducted in possible risk

factors included living area (urban or rural), consumption of raw meat, exposure to soil, contacting with cat or dog, education level (elementary school or above elementary school), intravascular drug use (IDU), water source (tap, well or river), man having sex with man (MSM), transfusion history and travelling history to endemic areas. Occupational population represents people who had been in frequent contact with pigs or pig products, including veterinarians, swine workers, slaughterhouse workers and pork sellers. Special populations are further categorized into four groups as followings: patients with acute hepatitis (caused by hepatitis B virus, hepatitis C virus or other unknown hepatitis), individuals with human immunodeficiency virus (HIV) infection, people who underwent hemodialysis and organ transplant recipients. Two independent reviewers (PL and JY) extracted data, with discrepancies and disagreements resolved by discussion. We extracted data on first author, country, continent, publication date, anti-HEV IgG prevalence, anti-HEV IgM prevalence, HEV RNA positivity, subgroup information of anti-HEV IgG prevalence and HEV-related risk factors using data extracting forms. When multiple publications were identified that reported on the same populations and outcomes, only the most representative and comprehensive study was included for further meta-analysis in order to avoid duplicate data. The quality of studies was assessed using the Joanna Briggs Institute checklist for prevalence studies, which enabled assessment of included studies in relation to risk of bias, rigour, and transparency.[24] Studies scoring 1-3 were defined as low quality, 4-6 as average quality, and 7-9 as high quality (Table S1). Studies were not excluded on the basis of their quality score to increase transparency and to ensure all available evidence in this area was reported.

Statistics analysis

After checking for consistency, the Metaprop module in the R-3.5.3 statistical software package was used for meta-analysis. A 95% confidence interval (95% CI) was estimated using Wilson score method, and pooled seroprevalence was calculated with the DerSimonian-Laird random-effects model with Freeman-Tukey double arcsine transformation. Heterogeneity across the included studies was assessed using the Cochran Q statistics and I^2 statistics, with I^2 statistics 25%-50%, 50%-75%, and >75% considered as mild, moderate, and severe heterogeneity, respectively. When heterogeneity was higher than 50%, a random-effect model will be used. ORs was used to report the risk factors for HEV infection. ORs and their 95% CI were extracted directly from studies when available, with adjusted ORs extracted preferentially over unadjusted ORs. If an included studies did not report ORs, crude ORs were calculated from extracted data. We then pooled the ORs using the DerSimonian and Laird random effect models, with the heterogeneity estimated from the Mantel-Haenszel model. Funnel plots and Egger regression test were used to assess potential publication biases. Additionally, we performed sensitivity analyses by using “metainf” in a random model to investigate the effects of population source and potentially unrepresentative samples. The estimated prevalence of anti-HEV IgG, IgM and HEV RNA infection was based on the global population of 7530000000 in 20th July, 2019 (https://population.io).

RESULTS

Global prevalence of HEV infection

Our search retuned 8153 records, of which 419 met the inclusion criteria (Fig. 1). In total, participants from 302 studies related to general population, 287 studies were pooled to estimate a global anti-HEV IgG seroprevalence of 12.47% (1099717 individuals included; 95% CI 10.42-14.67; I^2=100%) (Fig. 2A, Fig. S1). The pooled estimate of anti-HEV IgM seroprevalence based on 98 studies is 1.47% (479001 individuals; 95% CI 1.14-1.85; I^2=99%) (Fig. 2B, Fig. S2). The overall estimate of HEV RNA positive rate in the general population is 0.20% (3444752; 95% CI 0.15-0.25; I^2=98%) (Fig. 2C, Fig. S3). We also stratified data to estimate the HEV prevalence in 75 countries among six continents (excluding Antarctica). The highest anti-HEV IgG seropositivity rate was found in Africa (22377; 21.76%, 95% CI 13.05-31.98; I^2=100%), followed by Asia (681373; 15.80%, 95% CI 13.29-18.49; I^2=100%), Europe (132419; 9.31%, 95% CI 7.35-11.48; I^2=99%), North America (71989; 8.05%, 95% CI 5.47-11.09; I^2=99%), South America (14586; 7.28%, 95% CI 4.83-10.19; I^2=97%) and Oceania (1563; 5.99%, 95% CI 1.22-14.03; I^2=96%) (Fig. S4). Besides, the anti-HEV IgM seroprevalence was 3.09% (5001; 95% CI 1.49-5.24; I^2=93%), 1.86% (141565; 95% CI 1.34-2.46; I^2=98%), 0.79% (146322; 95% CI 0.30-1.51; I^2=99%), 0.22% (12197; 95% CI 0.00-0.74; I^2=91%), 2.43% (2680; 95% CI 0.43-6.00; I^2=96%) for Africa, Asia, Europe, North America and South America, respectively (Fig. S5). In addition, the HEV RNA positivity rate was 0.00% (278; 95% CI 0.00-0.35), 0.93% (727744; 95% CI 0.48-1.52; I^2=99%), 0.08% (2441774; 95% CI 0.05-0.11; I^2=95%), 0.00% (34761; 95% CI 0.00-0.02; I^2=45%), 0.00% (74131; 95% CI 0.00-0.01), 0.18% (1054; 95% CI 0.00-1.36; I^2=81%) for Africa, Asia, Europe, North America, Oceania and South America, respectively (Fig. S6). HEV prevalence varies substantially among countries, from 0.25% (Tanzania, 95% CI 0.00-0.97) to 74.76% (South Sudan, 95% CI 68.61-80.44) of anti-HEV IgG, from 0.00% (Mongolia, 95% CI 0.00-0.08; Bulgaria, 95% CI 0.00-0.13) to 19.83% (United Arab, 95% CI 16.35-23.56) of anti-HEV IgM, from 0.00% (Benin, Malawi, Australia, Canada, Brazil) to 6.75% (France, 95% CI 0.14-22.04) of HEV RNA positivity (Table 1, Fig. S1-S3). We also collected data of HEV genotypes, with the finding that HEV GT1 infection occasionally occurred in China and frequently in India, and GT3 was widely distributed in European countries. GT3 was also prevalent in Japan and Korea, whereas GT4 infection mainly emerged in China (Fig. 3, Table S2). Based on our comprehensive estimates, approximately 938991000 individuals corresponding to 1/8 of the global population have ever experienced HEV infection based on anti-HEV IgG positivity. Importantly, we estimated approximately 110691000 global individuals with current or recent HEV infection and 15060000 individuals with ongoing HEV infection based on anti-HEV IgM or viral RNA positivity, respectively.

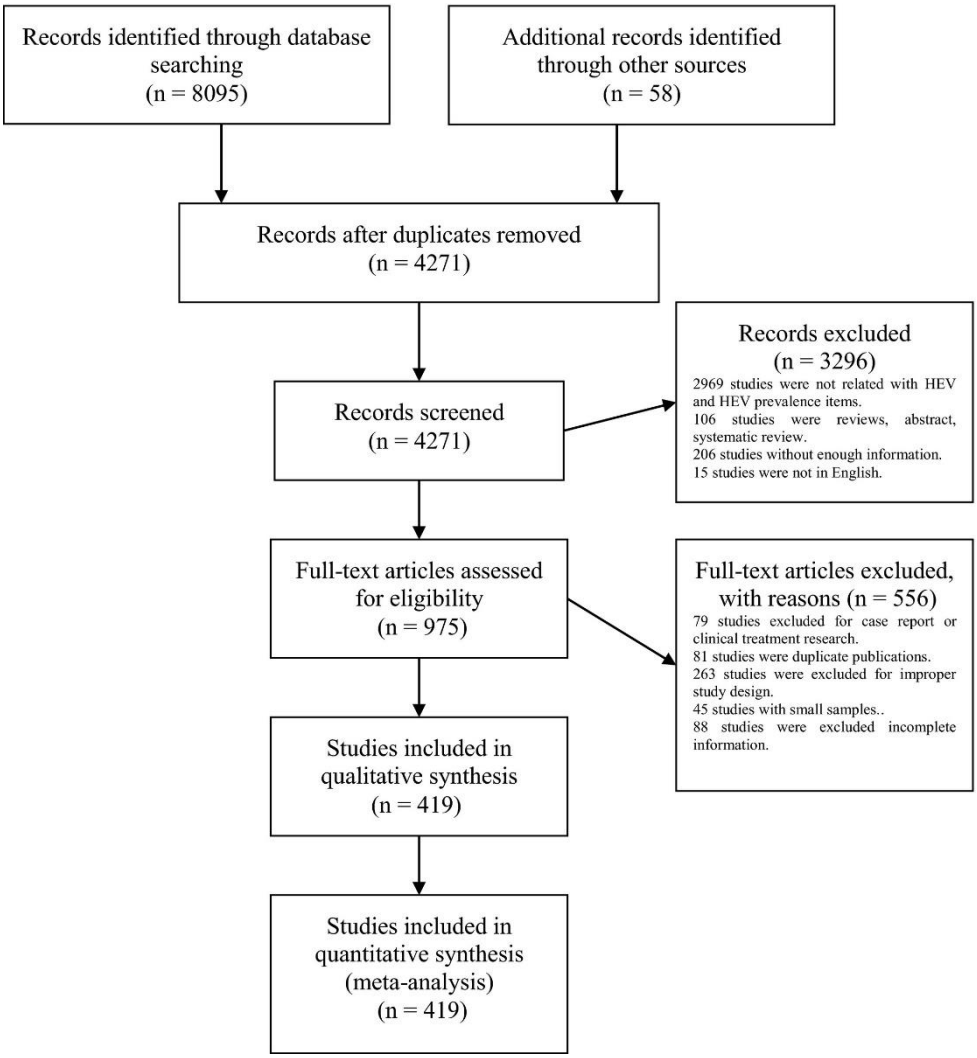

Figure 1. Study selection.

We next performed subgroup analysis of anti-HEV IgG positivity rate in general population. General population of six different continents were further divided into seven age groups, including age range of 0-9, 10-19, 20-29, 30-39, 40-49, 50-59 and above 60-year old. The corresponding pooled anti-HEV IgG positive rates are 7.73% (6977 individuals included; 95% CI 2.29-16.02; I^2=99%), 9.03% (14452 individuals; 95% CI 3.78-16.25; I^2=99%), 10.78% (33365; 95% CI 7.44-14.64; I^2=99%), 14.17% (23217; 95% CI 10.27-18.57; I^2=99%), 21.53% (21324; 95% CI 16.82-26.65; I^2=99%), 24.48% (17474; 95% CI 18.56-30.93; I^2=99%) and 27.47% (23924; 95% CI 21.07-34.36; I^2=99%), respectively (Fig. 4, Fig. S7-8). The positive rate is slightly higher in male (129569; 13.39%, 95% CI 11.34-15.59; I^2=99%) compared to female (120264; 12.25%, 95% CI 10.05-14.63; I^2=99%) (Fig. 4, Fig. S9). To clarify the HEV prevalence among regions with different levels of economic development, we firstly calculated the anti-HEV IgG prevalence in high income countries, upper-middle income countries, lower middle income countries, and low income countries. We estimated the anti-HEV IgG positivity of 8.84% (424905; 95% CI 6.79-11.14; I^2=100%) in high income countries, 12.79% (618638; 95% CI 10.81-14.92; I^2=100%) in upper-middle income countries, 19.04% (40593; 95% CI 13.25%-25.60%; I^2=100%) in lower middle income countries

and 30.44% (5781; 95% CI 16.60-46.39; I^2=99%) in low income countries (Fig. 4, Fig. S10). The pooled estimate of anti-HEV IgG seroprevalence was 14.83% (689452; 95% CI 12.98-16.77; I^2=100%) in developing countries compared to 8.59% (401513; 95% CI 6.46-10.99; I^2=100%) in developed countries (Fig. 4, Fig. S11). Of the global HEV prevalence during the period of 1993-2019, we estimated anti-HEV IgG positive rate of 9.43% (79998; 95% CI 6.11-13.37; I^2=100%) during 1993-2006 and 13.65% (1019719; 95% CI 11.15-16.35; I^2=100%) during 2007-2019 (Fig. 4, Fig. S12).

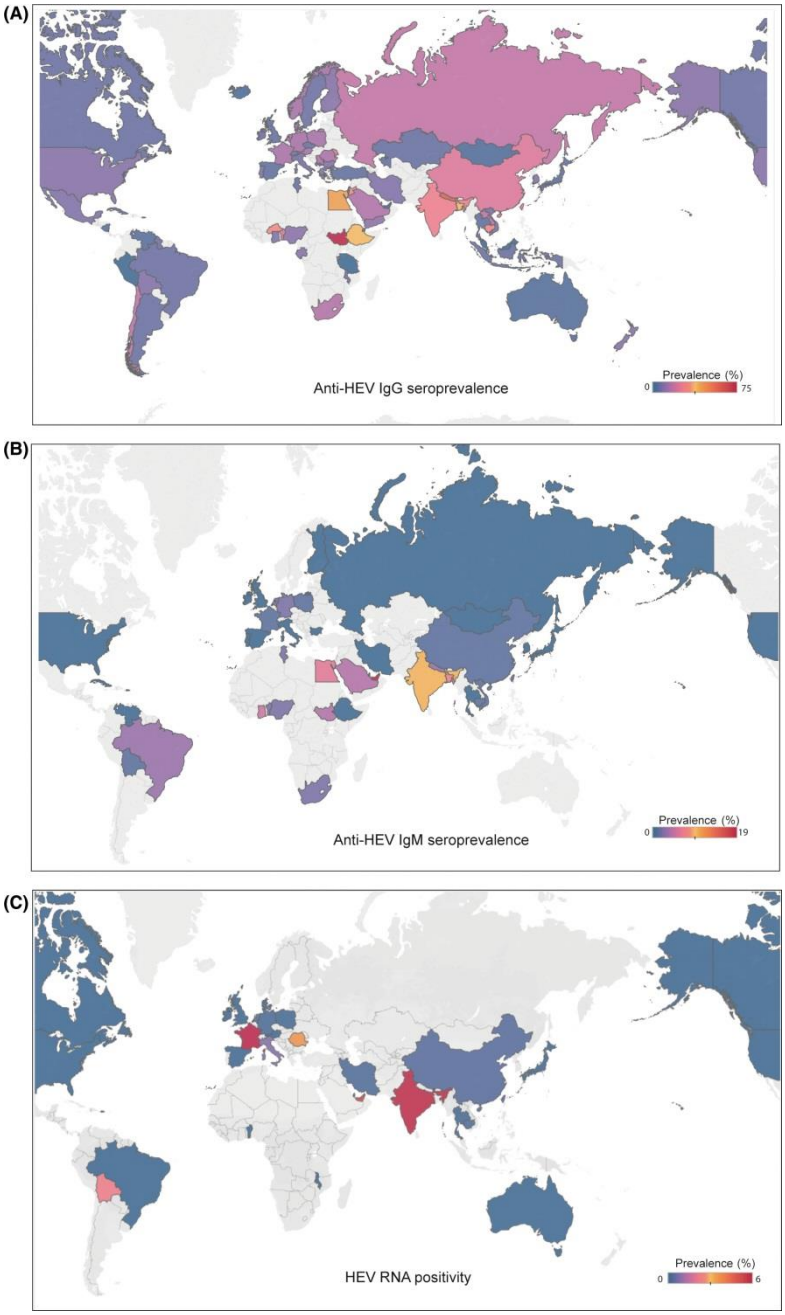

Figure 2. (A) The global seroprevalence of anti-HEV IgG antibody (B) The global seroprevalence of anti-HEV IgM antibody (C) The global prevalence of HEV RNA positivity.

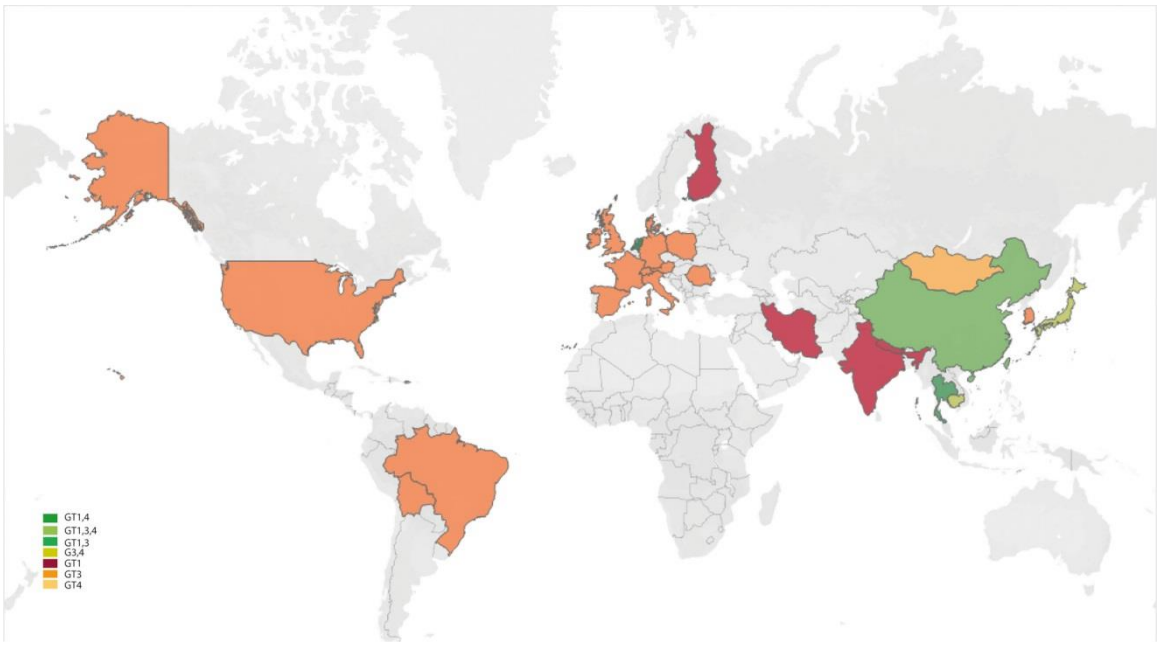

Figure 3. Hepatitis E virus genotype distribution in our study.

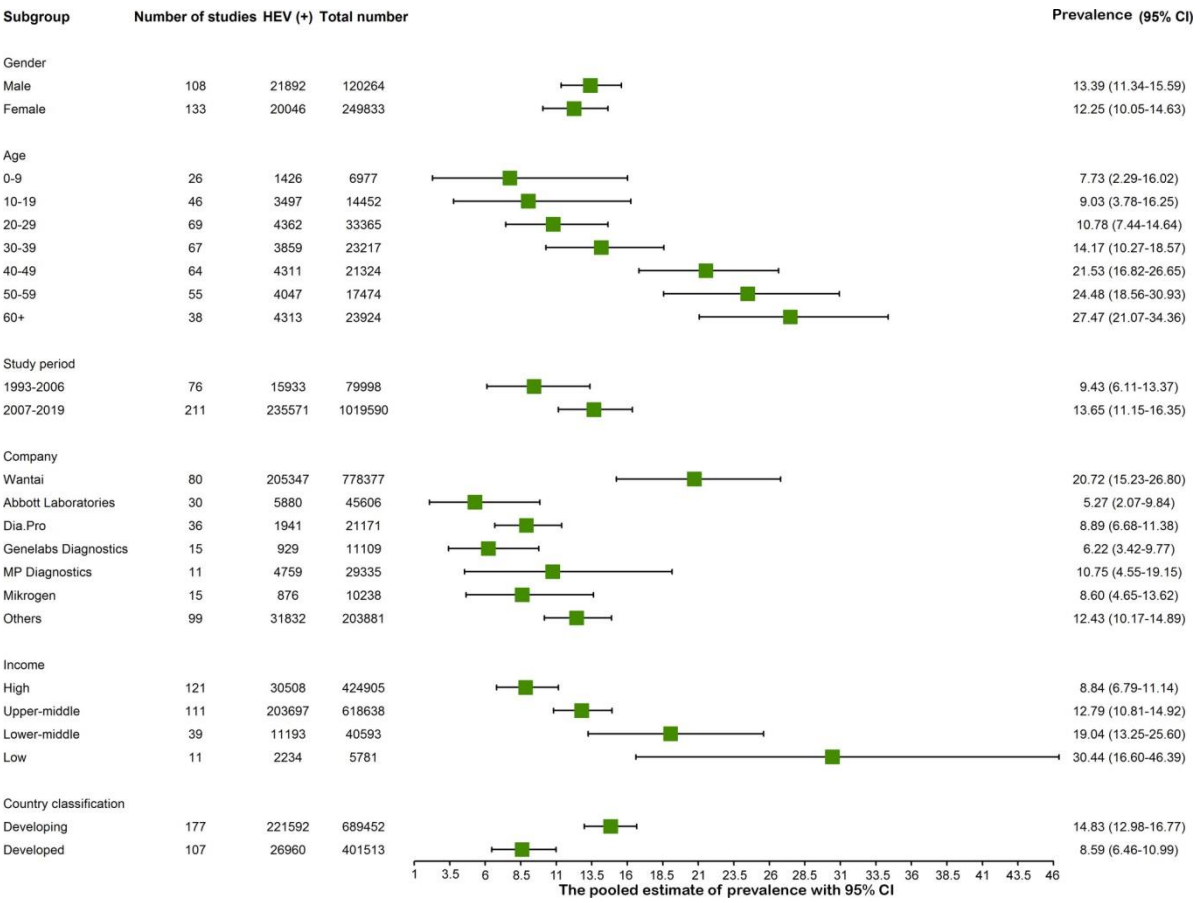

Figure 4. Anti-hepatitis E virus (HEV) IgG seroprevalence among six subgroups.

3.2 Prevalence of HEV infection in occupational population and special population

Anti-HEV IgG seroprevalence data from veterinarians, swine workers, slaughters, and pork sellers were collected to estimate the overall anti-HEV seroprevalence in occupational population. Based on 43 studies with 8776 occupational individuals, the overall seropositivity of anti-HEV IgG is 24.04% (95% CI 18.55-29.99; I^2=97%) (Fig. S13). In total, 126 studies were extracted data to analyze the prevalence in special populations. The overall anti-HEV IgG, anti-HEV IgM and viral RNA positive rates are 15.43% (95% CI 12.82-18.24; I^2=98%), 3.21% (95% CI 1.77-5.06; I^2=98%) and 1.10% (95% CI 0.53-1.87; I^2=97%), respectively (Fig. S14-S16). Among these special populations, patients with acute hepatitis have the highest positive rate of anti-HEV IgG (21.49%, 95% CI 12.65-31.92; I^2=99%), anti-HEV IgM (8.62%, 95% CI 4.16-14.51; I^2=99%) and viral RNA (5.57%, 95% CI 2.26-10.21; I^2=99%) (Fig. S17-S19). The anti-HEV IgG positive rates in two special groups are higher than that in general population, with 16.91% (95% CI 12.64-21.67; I^2=98%) in the HIV population, 13.10% (95% CI 9.34-17.39; I^2=96%) in hemodialysis population, while it is slightly lower in organ transplant recipients with 11.68% (95% CI 7.91-16.06; I^2=97%) seropositivity (Fig. S20-S27, Table S5).

3.3 Risk factors of HEV

We investigated the potential risk factors for HEV in the general population (Fig. S28). Significant rising effects on anti-HEV IgG seropositivity were observed in consumption of raw meat (OR 1.45, 95% CI 1.20-1.76, p=0.0001), exposure to soil (OR 1.52, 95% CI 1.24-1.86, p<0.0001), blood transfusion (OR 1.61, 95% CI 1.10-2.36, p=0.0138), travelling to endemic areas (OR 1.39, 95% CI 1.04-1.84, p=0.0244), contacting with dogs (OR 1.45, 95% CI 1.01-2.07, p=0.0416), living in rural areas (OR 0.80, 95% CI 0.65-0.98, p=0.0349) and receiving education less than elementary school (OR 1.71, 95% CI 1.41-2.07, p<0.0001). No statistically significant differences were identified for anti-HEV IgG positivity in respect to different water source (p=0.0909), IDU experience (p=0.4321), MSM experience (p=0.5576) and contacting with cats (p=0.4791) (Fig. S29-S39). Sensitivity analysis detected no study having an obvious effect influence the pooled estimates of HEV prevalence in the general population (Table S3).

3.4 Anti-HEV IgG detection rate of different ELISA kits

We finally analyzed the detection rates of the ELISA kits from six manufactures. The detection rates of anti-HEV IgG seropositivity vary dramatically, with the highest of Wantai assay (20.72%, 95% CI 2.07-9.84; I^2=100%) followed by MP Diagnostics (10.75%, 95% CI 4.55-19.15; I^2=100%), Dia.Pro (8.89%, 95% CI 6.68-11.38; I^2=97%), Mikrogen (8.60%, 95% CI 4.65-13.62; I^2=98%), Genelabs Diagnostics (6.22%; 95% CI 3.42-9.77; I^2=98%) and Abbott Laboratories (5.27%, 95% CI 2.07-9.84; I^2=100%) (Fig. S40, Table S4).

TABLE 1 Hepatitis E virus (HEV) prevalence in general population

		Anti-HEV IgG					Anti-HEV IgM Anti-HEV IgM					HEV RNA				
Continent	Country	No. of studies	Events	Tested (n)	Prevalence (%)	95% CI	No. of studies	Events	Tested (n)	Prevalence (%)	95% CI	No. of studies	Events	Tested (n)	Prevalence (%)	95% CI
Asia	China	42	200 221	579 696	22.68	19.67; 25.83	18	1186	88 587	1.76	1.29; 2.31	5	106	56 319	0.41	0.07;1.06
	Thailand	4	121	2632	4.82	0.30; 14.31	2	5	2057	0.12	0.00; 1.05	1	26	30 115	0.09	0.06;0.12
	Israel	3	133	7115	3.36	0.19; 10.22	..	..	..	..	..	..	..	..	..	..
	Saudi Arabia	3	428	2911	15.41	10.77; 20.70	1	39	900	4.33	3.10; 5.76	..	..	..	..	..
	Japan	8	1901	40 936	4.26	3.27; 5.37	5	32	27 478	0.30	0.06; 0.73	2	41	623 325	0.05	0.00;0.29
	Jordan	1	139	450	30.89	26.71; 35.23	..	..	..	..	..	..	..	..	..	..
	Kazakhstan	1	11	199	5.53	2.79; 9.12	..	..	..	..	..	..	..	..	..	..
	Korea	3	328	3969	9.30	4.87; 14.96	1	9	1030	0.87	0.40; 1.53	..	..	..	..	..
	Vietnam	2	44	833	7.25	0.39; 21.55	1	1	187	0.53	0.00; 2.08	..	..	..	..	..
	Yemen	1	38	356	10.67	7.68; 14.09	..	..	..	..	..	..	..	..	..	..
	Bangladesh	3	509	1707	36.87	17.16; 59.20	1	20	273	7.33	4.54; 10.71	..	..	..	..	..
	India	7	3160	14 136	27.15	19.31; 35.78	5	348	5354	10.18	2.08; 23.38	4	510	8462	6.59	0.22;20.71
	Indonesia	2	50	858	5.83	4.36; 7.49	..	..	..	..	..	..	..	..	..	..
	Mongolia	3	36	1486	2.70	0.06; 9.08	2	0	1237	0	0.00; 0.08	..	..	..	..	..
	Iran	20	1208	12 547	8.98	5.74; 12.86	5	38	4148	0.80	0.19; 1.82	2	7	2031	0.24	0.00;2.16
	Cambodia	3	1074	3173	28.93	14.46; 46.04	2	55	2305	1.31	0.01; 4.74	2	3	1169	0.25	0.05;0.63
	Singapore	1	30	219	13.70	9.48; 18.56	..	..	..	..	..	..	..	..	..	..
	Laos	1	38	210	18.10	13.20; 23.58	..	..	..	..	..	..	..	..	..	..
	Nepal	2	1344	2602	59.19	26.14; 88.13	1	54	1686	3.20	2.42; 4.10	..	..	..	..	..
	Qatar	1	1198	5854	20.46	19.44; 21.51	1	34	5854	0.58	0.40; 0.79	1	4	5854	0.07	0.02;0.15
	United Arab Emirates	..	..	..	..	..	1	93	469	19.83	16.35; 23.56	1	28	469	5.97	4.01;8.29
	Total	111	212 011	681 373	15.80	13.29; 18.49	46	1920	141 565	1.86	1.34; 2.46	18	725	727 744	0.93	0.48;1.52
Africa	Nigeria	2	56	588	10.17	5.32; 16.35	2	17	927	2.83	0.00; 17.56	..	..	..	..	..
	Burkina Faso	1	56	178	31.46	24.86; 38.46	..	..	..	..	..	..	..	..	..	..
	Burundi	1	18	129	13.95	8.54; 20.44	..	..	..	..	..	..	..	..	..	..
	Djibouti	1	14	112	12.50	7.05; 19.23	..	..	..	..	..	..	..	..	..	..
	Egypt	6	6670	14052	42.43	20.40; 66.19	1	6	100	6.00	2.22; 11.47	..	..	..	..	..
	Ethiopia	2	481	1232	37.09	26.85; 47.95	2	10	1232	0.80	0.38; 1.37	..	..	..	..	..
	Gabon	2	135	1083	10.23	4.02; 18.87	..	..	..	..	..	..	..	..	..	..
	Ghana	3	75	789	8.74	4.39; 14.38	3	44	789	5.87	0.06; 20.10	..	..	..	..	..
	Benin	1	62	278	22.30	17.61; 27.38	1	7	278	2.52	1.01; 4.68	1	0	278	0	0.00;1.32
	Malawi	1	80	397	20.15	16.36; 24.23	..	..	..	..	..	..	..	..	..	..

Continent	Country	Anti-HEV IgG					Anti-HEV IgM Anti-HEV IgM					HEV RNA				
		No. of studies	Events	Tested (n)	Prevalence (%)	95% CI	No. of studies	Events	Tested (n)	Prevalence (%)	95% CI	No. of studies	Events	Tested (n)	Prevalence (%)	95% CI
	South Africa	3	418	2243	16·00	1·55; 41·31	1	16	782	2·05	1·17; 3·16	..	..	..	..	..
	South Sudan	1	154	206	74·76	68·61; 80·44	1	9	206	4·37	2·01; 7·58	..	..	..	..	..
	Tanzania	1	1	403	0·25	0·00; 0·97	..	..	..	..	..	..	..	..	..	..
	Tunisia	1	37	687	5·39	3·82; 7·20	1	20	687	2·91	1·79; 4·30	..	..	..	..	..
	Total	26	8257	22 377	21·76	13·05; 31·98	12	129	5001	3·09	1·49; 5·24	1	0	278	0	0·00;0·35
Europe	Finland	1	37	385	9·61	6·87; 12·75	1	1	385	0·26	0·00; 1·02	..	..	..	..	..
	France	8	3978	17 778	14·51	6·80; 24·49	5	230	15 027	1·16	0·30; 2·57	3	32	917	6·75	0·14;22·04
	Germany	11	2146	11 045	14·35	6·69; 24·30	2	60	2183	2·86	0·00; 23·32	2	16	17 144	0·14	0·02;0·37
	Moldova	1	63	255	24·71	19·62; 30·18	..	..	..	..	..	..	..	..	..	..
	Greece	1	25	265	9·43	6·22; 13·24	..	..	..	..	..	..	..	..	..	..
	Turkey	10	225	4656	4·93	2·68; 7·81	..	..	..	..	..	..	..	..	..	..
	UK	7	706	9672	5·60	3·11; 8·76	3	25	96 341	0·36	0·00; 1·66	4	600	2 201 609	0·02	0·01;0·04
	Iceland	1	6	291	2·06	0·75; 4·01	..	..	..	..	..	..	..	..	..	..
	Ireland	2	73	1274	6·17	3·92; 8·90	1	2	1076	0·19	0·02; 0·53	1	10	24 985	0·04	0·02;0·07
	Italy	14	1690	19 488	7·28	4·54; 10·60	4	49	10 559	0·44	0·19; 0·78	2	12	10 363	0·83	0·00;7·27
	Czech	1	13	230	5·65	3·05; 9·00	..	..	..	..	..	..	..	..	..	..
	Denmark	2	296	1459	11·09	0·00; 57·44	..	..	..	..	..	1	11	25 637	0·04	0·02;0·07
	Austria	2	306	2200	13·91	12·49; 15·38	..	..	..	..	..	1	7	58 915	0·01	0·00;0·02
	Bulgaria	1	67	741	9·04	7·08; 11·21	1	0	741	0	0·00; 0·13	..	..	..	..	..
	Montenegro	1	24	400	6·00	3·89; 8·53	0·87·	..	..	..	..	..	..	..	..	..
	Netherlands	8	3521	25 786	16·07	6·09; 29·62	3	491	13 503	2·00	0·05; 6·63	4	96	67 041	0·40	0·03;1·18
	Norway	1	177	1263	14·01	12·16; 15·98	..	..	..	..	..	..	..	..	..	..
	Poland	4	1561	4497	14·17	2·07; 34·48	3	41	3470	1·02	0·52; 1·67	1	10	12 664	0·08	0·04;0·14
	Portugal	3	380	2812	8·72	2·20; 18·99	1	8	1656	0·48	0·21; 0·87	..	..	..	..	..
	Romania	1	22	148	14·86	9·61; 21·03	..	..	..	..	..	1	6	148	4·05	1·49;7·81
	Russia	1	62	341	18·18	14·27; 22·45	1	2	341	0·59	0·06; 1·67	..	..	..	..	..
	San Marino	1	33	2233	1·48	1·02; 2·02	..	..	..	..	..	..	..	..	..	..
	Serbia	2	50	726	8·46	0·95; 22·35	..	..	..	..	..	..	..	..	..	..
	Spain	7	2282	18 534	5·08	0·85; 12·58	1	7	1040	0·67	0·27; 2·16	3	7	22 351	0·03	0·01;0·06
	Sweden	2	14	205	6·51	2·40; 12·45	..	..	..	..	..	..	..	..	..	..
	Switzerland	4	803	5228	7·25	0·97; 18·62	..	..	..	..	..	..	..	..	..	..
	Total	97	18 560	132 419	9·31	7·35; 11·48	26	916	146 322	0·79	0·30; 1·51	23	807	2 441 744	0·08	0·05;0·11

		Anti-HEV IgG					Anti-HEV IgM Anti-HEV IgM					HEV RNA				
Continent	Country	No. of studies	Events	Tested (n)	Prevalence (%)	95% CI	No. of studies	Events	Tested (n)	Prevalence (%)	95% CI	No. of studies	Events	Tested (n)	Prevalence (%)	95% CI
Oceania	New Zealand	1	98	1013	9.67	7.93; 11.57	..	..	..	..	..	..	..	..	..	..
	Australia	1	17	550	3.09	1.81; 4.70	..	..	..	..	..	1	1	74 131	0	0.00;0.01
	Total	2	115	1 563	5.99	1.22; 14.03	..	..	..	..	..	1	1	74 131	0	0.00;0.01
North America	Cuba	3	74	1827	4.89	0.70; 12.55	1	5	1149	0.44	0.14; 0.90	..	..	..	..	..
	Mexico	6	535	4977	8.97	3.75; 16.14	..	..	..	..	..	..	..	..	..	..
	USA	12	7747	60 291	9.65	5.68; 14.53	3	12	11 048	0.16	0.00; 0.78	2	2	20 768	0.01	0.00;0.03
	Canada	2	252	4495	4.35	1.82; 7.91	..	..	..	..	..	1	0	13 993	0	0.00;0.01
	Nicaragua	1	17	399	4.26	2.50;6.46	..	..	..	..	..	..	..	..	..	..
	Total	24	8625	71 989	8.05	5.47; 11.09	4	17	12 197	0.22	0.00; 0.74	3	2	34 761	0	0.00;0.02
South America	Chile	1	82	469	17.48	14.18; 21.05	..	..	..	..	..	..	..	..	..	..
	Argentina	3	145	5831	5.92	1.29; 13.60	..	..	..	..	..	..	..	..	..	..
	Venezuela	1	23	611	3.76	2.40; 5.42	1	3	611	0.49	0.09; 1.20	..	..	..	..	..
	Bolivia	5	209	1940	9.50	3.19; 18.70	1	10	574	1.74	0.83; 2.97	1	3	123	2.44	0.47;5.89
	Brazil	10	315	4739	6.39	3.25; 10.49	4	50	1495	3.46	0.12; 11.09	2	0	931	0	0.00;0.10
	Guyana	1	64	996	6.43	4.99; 8.03	..	..	..	..	..	..	..	..	..	..
	Total	21	838	14 586	7.28	4.83; 10.19	6	63	2680	2.43	0.43; 6.00	3	3	1054	0.18	0.00;1.36
Multiple		6	3158	175 410	14.64	0.40; 43.67	4	18	171 236	0.15	0.00; 0.56	1	16	165 010	0.01	0.01;0.02
Total		287	251 564	1 099 717	12.47	10.42; 14.67	98	3063	479 001	1.47	1.14; 1.85	50	1554	3 444 752	0.20	0.15;0.25

Multiple: studies contained more than one countries.

4 DISCUSSION

It has been estimated that one third of the global population, representing over two billion people, live in HEV endemic areas at risk of infection.[12] This has been widely misinterpreted as that 2.3 billion of the population have been infected with HEV.[25] In fact, the true burden of hepatitis E remains largely unknown.[26] In this study, we have systematically and comprehensively assessed the global HEV prevalence by retrieving data from 75 countries of the six continents. We estimated that 12.47% of the global population, corresponding to approximately 939 million individuals, have experienced past-infection of HEV based on their seropositivity of anti-HEV IgG antibody. Africa and Asia have been previously recognized for the high prevalence of HEV.[27,28] Our estimates confirm the high seroprevalence rates of 21.76% and 15.80% in Africa and Asia, respectively. For Europe, we estimated a prevalence rate of 9.31%, which is substantially lower than a previous estimation of 16.90% from a meta-analysis performed in 2016.[14] A possible explanation for the disparity could be that they collected fewer studies and included small size populations, and thus is prone to cause more bias. In Americas, we observed a slightly higher seroprevalence rate in North (8.05%) compared to South (7.28%) America, which is consistent with the results from a recent meta-analysis.[13]

Of a technical note, it has been well-realized that there are substantial differences in sensitivity and specificity of the anti-HEV IgG ELISA kits from different manufactures.[29,30] Our results largely agree with the literature that the Wantai assay has the best performance and has been most widely used.[31] Thus, the use of different anti-HEV IgG ELISA kits may partially explain the disparities in estimates among different studies, and caution should be taken when interpreting the seroprevalence rate in this respect.

The *bona fide* disease burden of HEV lies in the actively infected patients. The global burden caused by GT 1 and 2 HEV in Africa and Asia has been mathematically modeled for 2005. Among the 4.7 billion people in these regions corresponding to 72.8% of the global population in 2005, it has been estimated as 20 million incident HEV infections, 3.4 million symptomatic cases, 70000 deaths, and 3000 stillbirths.[32] In 2011, WHO reported 14 million symptomatic cases annually worldwide with 300000 deaths and 5200 stillbirths.[33] Hypothetically, if both estimates are accurate, there would be about 10 million symptomatic cases annually from developed countries, which are mainly caused by the zoonotic GT3 strains. This clearly disagrees with the vast majority of the current literature that we do not expect the burden in respect to symptomatic infection would be three-times in developed compared to developing countries. In this study, we have estimated approximately 110 million individuals with recent/current infection based on anti-HEV IgM antibody positivity and 15 million with ongoing infection based on HEV RNA positivity. As viral RNA persists for a few weeks and anti-HEV IgM antibody for a few months,[34] the annually global infections are probably at a range of hundred(s) millions. However, the available data regarding anti-HEV IgM

antibody or viral RNA positivity are very limited. Thus, our estimates may have biases, and we were not able to further sub-analyze regional prevalence, genotype-specific burden or clinical outcome, which require future studies in these aspects.

Accumulating knowledge on HEV biology and transmission routes has facilitated the identification of risk factors for the infection. A wide range of domestic or wild animals have been recognized as reservoirs for the zoonotic strains. Consumption of uncooked meat or meat product from swine, wild boar or deer has been widely reported to cause GT3 HEV infection in European countries.[35,36] As expected, consumption of raw meat is an important risk factor revealed by our meta-analysis. This is in line with previous reports that human with occupational exposure to pigs are at a high risk of HEV infection.[37,38] In this study, we observed two-fold higher of anti-HEV seropositivity in occupational population who frequently contact with pig or pig products compared to the general population.

The host range for HEV is ever expanding and cross-species infections commonly occur.[7] Intriguingly, recent evidence has indicated that companion animals including dogs, cats, rabbits and horses might be accidental hosts for HEV and might constitute a source for HEV transmission to human.[10,11,39] Transmission of rat HEV to human has been recently reported in Hong Kong.[40] Dogs and cats are the most common household pets. Previous studies have reported that seroprevalence of HEV antibodies in dogs ranges from 0.8% in UK,[41] 6.79% in Brazil,[42] 17.8% to 36.55% in different regions of China,[10,11] 22.7% in India,[43] and 56.6% in Germany.[44] Interestingly, when comparing with the general population, veterinarians and dog farm staff who are frequently exposed to dogs have significantly higher anti-HEV antibody positivity.[10] The anti-HEV seroprevalence rates in cats have been reported to be 6.28% in China,[11] 8.1% in Korea,[45] and 33% in Japan.[46] In this study, we found that people who frequently contact with dogs have higher anti-HEV IgG seropositivity. This was not found in people who contact with cats, but the number of studies are very limited. These results call more attention to address the potential role of pets in HEV zoonotic transmission, although currently it remains unconfirmed whether pets are reservoirs, requiring further investigation.

Previous studies have indicated the differences of HEV seroprevalence between rural and urban areas.[47-49] We found that rural compared to urban residents have higher risk of HEV infection. This largely agrees with our findings that high exposure to soil is also a risk factor. In addition, we observed the high risk of HEV infection in individuals with lower education levels, consistent with previous studies.[50,51] Conceivably, this population are more likely living in rural arears with compromised sanitation conditions and more frequent exposure to animals or soil. Although we did not find differences of HEV prevalence in respect to different water source, this does not contradict to the fact that contaminated water is the main source of GT1 infection, especially during outbreak. In our study, we have excluded studies related to outbreak, and the number of included studies reporting water source is also very limited, which may cause bias.

Of note, there are some limitations of our study. Firstly, the number of available studies, in particular on anti-HEV IgM antibody and viral RNA positivity, are limited. We were also not able to further detailed sub-analyze regional prevalence, genotype-specific burden or clinical outcome. Secondly, we have focused on HEV prevalence, but did not estimate the incidence, which is also very relevant for assessing the disease burden. Thirdly, the assays used for HEV detection are heterogeneous in sensitivity and specificity, which may affect the estimates. Fourthly, publication bias existed in our study which was reflected in Funnel and Egger test (Fig. S41-S42).

In summary, we found that 1/8 of the global population, corresponding to over 900 million individuals, have ever encountered HEV infection. Importantly, 15-110 million individuals are experiencing recent or ongoing infection. Consuming raw meat, exposing to soil, blood transfusion, travelling to endemic areas, contacting with dogs, living in rural areas and receiving lower level of education were identified as risk factors for HEV infection. Thus, our results bear important implications for assessing the global burden and devising preventive measures for controlling HEV infection.

For supplementary file please refer to
https://onlinelibrary.wiley.com/action/downloadSupplement?doi=10.1111%2Fliv.14468&file=liv14468-sup-0001-Supinfo.pdf

Reference

1. Khuroo MS, Kamili S. Aetiology, clinical course and outcome of sporadic acute viral hepatitis in pregnancy. *J Viral Hepat.* 2003;10(1):61-69.
2. Kamar N, Selves J, Mansuy JM, et al. Hepatitis E virus and chronic hepatitis in organ-transplant recipients. *N Engl J Med.* 2008;358(8):811-817.
3. Zhou X, de Man RA, de Knegt RJ, Metselaar HJ, Peppelenbosch MP, Pan Q. Epidemiology and management of chronic hepatitis E infection in solid organ transplantation: a comprehensive literature review. *Rev Med Virol.* 2013;23(5):295-304.
4. Purdy MA, Harrison TJ, Jameel S, et al. ICTV Virus Taxonomy Profile: Hepeviridae. *J Gen Virol.* 2017;98(11):2645-2646.
5. Zhou JH, Li XR, Lan X, et al. The genetic divergences of codon usage shed new lights on transmission of hepatitis E virus from swine to human. *Infect Genet Evol.* 2019;68:23-29.
6. Wang Y, Chen G, Pan Q, Zhao J. Chronic Hepatitis E in a Renal Transplant Recipient: The First Report of Genotype 4 Hepatitis E Virus Caused Chronic Infection in Organ Recipient. *Gastroenterology.* 2018;154(4):1199-1201.
7. Meng XJ. Expanding Host Range and Cross-Species Infection of Hepatitis E Virus. *PLoS Pathog.* 2016;12(8):e1005695.
8. Westholter D, Hiller J, Denzer U, et al. HEV-positive blood donations represent a relevant infection risk for immunosuppressed recipients. *J Hepatol.* 2018;69(1):36-42.
9. Teshale EH, Grytdal SP, Howard C, et al. Evidence of person-to-person transmission of hepatitis E virus during a large outbreak in Northern Uganda. *Clin Infect Dis.* 2010;50(7):1006-1010.
10. Zeng MY, Gao H, Yan XX, et al. High hepatitis E virus antibody positive rates in dogs and humans exposed to dogs in the south-west of China. *Zoonoses Public Health.* 2017;64(8):684-688.
11. Liang H, Chen J, Xie J, et al. Hepatitis E virus serosurvey among pet dogs and cats in several developed cities in China. *PLoS One.* 2014;9(6):e98068.
12. Mirazo S, Ramos N, Mainardi V, Gerona S, Arbiza J. Transmission, diagnosis, and management of hepatitis E: an update. *Hepat Med.* 2014;6:45-59.
13. Horvatits T, Ozga AK, Westholter D, et al. Hepatitis E seroprevalence in the Americas: A systematic review and meta-analysis. *Liver Int.* 2018;38(11):1951-1964.
14. Hartl J, Otto B, Madden RG, et al. Hepatitis E Seroprevalence in Europe: A Meta-Analysis. *Viruses.* 2016;8(8).
15. Capai L, Falchi A, Charrel R. Meta-Analysis of Human IgG anti-HEV Seroprevalence in Industrialized Countries and a Review of Literature. *Viruses.* 2019;11(1).
16. Behzadifar M, Lankarani KB, Abdi S, et al. Seroprevalence of Hepatitis E Virus in Iran: A Systematic Review and Meta-analysis. *Middle East J Dig Dis.* 2016;8(3):189-200.
17. Hassan-Kadle MA, Osman MS, Ogurtsov PP. Epidemiology of viral hepatitis in Somalia: Systematic review and meta-analysis study. *World J Gastroenterol.* 2018;24(34):3927-3957.
18. Zhang L, Jiao S, Yang Z, et al. Prevalence of hepatitis E virus infection among blood donors in mainland China: a meta-analysis. *Transfusion.* 2017;57(2):248-257.
19. Huang X, Huang Y, Wagner AL, Chen X, Lu Y. Hepatitis E virus infection in swine workers: A meta-analysis. *Zoonoses Public Health.* 2019;66(1):155-163.
20. Hakim MS, Wang W, Bramer WM, et al. The global burden of hepatitis E outbreaks: a systematic review. *Liver Int.* 2017;37(1):19-31.
21. Aggarwal R. Diagnosis of hepatitis E. *Nat Rev Gastroenterol Hepatol.* 2013;10(1):24-33.
22. Takahashi M, Kusakai S, Mizuo H, et al. Simultaneous detection of immunoglobulin A (IgA) and IgM antibodies against hepatitis E virus (HEV) Is highly specific for diagnosis of acute HEV infection. *J Clin Microbiol.* 2005;43(1):49-56.
23. Moher D, Liberati A, Tetzlaff J, Altman DG, Group P. Preferred reporting items for systematic reviews and meta-analyses: the PRISMA statement. *J Clin Epidemiol.* 2009;62(10):1006-1012.
24. THE Joanna Briggs Institute. The Joanna Briggs Institute Critical Appraisal tools for use in JBI systematic reviews. Checklist for Systematic Reviews and Research Syntheses. https://joannabriggs.org/sites/default/files/2019-05/JBI_Critical_Appraisal-Checklist_for_Systematic_Reviews2017_0.pdf (accessed March 03, 2020).
25. Melgaco JG, Gardinali NR, de Mello VDM, Leal M, Lewis-Ximenez LL, Pinto MA. Hepatitis E: Update on Prevention and Control. *Biomed Res Int.* 2018;2018:5769201.
26. World Health Organization. SIXTY-SECOND WORLD HEALTH ASSEMBLY A62/22. https://apps.who.int/gb/ebwha/pdf_files/WHA62-REC1/WHA62_REC1-en.pdf (accessed March 03, 2020).
27. Yazbek S, Kreidieh K, Ramia S. Hepatitis E virus in the countries of the Middle East and North Africa region: an awareness of an infectious threat to blood safety. *Infection.* 2016;44(1):11-22.
28. Kmush B, Wierzba T, Krain L, Nelson K, Labrique AB. Epidemiology of hepatitis E in low- and middle-income countries of Asia and Africa. *Semin Liver Dis.* 2013;33(1):15-29.
29. Rossi-Tamisier M, Moal V, Gerolami R, Colson P. Discrepancy between anti-hepatitis E virus immunoglobulin G prevalence assessed by two assays in kidney and liver transplant recipients. *J Clin Virol.* 2013;56(1):62-64.
30. Wenzel JJ, Preiss J, Schemmerer M, Huber B, Jilg W. Test performance characteristics of Anti-HEV IgG assays strongly influence hepatitis E seroprevalence estimates. *J Infect Dis.* 2013;207(3):497-500.
31. Sommerkorn FM, Schauer B, Schreiner T, Fickenscher H, Krumbholz A. Performance of Hepatitis E Virus (HEV)-antibody tests: a comparative analysis based on samples from individuals with direct contact to domestic pigs or wild boar in Germany. *Med Microbiol Immunol.* 2017;206(3):277-286.
32. Rein DB, Stevens GA, Theaker J, Wittenborn JS, Wiersma ST. The global burden of hepatitis E virus genotypes 1 and 2 in 2005. *Hepatology.* 2012;55(4):988-997.
33. WHO. Viral hepatitis in the WHO countries of south-east Asia region. http://hepcasia.com/wp-content/uploads/2015/03/who_searo_viral-hepatitis-report.pdf. (accessed June 30, 2019).
34. Kamar N, Bendall R, Legrand-Abravanel F, et al. Hepatitis E. *Lancet.* 2012;379(9835):2477-2488.
35. Tei S, Kitajima N, Ohara S, et al. Consumption of uncooked deer meat as a risk factor for hepatitis E virus infection: an age- and sex-matched case-control study. *J Med Virol.* 2004;74(1):67-70.
36. Colson P, Romanet P, Moal V, et al. Autochthonous infections with hepatitis E virus genotype 4, France. *Emerg Infect Dis.* 2012;18(8):1361-1364.

37. Ivanova A, Tefanova V, Reshetnjak I, et al. Hepatitis E Virus in Domestic Pigs, Wild Boars, Pig Farm Workers, and Hunters in Estonia. *Food Environ Virol.* 2015;7(4):403-412.
38. Teixeira J, Mesquita JR, Pereira SS, et al. Prevalence of hepatitis E virus antibodies in workers occupationally exposed to swine in Portugal. *Med Microbiol Immunol.* 2017;206(1):77-81.
39. Sahli R, Fraga M, Semela D, Moradpour D, Gouttenoire J. Rabbit HEV in immunosuppressed patients with hepatitis E acquired in Switzerland. *J Hepatol.* 2019;70(5):1023-1025.
40. Sridhar S, Yip CC, Wu S, et al. Transmission of rat hepatitis E virus infection to humans in Hong Kong: a clinical and epidemiological analysis. *Hepatology.* 2020.
41. McElroy A, Hiraide R, Bexfield N, et al. Detection of Hepatitis E Virus Antibodies in Dogs in the United Kingdom. *PLoS One.* 2015;10(6):e0128703.
42. Vitral CL, Pinto MA, Lewis-Ximenez LL, Khudyakov YE, dos Santos DR, Gaspar AM. Serological evidence of hepatitis E virus infection in different animal species from the Southeast of Brazil. *Mem Inst Oswaldo Cruz.* 2005;100(2):117-122.
43. Arankalle VA, Joshi MV, Kulkarni AM, et al. Prevalence of anti-hepatitis E virus antibodies in different Indian animal species. *J Viral Hepat.* 2001;8(3):223-227.
44. Dahnert L, Conraths FJ, Reimer N, Groschup MH, Eiden M. Molecular and serological surveillance of Hepatitis E virus in wild and domestic carnivores in Brandenburg, Germany. *Transbound Emerg Dis.* 2018;65(5):1377-1380.
45. Song YJ, Jeong HJ, Kim YJ, et al. Analysis of complete genome sequences of swine hepatitis E virus and possible risk factors for transmission of HEV to humans in Korea. *J Med Virol.* 2010;82(4):583-591.
46. Okamoto H, Takahashi M, Nishizawa T, Usui R, Kobayashi E. Presence of antibodies to hepatitis E virus in Japanese pet cats. *Infection.* 2004;32(1):57-58.
47. Echevarria JM. Light and Darkness: Prevalence of Hepatitis E Virus Infection among the General Population. *Scientifica (Cairo).* 2014;2014:481016.
48. Alvarado-Esquivel C, Sanchez-Anguiano LF, Hernandez-Tinoco J. Seroepidemiology of hepatitis e virus infection in mennonites in Mexico. *J Clin Med Res.* 2015;7(2):103-108.
49. Caron M, Kazanji M. Hepatitis E virus is highly prevalent among pregnant women in Gabon, central Africa, with different patterns between rural and urban areas. *Virol J.* 2008;5:158.
50. Farshadpour F, Taherkhani R, Ravanbod MR, Eghbali SS, Taherkhani S, Mahdavi E. Prevalence, risk factors and molecular evaluation of hepatitis E virus infection among pregnant women resident in the northern shores of Persian Gulf, Iran. *PLoS One.* 2018;13(1):e0191090.
51. Oncu S, Oncu S, Okyay P, Ertug S, Sakarya S. Prevalence and risk factors for HEV infection in pregnant women. *Med Sci Monit.* 2006;12(1):CR36-39.

CHAPTER 6

Global prevalence, incidence and outcomes of non-alcoholic fatty liver disease

Jiaye Liu[1#*], Pengfei Li[1#], Wanlu Cao[1#], Qin Yang[1,2#], Ling Wang[1], Junyi Shen[3], Tianfu Wen[3], Xiaofang Zhang[4], Zhongren Ma[5], Wichor Bramer[6], Shaoli Lin[7], Marco J. Bruno[1], Mohsen Ghanbari[4,8], Maikel P. Peppelenbosch[1], Qiuwei Pan[1*]

In preparation

Abstract

Background & Aims

The increasing burden of non-alcoholic fatty liver disease (NAFLD) worldwide imposes an emerging public health issue. To obtain a comprehensive overview of NAFLD, we perform the current study with the aim to estimate the global prevalence, incidence, disease progression and clinical outcomes of NAFLD.

Approach & Results

A systematic search was conducted in five databases that screened articles in English language published from January 2000 to February 2020. Our search returned 59156 records, of which 578 studies fulfilled our inclusion criteria. The overall prevalence of NAFLD was 29.38% (95% CI 28.09-30.69) regardless of the diagnostic techniques. Looking at the group in which the diagnosis was made by ultrasound exclusively, the pooled prevalence was 30.49% (95% CI 29.55-31.43). NAFLD has become more prevalent during the latest 10 years (31.63%, 95% CI 30.23-33.04) compared to the previous decade (27.94%, 95% CI 26.23-29.69). The pooled estimation of NASH prevalence was 8.26% (95% CI 1.13-21.01), 46.49% (95% CI 35.93-57.20), 46.72% (95% CI 37.57-55.98) in general population, NAFLD patients and severe/morbidly obese patients, respectively. Based on a total of 110142 newly developed NAFLD patients, the pooled incident rate was estimated as 46.2 cases per 1000 person-years (95% CI 43.2-49.3). In patients with NAFLD, the incident rate of hepatocellular carcinoma was 1.4 (95% CI 0.9-2.0) cases per 1000 person-years. The overall pooled estimate of mortality was 23.9 (95% CI 13.5-37.1) death per 1000 person-years.

Conclusions

The prevalence of NAFLD is increasing globally. It is contributing to poor clinical outcomes including hepatocellular carcinoma and death. Rising awareness and urgent actions are warranted to control the NAFLD pandemic across the globe.

Introduction

Non-alcoholic fatty liver disease (NAFLD), once considered a disease of western developed world, now is affecting the global population.[1-5] Although NAFLD has a benign course in the majority of individuals, a subset of patients develop non-alcoholic steatohepatitis (NASH). NASH is a more serious form of liver damage which may further develop into end-stage liver diseases, including liver cirrhosis and hepatocellular carcinoma (HCC).[6-9] Due to its high prevalence in general population, even a small proportion of NAFLD patients developing end-stage liver disease will represent a sizable number and impose an emerging global health burden.[10-11]

Classical risk factors of NAFLD include age, sex, obesity resulted insulin resistance (IR), and development of metabolic syndromes (MetS).[12] The rise in the prevalence of NAFLD/NASH parallels with the epidemics of obesity during the last two decades.[13] Obesity, especially central obesity, is highly predictive for hepatic steatosis and disease progression as the prevalence rate is doubled in obese in comparison with lean NAFLD patients.[14] In morbid obesity, almost all patients have steatosis and more than one third present with NASH.[15] Moreover, the association with type 2 diabetes mellitus (T2DM) is particularly strong, being 3-9 times more frequent in NAFLD and 5 times higher in NASH patients as compared to the general population.[16] On the other hand, more than two third of T2DM patients present with NAFLD.[16-17] MetS is a cluster of metabolic abnormalities associated with cardiovascular mortality. One third of NAFLD patients have MetS and 80% have at least one of the components.[18-19]

Early studies have highlighted the emergence of the NAFLD epidemic,[3] but an up-to-date comprehensive meta-analysis regarding the evolving epidemiology of NAFLD from a global perspective is lacking. Therefore, this study aims to comprehensively estimate the global prevalence, incidence, disease progression and clinical outcomes of NAFLD by a systematic review and meta-analysis.

Materials and methods

Data source and searching strategy

A systematic search was conducted in Medline, Embase, Web of science, google scholar and Cochrane CENTRAL. Databases were searched for articles in the English language from January 2000 to February 2020. All searches from database were performed by a biomedical information specialist of the medical library, with an exhaustive set of search terms related to “non-alcoholic fatty liver disease”, “non-alcoholic steatohepatitis”, “prevalence”, “epidemiology” (The full search strategies are provided in the Supporting methods 1-3). Our analysis in this review was reported in accordance with PRISMA guidelines.[20]

Eligibility criteria

Inclusion criteria for the meta-analysis were as follows: (1) NAFLD diagnosed by imaging (ultrasound, computed tomography, and magnetic resonance imaging/spectroscopy, transient elastography), liver biopsy, and/or blood testing/predictive indices (fatty liver index or hepatic steatosis index); (2) the study was either a cross-sectional study or a baseline survey of longitudinal study; (3) the study provided information about sample size (> 30) and estimation of prevalence, incidence, disease progression or outcome (HCC or all-cause mortality, cancer-related, liver-specific, cardiovascular-related mortality) of NAFLD. Exclusion criteria for the meta-analysis were as follows: (1) the study was a review article, abstract, case report, correspondence, conference papers; (2) the study did not identify individuals with NAFLD; (3) individuals <18 years. (4) the study did not exclude other causes of liver disease, such as viral hepatitis B and C (HBV/HCV); (5) the study without reporting screening for excess alcohol consumption; (6) for NAFLD prevalence, incidence pooled estimates in general population, studies performed in patients, individuals from outpatient service were excluded; (7) the study reporting that individuals with preexisting disease, for example, human immunodeficiency virus (HIV) co-infected; (8) the study diagnosed NAFLD postmortem; (9) NASH studies were excluded if the diagnosis was not made by histological assessment; (10) a study unable to provide sufficient information for data extraction.

Data extraction, quality assessment and statistics analysis

Studies were screened based on pre-specified decision rules. Initial title and abstract screening was done independently by two reviewers (JL, PL), with a random 10% of studies checked by another two investigators (WC, QY). Full-text review was done independently by two authors (any two of JL, PL, WC and QY), with any discrepancies resolved by consensus or by a third reviewer (QP); consensus was reached in all instances. We extracted data at all levels reported in the study, including time of publication, study period, country or region, country or region income, the level of

country development, study categories, gender, age, living area (urban or rural), diagnostic techniques and prevalence or incidence of disease. Data were then cross checked for accuracy against the original source by one of four authors (JL, PL, WC or QY). Two authors (any two of JL, PL, WC and QY) independent reviewed and extracted data from the included studies by using a data extraction form specifically designed for current study. When duplicate data were identified, the duplicate with the smallest sample size or shortest duration of follow-up was excluded. We assessed the quality of included studies using an assessment scale based on the Newcastle-Ottawa Scale, which is comprised of three domains including selection, comparability and outcome. The Newcastle-Ottawa Scale assigns a maximum score of five for selection, two for comparability, and two for outcome. Studies scoring 1-3 were defined as low quality, 4-6 as average quality, and 7-9 as high quality (Supporting Table 1).[21] Studies were not excluded on the basis of their quality score to increase transparency and to ensure all available evidence in this area was reported. All statistics analysis were performed by using R 3.3.0 and Stata 15.0. More details are provided in Supporting methods 4.

Results

Study and patient characteristics

Our search retuned 59156 records, of which 578 studies fulfill our inclusion criteria (Figure 1). Among these included studies, 559 studies included epidemiological data, 16 studies documented disease progression and 16 studies reported clinical outcomes. The quality assessment scores for included studies are displayed in the Supporting Table 1. The mean quality score of all studies was 7.96 (range from 6-9). As a result, 553 high quality and 25 fair quality studies were further included in meta-analysis. The majority of these included studies had a cross-sectional design and most of them concerned data from health checkup's assessments within general population. The mean or median age of all participants ranged from 19.7 to 80.3 years and 21.4 to 80.0 years for NAFLD patients, respectively. The percentages of males ranged from 0% to 100% for the total study population as well as for NAFLD patients.

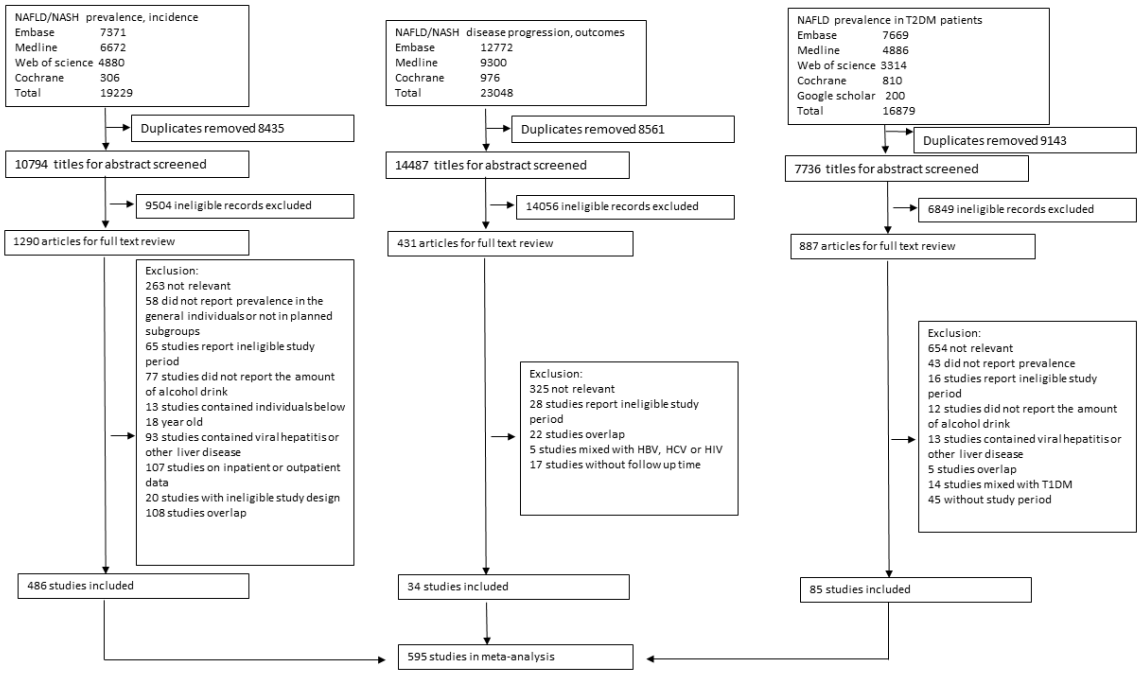

Figure 1. Study selection.

NAFLD prevalence

A total of 363 studies from 40 countries or regions (18 Asian countries and regions, 13 European countries, 4 North American countries, 3 South American countries, 2 African countries) comprised of 114406455 individuals reported NAFLD prevalence in general population. A total of 34347969 participants were diagnosed as NAFLD with a pooled estimated prevalence rate of 29.38% (95% CI 28.09-30.69) regardless of the diagnostic techniques (Supporting Table 2). By stratified data according to different continents, the highest NAFLD prevalence was found in South America with an

estimated rate of 31.31% (95% CI 25.81-37.08), followed by Europe (30.11%, 95% CI 26.89-33.42), Asia (29.92.%, 95% CI 28.87-30.98.), North America (24.28%, 95% CI 20.33.-28.47) and Africa (8.10%, 95% CI 0.85-21.72). NAFLD prevalence varied substantially among countries and regions, from 3.85% (Jamaica, 95% CI 0.75-9.21) to 59.85% (Guatemala, 55.08-64.54, Figure 2, Supporting Table 3). Clinical characteristics of participants in studies included for overall NAFLD prevalence analysis were listed in Supporting Table 4. Considering the diagnostic techniques for assessing NAFLD prevalence, 3 studies used liver biopsy (31.97%, 95% CI 14.12-53.13), 12 used computed tomography (CT, 18.07%, 95% CI 13.50-23.16), 30 used fatty liver index or hepatic steatosis index (26.93%, 95% CI 22.38-31.73), 4 studies used magnetic resonance imaging (MRI, 27.01%, 95% CI 24.87-29.20), 7 studies used transient elastography (TE, 29.63%, 95% CI 16.17-45.20), 12 used elevated liver enzyme (22.47%, 95% CI 17.11-28.33), and 295 studies used abdominal ultrasound (30.49%, 95% CI 29.55-31.43, Figure 3, Supporting Table 5). Since ultrasound was the most commonly used diagnostic technique, only these studies were included for the remaining analysis unless otherwise specified.

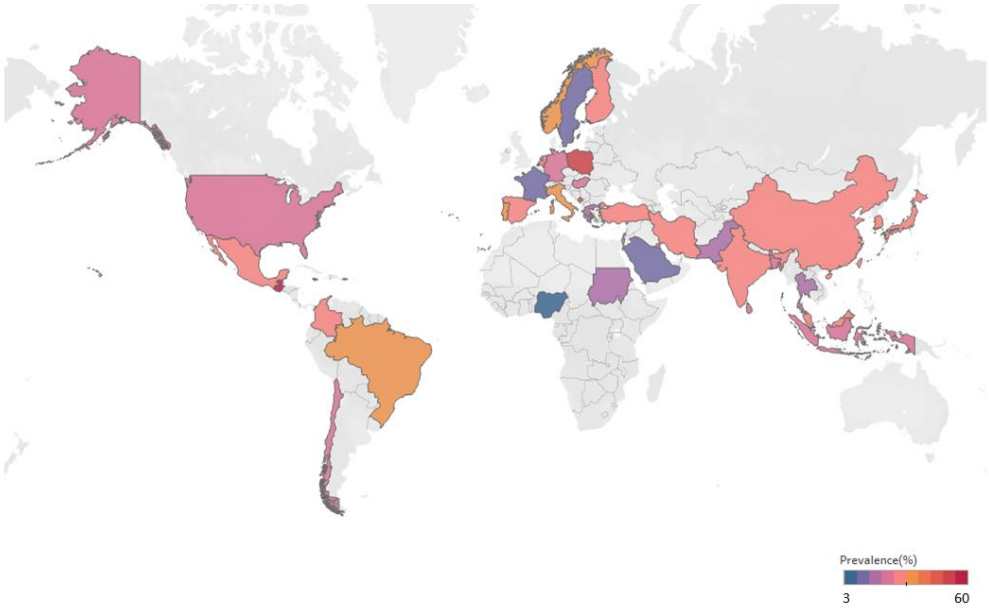

Figure 2. Prevalence of non-alcoholic fatty liver disease in general population regardless of diagnostic techniques.

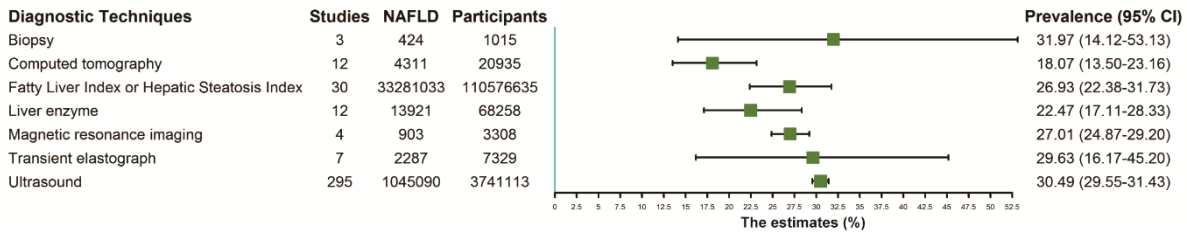

Figure 3. Prevalence of non-alcoholic fatty liver disease stratified by different diagnostic techniques.

Overall, 1045090 NAFLD patients from 31 countries or regions were diagnosed by ultrasound with overall prevalence rate of 30.49% (95% CI 29.55-31.43, Figure 4). USA had the highest prevalence rate of 51.11% (95% CI 46.25-55.95) and Nigeria with the lowest prevalence of 4.09% (95% CI 0.03-14.41). For countries or regions with more than three studies included, NAFLD was most prevalent in Taiwan (38.95%, 95% CI 31.53-46.63) and least prevalent in Japan (25.22%, 95% CI 22.17-28.27, Figure 5). Stratified data by continents, North America had the highest prevalence (40.33%, 95% CI 21.13-61.21), followed by Europe (32.23%, 95% CI 29.82-34.70), South America (31.31%, 95% CI 25.81-37.08), Asia (30.58%, 95% CI 29.60-31.57) and Africa (8.10%, 95% CI 0.85-21.72, Figure 5, Supporting Table 6). For subgroup analysis, NAFLD prevalence was further stratified by age, gender, sample size, country development, country income, study period and quality assessment score. The highest prevalence of NAFLD was found in the 40-60 age groups (38.10%, 95% CI 29.65-46.92, Figure 6 and Supporting table 7). The reported NAFLD prevalence was about 1.5 fold higher in males (36.96%, 95% CI 34.82-39.12) compared to females (23.85%, 95% CI 21.24-26.55, Figure 6 and Supporting table 7). The prevalence was slightly higher in developing countries (30.66%, 95% CI 29.01-32.33) than in developed countries (30.15%, 95% CI 28.99-31.31, Figure 6 and Supporting table 7). NAFLD prevalence was more prevalent in high income countries (31.19%, 95% CI 30.00-32.38) than in upper-middle income (30.53%, 95% CI 28.81-32.27) or lower-middle income countries (23.51%, 95% CI 16.80-30.97, Figure 6 and Supporting table 7). The prevalence had substantially increased from 27.94% (95% CI 26.23-29.69) during 2000-2009 to 31.63% (95% CI 30.23-33.04) during 2010-2020 (Figure 6, Supporting Table 7). Besides, we pooled estimates for the rate of comorbidities in NAFLD patients. Obesity was the most common comorbidity (67.36%, 95% CI 60.68-73.70), followed by Hypertriglyceridemia (52.36%, 95% CI 42.81-61.83), MetS (45.43%, 95% CI 38.75-52.18), hyperlipidemia (42.68%, 95% CI 40.38-45.00), hypertension (39.28%, 95% CI 37.59-40.98), cardiovascular disease (19.32%, 95% CI 8.06-33.96), diabetes (16.79%, 95% CI 15.83-17.77), chronic obstructive pulmonary disease (5.53%, 95% CI 1.59-11.66) and stroke (2.00%, 95% CI 0.00-11.74, Supporting Table 8). In addition, pooled estimates of the risk factors correlating with NALD prevalence are listed in Supporting Table 9. Individual parameters including advanced age (OR 1.02, 95% CI 1.02-1.02) and male sex (OR 2.39, 95% CI 2.303-2.487) were correlated with a higher risk of NAFLD development. Metabolic and biochemical parameters, such as increased body mass index (BMI, OR 1.01, 95% CI 1.01-1.01), central obesity (OR 1.13, 95% CI 1.13-1.14), elevated alanine aminotransferase (ALT, OR 1.03, 95% CI 1.03-1.03), aspartate aminotransferase (AST, OR 1.05, 95% CI 1.05-1.06), total cholesterol (OR 1.01, 95% CI 1.01-1.01), triglyceride (OR 1.01, 95% CI 1.01-1.01), insulin resistance (OR 1.01, 95% CI 1.01-1.01) are risk factors for NAFLD development. Furthermore, our pooled estimations indicated that obesity (OR 4.22, 4.13-4.30), diabetes (OR 1.86, 95% CI 1.69-2.04), MetS (OR 3.86, 3.46-4.30), hypertension (OR 2.38, 95% CI 2.33-2.44) and hyperlipidemia (OR 1.37, 1.26-1.49) were strong risk factors of NAFLD development (Supporting Figure 1).

We also attempted to calculate pooled estimates of NAFLD prevalence in normal or non-obese and overweight or obese individuals. As the cut off value defining normal, non-obese,

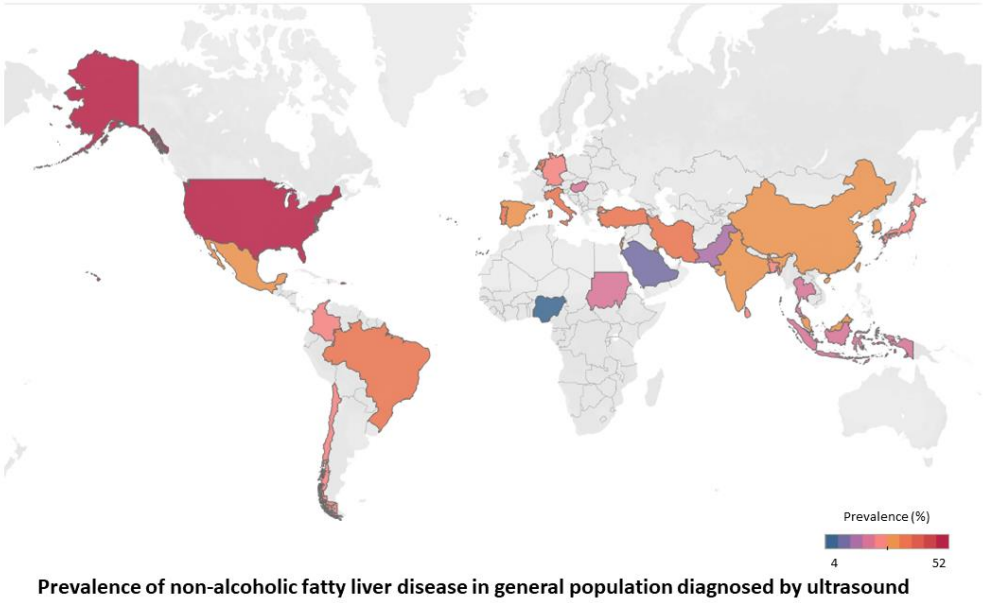

Figure 4. Prevalence of non-alcoholic fatty liver disease diagnosed by ultrasound.

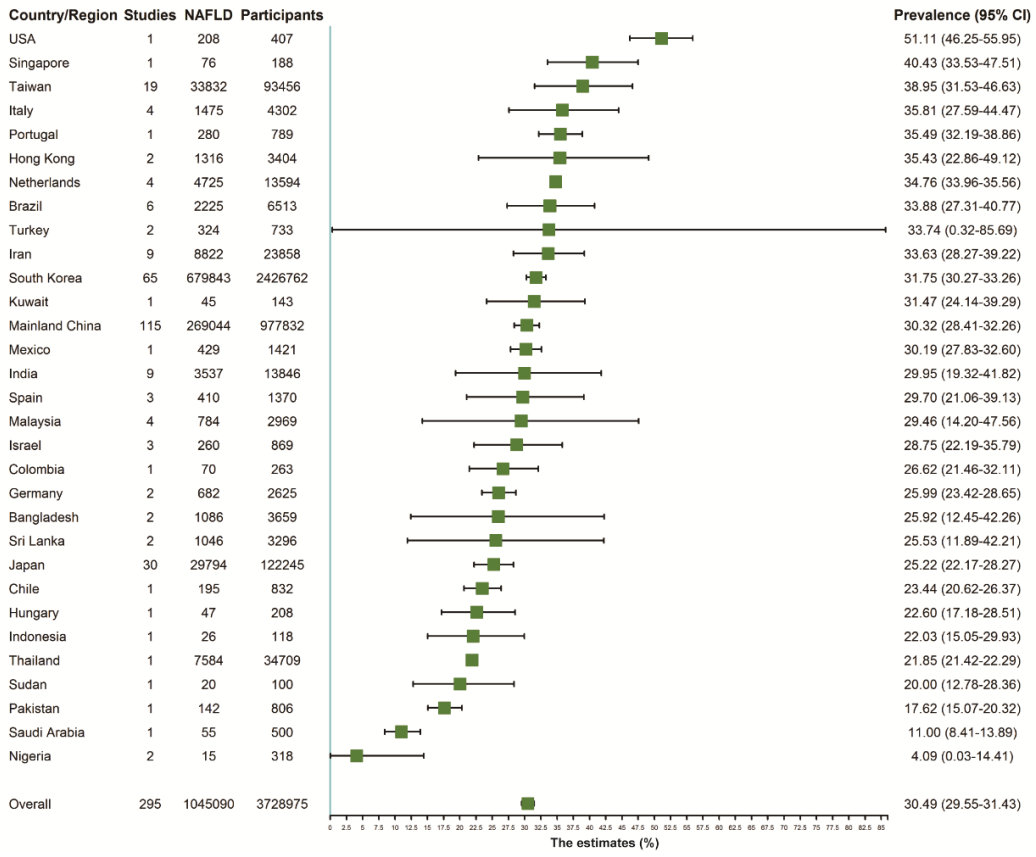

Figure 5. Prevalence of non-alcoholic fatty liver disease diagnosed by ultrasound stratified by countries and regions.

overweight and obese vary among different countries and continents. In accordance with many original publications, we estimated the pooled data by combining the overweight and obese groups. This resulted in 48 studies comprising of 537358 normal or non-obese participants with a pooled rate of 12.08% (95% CI 10.70-13.53, Supporting Figure 2, Table 10-11) compared to 46 studies comprising of 111999 overweight or obese participants with a rate of 54.49% (95% CI 50.94-58.02; Supporting Figure 3, Table 12-13). Moreover, we observed a particularly high NAFLD prevalence in severe or morbidly obese patients that had underwent bariatric surgery. A total of 7573 of such patients from 35 studies had underwent an intraoperative liver biopsy with a pooled NAFLD prevalence rate of 82.16% (95% CI 77.21-86.62; Supporting Figure 4, Table 14-15).

In addition, 82 studies comprising of 93446 T2DM patients yielded a NAFLD prevalence rate of 57.85% (95% CI 55.03-60.66). South America revealed the highest prevalence rate (75.64%, 95% CI 62.37-86.78), followed by North America (62.50%, 95% CI 49.55-74.59), Europe (62.42%, 95% CI 51.75-72.52), Asia (56.26%, 95% CI 52.76-59.72) and Africa (41.76%, 95% CI 17.13-68.83). For countries in which more than three studies were performed, NAFLD was most prevalent in Brazil (76.81%, 95% CI 60.27-89.93) and least prevalent in Nigeria (28.89%, 95% CI 4.55-63.29, Supporting Figure 5 and Supporting Table 16-17).

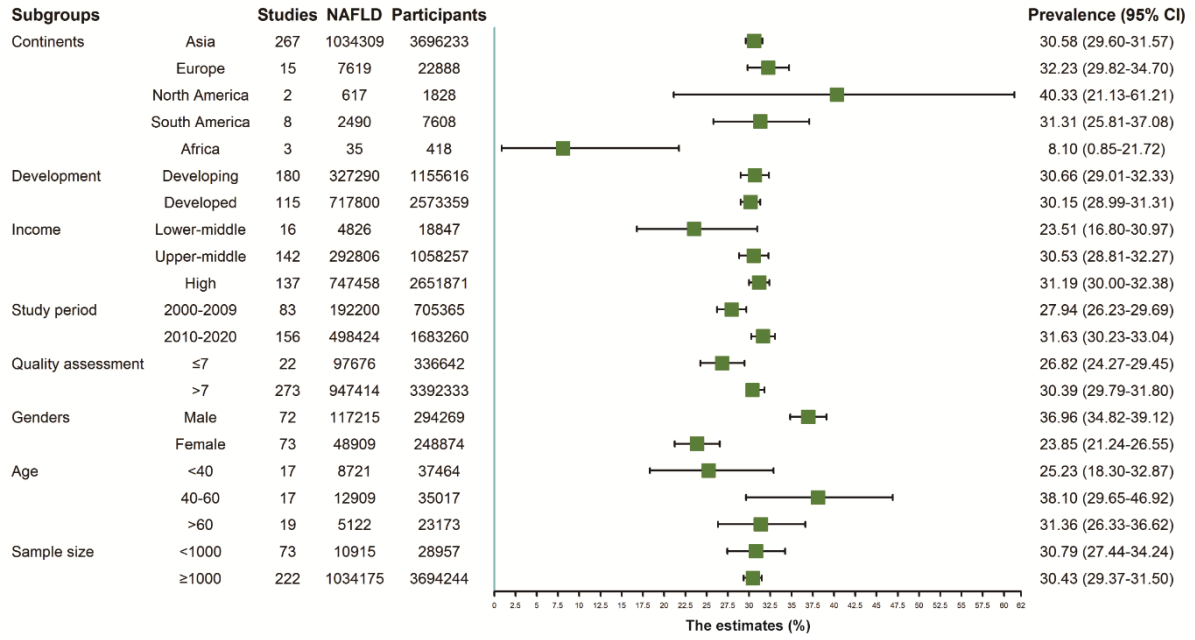

Figure 6. Subgroup analysis of prevalence of NAFLD diagnosed by ultrasound.

NASH prevalence

Diagnosis of NASH was based on histological features. Overall, there were 51 studies reporting NASH prevalence. Of these, 4 studies comprised of 1082 organ donor with a pooled NASH prevalence rate of 8.26% (95% CI 1.13-21.01) in general population (Supporting table 18-19). Twenty four studies including 108023 NAFLD patients with a

pooled prevalence rate of 46.49% (95% CI 35.93-57.20; Supporting figure 6 and Supporting Table 20-21). A total of 4574 severe or morbidly obese patients from 22 studies reported NASH prevalence of 46.72% (95% CI 37.57-55.98; Supporting figure 7 and Supporting Table 22-23).

NAFLD incidence

53 studies including 808713 individuals reported on the NAFLD incidence in the general population (mainland China [n=23], South Korea [n=20], Japan [n=5], Italy [n=2], Hong Kong [n=1], Israel [n=1], Germany [n=1], Table 1). Overall, 110142 newly developed NAFLD yielded a pooled incident rate of 46.2 cases per 1000 person-years (95% CI 43.2-49.3). The highest incident rate was reported in South Korea (49.1 cases per 1000 person-years, 95% CI 45.1-53.2) and lowest in Israel (28.0 cases per 1000 person-years, 95% CI 18.7-39.1, Supporting Table 24).

Disease progression and outcome

There were 16 studies reporting disease progression of non-NASH NAFLD and NASH patients (Table 2). The mean follow-up time ranged from 1.7 to 9.9 years. The pooled estimates of NAFLD remission rate was 50.4 cases per 1000 person-years (95% CI 37.9-64.5). The pooled newly developed rates of fibrosis, advanced fibrosis and cirrhosis were 93.7 (95% CI 55.4-140.8), 41.0 (95% CI 23.6-63.0), and 4.4 (95% CI 2.4-7.0) cases per 1000 person-years, respectively (Supporting Table 25-26). Eleven studies reported on the development of HCC (USA [n=4], South Korea [n=1], Israel [n=1], Italy [n=1], Hong Kong [n=1], UK [n=1], Japan [n=1], France and Hong Kong [n=1]), malignancy except HCC (South Korea [n=1], Italy [n=1], Israel [n=1], UK [n=1], France and Hong Kong [n=1]) or cardiovascular disease (Italy [n=1], UK [n=2], France and Hong Kong [n=1]) with the pooled rate of 1.4 (95% CI 0.9-2.0), 14.2 (95% CI 6.4-24.9), 20.2 (95% CI 6.2-41.9) cases per 1000 person-years, respectively (Table 3, Supporting Table 27). The annual overall mortality rate among patients with NAFLD was 23.9 (95% CI 13.5-37.1) cases per 1000 person-years. In addition, there were 4 studies that documented the overall cancer related mortality, 5 studies on liver-specific mortality and 8 studies on cardiovascular disease mortality with the rate of 1.5 (95% CI 0.2-3.9), 0.7 (95% CI 0.2-1.7) and 2.3 (95% CI 1.0-4.2) cases per 1000 person-years, respectively (Table 4, Supporting Table 28).

No significant publication bias was identified in the overall population (Egger's test, p=0.22) and subgroup analyses (Supporting table 29).

Table 1. Pooled NAFLD incidence rate, stratified by countries or regions.

Country/Region	Studies	Incident cases of NAFLD	Participants	Incident cases per 1000 person-years (95% CI)	I^2
China	23	24221	157394	49.0 (41.4-57.3)	99%
Hong Kong	1	76	565	34.5 (27.3-42.5)	-
Germany	1	605	2623	32.5 (30.0-35.1)	-
Israel	1	28	147	28.0 (18.7-39.1)	-
Italy	2	115	359	37.5(31.1-44.5)	0
Japan	5	3407	22407	32.8 (28.3-37.6)	89%
South Korea	20	81690	625218	49.1 (45.1-53.2)	99%
Overall	**53**	**110142**	**808713**	**46.2 (43.2-49.3)**	**99%**

Table 2. Incident rate of remission, fibrosis, advanced fibrosis and cirrhosis of non-alcoholic fatty liver disease stratified by countries or regions.

	Studies	Incident cases	Participants	Incident cases per 1000 person-years (95% CI)	I^2
NAFLD remission					
China	5	565	2750	49.8 (32.9-700.0)	97%
Japan	1	127	484	57.1 (47.8-67.1)	-
South Korea	3	315	1800	49.7 (24.4-83.2)	97%
Fibrosis development					
Taiwan	1	5	10	294.1 (108.4-525.5)	-
Croatia	1	201	507	156.2 (136.9-176.5)	-
Malaysia	1	18	35	80.4 (48.5-119.4)	-
Turkey	1	82	468	67.4 (54.0-82.2)	-
UK	1	45	108	63.1(46.4-82.1)	-
Advanced fibrosis development					
Taiwan	1	1	10	58.8 (1.5-286.9)	-
Malaysia	1	9	35	46.9 (21.7-87.1)	-
UK	1	6	27	33.7 (12.5-71.9)	-
Cirrhosis development					
Iceland	1	10	151	7.0 (3.3-11.9)	-
Malaysia	1	2	35	8.9 (0.8-25.4)	-
Turkey	1	16	468	8.5 (4.9-13.2)	-
USA	2	479	19361	2.8 (1.0-5.5)	97%

Table 3. Incident rate of hepatocellular carcinoma, other cancer types except hepatocellular carcinoma and cardiovascular among patients with non-alcoholic fatty liver disease stratified by countries or regions.

	Studies	Incident cases	Participants	Incident cases per 1000 person-years (95% CI)	I^2
Hepatocellular carcinoma					
Hong Kong	1	2	356	0.5 (0.1-1.6)	-
France and Hong Kong	1	21	2245	4.2 (2.6-6.1)	-
Israel	1	6	153	4.7 (1.7-9.1)	-
Italy	1	13	471	5.0 (2.7-8.1)	-
Japan	1	9	301	5.0 (2.3-8.8)	-
South Korea	1	13	8721	0.2 (0.1-0.4)	-
UK	1	19	1452	2.7 (1.6-4.0)	-
USA	4	983	571524	0.7 (0.3-1.2)	99%
Malignancy except HCC					
France and Hong Kong	1	142	2245	28.1 (23.7-32.9)	-
Israel	1	14	153	10.9 (6.0-17.3)	-
Italy	1	17	471	6.6 (3.8-10.1)	-
South Korea	1	427	8721	7.6 (6.9-8.3)	-
UK	1	157	1452	23.4 (19.9-27.1)	-
Cardiovascular disease					
France and Hong Kong	1	151	2254	29.9 (25.4-34.8)	-
Italy	1	8	471	3.1 (1.3-5.6)	-
UK	2	352	1773	25.8 (6.7-56.8)	99%

Table 4. Overall mortality, cancer-related mortality, liver-disease related mortality and cardiovascular disease related mortality among patients with non-alcoholic fatty liver disease stratified by countries or regions.

	Studies	Incident cases	Participants	Incident cases per 1000 person-years (95% CI)	I^2
Overall mortality					
Hong Kong	1	47	356	12.8 (9.4-16.7)	-
France and Hong Kong	1	56	2245	11.5 (8.7-14.6)	-
Israel	1	19	153	14.8 (8.9-22.1)	-
Italy	2	156	471	95.0 (0-492.5)	-
Japan	1	179	4073	6.3 (5.4-7.2)	-
Sri Lanka	1	41	851	4.8 (3.5-6.4)	-
South Korea	1	500	82899	49.7 (24.4-83.2)	97%
UK	2	309	1773	37.8 (28.7-48.0)	70%
Cancer-related mortality					
Italy	1	2	471	0.8 (0.1-2.2)	-
Sri Lanka	1	9	851	1.1 (0.5-1.9)	-
South Korea	1	211	82899	0.4 (0.4-0.5)	-
UK	1	38	1452	5.4 (3.8-7.2)	-
Liver disease-related mortality					
Italy	1	12	471	4.7 (2.4-7.7)	-
Japan	1	9	4073	0.3 (0.1-0.6)	-
Sri Lanka	1	4	851	0.5 (0.1-1.0)	-
South Korea	1	16	82899	0 (0-0.1)	-
UK	1	8	1452	1.1 (0.5-2.0)	-
Cardiovascular-related mortality					
Hong Kong	1	9	356	2.4 (1.1-4.3)	-
Italy	1	2	471	0.8 (0.1-2.2)	
Japan	1	9	4073	0.3 (0.1-0.6)	-
Sri Lanka	1	17	851	2.0 (1.2-3.1)	-
South Korea	1	89	82899	0.2 (0.2-0.2)	-
UK	2	58	1773	6.3 (4.8-8.0)	0

Discussion

In this systematic review and meta-analysis, we included 578 studies in order to comprehensively estimate the global prevalence, incidence, disease progression and outcomes of NAFLD. The overall prevalence of NAFLD in the general population is 29.38% (95% CI 28.09-30.69) regardless of the diagnostic techniques used to establish the diagnosis. Looking at the group in which the diagnosis was made by ultrasound exclusively, the pooled prevalence was 30.49% (95% CI 29.55-31.43). Importantly, the prevalence of NAFLD has substantially increased during the latest 10 years (31.63%, 95% CI 30.23-33.04) compared to the previous decade (27.94%, 95% CI 26.23-29.69). Except for Africa (8.10%, 95% CI 28.21-30.80) still maintaining a low prevalence, the other four continents show strikingly high NAFLD prevalence, regardless of the state of economic development.

Extensive studies have highlighted the importance of techniques in diagnosing NAFLD.[22-23] Arguments have been raised against the application of liver enzymes for diagnosing NAFLD because normal levels of these enzymes have been widely observed in the entire spectrum of NAFLD.[3] In line with this, we also observed that the prevalence of NAFLD diagnosed by elevation of liver enzymes yielded a substantially lower rate compared to that of liver biopsy and imaging modality based diagnosis. Interestingly, we also observed that the prevalence rate diagnosed by CT was lower than those of other imaging methodologies. Most of these studies targeted young or middle aged population, as they can tolerate to longer time of body examination. This bias in selecting younger population may explain the lower NAFLD prevalence. Ultrasound is the first-line and most widely used imaging test for NAFLD diagnosis with satisfactory sensitivity and specificity.[24-25] However, the accuracy of diagnosis by ultrasound substantially relies on the proficiency of the physician. Although liver biopsy is the gold standard, it is reserved for a specific patient population due to its invasiveness. Therefore, the uncertainty and variations in NAFLD diagnosis challenge the accurate estimation of the global prevalence.

Our pooled estimates of the odds ratios of risk factors are largely in line with previous studies with some subtle differences.[26-27] Male sex, obesity, development of MetS and hypertension are major risk factors. It has been proposed that lower prevalence in females may be attributable to the protective role of estrogen,[28] but lipid metabolism and fat distribution may also play a role.[29] Insulin resistance, diabetes, obesity, hypertension and hyperlipidemia are all conditions that may play a role in the development of MetS.[30] There is strong relation between the total number of the MetS components and the prevalence and severity of NAFLD.[31,32] A study from Japan proposed that MetS plays a central role in NAFLD development and remission.[33] Findings from Australia and Europe show that 85% NASH patients have at least three components of Mets.[34,35] Some other risk factors, such as sedentary lifestyle, diet habit or amount of exercise, cannot be included in our meta-analysis due to limited studies.

Several studies have reported regional data on NAFLD incidence. In Asia, NAFLD incidence rate was estimated as 50.9 cases per 1000 person-years, with the highest incidence observed in mainland China (63.0 cases per 1000 person-years) and the lowest in Japan (29.0 cases per 1000 person-years).[1] In Europe, a retrospective study including four countries observed doubled incidence rate comparing year 2015 with 2007.[36] In this study, the overall incidence was estimated as 46.2 cases per 1000 person-years.

Development of liver fibrosis or cirrhosis ultimately determine the clinical outcome of NAFLD patients. Although most NAFLD patients are not at risk of disease progression, a proportion will eventually progress to NASH. It has been estimated that 59.1% (95% CI 47.6-69.7) of NAFLD patients may develop with NASH.[3] In the current study, pooled prevalence of NASH in NAFLD patients is 45.48% (95% CI 35.21-55.96). However, there may be a selection and ascertainment bias because most of these NAFLD patients have at least one indication for liver biopsy. The overall prevalence of NASH in morbidly obese patients parallels of the prevalence of NASH among NAFLD patients. This finding is in line with two previous studies that the prevalence of NAFLD was 76% and 93% in obese people, and 37% and 26% of them progress to NASH, respectively.[37-38] Of note, we also estimated the pooled prevalence of NASH in organ donors showing a prevalence rate of 8.26% (95% CI 1.13-21.01), but numbers are small.

We found that the annual incidence of HCC was 1.3 cases per 1000 person-years, indicating an increase as compared to previously published estimates.[3] However, the exact HCC incidence is difficult to estimate because in some cases with NAFLD-related HCC the biological characteristics are distinctly different without preceding cirrhosis.[39] Also, some NAFLD/NASH patients that are co-infected with hepatitis B virus, hepatitis C virus or have other metabolic diseases cannot be included in this estimate of NALFD-related HCC incidence. Given the already high and ever-increasing burden of NAFLD and NASH, the incidence of related HCC is expected to grow. NAFLD/NASH related cirrhosis or HCC are becoming the leading indication for liver transplantation.[10,40] On another note, NAFLD is also associated with high incidence rate of other cancers (14.2 cases 1000 person-years, 95% CI 6.4-24.9), as well as cardiovascular disease (20.2 cases 1000 person-years, 95% CI 6.2-41.9). This may explain why a strikingly high overall death rate was observed in our study.

This study has several strengths. To our knowledge, this is the most comprehensive and up-to-date meta-analysis on the global epidemiology of NAFLD. By including large number of studies and individuals using stringent inclusion criteria, our estimates maximally recapitulate the real-world situation. Furthermore, we were able to include additional estimations for specific subpopulations and conditions such as NAFLD prevalence in morbidly obese patients, incidence of non-HCC malignancies, incidence of cardiovascular disease, and liver-specific and cardiovascular disease related death rates. There are also limitations in this study. Limited data from Africa and Oceania provided made it challenging to arrive at the accurate estimation for these continents.

The high heterogeneity underlying some of the source data in the current study cannot be fully explained. For subgroup analysis, we were only able to divide individuals into two broad categories, that is ‘normal or non-obese’ and ‘overweight or obese’ groups because studies all used different definitions to subdivide their populations. Pertaining disease progression and clinical outcome, some studies included NAFLD/NASH patients that also suffer from related complications (e.g. diabetes or cardiovascular disease) which may over-estimate the incidence and death rate of cardiovascular disease as well as the overall mortality rate. Last but not the least, a new terminology, “Metabolic associated fatty liver disease (MAFLD)”, has recently been proposed to replace “NAFLD”.[41-42] However, for this study, we decided not to adopt this new concept as it will take substantial debate and revision, before this new terminology will be fully accepted by the field.[43]

In summary, this meta-analysis shows that the global prevalence rate of NAFLD, a metabolic disease closely associated with hypertension, hyperlipidemia and diabetes, has risen to 29.38%. Nearly half of the individuals with NAFLD will progress to NASH, and ensuing cases that develop associated liver fibrosis, cirrhosis and HCC will impose a high demand on the healthcare system. Therefore, this substantial and ever growing burden of NAFLD, irrespective of geographic and socio-economic status, calls for attention and dedicated action from primary care physicians, specialists, health policy makers and the general public alike.

Supplementary file please refer to

https://drive.google.com/file/d/1pUMYCU2ndjtSYovhdkn0MDXR_G8kWH99/view?usp=sharing

Reference

1. Li J, Zou B, Yeo YH, Feng Y, Xie X, Lee DH, Fujii H, et al. Prevalence, incidence, and outcome of non-alcoholic fatty liver disease in Asia, 1999-2019: a systematic review and meta-analysis. Lancet Gastroenterol Hepatol 2019;4:389-398.
2. Zhou F, Zhou J, Wang W, Zhang XJ, Ji YX, Zhang P, She ZG, et al. Unexpected Rapid Increase in the Burden of NAFLD in China From 2008 to 2018: A Systematic Review and Meta-Analysis. Hepatology 2019;70:1119-1133.
3. Younossi ZM, Koenig AB, Abdelatif D, Fazel Y, Henry L, Wymer M. Global epidemiology of nonalcoholic fatty liver disease-Meta-analytic assessment of prevalence, incidence, and outcomes. Hepatology 2016;64:73-84.
4. Ye Q, Zou B, Yeo YH, Li J, Huang DQ, Wu Y, Yang H, et al. Global prevalence, incidence, and outcomes of non-obese or lean non-alcoholic fatty liver disease: a systematic review and meta-analysis. Lancet Gastroenterol Hepatol 2020.
5. Fan JG, Farrell GC. Epidemiology of non-alcoholic fatty liver disease in China. J Hepatol 2009;50:204-210.
6. Vernon G, Baranova A, Younossi ZM. Systematic review: the epidemiology and natural history of non-alcoholic fatty liver disease and non-alcoholic steatohepatitis in adults. Aliment Pharmacol Ther 2011;34:274-285.
7. Cai J, Zhang XJ, Li H. Progress and challenges in the prevention and control of nonalcoholic fatty liver disease. Med Res Rev 2019;39:328-348.
8. Sanyal A, Poklepovic A, Moyneur E, Barghout V. Population-based risk factors and resource utilization for HCC: US perspective. Curr Med Res Opin 2010;26:2183-2191.
9. Ratziu V, Bellentani S, Cortez-Pinto H, Day C, Marchesini G. A position statement on NAFLD/NASH based on the EASL 2009 special conference. J Hepatol 2010;53:372-384.
10. Wong RJ, Aguilar M, Cheung R, Perumpail RB, Harrison SA, Younossi ZM, Ahmed A. Nonalcoholic steatohepatitis is the second leading etiology of liver disease among adults awaiting liver transplantation in the United States. Gastroenterology 2015;148:547-555.
11. Younossi ZM, Blissett D, Blissett R, Henry L, Stepanova M, Younossi Y, Racila A, et al. The economic and clinical burden of nonalcoholic fatty liver disease in the United States and Europe. Hepatology 2016;64:1577-1586.
12. Singh S, Kuftinec GN, Sarkar S. Non-alcoholic Fatty Liver Disease in South Asians: A Review of the Literature. J Clin Transl Hepatol 2017;5:76-81.
13. Fazel Y, Koenig AB, Sayiner M, Goodman ZD, Younossi ZM. Epidemiology and natural history of non-alcoholic fatty liver disease. Metabolism 2016;65:1017-1025.
14. Bellentani S, Tiribelli C. The spectrum of liver disease in the general population: lesson from the Dionysos study. J Hepatol 2001;35:531-537.
15. Machado M, Marques-Vidal P, Cortez-Pinto H. Hepatic histology in obese patients undergoing bariatric surgery. J Hepatol 2006;45:600-606.
16. Anstee QM, Targher G, Day CP. Progression of NAFLD to diabetes mellitus, cardiovascular disease or cirrhosis. Nat Rev Gastroenterol Hepatol 2013;10:330-344.
17. Targher G, Bertolini L, Rodella S, Tessari R, Zenari L, Lippi G, Arcaro G. Nonalcoholic fatty liver disease is independently associated with an increased incidence of cardiovascular events in type 2 diabetic patients. Diabetes Care 2007;30:2119-2121.
18. Browning JD, Szczepaniak LS, Dobbins R, Nuremberg P, Horton JD, Cohen JC, Grundy SM, et al. Prevalence of hepatic steatosis in an urban population in the United States: impact of ethnicity. Hepatology 2004;40:1387-1395.
19. Marchesini G, Bugianesi E, Forlani G, Cerrelli F, Lenzi M, Manini R, Natale S, et al. Nonalcoholic fatty liver, steatohepatitis, and the metabolic syndrome. Hepatology 2003;37:917-923.
20. Moher D, Liberati A, Tetzlaff J, Altman DG, Group P. Preferred reporting items for systematic reviews and meta-analyses: the PRISMA statement. PLoS Med 2009;6:e1000097.
21. Wells GA SB, O'Connell D. The Newcastle-Ottawa Scale (NOS) for assessing the quality of nonrandomized studies in meta-analyses.
22. Younossi ZM, Loomba R, Anstee QM, Rinella ME, Bugianesi E, Marchesini G, Neuschwander-Tetri BA, et al. Diagnostic modalities for nonalcoholic fatty liver disease, nonalcoholic steatohepatitis, and associated fibrosis. Hepatology 2018;68:349-360.
23. Wong VW, Adams LA, de Ledinghen V, Wong GL, Sookoian S. Noninvasive biomarkers in NAFLD and NASH - current progress and future promise. Nat Rev Gastroenterol Hepatol 2018;15:461-478.
24. European Association for the Study of the L, European Association for the Study of D, European Association for the Study of O. EASL-EASD-EASO Clinical Practice Guidelines for the management of non-alcoholic fatty liver disease. J Hepatol 2016;64:1388-1402.
25. Hernaez R, Lazo M, Bonekamp S, Kamel I, Brancati FL, Guallar E, Clark JM. Diagnostic accuracy and reliability of ultrasonography for the detection of fatty liver: a meta-analysis. Hepatology 2011;54:1082-1090.
26. Rinella ME. Nonalcoholic fatty liver disease: a systematic review. JAMA 2015;313:2263-2273.
27. Loomba R, Sanyal AJ. The global NAFLD epidemic. Nat Rev Gastroenterol Hepatol 2013;10:686-690.
28. Villanueva-Ortega E, Garces-Hernandez MJ, Herrera-Rosas A, Lopez-Alvarenga JC, Laresgoiti-Servitje E, Escobedo G, Queipo G, et al. Gender-specific differences in clinical and metabolic variables associated with NAFLD in a Mexican pediatric population. Ann Hepatol 2019;18:693-700.
29. Lee YH, Kim SH, Kim SN, Kwon HJ, Kim JD, Oh JY, Jung YS. Sex-specific metabolic interactions between liver and adipose tissue in MCD diet-induced non-alcoholic fatty liver disease. Oncotarget 2016;7:46959-46971.
30. Yki-Jarvinen H. Non-alcoholic fatty liver disease as a cause and a consequence of metabolic syndrome. Lancet Diabetes Endocrinol 2014;2:901-910.

31. Wong VW, Chu WC, Wong GL, Chan RS, Chim AM, Ong A, Yeung DK, et al. Prevalence of non-alcoholic fatty liver disease and advanced fibrosis in Hong Kong Chinese: a population study using proton-magnetic resonance spectroscopy and transient elastography. Gut 2012;61:409-415.
32. Angulo P, Hui JM, Marchesini G, Bugianesi E, George J, Farrell GC, Enders F, et al. The NAFLD fibrosis score: a noninvasive system that identifies liver fibrosis in patients with NAFLD. Hepatology 2007;45:846-854.
33. Hamaguchi M, Kojima T, Takeda N, Nakagawa T, Taniguchi H, Fujii K, Omatsu T, et al. The metabolic syndrome as a predictor of nonalcoholic fatty liver disease. Ann Intern Med 2005;143:722-728.
34. Cusi K. Role of obesity and lipotoxicity in the development of nonalcoholic steatohepatitis: pathophysiology and clinical implications. Gastroenterology 2012;142:711-725 e716.
35. Kimura Y, Hyogo H, Ishitobi T, Nabeshima Y, Arihiro K, Chayama K. Postprandial insulin secretion pattern is associated with histological severity in non-alcoholic fatty liver disease patients without prior known diabetes mellitus. J Gastroenterol Hepatol 2011;26:517-522.
36. Alexander M, Loomis AK, Fairburn-Beech J, van der Lei J, Duarte-Salles T, Prieto-Alhambra D, Ansell D, et al. Real-world data reveal a diagnostic gap in non-alcoholic fatty liver disease. BMC Med 2018;16:130.
37. Ong JP, Elariny H, Collantes R, Younoszai A, Chandhoke V, Reines HD, Goodman Z, et al. Predictors of nonalcoholic steatohepatitis and advanced fibrosis in morbidly obese patients. Obes Surg 2005;15:310-315.
38. Lazo M, Clark JM. The epidemiology of nonalcoholic fatty liver disease: a global perspective. Semin Liver Dis 2008;28:339-350.
39. White DL, Kanwal F, El-Serag HB. Association between nonalcoholic fatty liver disease and risk for hepatocellular cancer, based on systematic review. Clin Gastroenterol Hepatol 2012;10:1342-1359 e1342.
40. Calzadilla-Bertot L, Jeffrey GP, Jacques B, McCaughan G, Crawford M, Angus P, Jones R, et al. Increasing Incidence of Nonalcoholic Steatohepatitis as an Indication for Liver Transplantation in Australia and New Zealand. Liver Transpl 2019;25:25-34.
41. Eslam M, Sanyal AJ, George J, International Consensus P. MAFLD: A Consensus-Driven Proposed Nomenclature for Metabolic Associated Fatty Liver Disease. Gastroenterology 2020.
42. Eslam M, Newsome PN, Sarin SK, Anstee QM, Targher G, Romero-Gomez M, Zelber-Sagi S, et al. A new definition for metabolic dysfunction-associated fatty liver disease: An international expert consensus statement. J Hepatol 2020.
43. The Lancet Gastroenterology H. Redefining non-alcoholic fatty liver disease: what's in a name? Lancet Gastroenterol Hepatol 2020;5:419.

CHAPTER 7

Estimating global prevalence of metabolic dysfunction-associated fatty liver disease in overweight or obese children and adolescents

Jiaye Liu, Ziyi Wang, Ling Wang, Yang Li, Tianfu Wen, Xiaofang Zhang, Zhongren Ma, Maarten F.M. Engel, Marco J. Bruno, Mohsen Ghanbari, Robert J. de Knegt, Wanlu Cao, Maikel P. Peppelenbosch, Qiuwei Pan

In preparation

Summary

Background Metabolic dysfunction-associated fatty liver disease (MAFLD) is a new terminology recently updated from non-alcoholic fatty liver disease (NAFLD). The discontinuity in nomenclature and disease definition hampers epidemiological understanding of MAFLD. In this study, we aim to perform a systematic review and meta-analysis to estimate the global prevalence of MAFLD in overweight or obese children and adolescents, by repurposing existing data on fatty liver disease.

Methods A systematic search was conducted in Medline, Embase, Web of science, Cochrane CENTRAL Databases and google scholar. We screened relevant articles in English language published until May 2020. By transforming data according to the new diagnosis criteria, the global prevalence of MAFLD was estimated in general and clinical populations. A 95% confidence interval was estimated using Wilson score method, and pooled prevalence was calculated using the DerSimonian-Laird random-effects model with Free-Tukey double arcsine transformations.

Findings Our search returned 35441 records, of which 156 studies fulfilled our inclusion criteria. The overall prevalence of MAFLD was 34.76% (95% CI 27.78-42.08) in general and 45.33% (95% CI 40.74-49.96) in clinical populations of overweight or obese children and adolescents regardless of the diagnostic techniques. Based on the most used ultrasound diagnosis, the pooled prevalence was 35.07% (95% CI 27.76-42.73) in general population and 46.82% (95% CI 41.47-51.20) in clinical population. For subgroup analysis, MAFLD prevalence was slightly higher in boys compared to girls (34.28% vs 25.48% in the general population; 51.33% vs 36.95% in a clinical setting). In the general population, higher prevalence was observed in developing compared to developed countries.

Interpretation MAFLD is highly prevalent in overweight or obese children and adolescents. Rising awareness and urgent actions are warranted as control of the global MAFLD pandemic appears necessary.

Introduction

Obesity has become a global pandemic, and especially the growing burden in pediatric population is more worrisome.[1] Approximately 400 million children and adolescents were estimated to be overweight or obese in 2016,[2] which will have substantial short- and long-term consequences. More specifically, these children are more likely to suffer from psychological comorbidities, cardiovascular disease, diabetes, cancers, musculoskeletal problems and liver complications.[3-5]

Fatty liver disease is one of the most common co-morbidities to obesity in pediatric population. Previous studies established that the prevalence of non-alcoholic fatty liver disease (NAFLD) in pediatric population ranges from 3% to 12%, but this rate can become as high as 70-80% in obese children.[6-7] Recently it has been proposed to revise the classical NAFLD definition and terminology in fatty liver disease to metabolic dysfunction-associated fatty liver disease (MAFLD).[8-9] This revised nomenclature is expected to have major impact on the reporting of the dynamics in disease diagnosis, guidelines for patient management, therapeutic development and the management of public health with respect to fatty liver disease. One of the major changes is the shift towards inclusionary diagnostic criteria, a diagnosis of MAFLD being based on detection of hepatic steatosis by histology, imaging or blood biomarker in addition to the presence of at least one of the following three conditions: overweight/obesity, presence of type 2 diabetes mellitus (T2DM), or evidence for metabolic dysregulation.

The resulting paradigm shift in disease definition urges re-assessing the burden of fatty liver disease, as many previous studies on NAFLD would become ineligible for estimating MAFLD epidemiology. A large proportion of existing data on fatty liver disease in overweight or obese population might, however, be repurposed for MAFLD epidemiology, by adjusting existing results to the new criteria. In this study, we performed a systematic review and meta-analysis to estimate the global prevalence of MAFLD in overweight and obese children and adolescents by exploring the existing epidemiological data of fatty liver disease.

Methods

Searching strategy and selection criteria

A systematic search was conducted in Medline, Embase, Web of science and Cochrane CENTRAL. Databases were searched for articles in the English language until May 2020. All searches from database were performed by a biomedical information specialist of the medical library, with an exhaustive set of search terms related to “fatty liver”, “hepatic steatosis”, “prevalence”, and “epidemiology” (The full search strategies are provided in the Appendix methods 1). We included studies that can be retrospectively transformed into reporting MAFLD prevalence in overweight or obese children or adolescents. The diagnosis of MAFLD was in accordance with the recent consensus on the criteria of diagnosing MAFLD. The detailed inclusion and exclusion criteria are provided in Appendix methods 2. Our analysis in this review was reported in accordance with PRISMA guidelines.[10]

Screen and selection

Studies were screened based on pre-specified decision rules. Initial title and abstract screening was done independently by two reviewers (JL, ZW), with a random 10% of studies checked by another two investigators (LW, YL). Full-text review was done independently by two authors (any two of JL, ZW, LW and YL), with any discrepancies resolved by consensus or by a third reviewer (QP); consensus was reached in all instances. We extracted data at all levels reported in the study, including time of publication, study period, country or region, country or region income based on World bank evaluation, the level of country development, study categories, gender, age, diagnostic techniques, body mass index (BMI) and prevalence of disease. Data were then crossly checked for accuracy against the original source by one of four authors (JL, ZW, LW or YL).

Data analysis

Two authors (any two of JL, ZW, LW and YL) independently reviewed and extracted data from the included studies by using a data extraction form specifically designed for this study. When duplicate data were identified, the duplicate with the smallest sample size or shortest duration of follow-up was excluded. We assessed the quality of included studies using an assessment scale based on the Newcastle-Ottawa Scale, which is comprised of three domains including selection, comparability and outcome. The Newcastle-Ottawa Scale assigns a maximum score of five for selection, two for comparability, and two for outcome.[11] Studies scoring 1-3 were defined as low, 4-6 as average, and 7-9 as high quality (Appendix Table 1). Studies were not excluded on the basis of their quality score to increase transparency and to ensure that all available evidence of this topic will be reported. Egger’s test was used to assess publication bias.

The main outcomes for this study were the global MAFLD prevalence for overweight or obese children and adolescents. To calculate MAFLD prevalence for each country and region, we estimated the pooled rate by using DerSimonian-Laird random-effects model with Free-Tukey double arcsine transformations. Heterogeneity across the included studies was assessed using the Cochran Q statistics and I^2 statistics, with I^2 statistics 25%-50%, 50%-75%, and >75% considered as mild, moderate, and severe heterogeneity, respectively. When heterogeneity was higher than 50%, a random-effect model will be used. Given that abdominal ultrasound was the most commonly used diagnostic technique, we further pooled the prevalence in studies with ultrasound as main diagnostic technique for estimating a more accurate rate. Subgroup analysis was done to further explore the source of heterogeneity which estimated the pooled rate by dividing individuals into covariates.

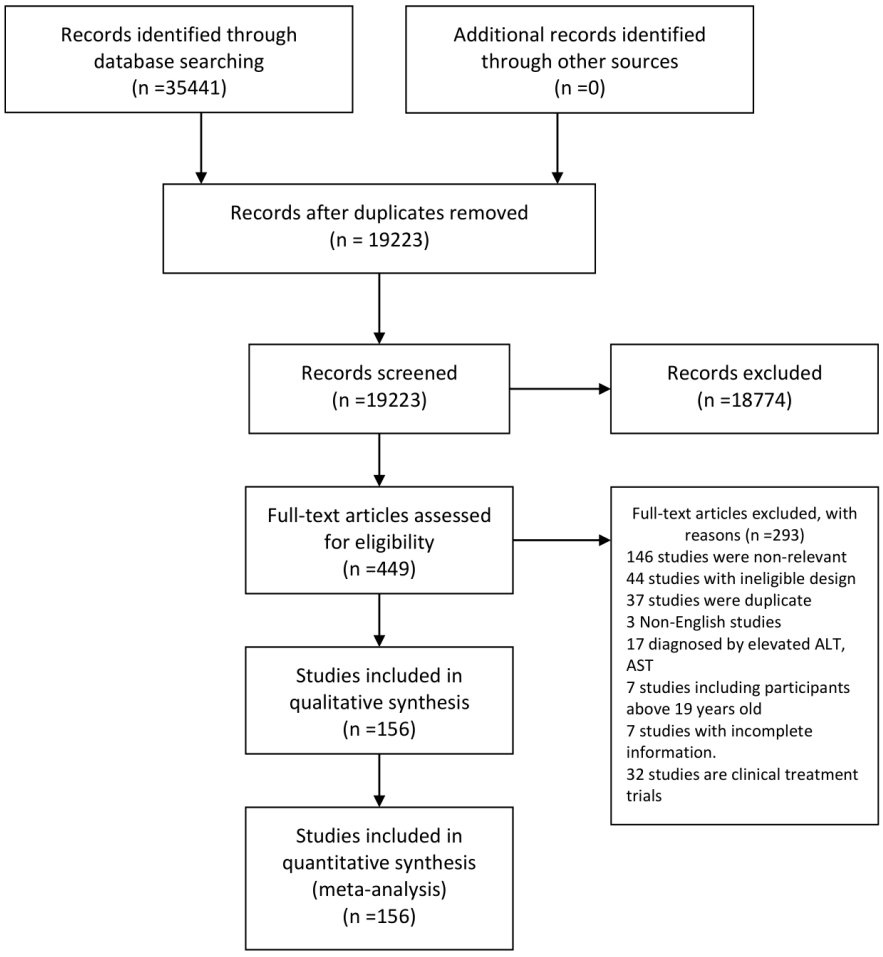

Figure 1. Study selection.

Results

Our search retuned 35441 records. After removing duplicates, 19223 studies were retained. By screening titles and abstracts, 18774 records were further excluded. Full text of the remaining 449 studies were assessed for eligibility, of which 293 were excluded. As a result, 156 studies from 32 countries and regions (Albania [n=1], Australia [n=2], Brazil [n=12], Mainland China [n=12], Canada [n=2], Chile [n=1], Colombia [n=2], Denmark [n=3], Egypt [n=4], Germany [n=5], Germany, Austria and Switzerland [n=1], Greece [n=2], Hong Kong [n=1], India [n=5], Iran [n=8], Israel [n=2], Italy [n=15], Japan [n=3], Malaysia [n=1], Mexico [n=2], Netherlands [n=4], Pakistan [n=1], Poland [n=5], Romania [n=2], Saudi Arabia [n=1], South Korea [n=7], Spain [n=6], Taiwan [n=8], Sri Lanka [n=1], Turkey [n=22], United Arab Emirates [n=1] and USA [n=14]) fulfill our inclusion criteria (Figure 1). The quality assessment score for included studies ranged from 6 to 9, with mean quality score as 7.46. A total of 147 high quality and 9 fair quality studies were included in the meta-analysis (Appendix Table 1). Characteristics of all included studies were listed in Appendix Table 1. The majority of these included studies had a cross-sectional design and most of them reported data from hospital or outpatient clinic settings. The mean or median age of participants across different studies ranged from 7.00 to 17.01 years, and the percentages of males ranged from 19.60% to 100%.

Among these included studies, 29 studies comprising 6095 individuals concerning MAFLD prevalence in overweight and obese children and adolescents from general population. The overall prevalence in this population was 34.76% (95% CI 27.78-42.08) regardless of diagnostic techniques. By stratifying data according to continents, the prevalence of MAFLD was 43.05% (95% CI 37.04-50.06), 40.89% (95% CI 34.54-47.39), 38.39% (95% CI 29.01-48.23), 24.09% (95% CI 16.51-32.57), and 22.86% (95% CI 11.65-36.46) in North America, Oceania, Asia, Europe and South America, respectively. The highest rate was observed in India (60.92%, 95% CI 54.60-67.07) and the lowest in Pakistan (10.45%, 95% 4.08-19.07, Figure 2). The majority of studies (89.66%) used ultrasound diagnosing MAFLD with the pooled prevalence rate of 35.07% (95% CI 27.76-42.73, Table 1, Appendix Figure S1). Subgroup analysis revealed that MAFLD was more prevalent in developing countries (38.69%, 95% CI 29.28-48.54) than developed countries (25.97%, 95% CI 18.66-34.00). In respect of the income of countries or regions, the pooled estimate prevalence of high, upper-middle and lower-middle countries or regions was 29.09% (95% 21.71-37.06), 40.94% (95% CI 27.92-54.64) and 40.71% (95% CI 9.91-76.22). Moreover, the MAFLD prevalence was 27.06% (95% CI 20.20-34.51) in participants below 10 years old and 43.65% (95% CI 27.66-60.34) in those above 10 years old. The pooled prevalence was 34.28% (95% CI 21.33-48.50) and 25.48% (95% CI 16.64-35.41) in boys and girls, respectively. Stratified participants by BMI, MAFLD prevalence was 22.87% (95% CI 14.49-32.47) in overweight participants and 38.91% (95% CI 29.42-48.83, Table 2) in obese participants.

A total of 127 studies comprising 36357 individuals were included for estimating MAFLD prevalence in overweight and obese patients from hospital or outpatient settings. The overall prevalence rate regardless of diagnostic techniques used was 45.33% (95% CI 40.74-49.96, Figure 3). The pooled regional prevalence estimates in this population were 59.82% (95% CI 43.61-56.02) for Asia, 38.69% (95% CI 31.09-46.58) for Europe, 52.20% (95% CI 33.32-70.77) for Africa, 47.34% (95% CI 31.99-62.95) for North America, 39.46% (95% CI 30.85-48.41) for South America and 67.44% (95% CI 59.08-75.28) for Oceania, though the number of studies for Oceania was limited. The prevalence varied substantially among different countries and regions, from 8.62% (Germany, Austria and Switzerland, 95% CI 8.09-9.18) to 86.67% (Japan, 95% CI 74.94-95.29). For countries or regions with more than

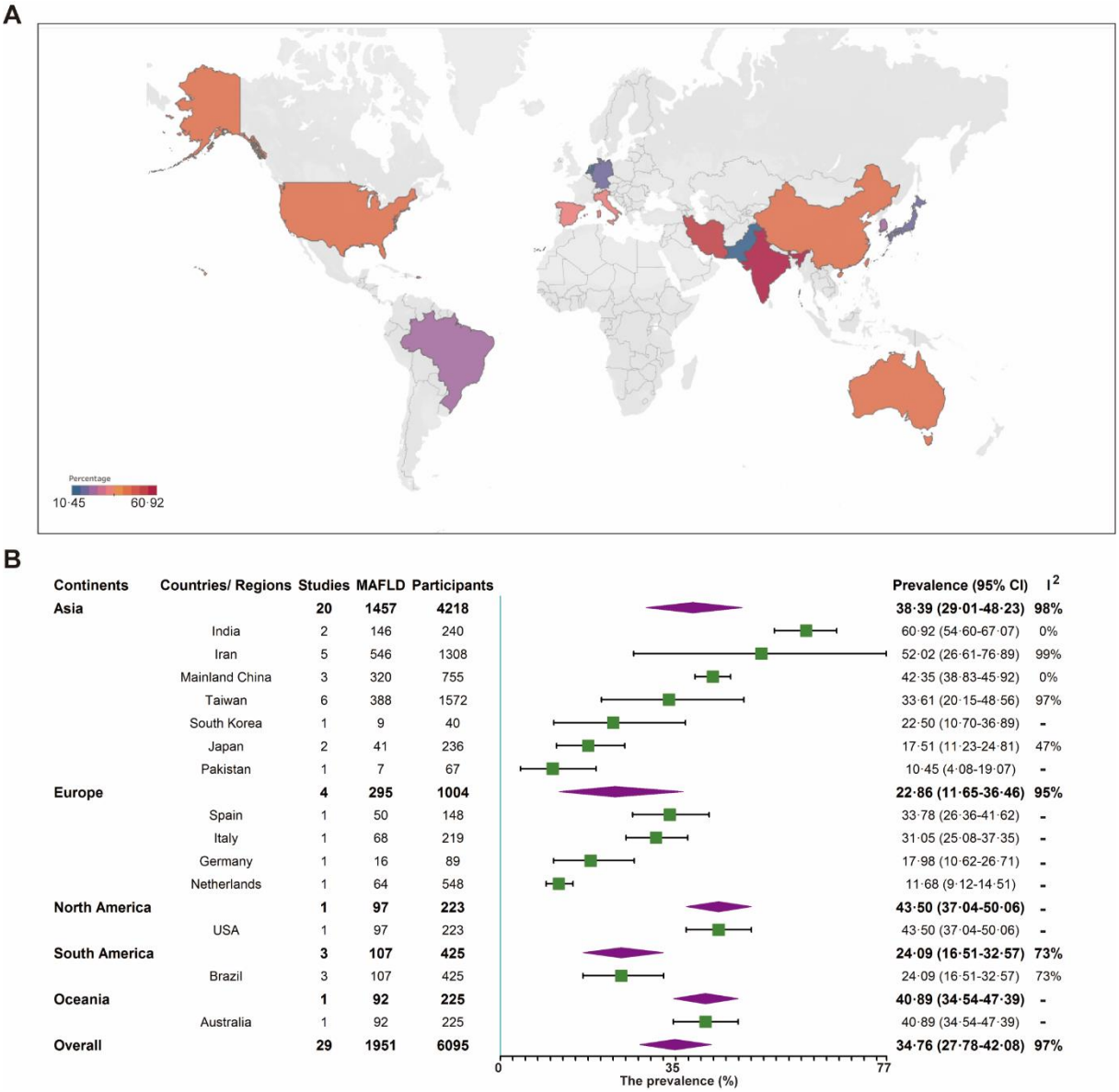

Figure 2. MAFLD prevalence in general population regardless of the diagnostic techniques. (A) Forest plot of MAFLD prevalence. (B) MAFLD prevalence in 14 countries and regions.

three studies included, MAFLD was most prevalent in Mainland China (54.09%, 95% CI 45.69-62.38) and the least in Germany (28.15%, 95% CI 25.76-30.60). Considering the diagnostic techniques, 96 studies used ultrasound (46.82%, 95% CI 41.47-52.20), 15 studies used magnetic resonance imaging (MRI, 34.48%, 95% CI 29.60-39.53), 11 studies used liver biopsy (46.94%, 95% CI 18.75-76.20), 5 studies used proton magnetic resonance spectroscopy (H-MRS, 50.23%, 95% CI 30.57-69.86), 1 studies used fatty liver index (FLI, 22.11%, 95% CI 16.60-28.16) and 1 studies used controlled attenuation parameter (CAP, 53.17%, 95% CI 44.41-61.85, Table 1). Since ultrasound was most commonly used, only these studies were included for the remaining analysis unless otherwise specified. For subgroup analysis, MAFLD was most prevalent in Mainland China (51.83%, 95% CI 41.98-61.62) and the least in Germany (28.15%, 95% CI 25.76-30.60, Appendix Figure S2). MAFLD prevalence was 48.44% (95% CI 42.58-54.32) in developing and 44.50% (95% CI 36.03-53.13) in developed countries. The pooled estimates among high, upper-middle and lower-middle countries.

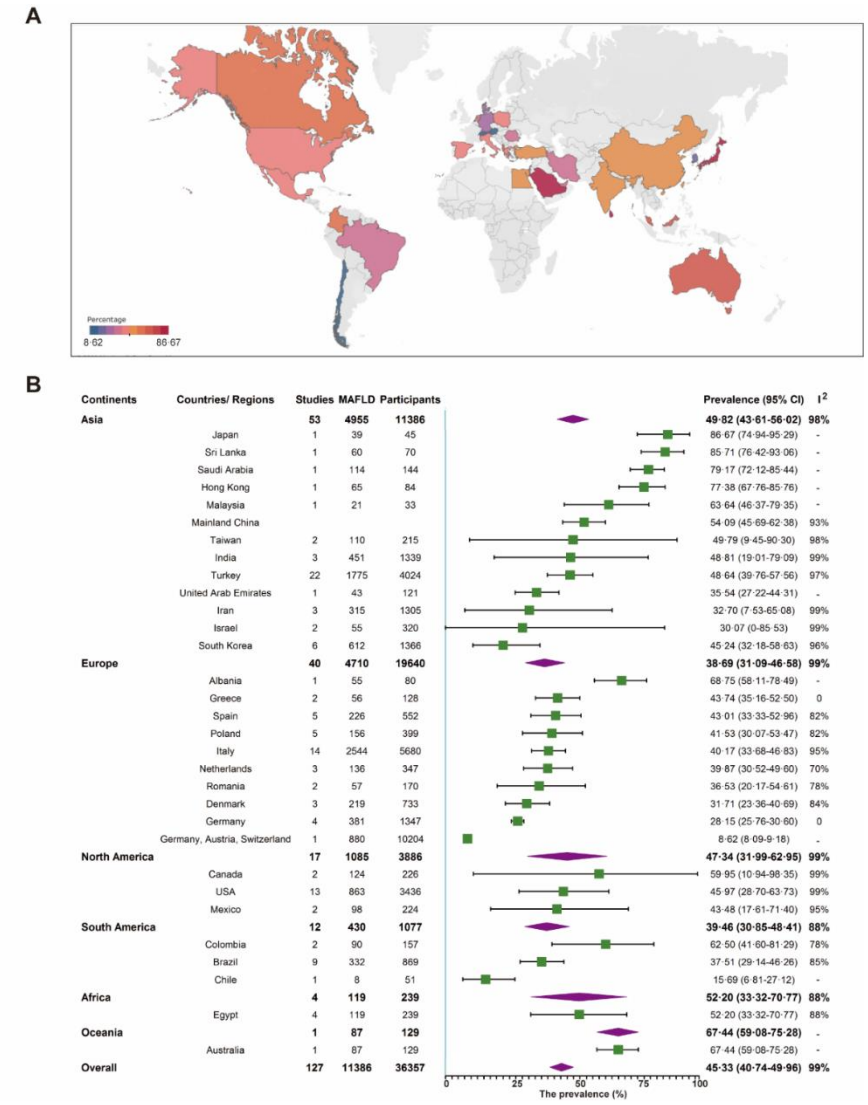

Figure 3. MAFLD prevalence in clinical population regardless of the diagnostic techniques. (A) Forest plot of MAFLD prevalence. (B) MAFLD prevalence in 31 countries and regions.

were 45.54% (95% CI 37.23-53.98), 47.76% (95% CI 41.62-53.92) and 48.81% (95% CI 19.01-79.09), respectively. Patients with age above 10 years old had a higher prevalence rate (46.12%, 95% CI 28.42-64.33) compared to those below 10 years old (34.00%, 95% CI 16.50-54.05). The prevalence was higher in boys (51.33%, 95% CI 45.06-57.59) than in girls (36.95%, 95% CI 30.31-43.83). Pooled estimates from six studies revealed a prevalence of 27.41% (95% CI 12.10-46.01) in overweight patients. Pooled analysis of 75 studies resulted in a rate of 48.32% (95% CI 41.83-54.84) in obese patients. There is a slightly increase of MAFLD prevalence when comparing study period before and after year 2010 (44.32%, 95% CI 33.42-55.51 versus 47.77%, 95% CI 42.32-53.25). MAFLD prevalence for studies with a quality assessment score above or below 8 points was 42.53% (95% CI 34.39-50.88) and 50.25% (95% CI 45.41-55.08), respectively. Studies with sample size less than 100 (41.85%, 95% 35.65-48.18) have a lower rate than those with over 100 participants (57.36%, 95% CI 51.15-63.46, Table 2).

Table 1. MAFLD prevalence by different diagnostic techniques in general and clinical populations.

	Studies	Individuals	Prevalence (95% CI)	I^2 (%)
General				
MRI	3	857	32.23% (9.44-60.78)	98%
US	26	5238	35.07% (27.76-42.73)	97%
Clinical*				
CAP	1	126	53.17% (44.41-61.85)	-
FLI	1	199	22.11% (16.60-28.16)	-
H-MRS	5	363	50.23% (30.57-69.86)	92%
Liver biopsy	9	2211	46.94% (18.75-76.20)	99%
MRI	15	2797	34.48% (29.60-39.53)	85%
US	96	30661	46.82% (41.47-51.20)	99%

MRI, magnetic resonance imaging; US, ultrasound; CAP, Controlled attenuation parameter; FLI, fatty liver index; H-MRS, proton magnetic resonance spectroscopy; *P<0.001 for difference across diagnostic methods.

Discussion

In this study, we performed a systematic review and meta-analysis based on existing epidemiology data on fatty liver disease in overweight or obese children and adolescents, but transformed the data to the new diagnosis criteria of MAFLD. We found the global MAFLD prevalence to be about 45% in clinical settings and 35% in the general population among overweight or obese children and adolescents aged between 1 and 19 years, regardless of the diagnostic techniques used. Based on the commonly used ultrasound methodology for diagnosis, we estimated a prevalence rate of 22.87% (95% CI 14.49-32.47) in overweight and 38.91% (95% CI 29.42-48.83) in

obese children and adolescents from the general population. These rates are 27.41% (95% CI 12.10-46.01) and 48.32% (95% CI 41.83-54.84) in the clinical setting of overweight or obese children and adolescents, respectively.

Table 2. Subgroup analysis of MAFLD prevalence in general and clinical populations based on ultrasound diagnosis.

	General population				Clinical population			
	Studies	**Prevalence (95% CI)**	**I^2**	**P**	**Studies**	**Prevalence (95% CI)**	**I^2**	**P**
Continents			97%	<0.01			99%	<0.01
Asia	19	37.98% (28.32-48.14)	98%		51	49.17% (42.84-55.52)	98%	
Europe	3	27.91% (19.85-36.74)	74%		29	40.45% (30.98-50.29)	99%	
Oceania	1	40.89% (34.54-47.39)	-		1	67.44% (59.08-75.28)	-	
Africa	-	-	-		2	60.00% (19.75-93.65)	96%	
North America	-	-	-		5	63.46% (42.28-82.29)	95%	
South America	3	24.09% (16.51-32.57)	73%		8	38.60% (29.56-48.05)	86%	
Development			97%	0.04			99%	0.46
Developed	7	25.97% (18.66-34.00)	86%		40	44.50% (36.03-53.13)	99%	
Developing	19	38.69% (29.28-48.54)	98%		56	48.44% (42.58-4.32)	97%	
Income			97%	0.29			99%	0.91
High	13	29.09% (21.71-37.06)	94%		43	45.54% (37.23-53.98)	99%	
Upper-middle	10	40.94% (27.92-54.64)	98%		50	47.76% (41.62-53.2)	97%	
Lower-middle	3	40.71% (9.91-76.22)	97%		3	48.81% (19.01-79.09)	99%	
Gender			90%	0.30			94%	<0.01
Boy	8	34.28% (21.33-48.50)	92%		23	51.33% (45.06-57.59)	92%	
girl	8	25.48% (16.64-35.41)	85%		23	36.95% (30.31-43.83)	93%	
Age			97%	0.07			99%	0.38
1< and≤10	4	27.06% (20.20-34.51)	65%		4	34.00% (16.50-54.05)	95%	

10<and≤19	10	43.65% (27.66-60.34)	98%		13	46.12% (28.42-64.33)	99%	
Study period				0.11			99%	0.59
Before 2010	14	29.23% (21.35-37.78)	94%		29	44.32% (33.42-55.51)	99%	
After 2010	10	43.61% (28.48-59.37)	98%		59	47.77% (42.32-53.25)	97%	
Sample size			97%	0.56			99%	<0.01
<100		30.71% (15.27-48.66)	94%		32	57.36% (51.15-63.46)	88%	
≥100	19	36.65% (28.29-45.43)	97%		64	41.85% (35.65-48.18)	99%	
Quality			97%	0.60			99%	0.12
<8	12	37.01 (23.71-51.37)	98%		53	50.25% (45.41-55.08)	95%	
≥8	14	32.77% (25.90-40.02)	94%		43	42.53% (34.39-50.88)	99%	
BMI								
Overweight	10	22.87% (14.49-32.47)	92%		6	27.41% (12.10-46.01)	98%	
Obese	20	38.91% (29.42-48.83)	96%		75	48.32% (41.83-54.84)	99%	

The terminology describing NAFLD and non-alcoholic steatohepatitis (NASH) was defined now 40 years ago.[12] This definition requires the exclusion of other causes of liver disease and the exclusion of detrimental alcohol consumption but the exact cut-offs in respect remains open to debate. Because of this ambiguity, it is now recognized fatty liver disease needs redefinition and thus renaming.[13] MAFLD is a new terminology recently proposed by a panel of international experts to replace NAFLD.[8-9] This updated nomenclature shifts towards an inclusionary diagnosis that does not require exclusion of alcohol intake or that of other liver diseases. As proposed, a diagnosis of MAFLD should be based on detection of liver steatosis with one of the following three conditions, overweight/obesity and/or presence of T2DM, and/or evidence of metabolic dysregulation.[8-9] A recent study has endeavored to compare MAFLD and NAFLD criteria in the real world using the large population-based National Health and Nutrition Examination Survey (NHANES) database. Although a diagnosis of MAFLD does not require exclusion of excessive alcohol consumption or other liver diseases, a similar prevalence rate as NAFLD was detected. However, MAFLD criteria were found to be more practical for identifying fatty liver disease patients with high risk of disease progression.[14] There are strong indications of a global acceptance and endorsement of the term MAFLD,[15] but the issue remains open to fierce debate. For example, it is reasonable to argue that currently there is no general consensus on the criteria to define ‘‘metabolic dysfunction”, and adding the new term “metabolic” does not fully

solve the ambiguity regarding etiologies of the disease.[16] We noticed, however, that MAFLD is relatively straightforward to be defined in the overweight or obese population. Globally, over 1.9 billion adults and about 400 million children and adolescents were overweight or obese in 2016.[2]

The prevalence of obesity has nearly tripled since 1975, and this parallels the growth of the fatty liver disease epidemic. Strong associations between obesity and prevalence of fatty liver disease are well-documented, both in children and adolescents.[17] A previous study attempted to depict the dynamic changes of NAFLD prevalence in adolescents aged 12-19 years using data from different periods of the NHANES database. Strikingly, the prevalence of NAFLD has increased from 3.9% in 1988-1994 to 10.7% in 2007-2010.[18] A recent meta-analysis estimated that the NAFLD prevalence rate in overweight or obese children from general population was 12.5% and 36%, respectively. NAFLD prevalence among children based on child obesity clinics has been reported as 34%,[7] but we observed a much higher (1.5-fold) rate of MAFLD in this population. This discrepancy may be attributed to differences in disease definition between NALFD and MAFLD, and/or population selection. NAFLD could represent an umbrella term for the multiple underlying sub-types which underestimates the prevalence of fatty liver disease.[19,20]

Extensive studies have highlighted the importance of technique in the diagnosis of fatty liver disease. Ultrasound has been the most used diagnostic method in both clinical and general populations and majorly contributes to the satisfactory sensitivity and specificity.[21,22] In the general population, we found no evidence of differences in MAFLD prevalence when analyzed with respect to different diagnostic techniques. In the clinical population, the prevalence of MAFLD diagnosed by H-MRS was higher than that by MRI or ultrasound. Interestingly, ultrasound and liver biopsy diagnoses yielded similar rates of MAFLD prevalence. Arguments have been raised against the application of liver enzymes for diagnosing fatty liver disease because occurrence of normal levels of these enzymes has been reported across the entire spectrum of NAFLD manifestations.[23,24] In line with this, the new diagnostic criteria of MAFLD no longer adopt elevated ALT and AST as markers for assessing fatty liver disease.

To our knowledge, this is the first study to comprehensively estimate the global epidemiology of MAFLD, even if clear limitations to our study exist. Firstly, there is a retrospective transformation of previous fatty liver disease data to the MAFLD epidemiological estimation. Any pre-existing bias in population selection will thus be copied to our results. Secondly, limited data are available for Africa and Oceania constituting a challenge to the accuracy for our estimates on these continents. There is limited data regarding race, ethnics, familial risk, epidemic factors and genetic variation, hence we could not perform further subgroup analysis. Fourthly, the high heterogeneity underlying some of the source data in the current study cannot be fully explained, and thus calls for caution. Finally, there are no consistent standards for defining overweight or obese across different countries and regions, which hampers interpretation.

In summary, this study has demonstrated a proof-of-concept on the feasibility of repurposing existing fatty liver disease data for estimating MAFLD burden. By including a large number of eligible studies across the globe, we a high prevalence rate of MAFLD in overweight or obese children and adolescents from both general or clinical populations. These findings should be interest for medical professionals and health policy makers interested in combating this disease. Given the retrospective nature of transforming previous data, future well-designed prospective studies are needed to better define the global epidemiology of MAFLD.

Reference

1. Lobstein T, Jackson-Leach R, Moodie ML, et al. Child and adolescent obesity: part of a bigger picture. *Lancet* 2015; **385**(9986): 2510-20.
2. Initiatives. D. 2018 Global Nutrition Report: Shining a Light to Spur Action on Nutrition. *Bristol: Development Initiatives Poverty Research Ltd; 2018* 2018; **https://globalnutritionreport.org/.**
3. Quek YH, Tam WWS, Zhang MWB, Ho RCM. Exploring the association between childhood and adolescent obesity and depression: a meta-analysis. *Obes Rev* 2017; **18**(7): 742-54.
4. Rankin J, Matthews L, Cobley S, et al. Psychological consequences of childhood obesity: psychiatric comorbidity and prevention. *Adolesc Health Med Ther* 2016; **7**: 125-46.
5. Friedemann C, Heneghan C, Mahtani K, Thompson M, Perera R, Ward AM. Cardiovascular disease risk in healthy children and its association with body mass index: systematic review and meta-analysis. *BMJ* 2012; **345**: e4759.
6. Alisi A, Feldstein AE, Villani A, Raponi M, Nobili V. Pediatric nonalcoholic fatty liver disease: a multidisciplinary approach. *Nat Rev Gastroenterol Hepatol* 2012; **9**(3): 152-61.
7. Anderson EL, Howe LD, Jones HE, Higgins JP, Lawlor DA, Fraser A. The Prevalence of Non-Alcoholic Fatty Liver Disease in Children and Adolescents: A Systematic Review and Meta-Analysis. *PLoS One* 2015; **10**(10): e0140908.
8. Eslam M, Sanyal AJ, George J, International Consensus P. MAFLD: A Consensus-Driven Proposed Nomenclature for Metabolic Associated Fatty Liver Disease. *Gastroenterology* 2020; **158**(7): 1999-2014 e1.
9. Eslam M, Newsome PN, Sarin SK, et al. A new definition for metabolic dysfunction-associated fatty liver disease: An international expert consensus statement. *J Hepatol* 2020; **73**(1): 202-9.
10. Moher D, Liberati A, Tetzlaff J, Altman DG, Group P. Preferred reporting items for systematic reviews and meta-analyses: the PRISMA statement. *PLoS Med* 2009; **6**(7): e1000097.
11. A Wells BS, D O'Connell, J Peterson, V Welch, M Losos, P Tugwell. The Newcastle-Ottawa Scale (NOS) for assessing the quality of nonrandomised studies in meta-analyses. (http://www.ohri.ca/programs/clinical_epidemiology/oxford.asp).
12. Kuchay MS, Misra A. From non-alcoholic fatty liver disease (NAFLD) to metabolic-associated fatty liver disease (MAFLD): A journey over 40 years. *Diabetes Metab Syndr* 2020; **14**(4): 695-6.
13. Fouad Y, Waked I, Bollipo S, Gomaa A, Ajlouni Y, Attia D. What's in a name? Renaming 'NAFLD' to 'MAFLD'. *Liver Int* 2020; **40**(6): 1254-61.
14. Lin S, Huang J, Wang M, et al. Comparison of MAFLD and NAFLD diagnostic criteria in real world. *Liver Int* 2020.
15. The Lancet Gastroenterology H. Redefining non-alcoholic fatty liver disease: what's in a name? *Lancet Gastroenterol Hepatol* 2020; **5**(5): 419.
16. Younossi ZM, Rinella ME, Sanyal A, et al. From NAFLD to MAFLD: Implications of a premature change in terminology. *Hepatology* 2020.
17. Non-alcoholic Fatty Liver Disease Study G, Lonardo A, Bellentani S, et al. Epidemiological modifiers of non-alcoholic fatty liver disease: Focus on high-risk groups. *Dig Liver Dis* 2015; **47**(12): 997-1006.
18. Welsh JA, Karpen S, Vos MB. Increasing prevalence of nonalcoholic fatty liver disease among United States adolescents, 1988-1994 to 2007-2010. *J Pediatr* 2013; **162**(3): 496-500 e1.
19. Yki-Jarvinen H, Luukkonen PK. Heterogeneity of non-alcoholic fatty liver disease. *Liver Int* 2015; **35**(12): 2498-500.
20. Lonardo A, Ballestri S, Targher G. "Not all forms of NAFLD were created equal". Do metabolic syndrome-related NAFLD and PNPLA3-related NAFLD exert a variable impact on the risk of early carotid atherosclerosis? *Atherosclerosis* 2017; **257**: 253-5.
21. European Association for the Study of the L, European Association for the Study of D, European Association for the Study of O. EASL-EASD-EASO Clinical Practice Guidelines for the Management of Non-Alcoholic Fatty Liver Disease. *Obes Facts* 2016; **9**(2): 65-90.
22. Hernaez R, Lazo M, Bonekamp S, et al. Diagnostic accuracy and reliability of ultrasonography for the detection of fatty liver: a meta-analysis. *Hepatology* 2011; **54**(3): 1082-90.
23. Mofrad P, Contos MJ, Haque M, et al. Clinical and histologic spectrum of nonalcoholic fatty liver disease associated with normal ALT values. *Hepatology* 2003; **37**(6): 1286-92.
24. Fracanzani AL, Valenti L, Bugianesi E, et al. Risk of severe liver disease in nonalcoholic fatty liver disease with normal aminotransferase levels: a role for insulin resistance and diabetes. *Hepatology* 2008; **48**(3): 792-8.

Supplementary file to

Estimating global prevalence of metabolic dysfunction-associated fatty liver disease in overweight or obese children and adolescents

Supplementary methods 1. Searching strategy for metabolic dysfunction-associated fatty liver disease in overweight or obese children and adolescents.

Database searched	Via	Records	Records after duplicates removed
Embase	Embase.com	11248	11075
Medline ALL	Ovid	10390	3157
Web of Science Core Collection	Web of Knowledge	8558	2260
Cochrane Central Register of Controlled Trials	Wiley	349	182
Other sources: Google Scholar (200 top ranked)		200	32
Additional	By searching NAFLD	4696	
Total		35441	19223

Embase

('fatty liver'/exp OR 'metabolic liver disease'/de OR 'steatohepatitis'/de OR (hepatosteato* OR steatohepat* OR AFLD OR NAFLD OR FLD OR ((fatty OR steato*) NEAR/3 (liver OR hepat*)) OR ((metabol*) NEAR/3 (liver OR hepat*) NEAR/3 (diseas* OR syndrom*))):ab,ti,kw) AND ('epidemiological data'/de OR 'epidemiology'/de OR 'geographic distribution'/de OR 'patient volume'/de OR prevalence/exp OR geography/de OR 'geographic names'/exp OR 'cross-sectional study'/de OR (epidemiolog* OR ((geograph* OR global*) NEAR/3 (distribut*)) OR (patient* NEAR/3 volume*) OR prevalen* OR population-based* OR cross-sectional*):ab,ti,kw) NOT ([animals]/lim NOT [humans]/lim) NOT ('case report'/de OR 'case report*':ti) NOT ([Conference Abstract]/lim) AND [english]/lim

Medline

(exp Fatty Liver/ OR Liver Diseases/me OR (hepatosteato* OR steatohepat* OR AFLD OR NAFLD OR FLD OR ((fatty OR steato*) ADJ3 (liver OR hepat*)) OR ((metabol*) ADJ3 (liver OR hepat*) ADJ3 (diseas* OR syndrom*))).ab,ti,kw.) AND (Epidemiological Monitoring/ OR Epidemiology/ OR Epidemiology.fs. OR exp Incidence/ OR exp Prevalence/ OR Geography/ OR exp Geographic Locations/ OR Epidemiologic Studies OR Cross-Sectional Studies/ OR (epidemiolog* OR ((geograph* OR global*) ADJ3 (distribut*)) OR (patient* ADJ3 volume*) OR prevalen* OR population-based* OR cross-sectional*).ab,ti,kw.) NOT (exp Animals/ NOT Humans/) NOT (Case Reports/ OR case report*.ti.)

NOT (news OR congres* OR abstract* OR book* OR chapter* OR dissertation abstract*).pt. AND english.la.

Cochrane

((hepatosteato* OR steatohepat* OR AFLD OR NAFLD OR FLD OR ((fatty OR steato*) NEAR/3 (liver OR hepat*)) OR ((metabol*) NEAR/3 (liver OR hepat*) NEAR/3 (diseas* OR syndrom*))):ab,ti) AND ((epidemiolog* OR ((geograph* OR global*) NEAR/3 (distribut*)) OR (patient* NEAR/3 volume*) OR prevalen* OR population-based* OR cross-sectional*):ab,ti)

Web of Science

TS=(((hepatosteato* OR steatohepat* OR AFLD OR NAFLD OR FLD OR ((fatty OR steato*) NEAR/2 (liver OR hepat*)) OR ((metabol*) NEAR/2 (liver OR hepat*) NEAR/2 (diseas* OR syndrom*)))) AND ((epidemiolog* OR ((geograph* OR global*) NEAR/2 (distribut*)) OR (patient* NEAR/2 volume*) OR prevalen* OR population-based* OR cross-sectional*)) NOT ((animal* OR rat OR rats OR mouse OR mice OR murine OR dog OR dogs OR canine OR cat OR cats OR feline OR rabbit OR cow OR cows OR bovine OR rodent* OR sheep OR ovine OR pig OR swine OR porcine OR veterinar* OR chick* OR zebrafish* OR baboon* OR nonhuman* OR primate* OR cattle* OR goose OR geese OR duck OR macaque* OR avian* OR bird* OR fish*) NOT (human* OR patient* OR women OR woman OR men OR man))) AND DT=(Article OR Review) AND LA=(English)

Google Scholar

hepatosteatosis|steatohepatitis|AFLD|NAFLD|FLD|"fatty|steatotic liver"|"liver|hepatic steatosis"|"metabolic liver disease" epidemiology|prevalence|"geographic|global distribution"|"patient volume"|"population based"|"cross sectional"

Additional searching for Non-alcoholic fatty liver disease

embase.com

('nonalcoholic fatty liver'/exp OR (((nonalcohol* OR non-alcohol*) NEAR/3 (fatty-liver* OR steatohepat* OR fld OR hepatosteato*)) OR ((nonalcohol* OR non-alcohol*) NEAR/3 steato* NEAR/3 (hepat* OR liver*)) OR nafld):ab,ti) AND ('epidemiological data'/de OR 'epidemiology'/de OR 'geographic distribution'/de OR incidence/exp OR 'patient volume'/de OR prevalence/exp OR geography/de OR 'geographic names'/exp OR (epidemiolog* OR ((geograph* OR global*) NEAR/3 (distribut*)) OR incidenc* OR (patient* NEAR/3 volume*) OR prevalen*):ab,ti) NOT ([animals]/lim NOT [humans]/lim) NOT ('case report'/de OR 'case report*':ti) NOT ([Conference Abstract]/lim) AND [english]/lim

Medline Ovid

(Non-alcoholic Fatty Liver Disease/ OR (((nonalcohol* OR non-alcohol*) ADJ3 (fatty-liver* OR steatohepat* OR fld OR hepatosteato*)) OR ((nonalcohol* OR non-alcohol*) ADJ3 steato* ADJ3 (hepat* OR liver*)) OR nafld).ab,ti.) AND (Epidemiological Monitoring/ OR Epidemiology/ OR Epidemiology.fs. OR exp Incidence/ OR exp Prevalence/ OR Geography/ OR exp Geographic Locations/ OR (epidemiolog* OR ((geograph* OR global*) ADJ3 (distribut*)) OR incidenc* OR (patient* ADJ3 volume*) OR prevalen*).ab,ti.) NOT (exp animals/ NOT humans/) NOT (case report/ OR case report*.ti.) NOT (news OR congres* OR abstract* OR book* OR chapter* OR dissertation abstract*).pt. AND english.la.

Web of science Core Collection

TS=(((((nonalcohol* OR non-alcohol*) NEAR/2 (fatty-liver* OR steatohepat* OR fld OR hepatosteato*)) OR ((nonalcohol* OR non-alcohol*) NEAR/2 steato* NEAR/2 (hepat* OR liver*)) OR nafld)) AND ((epidemiolog* OR ((geograph* OR global*) NEAR/2 (distribut*)) OR incidenc* OR (patient* NEAR/2 volume*) OR prevalen*)) NOT ((animal* OR rat OR rats OR mouse OR mice OR murine OR dog OR dogs OR canine OR cat OR cats OR feline OR rabbit OR cow OR cows OR bovine OR rodent* OR sheep OR ovine OR pig OR swine OR porcine OR veterinar* OR chick* OR zebrafish* OR baboon* OR nonhuman* OR primate* OR cattle* OR goose OR geese OR duck OR macaque* OR avian* OR bird* OR fish*) NOT (human* OR patient* OR women OR woman OR men OR man))) NOT TI=("case report*") AND LA=(english) AND DT=(article) Cochrane CENTRAL ((((nonalcohol* OR non-alcohol*) NEAR/3 (fatty-liver* OR steatohepat* OR fld OR hepatosteato*)) OR ((nonalcohol* OR non-alcohol*) NEAR/3 steato* NEAR/3 (hepat* OR liver*)) OR nafld):ab,ti) AND ((epidemiolog* OR ((geograph* OR global*) NEAR/3 (distribut*)) OR incidenc* OR (patient* NEAR/3 volume*) OR prevalen*):ab,ti)

Supplementary table 1. Characteristics for included studies.

Study	Country/ Region	Publication Year	Study Time	Study Design	Sample Source	Diagnostic Technique	MAFLD	Individuals	Body Mass Index	Quality
Adibi.A[1]	Iran	2009	2006-2007	Cross-sectional	Community	US	157	544	BMI >85th percentile with age- and sex-adjustment	8
Alavian.SM[2]	Iran	2008	2007	Cross-sectional	Community	US	45	267	BMI>25	8
Parray.IA[3]	India	2013	2008-2010	Cross-sectional	Community	US	23	42	Not specified	8
Pawar.SV[4]	India	2016	2016	Cross-sectional	Community	US	123	198	Overweight and obese was done using both Khadilkar criteria and Cole criteria	7
Geurtsen.M[5]	Netherlands	2019	2002-2006	Cross-sectional	Hospital	MRI	64	548	BMI >85th percentile	8
Kazemi.SA[6]	Iran	2016	2016	Cross-sectional	Community	US	104	145	BMI >85th percentile	7
Fu.CC[7]	Taiwan	2009	2002	Cross-sectional	Community	US	71	122	BMI >85th percentile	8
Khalkhali.HR[8]	Iran	2016	2013	Cross-sectional	School	US	132	150	BMI >85th percentile	7
Lin.M[9]	Taiwan	2017	2012-2013	Cross-sectional	Community	US	35	197	BMI >95th percentile	7
Lin.YC[10]	Taiwan	2012	2006-2011	Cross-sectional	Community	US	182	781	BMI >95th percentile	8
Tominaga.K[11]	Japan	1995	1989	Cross-sectional	School	US	20	138	BMI>18	7
Monteiro.PA[12]	Brazil	2014	2009	Cross-sectional	Community	US	45	145	According to the Cole criteria	8
Namakin.K[13]	Iran	2018	2018	Cross-sectional	Community	US	108	202	BMI >85th percentile	7
Nier.A[14]	Germany	2018	2009-2010	Cross-sectional	School	US	16	89	Not specified	8

Ramzan.M[15]	Pakistan	2009	2009	Cross-sectional	School	US	7	67	BMI >85th percentile	7
Fernandes.M[16]	Brazil	2010	2010	Cross-sectional	Community	US	14	90	BMI >95th percentile	7
Black.LJ[17]	Australia	2014	2006-2008	Prospective	School	US	92	225	BMI >85th percentile	8
Walker.RW[18]	USA	2013	2013	Cross-sectional	Community	MRI	97	223	BMI>25	8
Zhang.XM[19]	China	2015	2009-2011	Cross-sectional	Community	US	241	569	BMI >95th percentile	7
Tsuruta.G[20]	Japan	2010	2004-2007	Cross-sectional	School	US	21	98	BMI >85th percentile	8
Zhao.YZ[21]	China	2019	2017-2018	Cross-sectional	School	MRI	40	86	BMI >85th percentile	8
Dai.DL[22]	China	2017	2017	Cross-sectional	School	US	39	100	BMI >95th percentile	8
Huang.SC[23]	Taiwan	2013	2009	Cross-sectional	Community	US	42	203	BMI >85th percentile	7
Kim.IK[24]	South Korea	2008	2005	Cross-sectional	Community	US	9	40	BMI>25	7
Lin.YC[25]	Taiwan	2009	2006	Cross-sectional	Community	US	28	234	BMI >95th percentile	8
Monteiro.PA[26]	Brazil	2013	2010	Cross-sectional	Community	US	48	190	BMI >95th percentile	8
Berna.SJD[27]	Spain	2017	2013-2014	Cross-sectional	School	US	50	148	BMI z-score > 1	7
Shashaj.B[28]	Italy	2014	2011-2012	Cross-sectional	Community	US	68	219	BMI changed from normal weight to overweight or obesity in the previous 12 months according to the International Obesity Task Force	8
Kao.JT[29]	Taiwan	2008	1999-2005	Cross-sectional	School	US	30	35	CDC's BMI-for-age growth charts for girls and boys in the USA	8
Akcam.M[30]	Turkey	2013	2010-2011	Cross-sectional	Hospital	US	157	544	BMI >95th percentile	8
Alp.H[31]	Turkey	2013	2006	Cross-sectional	Hospital	US	45	267	BMI >95th percentile	6
Arenaza.L[32]	Spain	2019	2017	Cross-sectional	Hospital	US	23	42	overweight or obesity according to World Obesity Federation criteria	8
Arslan.N[33]	Turkey	2005	2005	Cross-sectional	Hospital	US	123	198	BMI of age- and sex matched children in the 50th percentile, then	6

									multiplied by 100. The ratio above 120 as obesity	
Boyraz.M[34]	Turkey	2013	2008-2012	Cross-sectional	Hospital	MRI	64	548	BMI >95th percentile	7
Fu.JF[35]	China	2011	2004-2009	Cross-sectional	Hospital	US	104	145	BMI >95th percentile	8
Atabek.ME[36]	Turkey	2014	2014	Cross-sectional	Hospital	US	71	122	BMI >95th percentile	8
Bedogni.G[37]	Italy	2012	2007-2009	Cross-sectional	Hospital	US	132	150	BMI >85th percentile	8
Belei.O[38]	Romania	2017	2015-2017	Cross-sectional	Hospital	US	35	197	BMI >95th percentile	7
Benetolo.P[39]	Brazil	2018	2014-2016	Cross-sectional	Hospital	US	182	781	BMI >95th percentile	7
Burgert.TS[40]	USA	2006	2004	Cross-sectional	Hospital	US	20	138	BMI>18	7
Cardoso.AS[41]	Brazil	2013	2009-2010	Cross-sectional	Hospital	US	45	145	BMI>Z score+2	7
Chan.DFY[42]	Hong Kong	2004	2000-2002	Cross-sectional	Hospital	US	108	202	BMI >85th percentile	7
Daar.G[43]	Turkey	2015	2013-2014	Cross-sectional	Hospital	US	16	89	Two standard deviations above the mean BMI for age and sex	7
Das.MK[44]	India	2017	2017	Cross-sectional	Hospital	US	7	67	BMI>18.5	8
Zusi.C[45]	Italy	2019	2019	Cross-sectional	Hospital	US	14	90	BMI >95th percentile	8
Costanzo.DI[46]	Italy	2019	2019	Cross-sectional	Hospital	US	92	225	BMI >85th percentile	8
Dursun.F[47]	Turkey	2019	2019	Cross-sectional	Hospital	MRI	97	223	BMI>25	8
Karaksy.HM[48]	Egypt	2011	2011	Cross-sectional	Hospital	US	241	569	BMI >95th percentile	7
Eminoglu.O[49]	Turkey	2008	2003-2005	Cross-sectional	Hospital	US	21	98	BMI >85th percentile	7
Erol.M[50]	Turkey	2016	2015	Cross-sectional	Hospital	MRI	40	86	BMI >85th percentile	7
Felix.DR[51]	Brazil	2016	2010-2013	Cross-sectional	Hospital	US	39	100	BMI >95th percentile	7
Ferraioli.G[52]	Italy	2017	2012-2016	Cross-sectional	Hospital	US	42	203	BMI >85th percentile	8
Fonvig.CE[53]	Denmark	2015	2009-2014	Cross-sectional	Hospital	US	9	40	BMI>25	8
Gheibi.S[54]	Iran	2019	2016-2017	Cross-sectional	Hospital	US	28	234	BMI >95th percentile	8
Hamza.RT[55]	Egypt	2016	2011-2013	Cross-sectional	Hospital	US	48	190	BMI >95th percentile	7
Han.XC[56]	China	2020	2020	Cross-sectional	Hospital	US	50	148	BMI z-score > 1	8

Hatipoglu.N[57]	Turkey	2016	2016	Cross-sectional	Hospital	US	68	219	BMI changed from normal weight to overweight or obesity in the previous 12 months according to the International Obesity Task Force	7
Hu.W[58]	China	2017	2012-2013	Cross-sectional	Hospital	US	84	169	BMI >95th percentile	8
Rivera.CJ[59]	Canada	2017	2009-2012	Cross-sectional	Hospital	US	93	400	BMI >95th percentile	8
Kalthenbach. TE[60]	Germany	2016	2000-2001	Cross-sectional	Hospital	MRI	40	110	BMI–standard deviation scores (BMI-SDS) based on German reference values.	8
Wiegand.S[61]	Germany, Austria and Switzerland	2010	2001-2009	Cross-sectional	Hospital	US	38	322	BMI >90th percentile	8
Zhang.HX[62]	China	2014	2009-2011	Cross-sectional	Hospital	US	217	451	Not specified	8
Kim.JY[63]	South Korea	2018	2004-2016	Cross-sectional	Hospital	US	587	861	BMI Z score >1	8
Kistler.KD[64]	USA	2010	2007	Cross-sectional	Hospital	US	38	217	BMI >85th percentile	8
Kodhelaj.K[65]	Albania	2014	2010	Cross-sectional	School	US	234	571	BMI >85th percentile	7
Labayen.I[66]	Spain	2018	2018	Cross-sectional	Hospital	US	36	125	BMI >85th percentile	8
Lee.JH[67]	South Korea	2017	2013	Cross-sectional	Hospital	MRI	14	50	BMI >85th percentile	8
Liang.S[68]	China	2017	2013-2015	Cross-sectional	Hospital	MRI	125	392	BMI >95th percentile	8
Mameli.C[69]	Italy	2018	2010-2017	Cross-sectional	Hospital	US	37	129	BMI Z score >1	8
De piano.A[70]	Brazil	2007	2007	Cross-sectional	Hospital	US	65	84	BMI>30	7
Mohammed.RZ[71]	Malaysia	2020	2015	Cross-sectional	Hospital	US	43	53	BMI >85th percentile	7
Ardakali.AT[72]	Iran	2014	2012	Cross-sectional	Hospital	US	215	961	BMI>18.5	7
Navarro.JM[73]	Spain	2013	2013	Cross-sectional	Hospital	US	347	514	BMI >95th percentile	8
Franzese.A[74]	Italy	1997	1997	Cross-sectional	Hospital	MRI	105	230	BMI >85th percentile	8
Guzzaloni.G[75]	Italy	2000	2000	Cross-sectional	Hospital	US	49	110	BMI >95th percentile	8
Oh.MS[76]	South Korea	2019	2015	Cross-sectional	Hospital	Biopy	33	76	BMI >85th percentile	7
Ozhan.B[77]	Turkey	2016	2016	Cross-sectional	Hospital	US	53	101	BMI >95th percentile	7

Pacifico.L[78]	Italy	2016	2007-2015	Cross-sectional	Hospital	US	62	107	BMI >85th percentile	8
Papandreou.D[79]	Greece	2012	2007-2011	Cross-sectional	Hospital	US	8	39	BMI >95th percentile	7
Pozzato.C[80]	Italy	2008	2006-2007	Cross-sectional	Hospital	FLI	44	199	According to the Cole criteria	7
Sagi.R[81]	Israel	2007	2003-2004	Cross-sectional	Hospital	MRI	89	287	BMI >90th percentile	8
Prokopowicz.Z[82]	Poland	2018	2012-2014	Cross-sectional	Hospital	US	69	747	LMS method based on Polish reference values	8
Radetti.G[83]	Italy	2006	2004	Cross-sectional	Hospital	US	40	50	BMI >95th percentile	7
Ruiz-Extremera.A[84]	Spain	2011	2011	Cross-sectional	Hospital	US	262	620	BMI >95th percentile	7
Schlieske.C[85]	Germany	2014	2014	Cross-sectional	Hospital	US	88	248	BMI >95th percentile	7
Damaso.AR[86]	Brazil	2008	2008	Cross-sectional	Hospital	US	40	71	BMI >95th percentile	7
Jung.JH[87]	South Korea	2015	2013-2014	Retrospective	Hospital	US	82	97	BMI >95th percentile	8
Sezer.OB[88]	Turkey	2016	2015	Cross-sectional	Hospital	US	99	332	BMI >95th percentile	7
Yildiz.I[89]	Turkey	2014	2012-2013	Cross-sectional	Hospital	US	880	10204	BMI >90th percentile	7
Pirgon.O[90]	Turkey	2013	2010-2011	Cross-sectional	Hospital	H-MRS	111	171	BMI >95th percentile	7
Cali.AMG[91]	USA	2007	2007	Cross-sectional	Hospital	US	192	352	BMI >90th percentile	6
Shi.JQ[92]	China	2017	2015	Cross-sectional	Hospital	Biopy	148	239	BMI >85th percentile	8
Torun.E[93]	Turkey	2014	2011-2013	Cross-sectional	Hospital	US	55	80	BMI >85th percentile	7
Ustyol.A[94]	Turkey	2017	2015-2016	Cross-sectional	Hospital	MRI	41	115	Not specified	8
Vakilishahrbabaki.HS[95]	Iran	2018	2016-2017	case-control	Hospital	US	144	242	BMI >85th percentile	7
Trico.D[96]	USA	2018	2018	Cross-sectional	Hospital	US	90	168	BMI >95th percentile	8
Wang.R[97]	China	2018	2015-2016	Cross-sectional	Hospital	US	46	213	BMI z score >1	8
Yang.HR[98]	South Korea	2016	2012-2014	Cross-sectional	Hospital	US	13	43	BMI>30	8
Silveira.LS[99]	Brazil	2013	2013	Cross-sectional	Hospital	US	21	33	BMI >85th percentile	8
Wasilewska.N[100]	Poland	2018	2018	Cross-sectional	Hospital	US	120	200	BMI >95th percentile	8
Yang.HR[101]	South Korea	2014	2006-2012	Cross-sectional	Hospital	US	50	144	BMI >95th percentile	8
Grønbæk.H[102]	Denmark	2012	2011	Cross-sectional	Hospital	US	38	72	An ideal body weight higher than 160% was	8

									considered as morbid obesity. All patients had an IBW over 120%.	
Saad.V[103]	Canada	2015	2008-2012	Cross-sectional	Hospital	US	157	375	BMI > 2 s.d. for chronological age	7
Zou.CC[104]	China	2005	2005	Cross-sectional	Hospital	US	41	212	BMI >85th percentile	6
Bohte.AE[105]	Netherlands	2011	2008-2010	Cross-sectional	Hospital	US	202	332	BMI >95th percentile	7
Chiloiro.M[106]	Italy	2008	2008	Cross-sectional	Hospital	US	268	596	BMI Z-score >2	6
Silva.KSH[107]	Sri Lanka	2006	2004-2005	Cross-sectional	Hospital	US	38	85	BMI >95th percentile	7
Denzer.C[108]	Germany	2009	2009	Cross-sectional	Hospital	MRI	14	60	BMI > 2 s.d. for chronological age	8
Hacihamdioglu.B[109]	Turkey	2011	2011	Cross-sectional	Hospital	US	35	58	BMI >85th percentile	6
Kim.JS[110]	USA	2012	2012	Cross-sectional	Hospital	US	34	108	BMI >97th percentile	6
El-Koofy.NM[111]	Egypt	2012	2012	Cross-sectional	Hospital	MRI	14	44	BMI >97th percentile	9
Ozkol.M[112]	Turkey	2010	2010	Cross-sectional	Hospital	US	57	127	BMI >95th percentile	7
Papandreou.D[113]	Greece	2008	2005-2006	Cross-sectional	Hospital	US	121	447	BMI >90th percentile	6
Perseghin.G[114]	Italy	2006	2006	Cross-sectional	Hospital	US	82	181	BMI >95th percentile	7
Reinehr.T[115]	Germany	2008	2008	Cross-sectional	Hospital	US	28	64	BMI >85th percentile	7
Tock.L[116]	Brazil	2006	2006	Cross-sectional	Hospital	US	58	113	BMI >95th percentile	7
Xanthakos.S[117]	USA	2006	2003-2005	Cross-sectional	Hospital	US	58	101	BMI >95th percentile	8
Boza.C[118]	Chile	2011	2006-2009	Cross-sectional	Hospital	US	45	87	BMI >95th percentile	9
Koot.BG[119]	Netherlands	2011	2004-2008	Cross-sectional	Hospital	MRI	12	49	BMI >95th percentile	8
Alqahtani.A[120]	Saudi Arabia	2017	2008	Cross-sectional	Hospital	US	43	117	BMI >95th percentile	9
Chociej.AB[121]	Spain	2018	2018	Cross-sectional	Hospital	US	85	109	BMI >95th percentile	8
Deeb.A[122]	United Arab Emirates	2018	2018	Cross-sectional	Hospital	US	80	228	BMI >95th percentile	8
Assuncao.SNF[123]	Brazil	2017	2015	Cross-sectional	Hospital	US	126	358	BMI >95th percentile	7
Goyal.P[124]	India	2018	2018	Cross-sectional	Hospital	MRI	209	503	BMI >95th percentile	8
Kirel.B[125]	Turkey	2012	2007-2010	Cross-sectional	Hospital	US	58	123	BMI >95th percentile	7

Martino.MD[126]	Italy	2016	2013-2014	Cross-sectional	Hospital	US	48	182	BMI >95th percentile	7
Yu.EL[127]	USA	2018	2018	Cross-sectional	Hospital	US	31	80	BMI >95th percentile	7
Szyboska.P[128]	Poland	2015	2015	Cross-sectional	Hospital	US	147	396	BMI >85th percentile	7
Pena-Velez.R[129]	Mexico	2019	2019	Cross-sectional	Hospital	US	49	117	BMI >95th percentile	8
Elkabany.ZA[130]	Egypt	2019	2019	Cross-sectional	Hospital	MRI	42	129	BMI >85th percentile	7
Ozsu.E[131]	Turkey	2019	2014-2015	Cross-sectional	Hospital	US	63	113	Body weight exceeded 120% stardard body weight	7
Hua.MC[132]	Taiwan	2019	2015-2017	Cross-sectional	Hospital	US	48	104	BMI z score of greater than 2 (95th percentile	8
Bonito.PD[133]	Italy	2019	2003-2016	Cross-sectional	Hospital	US	60	94	BMI >95th percentile	7
Jain.V[134]	India	2019	2012-2016	Cross-sectional	Hospital	US	60	70	BMI >95th percentile	7
Ortega.EV[135]	Mexico	2019	2015-2016	Cross-sectional	Hospital	US	149	532	BMI >90th percentile	7
Draijer.LG[136]	Netherlands	2019	2008-2010	Cross-sectional	Hospital	US	21	104	BMI >95th percentile	7
Kurku.H[137]	Turkey	2019	2016-2017	Cross-sectional	Hospital	MRI	16	41	BMI >85th percentile	7
Velez.RR[138]	Colombia	2018	2018	Cross-sectional	Hospital	Biopsy	15	33	BMI >85th percentile	7
Jackiewicz.MF[139]	Poland	2018	2018	Cross-sectional	Hospital	US	30	59	BMI >85th percentile	8
Bacha.F[140]	USA	2017	2017	Cross-sectional	Hospital	US	18	43	BMI >95th percentile	7
Balanescu.A[141]	Romania	2018	2017	Cross-sectional	Hospital	H-MRS	16	54	BMI >99th percentile	7
Lu.LP[142]	China	2017	2013-2015	Cross-sectional	Hospital	US	12	36	BMI >95th percentile	7
Chabanova.E[143]	Denmark	2017	2017	Cross-sectional	Hospital	US	38	73	BMI >95th percentile	8
Lee.SJ[144]	USA	2016	2016	Cross-sectional	Hospital	Biopsy	34	41	BMI >99th percentile	7
Sheldon.RD[145]	Colombia	2016	2016	Cross-sectional	Hospital	Biopsy	8	51	BMI 40 mg/kg2 or BMI 35 mg/kg2 with associated co-morbidities	9
Jin.R[146]	USA	2015	2015	Cross-sectional	Hospital	US	45	144	BMI>35 or BMI>30 with comorbidity	7
Chang.PF[147]	Taiwan	2015	2010-2012	Cross-sectional	Hospital	Biopsy	114	144	body mass index (BMI) of 40 kg/m2 (or multiple co-morbidities with a BMI	8

									43.5 kg/m2 or above the 99th percentile for age),	
Oksiuta.MK[148]	Japan	2014	2011-2012	Cross-sectional	Hospital	US	38	56	BMI >95th percentile	7
O'Sullivan.TA[149]	Austrilia	2013	2003-2005	Prospective	Hospital	US	43	121	BMI >85th percentile	8
Santoro.N[150]	USA	2014	2014	Cross-sectional	Hospital	US	56	100	BMI/i>+2	7
Lebensztejn.DM[151]	Poland	2010	2006-2007	Cross-sectional	Hospital	US	106	160	BMI>26	6
Demircioglu.F[152]	Turkey	2008	2004	Case-control	Hospital	US	66	161	BMI >95th percentile	7
Osborne.KNL[153]	USA	2008	2008	Cross-sectional	Hospital	MRI	40	65	BMI>30 or BMI >95th percentile	7
Shalitin.S[154]	Israel	2008	2004-2006	Cross-sectional	Hospital	Biopsy	27	93	BMI >95th percentile	8
Nichols.PH[155]	USA	2019	2010-2018	Cross-sectional	Hospital	MRI	106	408	BMI >85th percentile	7
Barretto.JR[156]	Brazil	2020	2019	Cross-sectional	Hospital	US	20	58	BMI Z-score >1	7

*US, ultrasound; CT, computed tomography; MRI, magnetic resonance imaging; FLI, fatty liver index; H-MRS, proton magnetic resonance spectroscopy; BMI, body mass index.

Supplementary Table 2. Egger's test for included studies.

Groups	P value
Studies in general population regardless of diagnostic technique	<0.01
Studies in general population diagnosed by ultrasound	0.39
Studies in special population from clinics regardless of diagnostic technique	<0.01
Studies in special population from clinics diagnosed by ultrasound	<0.01

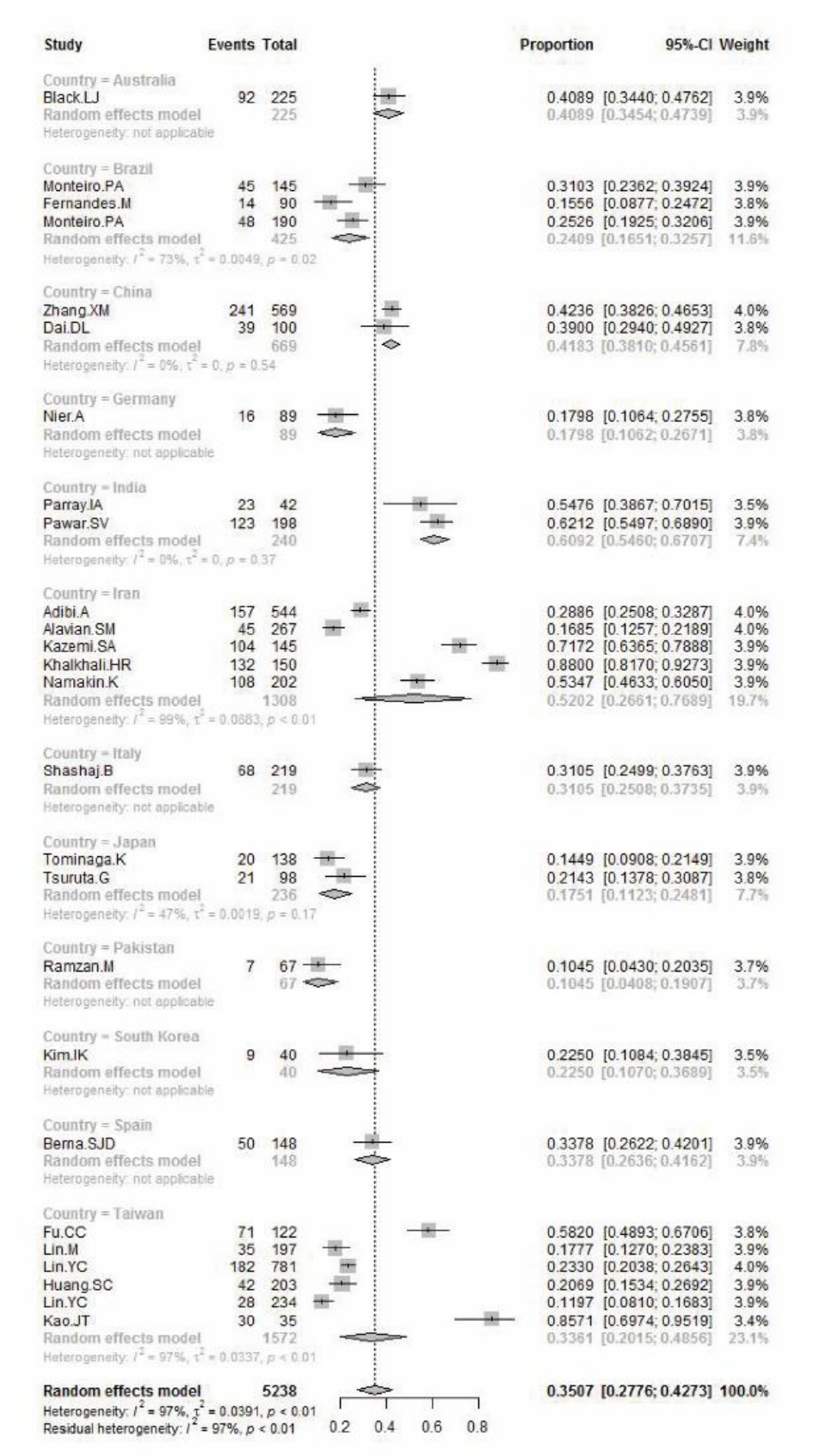

Supplementary Figure 1. MAFLD prevalence in general population diagnosed by ultrasound.

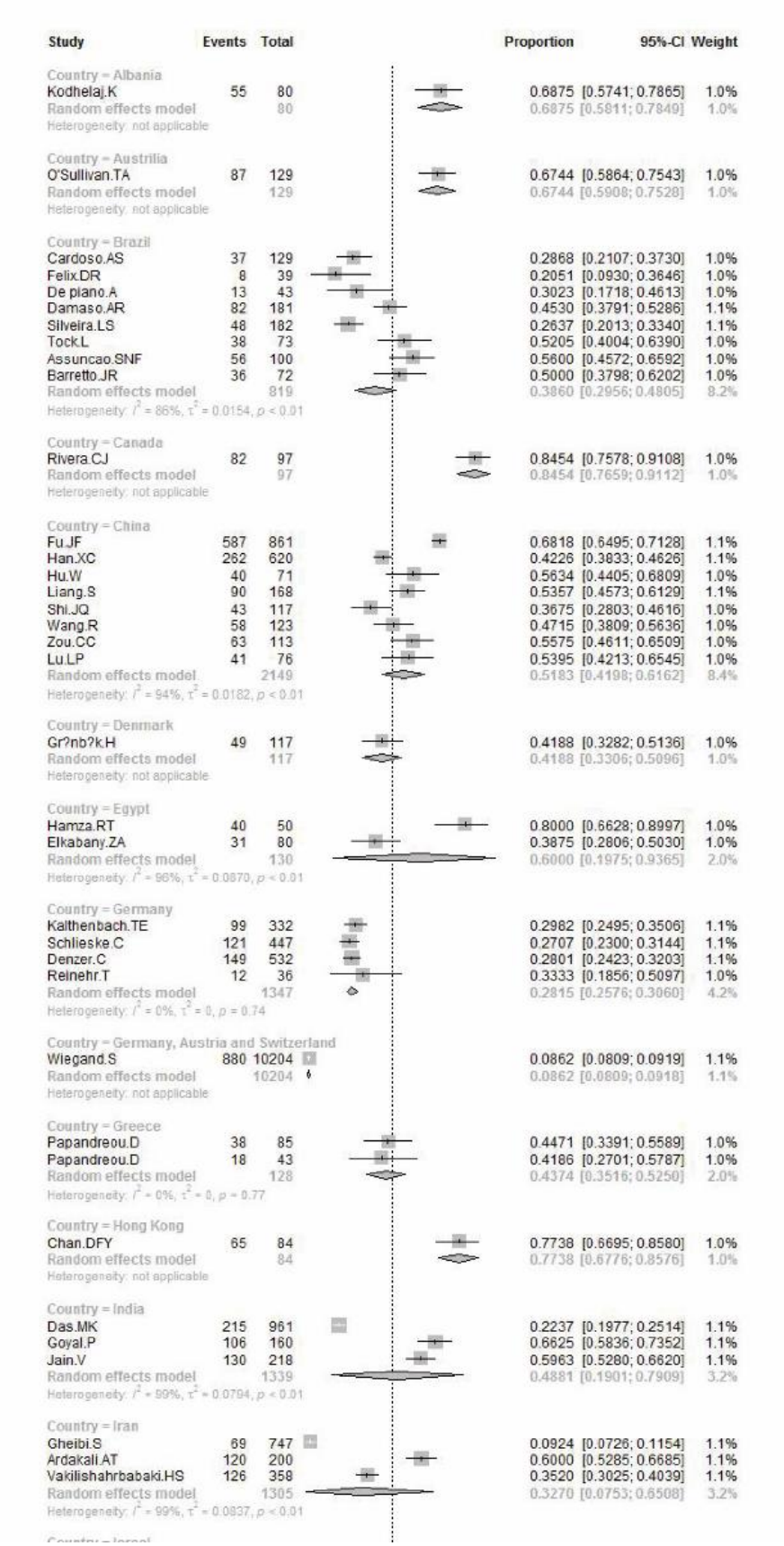
Study Events Total Proportion 95%-CI Weight
Country = Albania
Kodhelaj.K 55 80 0.6875 [0.5741; 0.7865] 1.0%
Random effects model 80 0.6875 [0.5811; 0.7849] 1.0%
Heterogeneity: not applicable
Country = Austrilia
O'Sullivan.TA 87 129 0.6744 [0.5864; 0.7543] 1.0%
Random effects model 129 0.6744 [0.5908; 0.7528] 1.0%
Heterogeneity: not applicable
Country = Brazil
Cardoso.AS 37 129 0.2868 [0.2107; 0.3730] 1.0%
Felix.DR 8 39 0.2051 [0.0930; 0.3646] 1.0%
De plano.A 13 43 0.3023 [0.1718; 0.4613] 1.0%
Damaso.AR 82 181 0.4530 [0.3791; 0.5286] 1.1%
Silveira.LS 48 182 0.2637 [0.2013; 0.3340] 1.1%
Tock.L 38 73 0.5205 [0.4004; 0.6390] 1.0%
Assuncao.SNF 56 100 0.5600 [0.4572; 0.6592] 1.0%
Barretto.JR 36 72 0.5000 [0.3798; 0.6202] 1.0%
Random effects model 819 0.3860 [0.2956; 0.4805] 8.2%
Heterogeneity: I^2 = 86%, τ^2 = 0.0154, p < 0.01
Country = Canada
Rivera.CJ 82 97 0.8454 [0.7578; 0.9108] 1.0%
Random effects model 97 0.8454 [0.7659; 0.9112] 1.0%
Heterogeneity: not applicable
Country = China
Fu.JF 587 851 0.6818 [0.6495; 0.7128] 1.1%
Han.XC 262 620 0.4226 [0.3833; 0.4626] 1.1%
Hu.W 40 71 0.5634 [0.4405; 0.6809] 1.0%
Liang.S 90 168 0.5357 [0.4573; 0.6129] 1.1%
Shi.JQ 43 117 0.3675 [0.2803; 0.4616] 1.0%
Wang.R 58 123 0.4715 [0.3809; 0.5636] 1.0%
Zou.CC 63 113 0.5575 [0.4611; 0.6509] 1.0%
Lu.LP 41 76 0.5395 [0.4213; 0.6545] 1.0%
Random effects model 2149 0.5183 [0.4198; 0.6162] 8.4%
Heterogeneity: I^2 = 94%, τ^2 = 0.0182, p < 0.01
Country = Denmark
Gr?nb?k.H 49 117 0.4188 [0.3282; 0.5136] 1.0%
Random effects model 117 0.4188 [0.3306; 0.5096] 1.0%
Heterogeneity: not applicable
Country = Egypt
Hamza.RT 40 50 0.8000 [0.6628; 0.8997] 1.0%
Elkabany.ZA 31 80 0.3875 [0.2806; 0.5030] 1.0%
Random effects model 130 0.6000 [0.1975; 0.9365] 2.0%
Heterogeneity: I^2 = 96%, τ^2 = 0.0870, p < 0.01
Country = Germany
Kalthenbach.TE 99 332 0.2982 [0.2495; 0.3506] 1.1%
Schlieske.C 121 447 0.2707 [0.2300; 0.3144] 1.1%
Denzer.C 149 532 0.2801 [0.2423; 0.3203] 1.1%
Reinehr.T 12 36 0.3333 [0.1856; 0.5097] 1.0%
Random effects model 1347 0.2815 [0.2576; 0.3060] 4.2%
Heterogeneity: I^2 = 0%, τ^2 = 0, p = 0.74
Country = Germany, Austria and Switzerland
Wiegand.S 880 10204 0.0862 [0.0809; 0.0919] 1.1%
Random effects model 10204 0.0862 [0.0809; 0.0918] 1.1%
Heterogeneity: not applicable
Country = Greece
Papandreou.D 38 85 0.4471 [0.3391; 0.5589] 1.0%
Papandreou.D 18 43 0.4186 [0.2701; 0.5787] 1.0%
Random effects model 128 0.4374 [0.3516; 0.5250] 2.0%
Heterogeneity: I^2 = 0%, τ^2 = 0, p = 0.77
Country = Hong Kong
Chan.DFY 65 84 0.7738 [0.6695; 0.8580] 1.0%
Random effects model 84 0.7738 [0.6776; 0.8576] 1.0%
Heterogeneity: not applicable
Country = India
Das.MK 215 961 0.2237 [0.1977; 0.2514] 1.1%
Goyal.P 106 160 0.6625 [0.5836; 0.7352] 1.1%
Jain.V 130 218 0.5963 [0.5280; 0.6620] 1.1%
Random effects model 1339 0.4881 [0.1901; 0.7909] 3.2%
Heterogeneity: I^2 = 99%, τ^2 = 0.0794, p < 0.01
Country = Iran
Gheibi.S 69 747 0.0924 [0.0726; 0.1154] 1.1%
Ardakali.AT 120 200 0.6000 [0.5285; 0.6685] 1.1%
Vakilishahrbabaki.HS 126 358 0.3520 [0.3025; 0.4039] 1.1%
Random effects model 1305 0.3270 [0.0753; 0.6508] 3.2%
Heterogeneity: I^2 = 99%, τ^2 = 0.0837, p < 0.01

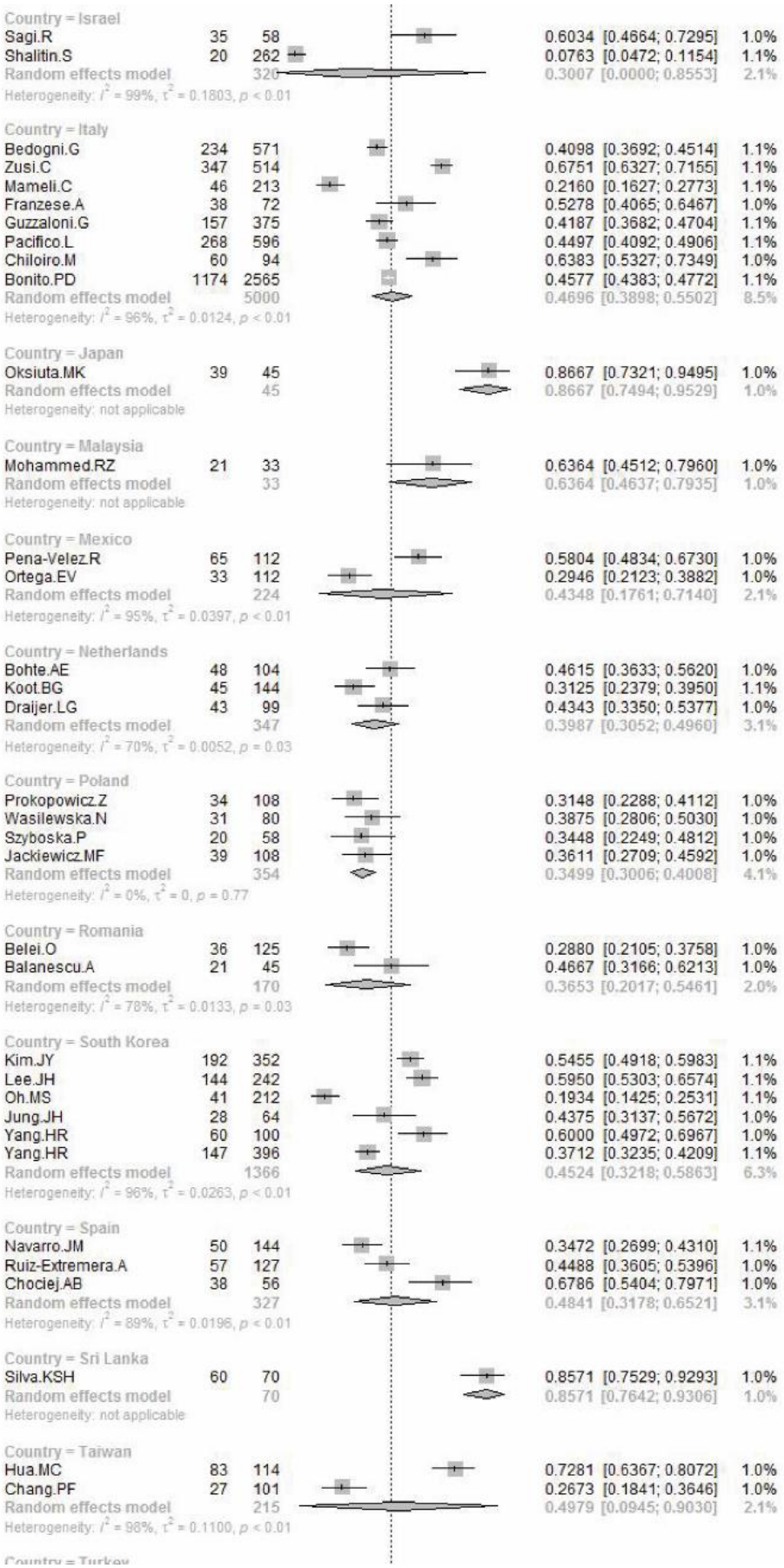
Country = Israel
Sagi.R 35 58 0.6034 [0.4664; 0.7295] 1.0%
Shalitin.S 20 262 0.0763 [0.0472; 0.1154] 1.1%
Random effects model 320 0.3007 [0.0000; 0.8553] 2.1%
Heterogeneity: I^2 = 99%, τ^2 = 0.1803, p < 0.01
Country = Italy
Bedogni.G 234 571 0.4098 [0.3692; 0.4514] 1.1%
Zusi.C 347 514 0.6751 [0.6327; 0.7155] 1.1%
Mameli.C 46 213 0.2160 [0.1627; 0.2773] 1.1%
Franzese.A 38 72 0.5278 [0.4065; 0.6467] 1.0%
Guzzaloni.G 157 375 0.4187 [0.3682; 0.4704] 1.1%
Pacifico.L 268 596 0.4497 [0.4092; 0.4906] 1.1%
Chiloiro.M 60 94 0.6383 [0.5327; 0.7349] 1.0%
Bonito.PD 1174 2565 0.4577 [0.4383; 0.4772] 1.1%
Random effects model 5000 0.4696 [0.3898; 0.5502] 8.5%
Heterogeneity: I^2 = 96%, τ^2 = 0.0124, p < 0.01
Country = Japan
Oksiuta.MK 39 45 0.8667 [0.7321; 0.9495] 1.0%
Random effects model 45 0.8667 [0.7494; 0.9529] 1.0%
Heterogeneity: not applicable
Country = Malaysia
Mohammed.RZ 21 33 0.6364 [0.4512; 0.7960] 1.0%
Random effects model 33 0.6364 [0.4637; 0.7935] 1.0%
Heterogeneity: not applicable
Country = Mexico
Pena-Velez.R 65 112 0.5804 [0.4834; 0.6730] 1.0%
Ortega.EV 33 112 0.2946 [0.2123; 0.3882] 1.0%
Random effects model 224 0.4348 [0.1761; 0.7140] 2.1%
Heterogeneity: I^2 = 95%, τ^2 = 0.0397, p < 0.01
Country = Netherlands
Bohte.AE 48 104 0.4615 [0.3633; 0.5620] 1.0%
Koot.BG 45 144 0.3125 [0.2379; 0.3950] 1.1%
Draijer.LG 43 99 0.4343 [0.3350; 0.5377] 1.0%
Random effects model 347 0.3987 [0.3052; 0.4960] 3.1%
Heterogeneity: I^2 = 70%, τ^2 = 0.0052, p = 0.03
Country = Poland
Prokopowicz.Z 34 108 0.3148 [0.2288; 0.4112] 1.0%
Wasilewska.N 31 80 0.3875 [0.2806; 0.5030] 1.0%
Szyboska.P 20 58 0.3448 [0.2249; 0.4812] 1.0%
Jackiewicz.MF 39 108 0.3611 [0.2709; 0.4592] 1.0%
Random effects model 354 0.3499 [0.3006; 0.4008] 4.1%
Heterogeneity: I^2 = 0%, τ^2 = 0, p = 0.77
Country = Romania
Belei.O 36 125 0.2880 [0.2105; 0.3758] 1.0%
Balanescu.A 21 45 0.4667 [0.3166; 0.6213] 1.0%
Random effects model 170 0.3653 [0.2017; 0.5461] 2.0%
Heterogeneity: I^2 = 78%, τ^2 = 0.0133, p = 0.03
Country = South Korea
Kim.JY 192 352 0.5455 [0.4918; 0.5983] 1.1%
Lee.JH 144 242 0.5950 [0.5303; 0.6574] 1.1%
Oh.MS 41 212 0.1934 [0.1425; 0.2531] 1.1%
Jung.JH 28 64 0.4375 [0.3137; 0.5672] 1.0%
Yang.HR 60 100 0.6000 [0.4972; 0.6967] 1.0%
Yang.HR 147 396 0.3712 [0.3235; 0.4209] 1.1%
Random effects model 1366 0.4524 [0.3218; 0.5863] 6.3%
Heterogeneity: I^2 = 96%, τ^2 = 0.0263, p < 0.01
Country = Spain
Navarro.JM 50 144 0.3472 [0.2699; 0.4310] 1.1%
Ruiz-Extremera.A 57 127 0.4488 [0.3605; 0.5396] 1.0%
Chociej.AB 38 56 0.6786 [0.5404; 0.7971] 1.0%
Random effects model 327 0.4841 [0.3178; 0.6521] 3.1%
Heterogeneity: I^2 = 89%, τ^2 = 0.0196, p < 0.01
Country = Sri Lanka
Silva.KSH 60 70 0.8571 [0.7529; 0.9293] 1.0%
Random effects model 70 0.8571 [0.7642; 0.9306] 1.0%
Heterogeneity: not applicable
Country = Taiwan
Hua.MC 83 114 0.7281 [0.6367; 0.8072] 1.0%
Chang.PF 27 101 0.2673 [0.1841; 0.3646] 1.0%
Random effects model 215 0.4979 [0.0945; 0.9030] 2.1%
Heterogeneity: I^2 = 98%, τ^2 = 0.1100, p < 0.01
Country = Turkey

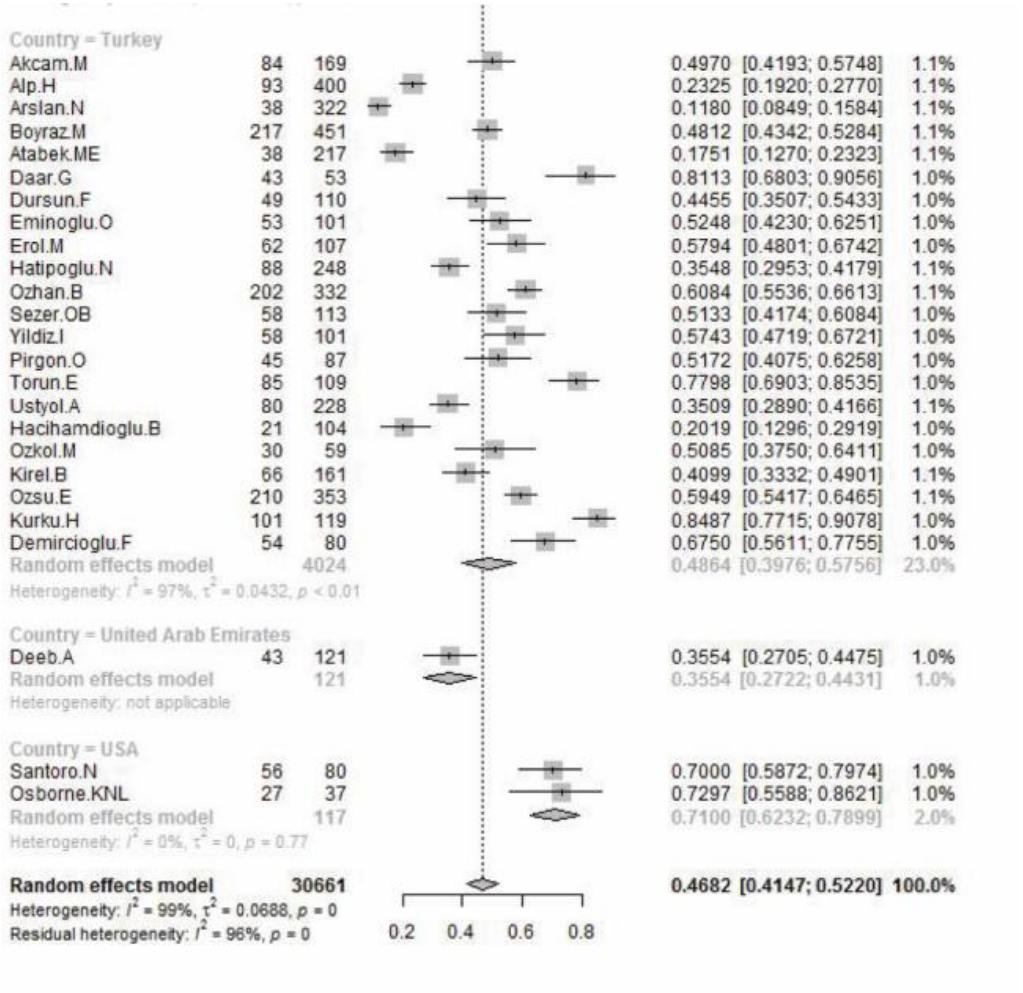

Supplementary figure 2. MAFLD prevalence in clinical population diagnosed by ultrasound.

Reference

1. Adibi A, Kelishadi R, Beihaghi A, Salehi H, Talaei M. Sonographic fatty liver in overweight and obese children, a cross sectional study in Isfahan. *Endokrynol Pol* 2009; **60**(1): 14-9.
2. Alavian SM, Mohammad-Alizadeh AH, Esna-Ashari F, Ardalan G, Hajarizadeh B. Non-alcoholic fatty liver disease prevalence among school-aged children and adolescents in Iran and its association with biochemical and anthropometric measures. *Liver Int* 2009; **29**(2): 159-63.
3. Parray IA. Ultrasonographic Prevalence of Non Alcoholic Fatty Liver Disease (Nafld) in Kashmir Valley School Children *Int J Sci* 2013; **2**(3): 229-301.
4. Pawar SV, Zanwar VG, Choksey AS, et al. Most overweight and obese Indian children have nonalcoholic fatty liver disease. *Ann Hepatol* 2016; **15**(6): 853-61.
5. Geurtsen ML, Santos S, Felix JF, et al. Liver Fat and Cardiometabolic Risk Factors Among School-Age Children. *Hepatology* 2019.
6. Kazemi SA. Assessment of the Relationship Between Prevalence of Reporting Fatty Liver Disease by Ultrasound and Body Mass Index in Children. *Iran J Pediatr* 2017; **27**(1): 1-4.
7. Fu CC, Chen MC, Li YM, Liu TT, Wang LY. The risk factors for ultrasound-diagnosed non-alcoholic fatty liver disease among adolescents. *Ann Acad Med Singapore* 2009; **38**(1): 15-7.
8. Khalkhali HR. Estimating Steatosis Prevalence in Overweight and Obese Children: Comparison of Bayesian Small Area and Direct Methods. *Int J Pediatrics* 2016; **4**(9): 3391-97.
9. Lin MS, Lin TH, Guo SE, et al. Waist-to-height ratio is a useful index for nonalcoholic fatty liver disease in children and adolescents: a secondary data analysis. *BMC Public Health* 2017; **17**(1): 851.
10. Lin YC, Chang PF, Chang MH, Ni YH. A common variant in the peroxisome proliferator-activated receptor-gamma coactivator-1alpha gene is associated with nonalcoholic fatty liver disease in obese children. *Am J Clin Nutr* 2013; **97**(2): 326-31.
11. Tominaga K, Kurata JH, Chen YK, et al. Prevalence of fatty liver in Japanese children and relationship to obesity. An epidemiological ultrasonographic survey. *Dig Dis Sci* 1995; **40**(9): 2002-9.

12. Monteiro PA, de Moura Mello Antunes B, Silveira LS, Christofaro DGD, Fernandes RA, Freitas IF. Body composition variables as predictors of NAFLD by ultrasound in obese children and adolescents. *BMC Pediatr* 2014; **14**(1).
13. Namakin K. Prevalence of Non-Alcoholic Fatty Liver Disease (NAFLD) and its Clinical Characteristics in Overweight and Obese Children in the South East of Iran, 2017. *Hepat Mon* 2018; **18**(12): e83525.
14. Nier A, Brandt A, Conzelmann IB, Ozel Y, Bergheim I. Non-Alcoholic Fatty Liver Disease in Overweight Children: Role of Fructose Intake and Dietary Pattern. *Nutrients* 2018; **10**(9).
15. Ramzan M. Sonographic Assessment of Hepatic Steatosis (Fatty Liver) in< School Children of Dera Ismail Khan City (NWFP) Pakistan. *Pak J Nutr* 2009; **8**(6): 797-9.
16. Fernandes MT, Ferraro AA, de Azevedo RA, Fagundes Neto U. Metabolic differences between male and female adolescents with non-alcoholic fatty liver disease, as detected by ultrasound. *Acta Paediatr* 2010; **99**(8): 1218-23.
17. Black LJ, Jacoby P, She Ping-Delfos WC, et al. Low serum 25-hydroxyvitamin D concentrations associate with non-alcoholic fatty liver disease in adolescents independent of adiposity. *J Gastroenterol Hepatol* 2014; **29**(6): 1215-22.
18. Walker RW, Sinatra F, Hartiala J, et al. Genetic and clinical markers of elevated liver fat content in overweight and obese Hispanic children. *Obesity (Silver Spring)* 2013; **21**(12): E790-7.
19. Zhang X, Wan Y, Zhang S, et al. Nonalcoholic fatty liver disease prevalence in urban school-aged children and adolescents from the Yangtze River delta region: a cross-sectional study. *Asia Pac J Clin Nutr* 2015; **24**(2): 281-8.
20. Tsuruta G, Tanaka N, Hongo M, et al. Nonalcoholic fatty liver disease in Japanese junior high school students: its prevalence and relationship to lifestyle habits. *J Gastroenterol* 2010; **45**(6): 666-72.
21. Zhao YZ, Gan YG, Zhou JL, et al. Accuracy of multi-echo Dixon sequence in quantification of hepatic steatosis in Chinese children and adolescents. *World J Gastroenterol* 2019; **25**(12): 1513-23.
22. Dai D, Wen F, Zhou S, et al. Association of MTTP gene variants with pediatric NAFLD: A candidate-gene-based analysis of single nucleotide variations in obese children. *PLoS One* 2017; **12**(9): e0185396.
23. Huang SC, Yang YJ. Serum retinol-binding protein 4 is independently associated with pediatric NAFLD and fasting triglyceride level. *J Pediatr Gastroenterol Nutr* 2013; **56**(2): 145-50.
24. Kim IK, Kim J, Kang JH, Song J. Serum leptin as a predictor of fatty liver in 7-year-old Korean children. *Ann Nutr Metab* 2008; **53**(2): 109-16.
25. Lin YC, Chang PF, Hu FC, Chang MH, Ni YH. Variants in the UGT1A1 gene and the risk of pediatric nonalcoholic fatty liver disease. *Pediatrics* 2009; **124**(6): e1221-7.
26. Monteiro PA, Mota J, Silveira LS, et al. Morphological and metabolic determinants of nonalcoholic fatty liver disease in obese youth: a pilot study. *BMC Res Notes* 2013; **6**: 89.
27. Berna-Serna JD, Sanchez-Jimenez R, Velazquez-Marin F, et al. Acoustic radiation force impulse imaging for detection of liver fibrosis in overweight and obese children. *Acta Radiol* 2018; **59**(2): 247-53.
28. Shashaj B, Bedogni G, Graziani MP, et al. Origin of cardiovascular risk in overweight preschool children: a cohort study of cardiometabolic risk factors at the onset of obesity. *JAMA Pediatr* 2014; **168**(10): 917-24.
29. Kao JT, Wang JH, Hung CH, et al. Changing aetiology of liver dysfunction in the new generation of a hepatitis B and C-endemic area: cross-sectional studies on adolescents born in the first 10 years after universal hepatitis B vaccination. *Liver Int* 2008; **28**(9): 1298-304.
30. Akcam M, Boyaci A, Pirgon O, Koroglu M, Dundar BN. Importance of the liver ultrasound scores in pubertal obese children with nonalcoholic fatty liver disease. *Clin Imaging* 2013; **37**(3): 504-8.
31. Alp H, Karaarslan S, Selver Eklioglu B, Atabek ME, Altin H, Baysal T. Association between nonalcoholic fatty liver disease and cardiovascular risk in obese children and adolescents. *Can J Cardiol* 2013; **29**(9): 1118-25.
32. Arenaza L, Medrano M, Oses M, et al. Dietary determinants of hepatic fat content and insulin resistance in overweight/obese children: a cross-sectional analysis of the Prevention of Diabetes in Kids (PREDIKID) study. *Br J Nutr* 2019; **121**(10): 1158-65.
33. Arslan N, Buyukgebiz B, Ozturk Y, Cakmakci H. Fatty liver in obese children: prevalence and correlation with anthropometric measurements and hyperlipidemia. *Turk J Pediatr* 2005; **47**(1): 23-7.
34. Boyraz M, Hatipoglu N, Sari E, et al. Non-alcoholic fatty liver disease in obese children and the relationship between metabolic syndrome criteria. *Obes Res Clin Pract* 2014; **8**(4): e356-63.
35. Fu JF, Shi HB, Liu LR, et al. Non-alcoholic fatty liver disease: An early mediator predicting metabolic syndrome in obese children? *World J Gastroenterol* 2011; **17**(6): 735-42.
36. Atabek ME, Selver Eklioglu B, Akyurek N. Which metabolic syndrome criteria best predict non-alcoholic fatty liver disease in children? *Eat Weight Disord* 2014; **19**(4): 495-501.
37. Bedogni G, Gastaldelli A, Manco M, et al. Relationship between fatty liver and glucose metabolism: a cross-sectional study in 571 obese children. *Nutr Metab Cardiovasc Dis* 2012; **22**(2): 120-6.
38. Belei O, Olariu L, Dobrescu A, Marcovici T, Marginean O. The relationship between non-alcoholic fatty liver disease and small intestinal bacterial overgrowth among overweight and obese children and adolescents. *J Pediatr Endocrinol Metab* 2017; **30**(11): 1161-8.
39. Benetolo PO, Fernandes MIM, Ciampo I, Elias-Junior J, Sawamura R. Evaluation of nonalcoholic fatty liver disease using magnetic resonance in obese children and adolescents. *J Pediatr (Rio J)* 2019; **95**(1): 34-40.
40. Burgert TS, Taksali SE, Dziura J, et al. Alanine aminotransferase levels and fatty liver in childhood obesity: associations with insulin resistance, adiponectin, and visceral fat. *J Clin Endocrinol Metab* 2006; **91**(11): 4287-94.
41. Cardoso AS, Gonzaga NC, Medeiros CC, Carvalho DF. Association of uric acid levels with components of metabolic syndrome and non-alcoholic fatty liver disease in overweight or obese children and adolescents. *J Pediatr (Rio J)* 2013; **89**(4): 412-8.
42. Chan DF, Li AM, Chu WC, et al. Hepatic steatosis in obese Chinese children. *Int J Obes Relat Metab Disord* 2004; **28**(10): 1257-63.
43. Daar G, Serin HI, Ede H, Husrevsahi H. Association between the corrected QT interval, carotid artery intima-media thickness, and hepatic steatosis in obese children. *Anatol J Cardiol* 2016; **16**(7): 524-8.
44. Das MK, Bhatia V, Sibal A, et al. Prevalence of Nonalcoholic Fatty Liver Disease in Normal-weight and Overweight Preadolescent Children in Haryana, India. *Indian Pediatr* 2017; **54**(12): 1012-6.
45. Zusi C, Mantovani A, Olivieri F, et al. Contribution of a genetic risk score to clinical prediction of hepatic steatosis in obese children and adolescents. *Dig Liver Dis* 2019; **51**(11): 1586-92.
46. Di Costanzo A, Pacifico L, Chiesa C, et al. Genetic and metabolic predictors of hepatic fat content in a cohort of Italian children with obesity. *Pediatr Res* 2019; **85**(5): 671-7.
47. Dursun F GN, Su Dur SM, Kirmizibekmez H. The relation between vitamin D level and hepatosteatosis in obese children. *North Clin Istanb* 2019; **6**(1): 28-32.

48. el-Karaksy HM, el-Koofy NM, Anwar GM, el-Mougy FM, el-Hennawy A, Fahmy ME. Predictors of non-alcoholic fatty liver disease in obese and overweight Egyptian children: single center study. *Saudi J Gastroenterol* 2011; **17**(1): 40-6.
49. Eminoglu TF, Camurdan OM, Oktar SO, Bideci A, Dalgic B. Factors related to non-alcoholic fatty liver disease in obese children. *Turk J Gastroenterol* 2008; **19**(2): 85-91.
50. Erol M, Bostan Gayret O, Tekin Nacaroglu H, et al. Association of Osteoprotegerin with Obesity, Insulin Resistance and Non-Alcoholic Fatty Liver Disease in Children. *Iran Red Crescent Med J* 2016; **18**(11): e41873.
51. Felix DR, Costenaro F, Gottschall CB, Coral GP. Non-alcoholic fatty liver disease (Nafld) in obese children- effect of refined carbohydrates in diet. *BMC Pediatr* 2016; **16**(1): 187.
52. Ferraioli G, Calcaterra V, Lissandrin R, et al. Noninvasive assessment of liver steatosis in children: the clinical value of controlled attenuation parameter. *BMC Gastroenterol* 2017; **17**(1): 61.
53. Fonvig CE, Chabanova E, Andersson EA, et al. 1H-MRS Measured Ectopic Fat in Liver and Muscle in Danish Lean and Obese Children and Adolescents. *PLoS One* 2015; **10**(8): e0135018.
54. Gheibi S. Prevalence and Predictors of Non-Alcoholic Fatty Liver Disease in Obese and Overweight Children in the Northwest of Iran. *Hepat Mon* 2019; **19**(10): e92199.
55. Hamza RT, Elfaramawy AA, Mahmoud NH. Serum Pentraxin 3 Fragment as a Noninvasive Marker of Nonalcoholic Fatty Liver Disease in Obese Children and Adolescents. *Horm Res Paediatr* 2016; **86**(1): 11-20.
56. Han X, Xu P, Zhou J, Liu Y, Xu H. Fasting C-peptide is a significant indicator of nonalcoholic fatty liver disease in obese children. *Diabetes Res Clin Pract* 2020; **160**: 108027.
57. Hatipoglu N, Dogan S, Mazicioglu MM, Kurtoglu S. Relationship between Neck Circumference and Non-Alcoholic Fatty Liver Disease in Childhood Obesity. *J Clin Res Pediatr Endocrinol* 2016; **8**(1): 32-9.
58. Hu W, Wang M, Yin C, Li S, Liu Y, Xiao Y. Serum complement factor 5a levels are associated with nonalcoholic fatty liver disease in obese children. *Acta Paediatr* 2018; **107**(2): 322-7.
59. Jimenez-Rivera C, Hadjiyannakis S, Davila J, et al. Prevalence and risk factors for non-alcoholic fatty liver in children and youth with obesity. *BMC Pediatr* 2017; **17**(1): 113.
60. Kaltenbach TE, Graeter T, Oeztuerk S, et al. Thyroid dysfunction and hepatic steatosis in overweight children and adolescents. *Pediatr Obes* 2017; **12**(1): 67-74.
61. Wiegand S, Keller KM, Robl M, et al. Obese boys at increased risk for nonalcoholic liver disease: evaluation of 16,390 overweight or obese children and adolescents. *Int J Obes (Lond)* 2010; **34**(10): 1468-74.
62. Zhang HX, Xu XQ, Fu JF, Lai C, Chen XF. Predicting hepatic steatosis and liver fat content in obese children based on biochemical parameters and anthropometry. *Pediatr Obes* 2015; **10**(2): 112-7.
63. Kim JY, Cho J, Yang HR. Biochemical Predictors of Early Onset Non-Alcoholic Fatty Liver Disease in Young Children with Obesity. *J Korean Med Sci* 2018; **33**(16): e122.
64. Kistler KD, Molleston J, Unalp A, et al. Symptoms and quality of life in obese children and adolescents with non-alcoholic fatty liver disease. *Aliment Pharmacol Ther* 2010; **31**(3): 396-406.
65. Kodhelaj K, Resuli B, Petrela E, Malaj V, Jaze H. Non-alcoholic fatty liver disease and non-alcoholic steatohepatitis in Albanian overweight children. *Minerva Pediatr* 2014; **66**(1): 23-30.
66. Labayen I, Ruiz JR, Arenaza L, et al. Hepatic fat content and bone mineral density in children with overweight/obesity. *Pediatr Res* 2018; **84**(5): 684-8.
67. Lee JH, Jeong SJ. What is the appropriate strategy for diagnosing NAFLD using ultrasonography in obese children? *World J Pediatr* 2017; **13**(3): 248-54.
68. Liang S, Cheng X, Hu Y, Song R, Li G. Insulin-like growth factor 1 and metabolic parameters are associated with nonalcoholic fatty liver disease in obese children and adolescents. *Acta Paediatr* 2017; **106**(2): 298-303.
69. Mameli C, Krakauer NY, Krakauer JC, et al. The association between a body shape index and cardiovascular risk in overweight and obese children and adolescents. *PLoS One* 2018; **13**(1): e0190426.
70. de Piano A, Prado WL, Caranti DA, et al. Metabolic and nutritional profile of obese adolescents with nonalcoholic fatty liver disease. *J Pediatr Gastroenterol Nutr* 2007; **44**(4): 446-52.
71. Mohamed RZ, Jalaludin MY, Anuar Zaini A. Predictors of non-alcoholic fatty liver disease (NAFLD) among children with obesity. *J Pediatr Endocrinol Metab* 2020; **33**(2): 247-53.
72. Taghavi Ardakani A SM, Kheirkhah D. Fatty liver disease in obese children in Kashan, Iran. *Caspian J of Pediatr* 2015; **1**(1): 17-21.
73. Navarro-Jarabo JM, Ubina-Aznar E, Tapia-Ceballos L, et al. Hepatic steatosis and severity-related factors in obese children. *J Gastroenterol Hepatol* 2013; **28**(9): 1532-8.
74. Franzese A, Vajro P, Argenziano A, et al. Liver involvement in obese children. Ultrasonography and liver enzyme levels at diagnosis and during follow-up in an Italian population. *Dig Dis Sci* 1997; **42**(7): 1428-32.
75. Guzzaloni G, Grugni G, Minocci A, Moro D, Morabito F. Liver steatosis in juvenile obesity: correlations with lipid profile, hepatic biochemical parameters and glycemic and insulinemic responses to an oral glucose tolerance test. *Int J Obes Relat Metab Disord* 2000; **24**(6): 772-6.
76. Oh MS, Kim S, Lee J, Lee MS, Kim YJ, Kang KS. Factors associated with Advanced Bone Age in Overweight and Obese Children. *Pediatr Gastroenterol Hepatol Nutr* 2020; **23**(1): 89-97.
77. Ozhan B, Ersoy B, Ozkol M, Kiremitci S, Ergin A. Waist to height ratio: a simple screening tool for nonalcoholic fatty liver disease in obese children. *Turk J Pediatr* 2016; **58**(5): 518-23.
78. Pacifico L, Bonci E, Andreoli GM, et al. The Impact of Nonalcoholic Fatty Liver Disease on Renal Function in Children with Overweight/Obesity. *Int J Mol Sci* 2016; **17**(8).
79. Papandreou D, Karabouta Z, Rousso I. Are dietary cholesterol intake and serum cholesterol levels related to nonalcoholic Fatty liver disease in obese children? *Cholesterol* 2012; **2012**: 572820.
80. Pozzato C, Radaelli G, Dall'Asta C, et al. MRI in identifying hepatic steatosis in obese children and relation to ultrasonography and metabolic findings. *J Pediatr Gastroenterol Nutr* 2008; **47**(4): 493-9.
81. Sagi R, Reif S, Neuman G, Webb M, Phillip M, Shalitin S. Nonalcoholic fatty liver disease in overweight children and adolescents. *Acta Paediatr* 2007; **96**(8): 1209-13.
82. Prokopowicz Z. Predictive Value of Adiposity Level, Metabolic Syndrome, and Insulin Resistance for the Risk of Nonalcoholic Fatty Liver Disease Diagnosis in Obese Children. *CAN J GASTROENTEROL* 2018; **2018**: 1-8.
83. Radetti G, Kleon W, Stuefer J, Pittschieler K. Non-alcoholic fatty liver disease in obese children evaluated by magnetic resonance imaging. *Acta Paediatr* 2006; **95**(7): 833-7.
84. Ruiz-Extremera A, Carazo A, Salmeron A, et al. Factors associated with hepatic steatosis in obese children and adolescents. *J Pediatr Gastroenterol Nutr* 2011; **53**(2): 196-201.

85. Schlieske C, Denzer C, Wabitsch M, et al. Sonographically measured suprailiac adipose tissue is a useful predictor of non-alcoholic fatty liver disease in obese children and adolescents. *Pediatr Obes* 2015; **10**(4): 260-6.
86. Damaso AR, do Prado WL, de Piano A, et al. Relationship between nonalcoholic fatty liver disease prevalence and visceral fat in obese adolescents. *Dig Liver Dis* 2008; **40**(2): 132-9.
87. Jung JH, Jung MK, Kim KE, et al. Ultrasound measurement of pediatric visceral fat thickness: correlations with metabolic and liver profiles. *Ann Pediatr Endocrinol Metab* 2016; **21**(2): 75-80.
88. Sezer OB, Bulus D, Hizli S, Andiran N, Yilmaz D, Ramadan SU. Low 25-hydroxyvitamin D level is not an independent risk factor for hepatosteatosis in obese children. *J Pediatr Endocrinol Metab* 2016; **29**(7): 783-8.
89. Yildiz I, Erol OB, Toprak S, et al. Role of vitamin D in children with hepatosteatosis. *J Pediatr Gastroenterol Nutr* 2014; **59**(1): 106-11.
90. Pirgon O, Cekmez F, Bilgin H, Eren E, Dundar B. Low 25-hydroxyvitamin D level is associated with insulin sensitivity in obese adolescents with non-alcoholic fatty liver disease. *Obes Res Clin Pract* 2013; **7**(4): e275-83.
91. Cali AM, Zern TL, Taksali SE, et al. Intrahepatic fat accumulation and alterations in lipoprotein composition in obese adolescents: a perfect proatherogenic state. *Diabetes Care* 2007; **30**(12): 3093-8.
92. Shi JQ, Shen WX, Wang XZ, Huang K, Zou CC. Relationship Between Immune Parameters and Non-alcoholic Fatty Liver Disease in Obese Children. *Indian Pediatr* 2017; **54**(10): 825-9.
93. Torun E, Aydin S, Gokce S, Ozgen IT, Donmez T, Cesur Y. Carotid intima-media thickness and flow-mediated dilation in obese children with non-alcoholic fatty liver disease. *Turk J Gastroenterol* 2014; **25 Suppl 1**: 92-8.
94. Üstyol A. Association of Serum Triglyceride-to-High-density Lipoprotein Cholesterol Ratio with Insulin Resistance and Non-alcoholic Fatty Liver Disease in Children and Adolescents. *Med Bull Hasek* 2017; **55**: 286-91.
95. Vakilishahrbabaki H-S. Association between Non-Alcoholic Fatty Liver Disease and Carotid Intima-Media Thickness in Overweight and Obese Children *J res med dent sci* 2018; **6**(3): 313-8.
96. Trico D, Caprio S, Rosaria Umano G, et al. Metabolic Features of Nonalcoholic Fatty Liver (NAFL) in Obese Adolescents: Findings From a Multiethnic Cohort. *Hepatology* 2018; **68**(4): 1376-90.
97. Wang R, Yang F, Qing L, Huang R, Liu Q, Li X. Decreased serum neuregulin 4 levels associated with non-alcoholic fatty liver disease in children with obesity. *Clin Obes* 2019; **9**(1): e12289.
98. Yang HR, Chang EJ. Insulin resistance, body composition, and fat distribution in obese children with nonalcoholic fatty liver disease. *Asia Pac J Clin Nutr* 2016; **25**(1): 126-33.
99. Silveira LS, Monteiro PA, Antunes Bde M, et al. Intra-abdominal fat is related to metabolic syndrome and non-alcoholic fat liver disease in obese youth. *BMC Pediatr* 2013; **13**: 115.
100. Wasilewska N, Bobrus-Chociej A, Harasim-Symbor E, et al. Increased serum concentration of ceramides in obese children with nonalcoholic fatty liver disease. *Lipids Health Dis* 2018; **17**(1): 216.
101. Yang HR, Yi DY, Choi HS. Comparison between a pediatric health promotion center and a pediatric obesity clinic in detecting metabolic syndrome and non-alcoholic fatty liver disease in children. *J Korean Med Sci* 2014; **29**(12): 1672-7.
102. Gronbaek H, Lange A, Birkebaek NH, et al. Effect of a 10-week weight loss camp on fatty liver disease and insulin sensitivity in obese Danish children. *J Pediatr Gastroenterol Nutr* 2012; **54**(2): 223-8.
103. Saad V, Wicklow B, Wittmeier K, et al. A clinically relevant method to screen for hepatic steatosis in overweight adolescents: a cross sectional study. *BMC Pediatr* 2015; **15**: 151.
104. Zou CC, Liang L, Hong F, Fu JF, Zhao ZY. Serum adiponectin, resistin levels and non-alcoholic fatty liver disease in obese children. *Endocr J* 2005; **52**(5): 519-24.
105. Bohte AE, Koot BG, van der Baan-Slootweg OH, et al. US cannot be used to predict the presence or severity of hepatic steatosis in severely obese adolescents. *Radiology* 2012; **262**(1): 327-34.
106. Chiloiro M, Riezzo G, Chiarappa S, et al. Relationship among fatty liver, adipose tissue distribution and metabolic profile in moderately obese children: an ultrasonographic study. *Curr Pharm Des* 2008; **14**(26): 2693-8.
107. de Silva KS, Wickramasinghe VP, Gooneratne IN. Metabolic consequences of childhood obesity--a preliminary report. *Ceylon Med J* 2006; **51**(3): 105-9.
108. Denzer C, Thiere D, Muche R, et al. Gender-specific prevalences of fatty liver in obese children and adolescents: roles of body fat distribution, sex steroids, and insulin resistance. *J Clin Endocrinol Metab* 2009; **94**(10): 3872-81.
109. Hacihamdioglu B, Okutan V, Yozgat Y, et al. Abdominal obesity is an independent risk factor for increased carotid intima- media thickness in obese children. *Turk J Pediatr* 2011; **53**(1): 48-54.
110. Kim JS, Le KA, Mahurkar S, Davis JN, Goran MI. Influence of elevated liver fat on circulating adipocytokines and insulin resistance in obese Hispanic adolescents. *Pediatr Obes* 2012; **7**(2): 158-64.
111. El-Koofy NM, Anwar GM, El-Raziky MS, et al. The association of metabolic syndrome, insulin resistance and non-alcoholic fatty liver disease in overweight/obese children. *Saudi J Gastroenterol* 2012; **18**(1): 44-9.
112. Ozkol M, Ersoy B, Kasirga E, Taneli F, Bostanci IE, Ozhan B. Metabolic predictors for early identification of fatty liver using doppler and B-mode ultrasonography in overweight and obese adolescents. *Eur J Pediatr* 2010; **169**(11): 1345-52.
113. Papandreou D, Rousso I, Malindretos P, et al. Are saturated fatty acids and insulin resistance associated with fatty liver in obese children? *Clin Nutr* 2008; **27**(2): 233-40.
114. Perseghin G, Bonfanti R, Magni S, et al. Insulin resistance and whole body energy homeostasis in obese adolescents with fatty liver disease. *Am J Physiol Endocrinol Metab* 2006; **291**(4): E697-703.
115. Reinehr T, Roth CL. Fetuin-A and its relation to metabolic syndrome and fatty liver disease in obese children before and after weight loss. *J Clin Endocrinol Metab* 2008; **93**(11): 4479-85.
116. Tock L, Prado WL, Caranti DA, et al. Nonalcoholic fatty liver disease decrease in obese adolescents after multidisciplinary therapy. *Eur J Gastroenterol Hepatol* 2006; **18**(12): 1241-5.
117. Xanthakos S, Miles L, Bucuvalas J, Daniels S, Garcia V, Inge T. Histologic spectrum of nonalcoholic fatty liver disease in morbidly obese adolescents. *Clin Gastroenterol Hepatol* 2006; **4**(2): 226-32.
118. Boza C, Viscido G, Salinas J, Crovari F, Funke R, Perez G. Laparoscopic sleeve gastrectomy in obese adolescents: results in 51 patients. *Surg Obes Relat Dis* 2012; **8**(2): 133-7; discussion 7-9.
119. Koot BG, van der Baan-Slootweg OH, Tamminga-Smeulders CL, et al. Lifestyle intervention for non-alcoholic fatty liver disease: prospective cohort study of its efficacy and factors related to improvement. *Arch Dis Child* 2011; **96**(7): 669-74.
120. Alqahtani A, Elahmedi M, Alswat K, Arafah M, Fagih M, Lee J. Features of nonalcoholic steatohepatitis in severely obese children and adolescents undergoing sleeve gastrectomy. *Surg Obes Relat Dis* 2017; **13**(9): 1599-609.
121. Bobrus-Chociej A, Flisiak-Jackiewicz M, Daniluk U, et al. Estimation of gamma-glutamyl transferase as a suitable simple biomarker of the cardiovascular risk in children with non-alcoholic fatty liver disease. *Acta Biochim Pol* 2018; **65**(4): 539-44.
122. Deeb A, Attia S, Mahmoud S, Elhaj G, Elfatih A. Dyslipidemia and Fatty Liver Disease in Overweight and Obese Children. *J Obes* 2018; **2018**: 8626818.

123. Assuncao SNF, Sorte N, Alves CAD, Mendes PSA, Alves CRB, Silva LR. Inflammatory cytokines and non-alcoholic fatty liver disease (NAFLD) in obese children and adolescents. *Nutr Hosp* 2018; **35**(1): 78-83.
124. Pooja G. Nutritional assessment in obese children with and without non-alcoholic fatty liver disease (NAFLD) in an Urban Area of Punjab, India. *Indian J Public Health De* 2018; **9**(12): 201-7.
125. Kirel B. Nonalcoholic fatty liver diseases in obese children and adolescents. *Turk Arch Ped* 2012; **47**: 172-8.
126. Di Martino M, Pacifico L, Bezzi M, et al. Comparison of magnetic resonance spectroscopy, proton density fat fraction and histological analysis in the quantification of liver steatosis in children and adolescents. *World J Gastroenterol* 2016; **22**(39): 8812-9.
127. Yu EL, Golshan S, Harlow KE, et al. Prevalence of Nonalcoholic Fatty Liver Disease in Children with Obesity. *J Pediatr* 2019; **207**: 64-70.
128. Szybowska P, Wojcik M, Starzyk JB, Sztefko K. Enhanced liver fibrosis (ELF) test in obese children with ultrasound-proven liver steatosis. *Neuro Endocrinol Lett* 2015; **36**(7): 700-5.
129. Pena-Velez R, Garibay-Nieto N, Cal YM-VM, et al. Association between neck circumference and non-alcoholic fatty liver disease in Mexican children and adolescents with obesity. *J Pediatr Endocrinol Metab* 2020; **33**(2): 205-13.
130. Elkabany ZA, Hamza RT, Ismail EAR, et al. Serum visfatin level as a noninvasive marker for nonalcoholic fatty liver disease in children and adolescents with obesity: relation to transient elastography with controlled attenuation parameter. *Eur J Gastroenterol Hepatol* 2019.
131. Ozsu E, Yazicioglu B. Obese boys with low concentrations of high-density lipoprotein cholesterol are at greater risk of hepatosteatosis. *Hormones (Athens)* 2019; **18**(4): 477-84.
132. Hua MC, Huang JL, Hu CC, Yao TC, Lai MW. Including Fibroblast Growth Factor-21 in Combined Biomarker Panels Improves Predictions of Liver Steatosis Severity in Children. *Front Pediatr* 2019; **7**: 420.
133. Di Bonito P, Valerio G, Licenziati MR, et al. High uric acid, reduced glomerular filtration rate and non-alcoholic fatty liver in young people with obesity. *J Endocrinol Invest* 2020; **43**(4): 461-8.
134. Jain V, Kumar A, Ahmad N, et al. Genetic polymorphisms associated with obesity and non-alcoholic fatty liver disease in Asian Indian adolescents. *J Pediatr Endocrinol Metab* 2019; **32**(7): 749-58.
135. Villanueva-Ortega E, Garces-Hernandez MJ, Herrera-Rosas A, et al. Gender-specific differences in clinical and metabolic variables associated with NAFLD in a Mexican pediatric population. *Ann Hepatol* 2019; **18**(5): 693-700.
136. Draijer LG, Feddouli S, Bohte AE, et al. Comparison of diagnostic accuracy of screening tests ALT and ultrasound for pediatric non-alcoholic fatty liver disease. *Eur J Pediatr* 2019; **178**(6): 863-70.
137. Kurku H, Atar M, Pirgon O, et al. Pubertal Status and Gonadal Functions in Obese Boys with Fatty Liver. *Metab Syndr Relat Disord* 2019; **17**(2): 102-7.
138. Ramirez-Velez R, Izquierdo M, Correa-Bautista JE, et al. Liver Fat Content and Body Fat Distribution in Youths with Excess Adiposity. *J Clin Med* 2018; **7**(12).
139. Flisiak-Jackiewicz M, Bobrus-Chociej A, Tarasow E, Wojtkowska M, Bialokoz-Kalinowska I, Lebensztejn DM. Predictive Role of Interleukin-18 in Liver Steatosis in Obese Children. *Can J Gastroenterol Hepatol* 2018; **2018**: 3870454.
140. Bacha F, Tomsa A, Bartz SK, et al. Nonalcoholic Fatty Liver Disease in Hispanic Youth With Dysglycemia: Risk for Subclinical Atherosclerosis? *J Endocr Soc* 2017; **1**(8): 1029-40.
141. Balanescu A, Balanescu P, Comanici V, et al. Lipid profile pattern in pediatric overweight population with or without NAFLD in relation to IDF criteria for metabolic syndrome: a preliminary study. *Rom J Intern Med* 2018; **56**(1): 47-54.
142. Lu LP, Wan YP, Xun PC, et al. Serum bile acid level and fatty acid composition in Chinese children with non-alcoholic fatty liver disease. *J Dig Dis* 2017; **18**(8): 461-71.
143. Chabanova E, Fonvig CE, Bojsoe C, Holm JC, Thomsen HS. (1)H MRS Assessment of Hepatic Fat Content: Comparison Between Normal- and Excess-weight Children and Adolescents. *Acad Radiol* 2017; **24**(8): 982-7.
144. Lee S, Kuk JL. Visceral fat is associated with the racial differences in liver fat between black and white adolescent boys with obesity. *Pediatr Diabetes* 2017; **18**(7): 660-3.
145. Sheldon RD, Kanosky KM, Wells KD, et al. Transcriptomic differences in intra-abdominal adipose tissue in extremely obese adolescents with different stages of NAFLD. *Physiol Genomics* 2016; **48**(12): 897-911.
146. Jin R, Le NA, Cleeton R, et al. Amount of hepatic fat predicts cardiovascular risk independent of insulin resistance among Hispanic-American adolescents. *Lipids Health Dis* 2015; **14**: 39.
147. Chang PF, Lin YC, Liu K, Yeh SJ, Ni YH. Heme oxygenase-1 gene promoter polymorphism and the risk of pediatric nonalcoholic fatty liver disease. *Int J Obes (Lond)* 2015; **39**(8): 1236-40.
148. Klusek-Oksiuta M, Bialokoz-Kalinowska I, Tarasow E, Wojtkowska M, Werpachowska I, Lebensztejn DM. Chemerin as a novel non-invasive serum marker of intrahepatic lipid content in obese children. *Ital J Pediatr* 2014; **40**: 84.
149. O'Sullivan TA, Oddy WH, Bremner AP, et al. Lower fructose intake may help protect against development of nonalcoholic fatty liver in adolescents with obesity. *J Pediatr Gastroenterol Nutr* 2014; **58**(5): 624-31.
150. Santoro N, Caprio S, Giannini C, et al. Oxidized fatty acids: A potential pathogenic link between fatty liver and type 2 diabetes in obese adolescents? *Antioxid Redox Signal* 2014; **20**(2): 383-9.
151. Lebensztejn DM, Kowalczuk D, Tarasow E, Skiba E, Kaczmarski M. Tumor necrosis factor alpha and its soluble receptors in obese children with NAFLD. *Adv Med Sci* 2010; **55**(1): 74-9.
152. Demircioglu F, Kocyigit A, Arslan N, Cakmakci H, Hizli S, Sedat AT. Intima-media thickness of carotid artery and susceptibility to atherosclerosis in obese children with nonalcoholic fatty liver disease. *J Pediatr Gastroenterol Nutr* 2008; **47**(1): 68-75.
153. Love-Osborne KA, Nadeau KJ, Sheeder J, Fenton LZ, Zeitler P. Presence of the metabolic syndrome in obese adolescents predicts impaired glucose tolerance and nonalcoholic fatty liver disease. *J Adolesc Health* 2008; **42**(6): 543-8.
154. Shalitin S, Phillip M. Frequency of cardiovascular risk factors in obese children and adolescents referred to a tertiary care center in Israel. *Horm Res* 2008; **69**(3): 152-9.
155. Nichols PH, Pan Y, May B, et al. Effect of TSH on Non-Alcoholic Fatty Liver Disease (NAFLD) independent of obesity in children of predominantly Hispanic/Latino ancestry by causal mediation analysis. *PLoS One* 2020; **15**(6): e0234985.
156. Barretto JR, Boa-Sorte N, Vinhaes CL, et al. Heightened Plasma Levels of Transforming Growth Factor Beta (TGF-beta) and Increased Degree of Systemic Biochemical Perturbation Characterizes Hepatic Steatosis in Overweight Pediatric Patients: A Cross-Sectional Study. *Nutrients* 2020; **12**(6).

CHAPTER 8

Estimating global prevalence of metabolic dysfunction-associated fatty liver disease in overweight or obese adults

Jiaye Liu; Ling Wang; Junyi Shen; Zhongren Ma;

Maikel P. Pepelenbosch; Qiuwei Pan

In preparation

Abstract

Background Metabolic dysfunction-associated fatty liver disease (MAFLD) is a new terminology recently updated from non-alcoholic fatty liver disease (NAFLD). The discontinuity in nomenclature and disease definition hampers epidemiological understanding of MAFLD. In this study, we aim to perform a systematic review and meta-analysis to estimate the global prevalence of MAFLD in overweight or obese adults from general population, by repurposing existing data on fatty liver disease.

Methods A systematic search was conducted in Medline, Embase, Web of science, Cochrane CENTRAL Databases and google scholar. We screened relevant articles in English language published until May 2020. By transforming data according to the new diagnosis criteria, the global prevalence of MAFLD was estimated in general population. A 95% confidence interval was estimated using Wilson score method, and pooled prevalence was calculated using the DerSimonian-Laird random-effects model with Free-Tukey double arcsine transformations.

Findings Our search returned 30745 records, of which 113 studies fulfilled our inclusion criteria. Based on the updated definition, we identified 1911077 overweight or obese adults who could be diagnosed as MAFLD. This resulted in an overall prevalence rate of 51.32% (95% CI 47.53-55.11) regardless of diagnostic techniques. Ultrasound was the most commonly used technique for the diagnosis with a prevalence rate of 52.72% (95% CI 50.38-55.06).

Interpretation MAFLD is highly prevalent in overweight or obese adults from general populations. Rising awareness and urgent actions are warranted as control of the global MAFLD pandemic appears necessary.

Introduction

Metabolic dysfunction-associated fatty liver disease (MAFLD) is a new terminology and is proposed to replace the older term non-alcoholic fatty liver disease (NAFLD), but involves a more broad definition of disease. This revised nomenclature appears to have major advantages for diagnosis, patient management, therapeutic development and public health when combating this disease. One of the major changes is shifting towards inclusionary diagnostic criteria, which removes ambiguity. As proposed, a positive diagnosis of MAFLD should be based on detection of hepatic steatosis by histology (biopsy), imaging or blood biomarker in addition to at least one of the following three criteria, namely overweight/obesity, presence of type 2 diabetes mellitus, or evidence of metabolic dysregulation.[1-2]

The resulting paradigm shift in defining fatty liver disease requires re-assessment of existing epidemiological data to fit the MAFLD criteria. The vast majority of the previous studies use NAFLD criteria and require reinterpretation.[3] Although fatty liver disease has a complex phenotype and has a complicated etiology, a substantial proportion of existing data on in the overweight or obese population might be repurposed for assessing MAFLD epidemiology. It is well-recognized that body mass index (BMI) is closely associated with the risk of fatty liver disease and is a critical determinant of adverse clinical outcomes.[4] In this study, we aim to estimate the global prevalence of MAFLD specifically in overweight and obese adults by performing a systematic review and meta-analysis through mining the existing epidemiological data on fatty liver disease.

Materials and Methods

A systematic search was conducted in Medline, Embase, Web of Science, Cochrane and google scholar database. We searched English articles from January, 2000 to May, 2020 (Supplementary methods 1).

Inclusion criteria for the meta-analysis were as follows: (1) hepatic steatosis detected by imaging (ultrasound, computed tomography, and magnetic resonance imaging/spectroscopy, transient elastography), liver biopsy, or blood predictive indices (fatty liver index); (2) the study included overweight or obese individuals; and (3) the study provided information on disease prevalence. Exclusion criteria were as follows: (1) the study was a review article, abstract, case report, correspondence, or conference paper; (2) did not identify individuals with MAFLD; (3) individuals <18 years; (4) performed in patients from outpatient service; (5) no sufficient information for data extraction. Data extraction, quality assessment as well as statistics analysis are detailed in supplementary methods 2 and table S1.

(A)

Continents	Countries	Studies	MAFLD	Participants	Prevalence (95% CI)	I^2
Asia		**83**	**1872470**	**2557274**	**52.51 (48.38-56.63)**	**100%**
	Indonesia	2	389	524	65.70 (40.94-86.71)	87%
	Sri Lanka	2	699	1211	57.79 (54.97-60.59)	0
	Hong Kong	2	294	524	56.58 (49.41-63.62)	63%
	Japan	9	8838	18197	55.46 (47.28-63.49)	99%
	South Korea	19	1801900	2414714	55.22 (47.66-62.65)	100%
	Malaysia	3	531	1009	52.59 (43.16-61.94)	85%
	Mainland China	28	50970	101816	52.32 (46.67-57.94)	100%
	India	3	398	782	51.12 (30.20-71.83)	97%
	Taiwan	7	4625	10680	49.75 (31.29-68.23)	100%
	Iran	5	3445	6484	46.44 (34.70-58.39)	98%
	Philippines	1	27	80	33.75 (23.75-44.53)	–
	Pakistan	1	235	719	32.68 (29.30-36.16)	–
	Thailand	1	119	534	22.28 (18.85-25.92)	–
Europe		**23**	**37285**	**85590**	**47.53 (41.00-54.11)**	**100%**
	Poland	1	1095	1344	81.47 (79.35-83.51)	–
	Austria	1	554	693	79.94 (76.88-82.84)	–
	Spain	2	343	734	56.41 (14.16-93.56)	99%
	Germany	4	1153	2282	54.06 (34.17-73.30)	99%
	Italy	5	841	10832	44.65 (29.89-59.90)	99%
	Netherlands	5	12166	23438	43.02 (27.03-59.79)	100%
	UK	1	601	1414	42.50 (39.94-45.09)	–
	France	1	15964	43292	36.88 (36.42-37.33)	–
	Portugal	1	58	191	30.37 (24.03-37.09)	–
	Finland	1	323	1135	28.46 (25.87-31.12)	–
	Sweden	1	55	226	24.34 (18.95-30.16)	–
North America		**5**	**961**	**2833**	**43.50 (25.50-62.43)**	**99%**
	Mexico	2	390	716	56.10 (43.61-68.21)	91%
	USA	3	571	2117	35.20 (15.71-57.68)	99%
South America		**2**	**361**	**534**	**65.42 (54.63-75.47)**	**79%**
	Brazil	2	361	534	65.42 (54.63-75.47)	79%
Overall		**113**	**1911077**	**2646231**	**51.32 (47.53-55.11)**	**100%**

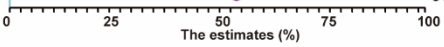

(B)

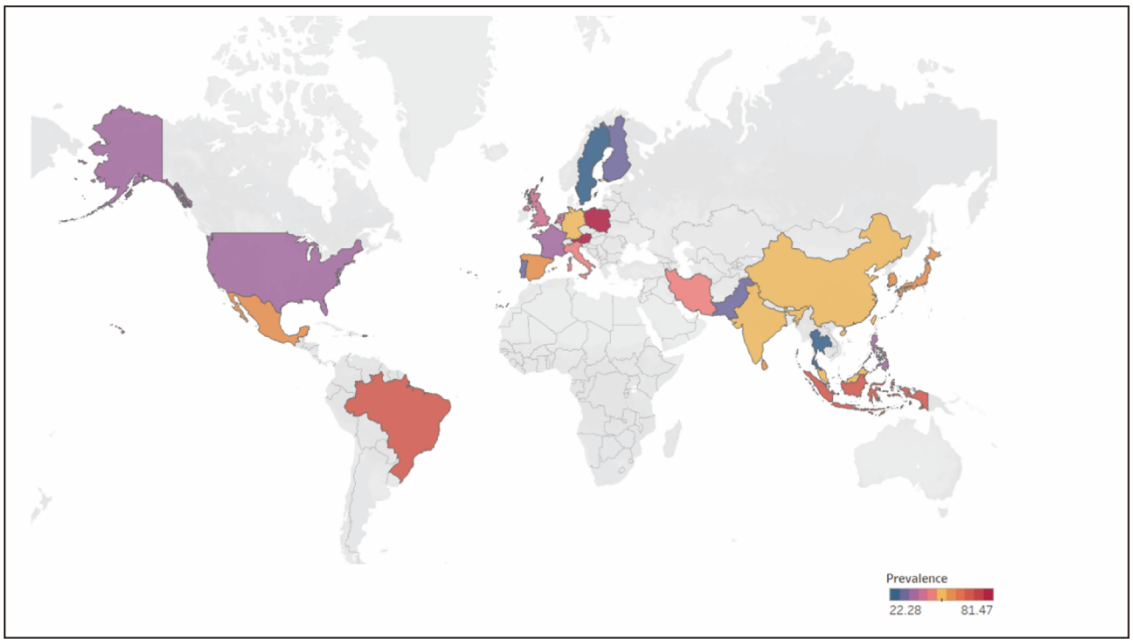

Figure 1. Global prevalence of MAFLD in overweight or obese adults. (A) Forest plot of MAFLD prevalence regardless of diagnostic techniques. (B) MAFLD prevalence in 27 countries and regions.

Results

Among the retrieved 30745 records, 113 eligible studies comprising 2646231 participants were finally included in the analysis (Supplementary Figure S1A, Table S1). Based on the updated definition, we identified 1911077 overweight or obese adults who could be diagnosed as MAFLD. This resulted in an overall prevalence rate of 51.32% (95% CI 47.53-55.11) regardless of diagnostic techniques (Figure 1). Stratified by different continents, South America led the highest prevalence (65.42%, 95% CI 54.63-75.47), followed by Asia (52.51%, 95% CI 48.38-56.63), Europe (47.53%, 95% CI 41.00-54.11) and North America (43.50%, 95% CI 25.50-62.43). MAFLD prevalence varied substantially among countries and regions, from 22.28% (Thailand, 95% CI 18.85-25.92) to 81.47% (Poland, 95% CI 79.35-83.51). Among countries or regions containing at least five relevant studies, Japan had the highest (55.46%, 95% CI 47.28-63.49) and Netherlands had the lowest (43.02%, 95% CI 27.03-59.79) of MAFLD prevalence in this population. Considering the diagnostic methods, one study used liver biopsy (51.36%, 95% CI 45.64-57.07), 10 with fatty liver index (54.38%, 95% CI 39.11-69.24), 4 used computed tomography (23.06%, 95% CI 18.42-28.06), one used proton magnetic resonance spectroscopy (53.18%, 95% CI 47.64-58.69), 3 used transient elastography (31.99%, 95% CI 19.20-46.33) and 92 studies used ultrasound (52.72%, 95% CI 50.38-55.06, Supplementary Figure S1B). Since ultrasound was the most commonly used diagnostic technique, only these studies were included for the remaining analysis (Supplementary Figure S1C). The prevalence was higher in developing countries (54.08%, 95% CI 49.84-58.29) than developed countries (50.99%, 95% CI 48.27-53.71). MAFLD was more prevalent in lower-middle income countries (57.98%, 95% CI 31.80-81.99) than that of upper-middles (53.60%, 95% CI 49.19-57.98) or high-income ones (51.51%, 95% CI 48.58-54.43). Notably, those diagnosed from 2010 to 2020 (56.11%, 95% CI 51.80-60.38) had a higher prevalence of MAFLD in overweight and obese adults than those diagnosed from 2000 to 2009 (51.50%, 46.80-51.69). Egger's test showed significant publication bias in the overall analyses ($P<0.05$) but not in subgroup analyses ($P=0.59$, Supplementary Figure S1D-F).

Discussion

To our knowledge, this is the first comprehensive meta-analysis on the global epidemiology of MAFLD in overweight and obese population. We estimate that the global prevalence of MAFLD among overweight or obese adults is over 50%. Alarmingly, the prevalence rate shows signs of even further increase, when older data is compared to more recent data.

Within the NAFLD population, it was recently estimated that 60% are lean or non-obese individuals,[5] and by inference 40% of this population should be overweight or obese. In the general population, global prevalence of NAFLD has been estimated as 25%

based on data from 1989 to 2015,[6] and a recent study calculated the prevalence of lean and non-obese NAFLD as 17%.[5] The estimation of NAFLD prevalence in obese population is far from accurate and ranges from 50-90%.[7] One study based on liver histology reported a prevalence of steatosis of 15% in non-obese individuals, 65% in persons with obesity, and 85% in extremely obese patients.[8] Because liver biopsy is only indicated for specific patients, these results cannot be generalized. Distinct from these historical studies, we now made a first step to quantify MAFLD epidemiology in overweight and obese adults. It is important to keep in mind that the relationship between MAFLD and BMI is complex and influenced by many factors, such as racial/ethnic background and genetic variations in specific genes and thus requires further in depth investigation.

There are some limitations in this study. The limited data available from Africa and Oceania might be a serious impediment with respect to the accuracy of the estimations. Furthermore, only little information is available with regard to the demographic and genetic characteristics in the included studies. High heterogeneity was observed in pooled estimates. Moreover, we could not perform subgroup analysis between overweight and obese individuals due to the scarcity of the available data.

In conclusion, MAFLD has a strikingly high prevalence rate in overweight and obese individuals. This calls for attention and dedicated action from primary care physicians, specialists, health policy makers and the general public alike.

Reference

1. Eslam M, et al. A new definition for metabolic dysfunction-associated fatty liver disease: An international expert consensus statement. J Hepatol 2020.
2. Eslam M, et al. MAFLD: A Consensus-Driven Proposed Nomenclature for Metabolic Associated Fatty Liver Disease. Gastroenterology 2020;158:1999-2014 e1.
3. Nobili V, et al. Comparison of the Phenotype and Approach to Pediatric vs Adult Patients With Nonalcoholic Fatty Liver Disease. Gastroenterology 2016;150:1798-810.
4. Loomis AK, et al. Body Mass Index and Risk of Nonalcoholic Fatty Liver Disease: Two Electronic Health Record Prospective Studies. J Clin Endocrinol Metab 2016;101:945-52.
5. Ye Q, et al. Global prevalence, incidence, and outcomes of non-obese or lean non-alcoholic fatty liver disease: a systematic review and meta-analysis. Lancet Gastroenterol Hepatol 2020.
6. Younossi ZM, et al. Global epidemiology of nonalcoholic fatty liver disease-Meta-analytic assessment of prevalence, incidence, and outcomes. Hepatology 2016;64:73-84.
7. Divella R, et al. Obesity, Nonalcoholic Fatty Liver Disease and Adipocytokines Network in Promotion of Cancer. Int J Biol Sci 2019;15:610-616.
8. Fabbrini E, et al. Obesity and nonalcoholic fatty liver disease: biochemical, metabolic, and clinical implications. Hepatology 2010;51:679-89.

Supplementary data for

Estimating global prevalence of metabolic dysfunction-associated fatty liver disease in overweight or obese adults

Table of contents

Supplementary methods 1. Searching strategy for metabolic dysfunction-associated fatty liver disease in overweight or obese adults.

Database searched	via	Years of coverage	Records	Records after duplicates removed
Embase	Embase.com	2000 - Present	11248	11075
Medline ALL	Ovid	2000 - Present	10390	3157
Web of Science Core Collection	Web of Knowledge	2000 - Present	8558	2260
Cochrane Central Register of Controlled Trials	Wiley	2000 - Present	349	182
Other sources: Google Scholar (200 top ranked)			200	32
Total			**30745**	**16706**

Embase

('fatty liver'/exp OR 'metabolic liver disease'/de OR 'steatohepatitis'/de OR (hepatosteato* OR steatohepat* OR AFLD OR NAFLD OR FLD OR ((fatty OR steato*) NEAR/3 (liver OR hepat*)) OR ((metabol*) NEAR/3 (liver OR hepat*) NEAR/3 (diseas* OR syndrom*))):ab,ti,kw) AND ('epidemiological data'/de OR 'epidemiology'/de OR 'geographic distribution'/de OR 'patient volume'/de OR prevalence/exp OR geography/de OR 'geographic names'/exp OR 'cross-sectional study'/de OR (epidemiolog* OR ((geograph* OR global*) NEAR/3 (distribut*)) OR (patient* NEAR/3 volume*) OR prevalen* OR population-based* OR cross-sectional*):ab,ti,kw) NOT ([animals]/lim NOT [humans]/lim) NOT ('case report'/de OR 'case report*':ti) NOT ([Conference Abstract]/lim) AND [english]/lim

Medline

(exp Fatty Liver/ OR Liver Diseases/me OR (hepatosteato* OR steatohepat* OR AFLD OR NAFLD OR FLD OR ((fatty OR steato*) ADJ3 (liver OR hepat*)) OR ((metabol*) ADJ3 (liver OR hepat*) ADJ3 (diseas* OR syndrom*))).ab,ti,kw.) AND (Epidemiological Monitoring/ OR Epidemiology/ OR Epidemiology.fs. OR exp Incidence/ OR exp Prevalence/ OR Geography/ OR exp Geographic Locations/ OR Epidemiologic Studies OR Cross-Sectional Studies/ OR (epidemiolog* OR ((geograph* OR global*) ADJ3 (distribut*)) OR (patient* ADJ3 volume*) OR prevalen* OR population-based* OR cross-sectional*).ab,ti,kw.) NOT (exp Animals/ NOT Humans/) NOT (Case Reports/ OR case report*.ti.) NOT (news OR congres* OR abstract* OR book* OR chapter* OR dissertation abstract*).pt. AND english.la.

Cochrane

((hepatosteato* OR steatohepat* OR AFLD OR NAFLD OR FLD OR ((fatty OR steato*) NEAR/3 (liver OR hepat*)) OR ((metabol*) NEAR/3 (liver OR hepat*) NEAR/3 (diseas* OR syndrom*))):ab,ti) AND

((epidemiolog* OR ((geograph* OR global*) NEAR/3 (distribut*)) OR (patient* NEAR/3 volume*) OR prevalen* OR population-based* OR cross-sectional*):ab,ti)

Web of Science

TS=(((hepatosteato* OR steatohepat* OR AFLD OR NAFLD OR FLD OR ((fatty OR steato*) NEAR/2 (liver OR hepat*)) OR ((metabol*) NEAR/2 (liver OR hepat*) NEAR/2 (diseas* OR syndrom*)))) AND ((epidemiolog* OR ((geograph* OR global*) NEAR/2 (distribut*)) OR (patient* NEAR/2 volume*) OR prevalen* OR population-based* OR cross-sectional*)) NOT ((animal* OR rat OR rats OR mouse OR mice OR murine OR dog OR dogs OR canine OR cat OR cats OR feline OR rabbit OR cow OR cows OR bovine OR rodent* OR sheep OR ovine OR pig OR swine OR porcine OR veterinar* OR chick* OR zebrafish* OR baboon* OR nonhuman* OR primate* OR cattle* OR goose OR geese OR duck OR macaque* OR avian* OR bird* OR fish*) NOT (human* OR patient* OR women OR woman OR men OR man))) AND DT=(Article OR Review) AND LA=(English)

Google Scholar

hepatosteatosis|steatohepatitis|AFLD|NAFLD|FLD|"fatty|steatotic liver"|"liver|hepatic steatosis"|"metabolic liver disease" epidemiology|prevalence|"geographic|global distribution"|"patient volume"|"population based"|"cross sectional"

Supplementary methods 2.

Studies were screened based on pre-specified decision rules. Initial title and abstract screening was done independently by two reviewers (JL and LW), with a random 10% of studies checked by another investigator (JS). Full-text review was done independently by two authors (JL and LW), with any discrepancies resolved by consensus or by a third reviewer (QP); consensus was reached in all instances. We extracted data at all levels reported in the study, including time of publication, study period, country or region, country or region income, the level of country development, study categories, diagnostic techniques and disease prevalence. Data were then crossly checked for accuracy against the original source by two authors (JL and LW). Two authors (JL and WL) independent reviewed and extracted data from the included studies by using a data extraction form specifically designed for current study. When duplicate data were identified, the duplicate with the smallest sample size or shortest duration of follow-up was excluded. We assessed the quality of included studies using an assessment scale based on the Newcastle-Ottawa Scale, which is comprised of three domains including selection, comparability and outcome. The Newcastle-Ottawa Scale assigns a maximum score of five for selection, two for comparability, and two for outcome. Studies scoring 1-3 were defined as low quality, 4-6 as average quality, and 7-9 as high quality (Supplementary Table S1). Studies were not excluded on the basis of their quality score to increase transparency and to ensure all available evidence in this area was reported. After checking for consistency, the Metaprop module in the R-3.5.3 statistical software package was used for meta-analysis. A 95% confidence interval (95% CI) was estimated using Wilson score method, and pooled prevalence was calculated with the DerSimonian-Laird random effects model with Free-Tukey double arcsine transformation. Heterogeneity across the included studies was assessed using the Cochran Q statistics and I^2 statistics, with I^2 statistics 25%-50%, 50%-75% and >75% considered as mild, moderate and severe heterogeneity, respectively. Egger regression test were used to assess potential publication biases. This study is reported in accordance with the Preferred Reporting Items for Systematic Reviews and Meta-Analysis (PRISMA).

Supplementary table S1. Charateristics for including studies.

Study	Country/ Region	Publication Year	Study Time	Study Design	Sample Source	Diagnostic Technique	MAFLD	Individuals	BMI	Quality assessment
Kwon.YM[1]	South Korea	2012	2003-2010	Cross-section	Health Check	US	3025	6036	≥25	8
Luo.ZX[2]	Mainland China	2015	2012	Cross-section	Health Check	US	6308	9546	≥25	8
Hamaguchi.M [3]	Japan	2012	2004-2008	Cross-section	Health Check	US	970	1441	≥25	8
Hsing. JC[4]	Mainland China	2019	2016	Cross-section	Community-based	FLI	467	1497	≥23	7
Lee.YH[5]	South Korea	2017	2008-2013	Cross-section	Health Check	HSI	2765	4653	≥25	8
Sung.KC [6]	South Korea	2012	2003-2008	Cross-section	Health Check	US	2317	4346	≥25	8
Fukuda.T[7]	Japan	2016	2003-2013	Cross-section	Health Check	US	591	1640	≥23	8
Nishioji.K[8]	Japan	2015	2011-2012	Cross-section	Health Check	US	394	575	≥25	8
Kim.SS [9]	South Korea	2018	2000-2010	Retrospective	Health Check	FLI	504	801	≥25	8
Li.C [10]	Mainland China	2018	2012-2013	Cross-section	Health Check	US	764	1048	≥24	8
Goh.SC[11]	Malaysia	2013	2000-2009	Cross-section	Health Check	US	329	661	≥23	8
Mansour.R [12]	Iran	2018	2017	Cross-section	Health Check	US	389	722	≥25	8
Teeratorn.N [13]	Thailand	2019	2013-2016	Prospective	Health Check	TE	119	534	≥23	8
VanWangner.LB [14]	USA	2020	2010-2011	Cross-section	Health Check	CT	128	790	≥30	8
Chung, GE [15]	South Korea	2015	2015	Cross-section	Health Check	US	780	1425	≥23	8
Yoshitaka.H [16]	Japan	2017	2003-2004	Cross-section	Health Check	US	243	663	≥23	8
Chen.CH [17]	Taiwan	2006	2003-2004	Cross-section	Health Check	US	291	945	≥25	8
Wei.JL [18]	Hong Kong	2015	2008-2010	Cross-section	Community-based	MRI	127	210	≥25	8
Yang.Z [19]	Mainland China	2016	2011-2012	Cross-section	Health Check	US	2901	4817	≥24	8
Lee.K [20]	South	2009	2005-	Cross-	Health	US	2524	4874	≥25	8

	Korea		2006	section	Check					
Du.T [21]	Mainland China	2017	2008-2010	Cross-section	Health Check	US	3783	6164	≥23	8
Kim.JY [22]	South Korea	2016	2004-2007	Cross-section	Health Check	US	96	194	≥25	8
Dassanayake.AS[23]	Sri Lanka	2009	2007	Cross-section	Community-based	US	669	1164	≥25	8
Jodi.S [24]	Iran	2018	2016	Cross-section	Health Check	US	45	70	≥25	8
Bhatt.SP [25]	India	2018	2012-2017	Cross-section	Health Check	US	168	240	≥23	8
Sinn.DH [26]	South Korea	2019	2003-2013	Cross-section	Health Check	US	13580	29479	≥25	8
Wu.J [27]	Mainland China	2020	2013-2014	Cross-section	Health Check	US	517	610	≥28	8
Huang.JF [28]	Taiwan	2019	2005-2016	Cross-section	Community-based	US	773	1212	≥24	8
Zhou.XH [29]	Mainland China	2018	2012-2013	Cross-section	Health Check	CT	628	2486	≥23	8
Kuhn.T [30]	Germany	2018	2015-2016	Cross-section	Hospitalized	MRI	75	143	≥25	6
Wang.L [31]	Mainland China	2016	2014	Cross-section	Health Check	US	1933	3473	≥24	8
Liu.J[32]	Mainland China	2016	2013-2014	Cross-section	Health Check	US	1331	2162	≥25	8
Alferink.LJ [33]	Netherlands	2019	2009-2014	Cross-section	Health Check	US	1204	2706	≥25	8
Kim.HJ [34]	South Korea	2004	2001	Cross-section	Health Check	US	106	308	≥25	8
Feldman.A[35]	Austria	2018	2007-2009	Cross-section	Health Check	US	554	693	≥30	8
Wang.J [36]	Taiwan	2015	2009	Cross-section	Health Check	US	814	3736	≥24	8
Hernandez.HR[37]	Mexico	2010	2007-2009	Cross-section	Health Check	US	228	457	≥30	8
Alferink.LJM [38]	Netherlands	2019	2000-2009	Cross-section	Health Check	US	1107	3270	≥25	8
Koehler.E [39]	Netherlands	2012	2009-2012	Cross-section	Health Check	US	994	2106	≥25	8
Choi.YJ [40]	South Korea	2018	2009-2012	Cross-section	Health Check	FLI	1676258	2184407	≥25	8
Omagari.K[41]	Japan	2002	2000	Cross-section	Health Check	US	405	698	≥25	8
Caballera.L [42]	Spain	2009	2007-2008	Cross-section	Health Check	US	176	530	≥25	8
Foster.T[43]	USA	2013	2000-	Cross-	Communi	CT	301	1113	≥25	8

			2002	section	ty-based					
Pinidiyapathirage.MJ[44]	Sri Lanka	2011	2010-2011	Cross-section	Community-based	US	30	47	≥25	8
Van den Berg. E[45]	Netherlands	2017	2006-2013	Cross-section	Health Check	FLI	8132	12494	≥25	8
Liu.M[46]	Mainland China	2017	2009-2013	Retrospective	Health Check	US	2643	11122	≥23	8
Kimura.T[47]	Japan	2015	2008-2009	Cross-section	Health Check	US	2554	6439	≥23	8
Shin.JY[48]	South Korea	2015	2009-2011	Cross-section	Health Check	US	2635	4403	≥25	8
Kim.G [49]	South Korea	2015	2008-2010	Cross-section	Health Check	US	2454	3711	≥25	8
Liu.PY[50]	Mainland China	2017	2008-2010	Cross-section	Health Check	US	2479	5470	≥24	8
Wang.Z[51]	Mainland China	2015	2010-2011	Cross-section	Health Check	US	680	1405	≥25	8
Yang.MH [52]	South Korea	2016	2008-2010	Cross-section	Health Check	US	1312	2958	≥23	8
Adriano.LS[53]	Brazil	2016	2009	Cross-section	Health Check	US	73	123	≥27	8
Li.WD[54]	Mainland China	2015	2008	Prospective	Health Check	US	796	1737	≥24	8
Wang.Y[55]	Mainland China	2018	2014-2016	Cross-section	Health Check	US	316	533	≥25	8
Lee.SW [56]	Taiwan	2018	2009	Cross-section	Hospitalized	US	285	1055	≥25	8
Li.L [57]	Mainland China	2015	2010	Cross-section	Health Check	US	250	393	≥25	8
Liu.F [58]	Mainland China	2018	2003-2004	Prospective	Health Check	US	474	791	≥23	8
Rinaldi.C[59]	Indonesia	2015	2013	Cross-section	Health Check	US	373	493	≥25	8
Tsai.CH [60]	Taiwan	2008	2004-2005	Cross-section	Health Check	US	280	430	≥24	8
Lankarani.KB [61]	Iran	2013	2010-2011	Cross-section	Health Check	US	147	479	≥25	8
Khammas.ASA [62]	Malaysia	2019	2015	Cross-section	Community-based	US	172	280	≥23	8
Oniki.K[63]	Japan	2015	2006-2012	Prospective	Health Check	US	64	72	≥25	8
Chang.Y [64]	South Korea	2019	2002-2014	Cross-section	Health Check	US	68447	123905	≥25	8
Gummesson.A [65]	Sweden	2018	2012	Cross-section	Health Check	CT	55	226	≥30	8
Yang.HJ [66]	South	2018	2002-	Cross-	Health	US	18751	31457	≥25	8

	Korea		2014	section	Check					
Nass.KJ[67]	Netherlands	2017	2006-2013	Cross-section	Health Check	FLI	729	2862	≥30	8
Gill.C [68]	USA	2017	2004-2007	Cross-section	Health Check	US	142	214	≥30	8
Hartleb.M [69]	Poland	2016	2007-2010	Cross-section	Community-based	FLI	1095	1344	≥25	8
Lee.JW[70]	South Korea	2019	2008-2013	Cross-section	Health Check	US	2518	4493	≥23	8
Abbas.Z[71]	Pakistan	2013	2010-2011	Cross-section	Health Check	US	235	719	≥23	8
Ostovaneh.MR [72]	Iran	2015	2008-2011	Cross-section	Health Check	US	2782	4939	≥25	8
Peng.K [73]	Mainland China	2017	2010	Cross-section	Health Check	US	1031	1539	≥28	8
Chavez-Tapia. N[74]	Mexico	2008	2005-2007	Cross-section	Health Check	US	162	259	≥30	8
Choi.SH [75]	South Korea	2015	2005-2013	Cross-section	Health Check	US	220	431	≥25	8
Chan.WK [76]	Malaysia	2014	2013	Cross-section	Health Check	US	30	68	≥25	8
Hu.XN [77]	Mainland China	2012	2011	Cross-section	Community-based	US	1605	2191	≥25	8
Lopez-Suarez.A [78]	Spain	2011	2006	Cross-section	Health Check	US	167	213	≥30	8
Tung.TH [79]	Taiwan	2011	2006	Cross-section	Health Check	US	865	1065	≥27	8
Das.K [80]	India	2010	2006-2008	Cross-section	Health Check	TE	79	248	≥23	8
Musso.G [81]	Italy	2007	2002-2007	Cross-section	Health Check	US	61	135	≥25	8
Hazim.A [82]	Indonesia	2019	2018	Cross-section	Health Check	US	16	31	≥25	8
Sogabe.M[83]	Japan	2014	2008-2012	Cross-section	Health Check	US	381	747	≥25	8
Leitao.J[84]	Portugal	2020	2012-2015	Cross-section	Community-based	US	58	191	≥30	8
Nabi.O[85]	France	2020	2012-2018	Cross-section	Health Check	FLI	15964	43292	≥25	8
Wu.LM[86]	Mainland China	2020	2016	Cross-section	Health Check	US	732	1454	≥25	6
Li.HB[87]	Mainland China	2020	2017	Cross-section	Community-based	US	2689	7260	≥23	8
Huang.J[88]	Mainland China	2019	2016-2018	Cross-section	Health Check	US	4155	7181	≥24	8
Suomela.E[89]	Finland	2015	2011	Cross-	Health	US	323	1135	≥25	8

				section	Check					
Hiramine.Y[90]	Japan	2010	2000-2007	Cross-section	Health Check	FLI	3236	5922	≥23	6
Lau.K[91]	Germany	2015	2008-2011	Cross-section	Health Check	US	629	1368	≥25	8
Lusong.MA[92]	Philippines	2008	2004	Cross-section	Health Check	US	27	80	≥30	8
Abeysekera.K[93]	UK	2020	2015-2017	Cross-section	Health Check	TE	601	1414	≥25	8
Chan.R[94]	Hong Kong	2015	2008-2010	Cross-section	Health Check	H-MRS	167	314	≥23	8
Chen.D[95]	Mainland China	2015	2012-2013	Cross-section	Health Check	US	11691	22000	≥23	8
Chiloiro.M[96]	Italy	2013	2001	Cross-section	Community-based	US	560	2195	≥25	6
Choi.JS[97]	South Korea	2018	2004-2011	Cross-section	Health Check	US	2590	5066	≥25	8
Choudhary.NS[98]	India	2016	2010-2016	Retrospective	Health Check	Biopsy	151	294	≥25	9
Colombo.S[99]	Italy	2010	2008-2009	Cross-section	Health Check	US	83	196	≥26	8
Conti.F[100]	Italy	2016	2006-2011	Cross-section	Community-based	US	123	203	≥25	8
Dai.H[101]	Mainland China	2009	2007	Cross-section	Health Check	US	130	306	≥25	6
Fan.JG[102]	Mainland China	2005	2002-2003	Cross-section	Health Check	US	522	1331	≥25	8
Guth.S[103]	Germany	2015	2006-2007	Cross-section	Health Check	US	131	379	≥25	8
Honarvar.B[104]	Iran	2017	2017	Cross-section	Community-based	US	82	274	≥25	8
Hu.XY[105]	Mainland China	2018	2017	Cross-section	Health Check	US	334	809	≥28	8
Huan.SL[106]	Mainland China	2016	2013-2014	Cross-section	Community-based	US	187	332	≥28	8
Huang.BX[107]	Mainland China	2015	2009-2010	Cross-section	Health Check	US	840	1836	≥24	8
Kim.SH[108]	South Korea	2011	2006-2007	Cross-section	Health Check	US	1195	1767	≥25	8
Kratzer.W[109]	Germany	2010	2002	Cross-section	Health Check	US	318	392	≥30	8
Leone.A[110]	Italy	2019	2010-2019	Cross-section	Health Check	FLI	4146	8103	≥25	8
Li.H[111]	Mainland China	2009	2007	Cross-section	Health Check	US	784	2323	≥25	7
Lin.YC[112]	Taiwan	2006	2004-2005	Cross-section	Health Check	US	1317	2237	≥24	8
Ndumele.CE[113]	Brazil	2011	2004-2006	Cross-section	Health Check	US	288	411	≥30	8

*US, ultrasound; CT, computed tomography; MRI, magnetic resonance imaging; FLI, fatty liver index; H-MRS, proton magnetic resonance spectroscopy; BMI, body mass index.

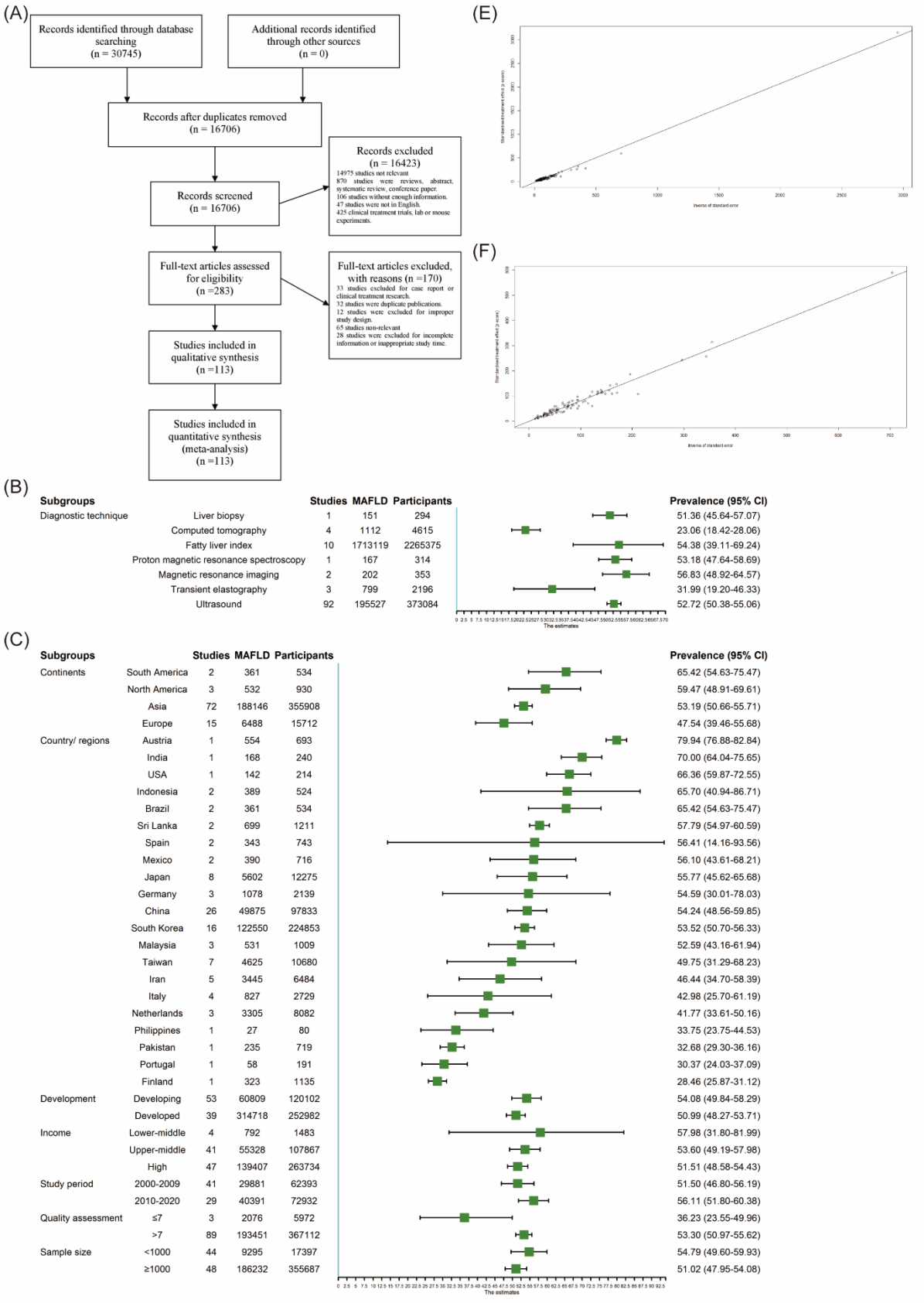

Supplementary Figure 1. (A) Study selection. (B) MAFLD prevalence stratified by different diagnostic methods. (C) Subgroup analysis for MAFLD diagnosed by ultrasound. (D) Egger's Test for all studies. (E) Egger's Test for studies diagnosed by ultrasound.

CHAPTER 9

Modeling liver cancer and therapy responsiveness using organoids derived from primary mouse liver tumors

Wanlu Cao, **Jiaye Liu,** Meng Li, Ling Wang, Monique M.A. Verstegen, Yuebang Yin, Buyun Ma, Kan Chen, Michiel Bolkestein, Dave Sprengers, Luc J. W. van der Laan, Michael Doukas, Jaap Kwekkeboom, Ron Smits, Maikel P. Peppelenbosch and Qiuwei Pan

Carcinogenesis. 2019 Mar 12;40(1):145-154.

Abstract

The current understanding of cancer biology and development of effective treatments for cancer remain far from satisfactory. This in turn heavily relies on the availability of easy and robust model systems that resemble the architecture/physiology of the tumors in patients to facilitate research. Cancer research *in vitro* has mainly been based on the use of immortalized 2D cancer cell lines for, which deviate in many aspects from the original primary tumors. The recent development of the organoid technology allowing generation of organ-buds in 3D culture from adult stem cells has endowed the possibility of establishing stable culture from primary tumors. Although culturing organoids from liver tumors is thought to be difficult, we now convincingly demonstrate the establishment of organoids from mouse primary liver tumors. We have succeeded in culturing 91 lines from 129 liver tissue/tumors. These organoids can be grown in long-term cultures *in vitro*. About 20% of these organoids form tumors in immunodeficient mice upon (serial) transplantation, confirming their tumorigenic and self-renewal properties. Interestingly, single cells from the tumor organoids have high efficiency of organoid initiation, and a single organoid derived from a cancer cell is able to initiate a tumor in mice, indicating the enrichment of tumor-initiating cells in the tumor organoids. Furthermore, these organoids recapitulate, to some extent, the heterogeneity of liver cancer in patients, with respect to phenotype, cancer cell composition and treatment response. These model systems shall provide enormous opportunities to advance our research on liver cancer (stem cell) biology, drug development and personalized medicine.

Keywords:

Tumor organoid, Liver tumor, Mouse, Anti-cancer research

Introduction

Liver cancer is one of the most common cause of cancer-related death worldwide with limited treatment options available [1]. Better understanding of the biology of liver cancer is urgently needed for facilitating the development of new therapies. However, this in turn heavily relies on the availability of easy and robust model systems that resemble the architecture and physiology of the tumors in patients. So far, the cancer research society has mainly used immortalized cancer cell lines that have been propagated in 2D culture as *in vitro* model for decades. Obviously, these cell lines behave very different from the original tumor in many aspects and cost long time to establish[2]. Primary cell culture of liver cancer cells from either human or mouse has proven to be very difficul[3]. Thus, innovative approaches enabling *in vitro* propagation of primary liver cancer cells that maximize the modeling capacity of the patient disease and treatment response will be of particular importance.

The recent development of the organoid technology has driven the stem cell research field moving forward[4,5] . Organoids are initiated *in vitro* from one or a few adult $Lgr5^{+}$ stem cells of a particular tissue/organ and self-organize into 3D structure[6,7]. They recapitulate the tissue architecture and lineage hierarchy, allow self-renewal and expansion of the stem cell population and empower different types of experimental manipulation[8]. Many types of cancers are believed to harbor a subset of cells, termed as tumor-initiating cells (TIC). Thus, it is conceivable that organoids could be cultured from tumor tissues, if sophisticated 3D cell culture techniques/conditions are employed. Indeed, tumor organoid models have been established from primary tumors of colorecta[9], pancreatic[10,11], prostate[12] and liver cancer[13] patients. This technology is now used to explore many aspects of cancer research, including studying oncogenic transformation, cancer stem cells, drug development and personalized treatment[14,15]. Our study has presented the successful establishment of malignant organoid models from mouse primary liver tumors, performed extensive characterization and demonstrated their applications in liver cancer research.

Method and material

Tumor/healthy organoid culture

Single cells were isolated from liver tumor tissues using a digestion solution: Collagenase type XI (0.5 mg/ml, Sigma-Aldrich), Dispase (0.2 mg/ml, Gibco), 1 % FBS in DMEM medium (Lonza) (37 °C, 30 min), then centrifuged (600 rpm, 10 min) to collect the cell pellets. Cells were directly mixed with matrigel (BD Bioscience), seeded on 24/48 well plates and kept at 37 °C for at least 30 min. After the matrigel formed a solid gel, medium was slowly added. Organoid culture medium was based on advanced DMEM/F12 (Invitrogen), which is supplemented with B27 (2% vol/vol) and N2 (1% vol/vol , Invitrogen), N-acetylcysteine (1.25 µM, Sigma-Aldrich), gastrin (10 nM, Sigma-Aldrich), EGF (50 ng/ml, Peprotech), R-spondin 1 (10% vol/vol, conditioned medium produced by 293T-H-RspoI-Fc cell line), FGF10 (100 ng/ml, Peprotech), nicotinamide (10 mM, Sigma-Aldrich) and HGF (50 ng/ml, Peprotech), as described previously[5]. For the initial 3 days, the organoids also need to be supplemented with Noggin (10% vol/vol, conditioned medium produced by 293T-HA-Noggin cell line) Wnt3a (30% vol/vol, conditioned medium produced by L-Wnt3a cell line)[5]. Medium was refreshed every 2-3 days and organoids were passaged in 1:2-1:10 split ratio once per week, or according to the growth of the organoids. The healthy liver-derived organoids were also isolated and cultured by using the same methodology as tumor organoid culture (stemness-keeping culture condition, without further differentiation).

Organoid allograft

Cold advanced DMEM/F12 medium was used to collect the organoids. Organoids were mechanically dissociated into pieces by pipetting (5-10 times) (collect enough amount of organoids from an entire 24-well plate, averagely 1×10^6-1×10^7). After centrifuging, organoids pellets (broken organoid pieces) were re-suspended in cold advanced DMEM/F12 medium and then mixed directly with matrigel in the ratio of 1:1 with a total volume of 100-200ul. 4-6 weeks old female NOG/JicTac (CIEA NOD.Cg-Prkdc-scid Il2rg-tm1Sug) mice were purchased from Taconic, and subcutaneously injected with the collected tumor organoids. Tumor formation was monitored weekly and mice were sacrificed to harvest tumor after visualizing the tumor (the tumor size reached 1cm). Tumor tissues were stored or cultured as described above. All animal experiments were approved by the Committee on the Ethics of Animal Experiments of the Erasmus Medical Center.

Single organoid formation assay and allograft assay

Cold advanced DMEM/F12 medium was used to collect the organoids. Organoids were mechanically dissociated into small pieces by pipetting (20-30 times) and further digested into single cells by TrypLE (Gibco, 37℃, 5-10 min). FACS sorter (BD FACSAriaTM II) was used to further isolate the single living cells. Propidiumiodide (PI) staining was used to exclude dead cells; FSC-Width with FSC-Area and then SSC-Width with SSC-Area gates were used to select the single cells. After mixing one single cell with matrigel, a droplet with in total volume of 5 µl was seeded in a well of 96-well plate for organoid initiation. After 1-3 weeks, single organoids were formed. Cold advanced DMEM/F12 medium was used to collect the single organoids. After removing the supernatant, matrigel was mixed with the organoid pellet and transplanted subcutaneously into the NOG mice directly. Tumor formation was monitored as described above.

Metabolic activity analyses for drug treatment

Different organoid lines were seeded separately in a 24/48-well plate. Sorafenib (1 uM) and Regorafenib (1 uM) was added to the organoid culture since the initial day. Drugs were refreshed every 2 days. At the day 7, organoids were incubated with Alamar Blue (Invitrogen, 1:20 in DMEM) for four hours, and then medium was collected for analysis of the metabolic activity of the cells. Absorbance was determined by using fluorescence plate reader (CytoFluor® Series 4000, Perseptive Biosystems) at the excitation of 530/25 nm and emission of 590/35. Each treatment condition was repeated for four times and matrigel only was used as blank control.

Karyotyping

Karyotyping was performed as previously described[16]. Briefly, cultures were incubated with 0.1 ug/ml Karyomax Colcemid (Gibco, 152120-012) for 24 h. Organoids were harvested by cold organoid basic medium and then kept on ice for 10 min. Then, TrypLE (Gibco) were added for digesting organoids into single cells. Cells were then incubated with KCL 0.0075 M hypotonic solution for 10 min in 37℃ incubator. Methanol: acetic acid (3:1, freshly prepared) was used for further fixation. Cells were dropped onto a microscope slide for visualization. Nuclei were mounted and stained using Vectashield with DAPI (Vector Labs). A minimum of 15 metaphases per sample were counted.

Statistical Analysis

Prism software (GraphPad Software) was used for all statistical analysis. For statistical significance of the differences between the means of two groups, we used Mann-Whitney U-test. For comparing two paired groups, we used Paired T-test. Differences were considered significant at a p value less than 0.05.

Results

Successful culture of organoids from mouse primary liver tumors

Diethylnitrosamine (DEN) is widely used as a carcinogen in experimental animal models, in particular for inducing liver tumors in mice. Similar to the gender disparity in patients, DEN also preferentially induce liver tumors in male mice[17]. Thus, we have mainly used male mice (53 male; 3 female) to induce liver tumor by DEN (Supplementary Figure 1 and Supplementary Figure 2). The livers were harvested for organoid culture (Figure 1A and Supplementary Figure 3). The numbers of visible tumors vary among the harvested mouse livers, ranging from zero to multiple tumors per liver (Supplementary Figure 1 and Supplementary Figure 4A). In total, we obtained 129 individual tissue/tumors from these mice, which were subjected to organoid culture (Figure 1A and Supplementary Figure 3). In general, small organoids could be visualized since post day 2-7 and passage was required around 7-14 days. We have succeeded in establishing organoid culture from 91 out of the 129 tumors, representing an efficiency of 70.5% (Supplementary Figure 2 and Supplementary Figure 4). The initiation efficiency varied from 0% to 100% among individual livers (Supplementary Figure 4B). For the rest 38 tissues that failed to form into organoids, 12 samples did initiate organoids but stopped proliferation at an early stage (maintained less than 3-4

weeks, 1-3 passages); whereas the other tumors had extensive necrosis and did not initiate any organoid from the start.

The successfully established lines could be maintained and propagated in 3D culture for at least 3 months, by passaging in the ratio of 1:2-1:4 for every 7 days. We further demonstrated that these tumor-derived organoids can be frozen, stored and re-cultured again without affecting their growth rate. With respect to the morphology, we (Figure 1C) and others[5] have observed that organoids derived from the healthy liver have a uniform bubble-like structure. In contrast, organoids derived from liver tumors presented diverse morphologies, ranging from bubble-like to condensed and flower-like, as well as an irregular sheet-like structure (Figure 1D-H). Interestingly, some cultures contained a mixture of organoids with different morphology (Supplementary Figure 5), which may reflect the heterogeneity of cell types within the tumors.

Tumorigenicity of expanded organoids in immunodeficient mice

To functionally assess whether these tumor-derived organoids are malignant, we performed the allograft assay in NOG immunodeficient mice as described previously (Figure 1A and Supplementary Figure 3)[18]. We have subcutaneously engrafted all the established 91 organoid lines and assessed their tumor formation ability *in vivo*. Within 4-16 weeks, 18 out of 91 (20%) lines initiated tumor formation in NOG mice (Figure 1A and Supplementary Table 1: The upper panel).

Organoids could be cultured again from these allograft tumors (Figure 1A-B and Supplementary Figure 3). These tumor organoids needed to be passaged every 5 days in the ratio of 1:5-1:10, indicating an increased speed of growth. Importantly, when engrafting into NOG mice, these organoids are capable to initiate tumors again, with relatively shorter time compared to engraftment of the primary tumor organoids (Figure 1B and Supplementary Table 1, allograft tumor vs. primary tumor: 35 days vs 40.6 days). These results firmly demonstrated that liver tumor derived organoids are malignant and tumorigenic with self-renewal capability. Furthermore, we have performed karyotyping for the organoid strains (Figure 2). The majority of the strains from the primary tumors and all the strains derived from allograft showed irregular chromosome numbers. In contrast, organoids from healthy livers stably maintain diploid/tetraploid/octoploid chromosome numbers in culture.

A single organoid derived from a single cancer cell is able to initiate tumor formation in mice

To further consolidate the ability to initiate tumor growth of the organoids, we performed an organoid formation assay with isolated single cells. We found that isolated single cells from the tumor organoids can efficiently re-initiate organoids (Figure 1A). More importantly, subcutaneous transplantation of a single tumor organoid derived from a

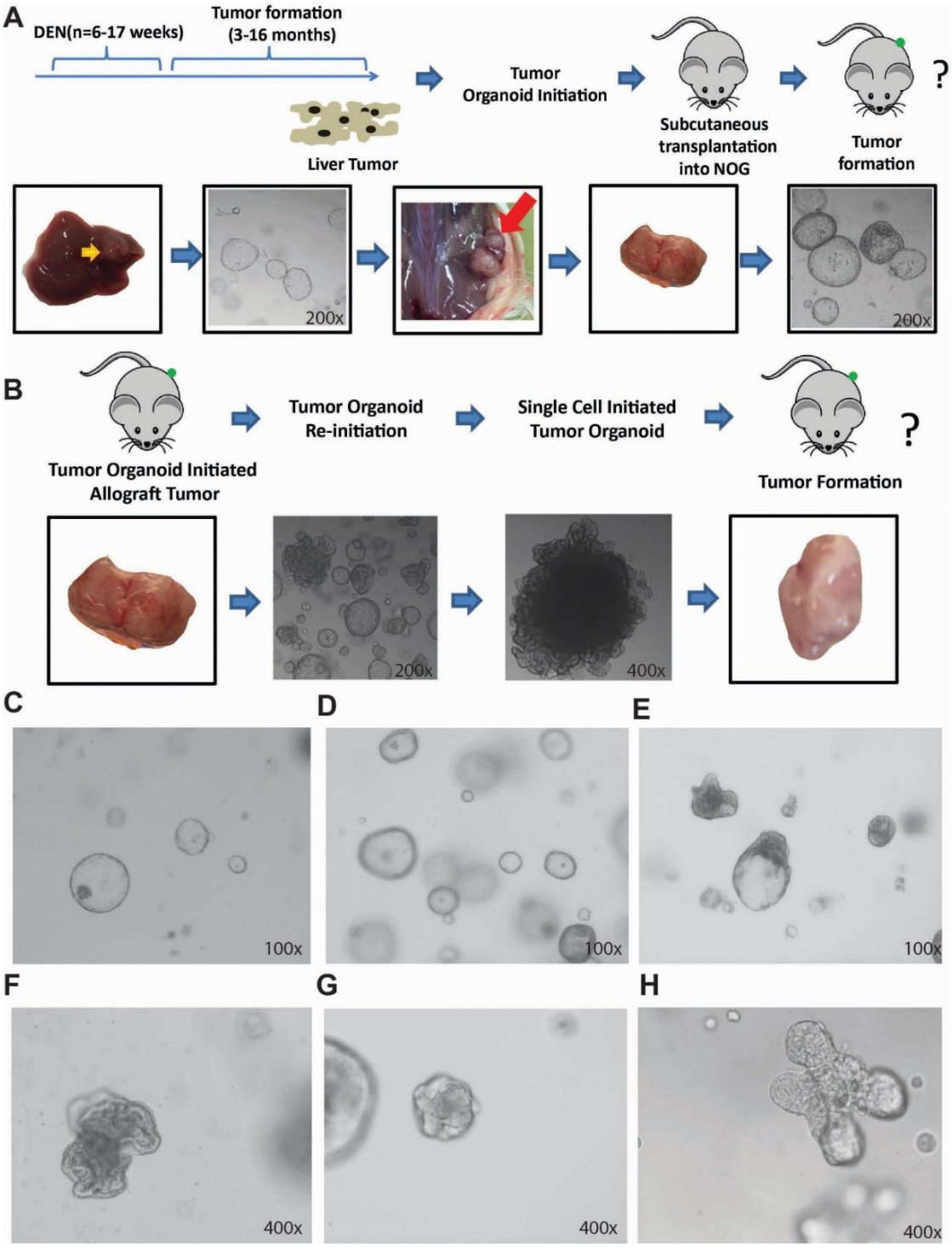

Figure 1. Establishment and characterization of organoid cultures from mouse liver tumors. (A) The upper panel: An outline of the experimental strategy used to establish primary tumor organoids. The lower panel: Representative pictures showing tumor organoids cultured from mouse primary liver tumors, and the formation of allograft tumor in NOG mice. The allograft tumors can be cultured into tumor organoids again. (B) The upper panel: An outline of the experimental strategy used to investigate single tumor organoid. The lower panel: Representative pictures showing that allograft tumor can initiate tumor organoids again. A single cell isolated from the tumor organoid can initiate a single organoid and then initiate tumor in NOG mice. (C) Example of normal liver organoids. (D-H) Liver tumor organoids with different morphologies.

single cell into immunodeficient NOG mice rapidly initiated tumor around two weeks, confirming their malignant property (Figure 1B and Supplementary Table 1: the lower panel). Furthermore, organoids can be re-cultured from those allograft tumors and exhibited progressive expansion for over 4 months. These results indicate that 3D tumor organoid system enriches the cells with the capacity of tumor initiating.

Classically, stem cell markers have been widely used to identify potential TIC, although it is an ever debating issue of defining qualified TIC markers[19]. Based on previous studies[19,20], we have profiled a panel of potential TIC markers, in comparison with organoids from normal liver stem cells. We found that the expression profile for stem cell/tumor stem cell markers varied from different strains (Supplementary file 1). Several markers, including *Bmi1*, *Lgr5*, *Oct4*, *Cd133*, *Hopx* and *Sox2* were upregulated in allograft strains compared to normal organoid or primary tumor-derived organoid strains (Figure 3). CD44 and Tert were downregulated in allograft strains. By paired analysis of the available paired strains, we observed the upregulation of *Bmi1*, *Lgr5* and *Muc5ac* and the downregulation of *Sox9* and *Ck7* (Supplementary Figure 6).

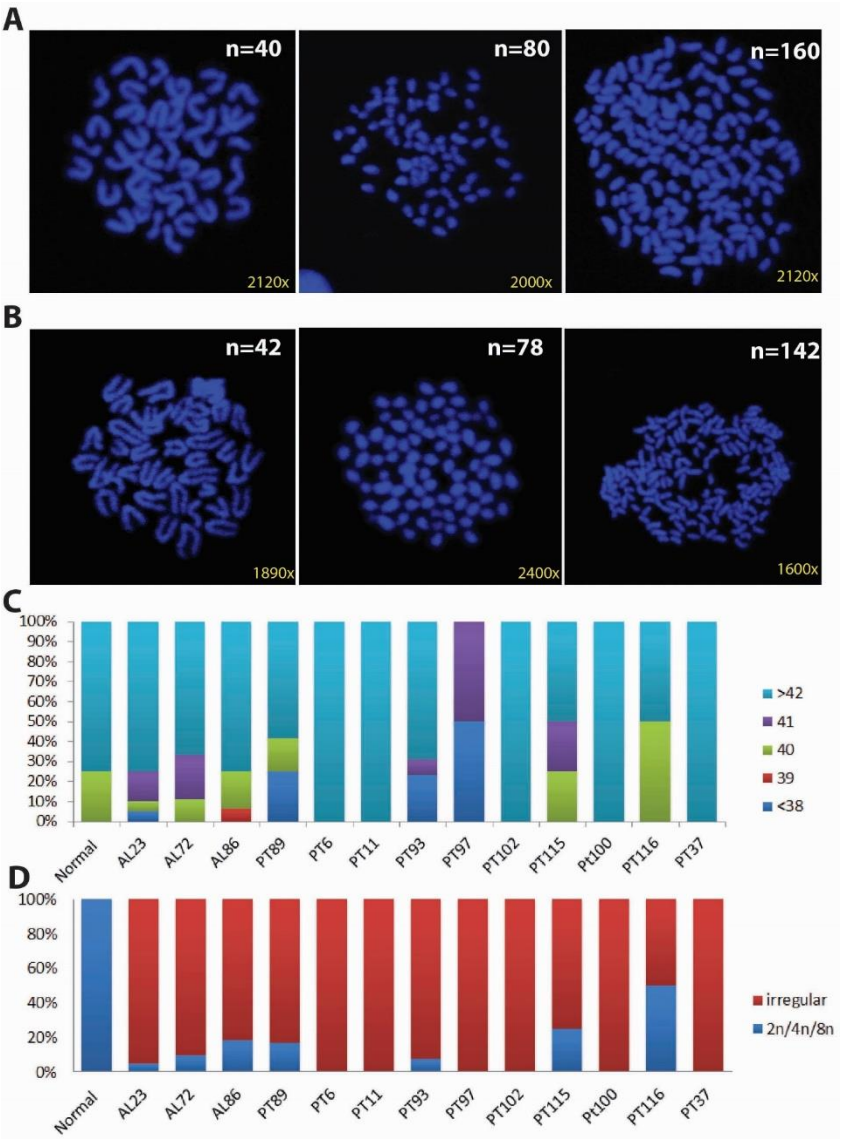

Figure 2. Karyotyping of normal and tumor organoids. (A-B) Representative images of organoid metaphases used for the ploidy analysis (A: normal chromosome number B: irregular chromosome number; Original magnification for organoids were 2800×). (C-D) Different analysis methods showing the percentage of ploidy per number of metaphases counted (at least 15 total), for normal organoid (N), allograft organoid (AL) and primary organoid (PT).

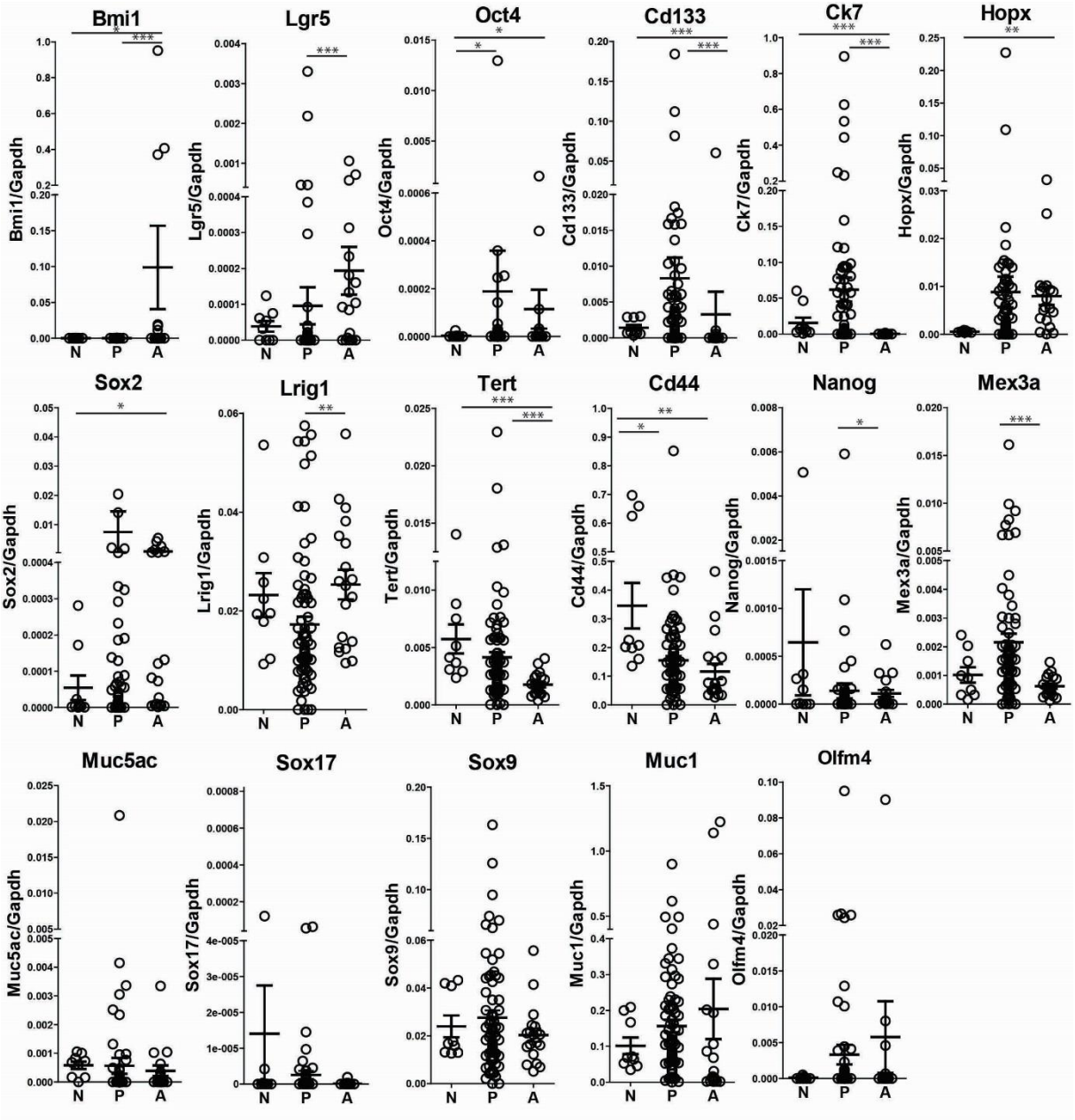

Figure 3. Comparison of the expression of progenitor/stem cell markers. N: normal liver organoid strains; P: strains from primary liver tumors; A: strains from allograft liver tumors (*P < .05; **P < .01; ***P < .001).

Tumor organoids express cholangiocyte and/or hepatocyte markers

In patients, primary liver cancer has been traditionally classified into three main types based on the tumor cell type. These are hepatocellular carcinoma (HCC), cholangiocarcinoma (CC) and hepatocellular-cholangiocarcinoma (CHCs). Although it

remains a challenge to differentiate these types, hepatocyte (e.g. AFP, HNF4α) or/and cholangiocyte (e.g. CEA, CK19, C-KIT, EpCAM) markers are often used as one of the approaches to distinguish these types of liver cancer[21]. In this respect, we have characterized the established tumor organoids and corresponding tissues by staining with HCC (AFP/HNF4α), CC (EpCAM/CK19) marker, H&E staining and Gomori's reticulin staining respectively (Figure 4, supplementary file 1-3). Among the 91 strains which were transplanted into the NOG mice, 25 were lost due to infection in culture or storage issue later on (Supplementary Figure 4, marked by yellow). Thus, we mainly focused on the rest 66 strains, as well as the 18 allograft strains. We found distinct expression patterns among different lines of established tumor organoids. Some with a subset of cells express AFP and Hnf4a, some express EpCAM and CK19, and others express both markers (Supplementary file 1). More importantly, some allograft strains maintained the expression profile as well as the histology, compared to the primary tissue/strains (Figure 5A); whereas the other strains did not (Figure 5B). These data indicate that murine tumor organoids may recapitulate the heterogeneity of liver cancer types in patients to some extent. Of note, given that the etiology of liver is diverse, DEN induced liver tumors in mice do not fully represent liver cancer in patients[17].

Assessment of anti-cancer drugs in the tumor organoid model

Current treatment options, in particular for advanced liver cancer, are very limited. Sorafenib is the only FDA-approved first-line systemic therapy for patients with advanced HCC, with improvement of patient survival for only 3 months[1]. Regorafenib is now emerging as a potential second-line therapy for HCC patients[22]. To explore the potential of using liver tumor organoid models for future drug development, we assessed the feasibility by testing the effects of Sorafenib and Regorafenib.

We used organoid lines established from nine allograft tumors, as well as four primary-tumor derived organoid strains. Overall, these two targeted therapies inhibited the growth of the organoids (Figure 6 and Supplementary figure 7). However, we also observed clear variations of the responsiveness among these organoids. Thus, we have classified the organoid strains into three groups. Group 1 is sensitive to both (Figure 6A and Supplementary figure 7A); whereas Group 2 is only sensitive to Sorafenib but not Regorafenib (Figure 6B and Supplementary figure 7B); and Group 3 is not sensitive to both (Figure 6C and Supplementary figure 7C). We further compared the expression profile of stem cell/tumor stem cell markers between Group 1 with the rest strains. We have observed low expression of Oct4 and high expression of Sox9 in Group 1 (Supplementary Figure 8).

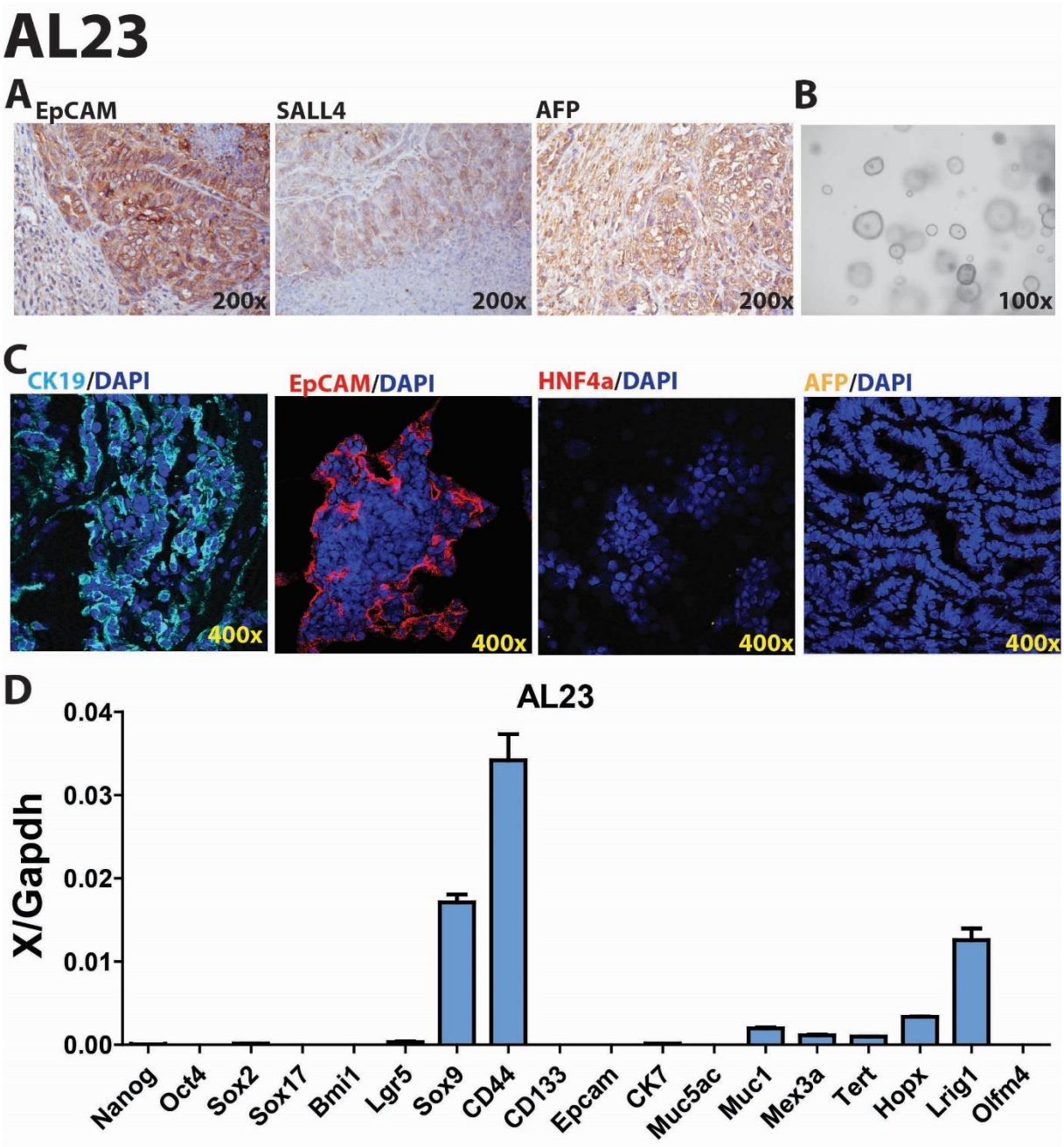

Figure 4. An example of the characterization of an organoid strain. (A) IHC straining for the allograft tissue of EpCAM (CC marker), SALL4 (poorly differentiated tumor marker) and AFP (HCC marker). (B) The morphology of organoid. (C) IF straining for the allograft organoid strain of CK19 (CC), EpCAM (CC), HNF4a(HCC) and AFP (HCC).(D) The expression profile for stem cell/tumor stem cell markers of the allograft organoid strains (n=3).

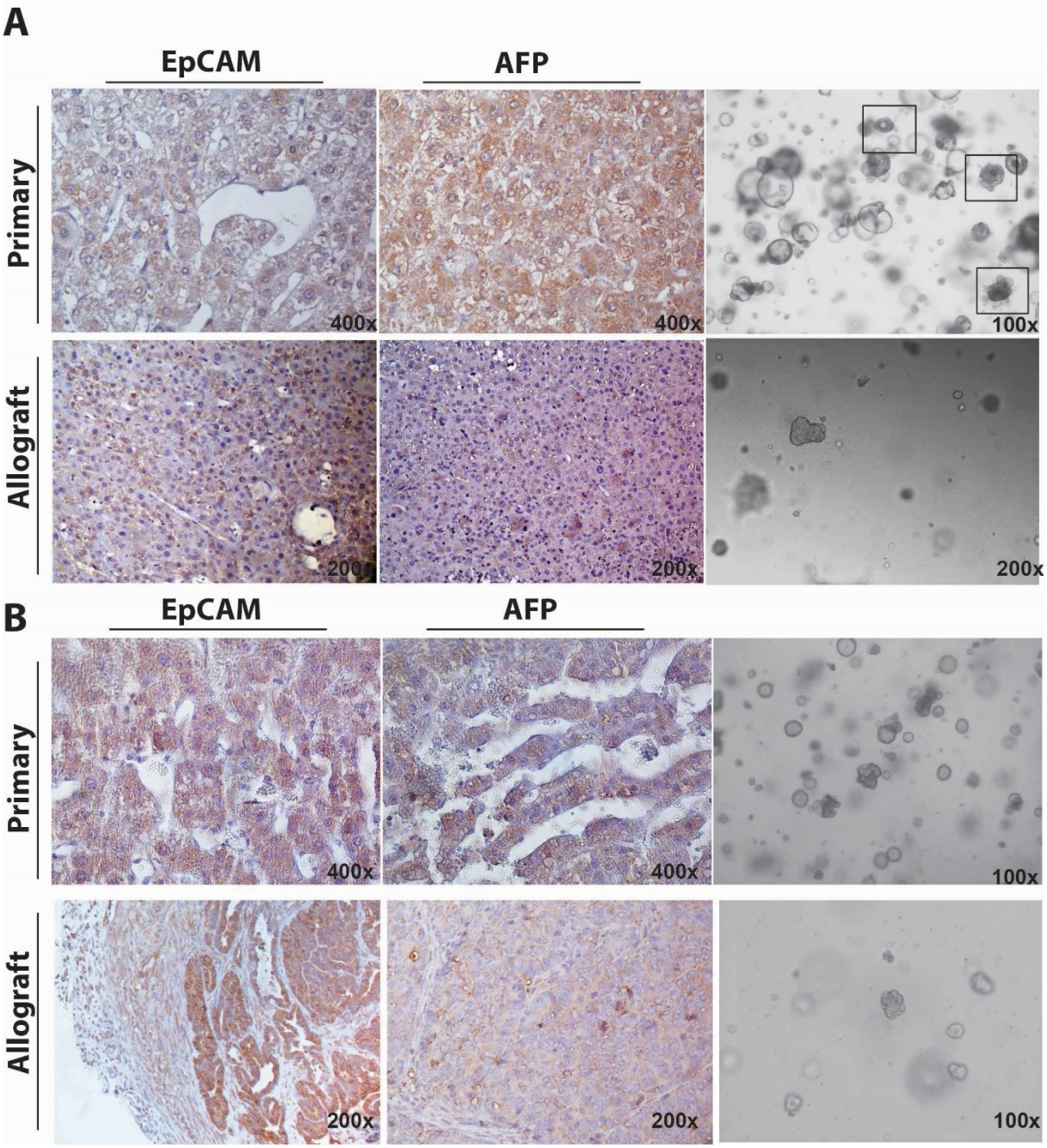

Figure 5. The characterization of organoid strains and corresponding tissue. (A) The tumor initiated by organoids showed similar histology and expression patterns of EpCAM and AFP compared to the primary tissue. Black box: the tumor organoid. (B) The tumor initiated by organoids showed different histology and expression profile of patterns of EpCAM and AFP compared to the primary tissue.

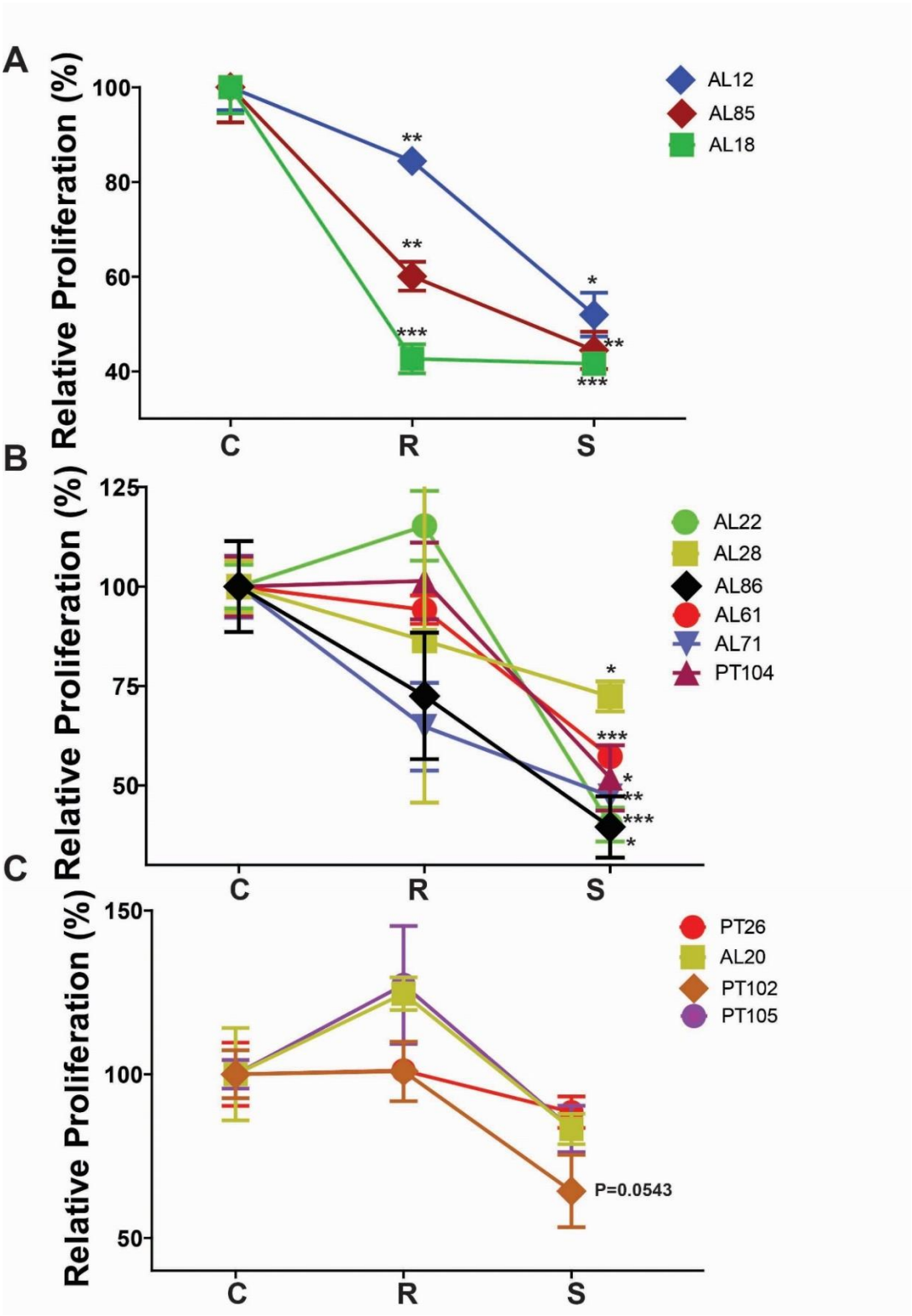

Figure 6. Tumor organoids in response to the treatment of the targeted therapeutics Sorafenib or Regorafenib. 13 tumor organoid lines (AL12, AL18, AL20, AL22, AL26, AL28, AL61, AL71, AL85, AL86, PT102, PT104 and PT105) were analyzed. At day 7, the Alamar blue assay was used to measure the growth of organoids. (*P < .05; **P < .01; ***P < .001, n=4). (A) Group 1: organoid strains which were both sensitive to Sorafenib and Regorafenib. (B) Group 2: organoid strains which were only sensitive to Sorafenib, but not Regorafenib. (C) Group 3: organoid strains which were not sensitive to both Sorafenib and Regorafenib.

Discussion

This study has demonstrated the establishment of organoids from primary mouse liver tumors. These organoids can be expanded in long-term cultures and initiate tumors in immunodeficient mice. Importantly, these organoids recapitulate, to some extent, the heterogeneity of liver cancer as seen in patients, with respect to phenotype, cancer cell composition and treatment response.

Classically, the *in vitro* investigation of liver cancer is based on cell lines, which have the following limitations: 1) limited number of established cell lines; 2) low efficiency of establishing new lines from primary tissues; 3) only aggressive tumors have high change to establish *in vitro* culture successfully. Thus, the majority of primary tissue (>90%) cannot be successfully culture *in vitro*, especially the benign or less aggressive tumors, which also should be further investigated. Except the traditional cell line culture model, several other methods have also been explored to model liver cancer *in vitro*. The rotating wall vessel bioreactor has been reported to be used to culture HCC cell lines. This system was further used to co-culture the liver tumor cells with colon carcinoma cells to form liver-tumor hybrid, as a model to mimic liver metastasis. In addition, 2D or 3D spheroid culture has been applied to culture HCC cell lines. However, the majority of those *in vitro* system focus on immortalized cell lines, rather than primary tissue.

We here adopted matrigel based 3D organoid culture system. This model allows investigation of healthy adult stem cells, as well as various types of diseases, in particular cancer. Successful examples have been reported in establishing organoids from colon, pancreas and prostate tumor tissues. A very recent study has reported the culture of organoids from a few liver cancer patients[13]. Here we reported that we have succeeded in establishing 91 lines from 128 mouse liver tissues/tumors. These organoids are capable of long-term culture and expansion *in vitro*. They are capable of initiating tumors in immunodeficient mice upon (serial) transplantation, confirming their tumorigenic, malignant and self-renewal properties. However, a subset of the tumor organoid strains did not initiate tumor in the current allograft transplantation model. First of all, we cannot exclude the possible existence of normal organoids among these organoid lines established from primary tumors. Secondly, the mouse model used for allograft transplantation retains part of the immune system which may inhibit tumor initiation[23].

There is substantial heterogeneity among different organoid strains, in respect to organoid morphology, tissue histology and marker expression. The diversity of morphology has previously also been observed in other types of tumor organoids, such as those derived from colorectal[9], pancreatic[10,11] and prostate[12] cancer. Interestingly, the tumor histology of the allograft and the corresponding primary tumor is not always matched (Supplementary Table 2, Supplementary Table 3 and Supplementary figure 9). One possible explanation is that the current liver organoid culture protocol more favors the growth of stem cell/cholangiocyte like cells[5,13,24]. Secondly, trans-

differentiation between hepatocyte and cholangiocyte has been well-recognized[25]. We speculate that with the current organoid culture approach we may drive the trans-differentiation of primary HCC cells into cholangiocarcinoma cells. Last but not the least, in case of a small tumor, tissue was prioritized for organoid culture, left no representative primary tumor tissue for histology evaluation.

Our results also support the notion that liver tumors contain TIC, and organoids may represent an innovative model system for studying these cancer cells. TIC is a rare cancer cell population, but is thought to be the engine of tumor formation, relapse, metastasis and chemo-resistance in many cancer types[19], including in liver cancer[26]. We envision that these tumor organoid models have potential to circumvent a major bottleneck in the TIC field as these cells are usually not able to be cultured *in vitro*. The current research is largely based on phenotypic description and tumor formation assays in immunodeficient mice[26]. Sophisticated *in vitro* culture of liver tumor organoids that are capable of long-term propagation *ex vivo*, as demonstrated in our study, provides a unique tool for the research field to advance in-depth research of liver TIC.

We further reveal the heterogeneity of individual lines as well as the differences in responsiveness between treatments. This provides proof-of-concept that organoids have the potential to be used as an *in vitro* model to study anti-cancer drug development in general, as well as for personalized medicine in cancer treatment. Furthermore, TIC have been proposed as attractive anti-cancer targets and recent studies have demonstrated the possibility and efficacy of targeting TIC in animal models. Different allograft organoid strains showed different expression patterns for the stem cell/tumor stem cell markers, which may be useful for further investigation of the specific tumor initiating cell/cancer stem cell populations (Supplementary figure 10). We believe that tumor organoid models have particular privileges as a platform for facilitating the development of TIC targeted therapies, given that these cells can be *ex vivo* cultured from primary tumor tissues.

Organoid model system shall provide enormous opportunities to advance the research on liver cancer/stem cell biology, drug development and personalized medicine. Of note, organoid systems do not mutually exclude the use of the classical cancer cell lines, but in fact complement each other. Finally, more efforts are urgently required to establish robust organoid models from patient liver tumors.

Reference

1 Ohlund D, Handly-Santana A, Biffi G, Elyada E, Almeida AS, Ponz-Sarvise M*, et al.* Distinct populations of inflammatory fibroblasts and myofibroblasts in pancreatic cancer. J Exp Med 2017;**214**:579-96.
2 Guo Y, Cordes KR, Farese RV, Jr., Walther TC. Lipid droplets at a glance. J Cell Sci 2009;**122**:749-52.
3 Collaborators GBDO, Afshin A, Forouzanfar MH, Reitsma MB, Sur P, Estep K*, et al.* Health Effects of Overweight and Obesity in 195 Countries over 25 Years. N Engl J Med 2017;**377**:13-27.
4 Gluchowski NL, Becuwe M, Walther TC, Farese RV, Jr. Lipid droplets and liver disease: from basic biology to clinical implications. Nat Rev Gastroenterol Hepatol 2017;**14**:343-55.
5 Olzmann JA, Carvalho P. Dynamics and functions of lipid droplets. Nat Rev Mol Cell Biol 2019;**20**:137-55.
6 Jackson CL. Lipid droplet biogenesis. Curr Opin Cell Biol 2019;**59**:88-96.
7 Yen CL, Stone SJ, Koliwad S, Harris C, Farese RV, Jr. Thematic review series: glycerolipids. DGAT enzymes and triacylglycerol biosynthesis. J Lipid Res 2008;**49**:2283-301.
8 Korber M, Klein I, Daum G. Steryl ester synthesis, storage and hydrolysis: A contribution to sterol homeostasis. Biochim Biophys Acta Mol Cell Biol Lipids 2017;**1862**:1534-45.
9 Ben M'barek K, Ajjaji D, Chorlay A, Vanni S, Forêt L, Thiam AR. ER Membrane Phospholipids and Surface Tension Control Cellular Lipid Droplet Formation. Dev Cell 2017;**41**:591-604 e7.
10 Salo VT, Belevich I, Li S, Karhinen L, Vihinen H, Vigouroux C*, et al.* Seipin regulates ER-lipid droplet contacts and cargo delivery. Embo J 2016;**35**:2699-716.
11 Salo VT, Li S, Vihinen H, Hölttä-Vuori M, Szkalisity A, Horvath P*, et al.* Seipin Facilitates Triglyceride Flow to Lipid Droplet and Counteracts Droplet Ripening via Endoplasmic Reticulum Contact. Dev Cell 2019;**50**:478-93 e9.
12 Chorlay A, Monticelli L, Veríssimo Ferreira J, Ben M'barek K, Ajjaji D, Wang S*, et al.* Membrane Asymmetry Imposes Directionality on Lipid Droplet Emergence from the ER. Dev Cell 2019;**50**:25-42 e7.
13 Kory N, Farese RV, Jr., Walther TC. Targeting Fat: Mechanisms of Protein Localization to Lipid Droplets. Trends Cell Biol 2016;**26**:535-46.
14 Wilfling F, Wang H, Haas JT, Krahmer N, Gould TJ, Uchida A*, et al.* Triacylglycerol synthesis enzymes mediate lipid droplet growth by relocalizing from the ER to lipid droplets. Dev Cell 2013;**24**:384-99.
15 Kuerschner L, Moessinger C, Thiele C. Imaging of lipid biosynthesis: how a neutral lipid enters lipid droplets. Traffic 2008;**9**:338-52.
16 Prévost C, Sharp ME, Kory N, Lin Q, Voth GA, Farese RV, Jr.*, et al.* Mechanism and Determinants of Amphipathic Helix-Containing Protein Targeting to Lipid Droplets. Dev Cell 2018;**44**:73-86 e4.
17 Sztalryd C, Brasaemle DL. The perilipin family of lipid droplet proteins: Gatekeepers of intracellular lipolysis. Biochim Biophys Acta Mol Cell Biol Lipids 2017;**1862**:1221-32.
18 Ozeki S, Cheng J, Tauchi-Sato K, Hatano N, Taniguchi H, Fujimoto T. Rab18 localizes to lipid droplets and induces their close apposition to the endoplasmic reticulum-derived membrane. J Cell Sci 2005;**118**:2601-11.
19 Pataki CI, Rodrigues J, Zhang L, Qian J, Efron B, Hastie T*, et al.* Proteomic analysis of monolayer-integrated proteins on lipid droplets identifies amphipathic interfacial α-helical membrane anchors. Proc Natl Acad Sci U S A 2018;**115**:E8172-E80.
20 Murphy DJ, Vance J. Mechanisms of lipid-body formation. Trends in Biochemical Sciences 1999;**24**:109-15.
21 Thiam AR, Farese RV, Jr., Walther TC. The biophysics and cell biology of lipid droplets. Nat Rev Mol Cell Biol 2013;**14**:775-86.
22 Gong J, Sun Z, Wu L, Xu W, Schieber N, Xu D*, et al.* Fsp27 promotes lipid droplet growth by lipid exchange and transfer at lipid droplet contact sites. J Cell Biol 2011;**195**:953-63.
23 Krahmer N, Guo Y, Wilfling F, Hilger M, Lingrell S, Heger K*, et al.* Phosphatidylcholine synthesis for lipid droplet expansion is mediated by localized activation of CTP:phosphocholine cytidylyltransferase. Cell Metab 2011;**14**:504-15.
24 Guo Y, Walther TC, Rao M, Stuurman N, Goshima G, Terayama K*, et al.* Functional genomic screen reveals genes involved in lipid-droplet formation and utilization. Nature 2008;**453**:657-61.
25 Valm AM, Cohen S, Legant WR, Melunis J, Hershberg U, Wait E*, et al.* Applying systems-level spectral imaging and analysis to reveal the organelle interactome. Nature 2017;**546**:162-7.
26 Greenberg AS, Coleman RA, Kraemer FB, McManaman JL, Obin MS, Puri V*, et al.* The role of lipid droplets in metabolic disease in rodents and humans. J Clin Invest 2011;**121**:2102-10.
27 Tauchi-Sato K, Ozeki S, Houjou T, Taguchi R, Fujimoto T. The surface of lipid droplets is a phospholipid monolayer with a unique Fatty Acid composition. J Biol Chem 2002;**277**:44507-12.
28 Zehmer JK, Bartz R, Bisel B, Liu P, Seemann J, Anderson RGW. Targeting sequences of UBXD8 and AAM-B reveal that the ER has a direct role in the emergence and regression of lipid droplets. Journal of cell science 2009;**122**:3694-702.
29 Olofsson S-O, Boström P, Andersson L, Rutberg M, Perman J, Borén J. Lipid droplets as dynamic organelles connecting storage and efflux of lipids. Biochimica et Biophysica Acta (BBA) - Molecular and Cell Biology of Lipids 2009;**1791**:448-58.
30 Bersuker K, Olzmann JA. Establishing the lipid droplet proteome: Mechanisms of lipid droplet protein targeting and degradation. Biochimica et biophysica acta Molecular and cell biology of lipids 2017;**1862**:1166-77.
31 Wang H, Lei M, Hsia RC, Sztalryd C. Analysis of lipid droplets in cardiac muscle. Methods Cell Biol 2013;**116**:129-49.
32 Tarnopolsky MA, Rennie CD, Robertshaw HA, Fedak-Tarnopolsky SN, Devries MC, Hamadeh MJ. Influence of endurance exercise training and sex on intramyocellular lipid and mitochondrial ultrastructure, substrate use, and mitochondrial enzyme activity. Am J Physiol Regul Integr Comp Physiol 2007;**292**:R1271-8.
33 Shaw CS, Jones DA, Wagenmakers AJ. Network distribution of mitochondria and lipid droplets in human muscle fibres. Histochem Cell Biol 2008;**129**:65-72.
34 Herms A, Bosch M, Reddy BJ, Schieber NL, Fajardo A, Rupérez C*, et al.* AMPK activation promotes lipid droplet dispersion on detyrosinated microtubules to increase mitochondrial fatty acid oxidation. Nat Commun 2015;**6**:7176.
35 Rambold Angelika S, Cohen S, Lippincott-Schwartz J. Fatty Acid Trafficking in Starved Cells: Regulation by Lipid Droplet Lipolysis, Autophagy, and Mitochondrial Fusion Dynamics. Developmental Cell 2015;**32**:678-92.
36 Benador IY, Veliova M, Liesa M, Shirihai OS. Mitochondria Bound to Lipid Droplets: Where Mitochondrial Dynamics Regulate Lipid Storage and Utilization. Cell Metabolism 2019;**29**:827-35.
37 Benador IY, Veliova M, Mahdaviani K, Petcherski A, Wikstrom JD, Assali EA*, et al.* Mitochondria Bound to Lipid Droplets Have Unique Bioenergetics, Composition, and Dynamics that Support Lipid Droplet Expansion. Cell metabolism 2018;**27**:869-85.e6.
38 Wang H, Sztalryd C. Oxidative tissue: perilipin 5 links storage with the furnace. Trends in Endocrinology & Metabolism 2011;**22**:197-203.

39 Wang H, Sreenivasan U, Hu H, Saladino A, Polster BM, Lund LM*, et al.* Perilipin 5, a lipid droplet-associated protein, provides physical and metabolic linkage to mitochondria. Journal of lipid research 2011;**52**:2159-68.
40 Zhu Y, Ren C, Zhang M, Zhong Y. Perilipin 5 Reduces Oxidative Damage Associated With Lipotoxicity by Activating the PI3K/ERK-Mediated Nrf2-ARE Signaling Pathway in INS-1 Pancreatic β-Cells. Front Endocrinol (Lausanne) 2020;**11**:166-.
41 Freyre CAC, Rauher PC, Ejsing CS, Klemm RW. MIGA2 Links Mitochondria, the ER, and Lipid Droplets and Promotes De Novo Lipogenesis in Adipocytes. Molecular Cell 2019;**76**:811-25.e14.
42 Joshi AS, Nebenfuehr B, Choudhary V, Satpute-Krishnan P, Levine TP, Golden A*, et al.* Lipid droplet and peroxisome biogenesis occur at the same ER subdomains. Nature Communications 2018;**9**:2940.
43 Shai N, Schuldiner M, Zalckvar E. No peroxisome is an island - Peroxisome contact sites. Biochim Biophys Acta 2016;**1863**:1061-9.
44 Joshi AS, Cohen S. Lipid Droplet and Peroxisome Biogenesis: Do They Go Hand-in-Hand? Front Cell Dev Biol 2019;**7**:92.
45 Zhou L, Yu M, Arshad M, Wang W, Lu Y, Gong J*, et al.* Coordination Among Lipid Droplets, Peroxisomes, and Mitochondria Regulates Energy Expenditure Through the CIDE-ATGL-PPARα Pathway in Adipocytes. Diabetes 2018;**67**:1935-48.
46 Singh R, Kaushik S, Wang Y, Xiang Y, Novak I, Komatsu M*, et al.* Autophagy regulates lipid metabolism. Nature 2009;**458**:1131-5.
47 Yang L, Li P, Fu S, Calay ES, Hotamisligil GS. Defective hepatic autophagy in obesity promotes ER stress and causes insulin resistance. Cell Metab 2010;**11**:467-78.
48 Jaber N, Dou Z, Chen JS, Catanzaro J, Jiang YP, Ballou LM*, et al.* Class III PI3K Vps34 plays an essential role in autophagy and in heart and liver function. Proc Natl Acad Sci U S A 2012;**109**:2003-8.
49 Settembre C, Ballabio A. Lysosome: regulator of lipid degradation pathways. Trends Cell Biol 2014;**24**:743-50.
50 Velázquez AP, Tatsuta T, Ghillebert R, Drescher I, Graef M. Lipid droplet–mediated ER homeostasis regulates autophagy and cell survival during starvation. Journal of Cell Biology 2016;**212**:621-31.
51 Eslam M, Newsome PN, Sarin SK, Anstee QM, Targher G, Romero-Gomez M*, et al.* A new definition for metabolic dysfunction-associated fatty liver disease: An international expert consensus statement. J Hepatol 2020.
52 Younossi ZM, Koenig AB, Abdelatif D, Fazel Y, Henry L, Wymer M. Global epidemiology of nonalcoholic fatty liver disease-Meta-analytic assessment of prevalence, incidence, and outcomes. Hepatology 2016;**64**:73-84.
53 Zhang CH, Zhou BG, Sheng JQ, Chen Y, Cao YQ, Chen C. Molecular mechanisms of hepatic insulin resistance in nonalcoholic fatty liver disease and potential treatment strategies. Pharmacol Res 2020:104984.
54 Chen K, Ma J, Jia X, Ai W, Ma Z, Pan Q. Advancing the understanding of NAFLD to hepatocellular carcinoma development: From experimental models to humans. Biochim Biophys Acta Rev Cancer 2019;**1871**:117-25.
55 Straub BK, Stoeffel P, Heid H, Zimbelmann R, Schirmacher P. Differential pattern of lipid droplet-associated proteins and de novo perilipin expression in hepatocyte steatogenesis. Hepatology 2008;**47**:1936-46.
56 Zhou L, Xu L, Ye J, Li D, Wang W, Li X*, et al.* Cidea promotes hepatic steatosis by sensing dietary fatty acids. Hepatology 2012;**56**:95-107.
57 Tang P, Low HB, Png CW, Torta F, Kumar JK, Lim HY*, et al.* Protective Function of Mitogen-Activated Protein Kinase Phosphatase 5 in Aging- and Diet-Induced Hepatic Steatosis and Steatohepatitis. Hepatol Commun 2019;**3**:748-62.
58 Su W, Wang Y, Jia X, Wu W, Li L, Tian X*, et al.* Comparative proteomic study reveals 17β-HSD13 as a pathogenic protein in nonalcoholic fatty liver disease. Proc Natl Acad Sci U S A 2014;**111**:11437-42.
59 Su W, Peng J, Li S, Dai Y-b, Wang C-j, Xu H*, et al.* Liver X receptor α induces 17β-hydroxysteroid dehydrogenase-13 expression through SREBP-1c. American Journal of Physiology-Endocrinology and Metabolism 2017;**312**:E357-E67.
60 Kim KH, Shin HJ, Kim K, Choi HM, Rhee SH, Moon HB*, et al.* Hepatitis B virus X protein induces hepatic steatosis via transcriptional activation of SREBP1 and PPARgamma. Gastroenterology 2007;**132**:1955-67.
61 Na TY, Shin YK, Roh KJ, Kang SA, Hong I, Oh SJ*, et al.* Liver X receptor mediates hepatitis B virus X protein-induced lipogenesis in hepatitis B virus-associated hepatocellular carcinoma. Hepatology 2009;**49**:1122-31.
62 Yasumoto J, Kasai H, Yoshimura K, Otoguro T, Watashi K, Wakita T*, et al.* Hepatitis B virus prevents excessive viral production via reduction of cell death-inducing DFF45-like effectors. J Gen Virol 2017;**98**:1762-73.
63 Miyanari Y, Atsuzawa K, Usuda N, Watashi K, Hishiki T, Zayas M*, et al.* The lipid droplet is an important organelle for hepatitis C virus production. Nature Cell Biology 2007;**9**:1089-97.
64 Filipe A, McLauchlan J. Hepatitis C virus and lipid droplets: finding a niche. Trends Mol Med 2015;**21**:34-42.
65 Lee JY, Cortese M, Haselmann U, Tabata K, Romero-Brey I, Funaya C*, et al.* Spatiotemporal Coupling of the Hepatitis C Virus Replication Cycle by Creating a Lipid Droplet- Proximal Membranous Replication Compartment. Cell Rep 2019;**27**:3602-17 e5.
66 Camus G, Schweiger M, Herker E, Harris C, Kondratowicz AS, Tsou C-L*, et al.* The hepatitis C virus core protein inhibits adipose triglyceride lipase (ATGL)-mediated lipid mobilization and enhances the ATGL interaction with comparative gene identification 58 (CGI-58) and lipid droplets. The Journal of biological chemistry 2014;**289**:35770-80.
67 Boulant S, Douglas MW, Moody L, Budkowska A, Targett-Adams P, McLauchlan J. Hepatitis C Virus Core Protein Induces Lipid Droplet Redistribution in a Microtubule- and Dynein-Dependent Manner. Traffic 2008;**9**:1268-82.
68 Tada T, Kumada T, Toyoda H, Sone Y, Takeshima K, Ogawa S*, et al.* Viral eradication reduces both liver stiffness and steatosis in patients with chronic hepatitis C virus infection who received direct-acting anti-viral therapy. Aliment Pharmacol Ther 2018;**47**:1012-22.
69 Hu B, Lin JZ, Yang XB, Sang XT. Aberrant lipid metabolism in hepatocellular carcinoma cells as well as immune microenvironment: A review. Cell Prolif 2020;**53**:e12772.
70 Balci NC, Befeler AS, Bieneman BK, Fattahi R, Saglam S, Havlioglu N. Fat containing HCC: findings on CT and MRI including serial contrast-enhanced imaging. Acad Radiol 2009;**16**:963-8.
71 Yamashita T, Honda M, Takatori H, Nishino R, Minato H, Takamura H*, et al.* Activation of lipogenic pathway correlates with cell proliferation and poor prognosis in hepatocellular carcinoma. Journal of Hepatology 2009;**50**:100-10.
72 Björnson E, Mukhopadhyay B, Asplund A, Pristovsek N, Cinar R, Romeo S*, et al.* Stratification of Hepatocellular Carcinoma Patients Based on Acetate Utilization. Cell Reports 2015;**13**:2014-26.
73 Menendez JA, Lupu R. Fatty acid synthase and the lipogenic phenotype in cancer pathogenesis. Nat Rev Cancer 2007;**7**:763-77.
74 Yasumoto Y, Miyazaki H, Vaidyan LK, Kagawa Y, Ebrahimi M, Yamamoto Y*, et al.* Inhibition of Fatty Acid Synthase Decreases Expression of Stemness Markers in Glioma Stem Cells. PLoS One 2016;**11**:e0147717.
75 Nieman KM, Kenny HA, Penicka CV, Ladanyi A, Buell-Gutbrod R, Zillhardt MR*, et al.* Adipocytes promote ovarian cancer metastasis and provide energy for rapid tumor growth. Nat Med 2011;**17**:1498-503.

76 Cao W, Li M, Liu J, Zhang S, Noordam L, Verstegen MMA*, et al.* LGR5 marks targetable tumor-initiating cells in mouse liver cancer. Nature communications 2020;**11**:1961.
77 Liu J, Dang H, Wang XW. The significance of intertumor and intratumor heterogeneity in liver cancer. Exp Mol Med 2018;**50**:e416.
78 Batlle E, Clevers H. Cancer stem cells revisited. Nat Med 2017;**23**:1124-34.
79 Tuveson D, Clevers H. Cancer modeling meets human organoid technology. Science 2019;**364**:952-5.
80 Broutier L, Mastrogiovanni G, Verstegen MM, Francies HE, Gavarro LM, Bradshaw CR*, et al.* Human primary liver cancer-derived organoid cultures for disease modeling and drug screening. Nat Med 2017;**23**:1424-35.
81 Cao W, Liu J, Wang L, Li M, Verstegen MMA, Yin Y*, et al.* Modeling liver cancer and therapy responsiveness using organoids derived from primary mouse liver tumors. Carcinogenesis 2019;**40**:145-54.
82 Giraldo NA, Becht E, Remark R, Damotte D, Sautes-Fridman C, Fridman WH. The immune contexture of primary and metastatic human tumours. Current Opinion in Immunology 2014;**27**:8-15.
83 Kalluri R. The biology and function of fibroblasts in cancer. Nature Reviews Cancer 2016;**16**:582-98.
84 Arnold JN, Magiera L, Kraman M, Fearon DT. Tumoral immune suppression by macrophages expressing fibroblast activation protein-alpha and heme oxygenase-1. Cancer Immunology Research 2014;**2**:121-6.
85 Weissmueller S, Manchado E, Saborowski M, Morris JPt, Wagenblast E, Davis CA*, et al.* Mutant p53 drives pancreatic cancer metastasis through cell-autonomous PDGF receptor beta signaling. Cell 2014;**157**:382-94.
86 Cadamuro M, Nardo G, Indraccolo S, Dall'olmo L, Sambado L, Moserle L*, et al.* Platelet-derived growth factor-D and Rho GTPases regulate recruitment of cancer-associated fibroblasts in cholangiocarcinoma. Hepatology 2013;**58**:1042-53.
87 Koliaraki V, Pallangyo CK, Greten FR, Kollias G. Mesenchymal Cells in Colon Cancer. Gastroenterology 2017;**152**:964-79.
88 Sugimoto H, Mundel TM, Kieran MW, Kalluri R. Identification of fibroblast heterogeneity in the tumor microenvironment. Cancer Biol Ther 2006;**5**:1640-6.
89 Record Owner NLM. Fibroblast-specific protein 1 identifies an inflammatory subpopulation of macrophages in the liver.
90 Liu AY, Zheng H, Ouyang G. Periostin, a multifunctional matricellular protein in inflammatory and tumor microenvironments. Matrix Biol 2014;**37**:150-6.
91 Multhaupt HA, Leitinger B, Gullberg D, Couchman JR. Extracellular matrix component signaling in cancer. Advanced Drug Delivery Reviews 2016;**97**:28-40.
92 Record Owner NLM. CD10<ovid:sup>+</ovid:sup>GPR77<ovid:sup>+</ovid:sup> Cancer-Associated Fibroblasts Promote Cancer Formation and Chemoresistance by Sustaining Cancer Stemness.
93 Fattovich G, Stroffolini T, Zagni I, Donato F. Hepatocellular carcinoma in cirrhosis: incidence and risk factors. Gastroenterology 2004;**127**:S35-50.
94 Ren J, Smid M, Iaria J, Salvatori DCF, van Dam H, Zhu HJ*, et al.* Cancer-associated fibroblast-derived Gremlin 1 promotes breast cancer progression. Breast Cancer Res 2019;**21**:109.
95 Xiong S, Wang R, Chen Q, Luo J, Wang J, Zhao Z*, et al.* Cancer-associated fibroblasts promote stem cell-like properties of hepatocellular carcinoma cells through IL-6/STAT3/Notch signaling. Am J Cancer Res 2018;**8**:302-16.
96 Fang T, Lv H, Lv G, Li T, Wang C, Han Q*, et al.* Tumor-derived exosomal miR-1247-3p induces cancer-associated fibroblast activation to foster lung metastasis of liver cancer. Nature communications 2018;**9**:191.
97 Chen WJ, Ho CC, Chang YL, Chen HY, Lin CA, Ling TY*, et al.* Cancer-associated fibroblasts regulate the plasticity of lung cancer stemness via paracrine signalling. Nature communications 2014;**5**:3472.
98 Ebbing EA, van der Zalm AP, Steins A, Creemers A, Hermsen S, Rentenaar R*, et al.* Stromal-derived interleukin 6 drives epithelial-to-mesenchymal transition and therapy resistance in esophageal adenocarcinoma. Proc Natl Acad Sci U S A 2019;**116**:2237-42.
99 Hu G, Wang S, Xu F, Ding Q, Chen W, Zhong K*, et al.* Tumor-Infiltrating Podoplanin+ Fibroblasts Predict Worse Outcome in Solid Tumors. Cell Physiol Biochem 2018;**51**:1041-50.
100 Su S, Chen J, Yao H, Liu J, Yu S, Lao L*, et al.* CD10(+)GPR77(+) Cancer-Associated Fibroblasts Promote Cancer Formation and Chemoresistance by Sustaining Cancer Stemness. Cell 2018;**172**:841-56 e16.
101 Lenos KJ, Miedema DM, Lodestijn SC, Nijman LE, van den Bosch T, Romero Ros X*, et al.* Stem cell functionality is microenvironmentally defined during tumour expansion and therapy response in colon cancer. Nat Cell Biol 2018;**20**:1193-202.
102 Clevers H. Modeling Development and Disease with Organoids. Cell 2016;**165**:1586-97.
103 Seino T, Kawasaki S, Shimokawa M, Tamagawa H, Toshimitsu K, Fujii M*, et al.* Human Pancreatic Tumor Organoids Reveal Loss of Stem Cell Niche Factor Dependence during Disease Progression. Cell Stem Cell 2018;**22**:454-67 e6.
104 Yamamura Y, Asai N, Enomoto A, Kato T, Mii S, Kondo Y*, et al.* Akt-Girdin signaling in cancer-associated fibroblasts contributes to tumor progression. Cancer Res 2015;**75**:813-23.
105 Orimo A, Gupta PB, Sgroi DC, Arenzana-Seisdedos F, Delaunay T, Naeem R*, et al.* Stromal fibroblasts present in invasive human breast carcinomas promote tumor growth and angiogenesis through elevated SDF-1/CXCL12 secretion. Cell 2005;**121**:335-48.
106 Record Owner NLM. Hepatic myofibroblasts promote the progression of human cholangiocarcinoma through activation of epidermal growth factor receptor.
107 Neufert C, Becker C, Tureci O, Waldner MJ, Backert I, Floh K*, et al.* Tumor fibroblast-derived epiregulin promotes growth of colitis-associated neoplasms through ERK. Journal of Clinical Investigation 2013;**123**:1428-43.
108 Vaquero J, Lobe C, Tahraoui S, Claperon A, Mergey M, Merabtene F*, et al.* The IGF2/IR/IGF1R Pathway in Tumor Cells and Myofibroblasts Mediates Resistance to EGFR Inhibition in Cholangiocarcinoma. Clin Cancer Res 2018;**24**:4282-96.
109 Grivennikov S, Karin E, Terzic J, Mucida D, Yu GY, Vallabhapurapu S*, et al.* IL-6 and Stat3 are required for survival of intestinal epithelial cells and development of colitis-associated cancer. Cancer Cell 2009;**15**:103-13.
110 Record Owner NLM. Interleukin-11 is the dominant IL-6 family cytokine during gastrointestinal tumorigenesis and can be targeted therapeutically.
111 Calon A, Espinet E, Palomo-Ponce S, Tauriello DV, Iglesias M, Cespedes MV*, et al.* Dependency of colorectal cancer on a TGF-beta-driven program in stromal cells for metastasis initiation. Cancer Cell 2012;**22**:571-84.
112 Gaggioli C, Hooper S, Hidalgo-Carcedo C, Grosse R, Marshall JF, Harrington K*, et al.* Fibroblast-led collective invasion of carcinoma cells with differing roles for RhoGTPases in leading and following cells. Nat Cell Biol 2007;**9**:1392-400.
113 Labernadie A, Kato T, Brugues A, Serra-Picamal X, Derzsi S, Arwert E*, et al.* A mechanically active heterotypic E-cadherin/N-cadherin adhesion enables fibroblasts to drive cancer cell invasion. Nat Cell Biol 2017;**19**:224-37.
114 Lau EY, Lo J, Cheng BY, Ma MK, Lee JM, Ng JK*, et al.* Cancer-Associated Fibroblasts Regulate Tumor-Initiating Cell Plasticity in Hepatocellular Carcinoma through c-Met/FRA1/HEY1 Signaling. Cell Reports 2016;**15**:1175-89.
115 Chen X, Song E. Turning foes to friends: targeting cancer-associated fibroblasts. Nat Rev Drug Discov 2019;**18**:99-115.

116 Meads MB, Gatenby RA, Dalton WS. Environment-mediated drug resistance: a major contributor to minimal residual disease. Nature Reviews Cancer 2009;**9**:665-74.
117 Paraiso KH, Smalley KS. Fibroblast-mediated drug resistance in cancer. Biochem Pharmacol 2013;**85**:1033-41.
118 Kumari N, Dwarakanath BS, Das A, Bhatt AN. Role of interleukin-6 in cancer progression and therapeutic resistance. Tumour Biol 2016;**37**:11553-72.
119 Roodhart JM, Daenen LG, Stigter EC, Prins HJ, Gerrits J, Houthuijzen JM*, et al.* Mesenchymal stem cells induce resistance to chemotherapy through the release of platinum-induced fatty acids. Cancer Cell 2011;**20**:370-83.
120 Lotti F, Jarrar AM, Pai RK, Hitomi M, Lathia J, Mace A*, et al.* Chemotherapy activates cancer-associated fibroblasts to maintain colorectal cancer-initiating cells by IL-17A. J Exp Med 2013;**210**:2851-72.
121 Wong PF, Wei W, Gupta S, Smithy JW, Zelterman D, Kluger HM*, et al.* Multiplex quantitative analysis of cancer-associated fibroblasts and immunotherapy outcome in metastatic melanoma. J Immunother Cancer 2019;**7**:194.
122 Nazareth MR, Broderick L, Simpson-Abelson MR, Kelleher RJ, Jr., Yokota SJ, Bankert RB. Characterization of human lung tumor-associated fibroblasts and their ability to modulate the activation of tumor-associated T cells. J Immunol 2007;**178**:5552-62.
123 Pinchuk IV, Saada JI, Beswick EJ, Boya G, Qiu SM, Mifflin RC*, et al.* PD-1 ligand expression by human colonic myofibroblasts/fibroblasts regulates CD4+ T-cell activity. Gastroenterology 2008;**135**:1228-37, 37 e1-2.
124 Joyce JA, Fearon DT. T cell exclusion, immune privilege, and the tumor microenvironment. Science 2015;**348**:74-80.
125 Tsai S, McOlash L, Palen K, Johnson B, Duris C, Yang Q*, et al.* Development of primary human pancreatic cancer organoids, matched stromal and immune cells and 3D tumor microenvironment models. BMC Cancer 2018;**18**:335.
126 Villanueva A. Hepatocellular Carcinoma. N Engl J Med 2019;**380**:1450-62.
127 White DL, Kanwal F, El-Serag HB. Association between nonalcoholic fatty liver disease and risk for hepatocellular cancer, based on systematic review. Clin Gastroenterol Hepatol 2012;**10**:1342-59 e2.

Supplementary data for

Modeling liver cancer and therapy responsiveness using organoids derived from primary mouse liver tumors

Table of contents

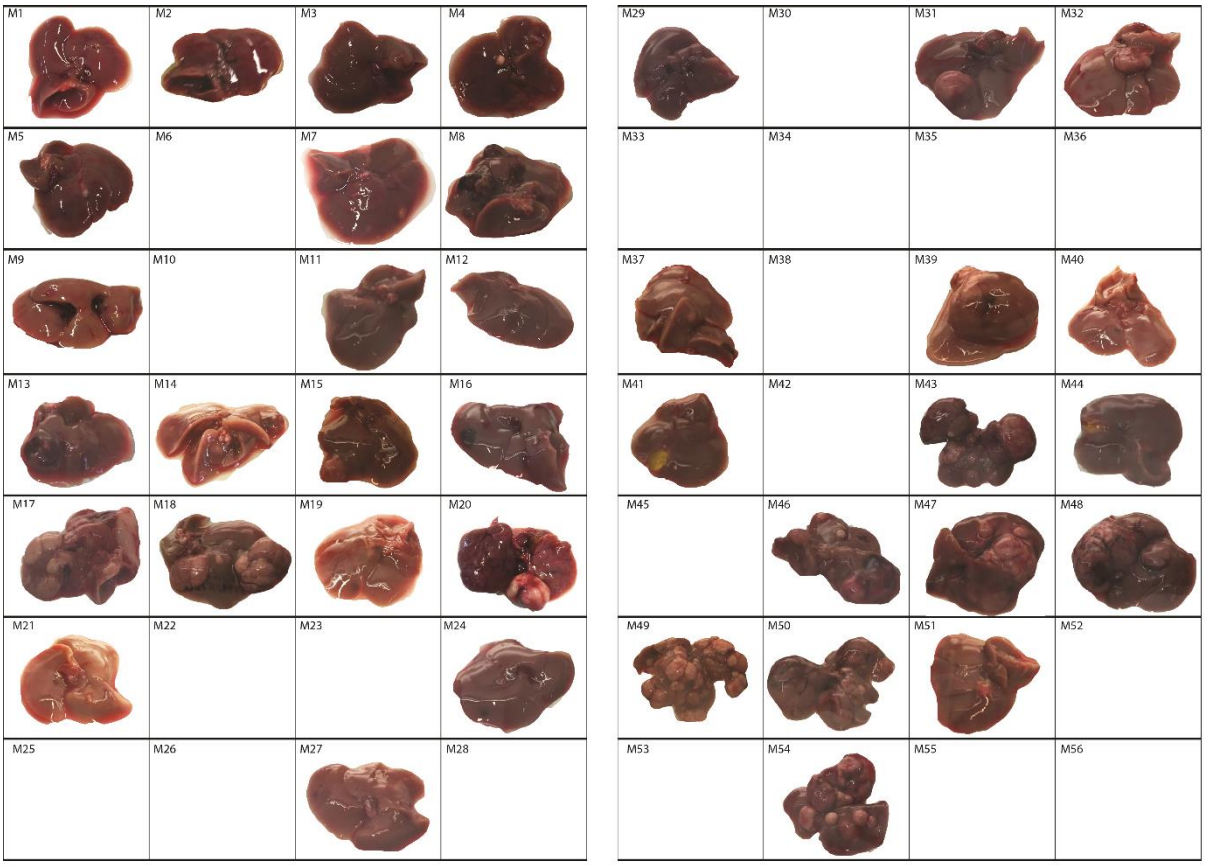

Supplementary Figure 1. The livers. The black squares are pictures of the corresponding livers which missed due to technical issue.

	Organoid Code	Mice Background	M/F	Primary Tumor Formation Time(Month)		Organoid Code	Mice Background	M/F	Primary Tumor Formation Time(Month)
1	PT1	B6	M	7	47	PT57	B6	M	10
2	PT2	B6/CD1	M	7	48	PT59	B6/CD1	M	14
3	PT3	B6/CD1	M	7	49	PT61	B6	M	14
4	PT6	B6	M	7	50	PT62	B6/CD1	M	15
5	PT7	B6	M	7	51	PT63	B6/C3H	M	8
6	PT8	B6	M	7	52	PT68	B6	M	8
7	PT9	B6	M	7	53	PT69	B6	M	8
8	PT10	B6	M	13	54	PT70	B6	M	8
9	PT11	B6	M	12	55	PT71	B6	M	15
10	PT12	B6/CD1	M	14	56	PT72	B6/C3H	M	7
11	PT13	B6/CD1	F	12	57	PT77	B6/CD1	M	14
12	PT14	B6/CD1	M	12	58	PT78	B6	M	8
13	PT15	B6/CD1	F	12	59	PT79	B6/C3H	M	8
14	PT16	B6	M	13	60	PT80	B6/C3H	M	7
15	PT17	B6	M	10	61	PT81	B6	M	15
16	PT18	B6	M	13	62	PT82	B6/C3H	M	7
17	PT19	B6	M	9	63	PT85	B6/C3H	M	7
18	PT20	B6/CD1	M	16	64	PT86	B6/C3H	M	8
19	PT21	B6/CD1	M	16	65	PT87	B6	M	15
20	PT22	B6	M	9	66	PT88	B6/C3H	M	8
21	PT23	B6/C3H	M	5	67	PT89	B6	M	15
22	PT24	B6	M	7	68	PT90	B6	M	15
23	PT25	B6/CD1	M	15	69	PT92	B6/CD1	M	15
24	PT26	B6	M	9	70	PT91	B6	M	15
25	PT27	B6	M	13	71	PT93	B6/CD1	M	15
26	PT28	B6	M	13	72	PT94	B6	M	15
27	PT29	B6	M	9	73	PT96	B6	M	15
28	PT30	B6	M	9	74	PT97	B6	M	15
29	PT31	B6	M	9	75	PT98	B6	M	15
30	PT32	B6	M	14	76	PT99	B6	M	15
31	PT35	B6	M	13	77	PT100	B6/C3H	M	8
32	PT36	B6	M	12	78	PT101	B6/C3H	M	8
33	PT37	B6	M	13	79	PT102	B6/CD1	M	14
34	PT38	B6	M	6	80	PT103	B6	M	13
35	PT39	B6/C3H	M	3	81	PT104	B6	M	13
36	PT40	B6	F	15	82	PT105	B6	M	13
37	PT41	B6	M	9	83	PT107	B6	M	15
38	PT42	B6	M	13	84	PT108	B6/CD1	M	15
39	PT43	B6	M	13	85	PT109	B6/CD1	M	15
40	PT44	B6	M	13	86	PT110	B6/CD1	M	16
41	PT45	B6	M	13	87	PT111	B6/C3H	M	7
42	PT46	B6	M	13	88	PT112	B6	M	15
43	PT47	B6	M	16	89	PT113	B6/CD1	M	15
44	PT49	B6	M	13	90	PT115	B6	M	15
45	PT51	B6	M	14	91	PT116	B6&C3H	M	8
46	PT52	B6/CD1	M	14					

Supplementary Figure 2. Tumor organoid lines. All the 91 tumor organoid lines, for the genetic background, gender and primary tumor formation time (counted since the time of first Den injection until the time to sacrifice the mice).

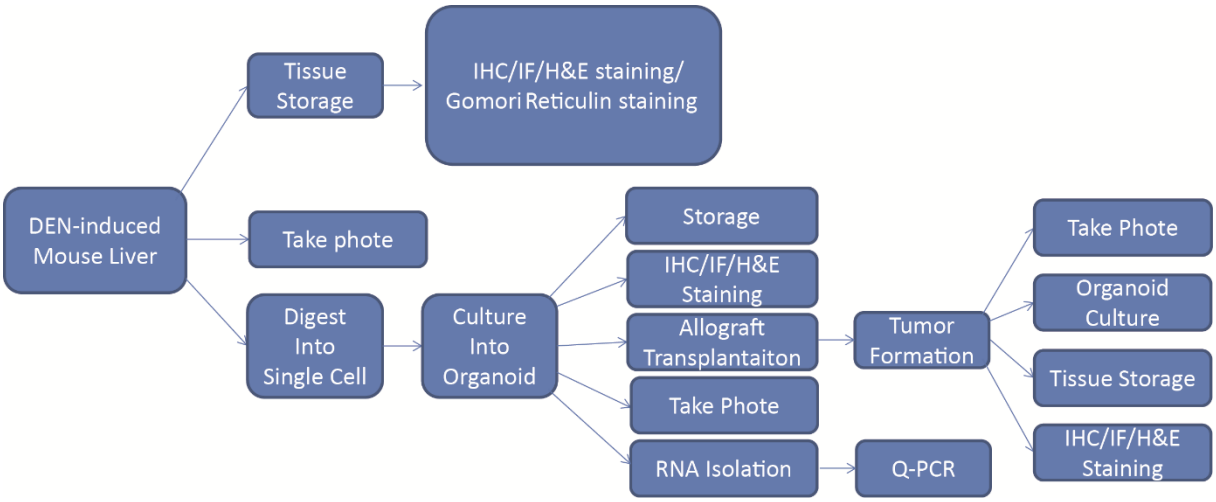

Supplementary Figure 3. The flowchart of the experimental design.

A

Mice Code	Organoid Code	Number of Initiated Organoid Stain	Tissue Number from each Mice	Initiation Efficiency(%)	Mice Code	Organoid Code	Number of Initiated Organoid Stain	Tissue Number from each Mice	Initiation Efficiency(%)	Mice Code	Organoid Code	Number of Initiated Organoid Stain	Tissue Number from each Mice	Initiation Efficiency(%)
M1	PT1	1	1	100		PT34				M39	PT68	4	4	100
M2	PT2	2	4	50		PT122					PT69			
	PT3					PT123					PT70			
	PT4					PT124					PT78			
	PT5				M20	PT32	1	1	100	M40	PT71	1	1	100
M3	PT6	2	2	100	M21	PT112	1	1	100	M41	PT72	1	1	100
	PT7				M22	PT116	1	1	100	M42	PT73	3	5	60
M4	PT8	3	3	100	M23	PT35	1	1	100		PT74			
	PT9				M24	PT36	1	1	100		PT92			
	PT24				M25	PT38	1	1	100		PT94			
M5	PT10	2	2	100	M26	PT39	1	1	100		PT115			
	PT16				M27	PT40	1	1	100	M43	PT75	3	8	37.5
M6	PT11	1	1	100	M28	PT42	1	6	16.7		PT76			
M7	PT12	1	5	20		PT125					PT81			
	PT53					PT126					PT90			
	PT54					PT127					PT95			
	PT55					PT128					PT107			
	PT56					PT60					PT117			
M8	PT13	2	2	100	M29	PT43	2	3	66.7		PT118			
	PT15					PT67				M44	PT88	1	1	100
M9	PT14	1	1	100		PT77				M45	PT113	1	1	100
M10	PT17	2	2	100	M30	PT96	1	1	100	M46	PT80	2	2	100
	PT57				M31	PT45	3	4	75		PT82			
M11	PT18	1	2	50		PT58				M47	PT85	1	1	100
	PT84					PT46				M48	PT87	3	3	100
M12	PT19	2	2	100		PT108					PT97			
	PT41				M32	PT47	2	2	100		PT98			
M13	PT20	2	2	100		PT44				M49	PT93	1	1	100
	PT21				M33	PT48	0	1	0	M50	PT99	1	1	100
M14	PT22	3	3	100	M34	PT49	2	2	100	M51	PT100	2	2	100
	PT26					PT51					PT101			
	PT31				M35	PT50	2	3	66.7	M52	PT102	1	1	100
M15	PT23	1	4	25		PT52				M53	PT103	3	3	100
	PT65					PT59					PT104			
	PT66				M36	PT61	1	2	50		PT105			
	PT83					PT114				M54	PT109	1	1	100
M16	PT25	1	1	100	M37	PT62	1	4	25	M55	PT110	1	1	100
M17	PT27	2	2	100		PT119				M56	PT111	1	1	100
	PT37					PT120								
M18	PT28	3	3	100		PT121								
	PT89				M38	PT63	3	5	60					
	PT91					PT64								
M19	PT29	2	7	28.6		PT79								
	PT30					PT86								
	PT33					PT106								

B

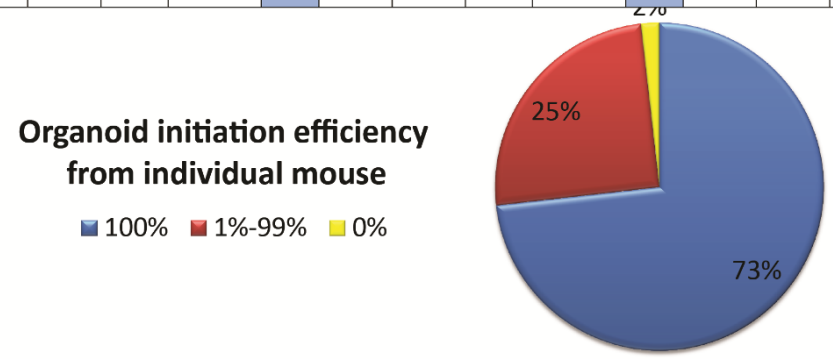

Supplementary Figure 4. The organoid strains grouped according to the mice. (A) The organoid strains which were successfully initiated and maintained are marked by green; The organoid strains which were successfully initiated (maintained over 3 months), transplanted into NOG mice for tumor initiation but lost afterward due to storage issue/infection are marked by yellow. (B) The distribution of the organoid initiation efficiency for individual mouse liver.

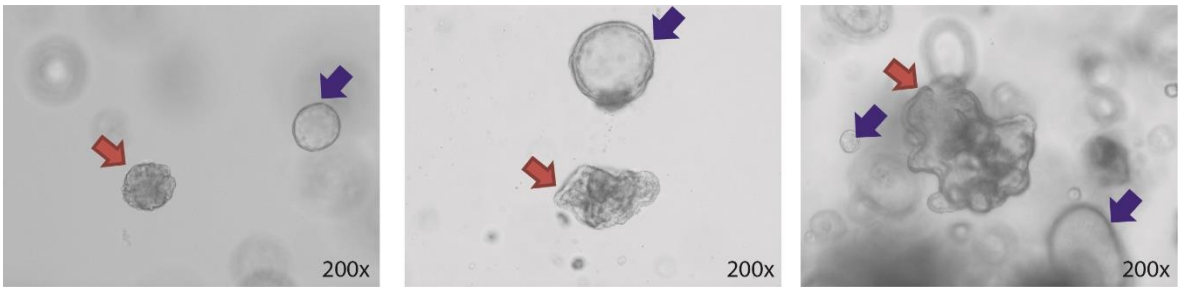

Supplementary Figure 5. Tumor organoids show mixed morphology. Red arrow: “tumor organoid” morphology; Blue arrow: “normal organoid” morphology.

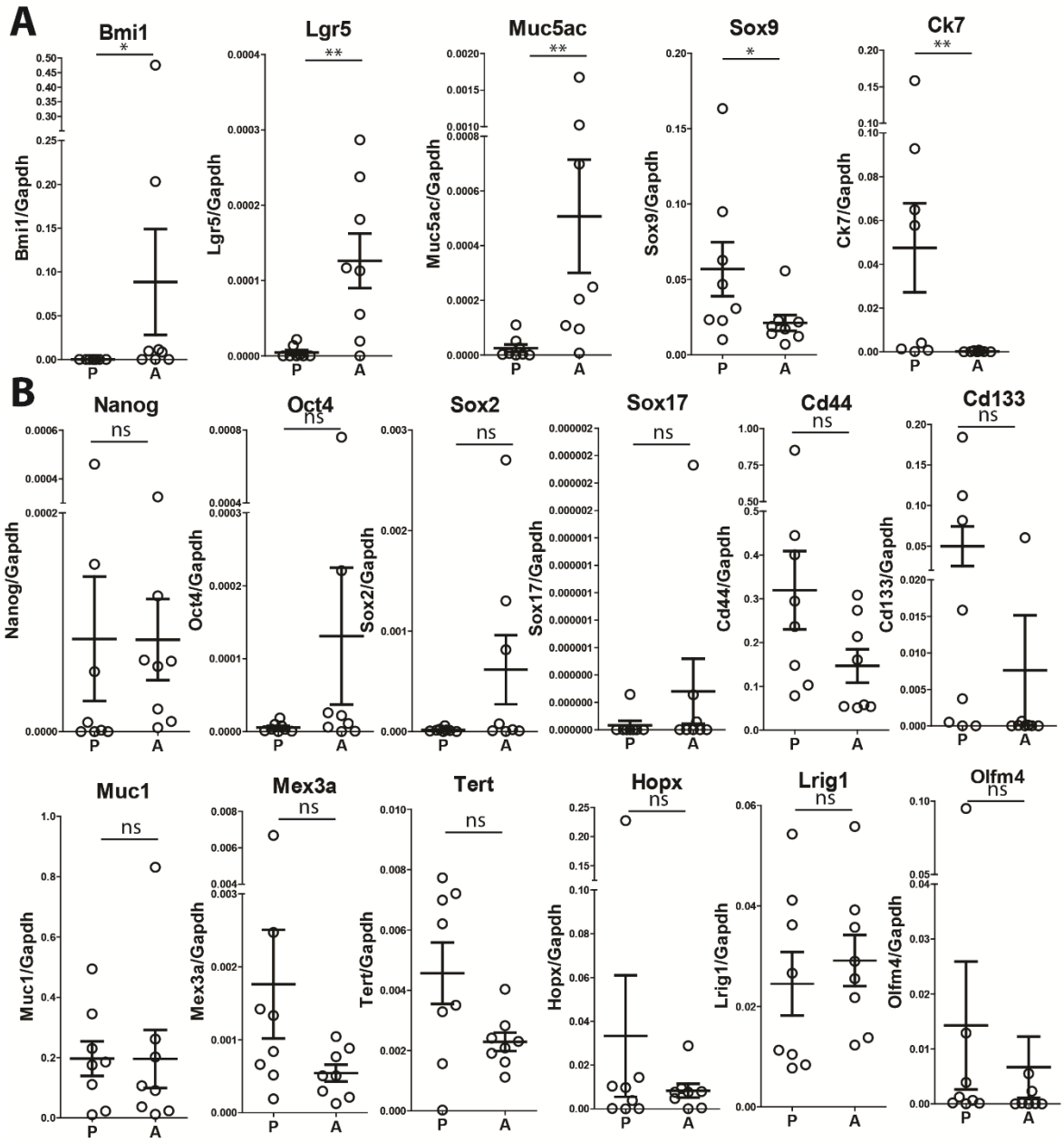

Supplementary Figure 6. The panel of progenitor cell markers which compared between paired primary organoid strains and corresponding allograft organoid strains (*P < .05; **P < .01; n = 8).

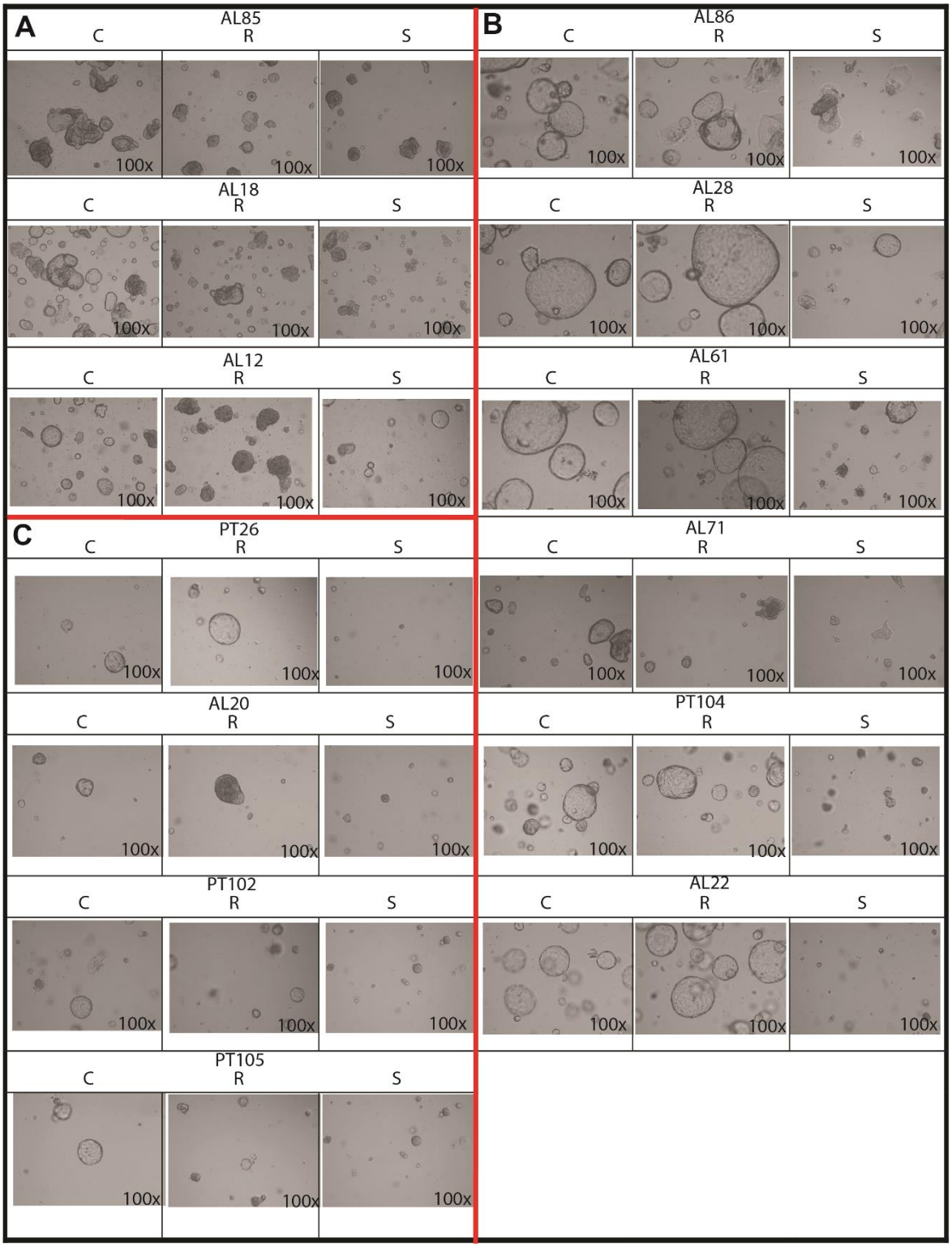

Supplementary Figure 7. Tumor organoids in response to the treatment of the targeted therapeutics Sorafenib or Regorafenib. (A) Representative pictures taken at day 7, showing that tumor organoids respond differently to the treatment (n=4). (A) Group 1: organoid strains which were both sensitive to Sorafenib and Regorafenib. (B) Group 2: organoid strains which were only sensitive to Sorafenib, but not Regorafenib. (C) Group 3: organoid strains which were not sensitive to both Sorafenib and Regorafenib.

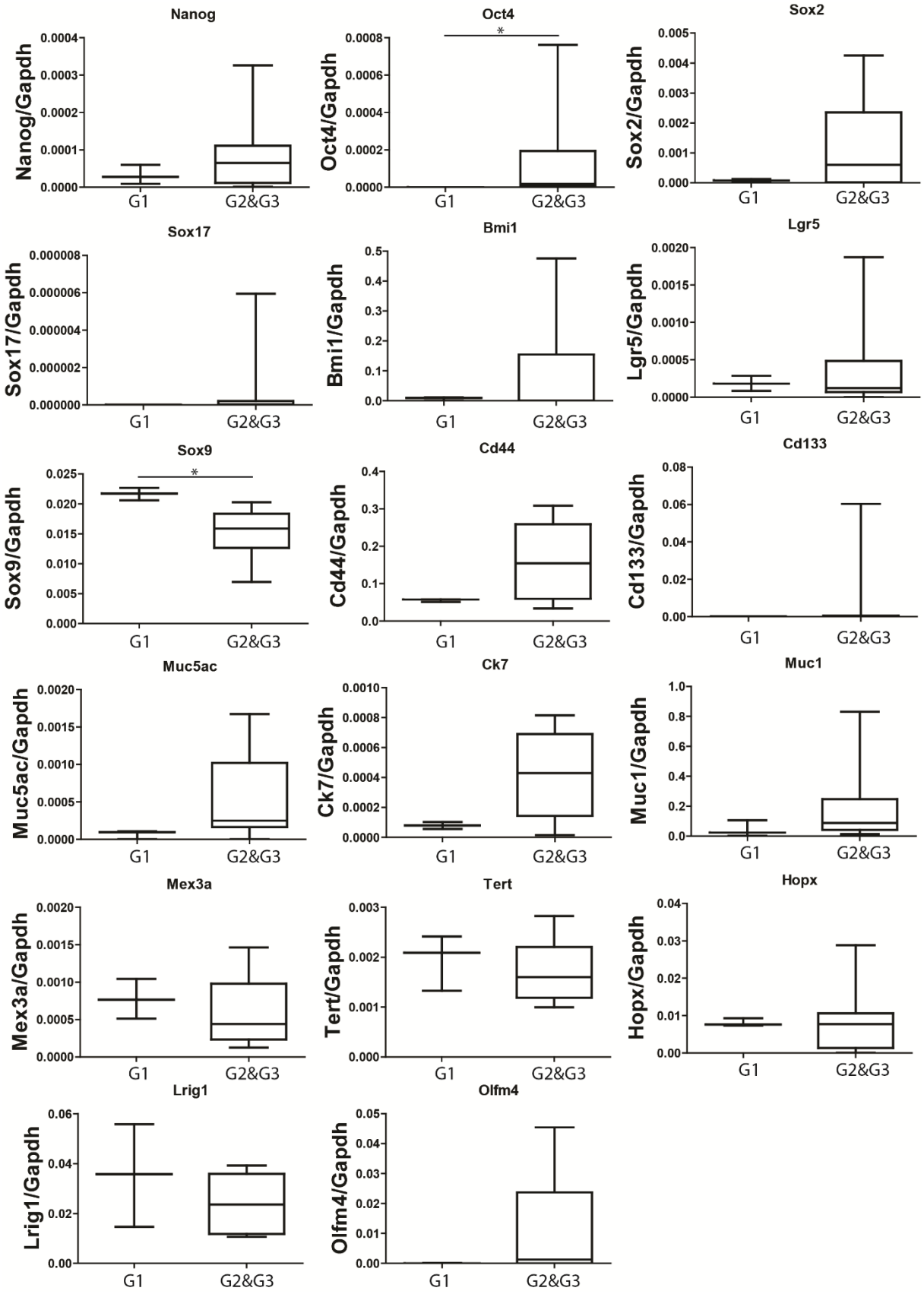

Supplementary figure 8: The panel of progenitor cell markers which compared between Group 1 (organoid strains which were sensitive to both treatment) and the rest strains (*P < .05; **P < .01).

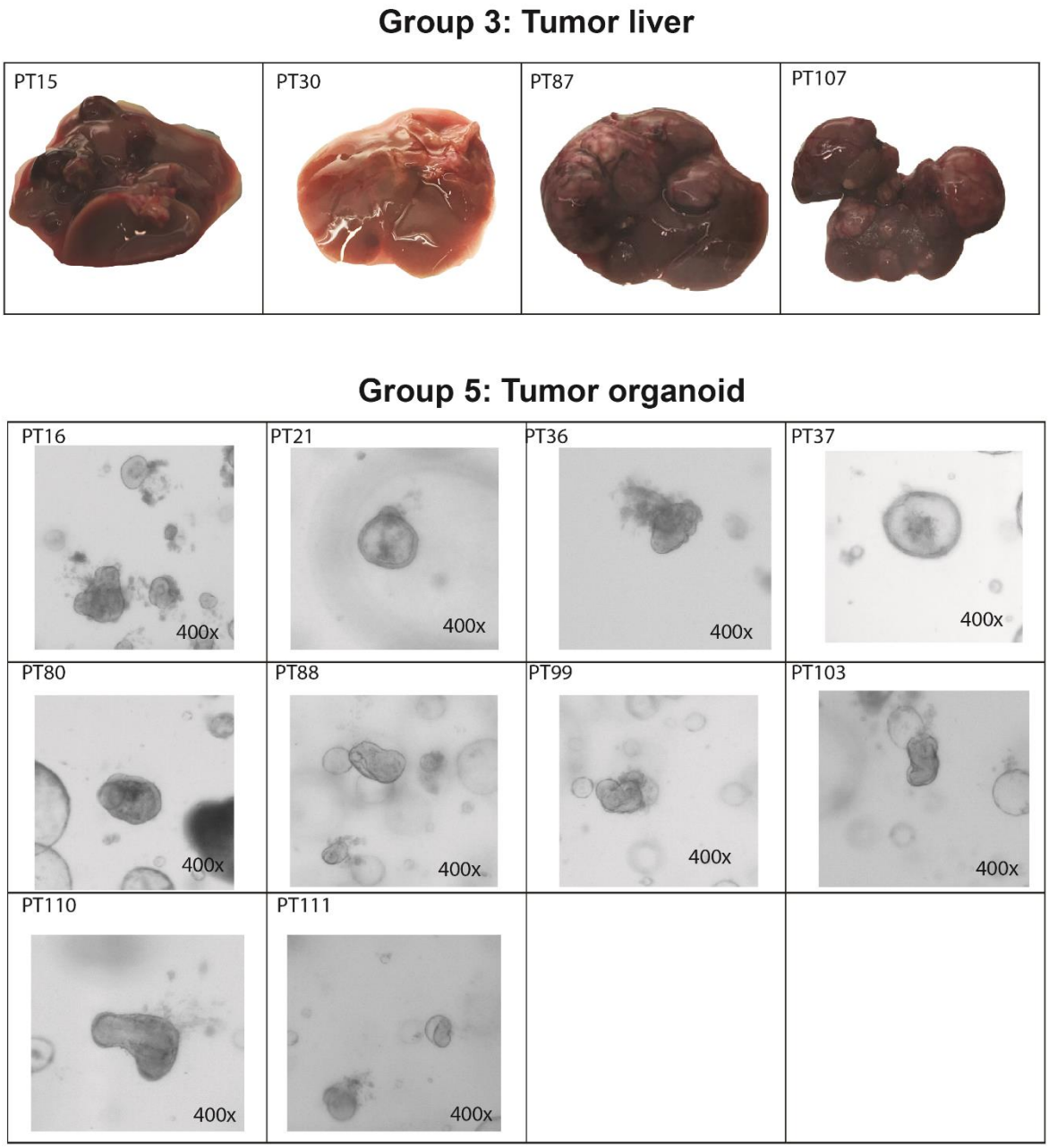

Supplementary figure 9: (A) Group 3: The organoid strains showed normal organoid morphology, normal tissue histology but liver tumor morphology. (B) Group 5: The organoid strains showed tumor organoid morphology but with normal histology.

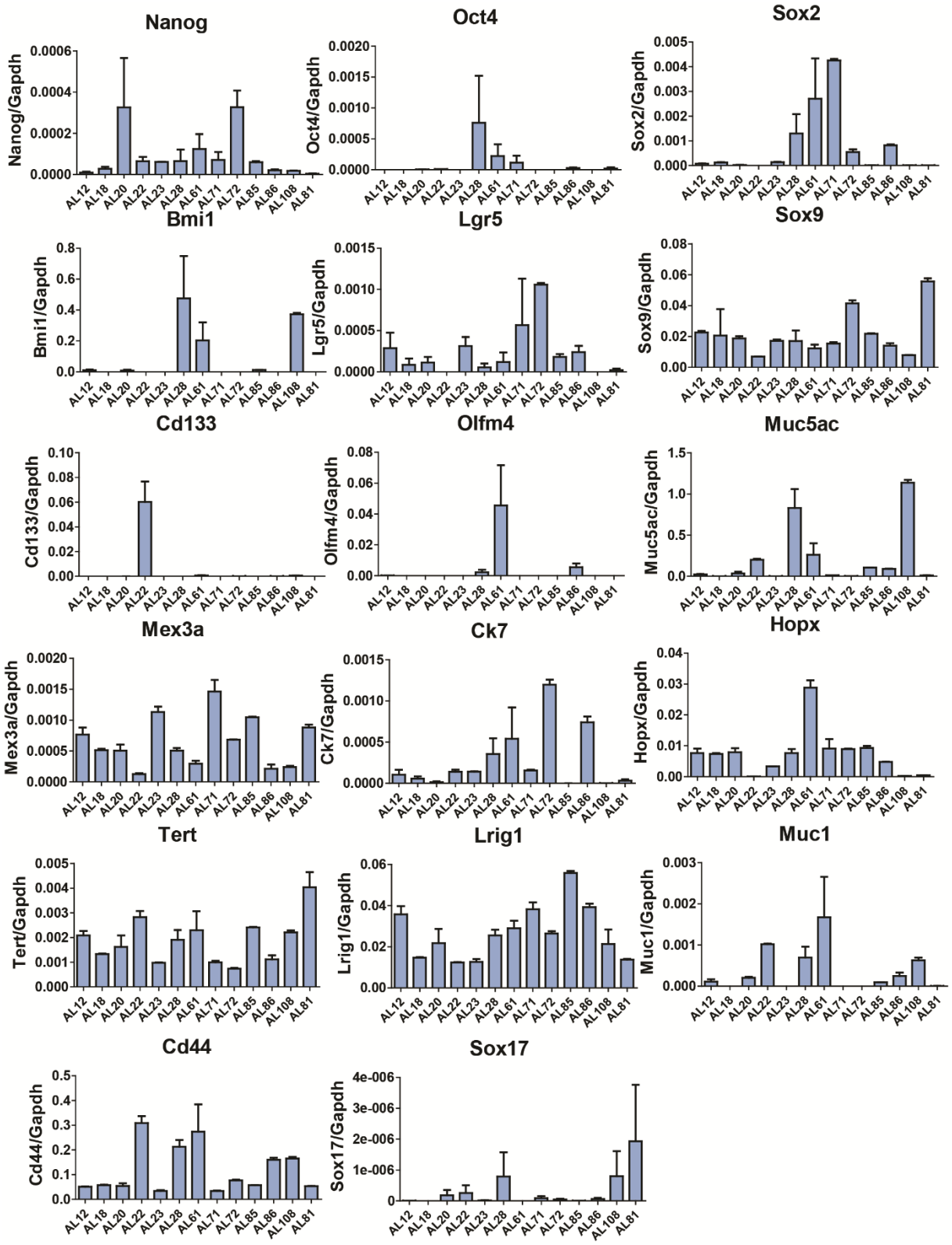

Supplementary figure 10: Allograft organoid strains have different profiles of stem cell/tumor stem cell expression.

Tumor Organoid Lines				
	Organoid Code	Primary Tumor Harvesting Time(Month)	Mice Background	Allograft Tumor Harvesting Time(Day)
1	PT12	14	B6/CD1	24
2	PT18	13	B6	58
3	PT20	16	B6/CD1	41
4	PT22	9	B6	58
5	PT23	5	B6/C3H	58
6	PT26	9	B6	58
7	PT28	13	B6	58
8	PT61	14	B6	36
9	PT71	15	B6	22
10	PT72	7	B6/C3H	22
11	PT81	15	B6	66
12	PT85	7	B6/C3H	40
13	PT86	8	B6/C3H	40
14	PT102	14	B6/CD1	33
15	PT104	13	B6	33
16	PT105	13	B6	33
17	PT108	13	B6	16
18	PT109	14	B6	36

Tumor Re-initiation From Allograft Tumor Derived Organoids		
	Organoid Code	2nd Allograft Tumor Harvesting Time (Day)
1	AT65	28
2	AT66	28
3	AT83	42
4	AT84	42

Tumor Initiation Of Single Organoids		
	Organoid Code	2nd Allograft Tumor Harvesting Time (Day)
1	AT50	14
2	AT53	22
3	AT54	22

Supplementary Table 1. Liver tumor organoid can initiate tumor. The upper panel: The primary tumor organoid lines which formed tumor in the NOG mice, and the corresponding information of tumor harvesting time and mouse strain; The middle panel: Tumor organoids derived from the allograft (1st allograft) can re-initiate tumor again (2nd allograft) in the NOG mice; The lower panel: The corresponding tumor harvesting time of single cell formed organoid derived allograft tumors.

Primary strain		Allograft strain	
PT12	Normal, Extramedullary hematopoiesis	AL12	CC or d/d mixed type
PT18	Normal	AL18	Cc with complex papillary structures
PT20	HCC, possibly also with an hemangioma	AL20	CC with complex papillary structures/villi structure.
PT22	HCC, possibly also with an vascular tumor	AL22	Not sure tumor type
PT23	HCC	AL23	CC
PT26	Hemangioma	AL26	Not sure tumor type
PT28	HCC	AL28	CC
PT61	Small HCC	AL61	CC
PT71	Normal	AL71	CC
PT72	Normal	AL72	CC or mixed type
PT81	HCC	AL81	HCC
PT85	HCC	AL85	CC or mixed type
PT86	HCC	AL86	CC
PT102	Normal	AL102	Maybe CC
PT104	CC	AL104	CC
PT105	HCC, with hemangioma	AL105	Not sure tumor type
PT108	HCC	AL108	Not sure tumor type
PT109	HCC tumor	AL109	Not sure tumor type

Supplementary Table 2: The histology for paired primary organoid strain (PT) and allograft organoid strain (AL). The green mark: the strains which showed consistent histology between primary and allograft tissues.

Group 1: Normal

Organoid code	Tissue Histology
PT1	Normal
PT2	Normal
PT3	Normal
PT6	Normal
PT7	Normal
PT10	Normal
PT14	Normal
PT19	Normal
PT24	Normal
PT25	Normal
PT35	Normal
PT39	Normal
PT57	Normal
PT89	Normal
PT91	Normal
PT96	Normal
PT112	Normal

Group 2: Tumor histology

Organoid code	Tissue Histology
PT8	HCC d/d mixed type
PT9	Mixed type
PT11	HCC(?), No obvious Portal traid
PT13	Necrosis, HCC
PT32	Necrosis, HCC
PT68	HCC
PT79	HCC
PT82	HCC
PT90	HCC
PT93	HCC
PT97	HCC With pale bodies (fibrinogen), Mallory hyaline
PT98	HCC, steatosis,pale bodies
PT100	HCC
PT101	HCC
PT115	HCC
PT116	HCC

Group 3: Tumor liver

Organoid code	Tissue Histology
PT15	Normal
PT30	Normal
PT87	Normal
PT107	Normal

Group 4: Other diseases

Organoid code	Tissue Histology
PT27	Necrosis, Fat liver
PT29	Hemangioma
PT31	A possible tumor
PT38	Gland structure, could be maglinant, cholangiocyte direction differentation
PT40	Steatosis liver
PT49	Fat liver
PT92	Necrosis
PT113	Necrosis tumor

Group 5: Tumor organoid

Organoid code	Tissue Histology
PT16	Normal
PT21	Normal
PT36	Normal
PT37	Fat liver
PT80	Necrosis
PT88	Normal
PT99	Normal
PT103	Normal
PT110	Normal
PT111	Normal

Supplementary Table 3: Different groups of organoids which grouped by liver morphology, histology, organoid morphology. Group 1: 17 out of 55 strains showed normal for all three aspect, thus considering as “Normal group” (30.9%); Group 2: 16 out of 55 showed tumor organoid morphology with tumor/”normal” histology, considering as tumor organoid group (29.1%). Group 3: 4 out of 55 showed normal organoid morphology with tumor liver morphology (7.3%); Group 4: 8 out of 55 showed “normal” organoid morphology but with normal/other disease histology (14.5%); Group 5: 10 out of 55 showed tumor organoid morphology but with normal/other disease histology (18.2%);

CHAPTER 10

LGR5 marks targetable tumor-initiating cells in liver cancer

Wanlu Cao, **Jiaye Liu,** Meng Li, Shaoshi Zhang, Lisanne Noordam, Monique M. A. Verstegen, Ling Wang, Buyun Ma, Shan Li, Wenshi Wang, Michiel Bolkestein, Michael Doukas, Kan Chen, Zhongren Ma, Marco Bruno, Dave Sprengers, Jaap Kwekkeboom, Luc J. W. van der Laan, Ron Smits, Maikel P. Peppelenbosch and Qiuwei Pan

Nat Commun. 2020 Apr 23;11(1):1961.

Abstract

Cancer stem cells (CSCs) or tumor-initiating cells (TICs) are thought to be the main drivers for disease progression and treatment resistance across various cancer types. Identifying and targeting these rare cancer cells, however, remains challenging and unproven with respect to therapeutic benefit. Here, we report the enrichment of LGR5 expressing cells, a well-recognized stem cell marker, in mouse liver tumors, and the upregulation of LGR5 expression in human hepatocellular carcinoma. Isolated LGR5 expressing cells from mouse liver tumors are superior in initiating organoids in 3D culture and forming tumors in immunodeficient mice upon engraftment compared to $LGR5^-$ cells, featuring candidate TICs. These cells are resistant to conventional treatment including sorafenib and 5-FU. Importantly, LGR5 lineage ablation significantly inhibits organoid initiation and tumor growth. The combination of LGR5 ablation with 5-FU, but not sorafenib, further augments the therapeutic efficacy *in vivo*. Thus, we have identified the $LGR5^+$ compartment as an important TIC population, representing a viable therapeutic target for combating liver cancer.

Keyword: LGR5; Tumor-initiating cells, Liver cancer; Anti-cancer target.

Introduction

The key concept underlying the cancer stem cell (CSC) or tumor-initiating cell (TIC) theory is that tumors are maintained through a hierarchical structure in which different cell populations have different functionalities in pathophysiology[1]. The bulk of a tumor is thought to consist of CSCs/TICs as well as rapidly proliferating cells. CSCs/TICs are responsible for tumor initiation, resistance to conventional treatment and distant metastasis. Rapidly proliferating cancer cells, thought to be derived from the tumor stem cell pool, are responsible for volume increment of the tumor[2]. A prediction based on this model is that ablation of the relatively small CSC compartment would ultimately result in cessation of tumor growth and metastasis, and provoke sensitization of the tumor to conventional treatment as well.

Within the framework of this theory, CSCs/TICs would be characterized by a large capacity for self-renewal, a potential for differentiation into different cell types that constitute the tumor, and a resistance to conventional treatment[1]. These key features largely overlap with those of normal stem cells, making it extremely difficult to specifically identify CSCs/TICs, but on the other hand would allow techniques traditionally used for identifying normal stem cells also to be applied for CSCs/TICs[3]. LGR5 (leucine-rich repeat-containing G protein-coupled receptor 5) evokes special interest as a potential marker for the CSC/TIC compartment in this respect. LGR5 is a well-characterized stem cell marker in several tissues/organs, including the small intestine, the colon and the liver[4,5,6]. In colon and intestine, the LGR5 stem cell pool constantly proliferates and differentiates into mature cell types to compensate for the loss of functional epithelial cells. Interestingly, these LGR5 stem cells also participate in the process of oncogenesis, acting as the cells-of-origin of intestinal cancer[7]. Importantly, LGR5 marks CSCs in colon cancer[8,9,10], intestinal cancer[11] and basal cell carcinoma[12]. In intestinal adenoma as well as malignant carcinoma, LGR5 cells account consistently for a ratio of 5-10% of tumor cells and fuel tumor growth[8,13]. Proof-of-concept showing that specific elimination of LGR5 cells delays tumor growth in colon cancer has been provided[9]. Given the essential role of CSCs/TICs, these cells are attractive targets for anti-cancer treatment, whereas their resistance to conventional therapies impedes the therapeutic development.

In contrast to the colon and intestine, LGR5 stem cells are absent in the homeostatic liver, but emerge upon tissue injury[4,14]. These liver LGR5 cells are likely to be an intermediate stem/progenitor cell population that responds to injury but they may have a limited contribution to tissue repair[14]. Whether an $LGR5^{+}$ compartment exists in liver cancer remains obscure and the possible importance of such a compartment in this disease is unexplored. Nevertheless, research into this possibility is urgently needed as liver cancer is one of the most common forms of malignancy worldwide, with nearly 800,000 cases reported yearly and it is characterized by a depressing lack of treatment options[15]. Hepatocellular carcinoma (HCC) and cholangiocarcinoma (CC) are the two main types of primary liver cancer. Currently, surgery remains the only potentially curative therapeutic strategy available but is well-known for its high recurrence rate

following tumor resection. Chemotherapy and targeted treatment are generally ineffective, with sorafenib providing some extension of life expectancy to HCC patients. The unusual treatment resistance of liver cancer is thought to be associated with the presence of CSCs/TICs, but this notion remains largely unproven[16]. Thus, we aimed to investigate whether LGR5 marks CSCs/TICs in liver cancer, and to explore the potential for therapeutic targeting of these cells. Our results show that in liver cancer an $LGR5^+$ compartment exists that is superior in tumor initiation and mediates therapy resistance. Targeting this compartment constitutes a rational novel avenue for combating this disease.

Results

Enrichment of LGR5 expressing cells in primary liver tumors

Homeostatic livers are reported to be devoid of LGR5$^+$ cells, but injury does induce such cells[14]. Whether LGR5$^+$ cells are present in liver cancer is largely unknown. By adopting *Lgr5-DTR-GFP* knock-in mice (**Fig. 1a**), we first investigated the presence of LGR5$^+$ cells (GFP co-expressing cells) in the healthy and injured liver, and during carcinogenesis. Carbon tetrachloride (CCl_4) was used to trigger liver injury. Diethylnitrosamine (DEN) was used to induce primary liver tumor formation (**Fig. 1b**, and **Supplementary Fig. 1**). Although LGR5 cells are absent in the homeostatic liver (**Fig. 1c**), either a single course or repeated administration of DEN can rapidly trigger the emergence of LGR5-GFP$^+$ cells (post DEN induction day 7; relative size of the LGR5-GFP$^+$ compartment following 1 X DEN: 0.025 ± 0.05%, n = 3 [mean ± SEM]; **Supplementary Fig. 2a-b**). Animals were monitored for liver tumor formation from 4 to 14 months post DEN induction (**Supplementary File. 1**). Analysis of the resulting hepatic neoplasms revealed stable presence of an LGR5$^+$ compartment in these liver tumors (**Fig. 1c**). The relative abundance of LGR5 cells in the tumors (**Supplementary File. 1** and **Supplementary Fig. 2c-d**) are significantly higher as compared to those in the tumor surrounding tissues (**Fig. 1d**) or as detected in CCl_4 injured livers (**Fig. 1c**). The LGR5 expression levels in the tumor cells show substantial variation, but are substantially and significantly higher compared to that in injured liver (**Fig. 1e**). Immunohistochemistry (IHC) and immunofluorescence (IF) staining of GFP expression further confirms the presence of an LGR5$^+$ compartment and enables detailed analysis of spatial distribution of LGR5-GFP$^+$ cells in the liver (IF: **Fig. 1f**; IHC: **Supplementary Fig. 2e-f**). Co-staining with hepatocyte marker (HNF4α) or cholangiocyte marker (CK19) revealed that a proportion of LGR5 cells in the tumor express HNF4α or CK19 (**Fig. 1g-h**), suggesting that LGR5$^+$ cells may give rise to both a HCC-like and a CC-like phenotype, the two main types of primary liver cancer. Thus, these data have demonstrated the presence of an LGR5$^+$ compartment in primary murine liver cancer.

To examine the clinical relevance, we investigated *LGR5* expression in human HCC tumors from our patient cohort (Erasmus MC cohort). We found that *LGR5* expression is significantly elevated in tumor tissues compared to the paired tumor free liver tissues (**Fig. 2a**), and also in some subpopulations of patients with specific etiologies of HCC (**Fig. 2b**). Survival analysis by predicting Kaplan-Meier curves revealed a tendency towards worse clinical outcome in patients with higher *LGR5* expression (**Fig. 2c**). Further analysis of online publically available datasets confirmed the upregulation of *LGR5* expression in HCC (**Supplementary Fig. 3a**), and possible association with clinical outcome especially in subpopulations of specific patients (**Supplementary Fig. 3b**). Interestingly, with data from the TCGA database and International Cancer Genome Consortium-France (LICA-FR) and International Cancer Genome Consortium-Japan (LIRI-JP), we found that the upregulation of *LGR5* expression is more pronounced in HCC tumors with β-catenin mutation (**Supplementary Fig. 4**). This is in line with LGR5 being a β-catenin target gene both in the intestine and liver[5,17].

Taken together, *LGR5* cells are enriched in both mouse and human liver tumors, and bear substantial clinical relevance.

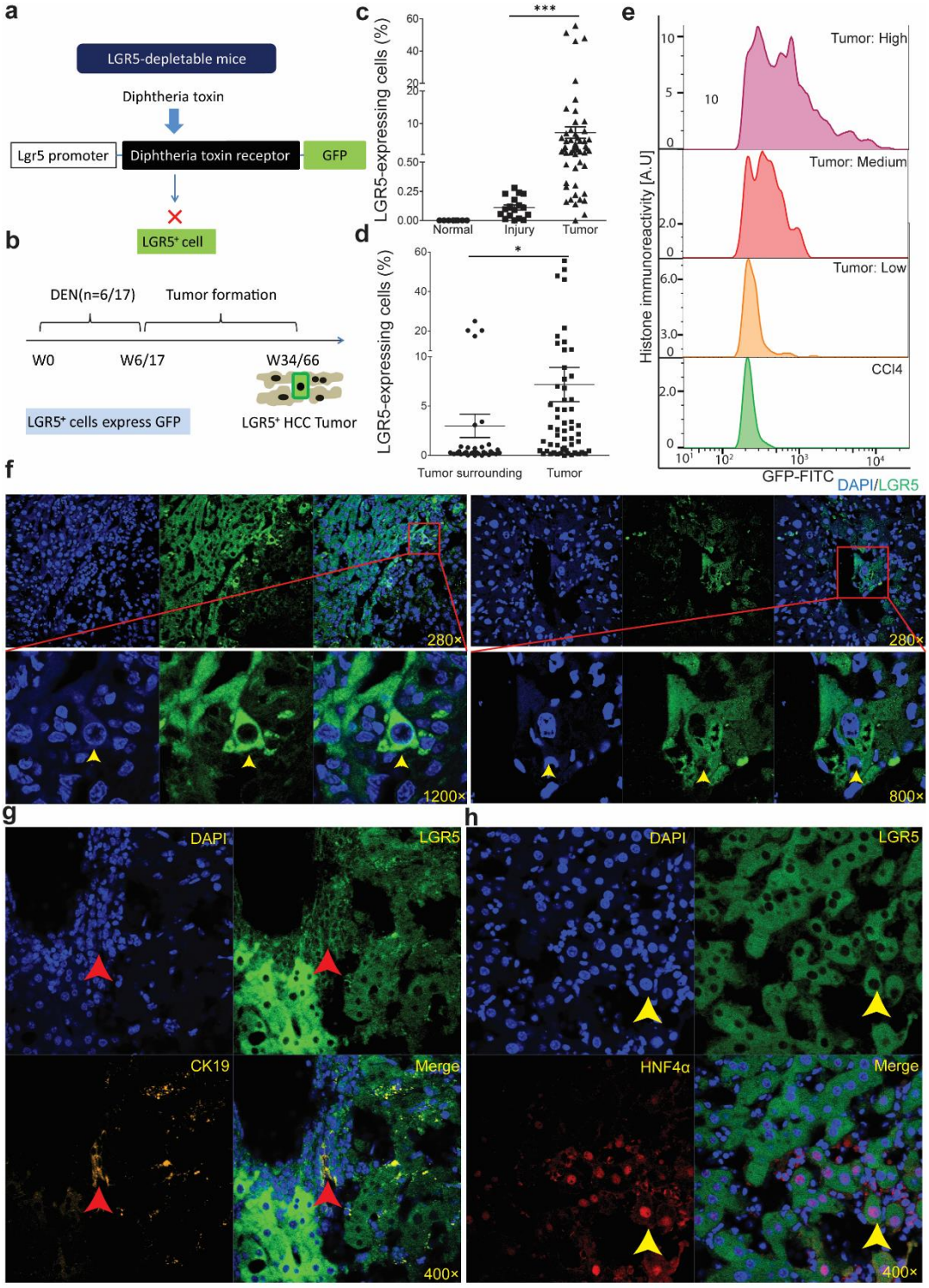

Fig. 1 Primary murine liver tumors are enriched with LGR5 expressing cells. a Principle of *Lgr5-DTR-GFP* transgenic mouse strategy used in this study. b Principle of the experimental strategy used to induce primary murine tumors in the context of this study. c The percentage of LGR5⁺ cells, as determined by flow cytometry, is significantly higher in liver tumors from DEN-treated (7.29 ± 1.76%, *n*

= 55) as compared to livers from untreated animals (0 ± 0 %, *n* = 8) or injured livers from CCl_4-treated animals (0.11 ± 0.022 %, *n* = 17) (Welch test, *P* = 0.0001). d The percentage of LGR5-GFP$^+$ cells is significantly increased in liver tumors (7.29 ± 1.76%, *n* = 55) as compared to the tumor-surrounding tissues (2.93 ± 1.15%, *n* = 34) of the same mice (Welch test, *P* = 0.0407). e Liver tumor-derived LGR5-GFP$^+$ cells showed increased fluorescence intensity when compared to LGR5-GFP$^+$ cells derived from CCl_4-injured livers. f Representative images showing LGR5-GFP$^+$ cells as present in liver tumors. Yellow arrow: LGR5-GFP$^+$ cell. DAPI: blue. g-h Representative confocal images showing the expression of the cholangiocyte marker (g, CK19, yellow) and the hepatocyte-specific marker (h, HNF4α, red) in LGR5-GFP expressing cells. Source data are provided as a Source Data file.

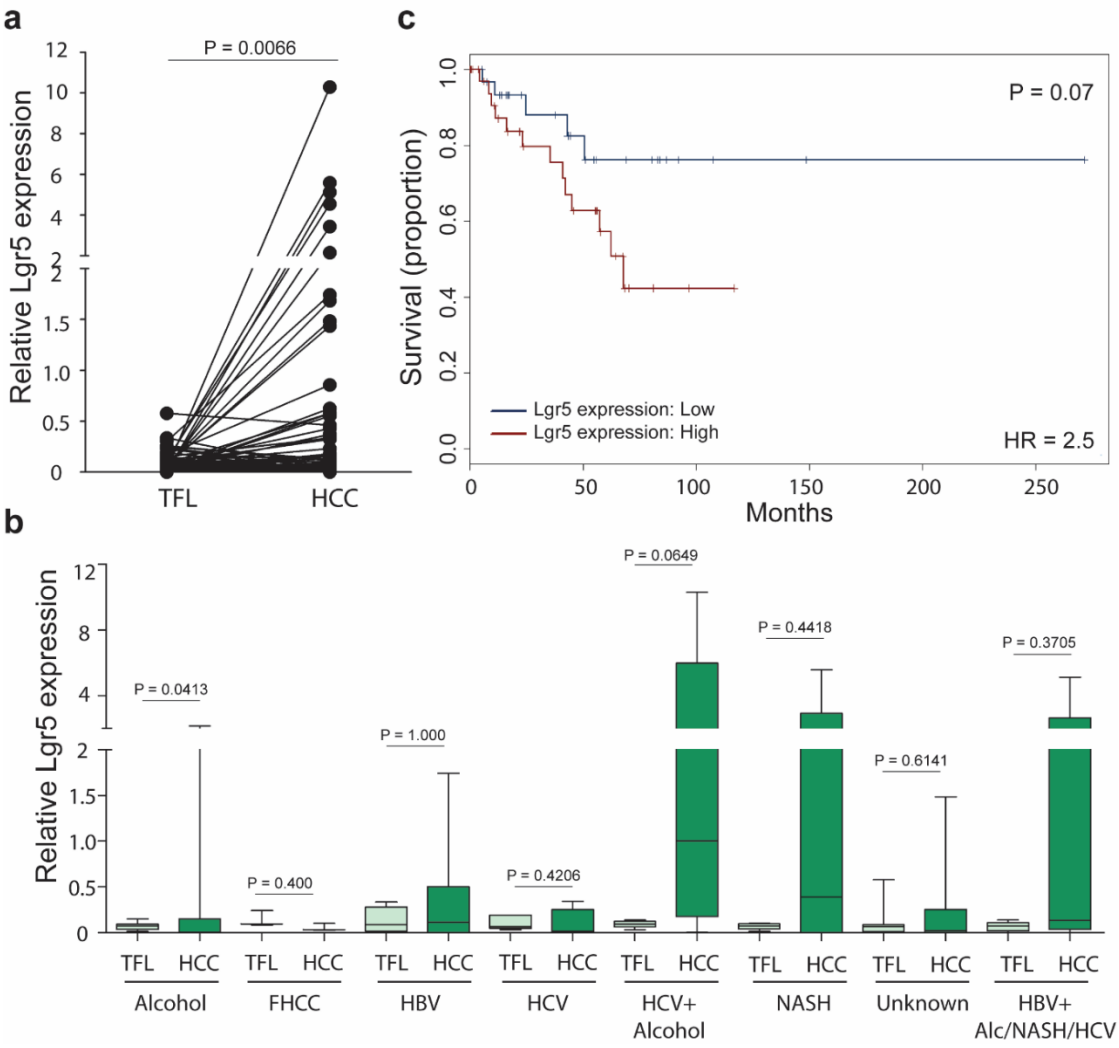

Fig. 2 The expression of *LGR5* is upregulated in human HCC tissues. a Upregulation of *LGR5* expression in HCC tissues (*n* = 74) compared with tumor free liver tissues (TFL, *n* = 75) from the Erasmus MC cohort (Paired T-test, *P* = 0.0066). *GUSB* (Beta-glucuronidases), *HPRT1* (hypoxanthine phosphoribosyltransferase 1) and *PMM1* (phosphomannomutase 1) were used as reference genes for normalization. b The expression of *LGR5* in HCC tissues compared with TFL stratified based on the etiologies of HCC (Paired T-test). FHCC: Fibrolamellar carcinoma; HBV: Hepatitis B virus; HCV: Hepatitis C virus; NASH: Non-alcoholic steatohepatitis. Alc: Alcohol. Patient number: Alcohol (*n* = 16); FHCC (*n* = 3); HBV (*n* = 9); HCV (*n* = 5); HCV + Alcohol (*n* = 6); NASH (*n* = 8); Unknown (*n* = 21); HBV + Alc/NASH/HCV (*n* = 5). c Kaplan-Meier curve of HCC patient survival with high (*n* = 37) and low (*n* = 37) *LGR5* expression (cut-off value based on median value – 0.047). Source data are provided as a Source Data file.

Preservation of LGR5 cells in liver tumor-derived organoids and allograft tumors

3D organoid cultures are robust model systems for studying the properties of (cancer) stem cells[18,19,20]. We have successfully established routine procedures[21] for creating organoid cultures from primary liver tumors of DEN-induced mice (**Supplementary Fig. 1**). In total, 89 tissues were obtained from 41 individual murine livers (**Supplementary File. 1**). 63 out of 89 (70.8%) tumor/tumor surrounding tissues successfully initiated organoids (8 out of 34 tumor surrounding tissues did not initiate organoid, 23.5%; 18 out of 55 tumor tissues did not initiate organoids, 32.7%). These organoids can be maintained and propagated in 3D culture for at least 5 months. Staining for CK19 and HNF4α demonstrates that these organoids either display a CC or HCC-like phenotype (**Fig. 3a-b**). Importantly, these cultured organoids maintain a population of LGR5 positive cells (**Fig. 3c**).

To investigate whether these organoid lines are malignant, we transplanted all the 63 strains into immunodeficient NOG mice (**Fig. 3d**). One to six months after allografting, eleven out of 63 organoid-strains formed palpable tumors in the immune deficient mice (17.5%). All contained an LGR5-GFP^{+} compartment as determined by FACS analysis of the tumors (**Fig. 3e**).

Following re-culture of cells obtained from these allograft tumors as organoids, we observed substantial diversity of the morphology (**Supplementary Fig. 5a-c**) and CK19/HNF4α expression in the corresponding allograft tumors (**Fig. 3f** and **Supplementary File. 2**). A population of LGR5-expressing cells were again observed in these organoid cultures (**Supplementary Fig. 5d**), in line with the existence of such a compartment in the allograft tumors from which these organoid cultures originated (IF: **Supplementary Fig. 5e**; IHC: **Supplementary Fig. 5f** and **Supplementary File. 2**). In addition, genome-wide transcriptomic analysis revealed a distinct gene expression signature between LGR5^{+} and LGR5^{-} cells, including TATA-box binding protein associated factor 7 like (Taf7l), Sialophorin (Spn), SRY-box 2 (Sox2), Nidogen-1(Nid1), Paralemmin 3 (Palm3), Alpha-1-microglobulin/bikunin precursor (Ambp), Membrane bound O-acyltransferase domain containing 4 (Mboat4) and Chymase 1 (Cma1), which had higher expression levels in LGR5^{+} compared with LGR5^{-} population. Kaplan-Meier curve analysis revealed that all these genes are associated with the survival of liver cancer patients (**Supplementary Fig. 6 and Supplementary File. 3-4**). Especially, Sox2 as a transcription factor is essential for maintaining self-renewal or pluripotency of undifferentiated embryonic stem cells, and has been reported as a marker for cancer stem cells in breast cancer and squamous-cell carcinoma[22]. Gene enrichment analysis of the 196 differentially expressed genes further revealed the involvement of metabolism-related pathways, including “Oxidation by Cytochrome P450”, “Calcium Regulation”, “Metapathway biotransformation” and “Purine metabolism”. There are also differentially expressed genes involved in immune

regulation, including “Macrophage markers pathway”, “Kit Receptor Signaling Pathway” and “IL-6 signaling Pathway”. Furthermore, LGR5^{+} cells had significantly differentially expressed genes involved in cell proliferation/migration, including “Chemokine signaling pathway”, “Matrix Metalloproteinases” and “PPAR signaling pathway”. Interestingly, there are differentially expressed genes enriched in “Wnt Signaling Pathway” and “G Protein Signaling Pathways”. Subsequent experiments were initiated to assess the exact functionality of LGR5 expressing cells.

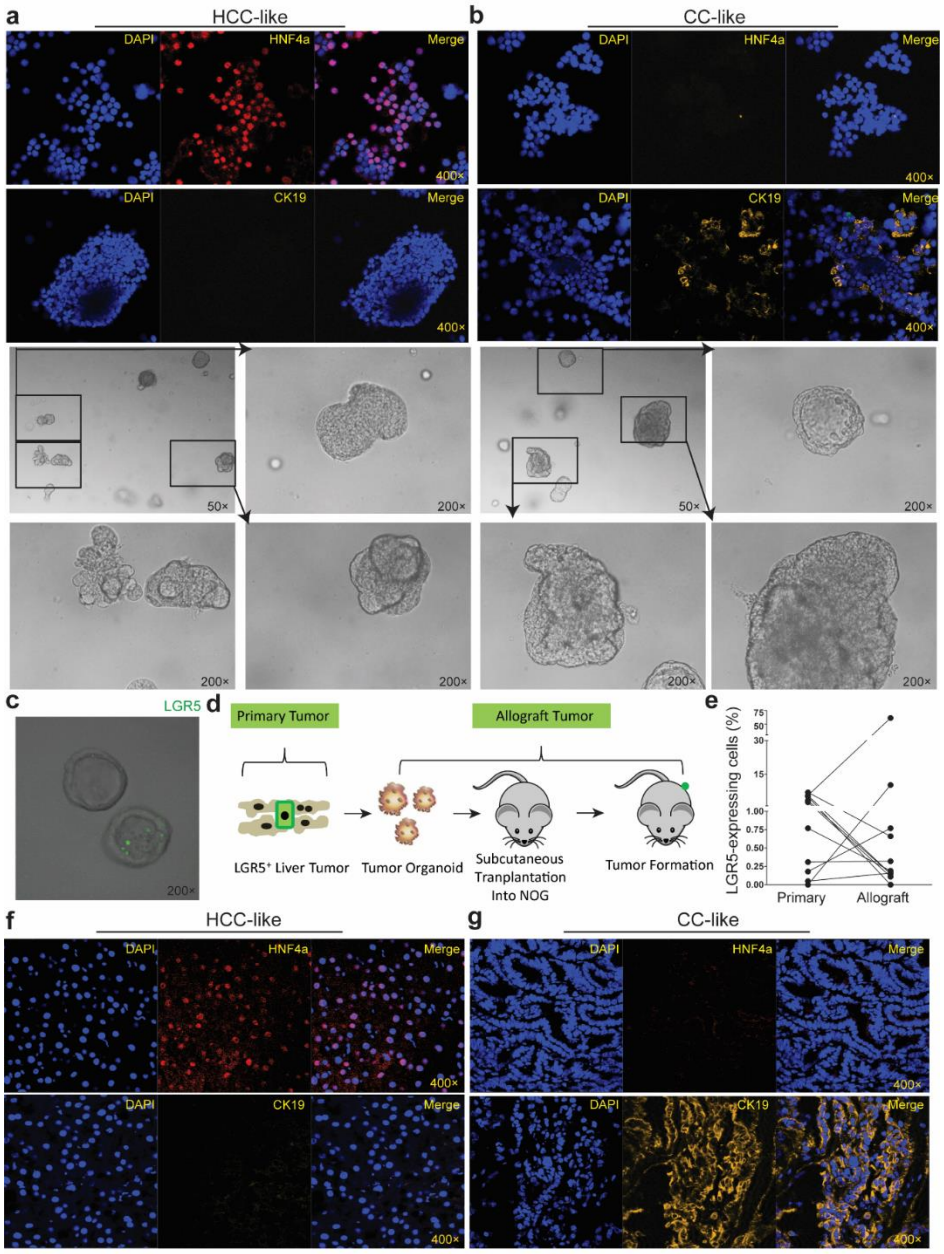

Fig. 3 Maintenance of LGR5 expressing cells in liver tumor organoids and allograft tumors. a-b Representative pictures showing organoid lines that predominately express the hepatocyte marker HNF4α (a) or the cholangiocyte marker CK19 (b) (Upper panels: IF staining; lower panels bright-field microscopic pictures). c Representative pictures showing the presence of LGR5 expressing cells in organoids. LGR5-driven GFP: Green. d An outline of the experimental strategy used to transplant tumor

organoid lines into immunodeficient mice. e The percentages of LGR5 expressing cells in allograft tumors and the corresponding primary tumors (Primary *vs.* Allograft: 2.8 ± 0.8% *vs*. 6.8 ± 5.6%, *n* = 11, *P* = 0.3577). f-g Representative pictures of allograft tumors that mainly express either the hepatocyte marker HNF4α (f) or the cholangiocyte marker CK19 (g). Source data are provided as a Source Data file.

Dissociated LGR5$^+$ cells from liver tumors are superior in organoid and tumor initiation compared to LGR5$^-$ cells

For functional comparison of LGR5$^+$ and LGR5$^-$ liver cancer cells, we first assessed their relative clonogenic ability using an organoid initiation assay. Employing FACS (the sorting strategy: **Supplementary Fig. 7a**), LGR5-GFP$^+$ and LGR5-GFP$^-$ cells were collected from 71 individual primary murine liver tissues, and cultured in 3D matrigel (**Fig. 4a** and **Supplementary File. 5**). After 2-3 weeks, we observed organoid formation from single cells (**Fig. 4b-d**). Importantly, LGR5-GFP$^+$ cells have stronger organoid formation ability compared to LGR5-GFP$^-$ cells (2.13 ± 0.67% vs. 0.07 ± 0.02%, n = 30) (**Supplementary File. 5**: detailed organoid initiation efficiency). In addition, we also observed that the initiation ability of LGR5$^+$ cells showed close correlation to collected cell number. The average numbers of LGR5$^+$ cells collected from tissues that did initiate organoid (1906 ± 442, n = 25) were significantly higher compared to the number that did not (171 ± 47, n = 46). This was not the case for LGR5$^-$ cells (28350 ± 8914, n = 60 vs. 13860 ± 3654, n = 11) (**Supplementary Fig. 7b-d**). This indicates that a sufficient cell number (>1000) is essential for successful organoid initiation of LGR5 expressing cells from liver tumors.

We next performed organoid initiation for cells derived from the allograft tumors (**Fig. 4e**). Similar as observed with primary tumors, LGR5$^+$ cells of allograft tumors initiate more organoids as compared to LGR5$^-$ cells (40.5 ± 10.2% vs. 9.8 ± 3.9%, n = 10) (**Fig. 4f**). Compared to cells isolated from primary tissues, allograft tumor cells are more potent with respect to their potential for organoid initiation (**Supplementary Fig. 7e-g**). Interestingly, organoids formed from a single LGR5-GFP$^+$ or LGR5-GFP$^-$ cell produce both LGR5 positive and negative offspring, suggesting possible self-formation of a hierarchical organization sustaining organoid growth and differentiation (**Supplementary Fig. 7h**).

The ultimate measure of potential functionality of LGR5$^+$ cells in pathophysiology is their capacity to form allograft tumors *in vivo* (**Fig. 4g**). Hence identical numbers of FACS sorted LGR5-GFP$^+$ and LGR5-GFP$^-$ cells derived from primary liver tumors were subcutaneously engrafted into NOG mice and tumor formation was monitored (**Supplementary File. 6**). As expected, LGR5$^+$ cells display a stronger capacity for tumor initiation as compared to LGR5$^-$ cells (LGR5$^+$ vs LGR5$^-$: 33.3% vs 11.1%) (**Fig. 4h, Supplementary File. 6**). Moreover, tumors initiated from LGR5$^+$ cells contain both LGR5 positive and negative populations (**Fig. 4i-n**). Additionally, we have performed a tumor formation assay for the cells that were derived from the allograft tumors (**Fig.**

4o). Again the LGR5^{+} compartment proved markedly more potent in this respect relative to the LGR5-GFP^{-} compartment (**Fig. 4p-q** and **Supplementary Table. 1**). Collectively, our results are best interpreted that liver tumor-derived LGR5^{+} cells constitute a *bona fide* TIC compartment.

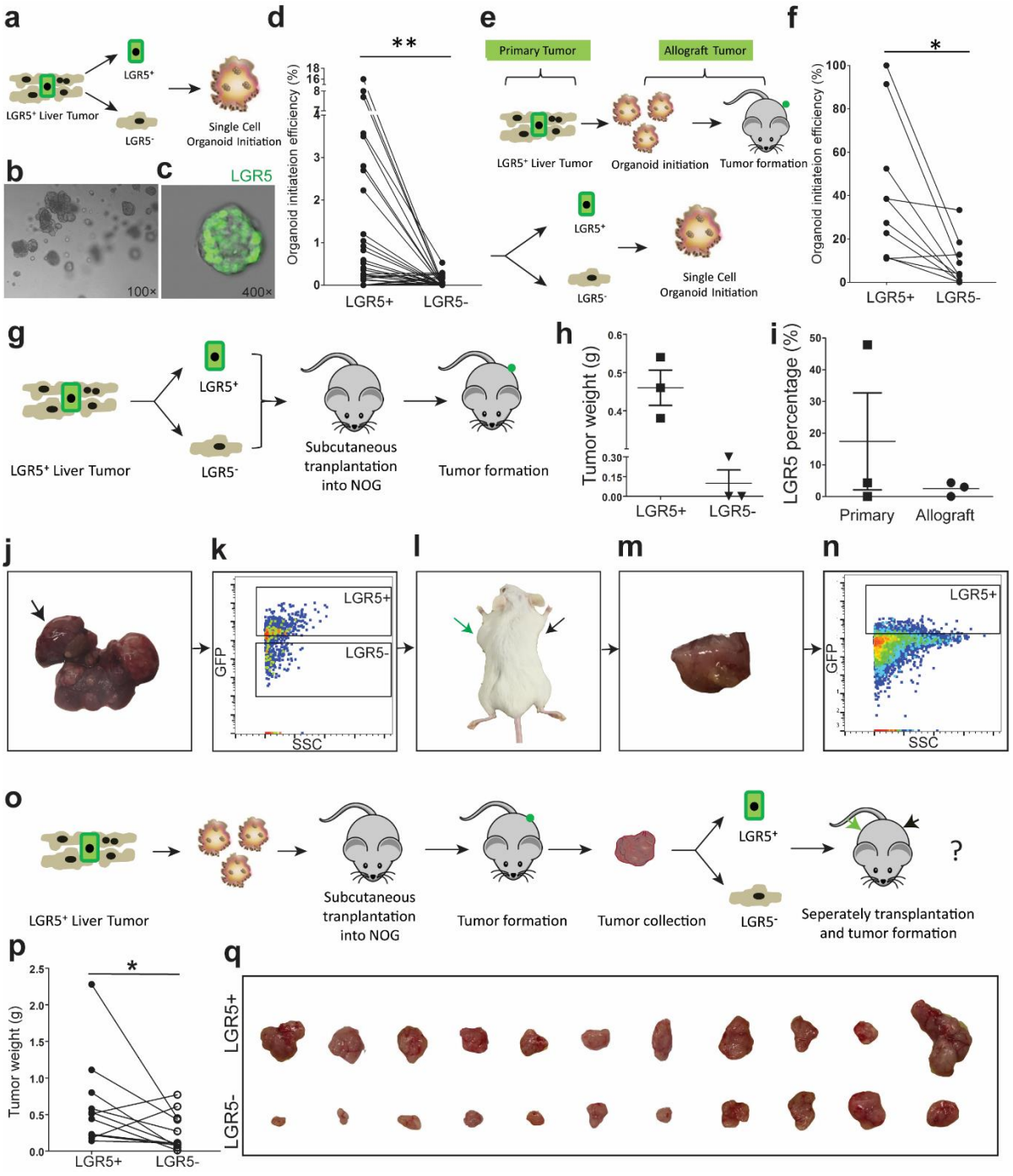

Fig. 4 Single LGR5^{+} cells from liver tumors are superior in organoid and tumor initiation. a An outline of the experimental strategy for studying *ex vivo* organoid initiation of cells derived from primary murine liver tumors. b A representative picture of organoids derived from single LGR5^{+} cells. c Representative confocal micrograph of a single LGR5^{+} cell-initiated organoid dominated by LGR5 expressing cells. LGR5-driven GFP: Green. d Organoid initiation efficiency of LGR5-GFP^{+} and LGR5-GFP^{-} cells, isolated

from primary liver tumors (LGR5$^+$ cells: 25 out of 71 tissues, 35.2%; LGR5$^-$ cells: 11 out of 71 tissues, 15.5%) (Paired T test, 2.13 ± 0.67 % *vs*. 0.065 ± 0.023 %, n = 30, P = 0.0048). e An outline of the experimental strategy used to study *ex vivo* organoid initiation of allograft tumor-derived cells. f Efficiency of organoid initiation by allograft liver tumor-derived LGR5-GFP$^+$ and LGR5-GFP$^-$ cells (Paired T test, 40.46 ± 10.19 % *vs.* 9.84 ± 3.93 %, n = 10, P = 0.0187). g Outline of the experimental strategy used to assess *in vivo* tumor initiation of cells isolated from primary murine liver tumors. h Weight of tumors initiated by LGR5$^+$ and LGR5$^-$ cells (LGR5$^+$ *vs.* LGR5$^-$: 0.46 ± 0.046 g *vs.* 0.10 ± 0.10 g, n = 3)(Formed tumor number: LGR5$^+$ cells--3 out of 9; LGR5$^-$ cells--1 out of 9). i LGR5 expression in single LGR5$^+$ cell-derived allograft tumors and corresponding primary tumors (17.42 ± 15.29 % *vs.* 2.47 ± 1.27 %, n = 3). j-n Representative pictures showing that LGR5-GFP$^+$ and LGR5-GFP$^-$ cells (k) were isolated from DEN-induced primary liver tumors (j). Then, LGR5-GFP$^+$ cells (green arrow) initiated allograft tumors in immunodeficient mouse (l-n). The initiated allograft tumors sustained LGR5 expression (n). o An outline of the experimental strategy for *in vivo* tumor initiation assay of cells isolated from allograft murine liver tumors. p Tumor weight of allografts initiated by LGR5-GFP$^+$ cells and LGR5-GFP$^-$ cells (isolated from allograft tumors). (0.64 ± 0.19 g *vs.* 0.27 ± 0.08 g, n = 11, P = 0.0418). q Macroscopic aspect of the tumors initiated by LGR5-GFP$^+$ cells and LGR5-GFP$^-$ cells (isolated from allograft tumors). Source data are provided as a Source Data file.

Anti-cancer treatment enriches LGR5 expressing cells

CSCs or TICs are presumed to be relatively resistant to conventional anti-cancer treatment. A prediction would thus be that in liver cancer the LGR5$^+$ cells would be more resistant to anti-cancer treatment as compared to the LGR5$^-$ cells. Hence we challenged tumor organoids with sorafenib, the FDA-approved drug for treating advanced HCC, and compared the relative potential of LGR5-GFP$^+$ and LGR5-GFP$^-$ cells to withstand such treatment (**Fig. 5a**). Treatment of tumor organoids with sorafenib significantly increased the percentage of LGR5 positive cells in the population (**Fig. 5b-d**). This effect became even more profound when the organoids were treated with the chemotherapeutic agent, 5-fluoro-uracil (5-FU) (**Fig. 5a-d**).

Subsequently the relative size of the LGR5$^+$ compartment following *in vivo* treatment with these therapeutic agents was assessed (**Fig. 5e**). Treatment with either sorafenib or 5-FU to mice bearing allograft tumors, formed by engrafting tumor organoids, substantially increased the fraction of the LGR5-GFP$^+$ cells in the tumors (**Fig. 5f**). Also when LGR5-GFP$^+$ and LGR5-GFP$^-$ cells were isolated from tumor organoids and used for organoid re-initiation, while subsequently being treated with 5-FU, the resulting cultures were dominated by LGR5-GFP$^+$ expressing cells, independent from whether LGR5-GFP$^+$ or LGR5-GFP$^-$ were used as starting material (**Fig. 5g**). Of note, LGR5$^+$ cells isolated from 5-FU-treated tumors retained the ability of organoid and tumor initiation (**Supplementary Fig. 8**). Interestingly, 5-FU treatment effectively rewired the transcriptome of LGR5$^+$ cells (**Fig. 5h**; **Supplementary Fig. 6 and 9**). Gene enrichment analysis of the 1464 differentially expressed genes between 5-FU treated compared to untreated LGR5$^+$ cells revealed the involvement of stem cell-related pathways, including “Wnt Signaling”, “Notch Signaling Pathway”, “ErbB signaling pathway”, “Hedgehog Signaling Pathway” and “BMP Signaling Pathway” (**Fig. 5i** and **Supplementary File. 3**). These pathways are commonly activated in many types of

solid tumors, associated with cancer initiation, progression and metastasis[23]. Interestingly, there are several pathways, including “TGF Beta Signaling Pathway”, “EGFR1 Signaling Pathway”, “PPAR signaling pathway”, “G1 to S cell cycle control”, “Mismatch repair”, “p53 signaling” and “Apoptosis Modulation/Apoptosis pathway”, are known to be implicated in anti-cancer treatment response and DNA damage response[24]. These results may partially explain the enrichment of LGR5 expressing cells upon 5-FU treatment. In conclusion, besides resistance, conventional anti-cancer treatment also triggers the generation and propagation of LGR5 expressing cells.

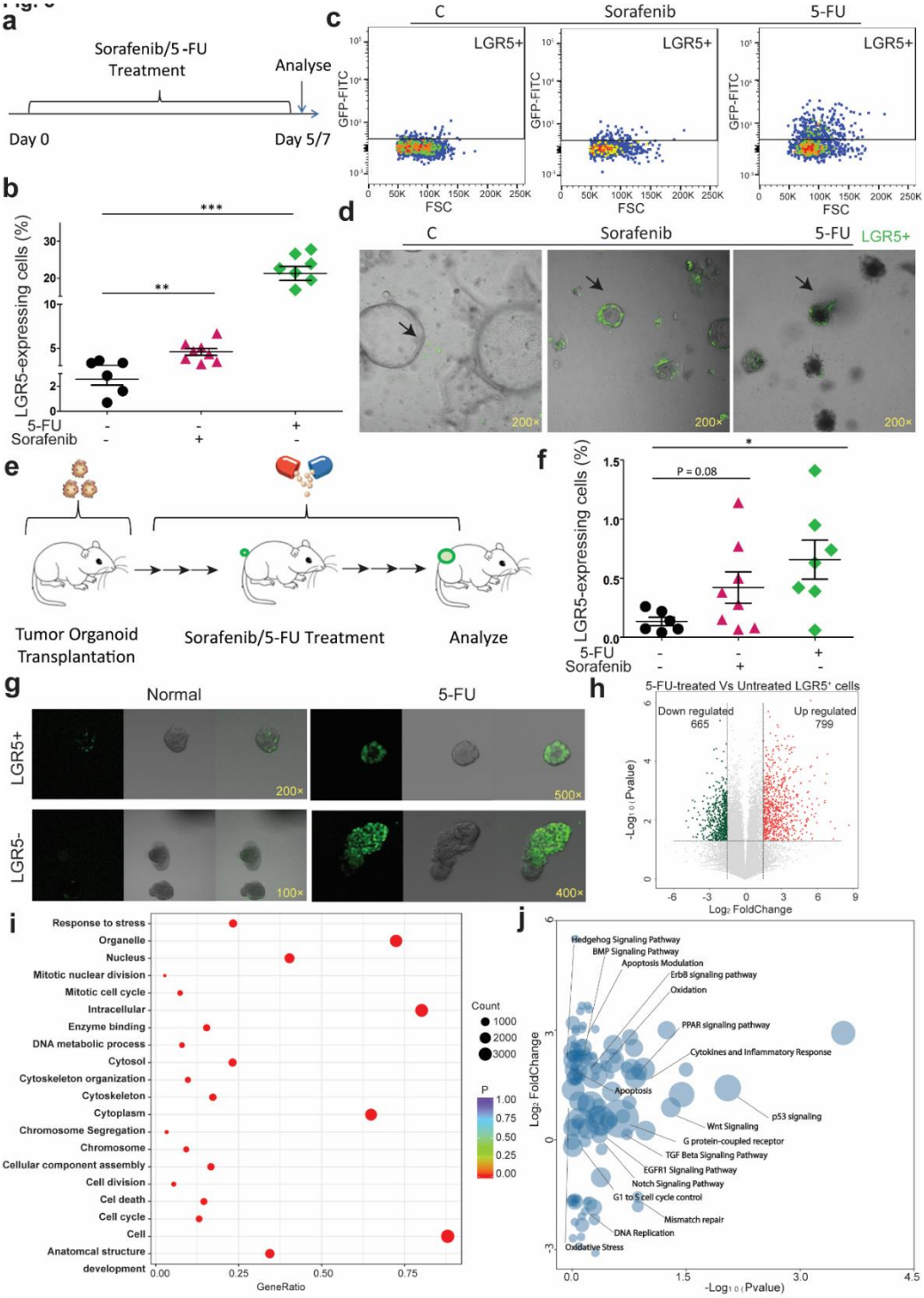

Fig. 5 Anti-cancer treatment selects for LGR5$^+$ cells. a Outline of the *ex vivo* experimental strategy used to assess the effects of drug treatment on the size of the LGR5$^+$ compartment. b The fraction of LGR5-GFP$^+$ cells is significantly increased upon treatment with sorafenib or 5-FU (vehicle control *vs.* 10 µM sorafenib *vs*. 10 µM 5-FU: 2.6 ± 0.5 % *vs*. 4.6 ± 0.4 % *vs*. 21.3 ± 1.9 %). c-d Representative FACS plots (c) and confocal pictures (d) demonstrating that the fraction of LGR5-GFP$^+$ cells is increased upon treatment with sorafenib or 5-FU. e An outline of the experimental strategy used for testing the effects of drug administration *in vivo*. f The percentages of LGR5-GFP$^+$ cells is increased upon administration of sorafenib or 5-FU to allografted animals (vehicle control *vs*. sorafenib *vs*. 5-FU: 0.13 ± 0.04 %, $n = 6$ *vs*. 0.42 ± 0.13 %, $n = 8$ *vs*. 0.66 ± 0.17 %, $n = 7$). g Representative confocal pictures showing that both single LGR5-GFP$^+$ and LGR5-GFP$^-$ cell-initiated organoids contain LGR5 expressing cells and the relative fraction of LGR5 expressing cells is increased in treatment resistant organoids. LGR5-driven GFP: Green. h A Volcano plot showing the most significantly differentially expressed genes between 5-FU treated/untreated LGR5$^+$ cells. i Gene enrichment analysis (with the library of Wiki2019) within the differentially expressed genes. Source data are provided as a Source Data file.

LGR5 lineage ablation inhibits organoid and tumor growth

From the results described above, we inferred that ablation of the LGR5$^+$ compartment should impair liver cancer growth. To experimentally test this notion, we exploited the co-expression of the diphtheria toxin receptor (DTR) in the *Lgr5-DTR-GFP* mice. This would allow us to specifically deplete the Lgr5-DTR-GFP$^+$ compartment through diphtheria toxin (DT) administration (**Fig. 1a**). We have previously optimized the concentrations of DT treatment (1-10 ng/ml) for LGR5 depletion, with organoids derived from healthy *Lgr5-DTR-GFP* mice[14]. Accordingly, we evaluated the effects on organoid initiation and proliferation (**Fig. 6a-b**), and sorafenib treatment served as a positive control. DT treatment inhibited the growth of tumor organoids in an effect that showed close correlation as to the effects on the numbers of LGR5-GFP$^+$ cells (**Fig. 6c-e**). DT treatment did not influence the growth of tumor organoids of genetically wild type (**Fig. 6c**: left panel).

We further assessed therapeutic targeting of LGR5 liver cancer cells *in vivo*. We first evaluated the effect of DT treatment after formation of visible tumors, following transplantation of tumor organoids into immunodeficient mice (**Supplementary Fig. 10a**). 5-FU and sorafenib served as the positive controls. The effects of LGR5 cell depletion on the growth of formed tumors was minor (**Supplementary Fig. 10c**: right panel and **10d**: right panel). In contrast, administration of DT immediately after transplantation of tumor organoids (**Fig. 6f**) efficiently delayed tumor initiation and inhibited their growth (**Fig. 6h**; **Supplementary Fig. 10c**: left panel and **10d**: left panel). Further analysis of the tumors confirmed the depletion of the LGR5-GFP$^+$ compartment in the DT treated animals (**Fig. 6g**). Also using absolute tumor size as a measure, DT-mediated depletion of the LGR5$^+$ compartment impaired tumor growth (**Fig. 6i**). The enrichment of stem cell markers also differed in control and DT-treated LGR5$^{+/-}$ cells (**Supplementary Fig. 11**). Interestingly, there was an inverse correlation between tumor size and the relative size of the LGR5-GFP$^+$ compartment at the end of the experiment (**Supplementary Fig. 10e-f**), indicating that LGR5 expressing cells are probably more active in the tumor initiation period. As control, DT treatment did not

influence initiation and growth of tumors formed from the wild type tumor organoids (**Supplementary Fig. 12a-b**). Thus, LGR5 lineage ablation impedes organoid and tumor initiation and further growth.

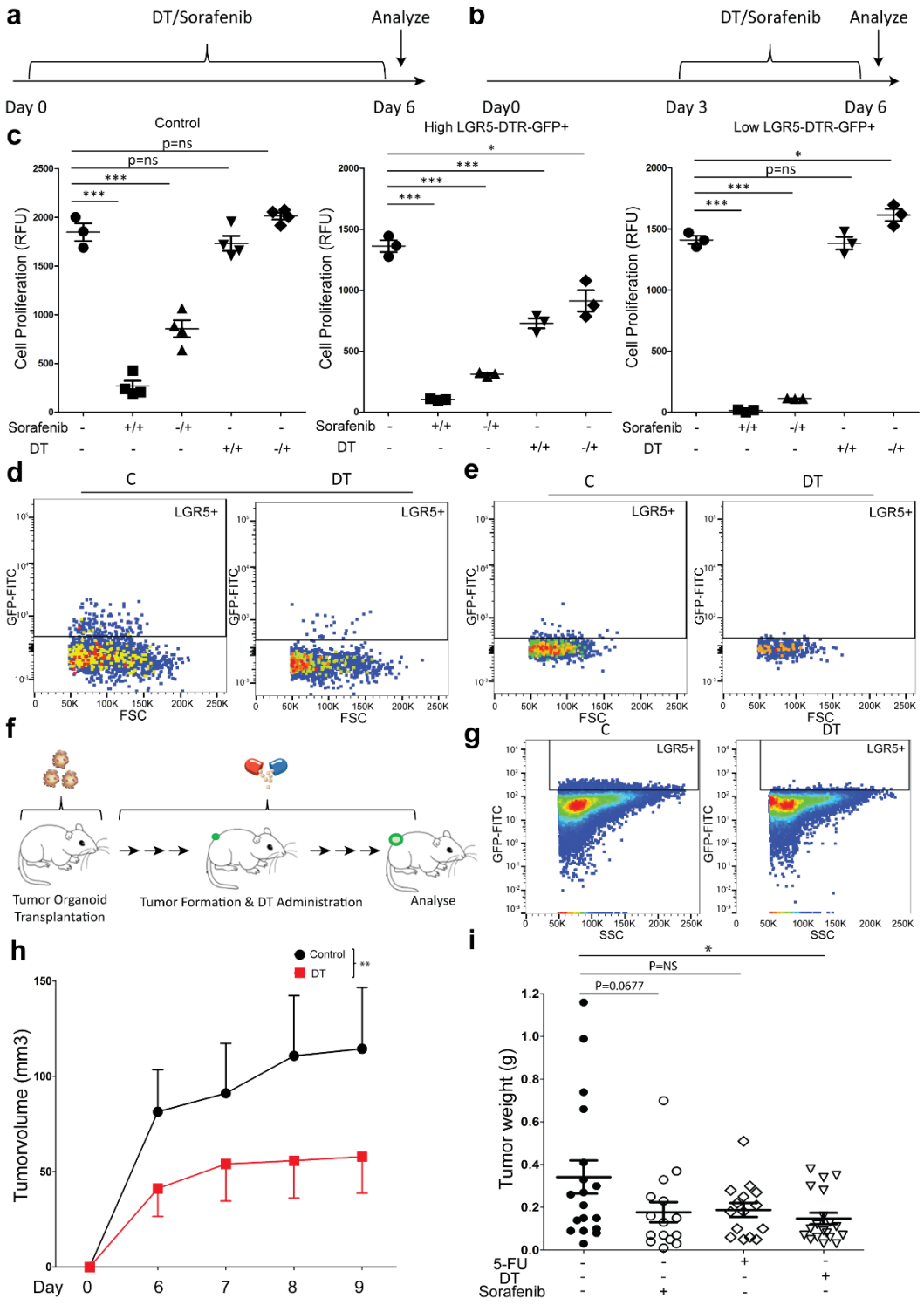

Fig. 6 LGR5 lineage ablation inhibits organoid and tumor growth. a-b The outlines of the *ex vivo* experimental strategy to assess the effects of anti-cancer drug treatment on (a)organoid initiation and delineate its temporal aspect (b) or during organoid expansion. c The response of wild type tumor organoids (Left) and Lgr5-DTR-GFP mice derived tumor organoids, with relatively high LGR5 expression (the percentage of LGR5 expression is higher than 1%)(Middle) or low LGR5 expression (the percentage

of LGR5 expression is lower than 1%) (Right) during regular expansion, to DT/sorafenib treatment. -/+: drug treatment during the expansion period; +/+: DT treatment since the initial culture day. d-e Representative FACS plots showing that LGR5-GFP$^+$ cells are depleted by DT treatment, for high LGR5 expression organoid strains (d) and low LGR5 expression organoid strains (e). f Outlines of the experimental strategy used to assess the efficacy of DT/sorafenib/5-FU administration on allograft tumors in mice. g Representative FACS plots from experiments validating the strategy to deplete LGR5$^+$ cells. h A representative growth curve showing the volumes of tumors derived from the vehicle control group and the DT-administrated group (n = 8). i, The weight of tumors from vehicle control, DT, 5-FU or sorafenib-treated groups, on the day of mice sacrifice (Control *vs*. sorafenib *vs*. 5-FU vs. DT: 0.34 ± 0.078 g, n = 18 *vs*. 0.18 ± 0.047g, n = 15 *vs*. 0.19 ± 0.033 g, n = 15 *vs*. 0.15 ± 0.027 g, n = 19). Source data are provided as a Source Data file.

Combination of LGR5 lineage ablation with chemotherapy enhances the anti-cancer efficacy

As LGR5$^+$ cells appear to mediate resistance against conventional anti-cancer treatment, it is rational to evaluate the combination of LGR5$^+$ lineage ablation with conventional anticancer treatment.

To experimentally test this notion, we first combined DT with sorafenib treatment. However, with different strategies of combination therapy, no enhanced anti-tumor activity was observed on allografted tumors (**Fig. 7**). We next tested the combination of 5-FU and DT. Allograft tumor-bearing mice were first subjected to 5-FU (which increases the relative size of the LGR5$^+$ compartment) followed by cessation of 5-FU therapy and start of DT treatment as to kill the LGR5$^+$ cells (**Fig. 8a** and **Supplementary Fig. 13a-c**). Indeed this approach is effective in combating allograft tumor formation (**Fig. 8b**) and is substantially superior to monotherapy with 5-FU, stand-alone DT treatment (**Fig. 8c-d** and **Supplementary Fig. 14a**) or initial treatment with DT followed by 5-FU therapy (**Supplementary Fig. 13d-h**). Simultaneous administration of 5-FU and DT (**Fig. 8e**) also resulted in robust anti-cancer effects (**Fig. 8f-h** and **Supplementary Fig. 14b**). Thus targeting the LGR5$^+$ compartment markedly enhances efficacy of conventional treatment aimed at combating liver cancer.

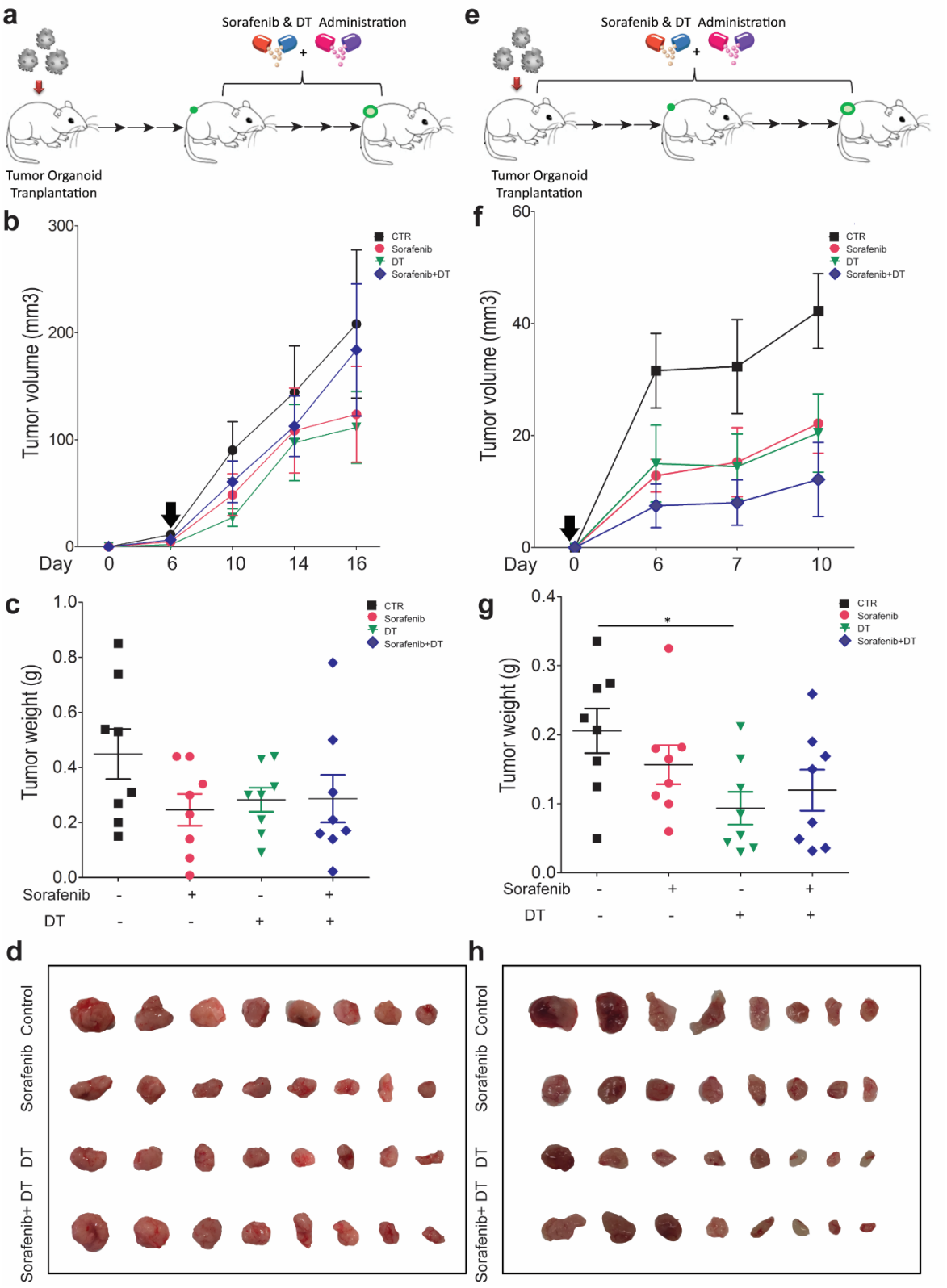

Fig. 7 Combination of LGR5 lineage ablation with sorafenib does not enhance the anti-cancer efficacy. a Outline of the experimental strategy to assess the combinatory effect of LGR5 lineage ablation with sorafenib. sorafenib and DT were administrated every other day for in total 10 days since visualization of tumor formation after organoid engraftment. b Representative growth curves showing tumor volumes in the vehicle control (CTR), sorafenib, DT, and sorafenib + DT treated groups. Black arrow: onset of administration. c Tumor masses from these four groups (CTR *vs.* sorafenib vs. DT. *vs*. sorafenib + DT:

0.45 ± 0.09 g, *n* = 8, vs. 0.25 ± 0.06 g, *n* = 8 *vs*. 0.28 ± 0.043 g, *n* = 8 *vs*. 0.29 ± 0.09, *n* = 8). d Images showing tumors from these four groups. e Outlines of the experimental strategy for assessing the effects of combining LGR5 lineage ablation and sorafenib treatment. sorafenib, DT or the combination were administered immediately since transplantation of the organoids every other day, for in total ten days. f, Representative growth curves showing tumor volumes of the four groups. Black arrow: onset of administration. g The tumor masses of these four groups (CTR *vs*. sorafenib *vs*. DT. *vs*. sorafenib + DT: 0.21 ± 0.03 g, *n* = 8 *vs*. 0.16 ± 0.03 g, *n* = 8 *vs*. 0.09 ± 0.02 g, *n* = 8 *vs*. 0.12 ± 0.03 g, *n* = 8). h Images showing the tumors from the different groups. Source data are provided as a Source Data file.

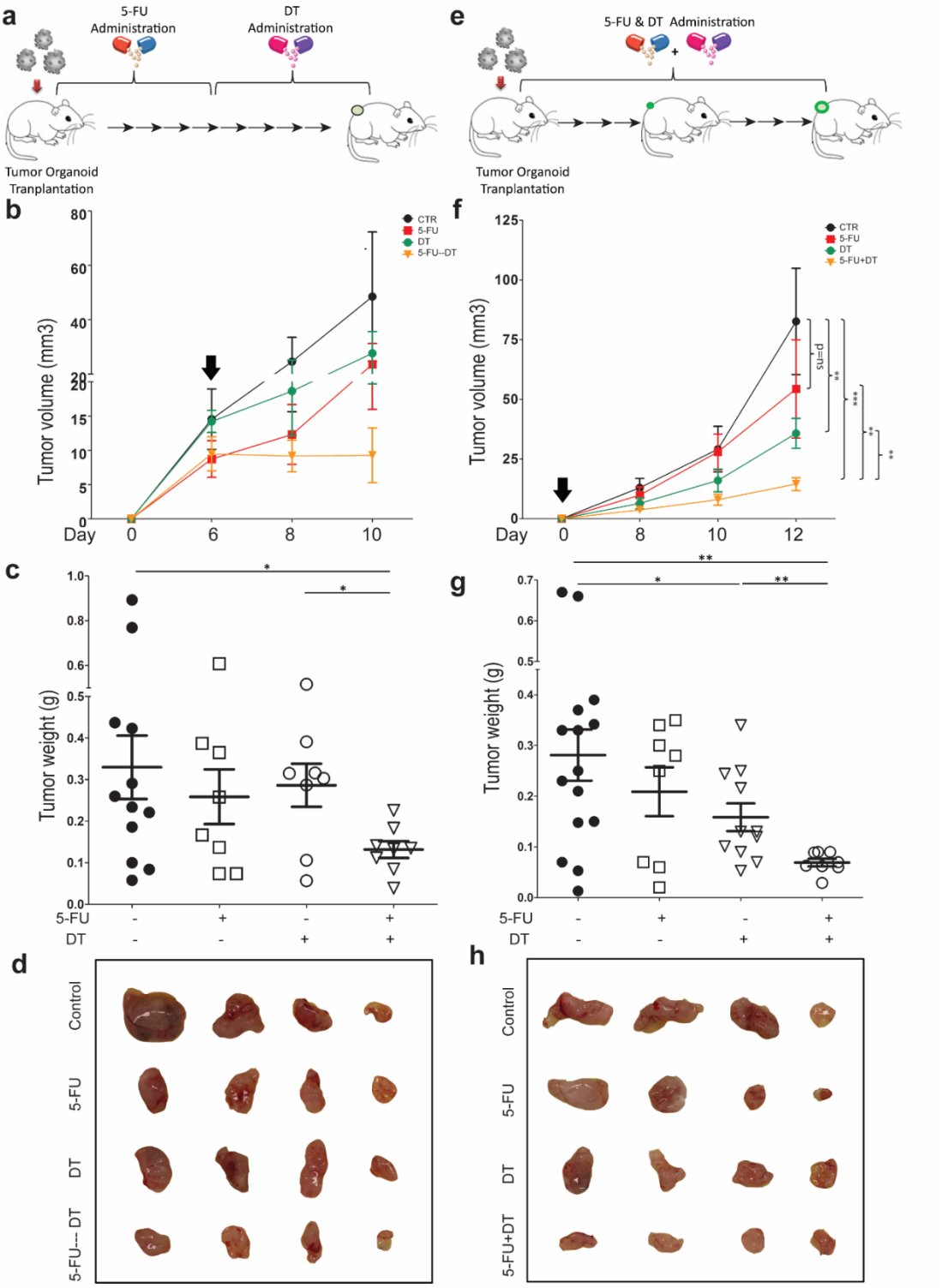

Fig. 8 Combination of LGR5 lineage ablation with 5-FU results in enhanced anti-cancer efficacy. a Outline of the experimental strategy to assess the combinatory effect of LGR5 lineage ablation with 5-FU. Following tumor organoid allografting, 5-FU was administrated for the first half of the experiment (every other day, for in total six days). DT was administrated for the second half of the experiment (every other day, for in total 6 days). b Representative growth curves showing tumor volumes in the vehicle control group (CTR), the 5-FU monotherapy group, the DT administration-only group, and the hybrid 5-FU/DT group. Black arrow: onset of administration. c Tumor masses from these four groups (Control *vs.* 5-FU vs. DT. *vs*. 5-FU-DT: 0.33 ± 0.076 g, *n* = 12 *vs*. 0.25 ± 0.066 g, *n* = 8 *vs*. 0.29 ± 0.052 g, *n* = 8 *vs*. 0.13 ± 0.020 g, *n* = 8). d Representative images showing tumors from these four groups. e Outlines of the experimental strategy for assessing the effects of combined LGR5 lineage ablation and 5-FU treatment. 5-FU, DT or the combination were administered since organoid engraftment every other day, for in total twelve days. f Representative growth curves showing tumor volumes of the four groups. Black arrow: onset of administration. g The tumor masses of these four groups (Control *vs*. 5-FU *vs*. DT. *vs*. 5-FU+DT: 0.28 ± 0.050 g, *n* = 15 *vs*. 0.21 ± 0.048 g, *n* = 8 *vs*. 0.16 ± 0.027 g, *n* = 11 *vs*. 0.069 ± 0.007 g, *n* = 8). h Representative images showing the tumors from the different groups. Source data are provided as a Source Data file.

Discussion

This study has demonstrated that liver cancer contains an LGR5^{+} compartment that has various hallmarks of TICs/CSCs, including an increased capacity for tumor organoid formation in culture and allograft formation in mice as well as resistance against conventional anti-cancer therapy. Functionally, these cells seem more important in tumor initiation, whereas the LGR5^{-} compartment appears to bear the proliferative burden. Simultaneously targeting both compartments as demonstrated in this study by 5-FU treatment in combination with DT-mediated ablation of the LGR5^{+} compartment was effective in combating experimental liver cancer. Thus, combining conventional therapy and LGR5^{+}-targeted therapy deserve to be further explored for the treatment of liver cancer in the clinic. Conceivably, this approach could be more effective for subset of patients with high levels of LGR5 expression, such as CTNNB1 mutated or alcohol-related HCC patients[25,26]. Although LGR5^{+}-targeting therapies are still largely in their infancy, the analogy with neuroendocrine tumors, which are successfully combated by radioactive somatostatin analogues (*e.g.* ^{177}Lu-Dotate) that target receptors with homology to LGR5[27], suggests that radioactive drugs (*e.g.* R-spondin) may be an option for treating liver cancer[28]. Our results, however, indicate that such therapy will be more effective when combined with particular conventional anti-cancer therapies.

Overexpression of LGR5 has been previously reported in patient HCC[17], and we confirmed that this is more pronounced in β-catenin mutated liver tumors. Although the elevation of LGR5 expression and potential association with clinical outcome have been observed in HCC patients, whether it can serve as an independent prognostic biomarker remains to be further investigated in specifically designed tumor marker prognostic studies in patients[29].

Of note, these early observations are based on mRNA expression, due to the lack of a reliable anti-LGR5 antibody. We now used transgenic mice in which LGR5-expressing cells co-express GFP and we can conditionally ablate these cells with the DT-DTR system[30]. This model allows for the identification and direct visualization of LGR5 expressing cells based on GFP expression, as well as isolation of LGR5-GFP$^+$ cells for further functional analyses and detailed characterization.

In intestinal adenomas, LGR5 marks 5-10% of the cells, which keep fueling the growth of established mouse adenomas[13]. We found that the percentages of LGR5-GFP$^+$ cells in murine liver tumors vary from 0.1% up to 55% (7.3 ± 1.8%, n = 55). Over 32% of the primary liver tumors harbor relatively high percentages (over 5%) (**Supplementary Fig. 2c**). In colon cancer, the percentage of LGR5 expressing cells has been reported to be associated with different background of the tumors, especially the accumulation of certain oncogenic mutations[8]. Thus, we speculate that the large variation of the abundance of LGR5 cells in liver tumors may also be related to different types of oncogenic mutations, although this hypothesis requires further investigation. Of note, DEN was used to induce primary liver cancer in this study and this compound is associated with the accumulation of liver β-catenin mutations[31]. Therefore, it is possible that our results are mainly relevant to liver cancers with deregulated Wnt/ß-catenin signaling and their importance requires future investigation in other mutational backgrounds (*e.g.* deregulated TSC/mTOR signaling)[32] as well.

Through a series of functional assays, in particular *in vitro* organoid initiation and *in vivo* tumor formation, we have demonstrated the importance of these LGR5 TICs in liver cancer. To define the potential for therapeutic targeting, we have performed LGR5 lineage ablation in organoids *in vitro* and in the tumor-bearing mouse model. Of note, the presence of LGR5 cells in tumors is likely dynamic. We observed large variations of their percentages among different primary liver tumors and allograft tumors generally contain lower numbers of LGR5 cells (less than 1%). In colorectal cancer, advanced stages compared to the early stages contain less LGR5 cells[33]. A speculative explanation could be that the tumors are derived from LGR5-positive stem cells, yet these cells are suppressed thereafter during tumor progression[33]. The dynamics could be essential for determining at which stage to target LGR5 TICs. When we performed LGR5 ablation in established tumors, we only observed a minor effect, probably due to a low percentage of LGR5 cells as well as their dispensable function at that stage, while depletion at the early stage yielded optimal anti-tumor effects. This result is in line with previous findings showing that LGR5 cells play distinct roles in primary and metastatic colon cancer[8].

Although we have demonstrated the feasibility and value of targeting LGR5 TICs in liver cancer, therapeutic ablation of these cells remains challenging. Resistance to conventional therapy is a common feature of CSCs[2]. We found that treatment with sorafenib or 5-FU enriches LGR5 cells, consistent with the findings in gastric[34] and colorectal cancer[35]. Different mechanisms may contribute to treatment resistance. Although LGR5 stem cells are generally fast-cycling in the intestine[36], the existence of

quiescent LGR5 cells have been reported in basal cell carcinoma, which mediate relapse after treatment[12]. Cell plasticity could be one of the potential mechanisms of treatment resistance. The loss of LGR5 stem cells in the intestine can be compensated by trans-differentiation from other stem cell pools[30], or through plasticity of their enterocyte-lineage daughters[37]. Cancer cell plasticity, shifting dynamically between a differentiated and a stemness state, has also been proposed as an important feature contributing to tumor progression, metastasis and therapeutic response[38]. We now have observed the induction of $LGR5^{+}$ from $LGR5^{-}$ liver cancer cells. This may implicates cell plasticity of LGR5 CSCs, but there could also be other mechanisms regulating the origin and expansion of LGR5 cells. Eventually, these LGR5 liver cancer cells may partially contribute to treatment resistance.

Currently, several innovative scenarios are being explored to therapeutically target CSCs, including antibody-drug conjugates[9], targeting quiescent CSCs[39] and inhibiting CSC-related pathways[2]. However, as discussed, different mechanisms could lead to treatment resistance[8]. Thus, combined therapies are likely necessary for this respect. With the intention to fully expand the stem cell pool, cetuximab has been used to first trigger the LGR5 population, followed by the ablation of these CSCs. This combined therapy has resulted in potent efficacy against colorectal cancer[10]. Similarly, we have observed that the combination of LGR5 lineage ablation with 5-FU chemotherapy can also lead to enhanced anti-liver cancer activity. However, combination of LGR5 lineage ablation with sorafenib did not yield enhanced anti-tumor activity. This is probably related to the mild effect of sorafenib in triggering the LGR5 CSC pool.

Lastly, a potential concern of such strategies is the possible harmful effects on normal LGR5 stem cells. In intestine, colon and skin, although LGR5 stem cells essentially contribute to tissue renewal at a daily basis[5,6], their loss can be compensated by trans-differentiation from other reserve stem cell pools[30,40] or through plasticity of their daughter cells[37]. Importantly, antibody conjugated drug targeting LGR5 CSCs in colon cancer has no major impact on the function of normal LGR5 stem cells[9]. In liver, LGR5 stem cells are absent during homeostasis, but only transiently activated upon injury likely without major contribution towards tissue repair[4,14]. Thus, we envision that our identification of targetable LGR5 TICs in liver cancer bears important implications for future therapeutic development.

Materials and Methods

Primary liver tumor model

Lgr5-DTR-GFP transgenic mice (kindly provided by Genentech) specifically co-express the diphtheria toxin (DT) receptor (DTR) and green florescent protein (GFP) under the control of the *Lgr5* promotor[30]. Thus, LGR5^{+} cells can be identified by GFP expression, and LGR5-GFP^{+} cells can be specifically depleted by DT administration. *Lgr5-DTR-GFP* transgenic mice (3-4 weeks) were administered with Diethylnitrosamine (DEN) by intraperitoneal injection (Sigma-Aldrich, i.p., 100 mg/kg) weekly for 6-17 weeks[41] . DEN is used to induce liver tumor in *Lgr5-DTR-GFP* transgenic mice and wild type mice, which could cause liver disease from basophilic foci, hyperplasic nodules, hepatocellular adenoma and finally lead to HCC[31,42,43]. Mice were sacrificed 3-16 months after the last DEN injection and livers/tumors were collected for further experiments (**Supplementary File. 1**: In total, 41 mice were monitored; 80.5%, 33 out of 41, mice formed liver tumors; the expression of LGR5 in each tumor/tumor surrounding tissues were also listed; **Supplementary Fig. 2g-h**). For each liver, biopsies were taken from the tumor and tumor surrounding tissue. If livers contain more than one tumors, individual tumors were collected and analyzed separately. For CCl_4 induced liver injury, *Lgr5-DTR-GFP* transgenic mice were weekly repeated administered with (6 or 17 weeks) intraperitoneal CCl_4 injection (10 µl/20 g body weight of 10% CCl_4 solution in corn oil or corn oil as control). All animal experiments were approved by the Committee on the Ethics of Animal Experiments of the Erasmus Medical Center.

HCC specimens and patient information

HCC specimens (paired tumor tissue and adjacent tumor free liver tissue) were collected from HCC patients undergoing tumor resection at the Erasmus Medical Center, The Netherlands. Samples were stored at -80℃ and then used for RNA extraction. 74 specimens were obtained from HCC patients and the corresponding clinica-pathological data are summarized in **Supplementary Table. 2**. HCC-specific survival was assessed in all patients and patients were stratified according to relative LGR5 expression (below and above median – 0.047). The Kaplan-Meier method was used to estimate survival outcome curves and the log-rank test was used to compare the survival between the two groups. The hazard ratio (HR) for HCC-specific survival was estimated using the Cox proportional hazards regression model. The study was approved by the medical ethical committee of Erasmus Medical Center. In addition, the study protocol conforms to the ethical guidelines of the 1975 Declaration of Helsinki.

Online database

For analysis of Lgr5 mRNA expression, data were retrieved from three independent HCC cohorts including The Cancer Genome Atlas (TCGA), Wurmbach[44], and Roessler[45]. For survival analysis based on Lgr5 mRNA expression, the TCGA cohort was used. For analysis of the relationship between gene mutation and Lgr5 expression, three independent cohorts were investigated, including TCGA, International Cancer Genome Consortium-France (LICA-FR) and International Cancer Genome Consortium-Japan (LIRI-JP).

Tumor organoid culture

Digestion solution II (37°C, 30 min, 500 µg/ml of collagenase type XI, 200 µg/ml of Dnase-1, 1% FBS in DMEM medium) (collagenase type XI: Sigma-Aldrich; Dnase-1: Sigma-Aldrich) was used to digest liver or tumor tissues into single cell suspension. Single cell suspension was directly mixed with matrigel (Corning BV) and then used for culturing, or sorted for further experiments. Sorted cells were also mixed

with matrigel and seeded for organoid initiation. Cells were cultured in organoid culture medium as previously described[4,14]. For the first 8-12 days, organoids were supplemented with 10 μM Y-27632 (Sigma-Aldrich), Noggin and Wnt3a conditioned medium. Medium was refreshed every 2 days and passage was performed in split ratios of 1:2-1:15 weekly. The proposed tumor organoid phenotypes is based on the expression of EpCAM/CK19 positive for CC-like and HNF4α/AFP positive for HCC-like phenotype.

Histology, immunohistochemistry and immunofluorescence

Liver or tumor was fixed in 4% paraformaldehyde (PFA) overnight at 4 °C. For immunofluorescence, samples were further dehydrated with 30% sucrose (Sigma-Aldrich, 4 °C, overnight), stored at -80 °C and then sectioned at 8 μm for further analysis. Images were acquired with a Zeiss LSM510META confocal microscope. For histology and immunohistochemistry, materials were dehydrated with 70% ethanol, embedded with paraffin, and sectioned at 4 μm for staining. Images were acquired with a Zeiss Axioskop 20 microscope. All antibodies are listed in **Supplementary Table. 3**.

Organoid-based allograft tumor model

Cold advanced DMEM/F12 medium was used to collect the organoids. After centrifuging, supernatant was discarded and organoid pellets (organoid fragmentation size: range from 5 ~ 150 μm) were mixed directly with matrigel in a ratio of 1:1 with a total volume of 200 μl. 4-6 weeks old female NOD.Cg-PrkdcSCIDIl2rgtm1Wjl/SzJ (NSG) mice, NOG/JicTac (CIEA NOD.Cg-Prkdc-scid Il2rg-tm1Sug) mice or nude mice (NMRI:BomTac-Nude) were purchased from Taconic, and subcutaneously injected with the collected tumor organoids. The characterization of phenotypes for murine allograft tumor is based on the expression of EpCAM/CK19 for CC-like and HNF4α/AFP for HCC-like phenotype (**Supplementary File 2**). Tumor dimensions were measured using calipers and tumor volume was calculated as 0.523 × length × width × width[9]. Tumor formation was monitored every other day and mice were sacrificed to harvest tumors after the tumor diameter reached approximately 2 cm. Tumor tissues were stored or cultured as described above.

Cell ablation by diphtheria toxin and treatment of 5-FU/sorafenib

To ablate $LGR5^+$ cells in organoids, DT (Calbiochem, 1-10 ng/ml) was added to organoid expansion/initiation medium, followed by further analysis[14]. For *in vivo* ablation, DT was administrated via intraperitoneal injection every other day (50 μg per kg body weight). If mice suffering from weight loss ≥ 10%, compared to the previous injection, the injection was omitted. 5-FU/sorafenib were also administrated via intraperitoneal injection every other day (5-FU/sorafenib: 30 mg per kg body weight) (sorafenib: Bio-Connect BV; 5-FU: Sigma-Aldrich).

qRT–PCR

For freshly FACS-sorted cells and HCC specimens, RNeasy Micro Kit (QIAGEN) was used to isolate RNA. For organoids, Machery-NucleoSpin RNA II kit (Bioké) was used. Quantification was measured with Nanodrop ND-1000 (Wilmington). RNA was then converted to cDNA by using a cDNA Synthesis kit (TAKARA BIO INC.). Real-time PCR reactions were performed with SYBRGreen-based real-time PCR (Applied Biosystems®) and amplified in a thermal cycler (GeneAmp PCR System 9700). For cells collected from murine tissues, glyceraldehyde 3-phosphate dehydrogenase (*Gapdh*) gene was used as reference. For quantification of LGR5 mRNA in human tumors and tumor-free liver tissues, *Gusb* (Beta-

glucuronidases), *Hprt1* (hypoxanthine phosphoribosyltransferase 1) and *Pmm1* (phosphomannomutase 1) were used as reference genes. All primers are listed in **Supplementary Table. 4**.

RNA sequencing

Total RNA was isolated using RNeasy Micro Kit (QIAGEN). The quantity of RNA was measured by a NanoDrop 2000. The collected RNA was further amplified by using SMARTer kit. Then, RNA sequencing was performed by Novogene with the paired-end 150bp (PE 150) sequencing strategy. Gene expression was analyzed. The identification of differentially expressed genes is based on $P < 0.05$ and absolute values of logFc > 1.5. GSEA with the library of Wiki2019 was performed to reveal the alteration of signaling pathways.

FACS analysis

For FACS analysis, single cells derived from liver tumors/tumor surrounding tissues or organoids were suspended in DMEM plus 2% FBS. Cell suspensions were analyzed using a BD FACSCalibur or BD FACSAria™ II. For FACS sorting, a BD FACSAria™ II cell sorter was used to isolate the target cell population. Propidium iodide (PI) staining was performed to exclude dead cells and CD45 staining was adopted for excluding leucocytes.

Metabolic activity analysis of organoids

Different organoid lines were seeded separately in a 24/48-well plate. sorafenib (10 μM) or 5-FU (10 μM) was added to the organoid culture since the initial day or post-initiation day 3, respectively. Drugs were refreshed every other day. At the day 6-7, organoids were incubated with Alamar Blue (Invitrogen, 1:20 in DMEM) for four hours (37 °C), and then medium was collected for analysis of the metabolic activity of the cells. Absorbance was determined by using fluorescence plate reader (CytoFluor® Series 4000, Perseptive Biosystems) at the excitation of 530/25 nm and emission of 590/35. Each treatment condition was repeated for four times and matrigel with medium only was used as blank control.

Statistical analysis.

Prism software (GraphPad Software) was used for all statistical analysis. For statistical significance of the differences between the means of groups, we used Mann-Whitney U-test; For statistical significance of the differences between groups with inequivalent sample sizes, we used Welch test (indicated in the legends); For statistical significance of the differences between paired samples, we used Paired T-test (indicated in the legends); For statistical significance of the differences between multiple independent groups, we used two-way ANOVA. Differences were considered significant at a *P* value less than 0.05.

References

1. Clevers, H. The cancer stem cell: premises, promises and challenges. Nat. Med. 17, 313–319 (2011).

2. Batlle, E. & Clevers, H. Cancer stem cells revisited. Nat. Med. 23, 1124–1134 (2017).

3. Ebben, J. D. et al. The cancer stem cell paradigm: a new understanding of tumor development and treatment. Expert Opin. Ther. Targets 14, 621–632 (2010).

4. Huch, M. et al. In vitro expansion of single Lgr5+ liver stem cells induced by Wnt-driven regeneration. Nature 494, 247–250 (2013).

5. Barker, N. et al. Identification of stem cells in small intestine and colon by marker gene Lgr5. Nature 449, 1003–1007 (2007).

6. Haegebarth, A. & Clevers, H. Wnt signaling, lgr5, and stem cells in the intestine and skin. Am. J. Pathol. 174, 715–721 (2009).

7. Barker, N. et al. Crypt stem cells as the cells-of-origin of intestinal cancer. Nature 457, 608–611 (2009).

8. de Sousa e Melo, F. et al. A distinct role for Lgr5+ stem cells in primary and metastatic colon cancer. Nature 543, 676–680 (2017).

9. Junttila, M. R. et al. Targeting LGR5+ cells with an antibody-drug conjugate for the treatment of colon cancer. Sci. Transl. Med. 7, 314ra186 (2015).

10. Shimokawa, M. et al. Visualization and targeting of LGR5+ human colon cancer stem cells. Nature 545, 187–192 (2017).

11. Yanai, H. et al. Intestinal cancer stem cells marked by Bmi1 or Lgr5 expression contribute to tumor propagation via clonal expansion. Sci. Rep. 7, 41838 (2017).

12. Sanchez-Danes, A. et al. A slow-cycling LGR5 tumour population mediates basal cell carcinoma relapse after therapy. Nature 562, 434–438 (2018).

13. Schepers, A. G. et al. Lineage tracing reveals Lgr5+ stem cell activity in mouse intestinal adenomas. Science 337, 730–735 (2012).

14. Cao, W. et al. Dynamics of proliferative and quiescent stem cells in liver homeostasis and injury. Gastroenterology 153, 1133–1147 (2017).

15. Bosch, F. X., Ribes, J., Diaz, M. & Cleries, R. Primary liver cancer: worldwide incidence and trends. Gastroenterology 127, S5–S16 (2004).

16. Yamashita, T. & Wang, X. W. Cancer stem cells in the development of liver cancer. J. Clin. Invest. 123, 1911–1918 (2013).

17. Yamamoto, Y. et al. Overexpression of orphan G-protein-coupled receptor, Gpr49, in human hepatocellular carcinomas with beta-catenin mutations. Hepatology 37, 528–533 (2003).

18. Broutier, L. et al. Human primary liver cancer-derived organoid cultures for disease modeling and drug screening. Nat. Med. 23, 1424 (2017).

19. Drost, J. & Clevers, H. Organoids in cancer research. Nat. Rev. Cancer 18, 407–418 (2018).

20. Nuciforo, S. et al. Organoid models of human liver cancers derived from tumor needle biopsies. Cell Rep. 24, 1363–1376 (2018).

21. Cao, W. et al. Modeling liver cancer and therapy responsiveness using organoids derived from primary mouse liver tumors. Carcinogenesis 40, 145–154 (2019).

22. Boumahdi, S. et al. SOX2 controls tumour initiation and cancer stem-cell functions in squamous-cell carcinoma. Nature 511, 246–250 (2014).

23. Nwabo Kamdje, A. H. et al. Developmental pathways associated with cancer metastasis: Notch, Wnt, and Hedgehog. Cancer Biol. Med. 14, 109–120 (2017).

24. Nussinov, R., Tsai, C. J. & Jang, H. A new view of pathway-driven drug resistance in tumor proliferation. Trends Pharm. Sci. 38, 427–437 (2017).

25. Boyault, S. et al. Transcriptome classification of HCC is related to gene alterations and to new therapeutic targets. Hepatology 45, 42–52 (2007).

26. Zucman-Rossi, J., Villanueva, A., Nault, J. C. & Llovet, J. M. Genetic landscape and biomarkers of hepatocellular carcinoma. Gastroenterology 149, 1226–1239 e1224 (2015).

27. Strosberg, J. et al. Phase 3 trial of (177)Lu-Dotatate for midgut neuroendocrine tumors. N. Engl. J. Med. 376, 125–135 (2017).

28. Koo, B. K. et al. Tumour suppressor RNF43 is a stem-cell E3 ligase that induces endocytosis of Wnt receptors. Nature 488, 665–669 (2012).

29. Sauerbrei, W., Taube, S. E., McShane, L. M., Cavenagh, M. M. & Altman, D. G. Reporting recommendations for tumor marker prognostic studies (REMARK): an abridged explanation and elaboration. J. Natl Cancer Inst. 110, 803–811 (2018).

30. Tian, H. et al. A reserve stem cell population in small intestine renders Lgr5- positive cells dispensable. Nature 478, 255–259 (2011).

31. Connor, F. et al. Mutational landscape of a chemically-induced mouse model of liver cancer. J. Hepatol. 69, 840–850 (2018).

32. van Veelen, W., Korsse, S. E., van de Laar, L. & Peppelenbosch, M. P. The long and winding road to rational treatment of cancer associated with LKB1/ AMPK/TSC/mTORC1 signaling. Oncogene 30, 2289–2303 (2011).

33. Zhou, X. et al. R-Spondin1/LGR5 activates TGFbeta signaling and suppresses colon cancer metastasis. Cancer Res. 77, 6589–6602 (2017).

34. Xi, H. Q. et al. Increased expression of Lgr5 is associated with chemotherapy resistance in human gastric cancer. Oncol. Rep. 32, 181–188 (2014).

35. Osawa, H. et al. Full-length LGR5-positive cells have chemoresistant characteristics in colorectal cancer. Br. J. Cancer 114, 1251–1260 (2016).

36. Basak, O. et al. Mapping early fate determination in Lgr5+ crypt stem cells using a novel Ki67-RFP allele. EMBO J. 33, 2057–2068 (2014).

37. Tetteh, P. W. et al. Replacement of lost Lgr5-positive stem cells through plasticity of their enterocyte-lineage daughters. Cell Stem Cell 18, 203–213 (2016).

38. da Silva-Diz, V., Lorenzo-Sanz, L., Bernat-Peguera, A., Lopez-Cerda, M. & Munoz, P. Cancer cell plasticity: impact on tumor progression and therapy response. Semin Cancer Biol. 53, 48–58 (2018). 39. Pascual, G. et al. Targeting metastasis-initiating cells through the fatty acid receptor CD36. Nature 541, 41–45 (2017).

40. Buczacki, S. J. et al. Intestinal label-retaining cells are secretory precursors expressing Lgr5. Nature 495, 65–69 (2013).

41. Tolba, R., Kraus, T., Liedtke, C., Schwarz, M. & Weiskirchen, R. Diethylnitrosamine (DEN)-induced carcinogenic liver injury in mice. Lab Anim. 49, 59–69 (2015).

42. Brown, Z. J., Heinrich, B. & Greten, T. F. Mouse models of hepatocellular carcinoma: an overview and highlights for immunotherapy research. Nat. Rev. Gastroenterol. Hepatol. 15, 536–554 (2018).

43. Dow, M. et al. Integrative genomic analysis of mouse and human hepatocellular carcinoma. Proc. Natl Acad. Sci. USA 115, E9879–E9888 (2018).

44. Wurmbach, E. et al. Genome-wide molecular profiles of HCV-induced dysplasia and hepatocellular carcinoma. Hepatology 45, 938–947 (2007).

45. Roessler, S. et al. A unique metastasis gene signature enables prediction of tumor relapse in early-stage hepatocellular carcinoma patients. Cancer Res. 70, 10202–10212 (2010).

Supplementary Information for:

LGR5 marks targetable tumor-initiating cells in mouse liver cancer

Table of contents

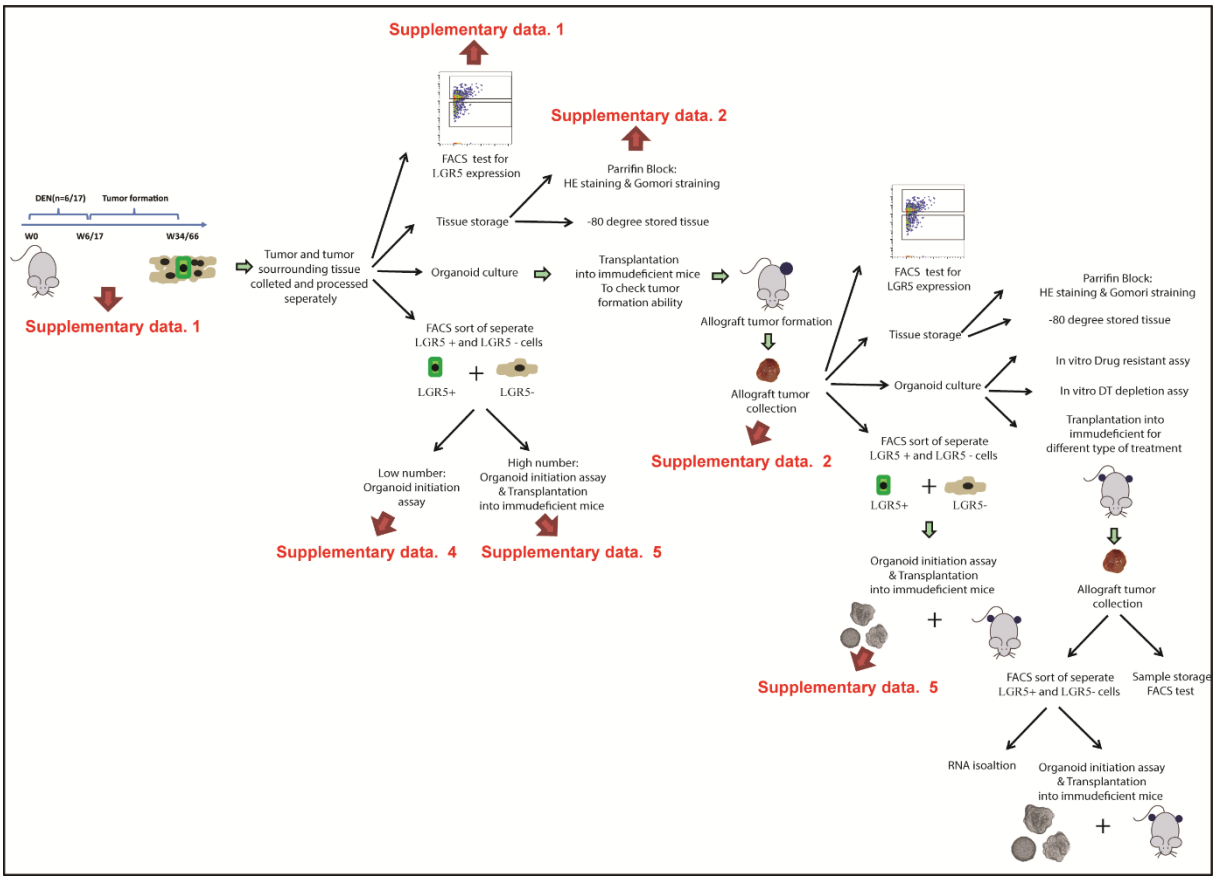

Supplementary Figure 1 | General flowchart of the experimental design.

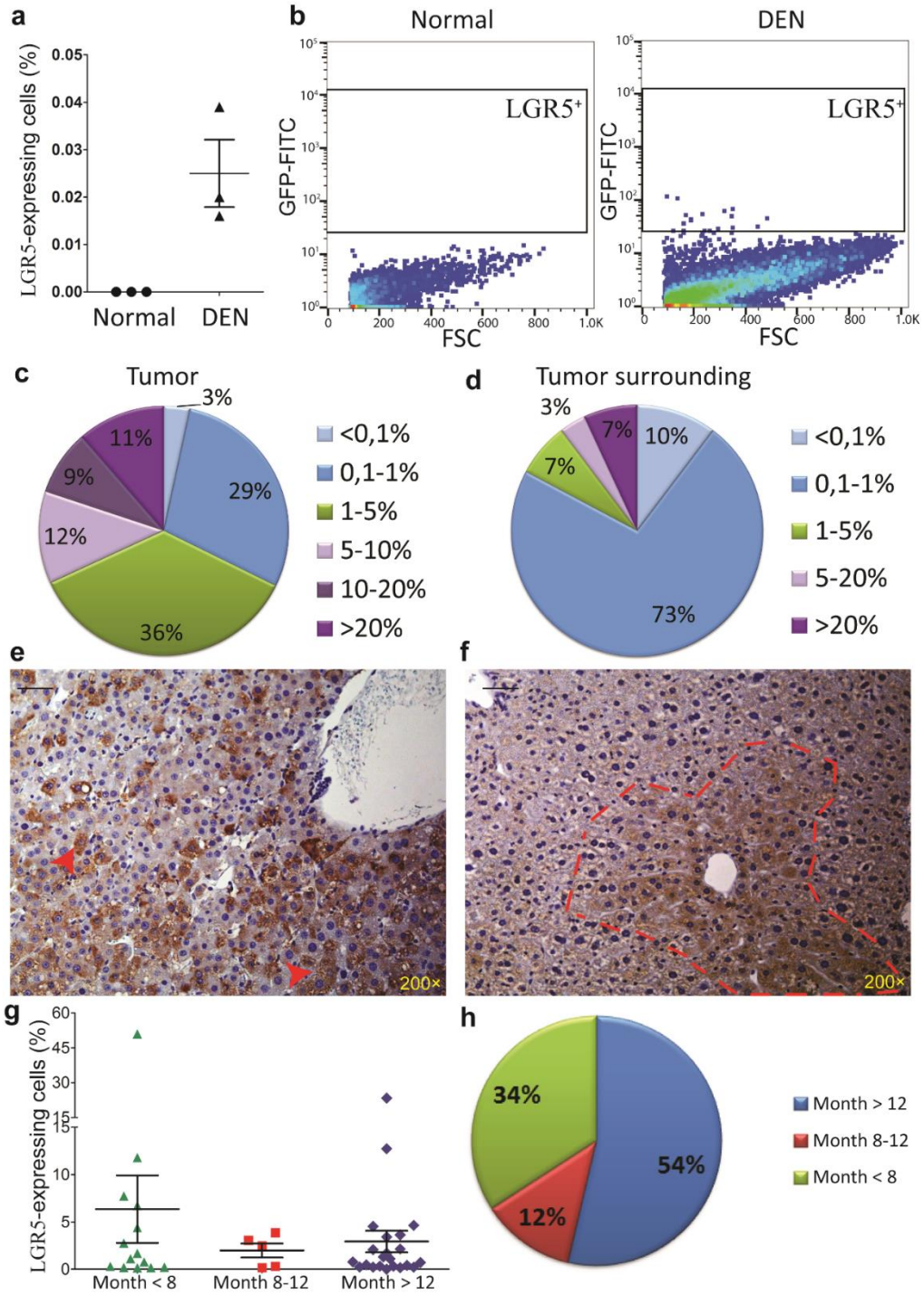

Supplementary Figure 2 | LGR5 expressing cells are present in the DEN-induced primary liver tumor. a, LGR5⁺ cells are present in the liver upon DEN administration (Post DEN induction day 7). **b**, Representative FACS plots showing that LGR5⁺ cells are present in the liver following DEN administration (Post DEN induction day 7). **c**, Relative LGR5⁺ fraction in DEN-induced liver tumors. **d**, Relative LGR5⁺ fraction in tissue bordering the DEN-induced liver tumors (denominated as surrounding). **e-f**, Representative immunohistochemistry pictures showing the microscopic aspect of the LGR5⁺ cells in liver cancer. Two types of LGR5⁺ cell distribution patterns are apparent, scattered LGR5⁺ cell distribution (**e**) and LGR5⁺ island-like clusters (**f**). The pictures show an anti-GFP immunohistochemistry staining in which LGR5⁺ cells are brown and nuclei are blue. Scale bar = 50µm**. g,** The percentage of LGR5-expressing cells within each tissue, grouped by tumor collection month (the month is counted since the first administration of DEN). Mean ± SEM. (**h**) Relative mice number fraction in all DEN-induced mice, grouped by tumor collection month. Source data are provided as a Source Data file.

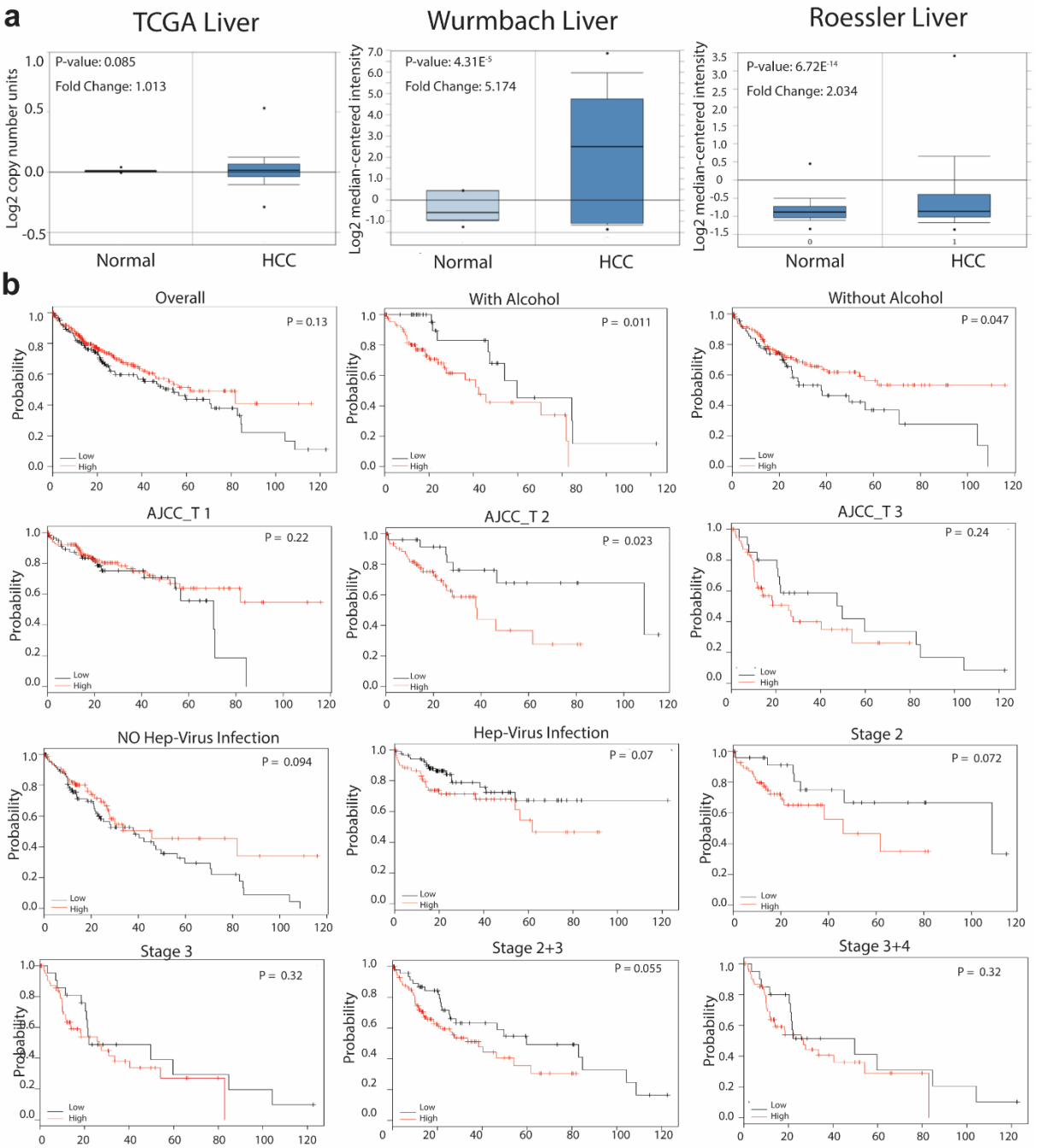

Supplementary Figure 3 | *LGR5* expression in HCC tissues and relation to patient outcome. a, The upregulated expression of *LGR5* in HCC tissues compared with normal tissues from TCGA Liver cohort (Normal vs. HCC: *n* = 115 vs. *n* = 97, *P* = 0.085, Fold change: 1.013), Wurmbach liver cohort (Normal vs. HCC: *n* = 10 vs. *n* = 35, *P* = 4.31E^{-5}, Fold change: 5.174) and Roessler liver cohort (Normal vs. HCC: *n* = 200 vs. *n* = 225, *P* = 6.72E-14, Fold change: 2.034). **b**, Kaplan-Meier curve for HCC of patients based on different etiology/tumor stage of HCC from TCGA Liver cohort. AJCC_T: American Joint Committee on Cancer (AJCC) tumor staging system; Stage: Barcelona Clinic Liver Cancer (BCLC) tumor staging system. Source data are provided as a Source Data file.

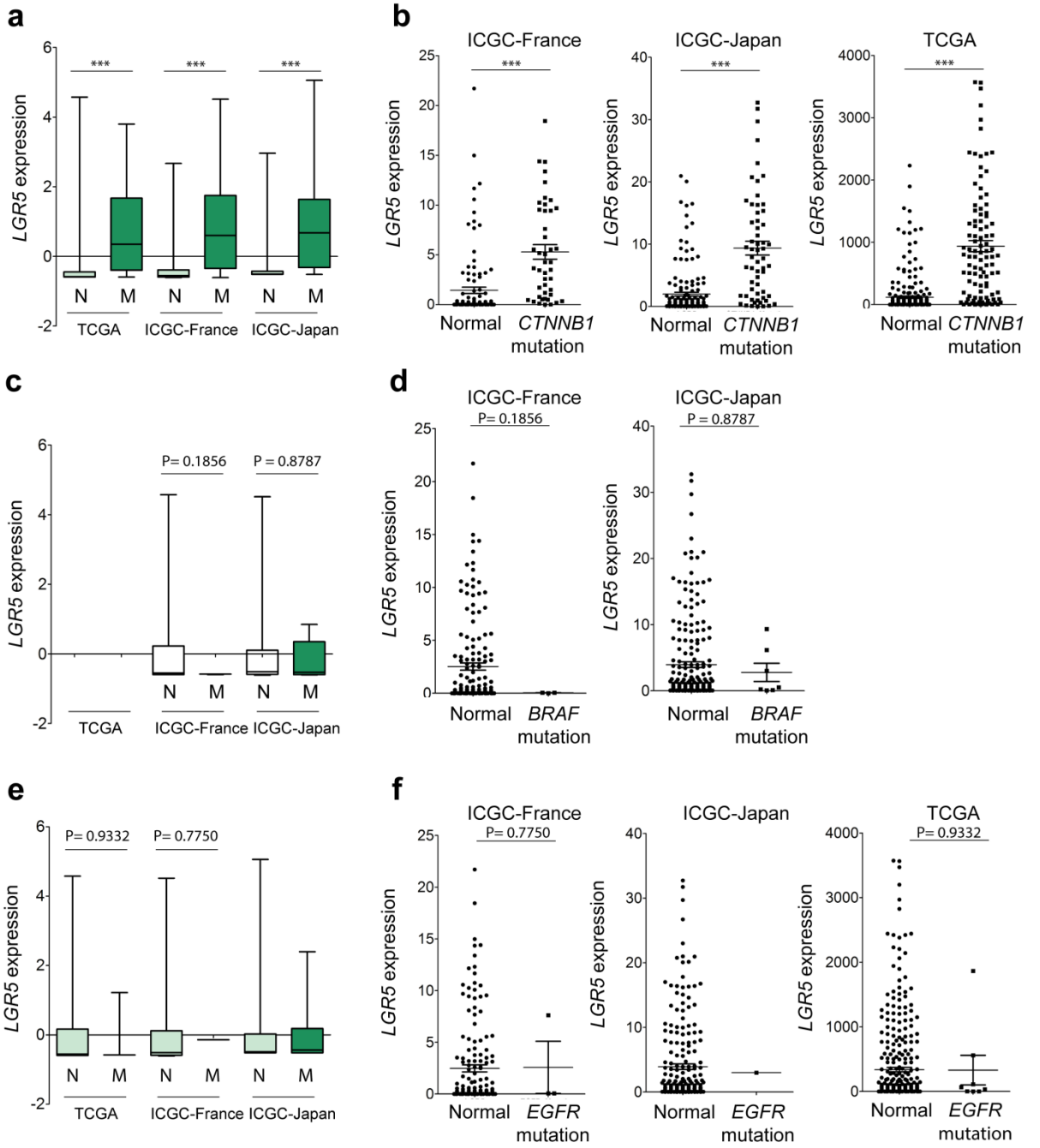

Supplementary Figure 4 | The expression level of *LGR5* is upregulated in *Ctnnb1* mutated HCC tumors. a-b, Upregulation of *LGR5* expression in *Ctnnb1* mutated compared to non-*Ctnnb1* mutated patient HCC tumors, in ICGC-France, ICGC-Japan and TCGA cohort. **c-d,** No significant difference of *LGR5* expression in *Braf* mutated compared to non-*Braf* mutated HCC tumors, in ICGC-France and ICGC-Japan cohort**. e-f,** No significant difference of *LGR5* expression in *Egfr* mutated compared to non-*Egfr* mutated HCC tumors, in ICGC-France, ICGC-Japan and TCGA cohort. Mean ± SEM. Source data are provided as a Source Data file.

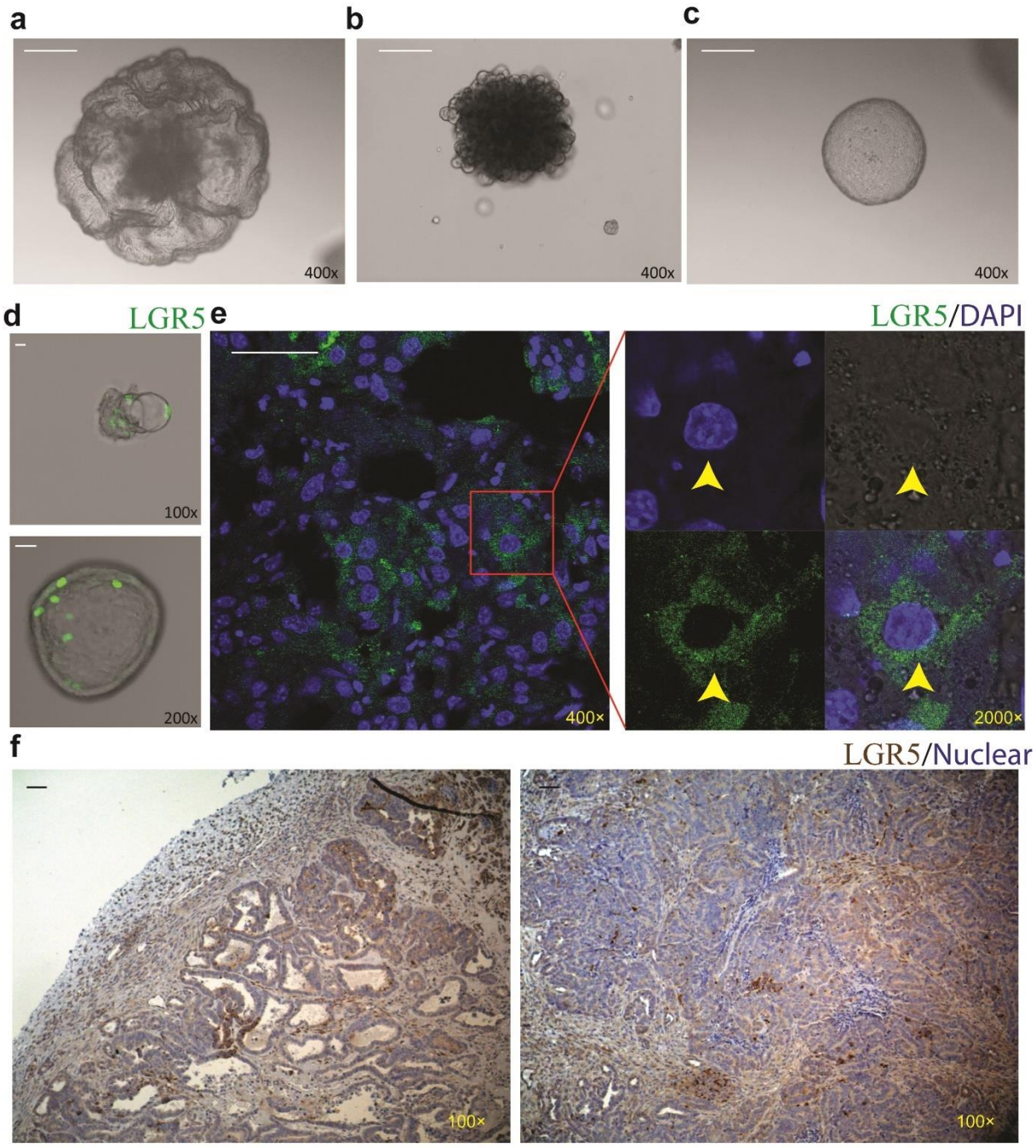

Supplementary Figure 5 | Allograft liver tumors maintain an LGR5⁺ compartment. a-c, 3-7 days after initiation of allograft tumor-derived cultures, small organoids were observed and subsequently passage was performed every 4-7 days, employing splitting ratios ranging from 1:4 to 1:10 as appropriate. Representative pictures show the different morphologies of the tumor organoids obtained, which include but also flower-like, irregular sheet-like structures (**a**), and grape-like, condensed phenotypes (**b**), and. relative normal hollow sphere-like aspects (**c**). **d**, Representative confocal pictures showing the maintenance of an LGR5⁺ compartment in tumor organoids (LGR5-driven GFP: green). **e**, Representative immunofluorescent pictures showing an LGR5⁺ compartment in allograft tumors (*LGR5*-driven GFP: green; DAPI: blue). **f**, Representative immunohistochemistry pictures showing expression of *LGR5* promotor-driven GFP in allograft tumors (anti-GFP immunohistochemistry: brown; nuclei: blue). Scale bar = 50µm.

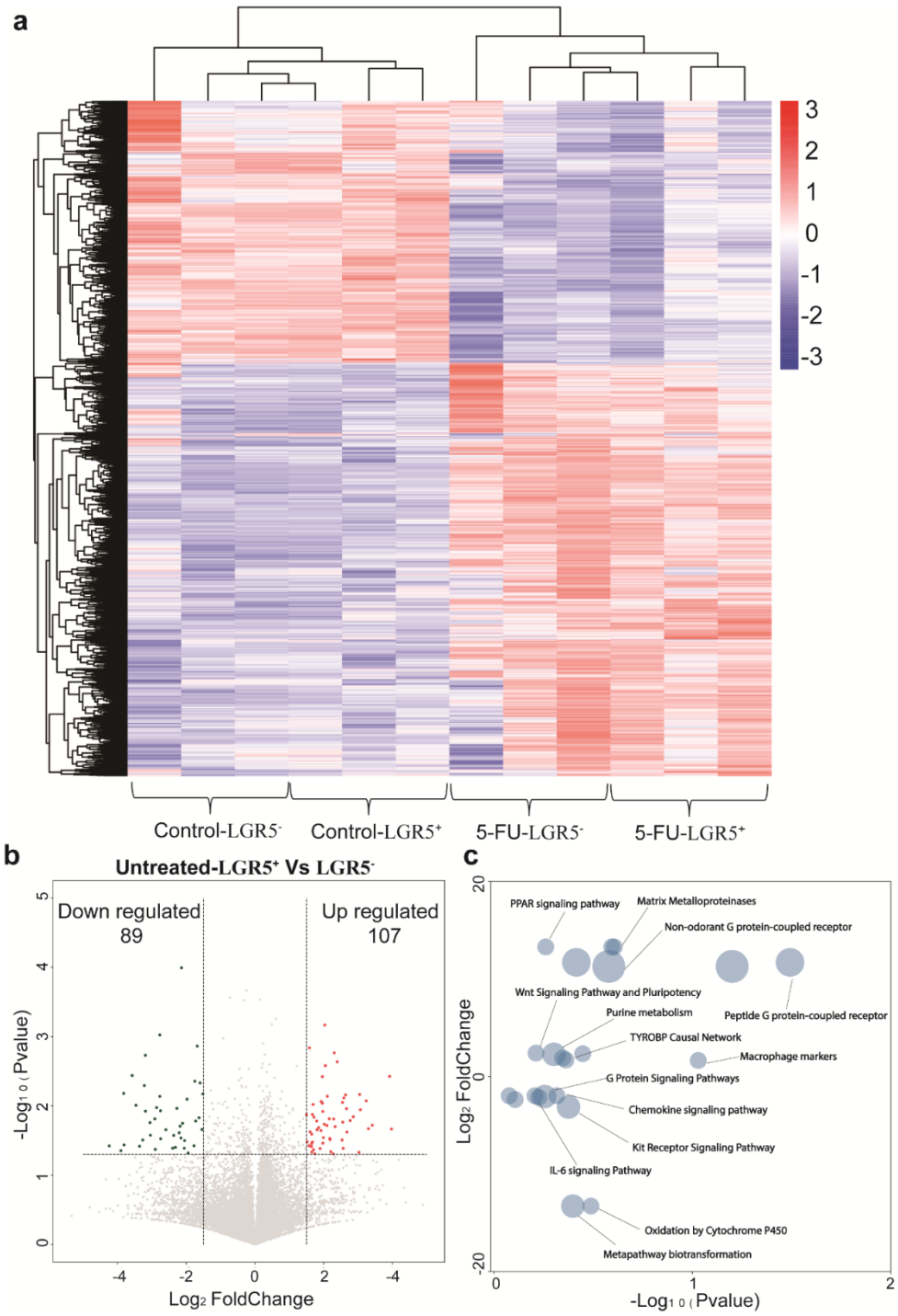

Supplementary Figure 6 | Genome-wide transcriptomic analysis of LGR5$^+$ and LGR5$^-$ cells by RNA-Seq. a, Hierarchical clustering showed a separation of all four different groups (Untreated LGR5$^+$ cells, Untreated LGR5$^-$ cells, 5-FU-treated LGR5$^+$ cells, 5-FU-treated LGR5$^-$ cells). **b**, A Volcano plot showing the most significantly differentially expressed genes between untreated LGR5$^+$ and LGR5$^-$ cells. **c**, GSEA with the library of Wiki2019 was performed to reveal the alteration of signaling pathways between untreated LGR5$^+$ and LGR5$^-$ cells. Source data are provided as a Source Data file.

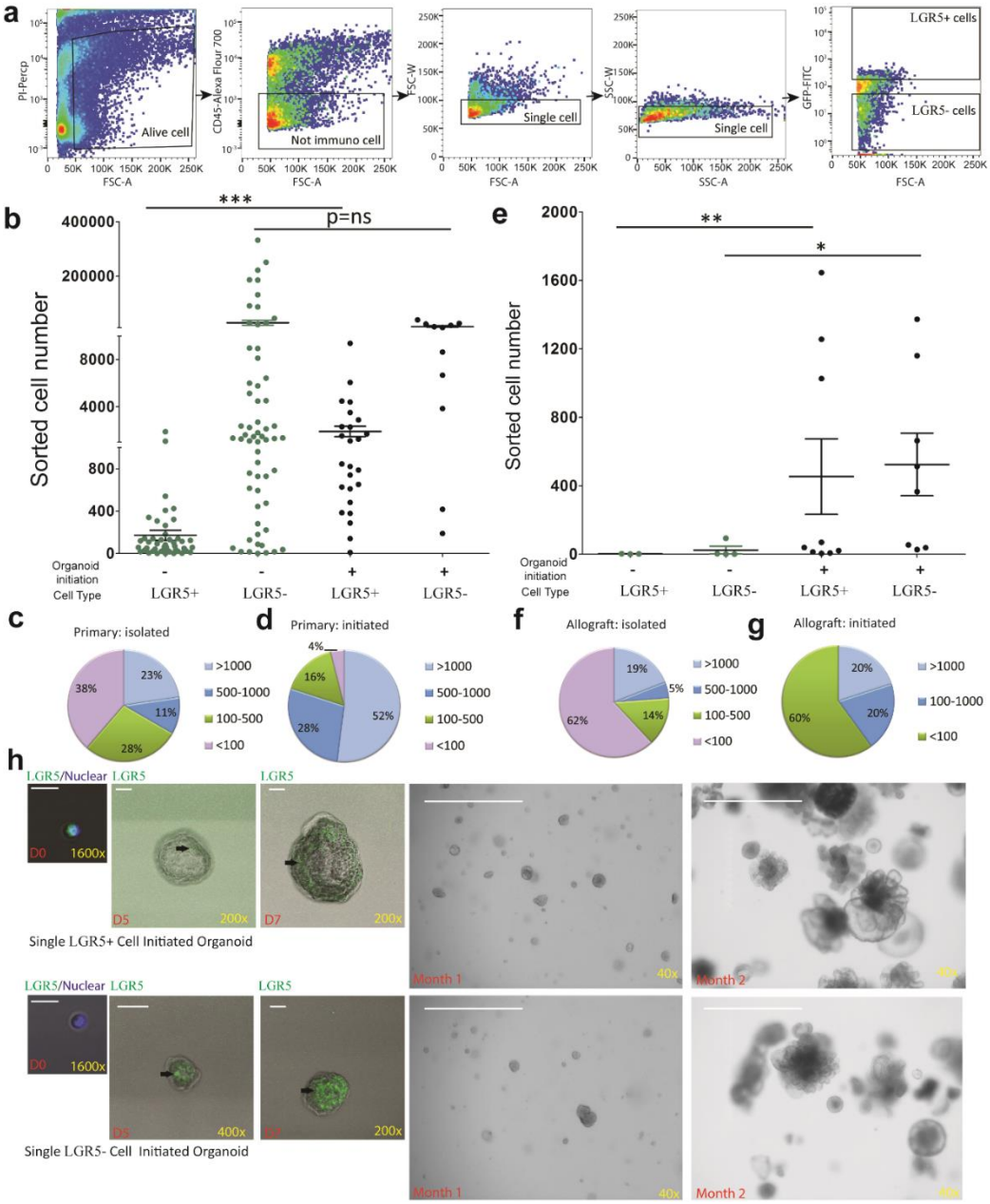

Supplementary Figure 7 | LGR5⁺ cells have stronger organoid initiation ability. a, The FACS test/sort strategy for isolating LGR5-GFP⁺ and LGR5-GFP⁻ cells obtained from liver/allograft tumors/organoids. **b**, The numbers of sorted LGR5-GFP⁺ and LGR5-GFP⁻ cells yielding successful (black dots) or failure of organoid initiation (green dots), employing material obtained from DEN-induced murine livers (LGR5⁺-non-initiation vs. LGR5⁻-non-initiation vs. LGR5⁺-initiation vs. LGR5⁻-initiation: 171.4 ± 47.1, n = 46 vs. 28350 ± 8914, n = 60 vs. 1906 ± 441.6, n = 25 vs. 13860 ± 3654, n = 11, Mean ± SEM). c, The distribution showing the percentage of the number of LGR5⁺ cells which were isolated from primary liver tumors. d, The cell number distribution for the sorted LGR5⁺ cells which can initiate organoid, from primary tumors. e, The exact sorted numbers for LGR5⁺ cells and LGR5⁻ cells , for organoid initiated (black dots) and non-organoid initiated (green dots), from allograft tumors (LGR5⁺-non-initiated vs. LGR5⁻-non-initiated vs. LGR5⁺-initiated vs. LGR5⁻-initiated: 2.0 ± 0.6, n = 3 vs. 24.3 ± 22.9, n = 4 vs. 453.7 ± 220.3, n = 9 vs. 524.3 ± 182.9, n = 8). **f**, Frequency distribution of the relative number of LGR5⁺ cells obtained from allograft liver tumors. **g**, Frequency distribution of the number of LGR5⁺ cells that display successful organoid initiation from material obtained from allograft tumors. **h**, Representative pictures tracing organoids initiation and growth from LGR5⁺ or LGR5⁻ cells. Black arrow: LGR5 expressing cells. Day0/5/7: Scale bar = 50μm; Month1/2: Scale bar = 1000μm. Source data are provided as a Source Data file.

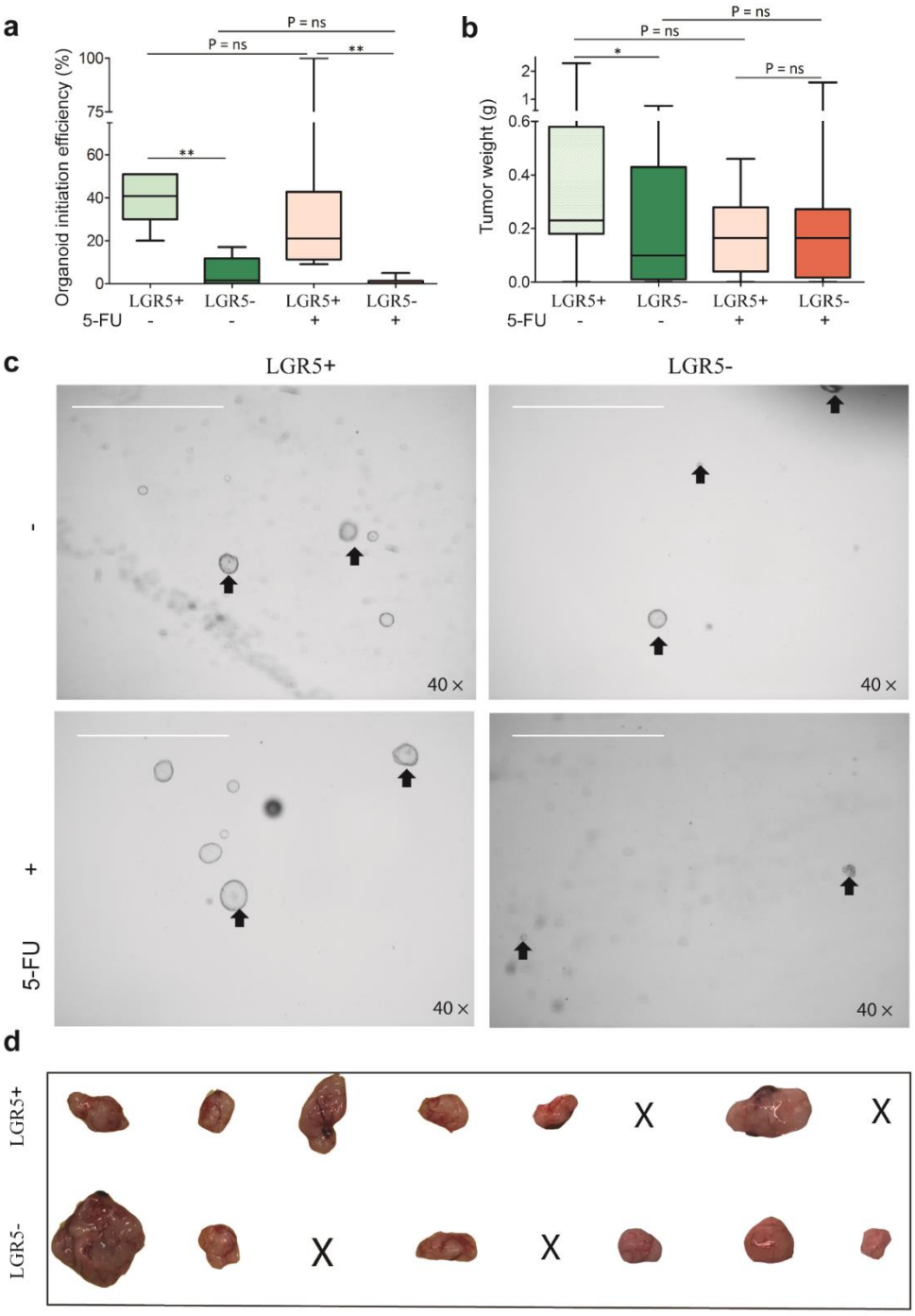

Supplementary Figure 8 | LGR5⁺ cells from 5-FU treated tumors can initiate organoid and tumor. **a,** The organoid initiation ability of untreated LGR5⁺ cells (39.5 ± 4.8 %, *n* = 6, Mean ± SEM), untreated LGR5⁻ cells (5.0 ± 2.9 %, *n* = 6), 5-FU-treated LGR5⁺ cells (31.2 ± 14.0 %, *n* = 6) and 5-FU-treated LGR5⁻ cells (0.8 ± 0.8 %, *n* = 6). **b,** The tumor initiation ability of untreated LGR5⁺ cells (0.50 ± 0.15 g, *n* = 15), untreated LGR5⁻ cells (0.21 ± 0.06 g, *n* = 15), 5-FU-treated LGR5⁺ cells (0.18 ± 0.05 g, *n* = 8) and 5-FU-treated LGR5⁻ cells (0.31 ± 0.19 g, *n* = 8). **c**, Representative picture showing the organoid initiation ability of above four groups. Black arrow: initiated organoids. Scale bar = 1000μm. **d**, Pictures showing 5-FU-treated LGR5⁺ cells and 5-FU-treated LGR5⁻ cells initiated tumors. Source data are provided as a Source Data file.

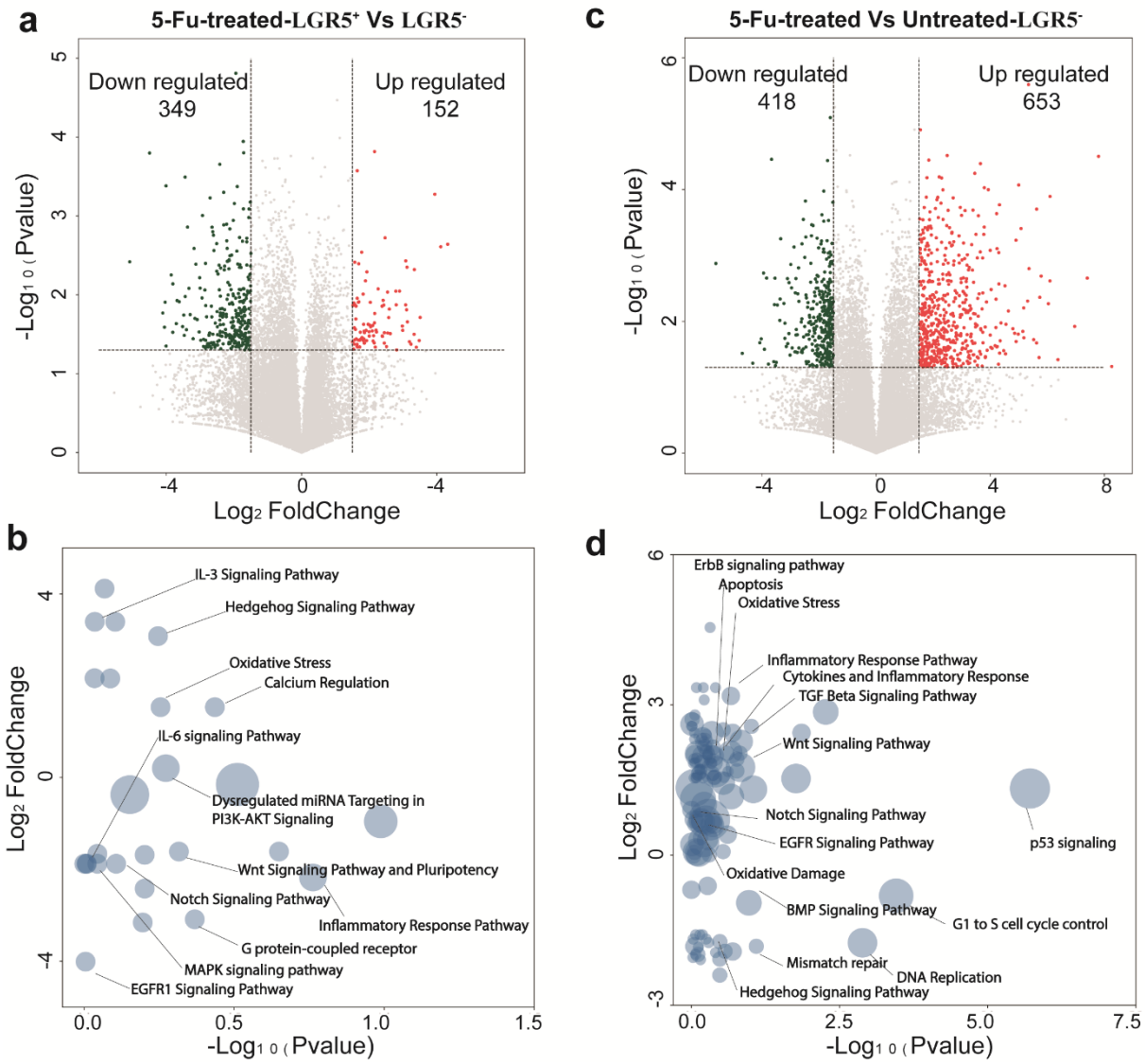

Supplementary Figure 9 | Genome-wide transcriptomic analysis of 5-FU treatment on LGR5$^{+/-}$ cells. a, A Volcano plot showing the most significantly differentially expressed genes between 5-FU treated LGR5^{+} cell/LGR5^{-} cells. **b**, Gene enrichment analysis (Wiki2019) of the differentially expressed genes between 5-FU treated LGR5^{+} cell/LGR5^{-} cells. **c**, A Volcano plot showing the most significantly differentially expressed genes between 5-FU treated/untreated LGR5^{-} cells. **d**, Gene enrichment analysis (Wiki2019) of the differentially expressed genes between 5-FU treated/untreated LGR5^{-} cells. Source data are provided as a Source Data file.

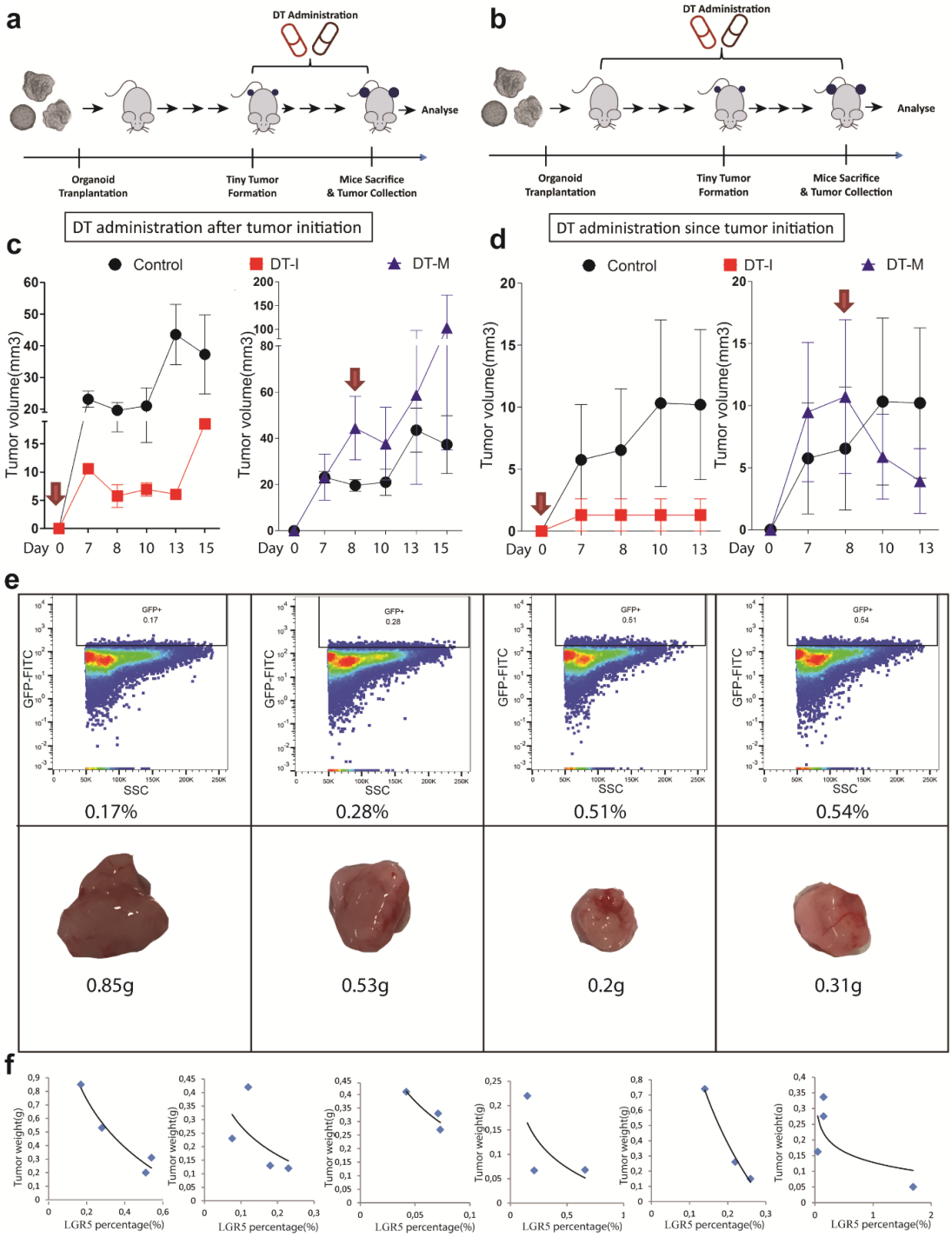

Supplementary Figure 10 | Targeting LGR5 impedes the tumor growth. a-b, Outline of the experimental strategies used to test the effect of DT administration during tumor growth (**a**) and at tumor initiation (**b**). **c-d**, Growth curves showing the effects of DT administration during the entire experimental period (Left, DT-I) and following DT intervention during tumor growth (Right, DT-M) for organoid strain 1 (**c**) and strain 2 (**d**). Mean ± SEM. Red arrow: onset of DT administration (n = 4 for each time point). **e**, Representative FACS pictures (upper channel, with LGR5-GFP$^+$ expression) and tumor pictures (lower channel, with tumor weights) showing that the same tumor strains, collected from a single mouse, shows variable LGR5 expression. **f**, tumors collected from six individual mice (transplanted with same strain and same amount of organoid; collected on the same day, non-treated tumors) showing that smaller tumors have relatively higher LGR5 expression. Source data are provided as a Source Data file.

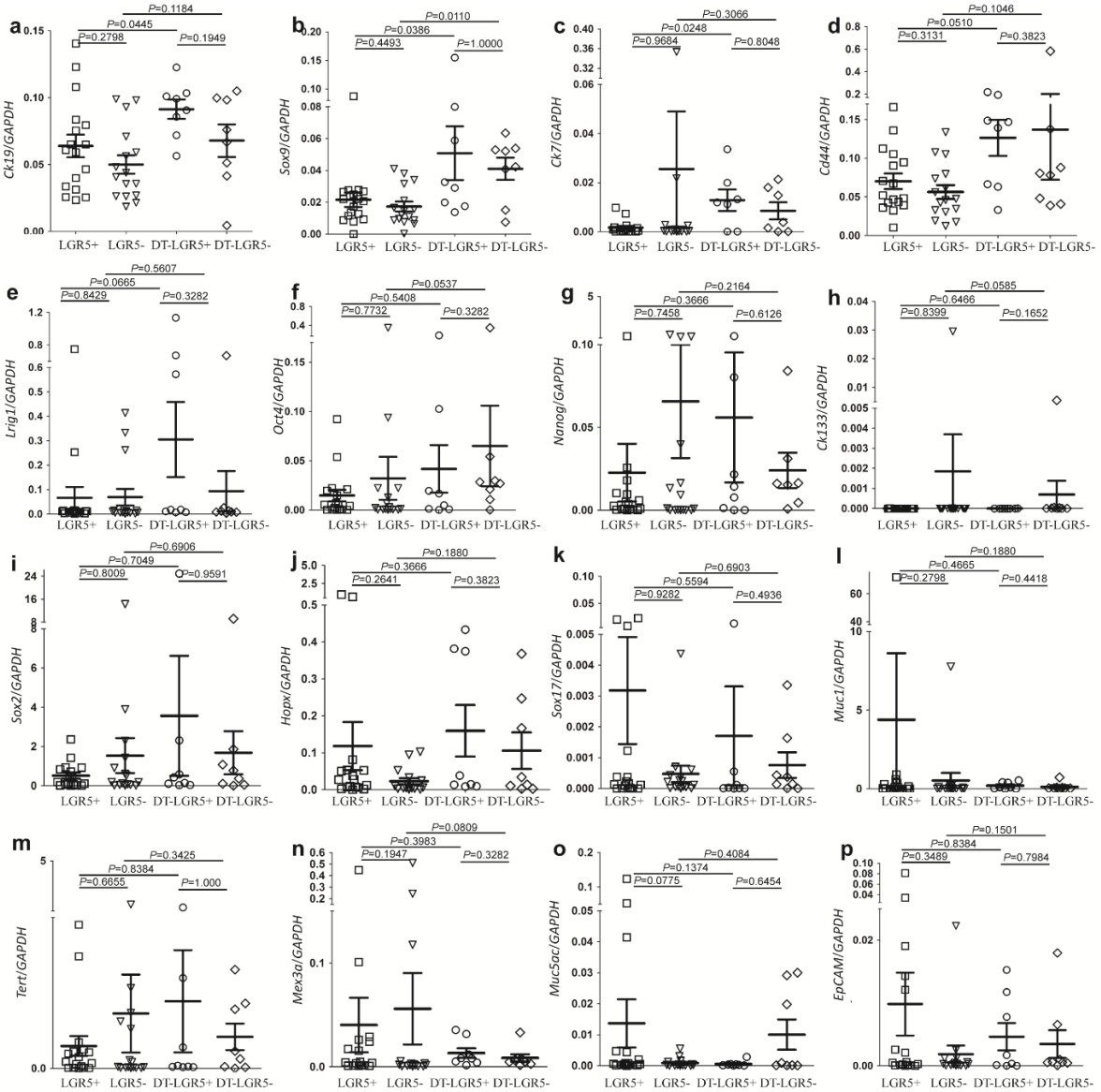

Supplementary Figure 11 | The expression profile of untreated/DT-treated LGR5^{+} and LGR5^{-} cells. **a-p,** The expression of stem cell/tumor stem cell markers in LGR5^{+}/LGR5^{-} and DT treated tumor isolated LGR5^{+}/LGR5^{-} cells was analyzed using qRT-PCR and related to a reference gene. Mean ± SEM. Source data are provided as a Source Data file.

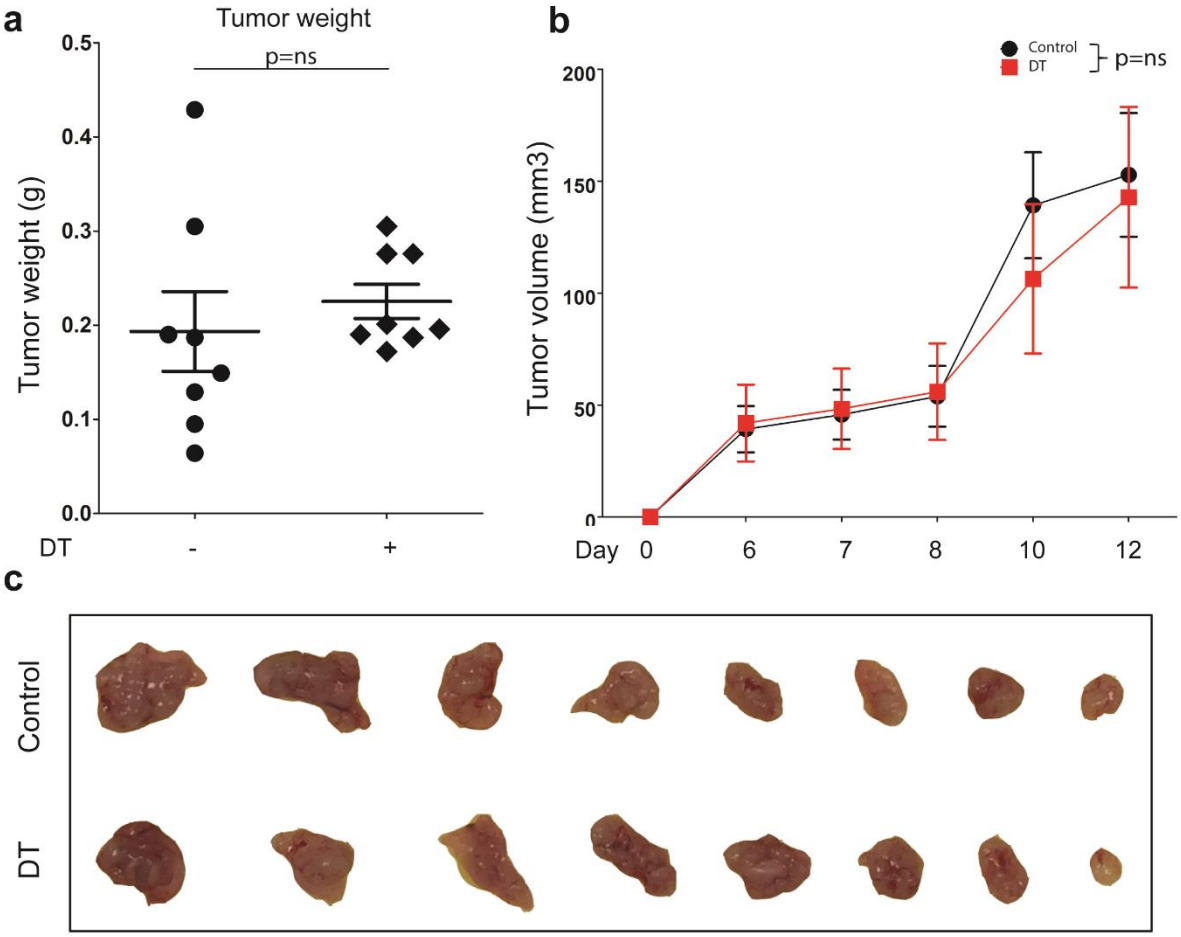

Supplementary Figure 12 | Wide type tumor organoids do not respond to DT administration. a, The weight of tumors initiated by wild type organoids from control, the DT-treated group following sacrifice of the animals involved (Control vs. DT: 0.19 ± 0.042 g vs. 0.23 ± 0.018 g, *n* = 8, *P* = ns, Mean ± SEM). **b,** Representative growth curve showing tumor volume in the control group and the DT-treated group (*n* = 4). **c,** Representative pictures showing the tumors from the control group and DT administrated group. Source data are provided as a Source Data file.

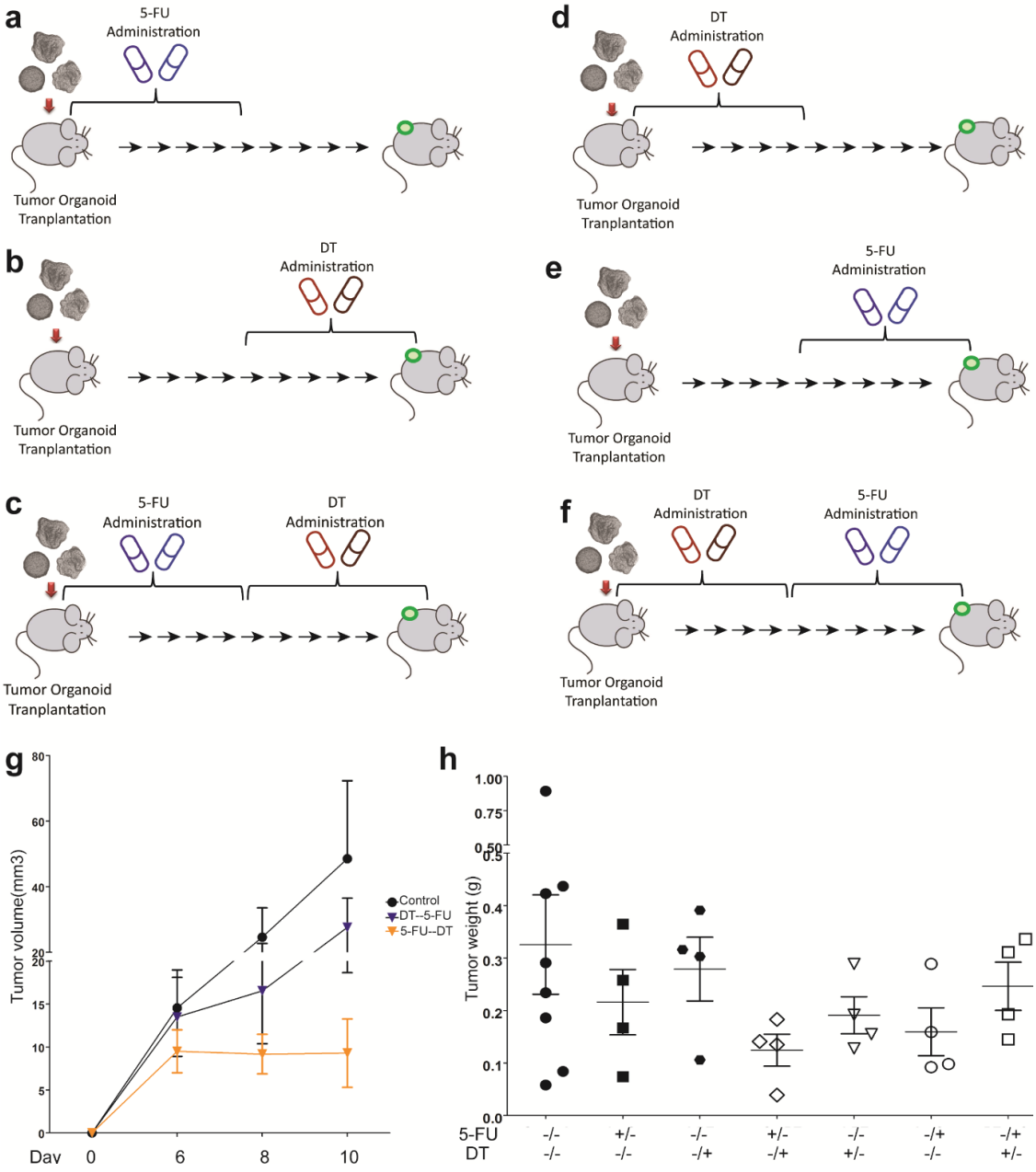

Supplementary Figure 13 | Effects of combining DT treatment with conventional anti-cancer therapy. a, 5-FU control: 5-FU was administrated during the first half of the experiment period and tumor volume was assessed continuously. **b**, DT control: animals were treated with DT during the second half of the experiment period and tumor volume was assessed continuously. **c**, Combination strategy 1: 5-FU was administrated during the first half and DT was treated during the second half of the experiment period. Tumor volume was assessed continuously. (**a** and **b** are the relevant control groups for **c**). **d**, DT control: DT was administrated during the first half of the experiment period and tumor volume was assessed continuously. **e**, 5-FU control: 5-FU was administrated during the second half of the experiment period and tumor volume was assessed continuously. **f**, Combination strategy 2: First DT was applied (first half of the experiment) followed by 5-FU treatment (second half of the experiment) (**d** and **e** are the relevant control groups for **f**). **g**, Representative growth curve showing tumor volumes of the control, Combination strategy 1 (5-FU--DT) and Combination strategy 2 (DT--5-FU) group (n = 4). **h**, Weight of tumors from the different groups described above at the end of the experiment. +/-: Treatment was administrated for the first half of the experiment; -/+: Treatment was administrated for the second half of the experiment; -/-: No treatment. Mean ± SEM. Source data are provided as a Source Data file.

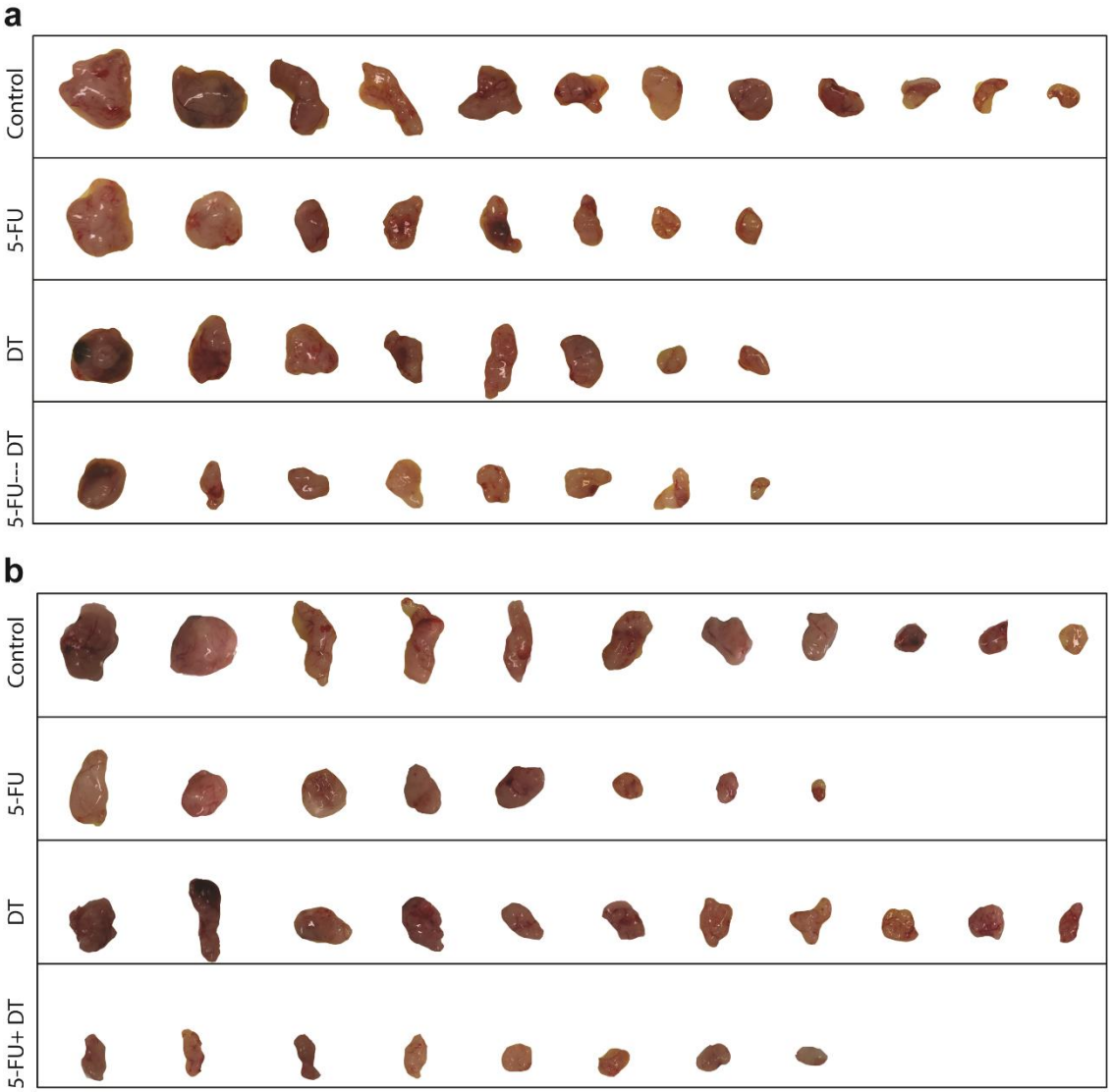

Supplementary Figure 14 | Combination of LGR5 lineage ablation with conventional therapy. a-b, Pictures showing the tumors from the different groups.

Supplementary Table 1 | Allograft tumor

Allograft Tumor						
Initiated Tumor Code	Isolated Cell Popualtion	Original Strain	Injected Cell Number	Initiated Tumor Weight(g)	Tumor Formation Time	Immunodeficient mice type
1	LGR5+	SAL1	72	0.58	23	Nude mice
	LGR5-		72	0.27	23	Nude mice
2	LGR5+	SAL1	57	0.44	23	Nude mice
	LGR5-		57	0.01	23	Nude mice
3	LGR5+	SAL1	90	0.14	23	Nude mice
	LGR5-		90	0.11	23	Nude mice
4	LGR5+	SAL1	167	0.22	23	Nude mice
	LGR5-		167	0.08	23	Nude mice
5	LGR5+	AL43	66	2.28	38	Nude mice
	LGR5-		66	0.45	38	Nude mice
6	LGR5+	AL43	53	1.11	38	NSG
	LGR5-		53	0.43	38	NSG
7	LGR5+	AL43	57	0.51	38	NSG
	LGR5-		57	0.77	38	NSG
8	LGR5+	SAL2	237	0.8	26	Nude mice
	LGR5-		237	0.05	26	Nude mice
9	LGR5+	SAL2	699	0.23	26	Nude mice
	LGR5-		699	0.1	26	Nude mice
10	LGR5+	SAL1	182	0.53	26	Nude mice
	LGR5-		182	0.09	26	Nude mice
11	LGR5+	SAL1	127	0.18	26	Nude mice
	LGR5-		127	0.61	26	Nude mice

Supplementary Table 2 | Clinical-pathological data of Erasmus cohort

Table. Patient characteristics	
Characteristic	**HCC patients (n=74)**
Age at surgery (years)	
Mean ± SD	60 ± 15,9
Median (range)	63 (11-82)
Sex – no. (%)	
Male	45 (60,8)
Female	29 (39,2)
Race – no. (%)	
White	61 (82,4)
African	6 (8,1)
Asian	6 (8,1)
Not reported	1 (1,4)
Etiology – no. (%)	
No known liver disease	21 (28,4)
Alcohol	16 (21,6)
Hepatitis B	9 (12,2)
NASH	8 (10,8)
Hepatitis C + Alcohol	6 (8,1)
Hepatitis B + Alc/HepC/NASH	5 (6,8)
Hepatitis C	5 (6,8)
Fibrolamellar HCC	3 (4,1)
Hemochromatosis + NASH	1 (1,4)
Hepatitis status – no. (%)	
Hepatitis B or C positive	25 (33,8)
Chronic Hepatitis B	14 (18,9)
Chronic Hepatitis C	12 (16,2)

Cirrhosis – no. (%)	
Yes	21 (28,4)
No	53 (71,6)
Tumor differentiation – no. (%)	
Good	8 (10,8)
Moderate	40 (54,1)
Poor	14 (18,9)
Unknown	12 (16,2)
Vascular invasion – no. (%)	
Yes	29 (39,2)
No	38 (51,4)
Unknown	7 (9,5)
Number of lesions – no. (%)	
1	40 (54,1)
>1	34 (45,9)
Size of largest lesion (cm)	
Mean ± SD	7,7 ± 5,6
Median (range)	6,1 (1-24)
AFP level before resection (ug/l)	
Mean ± SD	6661,1 ± 407289,4
Median (range)	8 (1-3118700)

Supplementary Table 3 | Antibody

Antibody	Antibody clone/ reference	Raised	Origin
CD45	56-0451-82	Mouse	eBioscience
AFP	SAB3500533-100UG	Goat	Sigma
HNF4a	ab41898	Mouse	Abcam
EpCAM	ab71916	Rabbit	Abcam
Cytokeratin 19	ab52625	Rabbit	Abcam
GFP	A-11122	Rabbit	Invitrogen/Life Technologies
Alexa Fluor® 488 AffiniPure Donkey Anti-Goat IgG (H+L)	705-545-147	Donkey	Bio-Connect
Donkey anti-Rabbit IgG (H+L) Secondary Antibody, Alexa Fluor® 594 conjugate	R37119	Donkey	Thermo fisher
Donkey anti-mouse IgG (H+L) Secondary Antibody, Alexa Fluor® 594 conjugate	R37115	Donkey	Thermo fisher

Supplementary Table 4 | Primer

Gene name	Gene Symbo	Sequence	
Leucine-rich repeat-containing G-protein coupled receptor 5	Mouse-*Lgr5*	Fw	CTG ACT TTG AAT GGT GCC TCG
		Re	ATG TCC ACT ACC GCG ATT AC
Cytokeratin-19	Mouse-*Krt19*	Fw	GTG AAG ATC CGC GAC TGG T
		Re	AGG CGA GCA TTG TC AAT CTG
Transcription factor SOX-9	Mouse-*Sox9*	Fw	CGA CTA CGC TGA CCA TCA GA
		Re	GAC TGG TTG TTC CCA GTG CT
CD133	Mouse-*Prom1*	Fw	TCT GTT CAG CAT TTC CTC AC
		Re	TCA GTA TCG AGA CGG GTC
CD44	Mouse-*CD44*	Fw	CGT CCA ACA CCT CCC ACT AT
		Re	AGC CGC TGC TGA CAT CGT
Keratin, type II cytoskeletal 7	Mouse-*Ck7*	Fw	ATC CGC GAG ATC ACC ATC
		Re	ATG TGT CTG AGA TCT GCG ACT
Leucine-rich repeats and immunoglobulin-like domains protein 1	Mouse-*Lrig1*	Fw	AAGGGAACTCAACTTGGCGAG
		Re	ACGTGAGGCCTTCAATCAGC
Octamer-binding transcription factor 4	Mouse-*Oct4*	Fw	CTGTAGGGAGGGCTTCGGGCAC TT
		Re	CTGAGGGCCAGGCAGGAGCAC GAG
Homeobox protein NANOG	Mouse-*Nanog*	Fw	AGGGTCTGCTACTGAGATGCTC TG
		Re	CAACCACTGGTTTTTCTGCCACC G
SRY (sex determining region Y)-box 2	Mouse-*Sox2*	Fw	GGCAGCTACAGCATGATGCAGG AGC
		Re	CTGGTCATGGAGTTGTACTGCA GG

Homeodomain-only protein	Mouse-*Hopx*	Fw	CATCCTTAGTCAGACGCGCA
		Re	AGGCAAGCCTTCTGACCGC
Telomerase reverse transcriptase	Mouse-*Tert*	Fw	GCAGGTGAACAGCCTCCAGACAG
		Re	TCCTAACACGCTGGTCAAAGGGAAGC
RNA-binding protein MEX3A	Mouse-*Mex3a*	Fw	ACACCACGGAGTGCGTTC
		Re	GTTGGTTTTGGCCCTCAGA
Mucin 5AC	Mouse-*Muc5ac*	Fw	GGACCAAGTGGTTTGACACTGAC
		Re	CCTCATAGTTGAGGCACATCCCAG
Epithelial cell adhesion molecule	Mouse-*Epcam*	Fw	CGCAGCTCAGGAAGAATGTG
		Re	TGAAGTACACTGGCATTGACG
SRY-box 17	Mouse-*Sox17*	Fw	GGCGCAGCAGAATCCAGA
		Re	CCACGACTTGCCCAGCAT
Cell surface associated or polymorphic epithelial mucin	Mouse-*Muc1*	Fw	CCCCAGTTGTCTGTTGGGGTC
		Re	GGATTCTACCACCACGGAGCC
Glyceraldehyde 3-phosphate dehydrogenase	Mouse-*Gapdh*	Fw	TCACCACCATGGAGAAGGC
		Re	GCTAAGCAGTTGGTGGTGCA
Beta-glucuronidases	Human-*GUSB*	Fw	CAGGTGATGGAAGAAGTGG
		Re	GTTGCTCACAAGGTCACAG
Hypoxanthine phosphoribosyltransferase 1	Human-*HPRT1*	Fw	GCTATAAATTCTTTGCTGACCTGCTG
		Re	AATTACTTTTATGTCCCCTGTTGACTGG
Phosphomannomutase 1	Human-*PMM1*	Fw	CGAGTTCTCCGAACTGGAC
		Re	CTGTTTTCAGGGCTTCCAC
Leucine-rich repeat-containing G-protein coupled receptor 5	Human-*LGR5*	Fw	TCAGTCAGCTGCTCCCGAAT
		Re	CGTTTCCCGCAAGACGTAAC

Supplementary Note:

Description for Supplementary Data

[1] Supplementary Data 1

Content:

The detailed information for *Lgr5-DTRGFP* mice which used to induce liver cancer, including:

1)The mice code

2)The mice background

3)Primary Code: The corresponding code of initiated primary organoid strain. Black mark: the tissue did not initiate an organoid strain or the strain was already lost due to infection in the following culture.

4)Post Den Time (Month): The sacrifice time after the induction of DEN.

5)DEN Administration (Week): Time passed between administration of DEN and sacrifice.

6)Tissue Type: S: tumor surrounding tissue; T: tumor tissue. S—T: initially marked with tumor surrounding tissue and then characterized as tumor.

7)Percentage of LGR5-expressing cells (%): The percentage of LGR5-expressing cells within each tissue.

8)Allograft Strains: The strain code which initiated allograft tumor in the immunodeficient mice.

Remarks: In total, 41 mice were monitored. 10 (mice code: 8,12,17,18,21,22,29,31,35,41) out of 41 mice liver did not show obvious tumor formation. After the following characterization, 2 (mice code: 8, 22) out of 10 were proven to be liver tumor.

Mouse Code	Mice Backgroud	Primary Code	Post Den Time (Month)	DEN Administration (Week)	Tissue Type	Percentage of LGR5-expressing cells (%)	Allograft Strains
M1	B6	PT1	7	6	S	0,28	
		PT2			T	0,16	
M2	B6	PT3	7	6	S	0,79	
		PT4			T	1,1	
M3	B6	PT5	12	6	S	0,16	
		PT6			T	0,18	
M4	B6	PT7	9	6	S	0,57	
		PT8			T1	5,66	AL8
		PT9			T2	0,32	
		PT10			T3	5,61	AL10
M5	B6	PT11	9	6	S	0,22	

		PT12			T	2,5	
M6	B6&C3H	PT13	5	17	S	0	AL13
		PT14			T	2,75	
M7	B6	PT15	13	6	S	0,4	
		PT16			T	2,07	
M8	B6	PT17	13	6	S--T	0,31	AL17
M9	B6	PT18	12	6	S	1,1	
		PT19			T	3,05	
M10	B6	PT20	15	6	S	0,85	
		PT21			T1	2,85	
		PT22			T2	1,43	
M11	B6	PT23	15	6	S	0,89	
		PT24			T	0,17	
Mouse Code	Mice backgroud	Primary code	Post Den time	DEN		Lgr5 expression	Allograft strains
M12	B6&C3H	PT25	3	11	S	0,18	
M13	B6	PT26	10	17	S	0,062	
		PT27			T	0,3	
M14	B6	PT28	13	6	S	0,33	
		PT29			T1	0,47	
		PT30			T2	2,15	
M15	B6	PT31	13	6	S	0	
		PT32			T1	0,45	
		PT33			T2	0,5	
M16	B6	PT34	13	6	S	0,12	
		PT35			T	1,71	

M17	B6	PT36	13	6	S	0,72	
M18	B6	PT37	13	6	S	0,24	
M19	B6	PT38	13	6	S	3,41	AL38
		PT39			T	1,11	
M20	B6	PT40	16	6	S	0,15	
		PT41			T	0,22	
M21	B6	PT42	14	6	S	0,33	
M22	B6&C3H	PT43	7	17	S--T	0,77	AL43
M23	B6&C3H	PT44	7	17	S	3,08	
		PT45			T1	3,29	
		PT46			T2	0,05	AL46
Mouse Code	Mice backgroud	Primary code	Post Den time	DEN		Lgr5 expression	Allograft strains
M24	B6&C3H	PT47	7	17	S	25	
		PT48			T1	46,1	
		PT49			T2	55,6	
		PT50			T3	51,2	
M25	B6	PT51	14	6	T	4,63	
M26	B6	PT52	14	6	S	0,021	
		PT53			T	0	
M27	B6&C3H	PT54	7	17	T	7,73	
M28	B6	PT55	8	17	S	20,3	
		PT56			T1	10,7	
		PT57			T2	1,67	
		PT58			T3	0,48	
		PT59			T4	4,66	

M29	B6	PT60	15	6	S	0,4	
M30	B6&C3H	PT61	8	17	T1	2,62	AL61
		PT62			T2	7,01	AL62
		PT63			T3	10,5	
M31	B6&C3H	PT64	8	17	S	0,3	
M32	B6	PT65	15	6	S	20,3	
		PT66			T1	1,04	
		PT67			T2	8,03	
M33	B6	PT68	15	6	T1	47,9	
		PT69			T2	17,4	
		PT70			T3	4,69	
Mouse Code	Mice backgroud	Primary code	Post Den time	DEN		Lgr5 expression	Allograft strains
M34	B6	PT71	15	6	S	17,4	
		PT72			T1	3,86	
		PT73			T2	21,6	
M35	B6	PT74	15	6	S	0,22	
M36	B6	PT75	15	6	S	0,25	
		PT76			T	3,41	
M37	B6	PT77	15	6	T1	1,41	
		PT78			T2	0,23	
		PT79			T3	0,65	
M38	B6&C3H	PT80	8	17	S	0,26	
		PT81			T	0,14	
M39	B6	PT82	13	6	T1	0,29	
		PT83			T2	5,13	

		PT84			T3	0,18	AL84
		PT85			T4	8.90	AL85
M40	B6&C3H	PT86	7	17	T1	14,6	
		PT87			T2	6,82	
		PT88			T3	13,9	
M41	B6&C3H	PT89	8	17	S	0,21	

Group Code	Group	Tissue Number	Lgr5 Expression
A	The collected mice liver tissue	89	5.583%
B	The mice liver which did not initiate tumor	8	0.325%
C	Tumor surrounding tissue	34	2.930%
D	Tumor tissue	55	7.294%

[2] Supplementary Data 2

Content:

The H&E/Gomori/EpCAM/AFP/CK19/GFP staining of primary/allograft tissues for all the allograft strains.

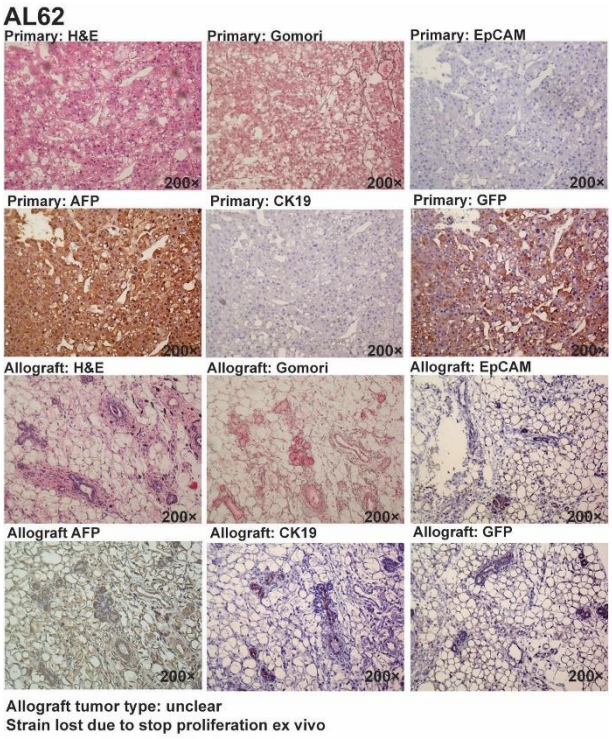

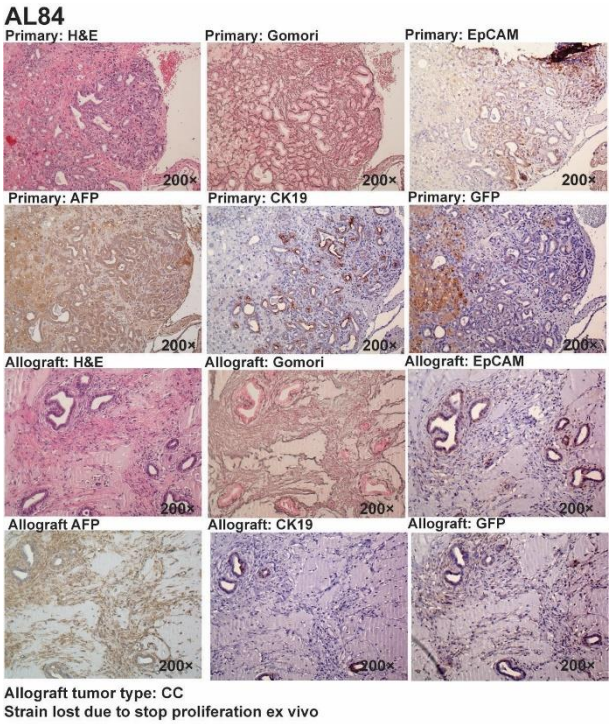

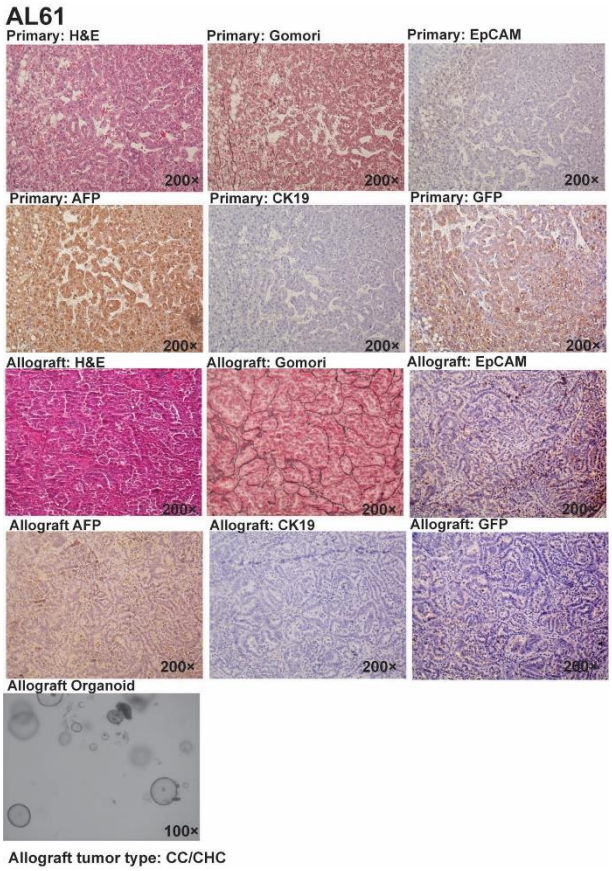

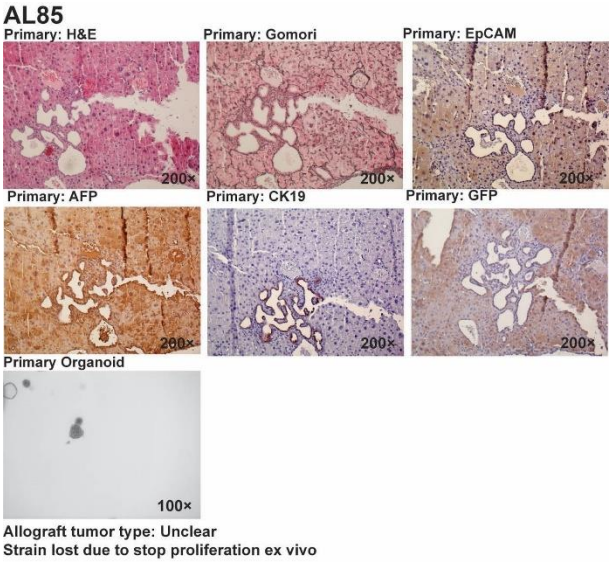

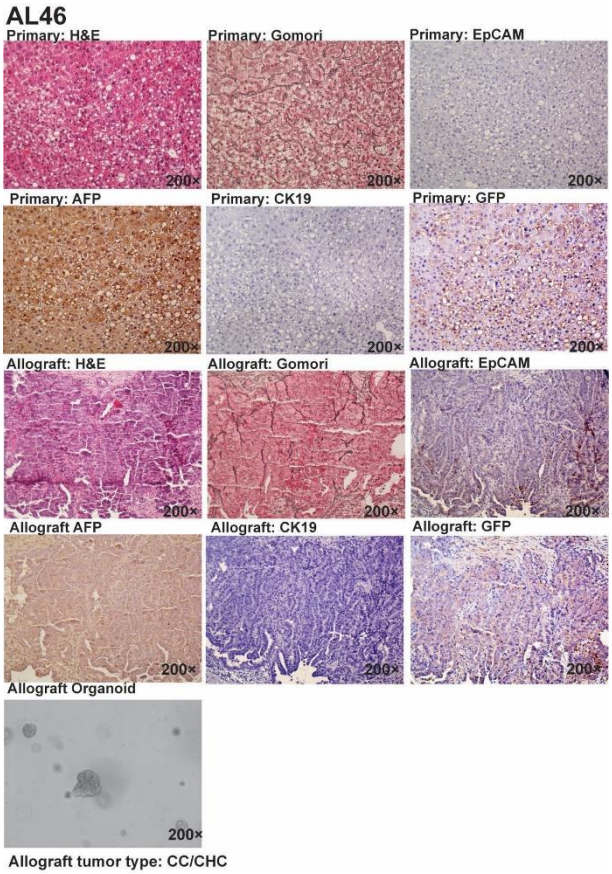
AL46
Primary: H&E
Primary: Gomori
Primary: EpCAM
Primary: AFP
Primary: CK19
Primary: GFP
Allograft: H&E
Allograft: Gomori
Allograft: EpCAM
Allograft AFP
Allograft: CK19
Allograft: GFP
Allograft Organoid
200×
Allograft tumor type: CC/CHC

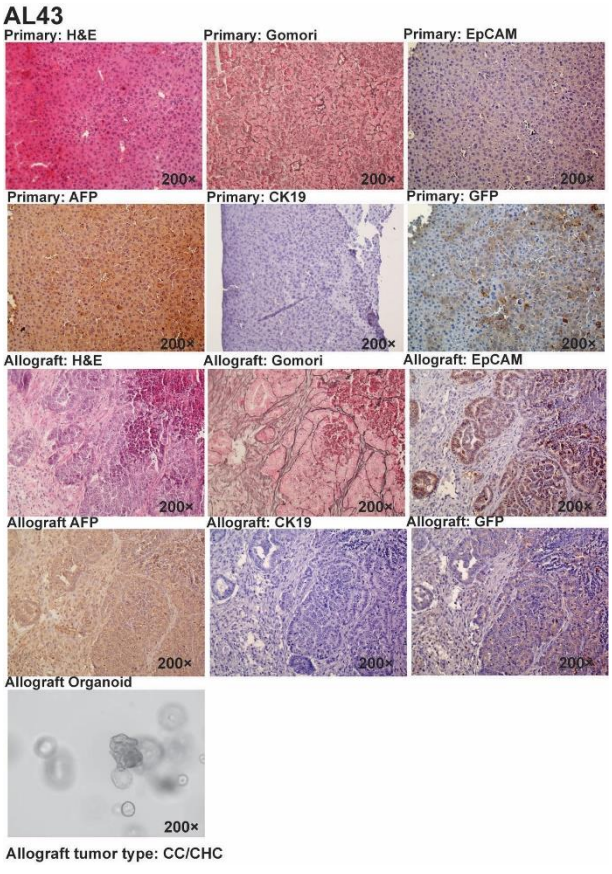
AL43
Primary: H&E
Primary: Gomori
Primary: EpCAM
Primary: AFP
Primary: CK19
Primary: GFP
Allograft: H&E
Allograft: Gomori
Allograft: EpCAM
Allograft AFP
Allograft: CK19
Allograft: GFP
Allograft Organoid
200×
Allograft tumor type: CC/CHC

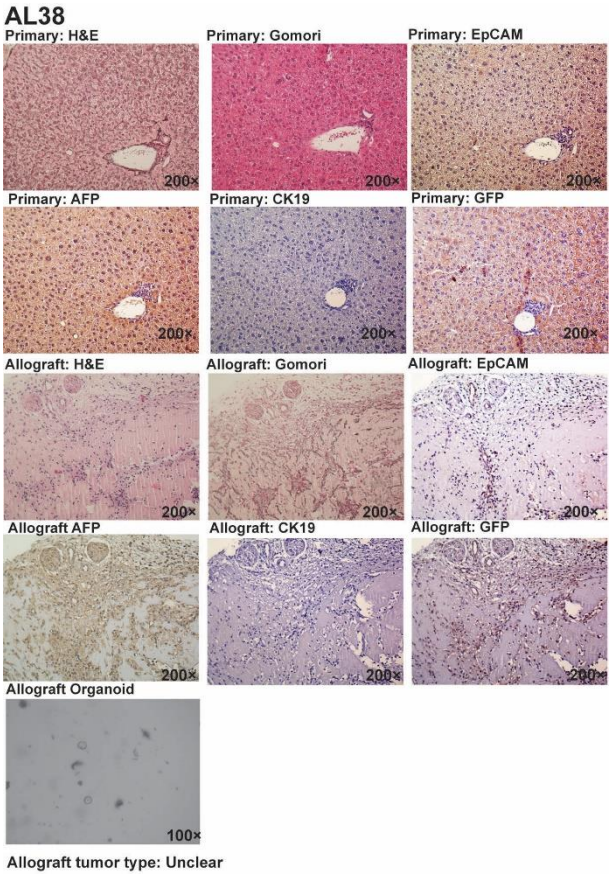
AL38
Primary: H&E
Primary: Gomori
Primary: EpCAM
Primary: AFP
Primary: CK19
Primary: GFP
Allograft: H&E
Allograft: Gomori
Allograft: EpCAM
Allograft AFP
Allograft: CK19
Allograft: GFP
Allograft Organoid
200×
100×
Allograft tumor type: Unclear

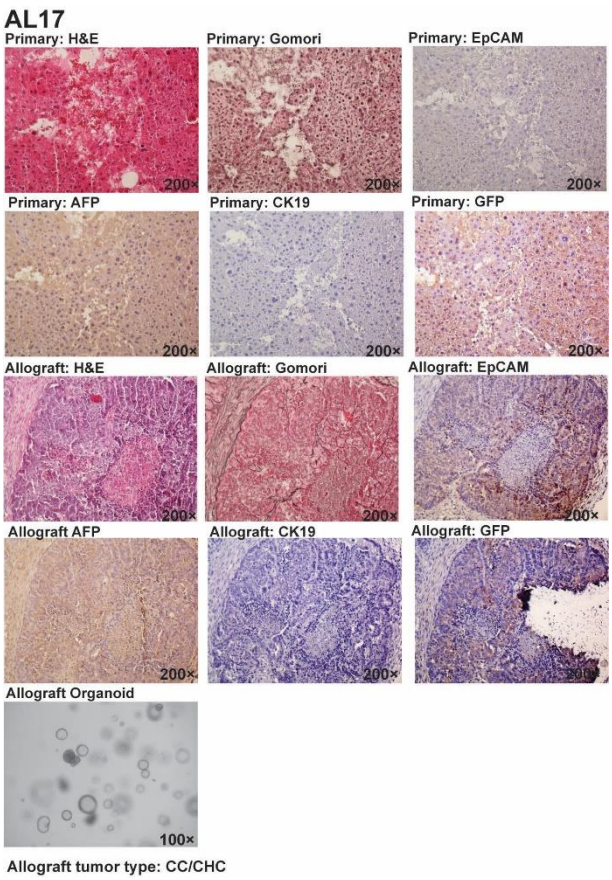
AL17
Primary: H&E
Primary: Gomori
Primary: EpCAM
Primary: AFP
Primary: CK19
Primary: GFP
Allograft: H&E
Allograft: Gomori
Allograft: EpCAM
Allograft AFP
Allograft: CK19
Allograft: GFP
Allograft Organoid
200×
100×
Allograft tumor type: CC/CHC

AL13

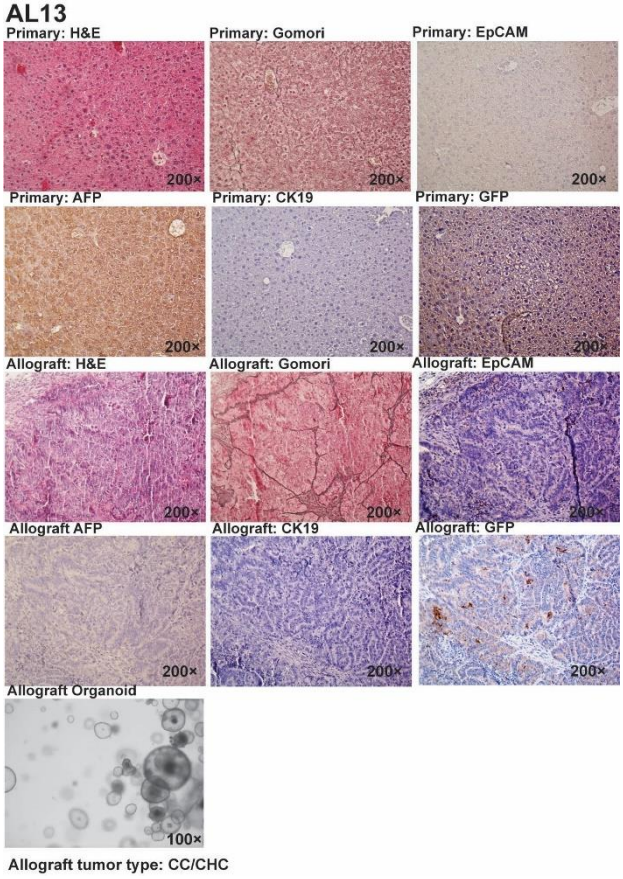

Allograft tumor type: CC/CHC

AL10

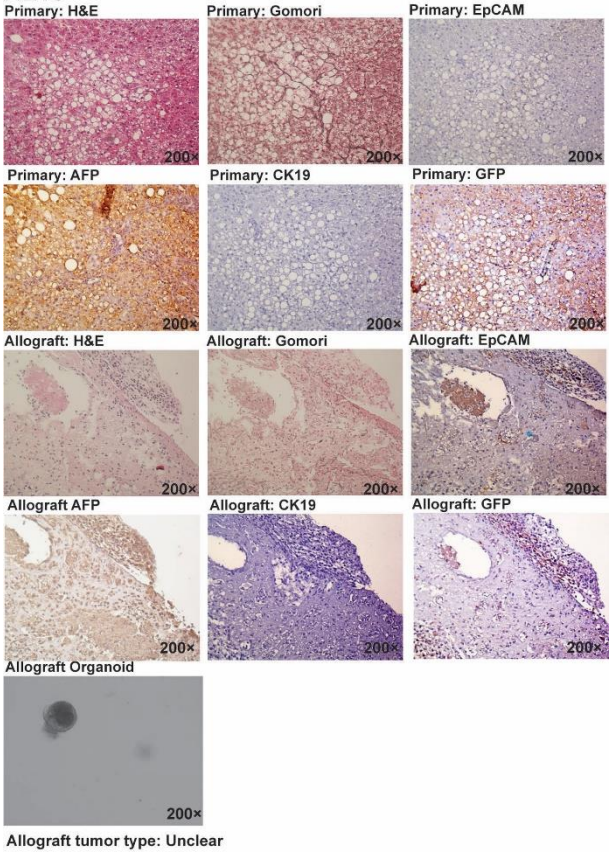

Allograft tumor type: Unclear

AL8

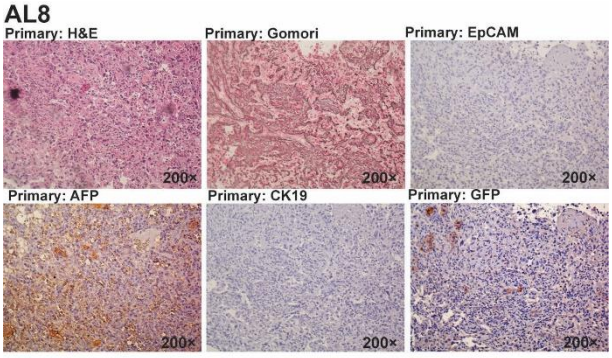

Allograft tumor type: Unclear
Strain lost due to stop proliferation ex vivo

SAL4

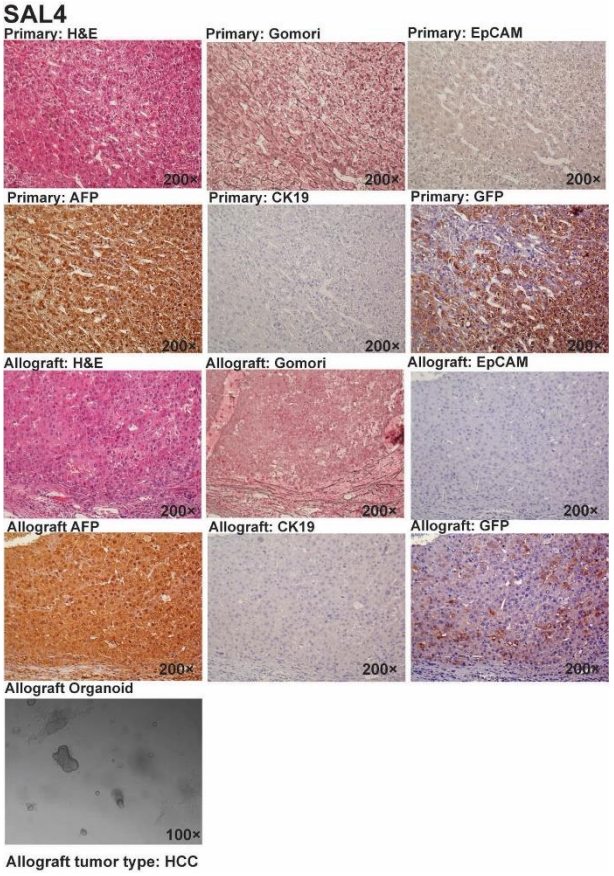

Allograft tumor type: HCC

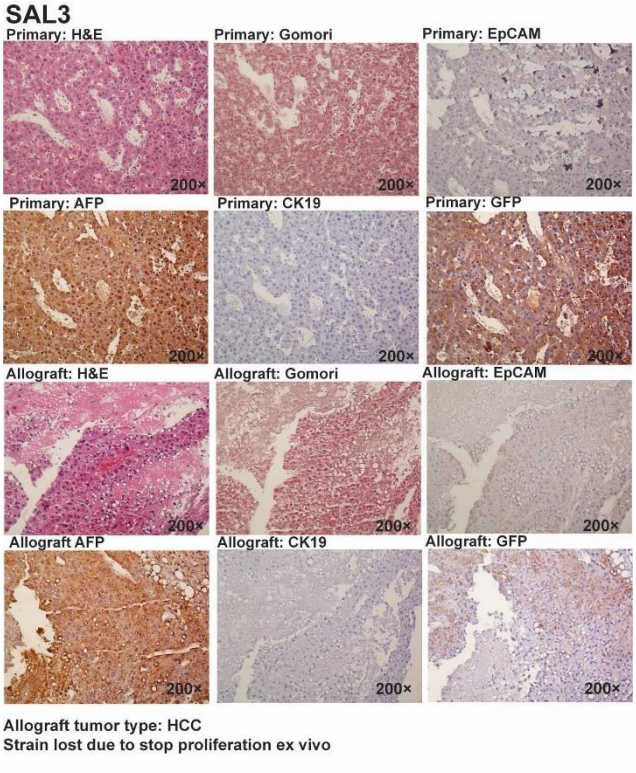

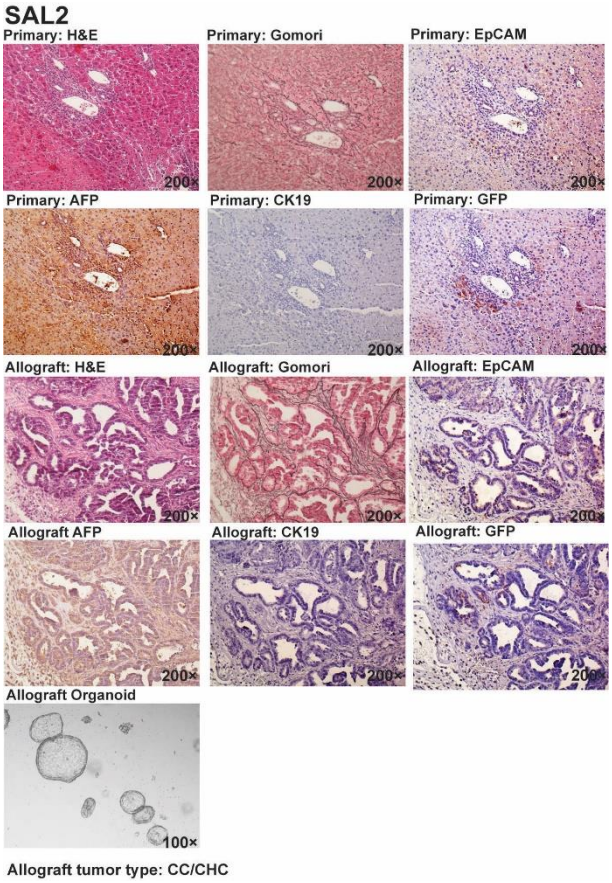

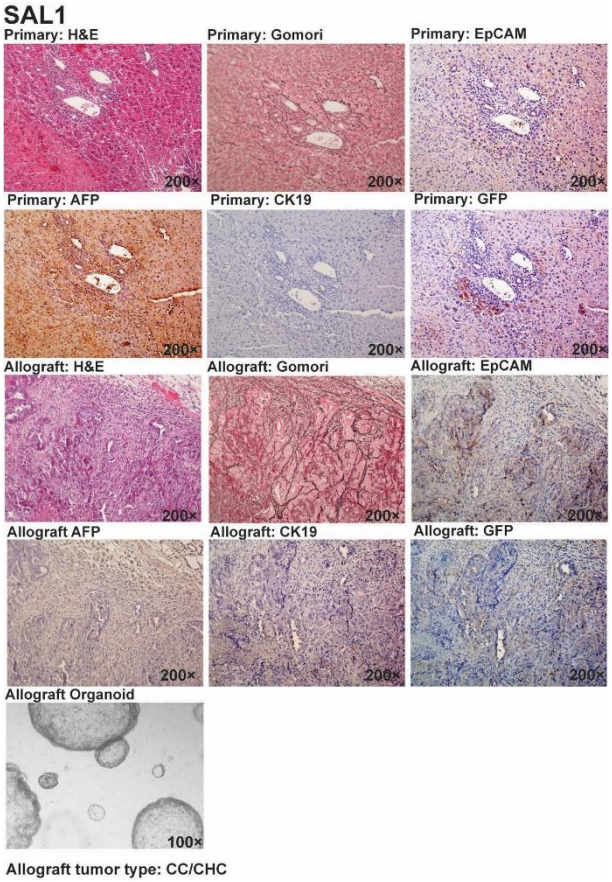

[3] Supplementary Data 3

Content:

Gene enrichment analysis of the differentially expressed genes between Untreated LGR5+ Vs. LGR5-, 5-FU-treated LGR5+ Vs. LGR5-, 5-FU-treated Vs. Untreated LGR5+ and 5-FU-treated Vs. Untreated LGR5- cells.

Treated LGR5+ Vs. LGR5-	
Pathway	**Genes**
Matrix Metalloproteinases WP441	MMP12;MMP9;MMP21
Glucocorticoid & Mineralcorticoid Metabolism WP495	HSD11B2;CYP21A1
Microglia Pathogen Phagocytosis Pathway WP3626	C1QA;FCER1G;NCF1
Striated Muscle Contraction WP216	TPM2;TCAP;TNNI3
Inflammatory Response Pathway WP458	COL1A1;CD28
Prostaglandin Synthesis and Regulation WP374	HSD11B2;ANXA8
Irinotecan Pathway WP475	UGT1A1
Osteoblast WP238	COL1A1
Estrogen metabolism WP1264	UGT1A1
Heart Development WP2067	HEY1;VEGFC
Calcium Regulation in the Cardiac Cell WP553	PRKCG;KCNB1;GJB6;ATP1B2;ADRB2
Glucuronidation WP1241	UGT1A1
Complement Activation, Classical Pathway WP200	C1QA
Eicosanoid Synthesis WP318	LTC4S
Hedgehog Signaling Pathway WP116	HHIP
GPCRs, Class B Secretin-like WP456	ADGRE1
Signal Transduction of S1P Receptor WP57	S1PR5
Spinal Cord Injury WP2432	MMP12;OMG;MMP9
Endochondral Ossification WP1270	COL10A1;MMP9
Dysregulated miRNA Targeting in Insulin/PI3K-AKT Signaling WP3855	COL1A1
Oxidative Stress WP412	UGT1A1
One Carbon Metabolism WP435	FOLH1
Peptide GPCRs WP234	CXCR3;CCR9
Eicosanoid metabolism via Lipo Oxygenases (LOX) WP4348	LTC4S
Monoamine GPCRs WP570	ADRB2
Retinol metabolism WP1259	NPC1L1
Parkinsons Disease Pathway WP3638	SNCAIP
Oxidation by Cytochrome P450 WP1274	CYP21A1
Oxidative Damage WP1496	C1QA
Non-odorant GPCRs WP1396	ADGRE1;CXCR3;CCR9;KISS1R;ADRB2;S1PR5
Metapathway biotransformation WP1251	UGT1A1;CYP21A1;HS3ST5
Wnt Signaling Pathway and Pluripotency WP723	PRKCG;HNF1A
Chemokine signaling pathway WP2292	NCF1;CXCR3;CCR9;PPBP
Wnt Signaling Pathway WP403	PRKCG
Lung fibrosis WP3632	MMP9
Complement and Coagulation Cascades WP449	C1QA
Alpha6-Beta4 Integrin Signaling Pathway WP488	COL17A1
GPCRs, Class A Rhodopsin-like WP189	GPR12;CXCR3;CCR9;ADRB2
Focal Adhesion WP85	COL1A1;VEGFC;THBS2
Adipogenesis genes WP447	PNPLA3;HNF1A
IL-2 Signaling Pathway WP450	CD53
Delta-Notch Signaling Pathway WP265	HEY1
GPCRs, Other WP41	ADRB2;S1PR5
Cytoplasmic Ribosomal Proteins WP163	RPL24
G Protein Signaling Pathways WP232	PRKCG
Amino Acid metabolism WP662	TAT
IL-6 signaling Pathway WP387	HNF1A
IL-3 Signaling Pathway WP373	MMP9
Neural Crest Differentiation WP2074	SNAI2
ESC Pluripotency Pathways WP339	HNF1A
Odorant GPCRs WP1397	GPR12;GPR61
Focal Adhesion-PI3K-Akt-mTOR-signaling pathway WP2841	COL1A1;ANGPT2;VEGFC;THBS2
Myometrial Relaxation and Contraction Pathways WP385	PRKCG
MAPK signaling pathway WP493	PRKCG
EGFR1 Signaling Pathway WP572	GM12260
PluriNetWork WP1763	PRKCG

Untreated LGR5+ Vs. LGR5-	
Pathway	Genes
Peptide GPCRs WP234	FPR1;SSTR1;TSHR
Myometrial Relaxation and Contraction Pathways WP385	MYL4;RGS5;ADCY4;RLN1
Macrophage markers WP2271	LYZ2
Matrix Metalloproteinases WP441	MMP8
Dopaminergic Neurogenesis WP1498	PITX3
Non-odorant GPCRs WP1396	FPR1;SSTR1;TSHR;CELSR3
Oxidation by Cytochrome P450 WP1274	CYP4X1
Striated Muscle Contraction WP216	MYL4
GPCRs, Class A Rhodopsin-like WP189	FPR1;SSTR1;TSHR
Metapathway biotransformation WP1251	CYP4X1;FMO2
Calcium Regulation in the Cardiac Cell WP553	RGS5;ADCY4
TYROBP Causal Network WP3625	HLX
Lung fibrosis WP3632	CMA1
Kit Receptor Signaling Pathway WP407	FGR
Purine metabolism WP2185	PNP2;ADCY4
PPAR signaling pathway WP2316	FABP2
Chemokine signaling pathway WP2292	FGR;ADCY4
G Protein Signaling Pathways WP232	ADCY4
Wnt Signaling Pathway and Pluripotency WP723	NKD2
IL-6 signaling Pathway WP387	FGR
GPCRs, Other WP41	CELSR3
Focal Adhesion WP85	FGR

[4] Supplementary Data 4

Content:

Gene: The differentially expressed genes between untreated LGR5+ cells and LGR5- cells.

Gene description: The gene description.

Survival Analyses: Online database (The Human Protein Atlas, http://www.proteinatlas.org/).

P value for Survival Analyses: Online database (The Human Protein Atlas, http://www.proteinatlas.org/).

Untreated LGR5+ vs. LGR5-			
Upregulated Gene	**Gene description**	**Survival Analyses**	**P value for Survival Analyses**
Gm11042			
AL589879.2			
1700003G13Rik			
Snord93			
Gm24325			
Gm8326			
Taf7l	TATA-box binding protein associated factor 7 like	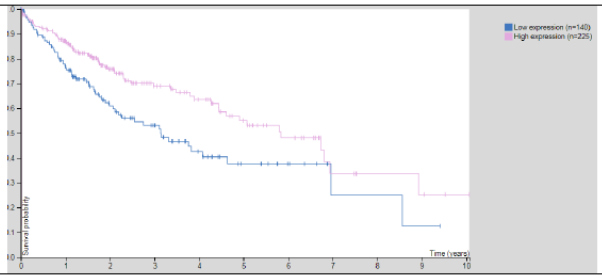	0.0039
Gm11977			
Gm24328			
Gm15558			
B230112G18Rik			
Gm42586			
Rpl36-ps7			
2210017I01Rik			
Gm43058			
Gm38321			
4833428L15Rik			
Tm6sf1	Transmembrane 6 superfamily member 1	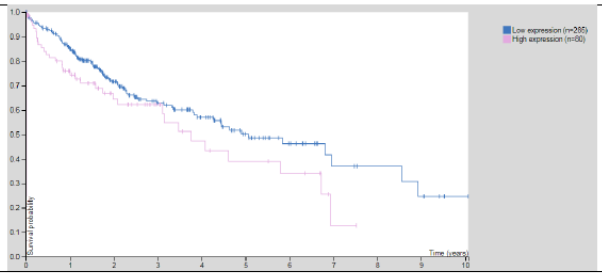	0.065
Gm18014			
Zfp572	Zfp572 zinc finger protein 572		
Kcnk4	Potassium two pore domain channel subfamily K member 4		

Spn	**Sialophorin**	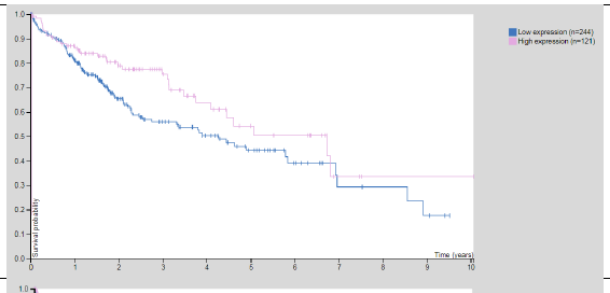	**0.040**
Smtnl1	**Smoothelin like 1**	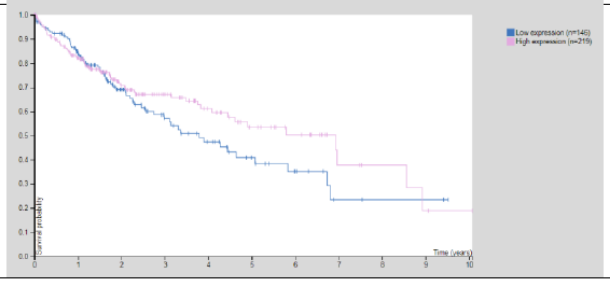	**0.22**
Gm12320			
Gm6976			
Gm24769			
Oas1h			
Tnfsfm13	**tumor necrosis factor (ligand) superfamily, membrane-bound member 13**		
Gm12227			
Gm12196			
Gm6568			
Gm15862			
Pitx3	**Paired like homeodomain 3**		
Rln1	**Relaxin 1**		
Fpr1	**Formyl peptide receptor 1**	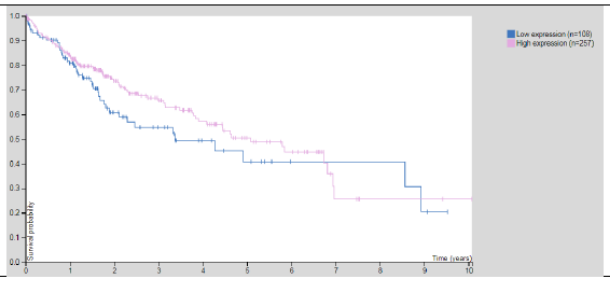	**0.20**
4933429H19Rik			
RP24-530N5.5			
Gm26899			
Ube4bos3			
Gm25445			
4933402D24Rik			
Mmp8	**Matrix**		

	metallopeptidase 8		
2300005B03Rik			
Fabp2	Fatty acid binding protein 2		
4930562D21Rik			
Gm38058			
Sox2	SRY-box 2	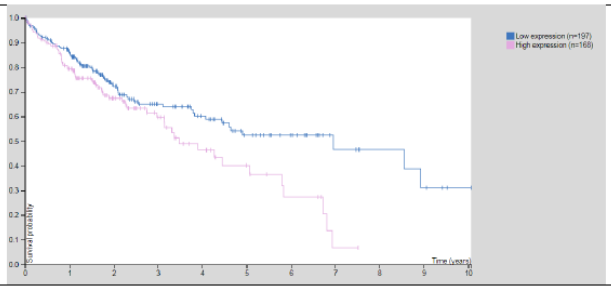	0.018
Gm4795			
Gm12043			
Dsg4	membrane proteins	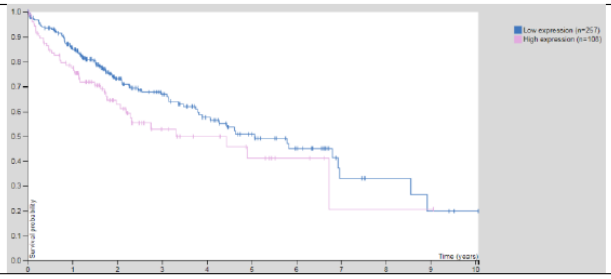	0.056
Gm15780			
Pnp2	Purine nucleoside phosphorylase		
Mcpt8	mast cell protease 8		
Nid1	Nidogen-1	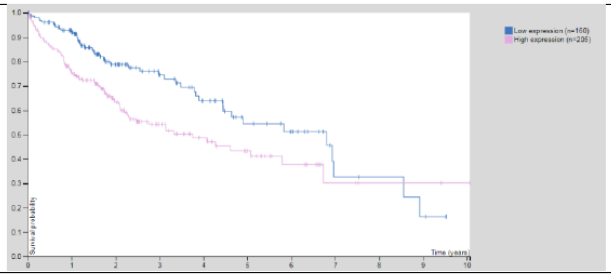	0.0024
Tshr	Thyroid stimulating hormone receptor		
Dnajb8	DnaJ heat shock protein family (Hsp40) member B8		
Nlrp4c	NACHT, LRR and PYD domains-containing protein 4C		
Gm10392			
Sstr1	Somatostatin		

	receptor 1		
Gm13578			
Gm14822			
Erich5	Glutamate rich 5	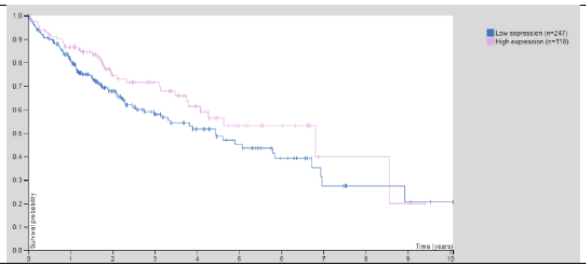	0.087
Gm18301			
6430571L13Rik			
Gm11465			
Gm15982			
Nkd2	Naked cuticle homolog 2		
Myl4	Myosin light chain 4		
Gm15964			
Gm42807			
Gm9765			
Gm16177			
Klhl3	Kelch like family member 3	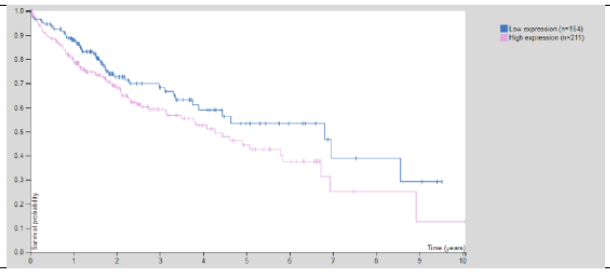	0.062
1700031P21Rik			
Gm24336			
Palm3	Paralemmin 3	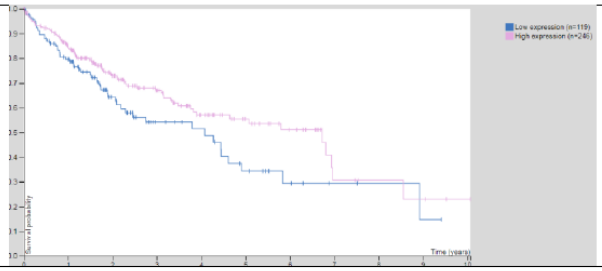	0.047
Gm14019			
Gm13110			
Gm42682			
Slc16a9	Solute carrier family 16 member 9		

Ambp	Alpha-1-microglobulin/bikunin precursor	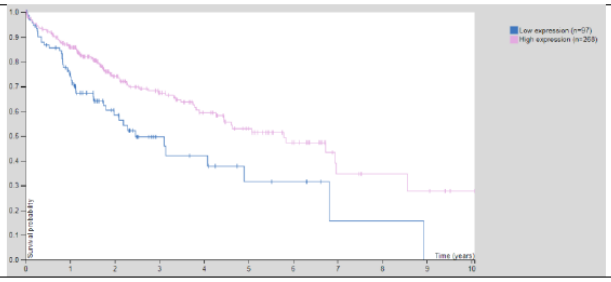	0.001
Gm37229			
Gm11764			
3110035E14Rik			
Gm6526			
Gm10030			
Mboat4	Membrane bound O-acyltransferase domain containing 4	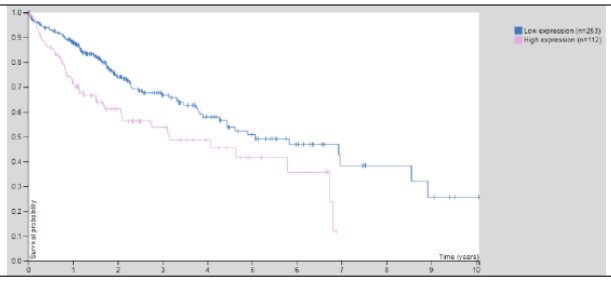	0.0019
Gm14379			
Cma1	Chymase 1	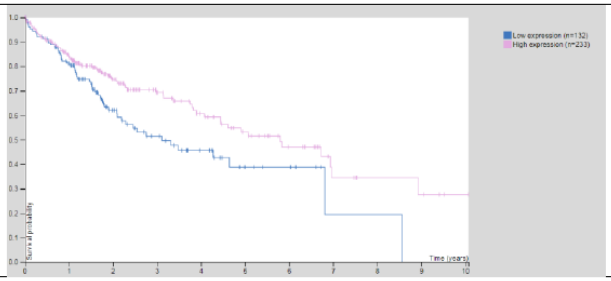	0.015
1600002D24Rik			
Gm5093			
Cd300lg	CD300 molecule like family member g		
Rab37	RAB37, member RAS oncogene family	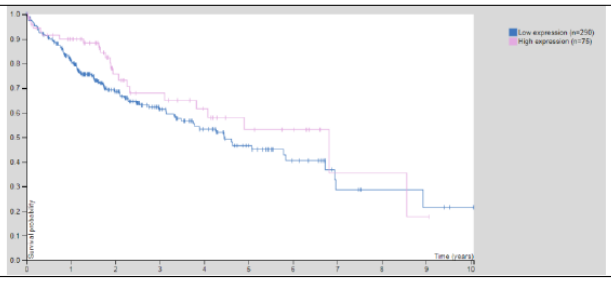	0.17
Gm28177			
Gm42500			
Hlx	H2.0 like homeobox		

Gm6226			
Gm37933			
Rai2	Retinoic acid induced 2		
Gm20056			
RP24-83C9.5			
Lyz2	Lysozyme C-2		
1700003M07Rik			
Gm5909			
Gm27033			
Gm13448			
Npm3-ps1			

[5] Supplementary Data 5

Content:

The detailed information for single cells isolated from DEN induced murine livers and allograft tumors, then used for organoid initiation, including:

1) Code: The corresponding tissues of DEN induced murine livers or allograft tumors. Green mark: the groups did initiate organoids after sorting.

2) Initiated organoid number for each group.

3) Organoid initiated efficiency (%) for each group.

Remarks: In total 89 tissues were collected. Among them, 71 tissues were sorted for following single cell initiation; 18 tissues were failed for the sort due to FACS machine issue or other technical reasons.

Primary Tissue						
Relative Organoid strain	**Isolated LGR5^{+} cell number**	**Initiated organoid number**	**Organoid initiated efficiency (%)**	**Isolated LGR5^{-} cell number**	**Initiated organoid number**	**Organoid initiated efficiency (%)**
PT1	0	0	0	1	0	0
PT2	1	0	0	7	0	0
PT3	10	1	10	17	0	0
PT11	307	0	0	8124	0	0
PT12	787	2	0.25	39066	20	0.05
PT13	24	0	0	332457	0	0
PT14	140	0	0	44901	0	0
PT15	58	0	0	186498	0	0
PT16	49	0	0	21632	0	0
PT17	59	0	0	221656	0	0
PT18	51	0	0	185640	0	0
PT19	81	0	0	8985	0	0
PT20	379	1	0.26	26090	75	0.29
PT21	611	1	0.16	13775	39	0.28
PT22	20	0	0	475	0	0
PT23	322	0	0	27748	0	0
PT24	3	0	0	8951	0	0
PT26	32	0	0	87	0	0
PT27	17	0	0	19104	30	0.16
PT28	17	0	0	8643	3	0.035
PT29	62	0	0	10809	22	0.20
PT30	124	0	0	6680	5	0.075
PT31	140	0	0	2692	0	0
PT32	41	0	0	6430	0	0
PT33	141	0	0	23853	10	0.042

PT34	36	0	0	2355	0	0
PT35	540	0	0	26689	0	0
PT36	265	0	0	86774	0	0
PT37	109	0	0	90979	0	0
PT38	1253	10	8.00	131695	0	0
PT39	1073	0	0	250982	0	0
PT40	115	0	0	1329	0	0
PT41	20	0	0	1464	0	0
PT42	181	0	0	1193	0	0
PT43	131	0	0	5998	0	0
PT44	71	0	0	76	0	0
PT45	740	3	0.41	1348	0	0
PT46	22	0	0	1485	0	0
PT47	2304	5	0.22	5356	0	0
PT48	845	1	0.12	859	0	0
PT49	482	1	0.21	418	1	0.24
PT50	385	2	0.52	444	0	0
PT51	140	5	3.57	189	1	0.53
PT52	12	0	0	594	0	0
PT53	1	0	0	180	0	0
PT54	6062	50	0.82	5767	0	0
PT55	407	0	0	2121	0	0
PT56	2282	364	16.0	3841	2	0.05
PT57	288	3	1.04	960	0	0
PT58	120	0	0	1613	0	0
PT59	821	23	2.8	758	0	0
PT60	30	0	0	1299	0	0
PT61	1879	0	0	2242	0	0
PT62	2881	10	3.5	4514	0	0
PT63	3510	27	7.7	1262	0	0
PT64	6	0	0	16	0	0
PT65	340	0	0	281	0	0
PT66	1425	0	0	1222	0	0
PT67	4404	3	0.00068	1026	0	0
PT68	9386	25	2.7	5129	0	0
PT69	93	0	0	128	0	0
PT70	1694	10	0.59	728	0	0
PT71	1526	14	0.92	1792	0	0
PT72	4482	6	0.13	4482	0	0
PT73	1101	4	0.36	1097	0	0
PT80	103	0	0	729	0	0
PT81	58	0	0	51	0	0
PT82	129	0	0	37	0	0

PT83	627	14	2.23	616	0	0
PT84	31	0	0	18	0	0
PT85	652	8	1.2	784	0	0

Allograft Tissue						
Relative Organoid strain	**Isolated $LGR5^+$ cell number**	**Initiated organoid number**	**Organoid initiated efficiency (%)**	**Isolated $LGR5^-$ cell number**	**Initiated organoid number**	**Organoid initiated efficiency (%)**
AL17	70	64	91.4	513	46	9,0
AL13	1026	233	22.7	663	5	0,8
SAL1	7	7	100	38	7	18,4
AL43	39	15	38.5	54	18	33,3
AL46	13	5	38.5	1	0	0,0
AL13.1	1646	180	10.9	1373	176	12,8
AL17.2	21	11	52.4	366	11	3,0
AL8.1	62	17	27.4	100	3	3,0
AL8.2	107	12	11.2	181	7	3,9
AL8.3	138	16	11.6	178	0	0,0

[6] Supplementary Data 6

Content:

The detailed information for single cells isolated from DEN induced murine livers, then injected directly into immunodeficient mice for tumor formation, including:

1) Code: The corresponding tissues of DEN induced murine livers and initiated allograft tumors. Green mark: the groups did initiate tumors after sorting.

2) Injected cell number for each group.

3) Pictures of primary tumors and corresponding allograft tumors.

	Tissue Code	Injected Cell Type	Injected Cell Number	Tumor initiation
1	PT47	$LGR5^+$ cells	3000	no
		$LGR5^-$ cells	3000	no
2	PT50	$LGR5^+$ cells	2000	SAL1
		$LGR5^-$ cells	2000	SAL2
3	PT63	$LGR5^+$ cells	2000	SAL3
		$LGR5^-$ cells	2000	no
4	PT65	$LGR5^+$ cells	6000	no
		$LGR5^-$ cells	6000	no
5	PT67	$LGR5^+$ cells	1000	no
		$LGR5^-$ cells	1000	no
6	PT68	$LGR5^+$ cells	16000	SAL4
		$LGR5^-$ cells	16000	no
7	PT72	$LGR5^+$ cells	5000	no
		$LGR5^-$ cells	5000	no
8	PT73	$LGR5^+$ cells	1000	no
		$LGR5^-$ cells	1000	no
	PT85	$LGR5^+$ cells	3000	no

9		LGR5$^-$ cells	3000	no

Tissue code	Primary tumor	Allograft Tumor
SAL1		
SAL2		
SAL3	Picture lacking	
SAL4		

CHAPTER 11

Cancer-associated fibroblasts provide a stromal niche for liver cancer organoids that confers trophic effects and therapy resistance

Jiaye Liu, Meng Li, Pengfei Li, Ling Wang, Zhouhong Ge, Lisanne Noordam, Ruby Lieshout, Monique M. A. Verstegen, Junhong Su, Qin Yang, Ruyi Zhang, Guoying Zhou, Lucia Campos Carrascosa, Dave Sprengers, Ron Smits, Jaap Kwekkeboom, Luc J. W. van der Laan, Maikel P. Peppelenbosch, Qiuwei Pan, Wanlu Cao

Cell Mol Gastroenter; Accepted

Abstract

Background & Aims: Cancer associated fibroblasts (CAFs) play a key role in cancer process, but the research progress is hampered by the paucity of preclinical models essential for mechanistic dissection of cancer cell-CAF interactions. Here, we aim to establish a 3D organotypic co-cultures of primary liver tumor-derived organoids with CAFs, and to understand their interactions and the response to treatment.

Methods: Liver tumor organoids and CAFs were cultured from murine and human primary liver tumors. 3D co-culture models of tumor organoids with CAFs and trans-well culture systems were established *in vitro*. A xenograft model was used to interrogate the cell-cell interactions *in vivo*. Gene expression analysis of CAF markers in our hepatocellular carcinoma (HCC) cohort and an online liver cancer database indicated the clinical relevance of CAFs.

Results: To functionally investigate the interactions of liver cancer cells with CAFs, we have successfully established murine and human 3D co-culture models of liver tumor organoids with CAFs. CAFs promoted tumor organoid growth in co-culture with direct cell-cell contact and in trans-well system via paracrine signaling. Vice versa, cancer cells secret paracrine factors regulating CAF physiology. Co-transplantation of CAFs with liver tumor organoids of mouse or human origin promoted tumor growth in xenograft models. Moreover, tumor organoids conferred resistance to clinically used anti-cancer drugs including Sorafenib, Regorafenib and Fluorouracil (5-FU) in the presence of CAFs, or the conditioned medium of CAFs.

Conclusions: We have successfully established murine and human 3D co-culture models and have revealed robust effects of CAFs in liver cancer nurturing and treatment resistance.

Key words: Liver tumor organoids; stromal cells; co-culture; cell-cell contact; paracrine effect.

Introduction

Liver cancer is one of the most common and deadly malignancies worldwide, and currently there are limited treatment options available. Heterogeneity within and between liver tumors greatly complicates disease progression and treatment response.[1] A subpopulation of cancer cells within tumors, termed cancer stem cells (CSCs), have been recognized to possess capacity for both self-renewal but also the potential for differentiation. This population of cells appears responsible for resistance to treatment in addition to tumor initiation and progression.[2] Although tumor biology of liver cancer in general remains poorly understood, hopes for obtaining better understanding of this disease have been fostered by the recent development of 3D organoids culture technology. Such cultures, initially derived from tissue-resident stem/progenitor cells, embryonic stem cells or induced pluripotent stem cells, has emerged as a new technology for stem cell research as they are capable of self-renewal and self-organization that recapitulate the functionality of the tissue-of-origin. Interestingly, this 3D culture system has been extended to culture a variety of primary cancer cells, providing insight into the role of CSCs in the cancer progress.[3] For liver cancer, tumor organoids that resemble hepatocellular carcinoma (HCC) or cholangiocarcinoma (CCA) have been successfully cultured from human tumor[4] or mouse tumor models.[5] In general, organoids are much easier to be cultured from CCA than HCC.

Cancer cells, in particular CSCs, actively interact with the tumor microenvironment. This microenvironment contains numerous cell types, including immune cells, fibroblasts and endothelial cells, and various factors including signaling molecules and extracellular matrix (ECM).[6] Among these components, a specialized group of fibroblasts called cancer associated fibroblasts (CAFs) are considered to be of unusual importance to tumor development. Previous studies have identified several CAF markers including alpha-smooth muscle actin (α-SMA), fibroblast associated protein (FAP), Vimentin, fibroblast specific protein 1 (FSP1), CD29, Caveonin 1 (CAV1), Desmin, platelet-derived growth factor receptor alpha (PDGFRA), platelet-derived growth factor receptor beta (PDGFRB), Gremlin1, Collagen, type I, alpha 1 (COL1A1), Periostin and C-X-C motif chemokine 12 (CXCL12).[7-14] CAFs can support tumor growth, metastasis and formation of cancer stem cell niches, and mediate immunosuppression and drug resistance by directly interacting with cancer cells or secreting a panel of factors and nutrients.[15] More than 80% of HCC patients have the background of liver cirrhosis,[16] and these livers are enriched with activated fibroblasts due to the chronic inflammation that characterize this disease. Thus, CAFs are assumed to play a prominent role in liver cancer even in the absence of formal proof.

In this study, we first develop a 3D co-culture system of primary liver tumor-derived organoids with CAFs of mouse or human origin. By using this system, we investigated the reciprocal interactions of cancer cells and CAFs, and the role that the CAF niche provided with respect to the nurturing of cancer cells and their importance for treatment resistance of liver cancer cells.

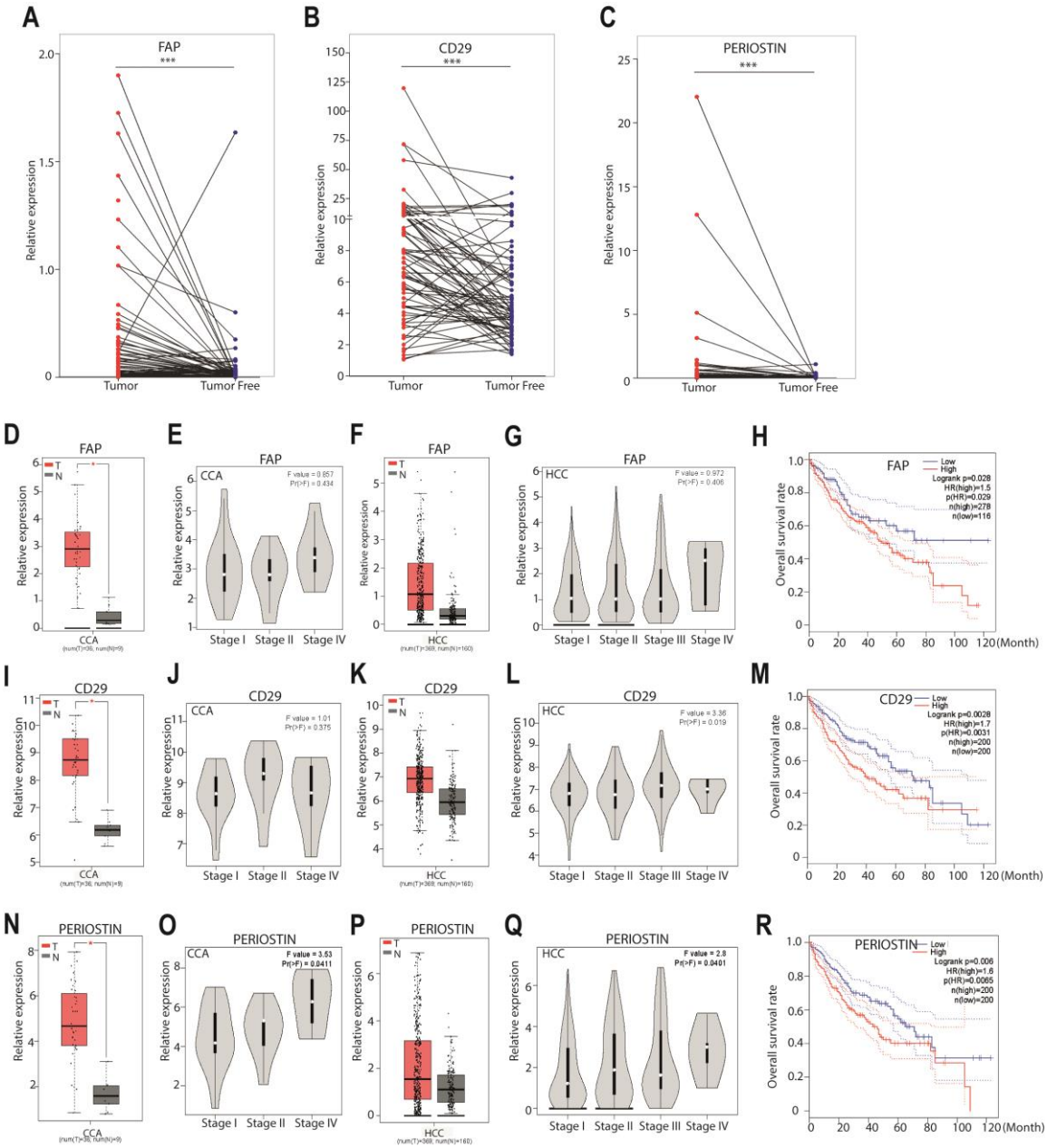

Figure 1. **Bioinformatics analysis between FAP, CD29 and Periostin gene expression and clinical relevance in liver cancer.** (A-C) Gene expression of CAF markers FAP, CD29 and Periostin in tumors compared to paired adjacent tumor free liver tissues in our HCC cohort (n = 75 HCC, Mann-Whitney *U* tests. ***p < 0.001). (D, I, N) Gene expression of CAF markers FAP, CD29 and Periostin in CCA compared to normal liver tissues in an online TCGA database (n = 9 for normal liver tissue; n = 36 for tumor tissue; One-way ANOVA; *p < 0.05). (F, K, P) Gene expression of CAF markers FAP, CD29 and Periostin in HCC compared to normal liver tissues in an online TCGA database (n = 160 for normal liver tissue; n = 369 for tumor tissue; One-way ANOVA; *p < 0.05). (E, J, O) The expression of FAP, CD29 and Periostin in different tumor stage of CCA (n = 36, One-way ANOVA). (G, L, Q) The expression of FAP, CD29 and Periostin in different tumor stage of HCC (n = 369, One-way ANOVA). (H, M, R) Overall survival assessed using the online TCGA database at www.gepia.com. The differences in survival related to CAFs markers CD29, FAP and Periostin mRNA expression were compared in each group involving in all patients (Log-rank test, FAP [n = 36 for CCA, n = 358 for HCC]; CD29 [n = 36 for CCA, n = 364 for HCC]; Periostin [n = 36 for CCA, n = 364 for HCC]). Dotted line indicated the 95% confidence interval. T, tumor tissues; N, normal liver tissue; CAF, cancer associated fibroblast; CCA, cholangiocarcinoma; HCC, hepatocellular carcinoma; FAP, fibroblast associated protein.

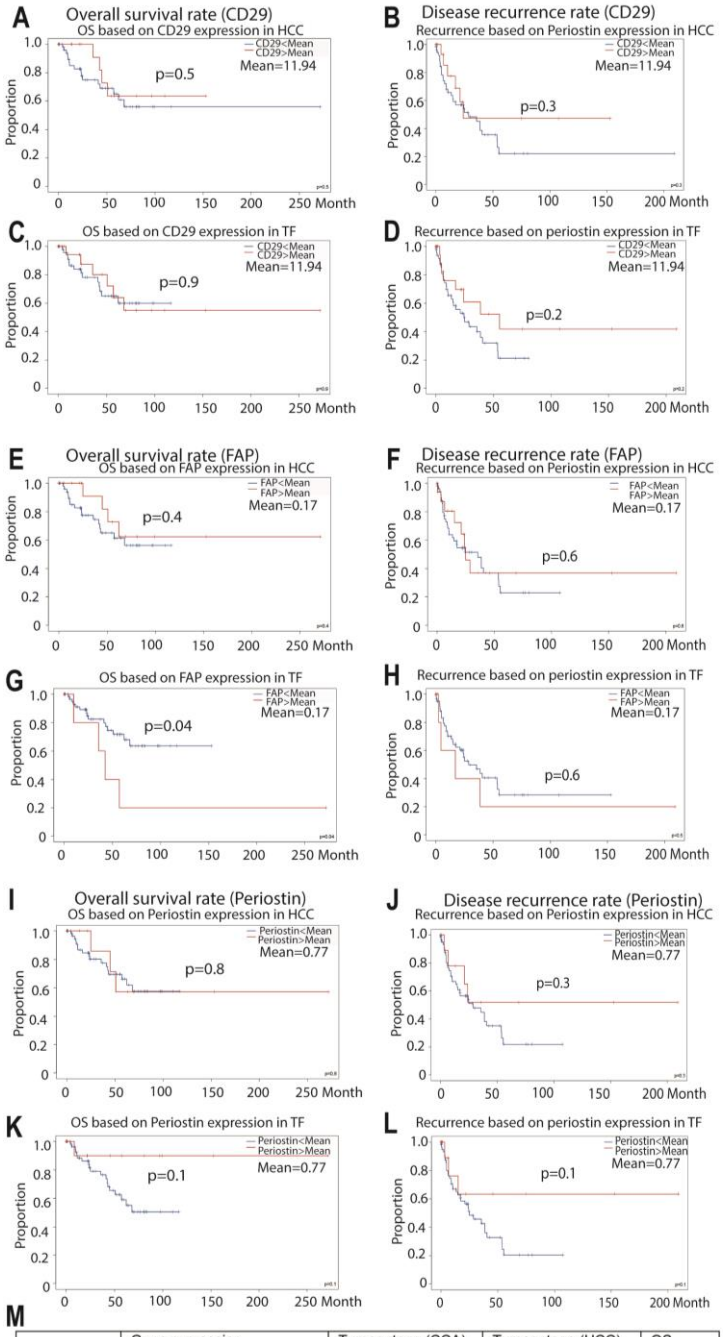

	Gene expression		Tumor stage (CCA)		Tumor stage (HCC)		OS
	CCA	HCC	F value	P value	F value	P value	P value
PDGFRB	T>N (<0.05)	T>N (<0.05)	0.26	0.78	0.56	0.65	0.71
Alpha-SMA	T>N (<0.05)	T>N (-)	1.11	0.34	0.41	0.74	0.27
S100A4	T>N (<0.05)	T>N (<0.05)	0.70	0.51	0.29	0.84	0.22
COL1A1	T>N (<0.05)	T>N (<0.05)	1.29	0.29	1.48	0.22	0.11
PDGFRA	T>N (-)	T<N (<0.05)	0.42	0.66	1.8	0.15	0.55
CXCL12	T<N (-)	T<N (<0.05)	0.32	0.73	1.2	0.30	0.41
CAV1	T>N (<0.05)	T>N (<0.05)	2.57	0.09	2.12	0.10	0.53
VIMENTIN	T>N (<0.05)	T>N (<0.05)	1.21	0.31	0.31	0.82	0.66

Figure 2. **Survival and recurrence analysis based on the gene expression of CD29, FAP and Periostin in our HCC cohort and bioinformatics analysis of other CAFs markers in GEPIA online database.** (A-L) Overall survival and disease free rate based on the gene expression of CD29, FAP and Periostin in tumor tissue or tumor free liver tissue of our HCC patients (Kaplan-Meier analysis, n = 75). (M) Bioinformatics analysis of PDGFRB, α-SMA,S100A4, COL1A1, PDGFRA, CXCL12, CAV1, VIMENTINE in GEPIA database. The gene expression of these markers in tumor and normal liver tissue (CCA: n = 9 for normal liver tissue; n = 36 for tumor tissue; HCC: n = 160 for normal liver tissue; n = 369 for tumor tissue; One-way ANOVA). Gene expression of these markers in different stages of liver tumors

(CCA: n = 36; HCC: n = 369, One-way ANOVA). The differences in survival related to CAFs markers PDGFRB, Alpha-SMA, FSP1, COL1A1, PDGFRA, CXCL12, CAV1 and Vimentin mRNA expression were compared in each group involving in all patients (Log-rank test, n = 36 for CCA, n = 364 for HCC). (-) Without statistical significant difference. CAF, cancer associated fibroblast; CCA, cholangiocarcinoma; HCC, hepatocellular carcinoma; FAP, fibroblast associated protein; FSP1, fibroblast-specific protein1; PDGFRA, platelet-derived growth factor receptor alpha; PDGFRB, platelet-derived growth factor receptor beta; COL1A1, collagen , type I, alpha 1; CXCL12, C-X-C motif chemokine ligand 12; CAV1, Caveolin 1; T, tumor tissues; N, normal liver tissue; OS, overall survival rate.

Results

Evidence for potential clinical significance of CAFs in liver cancer

We first examined the potential clinical relevance of CAFs in liver cancer patients. We quantified the mRNA expression of three well-recognized CAF markers including FAP[17, 18], CD29[19, 20] and Periostin[21, 22] in our HCC patient cohort. Their expression is significantly elevated in tumors compared to adjacent liver tissues of the same patients (n = 75, Figure 1A-C). We next analyzed the expression of these CAF markers using the online TCGA database. Consistently, FAP, CD29 and Periostin are upregulated in tumor compared to normal liver tissues (n = 196 for normal liver tissue; n = 405 for tumor tissue, including 369 HCC and 36 CCA, Figure 1D, F, I, K, N, P). This upregulation is more apparent in late stage of liver cancer (Figure 1E, G, J, L, O, Q). Importantly, high expression of FAP, CD29 or Periostin in tumor tissues is significantly associated with poor overall survival of the patients (Figure 1H, M, R). The patient number in our HCC cohort is too small for powerful statistical analysis of CAF markers in association with cancer-specific survival. Some of these markers showed similar trends in relation to patient survival in our cohort as observed in TCGA dataset, although they are not fully in accordance with the results from TCGA database (Figure 2A-L). Analysis of additional CAF markers revealed the upregulation of several other markers in tumor, although their expression is not associated with patient survival (Figure 2M). These results provided some evidence for potential clinical relevance of CAFs in liver cancer and promoted us to establish experimental models for further investigation.

Construction of 3D co-culture systems of liver tumor organoids with CAFs

For studying the interaction between cancer cells and CAFs, we first explored the construction of 3D organotypic co-culture systems of liver tumor organoids with CAFs. We have established 6 mouse tumor organoids from carcinogen N-nitrosodiethylamine (DEN) induced mouse liver tumors and 4 human CCA tumor organoids from resected patient CCA tumors as previously described.[4, 5] CAFs were isolated and cultured from DEN-induced liver tumors of red fluorescence-expressing Rosa 26-mT mice (Figure 3A), and tumors of HCC and CCA patients (Figure 3B). As a result, 2 mouse CAFs (2 out of 6 mice), 6 human CAFs (2 out of 3 CCA and 4 out of 10 HCC) were established. CAFs were enriched by plastic adherence and propagated in culture. Both mouse and human CAFs display an elongated, spindle-like morphology (Figure 3C). Immunofluorescence staining confirmed that most CAFs were positive for α-SMA and FAP (Figure 3D). We excluded the presence of other cell types including cancer cells, immune cells and endothelial cells by staining with the corresponding makers AFP, EpCAM, CD45 and CD31 (Figure 3D).

We have successfully established the murine and human 3D co-cultures of tumor organoids and CAFs. (Figure 4A-E). However, the co-cultured organoids and CAFs were not derived from the same mice or patients. After three days in co-culture, CAFs become further elongated and gradually formed net-like structure which encircled organoids (Figure 4E). Corresponding immunofluorescence images of the culture system of mouse origin are displayed, as these

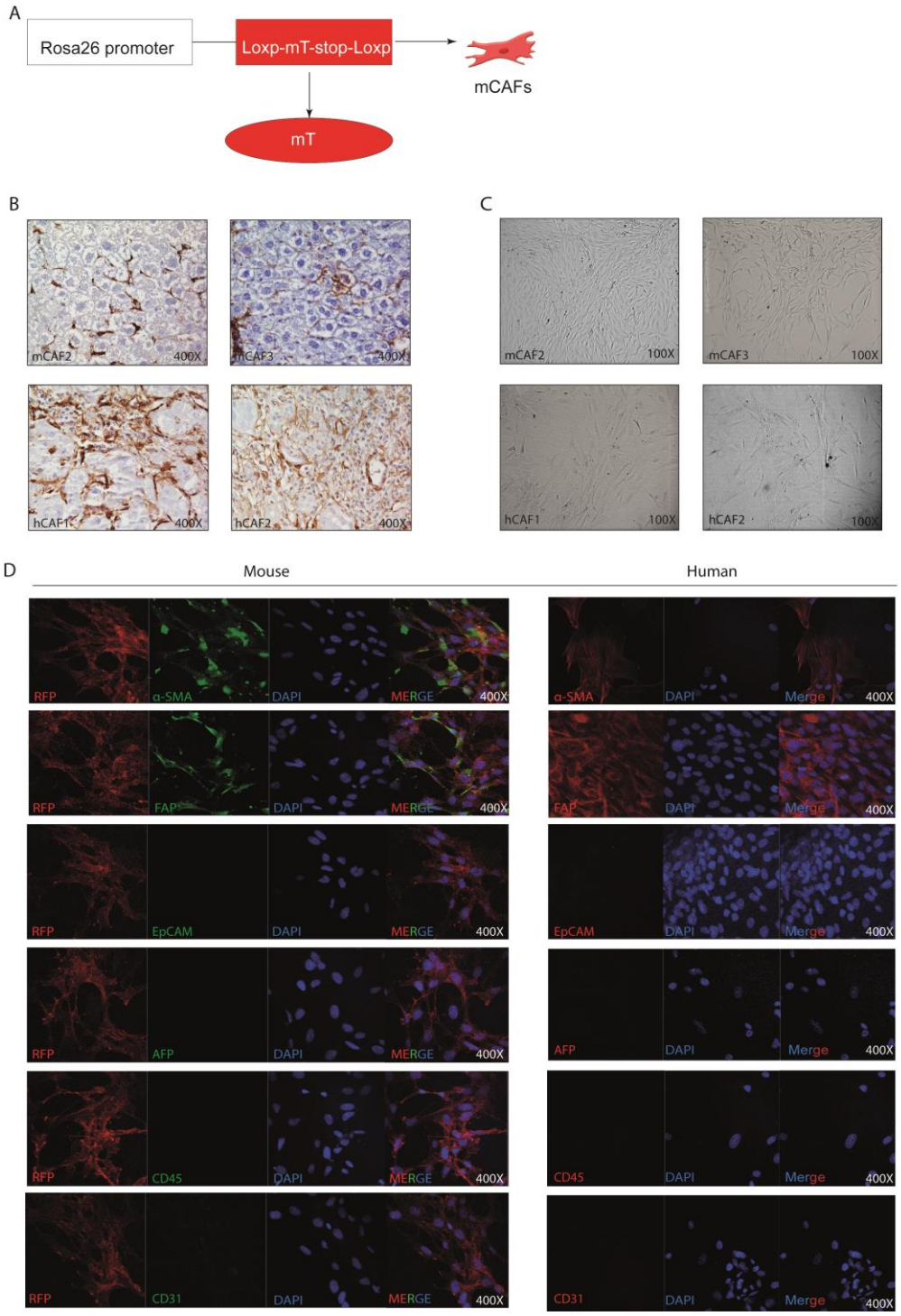

Figure 3. **Establishment of cancer associated fibroblasts.** (A) Rosa26-mT mouse treated with diethylnitrosamine (DEN) for 17 weeks, and waited 30 weeks for tumor formation. Then mouse CAFs were cultured according to our protocol. (B) Representative IHC staining of α-SMA in mouse and human primary tissue (magnification 400X). (C) Representative image of established human and mouse CAFs

(magnification 100X). (D) Representative IF staining of α-SMA, FAP, EpCAM, AFP, CD45 and CD31 in mouse and human CAFs (magnification 400X). IHC, immunohistochemistry; α-SMA, alpha smooth muscle actin; CAFs, cancer associated fibroblasts; IF, immunofluorescence; FAP, fibroblast associated protein; AFP, Alpha-fetoprotein; EpCAM, epithelial cell adhesion molecule.

CAFs were derived from red fluorescent protein (RFP) expression murine liver tumor (Figure 4F). By using immunofluorescence staining and 3D reconstructing the Z-stack of confocal images, we further confirmed that CAFs closely surrounded the organoids (Figure 4G and H).

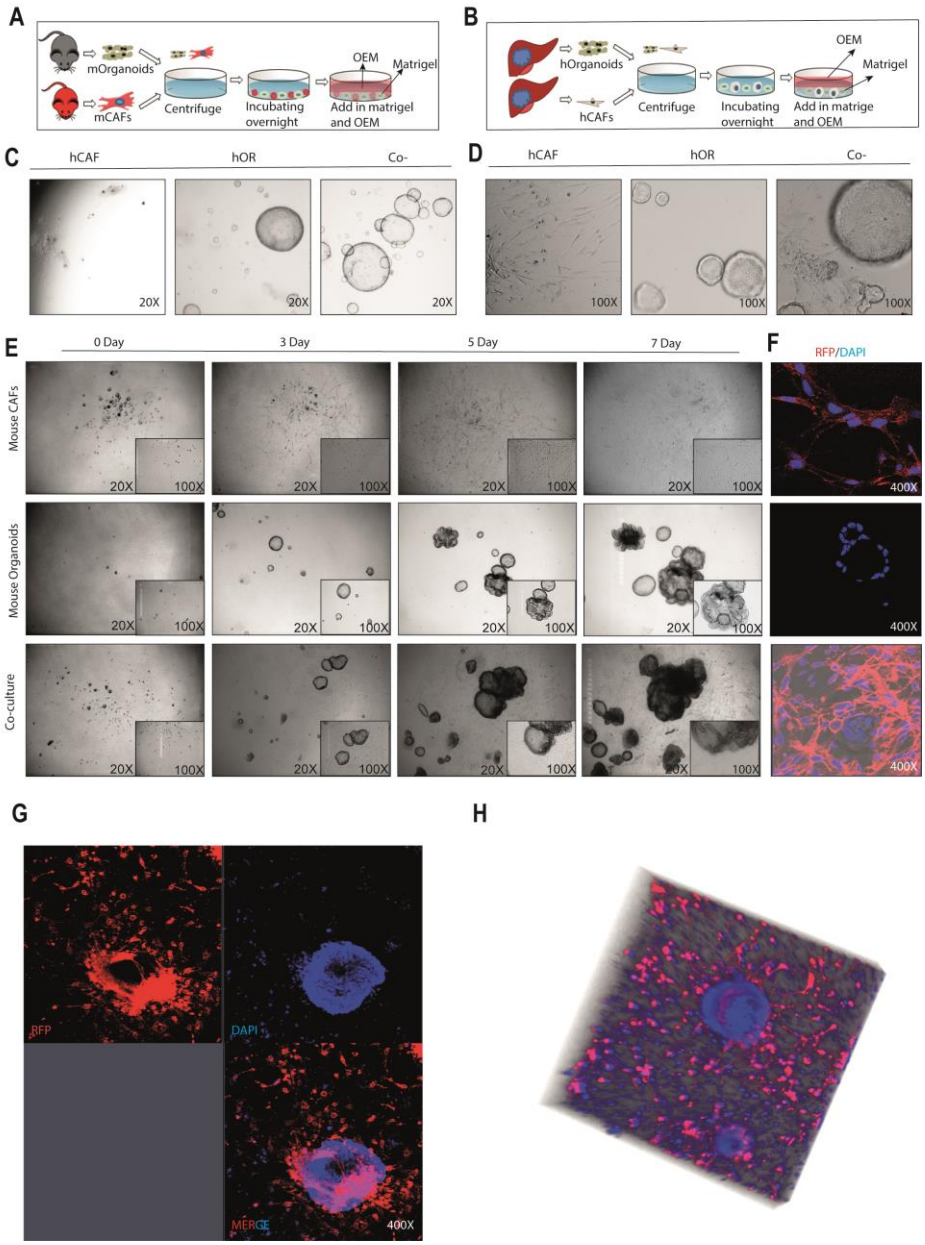

Figure 4. **Establishment of organoids and CAFs co-culture models of mouse and human origins.** (A-B) Schematic illustration of the co-culture models of murine and human origins. (C-D) Representative image of human CAFs, human organoids and co-cultures at day 10 (C, magnification 20X; D, magnification 100X). (E) Representative image of mouse CAFs, mouse organoids and co-cultures from day 0 to day 7 (magnification 20X, inset magnification 100X). (F) Representative IF staining of mouse CAFs, mouse organoids and co-cultures (magnification 400X). (G) Representative confocal image of mouse organoids and CAFs co-culture model (magnification 400X). (H) Representative 3D reconstruction of Z-stack of mouse organoids and CAFs co-culture model. CAFs, cancer associated fibroblasts; IF, immunofluorescence.

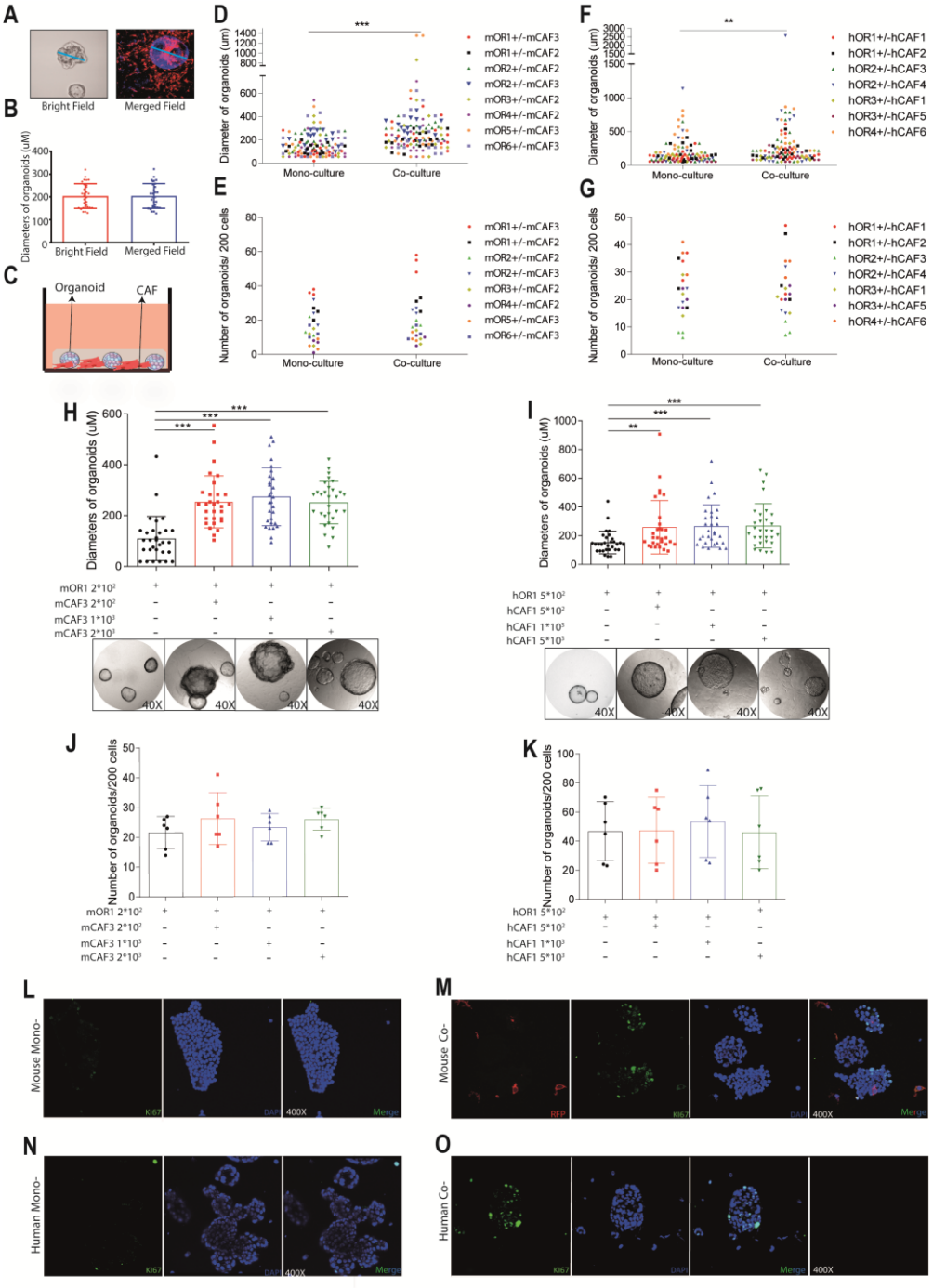

Figure 5. **The effects of CAFs on tumor organoids formation and growth.** (A-B) Measuring the diameter of organoids under immunofluorescence and bright field vision (n = 6. Five organoids for each well were randomly measured). (C) Mouse or human tumor organoids cultured with or without corresponding CAFs. (D) Diameters of mouse organoids cultured with or without mouse CAFs (n = 8 experimental settings with 3 biological replicates for each. Five organoids for each well were randomly measured). (E) Number of mouse organoids cultured with or without mouse CAFs (n = 8 experimental settings with 3 biological replicates for each) (F) Diameters of human organoids cultured with or without human CAFs (n = 7 experimental settings with 3 biological replicates for each. Five organoids for each well were randomly measured). (G) Number of human organoids cultured with or without mouse CAFs (n = 7 experimental settings with 3 biological replicates for each). (H-I) Diameters of formed organoids in mono- or co-cultures with different concentration between organoids and CAFs (n = 6; Five organoids for each well were randomly measured). (J-K) The number of formed organoids in mono- or co-cultures

with different concentration between organoids and CAFs (n = 6). (L) Ki67 staining for mouse organoids mono-culture (magnification 400X). (M) Ki67 staining for mouse organoids and CAFs co-culture (magnification 400X). (N) Ki67 staining for human organoids mono-culture (magnification 400X). (O) Ki67 staining for human organoids and CAFs co-culture (magnification 400X). (B, D-K) Data are expressed as means ± SD; Mann-Whitney *U* tests; **p < 0.01, ***p < 0.001.

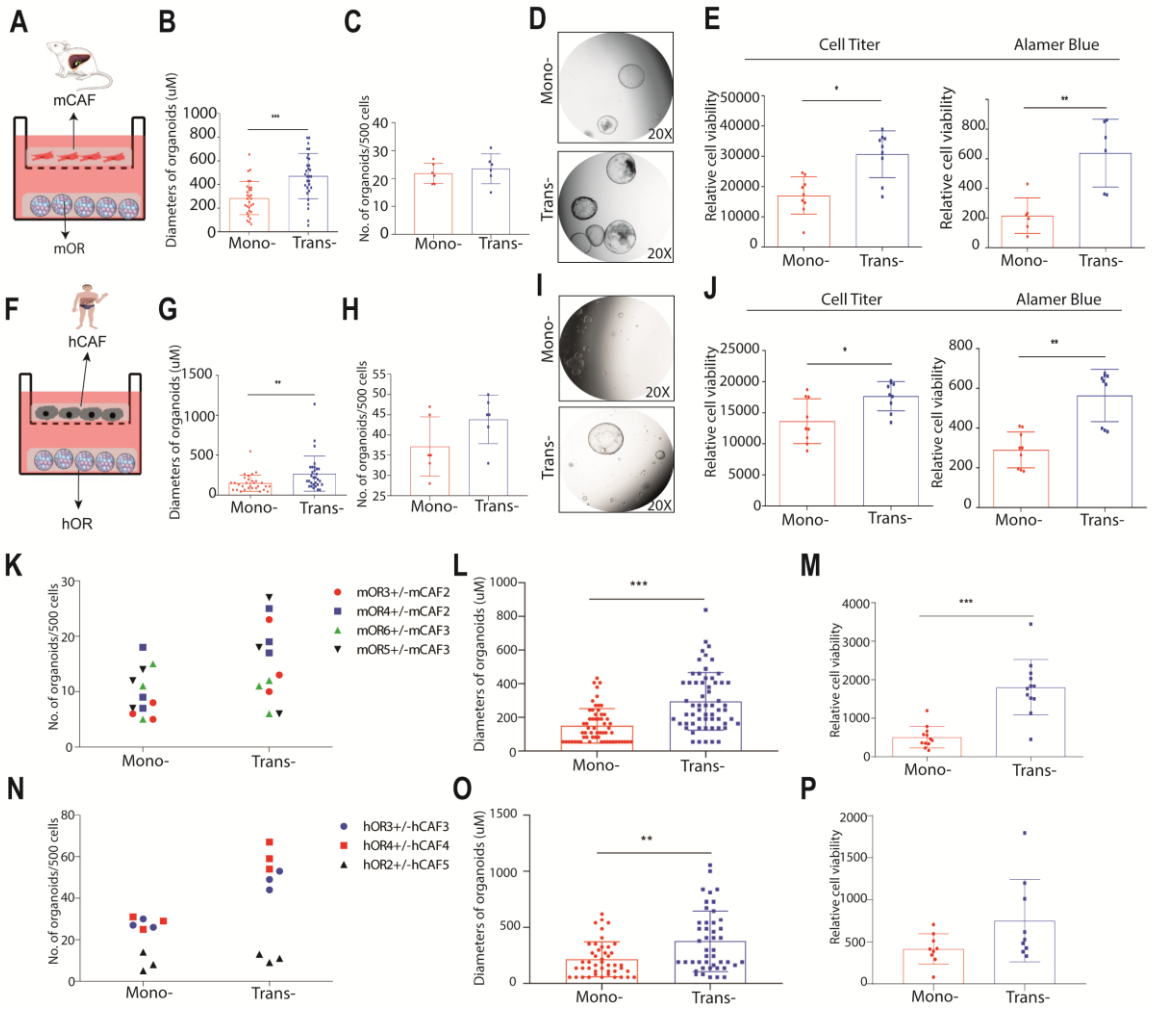

Figure 6. **The effects of CAFs on organoids in trans-well platform.** (A) Schematic illustration of trans-well culture platform for mouse cells. (B) Diameters of mouse organoids in trans-well platform with or without CAFs (n = 6; Five organoids for each well were randomly measured). (C) Number of mouse organoids in trans-well platform with or without CAFs (n = 6). (D) Representative images of mono-, co-cultured mouse organoids. (E) Growth of mouse liver tumor organoids determined by CellTiter (n = 9) and Alamar Blue Assay (n = 6). (F) Schematic illustration of trans-well culture platform for human cells. (G) Diameters of human organoids in trans-well platform with or without CAFs (n = 6; Five organoids for each well were randomly measured). (H) Number of human organoids in trans-well platform with or without CAFs (n = 6). (I) Representative images of mono-, co-cultured human organoids in trans-well platform. (J) Growth of human organoids determined by CellTiter and Alamar Blue Assay (n = 9). (K) The number of formed mouse tumor organoids in the presence or absence of CAFs in a trans-well system (n = 4 experimental settings with 3 biological replicates for each, Mann-Whitney *U* tests). (L) The size of formed mouse tumor organoids in the presence or absence of CAFs in a trans-well system (n = 4 experimental settings with 3 biological replicates for each. Five organoids for each well were randomly measured. (M) Growth of mouse liver tumor organoids determined by Alamar Blue Assay (n = 4 experimental settings with 3 biological replicates for each). (N) The number of formed human tumor organoids in the presence or absence

of CAFs in a trans-well system (n = 3 experimental settings with 3 biological replicates for each, Mann-Whitney *U* tests). (O) The size of formed human tumor organoids in the presence or absence of CAFs in a trans-well system (n = 3 experimental settings with 3 biological replicates for each. Five organoids for each well were randomly measured. (P) Growth of mouse liver tumor organoids determined by Alamar Blue Assay (n = 3 experimental settings with 3 biological replicates for each). (B, C, E, G, H, J, L, M, O, P) Data are expressed as means ± SD; Mann-Whitney *U* tests; *p < 0.05, **p < 0.01, ***p < 0.001. CAFs, cancer associated fibroblast.

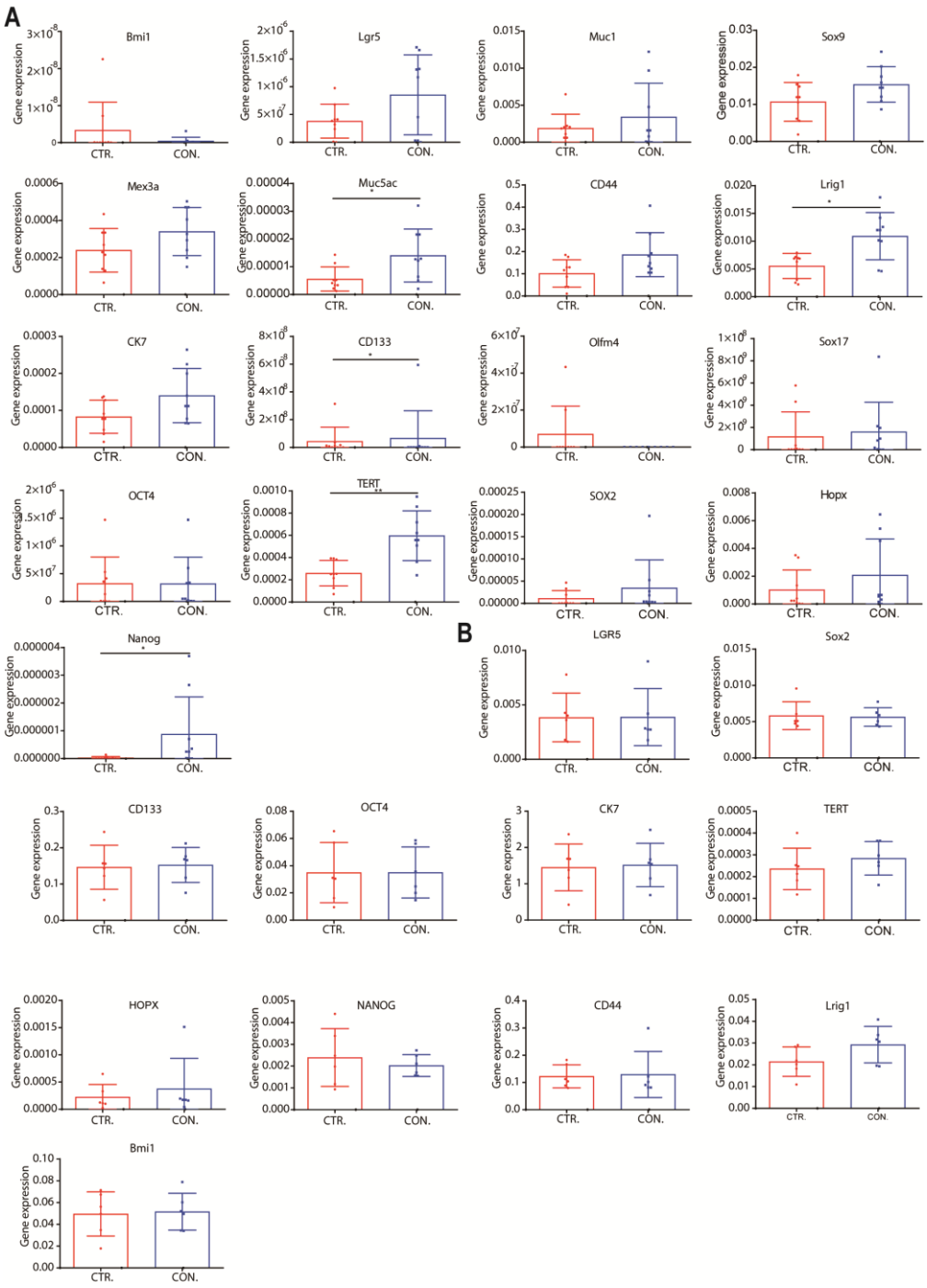

Figure 7. **The expression profile of stem cell markers in tumor organoids**. (A) Stem cell markers expression of mouse organoids in the presence or absence of CAFs conditioned medium (n = 9). (B) Stem cell markers expression of human organoids in the presence or absence of CAFs conditioned medium (n = 6). (A-B) Data are expressed as means ± SD; Mann-Whitney *U* tests; *p < 0.05, **p < 0.01. CAFs, cancer associated fibroblast; CTR, control; CON, conditioned.

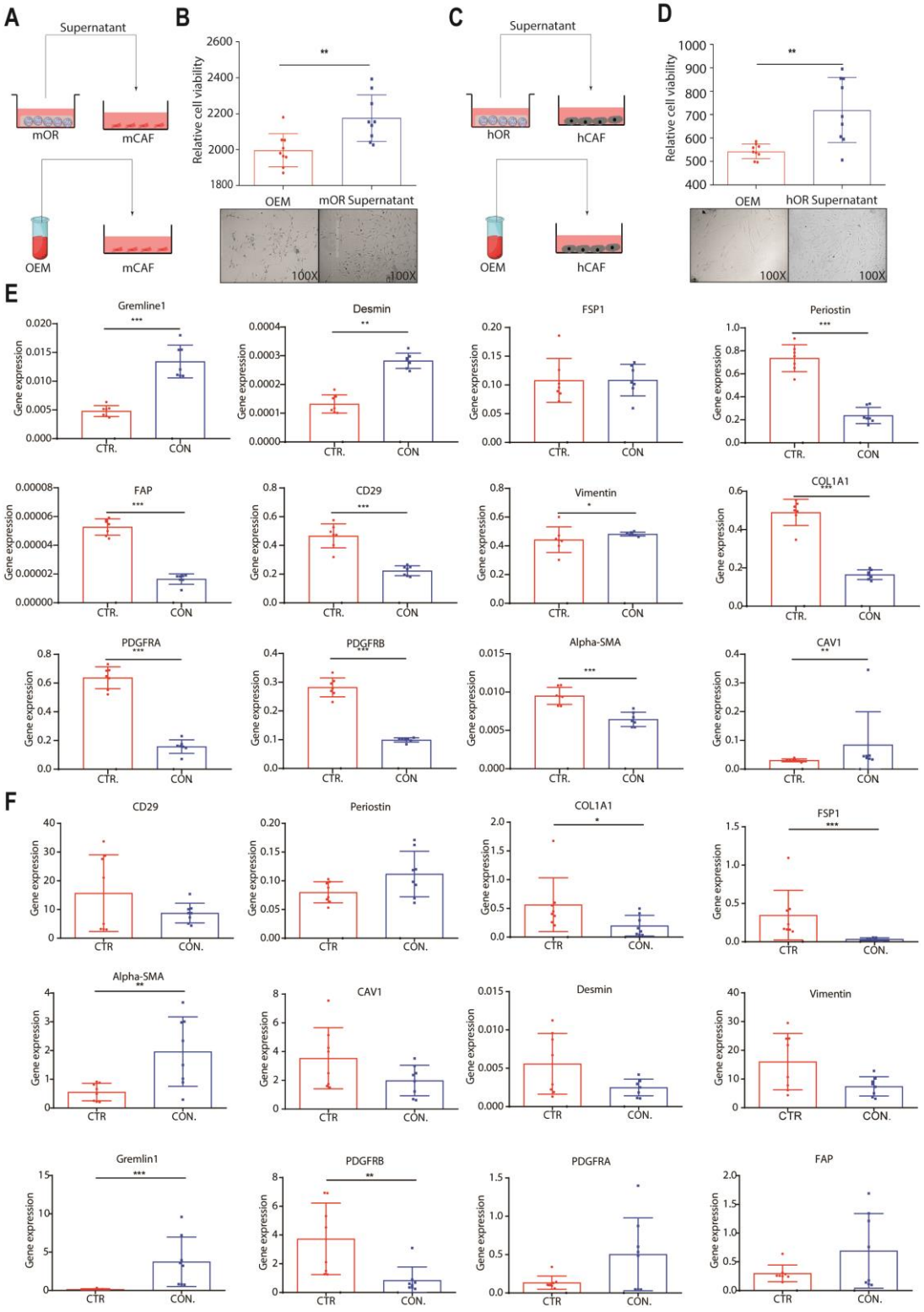

Figure 8. **Supernatant of organoids on the growth, morphology and gene expression of CAFs.** (A-B) Growth of mouse CAFs in the presence or absence of organoids conditioned medium (n = 9). (C-D) Growth of human CAFs in the presence or absence of organoids conditioned medium (n = 9). (E) Expression profile of mouse CAFs markers in the presence or absence of organoids conditioned medium (n = 8). (F) Expression profile of human CAFs markers in the presence or absence of organoids conditioned medium (n = 8). (B, D, E, F) Data were presented as Mean ± SD. Mann-Whitney U tests. *p < 0.05, **p < 0.01, ***p < 0.001. CAFs, cancer associated fibroblast; CTR, control; CON, conditioned.

CAFs promote the growth of organoids in co-culture

After co-culturing digested single murine organoid cells with CAFs for 7 days and those of human origin for 14 days, we counted the number of formed organoids and randomly measured the diameter of five organoids in each well (Figure 5A). We verified the accuracy of our measurement by measuring the diameter both under immunofluorescence and bright field vision (Figure 5B). We found that co-culturing CAFs enlarged the size of formed organoids, but did not affect the number (Figure 5C-G). This effect was already apparent at a 1:1 ratio input of organoid and CAF cells, but was not enhanced by further increasing the input of CAFs (Figure 5H-K). Enhanced expression of the cell proliferation marker Ki67 in co-cultured organoids further supports this promoting effect (Figure 5L-O). Therefore, these results suggest that CAFs may not regulate the efficiency of organoid initiation, but promote the growth of formed organoids in the co-culture system.

Reciprocal enhancement of CAFs and tumor organoids growth through paracrine signaling

The aforementioned results were demonstrated in the co-culture system, but this does not exclude the possibility of paracrine effects. To investigate this, we established a trans-well system in which CAFs were seeded on the top and organoids on the bottom layer (Figure 6A). After incubation for 10 days, we found that CAFs did not affect the number, but, reminiscent to co-culture, increased the diameter of formed organoids in the setting of cells of mouse origin (Figure 6B-D). Cell Titer Assay and Alamar Blue Assay further confirmed these results (Figure 6E). Same results were observed in the setting of other combination of mouse cells as well as cells of human origin (Figure 6F-P). Interestingly, several stem cell markers including Lrig1, Muc5ac, CD133, TERT, NANOG were upregulated in mouse organoids by the paracrine effect of CAFs (Figure 7A). But this was not observed in human organoids (Figure 7B).

Next, we examined the reverse effect by exposing CAFs to the conditioned medium of tumor organoids (Figure 8A and C). We found that education with soluble factors from tumor organoids significantly promoted the growth of CAFs (Figure 8B and D). Profiling a panel of potential CAFs makers revealed that gremlin1 was upregulated in both mouse and human CAFs (Figure 8E and F). Previous studies have documented that gremlin1 suppresses the function of bone morphogenetic proteins which may support cancer stemness.[23] Thus, CAFs and organoids reciprocally facilitate their growth at least partially through paracrine signaling.

CAFs promote the growth of organoids-formed tumors in mice

We have previously demonstrated that liver tumor organoids are capable of forming tumors upon subcutaneous transplantation in immunodeficient mice.[5] We thus investigated the effects of CAFs on organoids-based tumor formation and growth *in vivo* (Figure 9A). We found that co-transplantation of organoids with CAFs lead to more efficient tumor formation (12/12) than transplanting mouse organoids alone (9/12) (Figure 9B). More importantly, co-transplantation resulted in much larger tumors compared to transplanting organoids alone (tumor weight 0.60 ± 0.31g, n=12, VS. 0.33 ± 0.13g, n=9, $p<0.05$, Figure 9C). Immunohistochemistry and immunofluorescence staining confirmed the presence of CAFs in the tumor tissue of mice co-transplanted with CAFs (Figure 9D-F). Interestingly, CAFs are also abundantly present in the tumors of control mice transplanted with organoids alone (Figure 9D

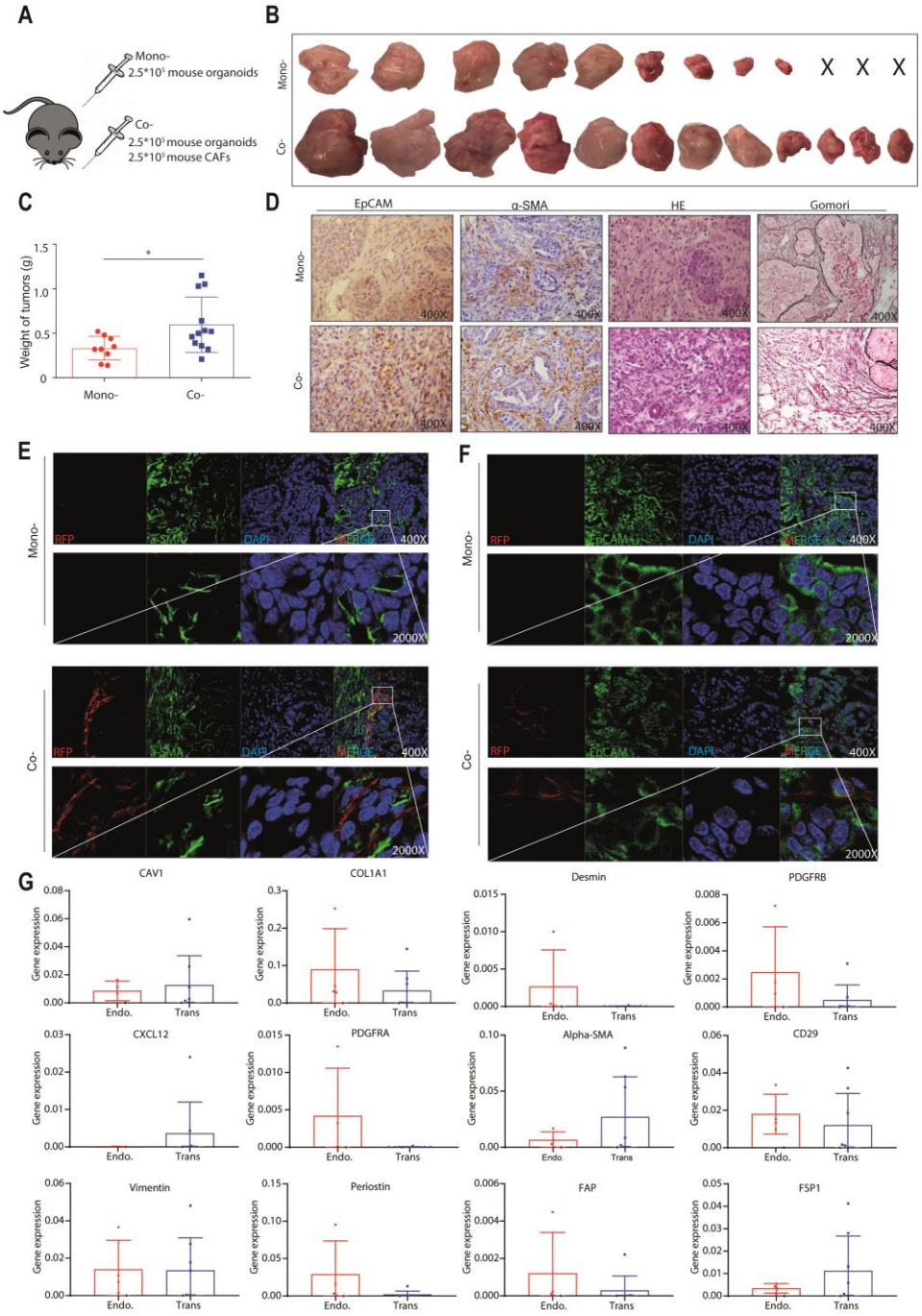

Figure 9. **Mouse CAFs promote the growth of mouse organoids formed tumors *in vivo*.** (A) 2.5*10^5 mouse tumor organoids together with or without 2.5*10^5 mouse CAFs were transplanted into NSG mouse. (B) Representative pictures showed the tumors from mono- and co-transplantation. (C) The weight of tumors from mono- or co-transplantation (n = 9 for xenografts from organoids transplantation only, n = 12 for xenografts from CAFs and organoids co-transplantation, *P < 0.05). (D) The representative immunohistochemistry staining of EpCAM, α-SMA, H&E and Gomori for tumors from mono- or co-transplantation (magnification 400X). (E) The representative confocal image of α-SMA expression for tumors from mono- or co-transplantation (magnification 400X, inset magnification 2000X). (F) The representative confocal image of EpCAM expression for tumors from mono- or co-transplantation (magnification 400X, inset magnification 2000X). (G) Expression profile of CAF markers for transplanted and endogenously recruited mouse CAFs (Endogenous, n = 4; Transplanted, n = 8). (C, G) Data were presented as mean ± SD, Mann-Whitney *U* tests. CAFs, cancer associated fibroblasts;

NSG, NOD scid gamma mouse; EpCAM, epithelial cell adhesion molecule; α-SMA, alpha smooth actin; H&E, hematoxylin and eosin; Endo, endogenous; Trans, transplant.

and E), suggesting that tumor organoids and the formed tumors can efficiently recruit endogenous CAFs. As the transplanted CAFs express RFP, we were able to separate the transplanted CAFs and endogenous CAFs by using FACS. The expression levels of some CAF markers are indeed substantially different but the pattern is not very clear (Figure 9G).

Consistently, co-transplantation with human CAFs also promoted tumor formation and growth of patient CCA organoids in mice (Figure 10A-C). Immunohistochemistry and immunofluorescence staining confirmed the presence of CAFs in the tumors (Figure 10D and F). We next isolated the *in vivo* educated human CAFs from the tumors and compared their gene expression with *in vitro* cultured CAFs. We found a distinct expression pattern of the CAF markers, showing a trend of enhanced expression of CAF markers in tumor educated CAFs (Figure 10G). Taken together, CAFs support organoids-based tumor formation and growth *in vivo*.

CAFs protect tumor organoids from drug treatment

We next examined the effects of CAFs on the response of tumor organoids to the anti-cancer drugs including Sorafenib, Regorafenib and Fluorouracil (5-FU). Mouse liver tumor organoids were treated with Sorafenib, Regorafenib or 5-FU in the presence or absence of CAFs (Figure 11A). Although the number of formed organoids are not significantly different, the diameters of organoids are significantly larger when co-culturing with CAFs compared with organoids alone (Figure 11B-H). Of note, most of the organoids that survived from the treatment were surround by CAFs (Figure 11I and J). These results were further confirmed in human liver tumor organoids, treated with Sorafenib, Regorafenib or 5-FU in the presence or absence of human CAFs (Figure 12A-H). Of note, treatment of Sorafenib, Regorafenib or 5-FU at 5 uMol/ml exerted moderate inhibition on cultured CAFs (Figure 11K, 12I).

To investigate whether these effects are related to paracrine signaling, both mouse and human organoids were exposed to conditioned medium of CAFs and treated with Sorafenib, Regorafenib or 5-FU (Figure 13A and K). Interestingly, organoids in the presence of CAF conditioned medium are more resistant to the treatment, as shown by higher half maximal inhibitory concentrations (IC50) (Figure 13B, E, H, L, O, R), and the morphological appearance (Figure 13C, F, I, M, P, S). A dynamic response of treatment at different time points revealed similar pattern of resistance in the presence of CAF conditioned medium (Figure 13D, G, J, N, Q, T). Taken together, these findings demonstrate that CAFs protect tumor organoids from anti-cancer treatment.

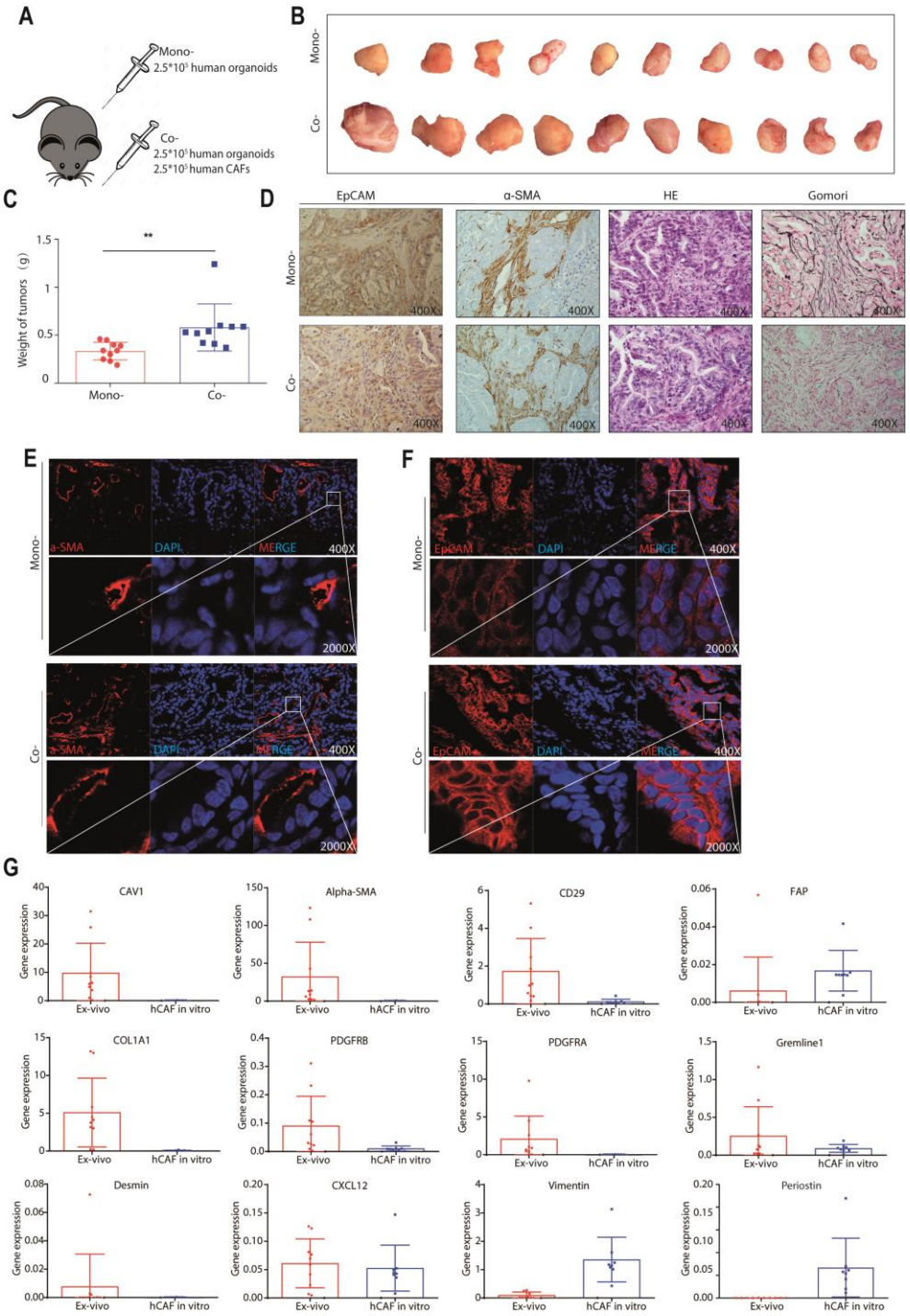

Figure 10. **Human CAFs promote the growth of patient CCA organoids formed tumors *in vivo*.** (A) 2.5*10^5 human tumor organoids together with or without 2.5*10^5 human CAFs were transplanted into NSG mouse. (B) Representative pictures showed the tumors from mono- and co-transplantation. (C) The weight of tumors from mono- or co-transplantation (n = 10 for both groups, **P < 0.01). (D) The representative immunohistochemistry staining of EpCAM, α-SMA, H&E and Gomori for tumors from mono- or co-transplantation (magnification 400X). (E) The representative confocal image of α-SMA expression for tumors of mono- or co-transplantation (magnification 400X, inset magnification 2000X). (F) The representative confocal image of EpCAM expression for tumors from mono- or co-transplantation (magnification 400X, inset magnification 2000X). (G) Expression profile of CAF markers for *in vivo* educated human CAFs from xenograft tumors compared to *in vitro* cultured CAFs (Educated n = 10, in-vitro n = 8). (C, G) Data were presented as mean ± SD, Mann-Whitney *U* tests. CAFs, cancer

associated fibroblasts; CCA, cholangiocarcinoma; NSG, NOD scid gamma mouse; EpCAM, epithelial cell adhesion molecule; α-SMA, alpha smooth actin; H&E, hematoxylin and eosin.

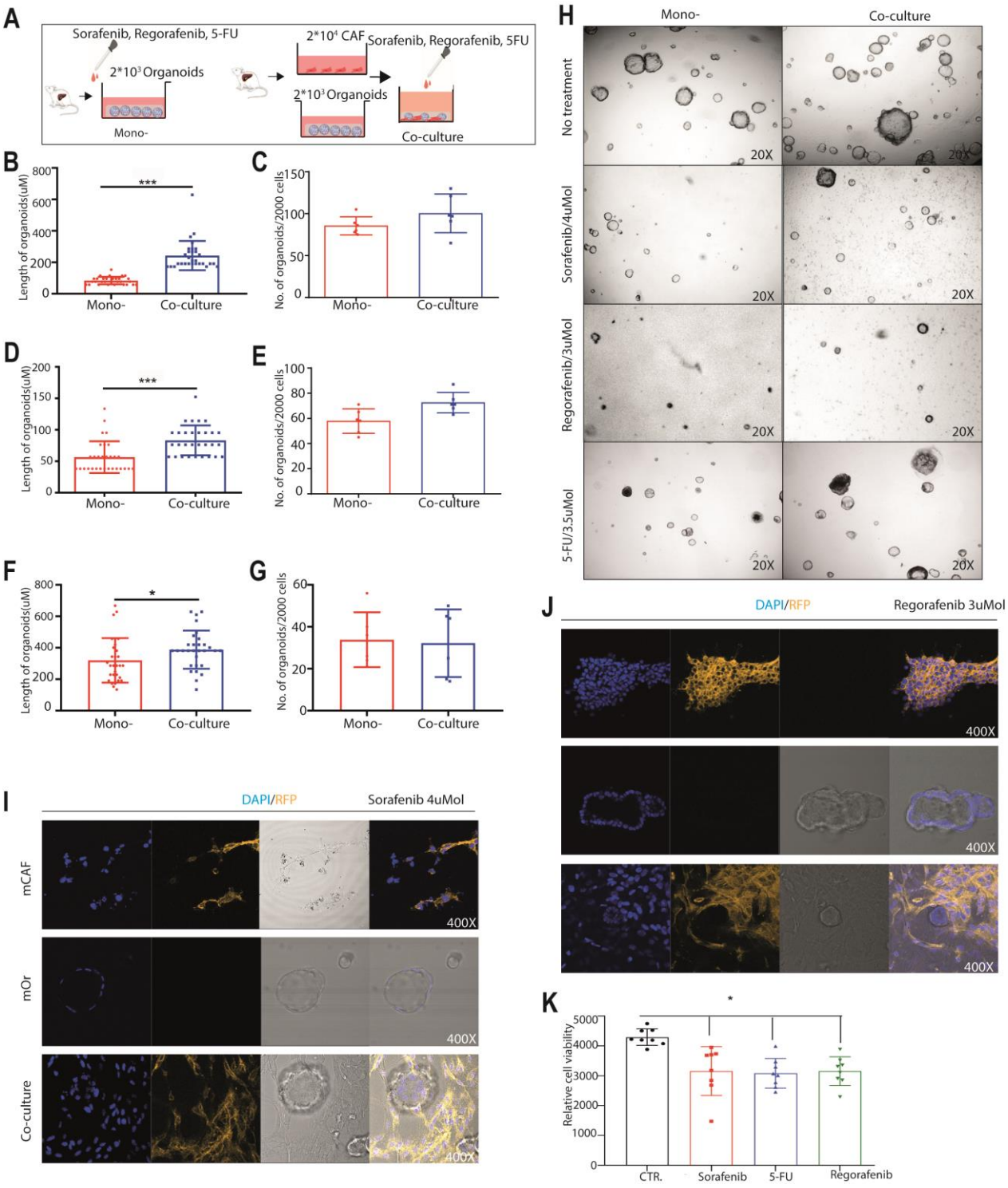

Figure 11. **Mouse organoids in the presence or absence of CAFs in response to anti-cancer drugs.** (A) An outline of the experimental strategy used to illustrate the drug administration on mouse tumor organoids with or without CAFs. (B-G) Mouse organoids in response to treatment of Sorafenib (4 uM/ml), Regorafenib (3 uM/ml) or 5-FU (3.5 uM/ml) with or without CAFs (n = 6). (H) Representative image of treatment for mouse mono-culture and co-culture (Magnification 20X). (I-J) Representative confocal image of mouse CAFs, organoids and co-cultures in response to treatment of Sorafenib and Regarafenib (Magnification 400X). (K) Mouse CAFs in response to anti-

cancer drugs (Sorafenib [5 uM/ml], Regorafenib [5 uM/ml], 5-FU [5 uM/ml]; n = 8). (B, D, F) Five organoids for each well were randomly measured. (B-G, K) Data were presented as mean ± SD, Mann-Whitney *U* tests, *p < 0.05, ***p < 0.001. CAFs, cancer associated fibroblast; 5-FU, Fluorouracil, CTR, control.

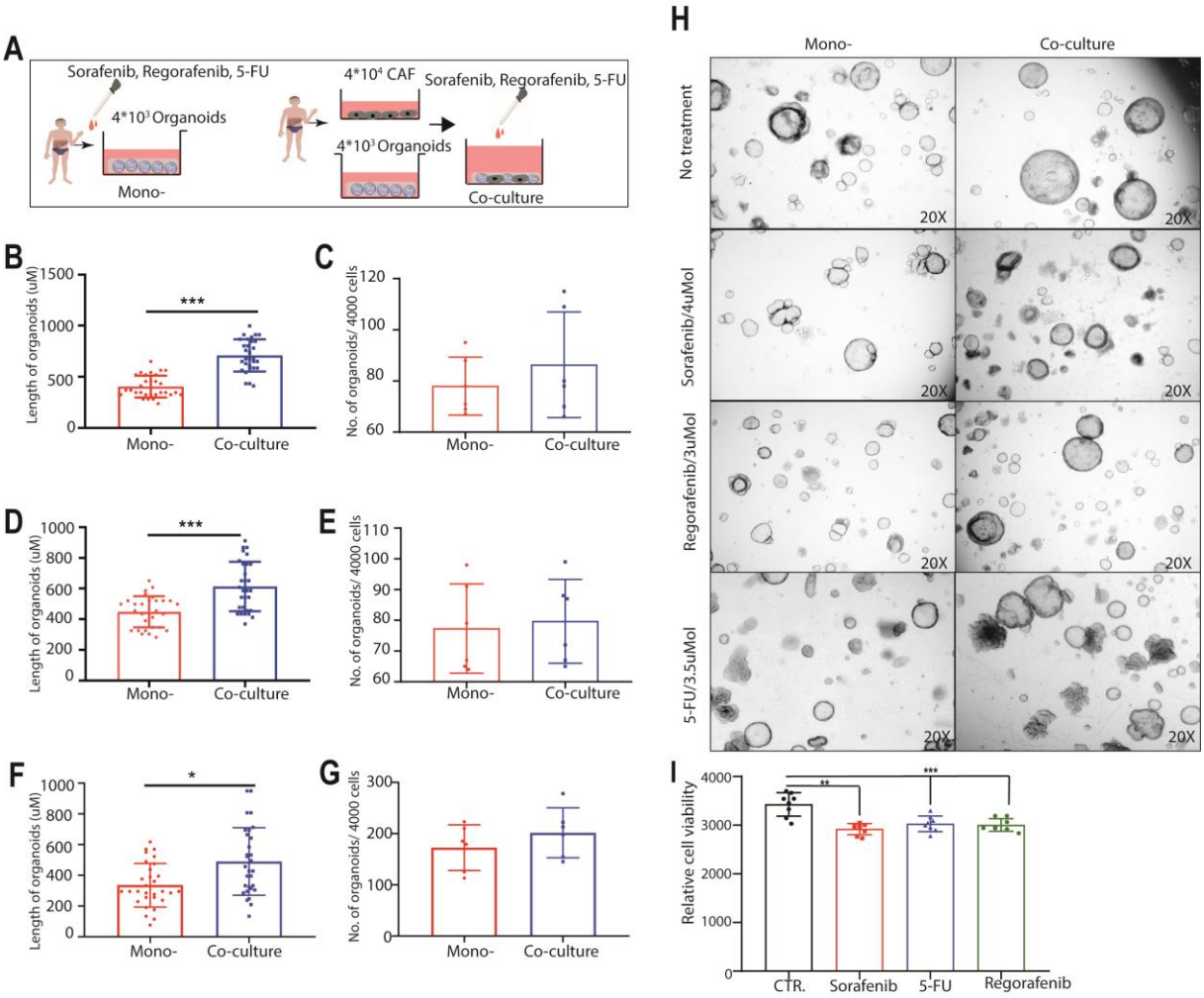

Figure 12. **Human organoids in the presence or absence of CAFs in response to anti-cancer drugs.** (A) An outline of the experimental strategy used to illustrate the drug treatment on human tumor organoids with or without CAFs. (B-G) Human organoids in response to treatment of Sorafenib (4 uM/ml), Regorafenib (3 uM/ml) or 5-FU (3.5 uM/ml) with or without CAFs. (H) Representative image of human mono-culture and co-culture with or without treatment (Magnification 20X). (I) Human CAFs in response to anti-cancer drugs (Sorafenib [5 uM/ml], Regorafenib [5 uM/ml], 5-FU [5 uM/ml]; n = 8). (B, D, F) Five organoids for each well were randomly measured. (B-G, I) Data were presented as mean ± SD, Mann-Whitney *U* tests, *p < 0.05, **p < 0.01, ***p < 0.001. CAF, cancer associated fibroblasts; 5-FU, Fluorouracil.

Discussion

CAFs as a vital component of the tumor microenvironment have been extensively demonstrated to support cancer development and progression, and to promote treatment resistance.[24, 25] The clinical significance of CAFs in disease progression, therapeutic response and patient outcome has been widely reported in various types of cancer.[26-28] In this study, we found that enhanced expression of CAF markers in liver tumors are associated

with poor patient outcome. Contemporary, a major challenge is how to dissect the interactions of cancer cells with CAFs in robust experimental models. We successfully established 3D co-culture systems of liver tumor organoids and CAFs of both mouse and human origins to study the interactions between these two cell types.

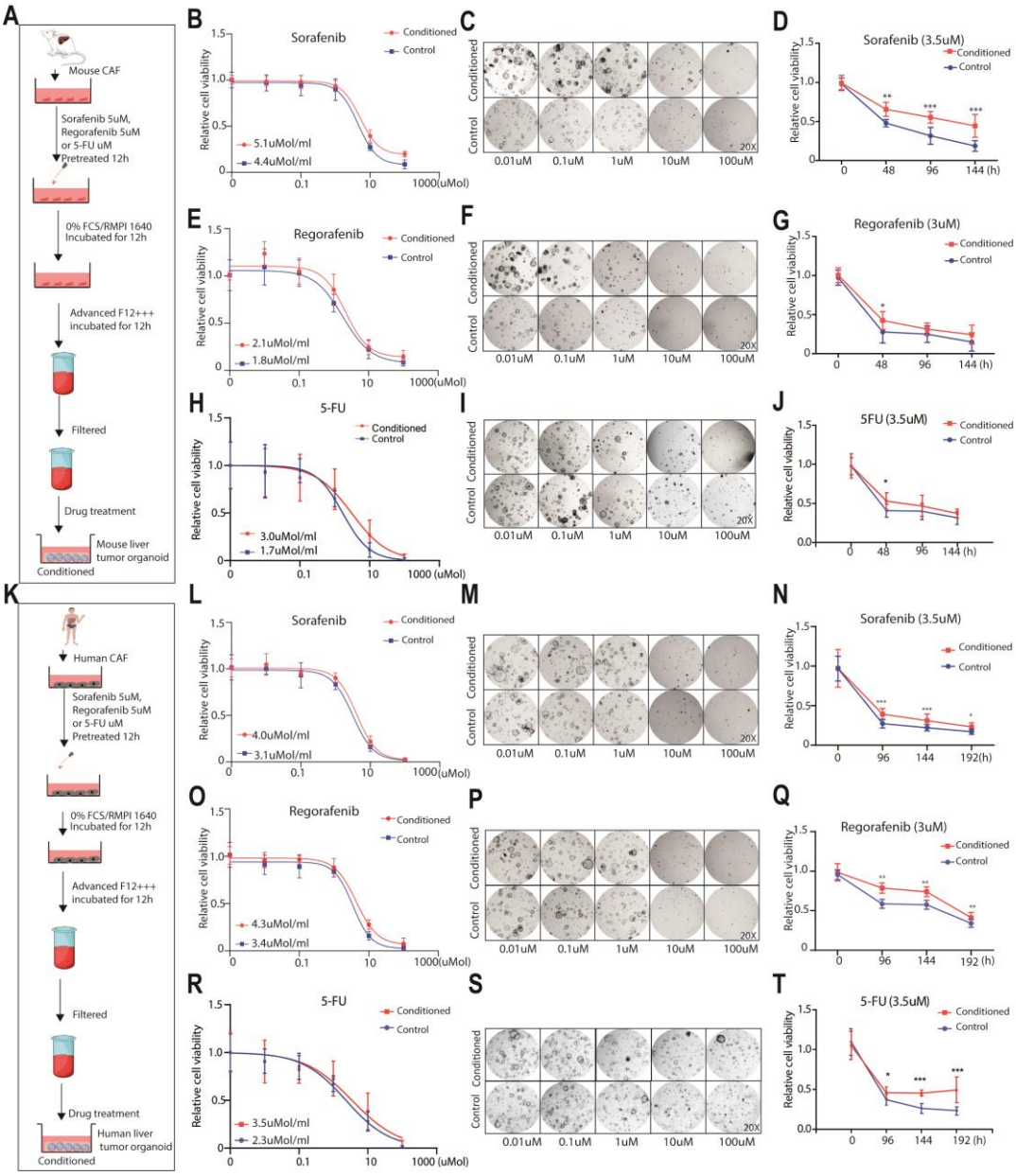

Figure 13. **Organoids in the presence or absence of CAFs conditioned medium in response to the anti-cancer treatment.** (A, K) An outline of the experimental strategy used to illustrate drug treatment on tumor organoids with or without conditioned medium of pretreated CAFs. (B, E, H, L, O, R) Organoids in the presence or absence of conditioned medium of pretreated CAFs were treated with a serial concentration of Sorafenib, Regorafenib or 5-FU, and the IC50 was determined (n = 9; Data were presented as mean ± SD). (C, F, I, M, P, S) Representative image of mouse or human tumor organoids in the presence or absence of conditioned medium of pretreated CAFs, treated with a serial concentrations of Sorafenib, Regorafenib or 5-FU for 10 days of mouse cells and 14 days of human cells (Magnification 20X). (D, G, J, N, Q, T) Cell viability assays were performed and measured at the indicated times, using mouse or human tumor organoids incubated with indicated anti-cancer drugs and parenthesized concentration in the presence or absence of conditioned medium of pretreated CAFs. n

= 9. Graphs show means ± SD of data normalized to *t* = 0,. Mann-Whitney *U* tests, *P < 0.05, **P < 0.01, ***P < 0.001. CAF, cancer associated fibroblasts; IC50, half maximal inhibitory concentration; 5-FU, Fluorouracil.

A prominent role of CAFs is thought to shape the stem cell niche to nurture CSCs, whereas the conventional 2D culture of immortalized cancer cell lines is far from satisfactory in recapitulating the properties of CSCs.[29, 30] The recent development of organoids technology that grows embryonic or adult mammalian stem cells-derived 3D organotypic structures *in vitro* has greatly facilitated stem cell research. This now has been extended to the culture of primary cancer cells that recapitulates the genomic and structural architecture of the tumor-of-origin, and especially CSC compartment.[31] Tumor organoids have been successfully established across variety of cancer types, including liver cancer.[4, 5, 32] The co-culture model of organoids with CAFs was first pioneered in pancreatic cancer, as pancreatic cancer has the most extensive stromal reaction accounting for up to 90% of the tumor volume.[33, 34] In this study, we established the co-culture of liver tumor organoids with CAFs. We first cultured organoids and CAFs from DEN-induced mouse liver tumors. We have recently shown that these organoids can recapitulate the heterogeneity of patient liver cancer types to some extent.[5] For patient liver cancer, organoids are much easier to be cultured from CCA compared to HCC,[4] and therefore we used CCA organoids for establishing the model. Our model systems shall enable the detailed study of interactions between liver cancer cells, especially CSCs, with CAFs.

CAFs secrete a variety of cytokines, chemokines and growth factors to create a tumor-permissive microenvironment.[35] Many factors like chemokine ligand 5 (CCL-5), CXCL12, transforming growth factor beta (TGFβ), insulin-like growth factors (IGF), epidermal growth factors (EGF), fibroblast growth factors (FGF), IL-6, IL-8, IL-10 and IL-11 secreted by CAFs have an essential role in regulating cancer development.[26, 29, 36-42] In addition to biochemical crosstalk, direct contact between CAFs and cancer cells also play a critical role in tumor progression. By extracellular matrix remodeling, CAFs facilitate the migration of cancer cells.[20] On the other hand, CAFs directly exert a pulling force on cancer cells through epithelial to mesenchymal transition (EMT) by mediating N-cadherin and E-cadherin expression.[43] These results are in accordance with our findings that CAFs confer growth advantages of tumor organoids in co-culture with cell-cell contact and in a trans-well system via paracrine signaling. Furthermore, co-transplantation with CAFs promotes organoids-based tumor formation and growth in mice. In pancreatic tumor organoids, a Wnt-non-producing subtype requires Wnt ligands from CAFs.[33] CAF-derived HGF has been reported to regulate liver tumor initiating cells via activation of FRAI in an Erk1, 2-dependent manner.[17] In our model, the exact contribution of paracrine signaling and physical interaction, and the underline molecular mechanisms, remain to be further explored.

Recruitment of fibroblasts to tumor stroma is regulated by multiple factors, which is highly context-dependent but remains not fully understood. It has been suggested that during tumor initiation, CAFs can be differentiated from the local fibroblast population of the epithelial stroma up on stimulation by transforming growth factor, whereas at later tumor progression stages, CAFs are mainly recruited from distal locations.[44-46] Thus, the origin of CAFs appears diverse and can be derived from different sources, such as tissue residual fibroblasts, bone marrow-derived cells, endothelial cells, pericytes, vascular smooth muscle cells, or even cancer cells that undergo EMT.[47-49] However, most of the previous studies suggest CAFs are non-cancer cells. In our study, we found our CAFs are negative for AFP and EpCAM, the

markers that are expressed by liver tumor organoids. Furthermore, we did not observe tumor formation by transplanting a large number of CAFs into flank of NSG immunodeficient mice. These results suggest that phenotypically and functionally our CAFs are not cancer cells. The different origin and different context may endow distinct phenotypes and functions of CAFs. This may partially explain our exploratory observation that *in vitro* cultured, transplanted and *in vivo* spontaneously recruited CAFs express different patterns of CAF markers.

Development of drug-resistance is a relentless clinical challenge for cancer treatment.[50] This re-enables tumor growth, cancer cell dissemination and early onset of metastasis. Studies on the mechanisms of therapy resistance have primarily focused on the intrinsic properties of tumor cells. Emerging evidence has redirected to the role of the organ/tumor-specific microenvironment for developing drug resistance. CAFs contribute to treatment resistance mainly through impaired drug delivery and biochemical signaling. Remodeled ECM by CAFs acts as a physical barrier to inhibit the uptake of anti-cancer drugs by increasing intratumoral interstitial fluid pressures and inducing vascular collapse.[51, 52] CAFs-derived soluble factors including IL-6, IL-17A, IGF1, IGF2 and nitric oxide can indirectly mediate the development of cancer treatment resistance.[51, 53-55] Our study revealed that co-culture with CAFs confer resistance of liver tumor organoids to the clinically used anti-cancer drugs including 5-FU, Sorafenib and Regorafenib. This effect was recapitulated by adding conditioned medium from CAFs. However, whether this effect occurs *in vivo* and the involved molecular mechanisms remain to be further studied.

A recent study has shown that the CAF population is implicated in immune dysregulation and associated with immunotherapy outcome in melanoma patients.[56] Interestingly, cultured CAFs from colon tumor, as well as lung cancer, have been reported to express immune checkpoint molecule programmed death 1 ligand 1/2, which strongly induce T cell exhaustion.[57, 58] CAFs may also indirectly regulate the immune response through ECM remodeling by acting as a barrier which block the access of immune cells to cancer cells.[59] A co-culture model with human pancreatic cancer organoids, matched stromal and immune cells has been recently developed. Thus, we call the further advance of our models by incorporating immune cells that shall enable the study of tumor-stroma and tumor immune interaction and the assessment of immunotherapeutic such as checkpoint inhibitors in the context of T-cell infiltration.[60] Because the clinical benefits of immune-based therapies for HCC are evident, and ongoing clinical trials will soon establish their role in management of HCC patients.

In summary, we have successfully established 3D co-culture models of liver tumor organoids with CAFs of mouse or human origin. We have revealed the robust effects of CAFs in liver cancer nurturing and treatment resistance. These model systems will be helpful for future research on the interactions of liver cancer cells with the stromal compartment and facilitate therapeutic development.

Materials and methods

Mouse liver tumor organoid culture

Mouse liver tumor organoids were cultured from DEN-treated LGR5-DTR-EGFP mice with histologically verified liver tumors. Tumor tissue was minced and digested with a digestion solution: Collagenase type XI (0.5 mg/ml, Sigmal Alrich, C9407), Dispase (0.2 mg/ml, Gibco, 17105041), 1% fetal bovine serum in Dulbecco's modified Eagle's medium (DMEM, 37°C, 30 mins, Lonza,). The tissue debris was allowed to settle, and the dissociated cells were pelleted and washed in Advanced DMEM/F12 (Invitrogen) and seeded in Matrigel (BD bioscience, 356231). After the Matrigel became solid, expansion medium was slowly added in. Mouse organoid expansion medium (OEM) was based on mouse organoid basic medium (OBM, Advanced DMEM/F12 supplemented with 1% Penicillin/Streptomycin [Life technologies, 15140122], 1% Glutamax [Westburg BV, BE-17-605E/U1], 10 mM HEPES [Westburg BV, be-17-737E]), B27 (2% vol/vol, Life Technologies Europe BV, 17504-001), N2 (1%, vol/vol, Life Technologies Europe BV, 17502001), N-acetylcysteine (1.25 μM, Sigma–Aldrich, A7250), gastrin (10 nM, Sigma Aldrich, G9145), epidermal growth factor (EGF, 50 ng/ml, PeproTech, AF-100-15), R-spondin 1 (10% vol/vol, conditioned medium produced by 293T-H-RspoI-Fc cell line), fibroblast growth factor 10 (FGF10, 100 ng/ml, PeproTech, 100-26), nicotinamide (10 mM, Sigma–Aldrich, N0636) and hepatocyte growth factor (HGF, 50 ng/ml, PeproTech, 167100-39-0500). For the initial 3 days, the organoids were cultured with organoid initiation medium (OIM) supplemented with Noggin (10% vol/vol, conditioned medium produced by 293T-HA-Noggin cell line), Wnt3a (10% vol/vol, conditioned medium produced by L-Wnt3a cell line), and Y-27632 (10.5 μM, Sigma-Aldrich, Y0503).

To passage, cold OBM was used to collect the organoids. Organoids were mechanically dissociated into small pieces by pipetting, and then seeded back into fresh Matrigel again. Passaging was performed at a ratio from 1:6~1:10 per week according to the growth of the organoids. To create frozen stocks, organoids were passaged and mixed with Freeze medium (90% FBS supplemented with 10% DMSO) using standard procedures. Cultures were thawed using standard thawing procedures, washed once with OBM, and seeded in Matrigel (Corning BV, 356231) with OIM for the first passage.

Isolation and culture of mouse CAFs

Mouse CAFs were isolated from DEN-induced Rosa26-mT mice with histologically verified liver tumors. CAFs were isolated by using an outgrowth isolation. Tissue from tumor edge was minced and digested with a digestion solution: Collagenase type XI (0.5 mg/ml, Sigmal Alrich, C7657), Dispase (0.2 mg/ml, Gibco, 17105041), 1% fetal bovine serum in Dulbecco's modified Eagle's medium (DMEM, Lonza) for 30 mins to 2 hours at 37°C in a water bath. Then the sample was filtered by using a filter tip and subsequently quenched in 10% FCS RPMI 1640 medium. The pellet that contained tumor debris was plated in a T25 flask and fibroblast was allowed to grow out and attached to the wall of the flask. To avoid cancer cell contamination, established cell culture was passed at least 3 generations. The medium was changed every 2 days. CAFs were sub-cultured when reaching 80% confluent, banked and used for experimental studies at passages 4-8. The fibroblasts were checked by using immunofluorescence of staining of the fibroblast markers α-SMA (1:1000, Abcam, ab124964), FAP (1:500, Abcam, ab28244) and negative staining for the HCC cell (AFP, 1:50, Sigma-Aldrich, SAB3500533), epithelial cell marker (EpCAM, 1:1000, Abcam, ab71916), endothelial marker (CD31, 1:50, Abcam, ab28364) and immune cell marker (CD45, 1:200, cell signalling, 13917) to exclude contamination of other cells types before subjected to experiments.

Human CCA organoids and CAF culture

OEM for culturing human CCA organoids was based upon OBM, B27(2% vol/vol), N2 (1% vol/vol, Invitrogen), N-acetylcysteine (1.25 μM), gastrin (10 nM), Rspo-1 conditioned medium (10% vol/vol), 10 mM nicotinamide, recombinant human EGF (50 ng/ml), recombinant human FGF10 (100 ng/ml), recombinant human HGF (25 ng/ml), 10 μM Forskolin (Bio-Techn, 1099), 5 μM A8301 (Bio-Techne, 2939/10), and 10 μM Y27632. Upon attainment of dense tumor-derived organoids (2-3 weeks after isolation), they were passaged by mechanical dissociation into small fragments via trituration with pipet, and transferred to fresh Matrigel in the previously defined OEM. Medium was refreshed every 2-3 days

and organoids were passaged in 1:2-1:10 split ratio according to the growth of the organoids. For isolation and culture of human CAFs from HCC and CCA tumors, the protocol was similar as isolation and culture of mouse CAFs.
The study was approved by the medical ethical committee of Erasmus Medical Center. In addition, the study protocol conforms to the ethical guidelines of the 1975 Declaration of Helsinki.

Co-culture of tumor organoids and CAFs
Cold organoid basic medium (OBM) was used to collect the organoids. Organoids were mechanically dissociated into small pieces by pipetting (20-30 times) and further digested into single cells by Trypsin-EDTA (gibco, 37°C, 2 mins). Fluorescence-activated cell sorting sorter (BD FACS AriaTM II) was used to further isolate the single living cells. Propidium iodide staining was used to exclude dead cells. Forward scattered light-width (FSC-Width) with FSC-Area and then side scattered light-width (SSC-Width) with SSC-Area gates were used to select the single cells. CAFs were collected when they were 80% confluent in the flask. After digesting into single cells, fluorescence-activated cell sorting sorter was used to further isolate the single living cells. For co-cultures, different concentrations between CAFs and tumor organoids cells were sorted into 48 wells or 96 wells plates with OBM contained 1% Matrigel. Then the cells were centrifuged in 1000rpm for three minutes and incubated in the plate overnight. The supernatant was removed on the second day and plastic surface of the wells was coated with Matrigel to provide biomatrix for 3D organoid growth. When Matrigel became solid, mouse OEM or human OEM were added. After co-culturing organoid cells with CAFs of mouse origin for 7 days and those of human origin for 14 days, the diameters of organoids was measured by using scale tool from ZenLightEdition Software.

Trans-well culture
For Trans-well culture, 1000 CAF cells were seeded on top of the trans-well membrane (1 µm pore size, Greiner Bio-One, 662610) and 500 single organoid cells growing in the lower compartment in 24-well plates for 10 days for mouse cells and 14 days for human cells.

Alamar blue assay
CAFs or organoids were incubated with Alamar Blue (Invitrogen, 1:20 in DMEM, DAL1100) for two hours (37°C), and then medium was collected for analysis of the metabolic activity of the cells. Absorbance was determined by using fluorescence plate reader (CytoFluor Series 4000, Perseptive Biosystems) at the excitation of 530/25 nm and emission of 590/35 nm. Matrigel with medium only was used as blank control.

Cell titer assay
After culturing organoids 10 days for mouse cells or 14 days for human cells in trans-well, a volume of CellTiter-Glo 3D reagent (Promega, G9681) equal to the volume of cell culture medium was added in each well. The contents were mixed vigorously for 5 minutes to induce cell lysis. The plate was incubated at room temperature for an additional 25 minutes to stabilize the luminescent signal, then luminescence was recorded.

Quantitative real-time RT-PCR
Total RNA was isolated using Macherey-Nagel NucleoSpin RNA II kit (Bioke, Leiden, Netherlands) and quantified using a Nanodrop ND-1000 (Wilmington, DE, USA). Quantification was measured with Nanodrop ND-1000 (Wilmington). RNA was then converted to cDNA by using a cDNA Synthesis kit (TAKARA BIO INC.). Real-time PCR reactions were performed with SYBRGreen-based real-time PCR (Applied Biosystems®) and amplified in a thermal cycler (GeneAmp PCR System 9700). For cells collected from murine tissues, glyceraldehyde 3-phosphate dehydrogenase (*Gapdh*) gene was used as reference. All qRT-PCR primers are listed in Table 1.
Organoids-based tumor formation assay in NSG mice
Five to six weeks old NSG immunodeficient mice were used for *in vivo* tumorigenesis assay. $2.5*10^5$ mouse or human organoids together with or without $2.5*10^5$ CAFs in 100 ul Matrigel subcutaneously

inoculated into the flanks of the mice. 2.5 million CAFs alone were injected as control. Tumor formation and tumor weight were examined and determined after 1-2 months. Mice were housed in a room maintained on a 12h light/dark cycle (light on at 6 a.m.) with food and water provided *ad libitum*. All animal experiments were approved by the Committee on the Ethics of Animal Experiments of the Erasmus Medical Center.

Flow cytometry assay and cell sorting

For FACS analysis, single cells derived from liver and organoids were suspended in DMEM plus 2% FBS. Cell suspensions were analyzed using a BD FACSCalibur or BD FACSAriaTM II. For FACS sort, a BD FACSAriaTM II cell sorter was used to isolate the target cell population. Single cell suspensions of tumor cells were labelled with PE anti-human CD140a Antibody (PDGFRα, 5 µl per million cells in 100 µl volume, Biolegend, 323506), Pacific Blue anti-human CD31 Antibody (2 µl per million cells in 100 µl volume Biolegend, 102422), FITC anti-human CD326 Antibody (EpCAM, 5 µl per million cells in 100 µl volume, Biolegend, 324204), Alexa Fluor 700 anti-human CD45 Antibody (1 µl per million cells in 100 µl volume, Biolegend, 135906) and PE anti-mouse CD140a Antibody (PDGFRα, 5 µl per million cells in 100 µl volume, Biolegend, 135906). For cell sorting, PDGFRα+ for CAFs were collected and processed for RNA extraction and qRT-PCR.

Immunofluorescence

CAFs were fixed in 4% paraformaldehyde (PFA) for 1 hour and permeabilised by incubation in PBS 0.2% Triton 100 (Sigma-Aldrich, X100) at room temperature for 20 minutes. Samples were blocked for 1 hour at room temperature in blocking buffer: 5% BSA PBS 0.05% Tween 20 (Sigma, P9416). Then cells were incubated with primary antibody anti-alpha-SMA (1:1000, Abcam, ab124964), anti-FAP (1:500, Abcam, ab28244), anti-EpCAM (1:1000, Abcam, Ab71916), anti-AFP (1:50, Sigmal-Aldrich, SAB3500533), anti-CD31 (1:50, Abcam, ab28364) and anti-CD45 (1:200, Cell signaling, 13917s) in blocking solution in a wet chamber overnight at 4°C. After three washes of 15 minutes in PBS, the samples were mounted and analyzed by using a Zeiss LSM510meta confocal.

Tissue histology, immunohistology and immunofluorescence

For histological analysis, tumors were dissected into 10% neutral buffered formalin, embedded in paraffin blocks and serial sections were taken. Paraffin-embedded tissue sections were rehydrated before antigen retrieval using pH 6 sodium citrate buffer. After blocking endogenous peroxidase (DAKO peroxidase block), sections were incubated with primary antibodies anti-Alpha-SMA (1:1000, Abcam, ab124964), anti-EpCAM (1:1000, Abcam, Ab71916) overnight. Then sections were incubated with second antibody for 1 h at room temperature. The slides were placed in DAB substrate (Abcam, ab64238) and incubated until desired color is achieved (30s - 3mins). Consequently, the slides were counterstained with haematoxylin. Images were acquired with a Zeiss Axioskop 20 microscope.

For immunofluorescence, samples were further dehydrated with 30% sucrose (Sigma-Aldrich, S0389, 4°C, overnight), stored at -80°C and then sectioned at 8 µm for further analysis. Images were acquired with a Zeiss LSM510meta confocal microscope.

Drug treatment

Organoids and CAFs were digested by using trypsin-EDTA into single cells. By using FACS sorting, 2000 mouse organoids or 4000 human organoids cells with or without CAFs in a 1:10 ratio were seeded and treated with Sorafenib (4 uMol/ml, Bi-connect BV, SC-357801A), Regorafenib (3 uMol/ml, Bio-connect BV, S1178) and 5-FU (3.5 uMol/ml, Sigmal Aldrich, F-6627) for 7 days. The number of formed organoids were counted and their diameters were measured.

To investigate the paracrine effect of CAFs on tumor organoids, Conditional medium of CAFs (about 70% confluent) was collected. In order to recapitulate the effects of anti-cancer drugs on CAFs in co-culture models, CAFs were primed by pretreating with 5 uM Sorafenib, 5 uM Regorafenib or 5 uM 5-FU in 10% FCS RMPI1640 medium for 12 h. Then the supernatant was removed and the cells were washed by PBS for three times. CAFs were then cultured in 0% FCS RMPI 1640 medium for another 12 h. After

removing medium and washing three times with PBS, 10 ml OBM was added and conditioned for 12 h. The supernatant were then collected and filtered by a 40um filter.
For IC50 analysis, 5000 mouse organoids or 10000 human organoids cells were cultured with conditioned or unconditioned medium with a series of concentrations of Sorafenib, Regorafenib or 5-FU for 10 days of mouse cells and 14 days of human cells. Cell viability was measured by Alamar blue assay. To study the dynamic response of treatment at different time points, 5000 mouse or human organoids cells were cultured with conditioned or unconditioned medium with Sorafenib (3.5 uMol/ml), Regorafenib (3 uMol/ml) and 5-FU (3.5 uMol/ml) for 0-192 h. Alamar blue assay was used to determine cell viability.

Online database

We used a database of GEPIA gene expression profiling interactive analysis (http://gepia.cancer-pku.cn/)[61] to evaluate the association of patient overall survival with the expression of target genes in tumor and normal liver tissue as well as at different stages of tumors.

Statistics analysis

Prism software (GraphPad Software 8.0) was used for all statistical analysis. Data were presented as mean ± standard deviation (SD). For comparing gene expression in tumor tissue and surrounding tissue from online database, One-way ANOVA was used to compare the difference between groups. For overall survival rate between high and low expression of genes, Log-Rank or Kaplan-Meier was used to compare the difference between groups. For statistical significance of the differences between groups, we used Mann-Whitney U-test. For Differences were considered significant at a *P* value less than 0.05. All authors had access to the study data and had reviewed and approved the final manuscript.

Reference

[1] Liu J, Dang H, Wang XW. The significance of intertumor and intratumor heterogeneity in liver cancer. Exp Mol Med 2018;50(1):e416.
[2] Batlle E, Clevers H. Cancer stem cells revisited. Nat Med 2017;23(10):1124-34.
[3] Tuveson D, Clevers H. Cancer modeling meets human organoid technology. Science 2019;364(6444):952-5.
[4] Broutier L, Mastrogiovanni G, Verstegen MM, Francies HE, Gavarro LM, Bradshaw CR, Allen GE, Arnes-Benito R, Sidorova O, Gaspersz MP, Georgakopoulos N, Koo BK, Dietmann S, Davies SE, Praseedom RK, Lieshout R, JNM IJ, Wigmore SJ, Saeb-Parsy K, Garnett MJ, van der Laan LJ, Huch M. Human primary liver cancer-derived organoid cultures for disease modeling and drug screening. Nat Med 2017;23(12):1424-35.
[5] Cao W, Liu J, Wang L, Li M, Verstegen MMA, Yin Y, Ma B, Chen K, Bolkestein M, Sprengers D, van der Laan LJW, Doukas M, Kwekkeboom J, Smits R, Peppelenbosch MP, Pan Q. Modeling liver cancer and therapy responsiveness using organoids derived from primary mouse liver tumors. Carcinogenesis 2019;40(1):145-54.
[6] Giraldo NA, Becht E, Remark R, Damotte D, Sautes-Fridman C, Fridman WH. The immune contexture of primary and metastatic human tumours. Current Opinion in Immunology 2014;27:8-15.
[7] Kalluri R. The biology and function of fibroblasts in cancer. Nature Reviews Cancer 2016;16(9):582-98.
[8] Arnold JN, Magiera L, Kraman M, Fearon DT. Tumoral immune suppression by macrophages expressing fibroblast activation protein-alpha and heme oxygenase-1. Cancer Immunology Research 2014;2(2):121-6.
[9] Weissmueller S, Manchado E, Saborowski M, Morris JPt, Wagenblast E, Davis CA, Moon SH, Pfister NT, Tschaharganeh DF, Kitzing T, Aust D, Markert EK, Wu J, Grimmond SM, Pilarsky C, Prives C, Biankin AV, Lowe SW. Mutant p53 drives pancreatic cancer metastasis through cell-autonomous PDGF receptor beta signaling. Cell 2014;157(2):382-94.
[10] Cadamuro M, Nardo G, Indraccolo S, Dall'olmo L, Sambado L, Moserle L, Franceschet I, Colledan M, Massani M, Stecca T, Bassi N, Morton S, Spirli C, Fiorotto R, Fabris L, Strazzabosco M. Platelet-derived growth factor-D and Rho GTPases regulate recruitment of cancer-associated fibroblasts in cholangiocarcinoma. Hepatology 2013;58(3):1042-53.
[11] Koliaraki V, Pallangyo CK, Greten FR, Kollias G. Mesenchymal Cells in Colon Cancer. Gastroenterology 2017;152(5):964-79.
[12] Sugimoto H, Mundel TM, Kieran MW, Kalluri R. Identification of fibroblast heterogeneity in the tumor microenvironment. Cancer Biol Ther 2006;5(12):1640-6.
[13] Record Owner NLM. Fibroblast-specific protein 1 identifies an inflammatory subpopulation of macrophages in the liver.
[14] Liu AY, Zheng H, Ouyang G. Periostin, a multifunctional matricellular protein in inflammatory and tumor microenvironments. Matrix Biol 2014;37:150-6.
[15] Multhaupt HA, Leitinger B, Gullberg D, Couchman JR. Extracellular matrix component signaling in cancer. Advanced Drug Delivery Reviews 2016;97:28-40.
[16] Fattovich G, Stroffolini T, Zagni I, Donato F. Hepatocellular carcinoma in cirrhosis: incidence and risk factors. Gastroenterology 2004;127(5 Suppl 1):S35-50.
[17] Lau EY, Lo J, Cheng BY, Ma MK, Lee JM, Ng JK, Chai S, Lin CH, Tsang SY, Ma S, Ng IO, Lee TK. Cancer-Associated Fibroblasts Regulate Tumor-Initiating Cell Plasticity in Hepatocellular Carcinoma through c-Met/FRA1/HEY1 Signaling. Cell Reports 2016;15(6):1175-89.
[18] Wang XM, Yu DM, McCaughan GW, Gorrell MD. Fibroblast activation protein increases apoptosis, cell adhesion, and migration by the LX-2 human stellate cell line. Hepatology 2005;42(4):935-45.
[19] Costa A, Kieffer Y, Scholer-Dahirel A, Pelon F, Bourachot B, Cardon M, Sirven P, Magagna I, Fuhrmann L, Bernard C, Bonneau C, Kondratova M, Kuperstein I, Zinovyev A, Givel AM, Parrini MC, Soumelis V, Vincent-Salomon A, Mechta-Grigoriou F. Fibroblast Heterogeneity and Immunosuppressive Environment in Human Breast Cancer. Cancer Cell 2018;33(3):463-79 e10.
[20] Gaggioli C, Hooper S, Hidalgo-Carcedo C, Grosse R, Marshall JF, Harrington K, Sahai E. Fibroblast-led collective invasion of carcinoma cells with differing roles for RhoGTPases in leading and following cells. Nat Cell Biol 2007;9(12):1392-400.
[21] Ratajczak-Wielgomas K, Grzegrzolka J, Piotrowska A, Gomulkiewicz A, Witkiewicz W, Dziegiel P. Periostin expression in cancer-associated fibroblasts of invasive ductal breast carcinoma. Oncol Rep 2016;36(5):2745-54.
[22] Underwood TJ, Hayden AL, Derouet M, Garcia E, Noble F, White MJ, Thirdborough S, Mead A, Clemons N, Mellone M, Uzoho C, Primrose JN, Blaydes JP, Thomas GJ. Cancer-associated fibroblasts predict poor outcome and promote periostin-dependent invasion in oesophageal adenocarcinoma. J Pathol 2015;235(3):466-77.
[23] Ren J, Smid M, Iaria J, Salvatori DCF, van Dam H, Zhu HJ, Martens JWM, Ten Dijke P. Cancer-associated fibroblast-derived Gremlin 1 promotes breast cancer progression. Breast Cancer Res 2019;21(1):109.
[24] Xiong S, Wang R, Chen Q, Luo J, Wang J, Zhao Z, Li Y, Wang Y, Wang X, Cheng B. Cancer-associated fibroblasts promote stem cell-like properties of hepatocellular carcinoma cells through IL-6/STAT3/Notch signaling. Am J Cancer Res 2018;8(2):302-16.
[25] Fang T, Lv H, Lv G, Li T, Wang C, Han Q, Yu L, Su B, Guo L, Huang S, Cao D, Tang L, Tang S, Wu M, Yang W, Wang H. Tumor-derived exosomal miR-1247-3p induces cancer-associated fibroblast activation to foster lung metastasis of liver cancer. Nature communications 2018;9(1):191.
[26] Chen WJ, Ho CC, Chang YL, Chen HY, Lin CA, Ling TY, Yu SL, Yuan SS, Chen YJ, Lin CY, Pan SH, Chou HY, Chen YJ, Chang GC, Chu WC, Lee YM, Lee JY, Lee PJ, Li KC, Chen HW, Yang PC. Cancer-associated fibroblasts regulate the plasticity of lung cancer stemness via paracrine signalling. Nature communications 2014;5:3472.
[27] Ebbing EA, van der Zalm AP, Steins A, Creemers A, Hermsen S, Rentenaar R, Klein M, Waasdorp C, Hooijer GKJ, Meijer SL, Krishnadath KK, Punt CJA, van Berge Henegouwen MI, Gisbertz SS, van Delden OM, Hulshof M, Medema JP, van Laarhoven HWM, Bijlsma MF. Stromal-derived interleukin 6 drives epithelial-to-mesenchymal transition and therapy resistance in esophageal adenocarcinoma. Proc Natl Acad Sci U S A 2019;116(6):2237-42.
[28] Hu G, Wang S, Xu F, Ding Q, Chen W, Zhong K, Huang L, Xu Q. Tumor-Infiltrating Podoplanin+ Fibroblasts Predict Worse Outcome in Solid Tumors. Cell Physiol Biochem 2018;51(3):1041-50.
[29] Su S, Chen J, Yao H, Liu J, Yu S, Lao L, Wang M, Luo M, Xing Y, Chen F, Huang D, Zhao J, Yang L, Liao D, Su F, Li M, Liu Q, Song E. CD10(+)GPR77(+) Cancer-Associated Fibroblasts Promote Cancer Formation and Chemoresistance by Sustaining Cancer Stemness. Cell 2018;172(4):841-56 e16.

[30] Lenos KJ, Miedema DM, Lodestijn SC, Nijman LE, van den Bosch T, Romero Ros X, Lourenco FC, Lecca MC, van der Heijden M, van Neerven SM, van Oort A, Leveille N, Adam RS, de Sousa EMF, Otten J, Veerman P, Hypolite G, Koens L, Lyons SK, Stassi G, Winton DJ, Medema JP, Morrissey E, Bijlsma MF, Vermeulen L. Stem cell functionality is microenvironmentally defined during tumour expansion and therapy response in colon cancer. Nat Cell Biol 2018;20(10):1193-202.
[31] Clevers H. Modeling Development and Disease with Organoids. Cell 2016;165(7):1586-97.
[32] Cao W, Li M, Liu J, Zhang S, Noordam L, Verstegen MMA, Wang L, Ma B, Li S, Wang W, Bolkestein M, Doukas M, Chen K, Ma Z, Bruno M, Sprengers D, Kwekkeboom J, L JWvdL, Smits R, Peppelenbosch MP, Pan Q. LGR5 marks targetable tumor-initiating cells in mouse liver cancer. Nature communications 2020;11(1):1961.
[33] Seino T, Kawasaki S, Shimokawa M, Tamagawa H, Toshimitsu K, Fujii M, Ohta Y, Matano M, Nanki K, Kawasaki K, Takahashi S, Sugimoto S, Iwasaki E, Takagi J, Itoi T, Kitago M, Kitagawa Y, Kanai T, Sato T. Human Pancreatic Tumor Organoids Reveal Loss of Stem Cell Niche Factor Dependence during Disease Progression. Cell Stem Cell 2018;22(3):454-67 e6.
[34] Ohlund D, Handly-Santana A, Biffi G, Elyada E, Almeida AS, Ponz-Sarvise M, Corbo V, Oni TE, Hearn SA, Lee EJ, Chio, II, Hwang CI, Tiriac H, Baker LA, Engle DD, Feig C, Kultti A, Egeblad M, Fearon DT, Crawford JM, Clevers H, Park Y, Tuveson DA. Distinct populations of inflammatory fibroblasts and myofibroblasts in pancreatic cancer. J Exp Med 2017;214(3):579-96.
[35] Yamamura Y, Asai N, Enomoto A, Kato T, Mii S, Kondo Y, Ushida K, Niimi K, Tsunoda N, Nagino M, Ichihara S, Furukawa K, Maeda K, Murohara T, Takahashi M. Akt-Girdin signaling in cancer-associated fibroblasts contributes to tumor progression. Cancer Res 2015;75(5):813-23.
[36] Orimo A, Gupta PB, Sgroi DC, Arenzana-Seisdedos F, Delaunay T, Naeem R, Carey VJ, Richardson AL, Weinberg RA. Stromal fibroblasts present in invasive human breast carcinomas promote tumor growth and angiogenesis through elevated SDF-1/CXCL12 secretion. Cell 2005;121(3):335-48.
[37] Record Owner NLM. Hepatic myofibroblasts promote the progression of human cholangiocarcinoma through activation of epidermal growth factor receptor.
[38] Neufert C, Becker C, Tureci O, Waldner MJ, Backert I, Floh K, Atreya I, Leppkes M, Jefremow A, Vieth M, Schneider-Stock R, Klinger P, Greten FR, Threadgill DW, Sahin U, Neurath MF. Tumor fibroblast-derived epiregulin promotes growth of colitis-associated neoplasms through ERK. Journal of Clinical Investigation 2013;123(4):1428-43.
[39] Vaquero J, Lobe C, Tahraoui S, Claperon A, Mergey M, Merabtene F, Wendum D, Coulouarn C, Housset C, Desbois-Mouthon C, Praz F, Fouassier L. The IGF2/IR/IGF1R Pathway in Tumor Cells and Myofibroblasts Mediates Resistance to EGFR Inhibition in Cholangiocarcinoma. Clin Cancer Res 2018;24(17):4282-96.
[40] Grivennikov S, Karin E, Terzic J, Mucida D, Yu GY, Vallabhapurapu S, Scheller J, Rose-John S, Cheroutre H, Eckmann L, Karin M. IL-6 and Stat3 are required for survival of intestinal epithelial cells and development of colitis-associated cancer. Cancer Cell 2009;15(2):103-13.
[41] Record Owner NLM. Interleukin-11 is the dominant IL-6 family cytokine during gastrointestinal tumorigenesis and can be targeted therapeutically.
[42] Calon A, Espinet E, Palomo-Ponce S, Tauriello DV, Iglesias M, Cespedes MV, Sevillano M, Nadal C, Jung P, Zhang XH, Byrom D, Riera A, Rossell D, Mangues R, Massague J, Sancho E, Batlle E. Dependency of colorectal cancer on a TGF-beta-driven program in stromal cells for metastasis initiation. Cancer Cell 2012;22(5):571-84.
[43] Labernadie A, Kato T, Brugues A, Serra-Picamal X, Derzsi S, Arwert E, Weston A, Gonzalez-Tarrago V, Elosegui-Artola A, Albertazzi L, Alcaraz J, Roca-Cusachs P, Sahai E, Trepat X. A mechanically active heterotypic E-cadherin/N-cadherin adhesion enables fibroblasts to drive cancer cell invasion. Nat Cell Biol 2017;19(3):224-37.
[44] Direkze NC, Hodivala-Dilke K, Jeffery R, Hunt T, Poulsom R, Oukrif D, Alison MR, Wright NA. Bone marrow contribution to tumor-associated myofibroblasts and fibroblasts. Cancer Res 2004;64(23):8492-5.
[45] Roni V, Habeler W, Parenti A, Indraccolo S, Gola E, Tosello V, Cortivo R, Abatangelo G, Chieco-Bianchi L, Amadori A. Recruitment of human umbilical vein endothelial cells and human primary fibroblasts into experimental tumors growing in SCID mice. Exp Cell Res 2003;287(1):28-38.
[46] Ishii G, Sangai T, Oda T, Aoyagi Y, Hasebe T, Kanomata N, Endoh Y, Okumura C, Okuhara Y, Magae J, Emura M, Ochiya T, Ochiai A. Bone-marrow-derived myofibroblasts contribute to the cancer-induced stromal reaction. Biochem Biophys Res Commun 2003;309(1):232-40.
[47] De Wever O, Mareel M. Role of tissue stroma in cancer cell invasion. J Pathol 2003;200(4):429-47.
[48] Elenbaas B, Weinberg RA. Heterotypic signaling between epithelial tumor cells and fibroblasts in carcinoma formation. Exp Cell Res 2001;264(1):169-84.
[49] Tomasek JJ, Gabbiani G, Hinz B, Chaponnier C, Brown RA. Myofibroblasts and mechano-regulation of connective tissue remodelling. Nat Rev Mol Cell Biol 2002;3(5):349-63.
[50] Chen X, Song E. Turning foes to friends: targeting cancer-associated fibroblasts. Nat Rev Drug Discov 2019;18(2):99-115.
[51] Meads MB, Gatenby RA, Dalton WS. Environment-mediated drug resistance: a major contributor to minimal residual disease. Nature Reviews Cancer 2009;9(9):665-74.
[52] Paraiso KH, Smalley KS. Fibroblast-mediated drug resistance in cancer. Biochem Pharmacol 2013;85(8):1033-41.
[53] Kumari N, Dwarakanath BS, Das A, Bhatt AN. Role of interleukin-6 in cancer progression and therapeutic resistance. Tumour Biol 2016;37(9):11553-72.
[54] Roodhart JM, Daenen LG, Stigter EC, Prins HJ, Gerrits J, Houthuijzen JM, Gerritsen MG, Schipper HS, Backer MJ, van Amersfoort M, Vermaat JS, Moerer P, Ishihara K, Kalkhoven E, Beijnen JH, Derksen PW, Medema RH, Martens AC, Brenkman AB, Voest EE. Mesenchymal stem cells induce resistance to chemotherapy through the release of platinum-induced fatty acids. Cancer Cell 2011;20(3):370-83.
[55] Lotti F, Jarrar AM, Pai RK, Hitomi M, Lathia J, Mace A, Gantt GA, Jr., Sukhdeo K, DeVecchio J, Vasanji A, Leahy P, Hjelmeland AB, Kalady MF, Rich JN. Chemotherapy activates cancer-associated fibroblasts to maintain colorectal cancer-initiating cells by IL-17A. J Exp Med 2013;210(13):2851-72.
[56] Wong PF, Wei W, Gupta S, Smithy JW, Zelterman D, Kluger HM, Rimm DL. Multiplex quantitative analysis of cancer-associated fibroblasts and immunotherapy outcome in metastatic melanoma. J Immunother Cancer 2019;7(1):194.
[57] Nazareth MR, Broderick L, Simpson-Abelson MR, Kelleher RJ, Jr., Yokota SJ, Bankert RB. Characterization of human lung tumor-associated fibroblasts and their ability to modulate the activation of tumor-associated T cells. J Immunol 2007;178(9):5552-62.

[58] Pinchuk IV, Saada JI, Beswick EJ, Boya G, Qiu SM, Mifflin RC, Raju GS, Reyes VE, Powell DW. PD-1 ligand expression by human colonic myofibroblasts/fibroblasts regulates CD4+ T-cell activity. Gastroenterology 2008;135(4):1228-37, 37 e1-2.
[59] Joyce JA, Fearon DT. T cell exclusion, immune privilege, and the tumor microenvironment. Science 2015;348(6230):74-80.
[60] Tsai S, McOlash L, Palen K, Johnson B, Duris C, Yang Q, Dwinell MB, Hunt B, Evans DB, Gershan J, James MA. Development of primary human pancreatic cancer organoids, matched stromal and immune cells and 3D tumor microenvironment models. BMC Cancer 2018;18(1):335.
[61] Tang Z, Li C, Kang B, Gao G, Li C, Zhang Z. GEPIA: a web server for cancer and normal gene expression profiling and interactive analyses. Nucleic Acids Res 2017;45(W1):W98-W102.

CHAPTER 12

General discussion and summary

In this thesis I have focussed on diverse but to certain extents related liver diseases. A common denominator might be that they either predispose or constitute cancer of the liver. Liver cancer, which mainly includes the disease entities cholangiocarcinoma (CCA) and hepatocellular carcinoma (HCC) display a rapid increase on an already high incidence and hence liver cancer has become a member of the group of most prevalent types of cancers globally.[1, 2] In view of the inadequacy of current options with respect to clinical management, it is not surprising to note that liver cancer constitutes one of the most common causes of oncological death and as a consequence this group of diseases is considered to be a major global public health challenge.[3] Progress with respect to better therapeutic options is frustratingly inadequate and slow.[4] The body of work in this dissertation was started from the idea that improved prevention and treatment of liver cancer needs improved understanding of not only the molecular and cellular factors governing its initiation and that determine treatment success, including side effects, but also the epidemiological factors driving nosidynamics (temporal changes in disease incidence). In this respect one should take into account that some inflammatory conditions like hepatitis C virus (HCV) infection, hepatitis E virus (HEV) or fatty liver disease predispose to cancer development. Thus I also undertook to start a quest for obtaining a better understanding of inflammatory disease in the liver. The preceding chapters have described the fruits resulting from all these endeavors, while in the present discussion, I strive to summarize these results and to discuss the main discoveries made in the light of the body of contemporary biomedical literature.

Full comprehension the overall approach taken requires an overview of existing relevant literature and thus prior providing an outline of this thesis, in Chapter 1, I provide a concise review on selected aspects of inflammatory disease and stem cells in the liver. In chapter 2, I further elaborate on this by interrogating the compendium of currently available biomedical literature on establishing how droplet dynamically interact with other cellular organelles to exert a variety of biological functions. This relates to chapter 3,4,5 where I investigate direct acting antiviral drugs (DAAs) for the treatment of Hepatitis C. Hepatitis C is an important inflammatory condition of the liver, and a precursor to cirrhosis and HCC. DAAs are highly effective and target viral RNA replication at the stage the virus co-localizes with lipid droplets. Unfortunately, in this thesis I was not able to study how my results on DAA and HCV replication relate to the co-localization of HCV core protein with lipid droplets, but I feel my results on the effectiveness and safety of direct-acting antivirals in eradicating HCV-GT1 in transplant recipients provide important groundwork for a future successor Ph.D student in this respect. Also my work on the proliferation promoted effect of direct-acting antivirals in hepatocellular carcinoma cells might be seen in this light. Moreover fatty liver disease (chapters 6,7,8) closely relates to lipid droplet formation and their growth, and thus my efforts on the prevalence, incidence, disease progression and clinical outcome of fatty liver disease may provide a solid foundation for a future successor to my work. As a future post doc in my host laboratory I might even be able to guide some of the efforts involved. As stated the final consequence of both viral hepatitis and fatty liver disease is cancer development and I attempted to make progress here as well. To this end I studied the role of cancer-associated fibroblasts (CAFs), the major component of tumor microenvironment, in proliferation and drug-resistant of liver tumor cells and the role of

LGR5-marked tumor initiating cells in liver cancer (chapter 9,10,11). Together I hope this thesis constitutes a valuable contribution to the scientific field of hepatic disease.

Hepatitis

HCV has either direct or indirect roles in carcinogenesis and is thought to act mainly through fibrosis in this respect, although viral effect on ß-catenin signaling in hepatocytes have also been proposed to be relevant.[5] Patients with advanced fibrosis or cirrhosis are at increased risk for carcinogenesis because chromosomal alterations that occur in fibrotic tissue are associated with tumor formation.[6] In addition, HCV may promote carcinogenesis through chronic inflammation or stimulation of hepatic stellate cells with subsequent fibrosis as a result. Chronic liver inflammation has been associated with a shift in the aspect of signaling by transforming growth factor beta resulting in a change from tumor suppression to fibrosis and carcinogenesis in response to this morphogen.[7] Ongoing inflammation provokes repeated cycles of cell death and regeneration in hepatic tissue [8] Such repeated cell cycling, especially in an inflammatory environment, is associated with accumulation of mutations that may transform hepatocytes to malignant cells through a multistage process. However, chronic inflammation by itself does not seem to promote carcinogenesis because patients with autoimmune liver disease, who have persistent chronic liver inflammation from the autoimmune process, rarely develop HCC. HCV nonstructural protein genes promote fibrosis partly through inducing transforming growth factor beta expression and activating hepatic stellate cells.[9] This has been demonstrated in cell culture systems where sera from HCV patients stimulate hepatic stellate cell proliferation, which subsequently leads to fibrosis.[9] In addition, HCV core protein may promote carcinogenesis. In a transgenic mouse model HCV core protein led to the development of HCC without the genetic aberrations typically seen in carcinogenesis, such as in colon cancer.[10] Previously, work in my host laboratory had shown that Hepatitis E virus infection induces mitochondrial fusion to facilitate viral replication by interfering with cell-autonomous innate immunity (Yijin Wang, thesis, ISBN: 978-94-6169-903-9). Interestingly, some studies also indicated that moderate tissue damage provoked by HEV infection could be in certain circumstances responsible of the progression of the chronic liver disease toward HCC. The importance of virus-induced inflammation in the context of liver cancer had, however, not been addressed prompting my further investigations in this respect.

To this end in Chapter 3, we compared the different combinations of DAAs in eradication of HCV GT1 recurrence for post-transplant organ recipients. Reinfection of liver allografts is universal in patients with pre-transplantation viremia and occurs at reperfusion, only a few hours after transplantation HCV RNA levels increase reaching peak levels by the fourth postoperative month. Changes induced by HCV infection of the graft can be demonstrated in 70-90% of recipients after 1 year and in 90-95% after 5 years, illustrating the universality of post-transplant HCV infection. Clinical course, severity of recurrent disease and outcome though are highly variable.[11] The most common pathological course is a kind of progressive chronic liver disease not dissimilar to that seen in the immunocompetent population (transplantation patients are routinely place on immunosuppressive regimens to prevent graft rejection), but are

characterized by higher viral loads and faster progression of fibrosis (which is a consequence of an early activation of stellate cells).[12] It is generally assumed that the immune response is the mediator of hepatocyte injury, but how this relates to immunosuppressive regimens these patients receive remains little understood and requires further investigation. The mean time interval from transplantation to the establishment of cirrhosis is 9.5 years. Due to this high speed of liver disease progression in these transplanted patients, re-transplantation is often necessary and hence HCV recurrence accounts for about 30-40% of elective re-transplantation. My results show that DAA treatment is clinically effective with respect to GT1 HCV recurrence in liver transplantation recipients. Of note, an unbalanced application of DAAs for GT1 HCV recurrence appears to exist when different regions are compared. There is a trend that use of first-class of DAAs is confined to European and North American countries. For many countries, even Japan is an example, cost-effectiveness more as achieving a sustained virological response (SVR) per se is the first consideration for clinicians.[13, 14] However, in Asian, Pacific, or African countries, HCV has a distinct epidemiology, also due to that DAA availability is subject to economic constraints and regulatory rules.[15] In our subgroup analysis of liver transplant recipients with SVR12 rate and fibrosis data (METAVIR Fibrosis Score), our detailed analysis supports the latest evidence-based guidelines that DAAs also can be effectively used in eradicating HCV in patients with advanced fibrosis or cirrhosis post LT.[16] We observed a higher SVR12 pooled estimate proportion in patients with mild fibrosis compared with those of advanced fibrosis or cirrhosis, with a trend favoring SVR12 in patients with mild fibrosis. Our results indicated that the capability of HCV eradication by DAAs may be correlated with the levels of liver fibrosis or cirrhosis. Therefore, I recommend DAA treatment early after transplantation.

In Chapter 4, I further explore this line of research and show that the DAA drug Sofosbuvir may induce a proliferation promoting effect of liver cancer cells in vitro. I observed increased single cell-based clonogenic capability in all four HCC cell lines. This is reflected by the significantly increased number and size of formed colonies. I interpret these unexpected results as having important implications and explaining as yet not-understood clinical observations. In fact, higher risk of HCC development has been observed in HCV patients with advanced diseases (e.g. cirrhosis),[17] or previously treated for HCC (e.g. ablation, resection, chemoembolization[18] or liver transplantation[19]). Although the effects seen in such studies are often poo-pooed by attributing such results to bias in selection, my results may indicate a direct promoting effect of DAAs on the rare preexisting transformed tumor cells in the cirrhotic liver, the residual HCC cells that are not completely eradicated by treatment, or the circulating tumor cells in the transplant patients. Despite the low number of these tumor cells, they are likely resemble the so called cancer stem cells that are resistance to chemo- or radiotherapy but responsible for tumor initiation, treatment relapse and recurrence after surgical operation.[20] Thus, DAAs are likely not to have a universal but rather specific effects on particular patients in respect to the risk of HCC development; whereas the current clinical studies are unable to fully resolve the ongoing debate. Complicating matters here is various studies indicate a role for immune cell dysfunction,[21-25], changes in the immune cytokine milieu [26, 27] and activation of angiogenesis [28] as well.

Thus, the distinct not mutually exclusive interpretations are possible and further investigations are necessary to address this issue.

Chapter 5 is a bit of the odd man out in this thesis as I discuss in this chapter global HEV seroprevalence. Although one-third of global population live in HEV endemic areas at risk of infection, the true burden of HEV among the world remains largely unknown. By retrieving data from 75 countries of the six inhabited continents, I estimated that 12.47% of the global population, corresponding to approximately 939 million individuals, has experienced past infection of HEV based on their seropositivity of anti-HEV IgG antibody. Our study reconfirms high seroprevalence of HEV in Asia and Africa.[29, 30] However, the HEV prevalence in Europe was lower than observed in a previous study.[31] The possible explanation for these disparities could be that these other reports involved collecting fewer studies and included relatively small size populations and were thus prone to more bias. Substantial differences in sensitivity and specificity of the anti-HEV IgG ELISA kits from different manufacturers is an important consideration as well.[32, 33] I largely agree with others that the Wantai assay has the highest sensitivity and fortunately this assay is the one that has been most widely used. Accumulating knowledge on HEV biology and transmission routes has facilitated the identification of risk factors for the infection. A wide range of domestic or wild animals have been recognized as reservoirs for the zoonotic strains. As expected, consumption of raw meat is an important risk factor revealed by my meta-analysis. This is in line with previous reports that humans with occupational exposure to pigs are at a high risk for HEV infection.[34, 35] The host range for HEV is ever expanding and cross-species infections commonly occur.[36] Intriguingly, recent evidence has indicated that companion animals including dogs, cats, rabbits and horses might be accidental hosts for HEV and might constitute a source for HEV transmission to human.[37-39] In this study, we found that people who frequently contact with dogs have higher anti-HEV IgG seropositivity. This was not found in people who contact with cats, but the number of studies is very limited. Previous studies have indicated the differences of HEV seroprevalence between rural and urban areas.[40-42] We found that rural compared to urban residents have higher risk of HEV infection. This largely agrees with our findings that high exposure to soil is also a risk factor. Thus, my results bear important implications for assessing the global burden and devising preventive measures for controlling HEV infection.

Fatty liver disease

Non-alcoholic fatty liver disease (NAFLD) was first described as a distinct clinical entity four decades ago. However, the condition has become the center of attention within hepatology owing to its high prevalence and growing contribution to the burden of end-stage liver disease in the general population. It is estimated that the burden of end-stage liver disease will increase 2–3 fold in both Western nations as well as in several Asian countries by 2030. Although fatty liver associated with metabolic dysfunction is common, there is no approved drug therapy. While pharmacotherapies are in

development, response rates appear unfortunately modest. The heterogeneous pathogenesis of metabolic fatty liver diseases and inaccuracies in terminology and definitions necessitate a reappraisal of nomenclature to inform clinical trial design and drug development. The old terminology NAFLD does not reflect current knowledge and metabolic (dysfunction) associated fatty liver disease "MAFLD" was suggested as a more appropriate overarching term. This opens the door for efforts from the research community to update the nomenclature and sub-phenotype the disease in order to accelerate the translational path to new treatments and this consideration drove import a significant part of the research effort described in this thesis.

In chapter 6, I included 578 studies and ventured to comprehensively estimate the global prevalence, incidence, disease progression and outcomes of NAFLD. The overall prevalence of NAFLD in the general population is 29.38% (95% CI 28.09-30.69) regardless of the diagnostic techniques employed to reach diagnosis. Extensive earlier work, however, suggested a principle importance of technique when diagnosing NAFLD. Arguments have been raised against the application of liver enzymes for diagnosing NAFLD because normal levels of these enzymes have been widely observed over the entire clinical spectrum of NAFLD and thus use of enzymes leads to underdiagnoses.[43] In line with this, I also observed that the prevalence of NAFLD diagnosed by elevation of liver enzymes yielded a substantially lower rate compared to that of liver biopsy and imaging modality based diagnosis. Ultrasound was the most commonly used diagnostic technique for NAFLD diagnosis with an observed rate of prevalence rate of 30.49% (95% CI 29.55-31.43). My pooled estimates of the odds ratios for risk factors are largely in line with previous studies with some subtle differences being noted by me.[44] Obesity, male sex, obesity, development of metabolic syndrome as well as hypertension appear major risk factors. More importantly, I observed an annual increase in the incidence of NAFLD-associated HCC which exceeded previously published estimates. However, exact HCC incidences are difficult to estimate because in some cases of NAFLD-related HCC there is no preceding cirrhosis.[45] Also, some NAFLD/NASH patients that are co-infected with hepatitis B virus, hepatitis C virus or have other metabolic diseases cannot be included in this estimate of NAFLD-related HCC incidence. Given the already high and ever increasing burden of NAFLD and NASH, the incidence of related HCC is expected to grow.

In chapter 7, a systematic review and a meta-analysis based on existing epidemiological data on fatty liver disease in overweight or obese children and adolescents, were pooled for estimating for MAFLD prevalence. The prevalence of obesity has nearly tripled since 1975, and this parallels the growth of the fatty liver disease epidemic. Strong associations between obesity and prevalence of fatty liver disease have been well-documented, both in children and adolescents.[46] A previous study attempted to visualize the dynamics in NAFLD prevalence in adolescents aged 12 to 19 years using data from different periods from the NHANES database. Strikingly, the prevalence of NAFLD has substantially risen from 3.9% in 1988-1994 to 10.7% in 2007-2010.[47] A recent meta-analysis estimated that the NAFLD prevalence rate in overweight or obese children from general population was 12.5% and 36%, respectively. NAFLD prevalence among children based on child obesity clinics has been reported to be 34%,[48] but we observed a much higher (1.5 fold) rate of MAFLD

in this population. This discrepancy may be attributed to differences in disease definition between NALFD and MAFLD, and/or population selection. NAFLD could represent an umbrella term for multiple underlying sub-types which underestimates the prevalence of fatty liver disease.[49]

In chapter 8, I attempted to estimate the global prevalence of MAFLD among overweight or obese adults and my results suggested that this prevalence exceeds 50%. Alarmingly, the prevalence rate is rising further even still, at least when the latest 10 years are compared to the preceding decade. Within the NAFLD population, recent estimates suggest that 60% are lean or non-obese individuals [50] and thus 40% are expected to be overweight or obese people. In the general population, global prevalence of NAFLD has been estimated to be 25%, as based on data from 1989 to 2015,[43]. A recent study calculated the prevalence of lean and non-obese NAFLD to be 17%.[50] Apparently, estimations of NAFLD prevalence in the obese population are far from accurate as these estimates range from 50% to 90%.[51] One study based on liver histology reported the prevalence of steatosis as being 15% in non-obese individuals, 65% in persons with obesity, and 85% in extremely obese patients.[52] Because liver biopsy is only indicated for specific patients, these results cannot be generalized. Distinct from these historical studies, I now made a first step to quantify MAFLD epidemiology in overweight and obese adults. Nevertheless, the relationship between MAFLD and BMI is complex influenced by many factors, such as racial/ethnic background and genetic variations in specific genes, thus requiring further in depth investigation.

Cancer stem cells

Comprehending the medical biology of cancer stem cells remains difficult, but may ultimately also lead to improved clinical management. In this thesis I tried to use organoids to obtain better understanding of cancer stem cells. To this end I exploited the still relatively new organoid technology. Organoids denominate stem cell derived organ-like 3D structures. Such organoids system do not only provide a promising platform for stem cell biology research, but might be used for modeling a wide range of diseases.[53] Stem cells in cancer are thought to underlie tumor initiation and growth, therapy resistance and tumor recurrence.[54] In my thesis I concentrated on LGR5, the leucine-rich-repeat-containing G-protein-coupled receptor 5, that marks a group of stem cells proliferating after liver injury induced by carbon tetrachloride (CCL4).[55] In intestinal and colorectal carcinoma, LGR5 marks a cancer stem cell population. The role of this group of stem cells in liver cancer remained, however, obscure at best.

My study established that LGR5 cells were induced by DEN injection (a procedure that evokes pre-cancerous liver damage often showing further progression). Furthermore, I observed that these LGR5 cells have a much stronger ability for tumor initiation (i.e. the capacity to form new organoids but also in vivo. I describe the findings involved in Chapter 9 and Chapter 10. I also reported that the fraction of LGR5 cells was significantly higher in tumor tissue when compared to the tissue surrounding the tumor (Chapter 10). To further demonstrate the function of LGR5 cells, we established a organoid culture system from primary liver tumors (Chapter 9). Employing this model, we observed that tumor LGR5 cells have stronger *in vitro* organoid initiation ability and

in vivo tumor initiation capability. We also revealed that LGR5 positive cells were more resistant to treatment, compared to LGR5 negative cells. More interestingly, the ablation of the LGR5 expression cells in liver tumor would impede the *in vivo* tumor formation. Studies in colon cancer have indicated that the reduction of the size of the LGR5 compartment impedes both the growth of the primary tumors as well as their metastasis.[56]

Cancer associated fibroblasts

Following my investigations of the liver cancer cells proper, I decided to explore the dependency of these cells on their environment. The cancer-associated fibroblasts (CAFs), which constitute a major component of tumor microenvironment, play a role in cancer progression but also in drug resistance of these cells in general.[57, 58] I attempted to determine their role in liver cancer by creating a model that is in essence a co-culture system of these CAFs and the cancer cells. I reasoned that by employing such cultures, I might be able to establish a 'more clinically relevant' tumor model that better mimics the actual situation as it occurs *in vivo.* Among the multitude of possible intercellular interactions of the cancer cells with their tumor microenvironment, the reciprocal interaction between fibroblasts and cancer cells is postulated to contribute to tumor initiation, but also progression and eventual metastasis, in many cancer types, although its role in liver cancer stays largely uncharacterized.[59, 60] Enticingly, these models could also be used to test anticancer agents.[61] Thus I decided to explore this angle of the liver cancer process.

In Chapter 11, I present an organoid-based co-culture model that combines tumor organoids with CAFs. I do observe that proliferation of tumor cells is significantly stimulated in these co-cultures when I compare these to the control group. Because I feel that the in vivo is more alike to co-cultures as compared to competing technologies, I think that the reciprocal interaction between the tumor organoids with the fibroblasts that I uncovered is best interpreted as that the co-culture system is more suitable for drug screening when compared to conventional technology. I addition, this system should help me dissecting the role of the tumor microenvironment in the liver cancer process. The mechanisms that may explain the trophic effects of co-culture include the induction of epithelial-to-mesenchymal transition (EMT) in the cancer cell compartment and this may predispose to metastasis. Furthermore, induction of increased stemness (which is associated with therapy resistance) and a metabolic reprogramming (which is a hallmark of cancer cells) are important here as well, I feel. In conjunction these CAF-mediated effects on the tumor cells can explain tumor progression and therapy failure.[62, 63] Disregarding the progress made in understanding CAF biology, I also feel my model can be of further importance to the field because most of the current investigations are based on in vitro assays and work involving a limited number of immortalized cell lines, whereas my model can work directly with cells obtained from patients and may also capture the variety in cell subtypes better. I thus hope that these studies may give more insight to the activity of CAFs and interaction between CAFs and cancer cells in turn producing superior therapy.

However, despite the large amount of work that has been done, more efforts are needed in this area. If, however, they prove successful, it may well prove possible to translate CAF-directed anti-cancer strategies from the bench to the clinic.

A further important point emerging from my studies is that the targeting of the cancer stem cell system is useful as it hampers the potential of the cancer for recovering from a chemotherapeutic insult. The apparent advantage of the specific targeting of cancer stem cells such as the LGR5 cells employed in this thesis is that it opens a window to a more superior clinical effect of patient management and potentially leads to long-term therapeutic benefit. If these observations can be extrapolated to other forms of oncological disease well, my studies might foster the generation a framework that allows developing novel therapeutic approaches for oncological disease in general.

Overall I have tried in this thesis to address many aspects of cancer and also inflammation in the field of hepatology and I hope the studies described in the above of this thesis will finally contribute to better management of such diseases.

Reference

1. Bray F, Ferlay J, Soerjomataram I, et al. Global cancer statistics 2018: GLOBOCAN estimates of incidence and mortality worldwide for 36 cancers in 185 countries. CA Cancer J Clin 2018;68:394-424.
2. Yang JD, Hainaut P, Gores GJ, et al. A global view of hepatocellular carcinoma: trends, risk, prevention and management. Nat Rev Gastroenterol Hepatol 2019;16:589-604.
3. Scudellari M. Drug development: try and try again. Nature 2014;516:S4-6.
4. Yang JD, Roberts LR. Hepatocellular carcinoma: A global view. Nat Rev Gastroenterol Hepatol 2010;7:448-58.
5. Wang W, Pan Q, Fuhler GM, et al. Action and function of Wnt/beta-catenin signaling in the progression from chronic hepatitis C to hepatocellular carcinoma. J Gastroenterol 2017;52:419-431.
6. El-Serag HB, Rudolph KL. Hepatocellular carcinoma: epidemiology and molecular carcinogenesis. Gastroenterology 2007;132:2557-76.
7. Matsuzaki K, Murata M, Yoshida K, et al. Chronic inflammation associated with hepatitis C virus infection perturbs hepatic transforming growth factor beta signaling, promoting cirrhosis and hepatocellular carcinoma. Hepatology 2007;46:48-57.
8. Hino O, Kajino K, Umeda T, et al. Understanding the hypercarcinogenic state in chronic hepatitis: a clue to the prevention of human hepatocellular carcinoma. J Gastroenterol 2002;37:883-7.
9. Schulze-Krebs A, Preimel D, Popov Y, et al. Hepatitis C virus-replicating hepatocytes induce fibrogenic activation of hepatic stellate cells. Gastroenterology 2005;129:246-58.
10. Moriya K, Fujie H, Shintani Y, et al. The core protein of hepatitis C virus induces hepatocellular carcinoma in transgenic mice. Nat Med 1998;4:1065-7.
11. Gane E. The natural history and outcome of liver transplantation in hepatitis C virus-infected recipients. Liver Transpl 2003;9:S28-34.
12. Bataller R, Brenner DA. Hepatic stellate cells as a target for the treatment of liver fibrosis. Semin Liver Dis 2001;21:437-51.
13. Ikegami T, Ueda Y, Akamatsu N, et al. Asunaprevir and daclatasvir for recurrent hepatitis C after liver transplantation: A Japanese multicenter experience. Clin Transplant 2017;31.
14. Honda M, Sugawara Y, Watanabe T, et al. Outcomes of treatment with daclatasvir and asunaprevir for recurrent hepatitis C after liver transplantation. Hepatol Res 2017;47:1147-1154.
15. Lim SG, Aghemo A, Chen PJ, et al. Management of hepatitis C virus infection in the Asia-Pacific region: an update. Lancet Gastroenterol Hepatol 2017;2:52-62.
16. European Association for the Study of the Liver. Electronic address eee. EASL Recommendations on Treatment of Hepatitis C 2016. J Hepatol 2017;66:153-194.
17. Reig M, Marino Z, Perello C, et al. Unexpected high rate of early tumor recurrence in patients with HCV-related HCC undergoing interferon-free therapy. J Hepatol 2016;65:719-726.
18. Conti F, Buonfiglioli F, Scuteri A, et al. Early occurrence and recurrence of hepatocellular carcinoma in HCV-related cirrhosis treated with direct-acting antivirals. J Hepatol 2016;65:727-733.
19. Yang JD, Aqel BA, Pungpapong S, et al. Direct acting antiviral therapy and tumor recurrence after liver transplantation for hepatitis C-associated hepatocellular carcinoma. J Hepatol 2016;65:859-860.
20. Batlle E, Clevers H. Cancer stem cells revisited. Nat Med 2017;23:1124-1134.
21. Casadei Gardini A, Conti F, Foschi FG, et al. Imbalance of Neutrophils and Lymphocyte Counts Can Be Predictive of Hepatocellular Carcinoma Occurrence in Hepatitis C-related Cirrhosis Treated With Direct-acting Antivirals. Gastroenterology 2018;154:2281-2282.
22. Chu PS, Nakamoto N, Taniki N, et al. On-treatment decrease of NKG2D correlates to early emergence of clinically evident hepatocellular carcinoma after interferon-free therapy for chronic hepatitis C. PLoS One 2017;12:e0179096.
23. Ning G, Li YT, Chen YM, et al. Dynamic Changes of the Frequency of Classic and Inflammatory Monocytes Subsets and Natural Killer Cells in Chronic Hepatitis C Patients Treated by Direct-Acting Antiviral Agents. Can J Gastroenterol Hepatol 2017;2017:3612403.
24. Meissner EG, Kohli A, Higgins J, et al. Rapid changes in peripheral lymphocyte concentrations during interferon-free treatment of chronic hepatitis C virus infection. Hepatol Commun 2017;1:586-594.
25. Langhans B, Nischalke HD, Kramer B, et al. Increased peripheral CD4(+) regulatory T cells persist after successful direct-acting antiviral treatment of chronic hepatitis C. J Hepatol 2017;66:888-896.
26. Villani R, Facciorusso A, Bellanti F, et al. DAAs Rapidly Reduce Inflammation but Increase Serum VEGF Level: A Rationale for Tumor Risk during Anti-HCV Treatment. PLoS One 2016;11:e0167934.
27. Debes JD, van Tilborg M, Groothuismink ZMA, et al. Levels of Cytokines in Serum Associate With Development of Hepatocellular Carcinoma in Patients With HCV Infection Treated With Direct-Acting Antivirals. Gastroenterology 2018;154:515-517 e3.
28. Faillaci F, Marzi L, Critelli R, et al. Liver Angiopoietin-2 Is a Key Predictor of De Novo or Recurrent Hepatocellular Cancer After Hepatitis C Virus Direct-Acting Antivirals. Hepatology 2018;68:1010-1024.
29. Yazbek S, Kreidieh K, Ramia S. Hepatitis E virus in the countries of the Middle East and North Africa region: an awareness of an infectious threat to blood safety. Infection 2016;44:11-22.
30. Kmush B, Wierzba T, Krain L, et al. Epidemiology of hepatitis E in low- and middle-income countries of Asia and Africa. Semin Liver Dis 2013;33:15-29.
31. Hartl J, Otto B, Madden RG, et al. Hepatitis E Seroprevalence in Europe: A Meta-Analysis. Viruses 2016;8.
32. Rossi-Tamisier M, Moal V, Gerolami R, et al. Discrepancy between anti-hepatitis E virus immunoglobulin G prevalence assessed by two assays in kidney and liver transplant recipients. J Clin Virol 2013;56:62-4.
33. Wenzel JJ, Preiss J, Schemmerer M, et al. Test performance characteristics of Anti-HEV IgG assays strongly influence hepatitis E seroprevalence estimates. J Infect Dis 2013;207:497-500.
34. Ivanova A, Tefanova V, Reshetnjak I, et al. Hepatitis E Virus in Domestic Pigs, Wild Boars, Pig Farm Workers, and Hunters in Estonia. Food Environ Virol 2015;7:403-12.
35. Teixeira J, Mesquita JR, Pereira SS, et al. Prevalence of hepatitis E virus antibodies in workers occupationally exposed to swine in Portugal. Med Microbiol Immunol 2017;206:77-81.
36. Meng XJ. Expanding Host Range and Cross-Species Infection of Hepatitis E Virus. PLoS Pathog 2016;12:e1005695.
37. Zeng MY, Gao H, Yan XX, et al. High hepatitis E virus antibody positive rates in dogs and humans exposed to dogs in the south-west of China. Zoonoses Public Health 2017;64:684-688.

38. Liang H, Chen J, Xie J, et al. Hepatitis E virus serosurvey among pet dogs and cats in several developed cities in China. PLoS One 2014;9:e98068.
39. Sahli R, Fraga M, Semela D, et al. Rabbit HEV in immunosuppressed patients with hepatitis E acquired in Switzerland. J Hepatol 2019;70:1023-1025.
40. Echevarria JM. Light and Darkness: Prevalence of Hepatitis E Virus Infection among the General Population. Scientifica (Cairo) 2014;2014:481016.
41. Alvarado-Esquivel C, Sanchez-Anguiano LF, Hernandez-Tinoco J. Seroepidemiology of hepatitis e virus infection in mennonites in Mexico. J Clin Med Res 2015;7:103-8.
42. Caron M, Kazanji M. Hepatitis E virus is highly prevalent among pregnant women in Gabon, central Africa, with different patterns between rural and urban areas. Virol J 2008;5:158.
43. Younossi ZM, Koenig AB, Abdelatif D, et al. Global epidemiology of nonalcoholic fatty liver disease-Meta-analytic assessment of prevalence, incidence, and outcomes. Hepatology 2016;64:73-84.
44. Rinella ME. Nonalcoholic fatty liver disease: a systematic review. JAMA 2015;313:2263-73.
45. White DL, Kanwal F, El-Serag HB. Association between nonalcoholic fatty liver disease and risk for hepatocellular cancer, based on systematic review. Clin Gastroenterol Hepatol 2012;10:1342-1359 e2.
46. Non-alcoholic Fatty Liver Disease Study G, Lonardo A, Bellentani S, et al. Epidemiological modifiers of non-alcoholic fatty liver disease: Focus on high-risk groups. Dig Liver Dis 2015;47:997-1006.
47. Welsh JA, Karpen S, Vos MB. Increasing prevalence of nonalcoholic fatty liver disease among United States adolescents, 1988-1994 to 2007-2010. J Pediatr 2013;162:496-500 e1.
48. Anderson EL, Howe LD, Jones HE, et al. The Prevalence of Non-Alcoholic Fatty Liver Disease in Children and Adolescents: A Systematic Review and Meta-Analysis. PLoS One 2015;10:e0140908.
49. Yki-Jarvinen H. Nutritional Modulation of Non-Alcoholic Fatty Liver Disease and Insulin Resistance. Nutrients 2015;7:9127-38.
50. Ye Q, Zou B, Yeo YH, et al. Global prevalence, incidence, and outcomes of non-obese or lean non-alcoholic fatty liver disease: a systematic review and meta-analysis. Lancet Gastroenterol Hepatol 2020;5:739-752.
51. Divella R, Mazzocca A, Daniele A, et al. Obesity, Nonalcoholic Fatty Liver Disease and Adipocytokines Network in Promotion of Cancer. Int J Biol Sci 2019;15:610-616.
52. Fabbrini E, Sullivan S, Klein S. Obesity and nonalcoholic fatty liver disease: biochemical, metabolic, and clinical implications. Hepatology 2010;51:679-89.
53. Huch M, Dorrell C, Boj SF, et al. In vitro expansion of single Lgr5+ liver stem cells induced by Wnt-driven regeneration. Nature 2013;494:247-50.
54. Sun JH, Luo Q, Liu LL, et al. Liver cancer stem cell markers: Progression and therapeutic implications. World J Gastroenterol 2016;22:3547-57.
55. Cao W, Chen K, Bolkestein M, et al. Dynamics of Proliferative and Quiescent Stem Cells in Liver Homeostasis and Injury. Gastroenterology 2017;153:1133-1147.
56. Shimokawa M, Ohta Y, Nishikori S, et al. Visualization and targeting of LGR5(+) human colon cancer stem cells. Nature 2017;545:187-192.
57. Becker LM, O'Connell JT, Vo AP, et al. Epigenetic Reprogramming of Cancer-Associated Fibroblasts Deregulates Glucose Metabolism and Facilitates Progression of Breast Cancer. Cell Rep 2020;31:107701.
58. Allaoui R, Bergenfelz C, Mohlin S, et al. Cancer-associated fibroblast-secreted CXCL16 attracts monocytes to promote stroma activation in triple-negative breast cancers. Nat Commun 2016;7:13050.
59. Houthuijzen JM, Jonkers J. Cancer-associated fibroblasts as key regulators of the breast cancer tumor microenvironment. Cancer Metastasis Rev 2018;37:577-597.
60. Friedrich J, Seidel C, Ebner R, et al. Spheroid-based drug screen: considerations and practical approach. Nat Protoc 2009;4:309-24.
61. Aref AR, Huang RY, Yu W, et al. Screening therapeutic EMT blocking agents in a three-dimensional microenvironment. Integr Biol (Camb) 2013;5:381-9.
62. Kalluri R. The biology and function of fibroblasts in cancer. Nat Rev Cancer 2016;16:582-98.
63. Su S, Chen J, Yao H, et al. CD10(+)GPR77(+) Cancer-Associated Fibroblasts Promote Cancer Formation and Chemoresistance by Sustaining Cancer Stemness. Cell 2018;172:841-856 e16.

CHAPTER 13

Nederlandse samenvatting

Dutch summary

Nederlandse samenvatting.

De lever, een groot lichtbruin orgaan dat rechtsboven in de buik onder het middenrif gelegen is, vormt één van de belangrijkste structuren van het lichaam. Het orgaan dat vaak terecht beschreven wordt als de biochemische fabriek van het lichaam, vervult talrijke functies, met name bij de verwerking en afvoer van afvalstoffen, de productie en opslag van energie en de productie van belangrijke eiwitten. Ongelukkigerwijze, kan de lever ook ziek worden en zo dan ook de bron zijn van veel menselijke ellende en verdriet. Met mijn promotieonderzoek en dit proefschrift heb ik een bijdrage proberen te leveren aan het gevecht van de mensheid tegen ziekte in de lever. Met name concentreer ik mij hierbij op twee vormen van virale infectie van de lever (Hepatitis C en Hepatitis E), ziekte door vervetting van de lever en leverkanker. Ik doe dit middels literatuur studies, epidemiologische analyses en biologische experimentatie.

In dit proefschrift geef ik eerst een rechtvaardiging van de gekozen strategie (**hoofdstuk één**) en probeer ik met name de keuzes die ik heb gemaakt in dit onderzoek uit te leggen. Vervolgens voer ik een literatuurstudie uit naar functie en belang van intracellulaire vetdruppeltjes voor het functioneren van de levercellen (de zogenaamde hepatocyten). In de darm wordt voedsel opgenomen en dit wordt vervolgens door de lever verwerkt. Een gedeelte van de energie die vervolgens beschikbaar komt in de levercel, wordt dan omgezet in triglyceriden en die worden of afgegeven aan het lichaam, of opgeslagen in vetdruppeltjes in de levercel. In **hoofdstuk twee** beschrijf ik een literatuurstudie naar het belang van deze vetdruppels voor het functioneren van de lever in gezondheid en ziekte. Het blijkt dat sommige virussen deze vetdruppeltjes gebruiken als een stellage waarop zij gedurende hun levenscyclus nieuwe virusdeeltjes kunnen bouwen. Daarmee worden dergelijke vetdruppeltjes ook meteen een interessant aangrijppunt bij de behandeling van virusziekten in de lever.

In **hoofdstuk drie** werk ik het probleem van virusinfectie van de lever verder uit. Hier concentreer ik mij in eerste instantie op het Hepatitis C virus. Zo'n hepatitis C-infectie is meestal asymptomatisch en wordt in de meerderheid van de gevallen (70%) ongemerkt chronisch. Bij een kwart van de mensen die de chronische vorm van Hepatitis C hebben, ontwikkelt zich verlittekening van de lever en uit deze groep krijgt dan weer ongeveer 2-5% per jaar leverkanker. Mensen krijgen pas 20 of 30 jaar na de initiële besmetting klachten, wanneer de lever al onherstelbaar is aangetast. Er zijn verschillende virusstammen, maar in dit hoofdstuk concentreer ik mij op het zogenaamde genotype 1 en beperk ik mij tot die patiënten die vanwege verlittekening van de lever door het hepatitis C virus een levertransplantatie hebben ondergaan. De nieuw lever van dergelijke patiënten wordt vrijwel altijd geherinfecteerd door het virus en ik onderzoek welke antivirale middelen het best toegepast kunnen worden. De resultaten werden gepubliceerd in het vaktijdschift *Transplantation Infectious Disease.*

In **hoofdstuk vier** bouw ik op deze resultaten verder. Merkwaardigerwijze helpen antivirale middelen niet bij het beschermen tegen het ontstaan van leverkanker, zelfs al wordt de virale infectie wel efficiënt bestreden. In dit hoofdstuk doe ik experimenten waarbij ik levercellen behandel met een antiviraal middel en ik laat zien dat dergelijke middelen zelf het kankerproces kunnen bevorderen. Het gunstig effect van het bestrijden van het virus zou dus wel eens teniet kunnen worden gedaan door effecten van het medicijn zelf op het kankerproces. Deze resultaten publiceerde ik in het vaktijdschrift *Clinics and Research in Hepatology and Gastroenterology*.

In **hoofdstuk vijf** richt ik mijn aandacht op een ander virus dat de lever infecteert, het Hepatitis E virus. Het hepatitis E-virus veroorzaakt meestal milde klachten maar kan zich tot een chronische infectie ontwikkelen bij sterk verminderde weerstand zoals transplantatiepatiënten. Daarnaast wordt in ontwikkelingslanden tot ernstige ziekte en sterfte tijdens de zwangerschap gezien. In dit hoofdstuk, dat gepubliceerd in het vooraanstaande vaktijdschrift *Liver International*, breng ik de ernst van het probleem middels een wereldwijde epidemiologische analyse in kaart.

In de volgende drie hoofdstukken richt ik mijn pijlen dan op leververvetting. Leververvetting is de meest voorkomende aandoening van de lever in de Westerse wereld. Door een slechte voeding en een ongezonde levensstijl hoopt vet zich op in de lever. Als er niets gebeurt aan de onderliggende oorzaken, vervet de lever steeds verder, met leverontsteking tot gevolg. Uiteindelijk leidt dit weer tot ernstige schade aan de lever en soms tot levensbedreigend leverfalen, met een levertransplantatie nog als enige behandelmogelijkheid. **Hoofdstuk zes** is een algemene epidemiologische analyse van dit probleem, terwijl in **hoofdstuk zeven** meer naar kinderen en pubers wordt gekeken, terwijl in **hoofdstuk acht** specifiek naar volwassen met overgewicht worden onderzocht. Samen geven ze een goed beeld van de betrokken problematiek.

Zowel virale leverinfectie alsook leververvetting kunnen leiden tot leverkanker en de laatste experimentele hoofdstukken uit dit proefschrift gaan hierover. In **hoofdstuk negen** laat ik zien hoe je organoïden kan gebruiken bij ontwerpen van betere therapie voor leverkanker. Organoïden zijn in een kweekschaal uit stamcellen gegroeide structuren die belangrijke aspecten van organen kunnen modelleren, maar ook kanker uit dergelijke organen. Ik laat zien dat dit ook voor leverkanker kan. Ik kon deze resultaten publiceren in het vooraanstaande vaktijdschrift *Carcinogenesis.* Vervolgens heb ik dit systeem geëxploiteerd om te onderzoeken of het uitschakelen van een bepaald stamceltype, de zogenaamde LGR5-positieve cel, waarde had bij het behandelen van leverkanker. Ik liet zien dat chemotherapie alleen niet in staat was leverkanker te bestrijden. Ook louter het uitschakelen van de LGR5-positieve cel had weinig effect. Werden beide behandelingen gecombineerd, dan werd de leverkanker wel effectief bestreden. Deze veelbelovende resultaten, te vinden in **hoofdstuk tien**, werden gepubliceerd in het vooraanstaande wetenschappelijke tijdschrift *Nature Communications.* Een laatste studie (**hoofdstuk 11**) richt zich niet op de kankercellen zelf, maar juist op de bindweefselcellen die de kankercellen omringen. Ik kon laten zien dat deze cellen een belangrijke rol vervullen bij het voeden en verzorgen van de

kankercellen, vooral tijdens chemotherapie. Deze cellen vormen dus een verder aangrijpingspunt voor mogelijke nieuwe therapie. Deze resultaten heb ik ook gepubliceerd en wel in het vooraanstaande vaktijdschrift *Cellular and Molecular Gastroenterology and Hepatology*.

In **hoofdstuk 12** probeer ik alle data die ik heb verzameld tijdens mijn promotieonderzoek te integreren en te bediscussiëren in het licht van het corpus aan contemporaine biomedische wetenschappelijke literatuur. Ik hoop daarmee een bijdrage te hebben geleverd aan betere behandeling van ziekten van de lever, of althans een fundament te hebben geschapen waarmee een opvolger van mij aan de slag kan gaan.

Appendix

Acknowledgements

Publications

PhD portfolio

Curriculum Vitae

Acknowledgements

To obtain a PhD degree is a long journey full of unknowns and indeterminants. I would like to thank all people who walked this road with me.

First and foremost, I would like to give my wholehearted appreciation to my promotor, Prof. Dr. Maikel P Peppelenbosch, for offering me the precious opportunity to pursue my PhD and your four-year of supervising with great patience and sharing your immense knowledge with me. You are a legendary scientist full of innovative and creative ideas. Without your help, I can never obtain survival from my PhD and finally present this thesis.

I am also deeply indebted to my co-promoter Dr. Qiuwei Pan for his fundamental role in pursuing my doctoral work. His encouragement, support, and guidance throughout my PhD study made me finally grow up from a pupil to an adult. You are such a brilliant, hard-working and humble scientist, a model that I hook up to. Your enthusiasm in science really motivated me a lot.

I also want to express my deepest gratitude to my colleague Wanlu Cao for your encouragement and endless support. Four years before, I came to Holland to start my PhD like a blank paper. It is you that step by step taught me how to be a qualified scientist. You are strict, unyielding and sometimes could be stubborn. However, I really feel that I am a lucky star that I can meet you. Thanks for your time on me.

To Ron, you are such a knowledgeable, kindness and patient person. You did give us support like an uncle liver in neighborhood. You are an encyclopedia that no matter what kind of question, you can always give us the best answer.

To Luc, thank you for your brilliant comments and suggestions for my projects and papers. You are such a gentle and brilliant person with a big-picture thinking in research area. It was an enjoyable time full with interesting discussions and meetings.

To Gwenny, it is a splendid experience to work with and study from you. It was generous of you to give so much kind advice on my projects. I learned not only from the answers you gave to my questions but also a strict attitude to seek the truth.

To Jaap and Dave, thanks for the professional suggestion, insightful comments and encouragement, but also for the mind-blowing questions. Wish all the best to you.

To Monique, thanks for countless of help and patience you provided. I will miss the time and best wishes to you and your family.

To Auke and Leonie, there are too many times you helped me out with my problems. I could not have imagined how the lab would be without you. Thanks so much and wish the best to you and your family.

My greatest gratitude also goes to Anthonie, Henk and Petra. You are always supportive when I sought your help. I am grateful for every experience and lesson I learned.

To Zhouhong, Sunny and Estella, thanks for your continuous support for work, time after time. May your guys have a brilliant future.

To Ruby, Floris, Yorke, thanks for your valuable suggestions and your help during our weekly meetings and project discussions.

To Suk Yee, thanks for providing professional help with translation, all extraordinary patience and a constant sunshine smile.

To Yang, Peifa, Yunlong, Ruyi, Zhijiang, Shaojun, Yining, I am extremely grateful for staying and working with your guys. Thanks for all the patience, encouragement and support.

To Shan, Buyun, Meng, Wenhui, Wenshi, Changbo, Wen, I feel so lucky to work with you during the past years. Thanks for the constant encouragement and valuable suggestions.

To my paranimfen Ling and Pengfei, I would like to express my heartfelt gratitude for all the support. You helped me out of my difficulties and supported me without a word of complaint.

To all the others from MDL, thanks for your kindly help and time for my 4 years here. I really appreciated that.

To all the co-authors, thanks for your contributions to my thesis and the journal publications.

Financial support from China Scholarship Council made a dream come true, thanks for the generous support from home.

To Edith Leuthi, tnanks for your splendid design for the layout of cover.

To all honorable MDL members who have left and who are present, thanks for all the happy time and unconditional help. Best wishes to all!

最后感谢我的家人，是你们的陪伴和支持给了我坚持下去的勇气和信心。把这篇毕业论文献给你们！

List of publications

Jiaye Liu, Meng Li, Pengfei Li, Ling Wang, Zhouhong Ge, Lisanne Noordam, Ruby Lieshout, Monique M. A. Verstegen, Buyun Ma, Junhong Su, Qin Yang, Ruyi Zhang, Guoying Zhou, Lucia Campos Carrascosa, Dave Sprengers, Ron Smits, Jaap Kwekkeboom, Luc J. W. van der Laan, Maikel P. Peppelenbosch, Qiuwei Pan, Wanlu Cao; Cancer-associated fibroblasts provide a stromal niche for liver cancer organoids that confers trophic effects and therapy resistance. ***Cell Mol Gastroenterol Hepatol****.* 2020; Accepted.

Liu, J.; Ma, B.; Cao, W.; Li, M.; Bramer, W.M.; Peppelenbosch, M.P.; Pan, Q. Direct-acting antiviral agents for liver transplant recipients with recurrent genotype 1 hepatitis C virus infection: Systematic review and meta-analysis. ***Transpl Infect Dis*** 2019, *21*, e13047, doi:10.1111/tid.13047.

Liu, J.; Cao, W.; Ma, B.; Li, M.; Peppelenbosch, M.P.; Pan, Q. Sofosbuvir directly promotes the clonogenic capability of human hepatocellular carcinoma cells. ***Clin Res Hepatol Gastroenterol*** 2019, 43, e79-e81, doi:10.1016/j.clinre.2018.11.016.

Li, P*.; **Liu, J.*#;** Li, Y.; Su, J.; Ma, Z.; Bramer, WM; Cao, W.; De Man, R.; Peppelenbosch, M.P.; Pan, Q#. The global epidemiology of hepatitis E virus infection: A systematic review and meta-analysis. ***Liver Int***. 2020;40:1516-1528. DOI: 10.1111/liv.14468

Jiaye Liu, Pengfei Li, Wanlu Cao, Qin Yang, Ling Wang, Junyi Shen, Tianfu Wen, Xiaofang Zhang, Zhongren Ma, Wichor Bramer, Shaoli Lin, Marco J. Bruno, Mohsen Ghanbari, Maikel P. Peppelenbosch, Qiuwei Pan: Global prevalence, incidence and outcomes of non-alcoholic fatty liver disease: systematic review and meta-analysis; ***Submitted***

Jiaye Liu, Ziyi Wang, Ling Wang, Yang Li, Tianfu Wen, Xiaofang Zhang, Zhongren Ma, Maarten F.M. Engel, Marco J. Bruno, Mohsen Ghanbari, Robert J. de Knegt, Wanlu Cao, Maikel P. Peppelenbosch, Qiuwei Pan Estimating global prevalence of metabolic dysfunction-associated fatty liver disease in overweight or obese children and adolescents: systematic review and meta-analysis; ***Submitted***

Jiaye Liu; Ling Wang; Junyi Shen; Zhongren Ma; Maikel P. Pepelenbosch; Qiuwei Pan; Estimating global prevalence of metabolic dysfunction-associated fatty liver disease in overweight or obese adults; ***Submitted***

Cao, W.; **Liu, J**.; Li, M.; Zhang, S.; Noordam, L.; Verstegen, M.M.A.; Wang, L.; Ma, B.; Li, S.; Wang, W., et al. LGR5 marks targetable tumor-initiating cells in mouse liver cancer. ***Nat Commun*** 2020, *11*, 1961, doi:10.1038/s41467-020-15846-0.

Cao, W.; **Liu, J**.; Wang, L.; Li, M.; Verstegen, M.M.A.; Yin, Y.; Ma, B.; Chen, K.; Bolkestein, M.; Sprengers, D., et al. Modeling liver cancer and therapy responsiveness using organoids derived from primary mouse liver tumors. ***Carcinogenesis*** 2019, *40*, 145-154, doi:10.1093/carcin/bgy129.

Ma, Z; **Liu, J**; Pan, Q. Overwhelming COVID-19 Clinical Trials: Call for Prospective Meta-Analyses. ***Trends Pharmacol. Sci***. https://doi.org/10.1016/j.tips.2020.05.002

Li P, **Liu J**, Ma Z, Bramer WM, Pepelenbosch MP, Pan Q. Estimating global epidemiology of low pathogenic human coronaviruses relating to the COVID-19 context [published online ahead of print, 2020 Jun 4]. ***J Infect Dis***. 2020;jiaa321. doi:10.1093/infdis/jiaa321

Shen J, **Liu J**, Li C, Wen T, Yan L, Yang J. The Impact of Tumor Differentiation on the Prognosis of HBV-Associated Solitary Hepatocellular Carcinoma Following Hepatectomy: A Propensity Score Matching Analysis. ***Dig Dis Sci***. 2018;63(7):1962-1969. doi:10.1007/s10620-018-5077-5

Shen J, **Liu J**, Li C, Wen T, Yan L, Yang J. The prognostic significance of serum HBeAg on the recurrence and long-term survival after hepatectomy for hepatocellular carcinoma: A propensity score matching analysis. ***J Viral Hepat***. 2018;25(9):1057-1065. doi:10.1111/jvh.12911

Yang Q, **Liu J**, Ma W,. Efficacy of Different Endoscopic Stents in the Management of Postoperative Biliary Strictures: A Systematic Review and Meta-analysis. ***J Clin Gastroenterol***. 2019;53(6):418-426. doi:10.1097/MCG.0000000000001193

Li C, **Liu J**, Peng W,. Liver resection *versus* transplantation for multiple hepatocellular carcinoma: a propensity score analysis. ***Oncotarget.*** 2017;8(46):81492-81500. Published 2017 Sep 2. doi:10.18632/oncotarget.20623

Meng Li, Ling Wang, Yijin Wang, Shaoshi Zhang, Guoying Zhou, Ruby Lieshout, Buyun Ma, **Jiaye Liu** , Changbo Qu , Monique M A Verstegen, Dave Sprengers, Jaap Kwekkeboom, Luc J W van der Laan, Wanlu Cao, Maikel P Peppelenbosch, Qiuwei Pan. ***Cells*.** 2020 Jan 4;9(1):121

Miao, Z.; Zhang, S.; Ou, X.; Li, S.; Ma, Z.; Wang, W.; Peppelenbosch, M.P.; **Liu, J.**; Qiuwei Pan. Estimating the global prevalence, disease progression and clinical outcome of hepatitis delta virus infection; ***J Infect Dis*** 2020 Apr 27;221(10):1677-1687. doi: 10.1093/infdis/jiz633.

Chen, K.; Sheng, J.; Ma, B;. Cao, W.; Hernanda, P.Y.; **Liu, J.**; Boor. P.; Tjon, A.; Felczak, K.; Sprengers, D.; Pankiewicz, KW.; Metselaar, H.J.; Ma, Z.; Kwekkeboom, J.; Peppelenbosch, M.P.; Pan, Q; Suppression of Hepatocellular Carcinoma by Mycophenolic Acid in Experimental Models and in Patients. ***Transplantation***. 2019 May;103(5):929-937.doi: 10.1097/TP.0000000000002647.

Ma, B.; Chen, K.; Liu, P.; Li, M.; **Liu, J**.; Sideras, K.; Sprengers, D.; Biermann, K.; Wang, W.; JNM, I.J., et al. Dichotomal functions of phosphorylated and unphosphorylated STAT1 in hepatocellular carcinoma. ***J Mol Med (Berl)*** 2019, *97*, 77-88, doi:10.1007/s00109-018-1717-7.

PhD portfolio

Name of PhD student:	Jiaye Liu
EMC:	Department of Gastroenterology and Hepatology
PhD period:	October 2016 – Dec 2020
Promotor:	Prof. Dr. Maikel P Peppelenbosch
Co-promotor:	Dr. Qiuwei Pan

PhD training

Seminars

2016-2020, Weekly MDL seminar program in experimental gastroenterology and hepatology (attending) (42 weeks/year) (ETCS, 9.0);

2016-2020, Weekly MDL seminar program in experimental gastroenterology and hepatology (presenting) (2 times/year) (ETCS, 4.6);

2016-2020, Biweekly research group education (attending) (21 times/year) (ETCS, 4.3);

2016-20120, Biweekly research group education (presenting) (21 times/year) (ETCS, 4.6)

General academic and research skills: courses

2016 The survival analysis course (ETCS, 0.6);

2018 Introduction to laboratory animal science (ETCS, 4.0);

2016 The basic introduction of SPSS (ETCS, 1.0)

2016 The translational basic and translational oncology (ETCS, 1.8)

Special lectures and conferences

2017 The European Association for the Study of the Liver, Paris, the France (Poster presentation)

2020 The European Association for the Study of the Liver, London, UK (Poster presentation)

2020 The Erasmus Medical Center Molecular Medicine Day, Rotterdam, the Netherlands

Academic awards

China Scholarship Council (CSC) Scholarship (201506100033)

2020 The European Association for the Study of the Liver, London, UK (Young investigator)

Curriculum vitae

Jiaye Liu was born in Sep. 25th, 1989, in Chongqing, Chongqing province, China. He grew up with his beloved parents.

In 2008, he graduated from high school of his hometown and went to the Chongqing medical University of Chongqing. After obtaining the medical degree in 2013, He started a master study on clinical cancer research under the supervision of Prof. Tianfu Wen and graduated three years later.

In 2016, he had an opportunity to start his PhD research under the supervision of Prof. Maikel P Peppelenbosch and Dr. Qiuwei Pan at the department of Gastroenterology and hepatology, Erasmus Medical Center, the Netherlands. With the financial support of China Scholarship Council, he focused his study on inflammation and stem cells in liver disease.